J. LINDHARD

# ON THE THEORY OF MEASUREMENT AND ITS CONSEQUENCES IN STATISTICAL DYNAMICS

Det Kongelige Danske Videnskabernes Selskab
Matematisk-fysiske Meddelelser **39**, 1


Kommissionær: Munksgaard
København 1974

# CONTENTS



## Synopsis


It is attempted to analyse questions of probability common to statistical physics, mathematical statistics, and measurements. Idealized measurements may be used as a starting-point and general irreversible equations of motion of a field as an aid in the analysis. When a field remains independent of a measurement, the measurement contains a simple statement about the field. It is found that the statement is in terms of, not an absolute entropy, but a relative entropy measuring the field with respect to observed frequencies, or in terms of other relative degradation functions. This central question is elucidated further by irreversible equations of motion, showing that only relative entropy, or degradation functions, have the necessary monotonic behaviour. The frequent use of absolute entropy in various disciplines is commented upon. It is found, however, that a new absolute function of the field exists for time-independent equations of motion. Fields dependent on the measurement are also analysed. It is shown how an effective time reversibility in equilibrium may result from irreversible equations of motion.

It turns out to be necessary to look into a celebrated issue in mathematical statistics. This is done separately in § 5, where it is shown how probability statements of outcome of measurements may be inverted to statements about the field from given experimental results. The discussion concerns discrete variables and one-way continuum variables.



PRINTED IN DENMARK
BIANCO LUNOS BOGTRYKKERI A/S
ISBN 87 7304 029 0

## § 1. Introduction

I should begin by forewarning the reader. I am to be concerned with measurements in physics, but will be in danger of conjuring up mathematical fictions rather than events of the real world, since the measurements are conceived in terms of probabilistic Gedankenexperimente. However this may be, the main purpose of the study of measurements is to obtain a stepping stone to fundamental concepts and methods in the dynamics of physical systems.

The present paper has, apparently, a simple pattern. The introduction is mainly concerned with a classification of fields and measurements, and the equations of motion are mentioned briefly. One class of measurements is that where the field remains independent of a measurement, as treated in § 2. At first I discuss direct measurements of an independent field, a subject connected with familiar mathematical statistical methods, like the simple theory of errors. Next, from the measurements one may want to determine the independent field at earlier and later times, and we shall look into the interesting difference between the two cases. Above all, measurements of independent fields lead directly to degradation functions, like entropy, as measures of probability, but in a more general sense than usually conceived. In fact, as shown in § 3, functions like entropy are not absolute measures of a probability field but only relative measures of one field with respect to another one. One absolute function of the field does exist, however, if the equations of motion are time-independent. In the second class of measurements the field depends on the measurement, as discussed in § 4. For successive measurements the properties of Markov chains are obtained in the simpler cases. Dependent fields give possibility of analyzing a basic situation in statistical mechanics, and it is shown how irreversible equations of motion can result in time reversibility in equilibrium.

The first subject mentioned above, i.e. the familiar direct measurement based on the theory of errors or similar statistical methods, turns out to contain unsuspected and treacherous pitfalls. This is because probability statements in measurements are not the desired ones about the unknown

field. Such problems are well-known in mathematical statistics but mainly ignored in physics; they have led to a schism connected with a celebrated suggestion by BAYES. It is necessary, therefore, to look into the probability content of basic measurements. In order not to confuse the main issue of this paper, I have stated the relevant results briefly in § 2. The detailed analysis is postponed to § 5, where it is shown how measurements can yield probability statements as regards the parameters in the theory.

It might be asked why one should discuss, in such detail, abstract measurements as well as an abstract theory, with emphasis laid on probability and irreversibility. A general reason — already inherent in the question — is that probability in physics, primarily in statistical mechanics but also in quantum mechanics, gives rise to much more serious and profound problems than often envisaged. I need not remind of the remarkable differences in point of view in BOLTZMANN's and GIBBS' treatments of statistical mechanics, of the discussions between EINSTEIN and BOHR on quantum theory, or of the more recent information theory approach where the existence of an absolute entropy is claimed before the laws of physics are invoked. It should be emphasized, however, that any measurement is intimately connected with probability and constitutes by itself an irreversible process. On the one hand, if one wants to analyse the basic interpretation of quantum theory it is particularly important to account consistently for probability concepts and for irreversibility. On the other hand, for practical purposes it is useful to formulate a simple general theory, even though it necessitates somewhat abstract concepts. I am well aware that these remarks are somewhat scattered, and that the following discussion too consists of scattered solutions of the major problems aimed at.

**Terminology and equations of motion**

It might be useful, before completing the introductory discussion, to explain some basic concepts and terminology connected with the equations of motion of the field. The term 'statistical dynamics' is meant to indicate that there is an arrow on the time variable in the equations of motion, and that a field usually has conservation and is non-negative. The general description is discussed in detail in a previous paper[12], in the following referred to as SSD. I do not invoke the Hamiltonian equations of motion but use a more general formulation where irreversibility is explicit. If so desired, the reader may consider it as retarded solutions of the equations of motion, as exemplified by Brownian motion of a Hamiltonian system.

We are concerned with a coordinate variable, which may be discrete ($j = 1,2,3,\ldots n$), or continuous. Consider, for definiteness, a discrete variable and introduce an initial field $\bar{A} = (A_1, A_2, A_3, \ldots, A_n)$ where $A_j \geq 0$ and $\sum_j A_j = 1$. In a linear theory, a final field $\bar{a} = (a_1, a_2, a_3, \ldots, a_n)$ is then determined by $\bar{A}$ and by transition rates $T_{kj}$ from state $j$ to state $k$ by

$$\bar{a} = \bar{\bar{T}} \cdot \bar{A}, \text{ or } a_k = \sum_j T_{kj} A_j, \tag{1.1}$$

where we must assume $T_{kj} \geq 0$ in order that $a_k \geq 0$, and $\sum_k T_{kj} = 1$, so that $\sum_k a_k = 1$.

The propagator $\bar{\bar{T}}$ should be considered as resulting from equations of motion of type of

$$\frac{\partial}{\partial t} a_k(t) = \sum_j \{G_{kj}(t) a_j(t) - G_{jk}(t) a_k(t)\}, \tag{1.2}$$

where $G_{kj}(t) \geq 0$. In (1.1) the fields $\bar{A}$ and $\bar{a}$ can then be, respectively, $\bar{a}(t')$ and $\bar{a}(t'')$, $t'' \geq t'$, so that $T_{kj} = T_{kj}(t'',t')$. In the case of continuum variables the above equations remain valid if $j \to x'$, $k \to x''$, so that e.g., $T = T(x'',t'';x',t')$ and $a_k(t) \to a(x,t)$. If the coefficients $G$ in (1.2) are time-independent, the propagator is a function of the time difference only, $T = T(x'',x',t'' - t')$, and there is a unique equilibrium for indivisible systems (cf. SSD). A main point is that $T(x'',t'';x',t')$ does not exist for $t'' < t'$, and for discrete variables the propagator $T_{kj}$ does not fulfill the rule of non-negative fields when $t'' < t'$.

Note that the variable $t$ need not be time, so that any one-way variable will do as well. One example is the path length moved by a particle suffering collisions and being possibly slowed down. Transformations between one-way variables are exhibited in § 5.

**Measurements and interpretation of fields**

Measurements are irreversible processes. I shall not here investigate this basic aspect of measurements but only note that it is not at variance with the above-mentioned irreversible equations of motion. The problem with which we shall be concerned is the probability property of measurements. In fact, in the following it will be supposed that a measurement is a more or less imperfect sampling, in the sense of mathematical statistics. Though plausible, also this assumption would seem to require an explanation, concerning its consistency and its connection to the theory of physics. I refrain from a closer discussion but, in part, the consistency will be elucidated.

It is useful to make a classification of measurements, and of the field to be measured. First, one may want to find from a measurement the immediate value of the field, $\bar{a}(t)$. This is clearly the simplest case, and there is also little difficulty in finding from it the field at a later time. Second, in many physical problems one asks preferably for a previous field $\bar{a}(t - \tau)$, as introduced above. One is here up against the difficulty that, whereas $\bar{a}(t)$ may be determined from $\bar{a}(t - \tau)$ according to (1.1), the inverse determination of $\bar{a}(t - \tau)$ is not straightforward, mainly because a propagator backwards in time does not exist. There is thus no symmetry between past and future, and it becomes more difficult to predict the past than the future.

As to the interpretation of the field, $\bar{a} = \bar{a}(t)$, and its relation to measurements, one may meet with several situations. We confine the discussion to two major cases. In these classifications I distinguish between properties of the measurements and properties of the field. The distinction is convenient but not strictly correct. In the end, most of the properties of the field, like its independence, are determined by the measurement and by the parameters one decides to measure.

**Independent field**

In one type of field measurement the field remains independent of the measurement. A familiar phenomenon of this kind is an incoming current of identical, but independent, particles, which suffer collisions in a gas. The incoming current is supposed to have a steady probability distribution in space and in momentum. One measures each time on a new particle, but on the same probability distribution. A similar example of independent fields is observations of the spectral distribution of electromagnetic radiation from a star.

One may perform measurements at various time instances and collect information about the field. By time is meant the independent one-way variable of the field, e.g., the path length moved or the time variable for each particle. The spatial variable of the field can be coordinate space, momentum space, or phase space; and it may alternatively be considered as a discrete variable, for instance when counters are used. Each measurement concerns a new particle whose behaviour is independent of the others but governed by the same field $a(x,t)$. The theory of independent fields is discussed in § 2.

**Dependent field**

In the second case the field depends on the measurement. Consider the above-mentioned current of particles through a gas, or a Brownian motion. One may measure the generalized coordinates of a particle at a certain time, and ask for the new probability distribution of it at subsequent and even at prior times. This case is to be discussed in some detail. However, this case may also be conceived in a more general way. The 'particle' may be a small or large physical system and its distribution is then the ensemble of Gibbs, but now governed by explicitly irreversible equations of motion. From a mathematical point of view the measurements of dependent fields can have connections to Markov processes, as we shall see. Measurements of a dependent field may alternatively be considered as preparations of a system in a more or less well-defined state. But it should be remembered that the

basic preparation of systems, before performing experiments, is to let them achieve equilibrium, whereby a quite definite state is obtained with comparative ease. The dependent field is treated in § 4.

The above division into classes of fields and measurements appears to be useful. Still, in actual measurements one may be concerned with, say, a mixture of independent and dependent fields. Thus, in measurements of Brownian motion, SVEDBERG observed the number of particles in a small volume at successive time instances. For particles which enter the volume one is concerned with the independent field, while for those which have been observed it is the dependent field.

Usually, the field is normalized to unity or to a certain particle number, and so is the measurement. This holds particularly for the case of dependent fields. But often the field or the measurement does not represent a fixed number of particles. Fields of this kind correspond to the grand ensemble of Gibbs, with particular mathematical simplifications. Measurements without a fixed number of particles are familiar in the form of Poisson distributions.

## § 2. Measurements of Independent Fields

The concept of measurement of independent fields was explained in the introduction. In some respects this case is the simplest one. In fact, when the field is independent one may perform an arbitrary number of measurements of the same field, and none of the results will be influenced by any of the others. I consider primarily the simpler case of measurement of the immediate field $\bar{a}$, but will take up measurements of previous and later fields at the end of this chapter.

### Probability by measurement of immediate field

Direct measurements of an independent field are closely connected to a subject treated extensively in textbooks on statistical methods and probability. Furthermore, if one is concerned with a large number of recordings there is little difficulty in interpreting the results in a straight-forward way. Yet, the simple measurements contain a celebrated problem and other difficulties which have to be discussed and clarified, because of their importance to measurements in physics. These difficulties arise since a normal statistical statement gives only the probabilities of various outcomes, assuming the parameters (the field $\bar{a}$) to be known. In a measurement, on the contrary, one wants a statement, possibily a probability statement, as regards the unknown parameters for a given outcome. I call this the question of inversion of

probability. The question was raised by BAYES in 1763[1] but even in present mathematical statistics there are several schools of thought about it.

In order not to confuse the main issue of the present paper, I now give merely a summary discussion of the direct measurement, with preliminary statements as to the inversion of probability. A more detailed analysis is necessary but it is postponed to § 5, at the end of the paper.

The discussion of measurements is rather different for fields, $a_k$, depending on a discrete coordinate variable, and fields $a(x)$ with a continuum variable. For the present I confine the discussion to discrete variables, where the number of unknown quantities to be determined is explicitly finite. The field is $\bar{a} = (a_1, a_2, \ldots, a_n)$, $\sum a_i = 1$, and thus any function, $f_i$, depending on the discrete variable $i$ has a value (average) $\langle f \rangle = \sum f_i \cdot a_i$.

The elementary measurement is taken to be a single count in one of the $n$ places. To the $i$'th outcome is ascribed a probability, assumed to be given by the number $a_i$. Let $N$ elementary measurements be performed. The basic assumptions are that the measurements are independent and indistinguishable. From independence it follows, first, that all measurements have the same probability field $\bar{a}$ and, second, that the probability of a composite event is the product of the individual probabilities. It is thus possible to assign a probability to every set of measurements. The assumption of indistinguishable measurements is merely a simplification, implying that any ordering of the events is immaterial and that only the total number of recordings, $N_i$, in each of the $n$ places is of significance. Thus, it follows that the result of $N$ measurements* is completely specified by $\overline{N} = (N_1, N_2, \ldots, N_n)$, where $N_i = 0,1,2, \ldots$ and $\sum N_i = N$.

From the above it can be concluded that the probability of $\overline{N}$, for given $\bar{a}$ and $N$, is the familiar formula

$$P_{\bar{a},N}(\overline{N}) = \frac{N!}{N_1!N_2! \ldots N_n!} a_1^{N_1} a_2^{N_2} \ldots a_n^{N_n}. \tag{2.1}$$

Again, a function $f(\overline{N})$ has a value given by $\langle f \rangle = \sum_{\overline{N}} f(\overline{N}) P_{\bar{a},N}(\overline{N})$, the summation being over all $\overline{N}$ belonging to $N$. In particular, it is observed that (2.1) implies $\langle N_i/N \rangle = a_i$. The main significance of (2.1) is the rules of probability contained in it. In addition to the discussion above, it may be mentioned that (2.1) obeys the rule of additivity of probabilities. Thus, (2.1)

* Note that the distinction between a single measurement and $N$ measurements is usually a convention. The $N$ measurements may be conceived as, and may actually be, a single measurement, i.e. one $N$-measurement.

is one of the terms in $(a_1 + a_2 + \ldots + a_n)^N = 1^N$, and here one can join elements, $a_{12} = a_1 + a_2$, if the counts are joined, $N_{12} = N_1 + N_2$.

These remarks are meant to illustrate the uniquely defined properties of probabilities for outcome of measurements. The main features are those of mass distributions. It is not necessary to invoke a connection between probabilities and frequencies belonging to real measurements. Instead, in the mathematical limit of $N \to \infty$ the numbers $N_i/N$ converge towards $a_i$, since according to (2.1) $\langle (N_i/N)^s \rangle \to a_i^s$, for $s \geq 0$.

The measurement described by (2.1) concerns a fixed number of counts, $N$. It is often convenient to relax this bond. Calculations can be simpler if the $N_i$ are completely independent. In fact, many physical measurements are just of this kind. Thus, one may have $n$ identical counters measuring intensities of a scattered beam. The intensities are proportional to $a_i$. If all counters are open during the same time interval, the individual countings are independent and have probabilities $p_{a_j, M}(N_j)$, where

$$p_{a_j, M}(N_j) = \frac{(Ma_j)^{N_j}}{N_j!} e^{-Ma_j}, \quad j = 1, 2, \ldots, n. \tag{2.2}$$

The probabilities (2.2) are the familiar Poisson distributions. The total probability is

$$P_{\bar{a}, M}(\bar{N}) = \prod_{j=1}^{n} p_{a_j, M}(N_j) = e^{-M} \prod_{j=1}^{n} \frac{(Ma_j)^{N_j}}{N_j!}, \tag{2.3}$$

which formula is not unlike (2.1). The parameter $M$ is also the total average number of counts, $M = \sum_j \langle N_j \rangle$, and it is proportional to the time during which the counters are open. The measurements (2.1) and (2.2) are analogous to the statistical mechanical concepts of petit ensembles and grand ensembles, respectively.

**Distribution of immediate field from measurement**

I now turn to the actual problem of inversion of probability, i.e. the possibility of a probability statement as regards $\bar{a}$ for a given observation $\bar{N}$. It should be emphasized from the start that the experiment stated in (2.1) does not—when unmodified—allow of unique inversion of probability. In § 5 it will be shown how a slight modification leads to inversion of probability, and also how inversion obtains in the continuum case without modification of the experiment. The aim here is merely to quote from § 5 the results as

regards inversion of probability, for a discrete variable. Still, it seems appropriate to accompany the formulae by qualitative arguments which, I hope, make the results plausible. In addition, such arguments emphasize that, for large $N_i$, there is little difference between the various points of view on inversion.

Suppose for simplicity that $n = 2$ in (2.1), so that there is only one parameter, $a_1$, since $a_2 = 1 - a_1$. In the limit of large $N$, the formula (2.1) then becomes

$$P_{a_1, N}(N_1) \propto \exp\left\{-\left(\frac{N_1}{N} - a_1\right)^2 \Big/ 2\sigma^2\right\},$$

where $\sigma^2 \sim a_1 (1 - a_1)/N \sim (N_1/N)(1 - N_1/N)/N$ may be considered as a constant. If $N_1/N$ is taken to be a continuum variable, the distribution is Gaussian in the variable $a_1 - N_1/N$, and thus the unknown parameter $a_1$ has a Gaussian distribution about $N_1/N$.

Because of the above asymptotic results, the direct probability (2.1) will in some respects correspond to a probability of $\bar{a}$ for given $\bar{N}$. Introduce therefore a factor taking account of this contribution,

$$L_{\bar{N}}(\bar{a}) = a_1^{N_1} a_2^{N_2} \ldots . a_n^{N_n} = \exp\Big(\sum_{i=1}^{n} N_i \log a_i\Big). \tag{2.4}$$

The quantity $L$ in (2.4) is often called likelihood, a term introduced by R. A. FISHER[8], in order to emphasize that one is not concerned with a probability. But in contrast to the original notion of FISHER, the likelihood is here part of a distribution of the field $\bar{a}$.

The differential distribution af $\bar{a}$ may be written on the form, cf. (5.22),

$$\tilde{P}_{\bar{N}}(\bar{a}) \cdot \frac{da_1}{a_1} \cdot \frac{da_2}{a_2} \cdot \ldots \cdot \frac{da_n}{a_n} \cdot \delta\Big(\sum_i a_i - 1\Big), \tag{2.5}$$

where the $\delta$-function takes care of the bond between the values of $a_i$. The integral of (2.5) over all values of $a_i$ ($0 \leq a_i \leq 1$) is normalized to unity.

Write next $\tilde{P}$ as

$$\tilde{P}_{\bar{N}}(\bar{a}) = C \cdot L_{\bar{N}}(\bar{a}) \cdot w(\bar{a}), \tag{2.6}$$

where $w(\bar{a})$ is an uncertainty factor and $C$ accounts for normalization.

The distribution $\tilde{P}_{\bar{N}}(\bar{a})$ is bracketed within a relatively narrow interval of probability distributions. This is expressed by the uncertainty factor $w(\bar{a})$ in the following way

$$w(\bar{a}) = a_1^{\xi_1} a_2^{\xi_2} \cdot \ldots \cdot a_n^{\xi_n},$$

where

$$\sum_{i=1}^{n} \xi_i = 1, \quad 0 < \xi_i < 1. \qquad (2.7)$$

The value of the normalization constant $C$ in (2.6) is seen to be

$$C(\overline{N} + \overline{\xi}) = \frac{\Gamma(N + \sum \xi_i)}{\Gamma(N_1 + \xi_1)\Gamma(N_2 + \xi_2) \ldots \Gamma(N_n + \xi_n)}. \qquad (2.8)$$

The factor $w$ thus represents an uncertainty in the probability, but the uncertainty is usually quite negligible. Its magnitude can be ascertained in the estimate of any average by varying $\overline{\xi}$ in (2.7).

Note that the distribution $\tilde{P}_N(\bar{a})$, according to (2.4), (2.5), (2.6), and (2.7), obeys the same rule of composition as (2.1). Thus, if $a_1$ and $a_2$ are combined to one variable, $a_{12} = a_1 + a_2$, by integrating away one variable in (2.5), then one obtains again the same formulae with one variable less and $N_{12} = N_1 + N_2$, as it should be.

In the following I make use of the likelihood (2.4) with $C = C(\overline{N})$ as a sufficiently well-defined representation of inverse probability, the small uncertainty in $w$ being tacitly understood.

**Degradation functions and accuracy of field**

The likelihood represents approximately the probability of a field $\bar{a}$ for a given measurement $\overline{N}$, when $N$ is large. It may be reformulated in the following way. Let $\overline{\nu} = (\nu_1, \nu_2, \ldots \nu_n)$, such that $\sum_i \nu_i = 1$, introduce a quantity $S_{\overline{\nu}}(\bar{a}')$ by

$$S_{\overline{\nu}}(\bar{a}') = \sum_{j=1}^{n} \nu_j \log \frac{a_j'}{\nu_j} \leq 0, \qquad (2.9)$$

and call it the relative entropy of $\bar{a}'$ with respect to $\overline{\nu}$. The relative entropy is equal to zero only when $a_j' = \nu_j$ for all $j$, i.e. $\bar{a}' = \overline{\nu}$. If we introduce $\nu_i = N_i/N$, and disregard the uncertainty factor $w$, we can express the distribution (2.5), (2.6) in terms of the likelihood

$$\tilde{P}_{\overline{N}}(\bar{a}') \simeq C(\overline{N}) L_{\overline{N}}(\bar{a}') \simeq \exp(N S_{\overline{\nu}}(\bar{a}')). \qquad (2.10)$$

When $N$ is large one finds that (2.1), from STIRLING's formula, is also represented by (2.10). It is obvious that, when $N$ becomes large, the field $\bar{a}$

and the measured frequency $\bar{\nu}$ deviate less and less from one another. In this limit we may expand in (2.9), assuming $\bar{\nu} \approx \bar{a}$, and find

$$S_{\bar{\nu}}(\bar{a}') \cong -\sum_j \frac{(a_j' - \nu_j)^2}{2\nu_j} = -\sum_j \frac{a_j'^2}{2\nu_j} + \frac{1}{2} \cong -4(1 - \sum_j (a_j' \nu_j)^{1/2}). \tag{2.11}$$

The above formulae may be used to find how closely an $N$-measurement determines a field. To this end suppose that the field is $\bar{a}$. We make an $N$-measurement with outcome $\bar{N}$, and obtain a normalized likelihood $\tilde{P}_{\bar{N}}(\bar{a}') = C(\bar{N}) \cdot L_{\bar{N}}(\bar{a}')$ for the field being $\bar{a}'$. If we average over all possible outcomes $N_i$, with normalized probability (2.1) and $\sum_i N_i = N$, we find the probability of $\bar{a}'$, for a given $\bar{a}$. Thus

$$\left.\begin{aligned} \tilde{P}_{\bar{a}}(\bar{a}') = \sum_{N_1, N_2 \ldots} & \frac{N!}{N_1! \ldots . N_n!} \frac{(N-1)!}{(N_1 - 1)! \ldots . (N_n - 1)!} \\ & \cdot (a_1 a_1')^{N_1} \ldots . (a_n a_n')^{N_n}. \end{aligned}\right\} \tag{2.12}$$

Introduce here STIRLING's formula in the form $N! \cong (2\pi N)^{1/2} N^N e^{-N}$, and neglect small terms which are in fact of order of magnitude of the uncertainty in $w$.

The important thing to notice is that (2.12) is symmetric in $\bar{a}$ and $\bar{a}'$, and since only one degradation function, (3.4), is symmetric in the variables we should use that, i.e.

$$D_{\bar{a}}^{(-1/2)}(\bar{a}') = \sum_i (a_i a_i')^{1/2}. \tag{2.13}$$

In fact, introduce in (2.12) the quantity $\alpha_j = (a_j a_j')^{1/2} / (\sum_k (a_k a_k')^{1/2})$, where $\sum_j \alpha_j = 1$, and find

$$\tilde{P}_{\bar{a}}(\bar{a}') \cong \sum_{N_j} (2\pi)^{-n+1} \prod_i \left(\frac{N\alpha_i}{N_i}\right)^{2N_i} \cdot (D_{\bar{a}}^{(-1/2)}(\bar{a}'))^{2N},$$

or, replacing the summations by integrations over $\nu_i = N_i/N$,

$$\left.\begin{aligned} \tilde{P}_{\bar{a}}(\bar{a}') \cong (D_{\bar{a}}^{(-1/2)}(\bar{a}'))^{2N} & \cong \exp\{-2N(1 - D_{\bar{a}}^{(-1/2)}(\bar{a}'))\} \\ & = \exp\{-N \sum_i (a_i^{1/2} - a_i'^{1/2})^2\}. \end{aligned}\right\} \tag{2.14}$$

It is not surprising that (2.14) is essentially the square root of (2.10) if $a_i$ is replaced by $\nu_i$. Eq. (2.14) was derived on the assumption that $N$ is large. But in this limit $a_i'$ is close to $a_i$, and then the uncertainty implied

by $w(\bar{a}')$ in (2.7) becomes quite small. Therefore, (2.14) closely represents a probability and the small uncertainty may be estimated. One may thus use (2.14) to find how large $N$ has to be in order that a given accuracy obtains.

If a Poisson measurement (2.2) were used instead of the $N$-measurement, the calculation would be slightly simplified. Still, the main result, i.e. the appearance of $D^{(-1/2)}$, comes about in a surprisingly simple way in the above derivation of (2.14).

From the result (2.14) it may be concluded that degradation functions like (2.13) should tend monotonically to unity with time. Thus, suppose that one chooses to make an $N$-measurement, with a very large value of $N$, in order to be able to distinguish between two fields $\bar{a}$ and $\bar{a}'$. Let the fields obey the equation of motion (1.2). Such equations of motion contain a smearing of the fields so that with increasing time it should become less easy to distinguish between them. One expects therefore that an $N$-measurement gives inferior distinction if performed at a later time instant. But this means that $D^{(-1/2)}$ in (2.13) always tends towards unity. In fact, this monotonic behaviour is proven generally in § 3, cf. (3.13).

**Independent field before and after measurement**

In this section it is still assumed that an $N$-measurement is performed at time $t$. With given equations of motion one asks for statements as to the fields at earlier and later times, to be called respectively the previous and the later fields.

Consider the simple case of the later field. Let the field at time $t$, $\bar{a}(t)$, have a given distribution, e.g., (2.5). The later field, $\bar{a}(t+\tau)$ with $\tau > 0$, is easily obtained, because it is uniquely given by the propagator of the equations of motion, (1.1), $\bar{a}(t+\tau) = \overline{\overline{T}}(t+\tau,\ t) \cdot \bar{a}(t)$. Indeed, the estimate of the value of any function $f(\bar{a}(t+\tau))$ is obtained as an average over (2.5), i.e. $\langle f(\overline{\overline{T}}(t+\tau,t) \cdot \bar{a}(t))\rangle$.

Quite apart from such results, the mere fact that $t+\tau$ is later than $t$ reduces the freedom of choice of $\bar{a}(t+\tau)$. Consider thus the two differential volume elements $d^{(n)}a(t) = da_1(t) \cdot da_2(t) \ldots . da_n(t)$ and its time transform $d^{(n)}a(t+\tau)$. Because of the linear equations of motion their connection is established directly. Note that the $\delta$-function in (2.5) may be left out because it is conserved, the sum $\sum a_i$ being a constant of the motion. From (1.1) the volume elements are found to be connected by the determinant of the propagator matrix,

$$d^{(n)}a(t+\tau) = |\overline{\overline{T}}(t+\tau,t)|\, d^{(n)}a(t), \tag{2.15}$$

where it is readily shown that

$$|\,\overline{\overline{T}}(t+\tau,t)\,| = \exp\left\{-\sum_{k\neq j}^{n}\int_{t}^{t+\tau} G_{kj}(t')\,dt'\right\}. \tag{2.16}$$

For time-independent equations of motion the determinant (2.16) decreases exponentially with $\tau$,

$$|\,\overline{\overline{T}}(t+\tau,t)\,| = \exp\left\{-\tau\sum_{s=0}^{n-1}\lambda_s\right\}, \tag{2.16'}$$

$\lambda_s$ being the eigenvalues of the equation of motion, cf. SSD.

It follows that the available volume in $\bar{a}$-space shrinks with time, decreasing exponentially according to (2.16′) and exceedingly fast when $n$ is large. Moreover, the equation (2.16′) indirectly expresses the fact that, whatever the initial field $\bar{a}(t)$, the later field for large $\tau$ must approach the equilibrium field $\bar{a}^0$.

More delicate problems arise in connection with determination—from a measurement at time $t$—of a previous field, $\bar{a}(t-\tau)$, where therefore $\bar{a}(t) = \overline{\overline{T}}(t,t-\tau)\bar{a}(t-\tau)$. One difficulty is that the inverse propagator does not exist, as is more obvious in the continuum case. In the discrete case, the equations (2.15) and (2.16′) make it clear that if the field did exist at time $t-\tau$, the measured field at time $t$ has a strongly confined region of permissible values.

Another difficulty is that the field at time $t$ is itself influenced by the previous existence of the field. In the extreme case where the field is known to exist at time $-\infty$, the field at $t$ must be the equilibrium field $\bar{a}^0$, and it would be futile to attempt a measurement, unless the equilibrium is unknown. Suppose instead that the field is known to exist at time $t-\tau$. In attempting to find $\bar{a}(t)$ one should in (2.5) express this field in terms of the unknown $\bar{a}(t-\tau)$, the differential volume element being given by (2.15). Therefore (2.5) becomes

$$\left.\begin{aligned} &\tilde{P}_N(\overline{\overline{T}}(t,t-\tau)\cdot\bar{a}(t-\tau))\cdot|\,\overline{\overline{T}}(t,t-\tau)\,|\,d^{(n)}a(t-\tau)\cdot \\ &\cdot\delta(\sum_i a_i(t-\tau)-1)\cdot\prod_{j=1}^{n}\Big\{\sum_l T_{jl}(t,t-\tau)\cdot a_l(t-\tau)\Big\}^{-1}, \end{aligned}\right\} \tag{2.17}$$

stating indirectly the distribution of $\bar{a}(t)$.

As to the determination of the field at earlier times, the distribution of the field at $t-\tau$ is given directly by (2.17), unless it is known to exist before $t-\tau$. Look apart from the latter subtlety and suppose also that $N$ is large

so that the likelihood (2.4) gives the dominating probability factor. The probability for $\bar{a}(t-\tau)$ is then essentially given by (2.10), i.e.

$$C(\bar{N}) \cdot L_{\bar{N}}(\bar{\bar{T}} \cdot \bar{a}(t-\tau)) \simeq \exp\left\{N \sum_{j=1}^{n} \nu_j \log \frac{\sum_{k=1}^{n} T_{jk}(t, t-\tau) a_k(t-\tau)}{\nu_j}\right\}, \quad (2.18)$$

where $\nu_j = N_j/N$.

These brief remarks were meant to indicate the problems connected with previous fields, when the fields are independent. But such cases are quite common in practical measurements, and ad hoc procedures are often used for their solution. A basic property of $\bar{a}(t-\tau)$ is that its components are non-negative, and any prescription which takes account of this can give quite good estimates.

For dependent fields, the corresponding questions of earlier and later times have somewhat different implications, as discussed in § 4.

## § 3. The Relative Degradation Functions and Their Change with Time

It seems proper to indicate a few of the reasons why it may be rewarding to undertake the following, somewhat lengthy, study of relative degradation functions (cf. SSD) and their time behaviour.

First, we have already seen that several of the degradation functions come into play if we make a measurement and ask for the probability of a field, or if we want to distinguish between two fields by a measurement. The degradation functions in question were relative in the sense that they measured one field with respect to another one. Now, we were also concerned with the change in time of fields, where the irreversible equations of motion must lead to a smearing of fields, so that in some sense they approach each other. The quantitative expression for such a tendency, if it has a meaning at all, should apparently be sought for in the degradation functions. Again, the tendency should not depend on the existence of an equilibrium distribution or on time-independence of the equations of motion.

Second, in statistical mechanics the function entropy is used extensively and connected to absolute probabilities. In the theory of information the entropy is often claimed to be a unique measure of information, and this has been used as a basis for an alternative approach to statistical mechanics. It seems important to investigate such claims, and to look into the role of the other degradation functions since they have the same general properties

as entropy. To this end, the time behaviour of the functions will be studied on the basis of quite general equations of motion.

It turns out, above all, that neither the entropy nor the other degradation functions have consistent meaning if regarded as absolute functions; they are relative functions measuring one dynamic field with respect to another one. The reader may also notice that the preceding discussion of measurements, albeit idealized ones, led to relative degradation functions only.

**Degradation functions**

I now attempt a precise discussion of the degradation functions. This family of functions was derived in SSD. They are averages of functions depending on the field $a$, with the property of separability for independent systems. In SSD we considered only degradation functions for the equilibrium field with respect to a time-dependent field. Since I now drop the assumption of time-independent equations of motion, an equilibrium field does not necessarily exist. Consider continuum variables—discrete variables being a special case of this—and introduce the relative degradation function of $n$'th order for the field $a_2(x,t)$ with respect to $a_1(x,t)$,

$$D^{(n)}_{a_1(x,t)}(a_2(x,t)) = \int dx\, a_1(x,t)\left(\frac{a_1(x,t)}{a_2(x,t)}\right)^n, \quad -\infty < n < \infty, \tag{3.1}$$

where the integration extends over the total volume, and where, as indicated, $n$ is any number on the real axis. The functions $a_1$ and $a_2$ are positive and

$$\int a_1(x,t)\,dx = \int a_2(x,t)\,dx = 1. \tag{3.2}$$

It may be noted that

$$D^{(n)}_{a_1}(a_2) = D^{(-1-n)}_{a_2}(a_1), \tag{3.3}$$

and, in particular, the only symmetric function is

$$D^{(-1/2)}_{a_1}(a_2) = \int dx\{a_1(x,t)\,a_2(x,t)\}^{1/2}. \tag{3.4}$$

Because of (3.2), the degradation functions with $-1 \leq n \leq 0$ are always finite. For other values of $n$ the functions may initially be infinite, corresponding to one of the fields being zero in a part of $x$-space. The degradation functions $D^{(0)}$ and $D^{(-1)}$ are equal to unity, representing only normalization. At these values of $n$ the entropies appear. Thus, consider the relative entropy

$$S_{a_1}(a_2) = \int dx\, a_1(x,t) \log \frac{a_2(x,t)}{a_1(x,t)}. \tag{3.5}$$

It is alternatively given by

$$S_{a_1}(a_2) = -\frac{1}{n}(D^{(n)}_{a_1}(a_2) - 1)|_{n\to 0}. \tag{3.6}$$

Beside the familiar entropy (3.5) and the symmetric function $D^{(-1/2)}$ in (3.4), special mention should be made of one further degradation function. If the order is $n = 1$ in (3.1), one gets the simple result

$$D^{(1)}_{a_1}(a_2) = \int dx \frac{\{a_1(x,t)\}^2}{a_2(x,t)} = 1 + \int dx \frac{\{a_1(x,t) - a_2(x,t)\}^2}{a_2(x,t)}.$$

This function is used extensively in mathematical statistics,[8,6] and is often called the $\chi^2$-function. The field $a_1$ is then—in the discrete case—a measured frequency, while $a_2$ is a probability field.

Some inequalities are immediately found for the degradation functions. They are all equal to unity if and only if $a_1 \equiv a_2$, and generally

$$\left.\begin{aligned} &D^{(n)}_{a_1}(a_2) \geq 1, \quad \text{for} \quad n > 0 \quad \text{or} \quad n < -1, \\ &0 \leq D^{(n)}_{a_1}(a_2) \leq 1, \quad \text{for} \quad -1 < n < 0. \end{aligned}\right\} \tag{3.7}$$

This may be shown by means of an auxiliary function $f_n(\xi)$, where $n$ is a real number,

$$f_n(\xi) = \xi^{n+1} - (n+1)(\xi - 1) - 1, \quad 0 \leq \xi \leq \infty, \tag{3.8}$$

so that $f_n = 0$ for $\xi = 1$. Obviously, when $\xi \neq 1$,

$$\left.\begin{aligned} &f_n(\xi) > 0, \quad \text{if} \quad n > 0 \quad \text{or if} \quad n < -1, \\ &f_n(\xi) < 0, \quad \text{if} \quad -1 < n < 0. \end{aligned}\right\} \tag{3.9}$$

Since $D^{(n)}_{a_1}(a_2) = \int dx\, a_2 f_n(a_1/a_2) + 1$, and since the $D$-functions are positive, the inequalities (3.7) follow from (3.9). It is seen from (3.7) and (3.6) that $S_{a_1}(a_2) \leq 0$.

**Time dependence**

Consider equations of motion of type of (1.2) in a continuum space with arbitrary dimensionality, cf. also SSD,

$$\frac{\partial}{\partial t} a(x,t) = \int dy \{ G(x,y,t)\, a(y,t) - G(y,x,t)\, a(x,t) \}, \tag{3.10}$$

where $G$ is non-negative. In case of a differential equation in space, it can at most be of second order, i.e. of type of a diffusion equation. The bonds on the possible linear equations (as expressed by (3.10) with $G \geq 0$) arise when $a(x,t)$ is required to remain non-negative and to have conservation (3.2). Demand, for simplicity, that the system is indivisible, which means that any point $x'$ within the system communicates with any other point $x''$, so that it cannot be subdivided into independent parts.

We ask for the time derivative of a degradation function (3.1). It contains the time derivatives $\dot{a}_1(x,t)$ and $\dot{a}_2(x,t)$, for which we insert the values given by (3.10). If $G(y,x,t)$ is taken outside as a common factor, the function $f_n$ from (3.8) obtains directly, and we get

$$\frac{\partial}{\partial t} D^{(n)}_{a_1(x,t)}(a_2(x,t)) = -\int dx \int dy\, G(y,x,t)\, a_1(x,t) \left\{ \frac{a_1(y,t)}{a_2(y,t)} \right\}^n \frac{1}{\xi} f_n(\xi), \tag{3.11}$$

where

$$\xi = \frac{a_1(x,t)\, a_2(y,t)}{a_2(x,t)\, a_1(y,t)}. \tag{3.12}$$

It follows then from (3.9) that, unless $a_1 \equiv a_2$,

$$\left.\begin{aligned} &\frac{\partial}{\partial t} D^{(n)}_{a_1}(a_2) < 0, \quad \text{for} \quad n > 0 \quad \text{or} \quad n < -1, \\ &\frac{\partial}{\partial t} D^{(n)}_{a_1}(a_2) > 0, \quad \text{for} \quad -1 < n < 0, \\ \text{and} \quad &\frac{\partial}{\partial t} S_{a_1}(a_2) > 0. \end{aligned}\right\} \tag{3.13}$$

The above demand of an indivisible system is a sufficient condition for the validity of (3.13) but not by far a necessary condition. A weaker, and still sufficient, condition is that for any pair $(x',x'')$ at least one of the points communicates with the other one. This includes one-way systems like (5.7). In any case, equation (3.13) has rather general validity in statistical dynamics, including time-dependent equations of motion and other systems without an equilibrium. It applies for Brownian motion, and the only

notable exception is a first order differential equation in the space $x$. This is essentially the Hamiltonian equations of motion in phase space, for which all degradation functions remain constant in time (cf. SSD).

**Ambiguity of absolute measure of information**

Consider the question of entropy as a measure of information. For definiteness suppose that we are concerned with a discrete variable, $j = 1, 2, \ldots, n$, with corresponding probabilities $p_j$, and that to these belong an absolute measure of information equal to $H$, where $-H$ is statistical entropy, $H = \sum_j p_j \log p_j$, cf. e.g., SHANNON[17] or JAYNES[9]. Now, it is perfectly permissible to let any equation of motion, such as (1.2) or (3.10), act upon the $p_j$. This means that there is a transmission through some medium with a slight smearing of the distribution in question, and it must be demanded that the measure of information cannot increase by such processes. In order to see clearly the ambiguity in $H$ and in $\partial H/\partial t$, introduce another function $s_p(P) = -\sum_j p_j \log(p_j/P_j)$. Put $P_j = 1/n$, so that $s_p(P)$ is equal to $-H$ plus a fixed number ($\log n$) for any value of $p_j$. We find the time behaviour of $s_p(P)$ by letting both $p_j$ and $P_j$ change with time according to the same equations of motion (3.10). Then we have a function which can only increase with time, according to (3.13). Returning to the original $H$, i.e. a function only of $p_j$, we observe that $H$ does not necessarily decrease; it may just as well increase. This implies that $H$ cannot be used as an unambiguous measure of information. The relativity in entropy is also seen easily for a continuum variable, $x$, already because arbitrariness in the choice of variable (replace $x$ by e.g., $y = x^3$) necessitates a comparison of $p(x)$ with another field, $P(x)$.

For physical systems a definite description can obtain. Thus, if the equations of motion are time-independent and the system is confined to an energy shell, there may be only one equilibrium distribution, i.e. $P = \text{const.}$ within available phase space or quantum states. Entropy can then measure a distribution relative to equilibrium. But just for this reason entropy does not determine the equilibrium distribution (in contrast to the $\Theta$-function, cf. below).

The above does not mean that the results in the theory of communication, as based on an $H$-function for coding frequencies, are in error but only that they can not be used universally, in particular as regards connection to entropy. The criticism applies, however, if one turns the tables and tries to use information theory as a starting-point for statistical mechanics or

measurements.[2, 11] In such attempts JAYNES[9] has introduced a further recipe of an a priori distribution, based on absolute entropy and with connection to Bayesian concepts[14, 10, 5]. ROWLINSON[16] mentions some shortcomings of this a priori distribution, exemplified by the die of JAYNES.

Quite apart from the above lack of uniqueness of entropy as absolute measure of information, there are other deficiencies in this measure. For it is not clear beforehand why entropy should be singled out to the exclusion of the other degradation functions, which all have the same general properties (additivity for independent fields, and composition rules). On the contrary, we found previously that statements of the field from measurements contain not only relative entropy but other relative degradation functions as well.

**The $\Theta$-function**

The degradation functions are quite general functions of a field, based only on separability for independent fields. They are not necessarily connected with time dependence of a field or with any equation of motion (cf. e.g. the $\chi^2$-function in mathematical statistics). For some purposes it is a disadvantage that they are relative functions, measuring one field with respect to another one. This circumstance is sometimes obscured when a well-defined equilibrium field exists.

It may thus be well-advised to look for functions which are absolute measures of fields, even though their applicability be less general. I shall consider an interesting function of this kind, to be called the $\Theta$-function.

Let there be a field $a(x,t)$, following an equation of motion of type of (3.10), for instance. Suppose that the equation of motion is time-independent, i.e. $G$ in (3.10) does not depend on $t$. This is clearly a basic situation for systems in physics. Consider a degradation function of $n$'th order, measuring $a(x,t)$ with respect to the field taken a time $\tau$ later, $a(x,t+\tau)$. In the limit of small values of $\tau$ one obtains by expansion

$$D^{(n)}_{a(x,t+\tau)}(a(x,t)) = 1 + \frac{n(n+1)}{2}\tau^2\Theta(a(x,t)) + \ldots, \tag{3.14}$$

where $\Theta$ is given by

$$\Theta(a(x,t)) = \int dx \frac{\{\dot{a}(x,t)\}^2}{a(x,t)}. \tag{3.15}$$

When (3.10) is introduced in (3.15), $\Theta$ is seen to be explicitly a function of one field only, in contrast to the degradation functions. It follows directly

from (3.15) that $\Theta$ is additive for independent fields; when $a = a_1(x,t)a_2(y,t)$ then $\Theta(a) = \Theta(a_1) + \Theta(a_2)$. This property is inherited from the degradation functions through (3.14).

Clearly, $\Theta$ is larger than or equal to zero, the equality sign holding only in equilibrium. Moreover, the degradation functions $D^{(n)}$ were shown to change monotonically with time towards 1. It therefore follows from (3.14) and (3.13) that $\Theta$ as a function of time decreases towards zero, if $G$ in (3.10) is independent of $t$,

$$\frac{\partial}{\partial t}\Theta(a(x,t)) < 0, \quad \text{unless} \quad a(x,t) = a^0(x). \tag{3.16}$$

An obvious application of $\Theta$ is therefore, inserting the equation of motion in (3.15), to find the equilibrium field by variational methods, $\delta\Theta = 0$. It is not the aim here, however, to study such problems but only to point out the noteworthy properties of the $\Theta$-function.

## § 4. Dependent Fields

In the previous case of independent fields there was for instance a constant source of the field, and one could make an unlimited number of measurements, thereby improving the knowledge of the field.

The case of a dependent field is in some respects quite different. It affords further insight in physical problems and has connection to measurements as well as to basic theoretical concepts. Measurements of a dependent field may influence strongly the value of the field. Thus, one may make an observation on a Brownian particle, e.g., by ascertaining its position, and thereby obtain new statements as to its behaviour in time and as to the results of other measurements. When a measurement is made, it can be of interest to follow the system both forwards and backwards in time. Measurements of dependent fields may alternatively be considered as preparation of a specific configuration of the system, being thus part of an experimental setup.

It is convenient to make a separation between complete and incomplete measurements of a dependent field. In a complete measurement all coordinates of the system are recorded exactly. Incomplete measurements may observe all coordinates in an approximate manner, or may record exactly a few of the coordinates only.

I employ the following terminology. The field in the absence of measurements is called the original field. The field as modified by measurements is

the dependent field, labelled by a star. The dependent field after the measurement is called the subsequent field, whereas the dependent field before the measurement is described as the prior field.I f one wishes to visualize these concepts in a simple way, he may suppose that the systems measured have labels so that they can be recognized at all times.

In the following I consider the general case of continuum variables, with discrete variables as an obvious specialization. Suppose that the normalized field, at time $t = 0$, is $a(x,0)$. It obeys the equations of motion (1.1), (1.2), or (3.10), so that for $t \geq 0$

$$a(x,t) = \int dx' \, T(x,t;x',0)\, a(x',0). \tag{4.1}$$

**Complete measurement**

Suppose that a measurement is made at time $t_1$ with the unique result that the particle is at position $x_1$ (for instance a certain point in phase space). This complete measurement implies of course an unwarranted accuracy, but that is of no consequence in the present derivation. In fact, one might instead consider a probability statement with a certain width around $x_1$. Note also that in the corresponding discrete case it is completely justified to suppose that the system is observed at a definite position $k$.

The distribution of the system as determined by the measurement we call $a^*(x, t)$ so that

$$a^*(x,t_1) = \delta(x - x_1). \tag{4.2}$$

The probability of obtaining the measurement (4.2) is represented by the value of the original field, $a(x_1, t_1)$ from (4.1).

It is easy to find the field subsequent to the measurement, since by the equations of motion (4.1) acting on (4.2) one gets

$$\left.\begin{aligned} a^*(x_2,t_2) &= \int dx' \, T(x_2,t_2;x',t_1)\, a^*(x',t_1) \\ &= T(x_2,t_2;x_1,t_1), \qquad t_2 \geq t_1. \end{aligned}\right\} \tag{4.3}$$

Eq. (4.3) is the probability of obtaining $x_2$ at time $t_2$ if one has $x_1$ at $t_1$. If we multiply (4.3) by the probability $a(x_1, t_1)$ of $x_1$ at $t_1$, we obtain the combined probability of the two events

$$P(x_2,t_2,x_1,t_1) = T(x_2,t_2;x_1,t_1)\, a(x_1,t_1), \quad t_2 \geq t_1. \tag{4.4}$$

The result (4.4) may be extended to any number of subsequent measurements by multiplication with the appropriate propagators $T(x_{i+1}, t_{i+1};$

$x_i$, $t_i$). Therefore, one is concerned with a Markov chain[7], as is characteristic of complete measurements of a dependent field. But the more common case of incomplete measurements of a dependent field (cf. below) does not have this Markov property in full.

We next ask for the field backwards in time, as modified by the measurement at $t_1$, and call it the prior field. It is already determined by the previous considerations. The total probability of the two events at times $t_1$ and $t_2$ is given by (4.4) and we can obtain $t_2 < t_1$ by exchanging indices 1 and 2 in this formula, i.e. $T(x_1, t_1; x_2, t_2)a(x_2, t_2)$. The undisturbed probability of $x_1$ at $t_1$ with the original field is $a(x_1, t_1)$. By dividing into the product we obtain the probability of $x_2$ at $t_2$ if $x_1$ at $t_1$, i.e. the prior field

$$a^*(x_2, t_2) = \frac{1}{a(x_1, t_1)} T(x_1, t_1; x_2, t_2) a(x_2, t_2), \quad t_2 \leq t_1. \tag{4.5}$$

Note that $a^*(x_2, t_2)$ is normalized to unity. The formula (4.5) is also familiar for Markov chains (cf. Doob[7]). Observe also that, unless $a$ is the equilibrium field, it may cease to exist when $t_2 \to -\infty$, so that $t_2$ in (4.5) attains a lower limit too.

**Time reversibility in equilibrium**

Let us suppose, first, that the equations of motion are time-independent, so that $T(x_2, t_2; x_1, t_1) = T(x_2, x_1, t_2 - t_1)$. Second, let the original field be the equilibrium field, $a(x, t) = a^0(x)$, and thus independent of time. In fact, this is usually the most convenient way of preparing a system in a well-defined state; if it is left undisturbed for some time the equilibrium is attained with any desired degree of accuracy. When the original field is $a^0(x)$ the prior field (4.5) becomes

$$a^*(x_2, t_2) = \frac{1}{a^0(x_1)} T(x_1, x_2, t_1 - t_2) a^0(x_2), \quad t_2 \leq t_1. \tag{4.6}$$

When $t_2 \to -\infty$, the prior field (4.6) approaches the equilibrium field $a^0(x_2)$, because $T(x_1, x_2, \infty) = a^0(x_1)$. Likewise, the subsequent field (4.3) tends to $a^0(x_2)$ for $t_2 \to +\infty$.

The case considered here has particular interest because it allows a new approach to a familiar problem in the discussion of statistical mechanics near equilibrium. In that connection one often makes use of the conceptions of microscopic reversibility and macroscopic irreversibility. The Onsager

relations[3,15] between thermodynamic parameters are then considered as a consequence of microscopic reversibility, the latter being due to time reversibility of the Hamiltonian equations of motion.

The present equations of motion of statistical dynamics are much simpler in having no need of distinction between a macroscopic and a microscopic region, the motion being always irreversible. We can, however, now consider the question of effective time reversibility in equilibrium for a dependent field, on the basis of (4.6) and (4.3). To this end, consider the dependent field at times $t_2 = t_1 \pm \tau$,

$$\left.\begin{aligned} a^*(x_2, t_1 + \tau) &= T(x_2, x_1, \tau), \\ a^*(x_2, t_1 - \tau) &= \frac{1}{a^0(x_1)} T(x_1, x_2, \tau) a^0(x_2). \end{aligned}\right\} \tag{4.7}$$

We demand effective time reversibility in equilibrium, i.e. always

$$a^*(x_2, t_1 + \tau) = a^*(x_2, t_1 - \tau), \tag{4.8}$$

and obtain from (4.7) the condition

$$T(x_2, x_1, \tau) \cdot a^0(x_1) = T(x_1, x_2, \tau) a^0(x_2) \quad \text{for all} \quad \tau > 0. \tag{4.9}$$

The condition (4.9) requires that — in equilibrium — the rate of transition from any space point to any other point during any finite time $\tau$ is equal to the opposite rate. This property was called spatial reversibility in SSD. It was shown there that (4.9) is completely equivalent to a demand of spatial reversibility of the elementary transition rates, cf. (3.10),

$$G(x_2, x_1) a^0(x_1) = G(x_1, x_2) a^0(x_2) \tag{4.10}$$

for all $x_1$, $x_2$. It does not matter if $G(x_1, x_2) = 0$ for many $x_2 \neq x_1$, or for all $x_2 \neq x_1$, i.e. the limit where differential equations obtain from (3.10). The demand is merely that the system is indivisible, and thus has a unique equilibrium $a^0(x)$, and that (4.10) is fulfilled.

The demand of effective time reversibility in equilibrium leads to, e.g., the Onsager relations. But it is not necessarily connected with time reversibility of the equations of motion. On the contrary, according to (4.10) it poses a simple condition on the equations of motion. This condition is easily fulfilled by differential equations of motion, like Brownian motion. The situation is illustrated by the two following examples.

**Example; Brownian motion**

Consider Brownian motion of a particle in momentum space without external forces.[4] In this case momentum space gives a complete account of the behaviour, if we abstain from asking about the motion in coordinate space. Assume therefore that the equation of motion is

$$\frac{\partial}{\partial t} a(p,t) = \frac{\partial}{\partial p} D\left\{\frac{\beta p}{M} + \frac{\partial}{\partial p}\right\} a(p,t), \tag{4.11}$$

where $D$ and $\beta$ are constants. The equilibrium of (4.11) is given by the Maxwell distribution

$$a^0(p) = (\beta/2\pi M)^{1/2} \exp(-\beta p^2/2M). \tag{4.12}$$

According to SSD, p. 29, the equation (4.11) leads to spatial reversibility. In order to see this explicitly, find the propagator $T(p,p_0,\tau)$ belonging to (4.11). It is

$$T(p,p_0,\tau) = \left\{\frac{\beta}{2\pi M(1-e^{-2\lambda\tau})}\right\}^{1/2} \exp\left\{-\frac{\beta}{2M}\frac{(p-p_0 e^{-\lambda\tau})^2}{1-e^{-2\lambda\tau}}\right\}, \tag{4.13}$$

where the damping time is $\lambda^{-1} = M/(D\beta)$.

It follows from (4.13) and (4.12) that

$$\frac{1}{a^0(p)} T(p,p_0,\tau) = \frac{1}{a^0(p_0)} T(p_0,p,\tau), \tag{4.14}$$

i.e. spatial reversibility in momentum space.

Now, if the particle is measured to have momentum $p_0$ at a certain time $t$, then (4.13) represents its distribution in $p$ at a time $t + \tau$. But if the original distribution was the equilibrium (4.12), then it follows from (4.14), (4.6) and (4.3) that the distribution of the measured particle is also (4.13) at a time $t - \tau$. There is thus time reversibility in equilibrium because of the reversibility in momentum space for the time irreversible equation of motion (4.11). With this example we are getting close to statistical dynamics in phase space, where the Hamiltonian equations of motion play a part. In fact, with a view to this we can formulate another symmetry property of (4.11). Note that in (4.13)

$$T(-p,-p_0,\tau) = T(p,p_0,\tau). \tag{4.15}$$

Therefore (4.14) becomes, because of (4.12),

$$\frac{1}{a^0(p)} T(p,p_0,\tau) = \frac{1}{a^0(-p_0)} T(-p_0,-p,\tau). \tag{4.16}$$

This result is the one which remains valid in statistics in phase space.

**Counterexample: Multiple scattering with damping**

It is instructive to consider a case without spatial reversibility, for continuum variables. The purpose is not merely to show that mathematically simple counter-

examples may be found. It is, rather, to make clear that absence of reversibility in, e.g., momentum space is not only possible but even quite common in familiar problems from physics.

Small angle multiple scattering is equivalent to motion in transverse momentum space. The previous paper, SSD, contains several exact solutions of such integral equations. The simplest case of this kind corresponds, approximately, to classical scattering by $R^{-2}$-potentials. Let us in this case introduce a damping of the transverse motion, proportional to transverse momentum and due to slowing-down effects. This is not unlike what may happen in e.g., proper channelling[13].

The desired equation of motion in momentum space is, if we simplify to the one-dimensional case,

$$\frac{\partial}{\partial t} a(p,t) = \lambda \frac{\partial}{\partial p} \{p a(p,t)\} + C \int_{-\infty}^{\infty} \frac{d\eta}{\eta^2} \{a(p+\eta,t) - a(p,t)\}, \tag{4.17}$$

where $p$ is the small transverse momentum, and $\eta$ the change of transverse momentum by scattering. The equilibrium belonging to (4.17) is

$$a^0(p) = \frac{C/\lambda}{p^2 + \pi^2 (C/\lambda)^2}. \tag{4.18}$$

It is not difficult to find the propagator $T(p,p_0,\tau)$ belonging to (4.17),

$$T(p,p_0,\tau) = \frac{(1-e^{-\lambda\tau}) \cdot (C/\lambda)}{(p - p_0 e^{-\lambda\tau})^2 + \pi^2 (1-e^{-\lambda\tau})^2 (C/\lambda)^2}, \tag{4.19}$$

which formula has several features in common with the corresponding one for Brownian motion, (4.13). But there is not spatial reversibility, since (4.18) and (4.19) do not fulfill (4.14). In fact, suppose that the system is in equilibrium, and that at $t$ the momentum is measured to be $p_0$. The subsequent field, (4.3), is then given by (4.19)

$$a^*(p,t+\tau) = T(p,p_0,\tau), \tag{4.20}$$

but the prior field is, according to (4.6),

$$a^*(p,t-\tau) = \frac{p_0^2 + \pi^2 (C/\lambda)^2}{p^2 + \pi^2 (C/\lambda)^2} \cdot \frac{(1-e^{-\lambda\tau}) \cdot (C/\lambda)}{(p_0 - p e^{-\lambda\tau})^2 + \pi^2 (1-e^{-\lambda\tau})^2 (C/\lambda)^2}. \tag{4.21}$$

The formulae (4.21) and 4.20) are quite dissimilar; note in particular that, for $p \to \infty$, $a^*(p,t-\tau)/a^*(p,t+\tau) \to 0$. This result illustrates also how transient equilibrium distributions in physical systems may fail to give effective time reversibility, when integro-differential equations of motion are involved.

**Incomplete measurement**

As a supplement to the previous complete measurement of a dependent field let us discuss briefly the consequences of incomplete measurements. As an example, a number of particles may perform Brownian motion, the

instantaneous state of each particle being given by a point in phase space. An incomplete measurement might be to record only one momentum component of a particle. This case being quite simple, I shall instead look into the alternative problem where a measurement is only approximate.

Let the original field be given by (4.1) as before. Consider an incomplete measurement in the sense that it gives only a probability statement about the coordinates of the system. For definiteness, suppose that one has a counter measuring at time $t_1$, with its centre placed at $x_1$. If a particle passes the point $x$ at $t_1$, the counter gives off a signal with probability $f(x - x_1)$. Only the relative probabilities of signals matter for the present, so assume that $\int dx f(x - x_1) = 1$. But it should be realized that successive measurements imply a decrease which can have serious consequences.

We ask for the value of the prior field $a^*(x_2, t_2)$, $t_2 < t_1$, when an observation is made with the counter at time $t_1$, given the original field $a(x,t)$. If a particle starts from $x_2$ at $t_2$ its probability of reaching $x$ is $T(x, t_1, x_2, t_2)$. Its probability of being recorded is therefore $\int dx f(x - x_1) T(x,t_1 ; x_2, t_2)$. Moreover, the original probability of arriving at $x_2$, $t_2$ is $a(x_2, t_2)$ and, if this is multiplied into the integral, one gets the total probability of recording a particle having passed through $x_2$, $t_2$. Now, this is also—apart from a constant of normalization—the probability that the particle was at $x_2$, $t_2$, when it is recorded at time $t_1$; in fact, the latter result expresses merely the theorem of BAYES[7,10,14]. The prior field is therefore

$$a^*(x_2, t_2) = C^{-1} \int dx f(x - x_1)\, T(x, t_1; x_2, t_2)\, a(x_2, t_2), \quad t_2 \leq t_1, \tag{4.22}$$

with

$$C = \int dx_2 \int dx f(x - x_1) T(x, t_1; x_2, t_2)\, a(x_2, t_2) = \int dx f(x - x_1)\, a(x, t_1). \tag{4.23}$$

When the two times are equal, $t_2 = t_1$, (4.22) becomes, since $T(x,t_1; x_2,t_1) = \delta(x - x_2)$,

$$a^*(x_2, t_1) = C^{-1} f(x_2 - x_1)\, a(x_2, t_1), \tag{4.24}$$

and this result is more easily obtained by a direct argument.

By means of the propagator (4.1) acting on (4.24) the subsequent field obtains,

$$a^*(x_2, t_2) = C^{-1} \int dx\, T(x_2, t_2; x, t_1) f(x - x_1)\, a(x, t_1), \quad t_2 \geq t_1. \tag{4.25}$$

In a general sense, therefore, the results for incomplete measurements of dependent fields do not deviate from those for complete measurements,

except in being more complicated. In particular, the results concerning effective time reversibility in equilibrium, as expressed in (4.9) and (4.10), remain valid for incomplete measurements, i.e. when (4.22) and (4.25) hold.

## § 5. Inversion of Probabilities

The direct probability for a discrete variable was illustrated in (2.1) and (2.3), where the probabilities of various events $\bar{N}$ were found when the independent field $\bar{a}$ was given. The problem of inversion consists in finding what statement may be made about the field $\bar{a}$ when some event $\bar{N}$ is observed. This statement is, at most, a probability distribution of the field.

In the following I therefore suppose that no more than the direct probability is known for a complete set of events and for any field. I ask whether an inverse probability follows uniquely from it. We shall find that in some cases there is in fact a unique solution, while in other cases the solution has an uncertainty. This is quite similar to the results in usual inversion problems in mathematics.

It appears necessary to state the basic problems and their solution in some detail, because one may easily be led astray in these questions. In fact, the difficulties met with have led to various schools of thought in mathematical statistics, since the time when BAYES[1)] drew attention to the problem. In consequence, a number of concepts of different content are used in the literature. They range from the cautious use of 'likelihood', not conceived as a probability,[8)] to the introduction of 'a priori probabilities',[10,14)] which are not part of the problem as stated above.

More specifically, the following discussion takes up two major problems. The first one is the question of inversion of probability between continuum variables, to be studied in some detail for one-way variables. The second problem concerns a discrete variable, e.g., a true discrete variable like the number of alpha-particles emitted by a radioactive specimen, or an artificial one created by dividing a continuum variable into a number of intervals for the purpose of measurement. With a discrete variable one does not have a unique inversion of probability but a latitude appears as we shall see.

A third major problem concerns actual interpretation, in a given experiment, of an inversion statement about the field. This problem can be the most intriguing one. Thus, if one asks for a statement concerning an unknown parameter $\lambda$, the latter need not be, say, a stochastic quantity since it can have a fixed unknown value. Of course, it can then be difficult to have a realizable frequency interpretation of the probability of $\lambda$; but that may

occur for direct probabilities too. The more subtle difficulties are connected with other properties of probability, like independence and composition rules.

To sum up: I shall consider merely the well-defined question of what inversion statement is permitted when just the direct probabilities are known. I do not attempt to introduce a systematic and comprehensive theory, selecting instead suitable examples, which also illustrate actual applications. Whereas the aim is discrete variables, I solve first the simple case of one-way continuum variables.

**One-way distribution in continuum case, and its inversion**

Inversion of probability is a generalization of inversion of a function.* Thus, consider two variables, $t$ and $x$, and a curve $x = f(t)$ in the $t$–$x$ plane. The basic case for inversion of the function $f(t)$ obtains when it increases monotonically with $t$, because then the inversion $t = f^{-1}(x)$ is unique. We may suppose that $0 \leq t < \infty$, that $f(0) = 0$, and that there is no upper bound of $f(t)$; this does not imply a limitation of the results. If $f(t)$ were not monotonically increasing, one would have a more complicated problem of inversion. In particular, if $f(t)$ were constant in an interval $t_1 \leq t \leq t_2$, there would be no unique inversion when $x = f(t_1)$. As we shall see, the one-way variables in probability theory—or in statistical dynamics—are the analogue of monotonically increasing functions.

Consider the general case of a distribution of mass, with density $\varrho = \varrho(x, t)$, where $\varrho$ is defined for $0 \leq t < \infty$, $0 \leq x < \infty$, and $\varrho \geq 0$. If I regard the mass distribution as a probability distribution of $x$ for a given $t$, I write $P_t(x) \equiv \varrho(x, t)$. The distribution is assumed to have conservation, or

$$\int_0^\infty dx\, \varrho(x,t) = 1, \quad 0 \leq t < \infty. \tag{5.1}$$

It follows from the conservation (5.1) that, at the point $x$ at time $t$, one may introduce a current $j(x, t)$ as

$$j(x,t) = -\frac{\partial}{\partial t}\int_0^x \varrho(x',t)\,dx' \equiv -\frac{\partial}{\partial t} M(x,t), \tag{5.2}$$

or

* Because of this simple connection I use the term 'inversion' of probability. I should mention that, in mathematical statistics, the word 'inversion' is sometimes used in a different sense.[8, 10]

$$\frac{\partial}{\partial t}\varrho(x,t) + \frac{\partial}{\partial x}j(x,t) = 0. \tag{5.3}$$

I shall suppose that, for all $t$ and $x$, the function $j(x, t)$ in (5.2) is non-negative,

$$j(x,t) > 0, \quad \text{when} \quad \varrho(x,t) > 0. \tag{5.4}$$

This means that the distribution $\varrho(x, t)$ always moves in the direction of the positive $x$-axis, where motion stands for change when $t$ increases. Eq. (5.4) therefore implies that $x$ is a one-way variable, and that the distribution behaves similarly as the monotonous function $f(t)$.

Make now the following three assumptions as to the density $\varrho(x, t) \equiv P_t(x)$. First, suppose that $\varrho(x, 0) = \delta(x)$, so that at time $t = 0$ the distribution starts at the origin. Second, assume that there is not a finite probability placed on the $t$-axis outside the origin, i.e. $\varrho(x, t)$ can not contain a component of type of, say, $\delta(x) \cdot e^{-t/\tau}$. Third, assume for convenience that $\varrho(x, t \to \infty) \to 0$ at any fixed $x$, so that the distribution moves to infinitely large values of $x$ when $t \to \infty$. The third demand, together with (5.2), implies that

$$\int_0^\infty dt\, j(x, t) = 1. \tag{5.5}$$

It is thus plausible that $j(x, t)$ is a probability density. Actually, when (5.4), (5.5) and the three assumptions are fulfilled, there exists a probability density of $t$ for given $x$

$$P_x(t) \equiv j(x,t) = -\frac{\partial}{\partial t}\int_0^x dx'\,\varrho(x',t) = -\frac{\partial}{\partial t}M(x,t). \tag{5.6}$$

I call $P_t(x)$ and $P_x(t)$ the direct and inverse densities connecting one-way variables $x$ and $t$. The above curve $x = f(t)$ is a rather special example of this kind, since $P_t(x) = \delta(x - f(t))$ and $P_x(t) = f'(t)\delta(x - f(t)) \geq 0$.

Let me show, by a simple argument, that (5.6) is the inverse probability. Thus, approximate the density $\varrho(x, t)$ by a set of $N$ successive curves $f_i(t)$, all starting at the origin, increasing monotonically with $t$ without intersection, and tending to infinity for $t \to \infty$. Each of the curves is given a probability weight $1/N$, so that the total weight is 1. We may determine $f_i(t)$ by $i/N = \int_0^{f_i} \varrho(x,t)dx \equiv M(f_i, t)$, whereby the previous assumptions secure that the curves have the desired properties. The total density belonging to the set of curves is $P_t^N(x) = \sum_{i=1}^{N} \delta(x - f_i(t))/N$, but this can be inverted to $P_x^N(t) =$

$\sum_i f_i'(t)\delta(x - f_i(t))/N$, where $f_i'(t) > 0$ since $j(x,t)$ is positive. In the limit of $N \to \infty$, the inverse probability $P_x^N(t)$ becomes $P_x(t)$ in (5.6) which then is the inverse of $P_t(x)$. In order to have uniqueness we must in particular require that the derivative of the first curve, $f_1'(t)$, remains different from zero for any value of $N$; but that is a consequence of the second assumption above. If this assumption were not fulfilled, one would meet with problems like those belonging to discrete variables (cf. p. 35). Note, finally, that when $P_x(t)$ in (5.6) is the inverse of $P_t(x)$, then $P_t(x)$ is also the inverse of $P_x(t)$.

**One-way equation of motion**

Consider now an example of equations of motion for one-way variables. Suppose that the distribution $\varrho(x, t)$, with initial condition $\varrho(x, 0) = \delta(x)$, obeys the integro-differential equation

$$\frac{\partial}{\partial t}\varrho(x,t) = \int_0^\infty g(\eta)\,d\eta\{\varrho(x-\eta,t) - \varrho(x,t)\}, \tag{5.7}$$

where $g(\eta)$ is non-negative. Accordingly, $\varrho(x, t)$ remains non-negative, and it also has conservation, $\int dx\varrho(x, t) = \text{const}$. The equation (5.7) is somewhat specialized in being invariant towards displacements along both $t$-axis and $x$-axis (cf. SSD, in particular § 6). Since only positive values of $\eta$ occur in (5.7), it is obvious that the distribution always moves in the positive $x$-direction and (5.4) is fulfilled.

There are some conditions on $g(\eta)$ in (5.7). In order to have convergent results, so that $\varrho$ does not move promptly to infinity, there are a few demands on $g(\eta)$. It is required that $q_\varepsilon = \int_\varepsilon^\infty g(\eta)\,d\eta$ has a finite value but, when $\varepsilon \to 0$, $q_\varepsilon$ is allowed to diverge. This corresponds to a collision cross section which diverges for soft collisions, if we consider $g(\eta)d\eta$ as being proportional to a differential collision cross section. The divergence can not be too strong, because $\int_0^\varepsilon \eta g(\eta)\,d\eta$ must have a finite value so as to avoid prompt motion to $x = \infty$. The basic solutions of (5.7) are the propagators, i.e. functions which initially are $\varrho(x, t = 0) = \delta(x)$, corresponding to the first assumption. They have the property $\varrho(x, t_1 + t_2) = \int_0^x \varrho(x - x', t_1)\,\varrho(x', t_2)dx'$. In order that the second assumption on p. 30 be fulfilled, so that no part of the distribution remains on the $t$-axis, there is a requirement of $g(\eta)$. We must demand

$$q_\varepsilon = \int_\varepsilon^\infty g(\eta)\,d\eta \to \infty \quad \text{for } \varepsilon \to 0, \tag{5.8}$$

so that the corresponding transition cross section diverges. This is obvious, since if $q_0$ were finite, part of the distribution would remain on the $t$-axis, in fact $\exp(-q_0 t)\delta(x)$.

**Explicit solution of inversion**

We have thus found that the distribution (5.7) with the condition (5.8) can be inverted by eq. (5.6). Consider a specialized case of (5.7), where $g(\eta)$ obeys a power law,

$$g(\eta) = C_n/\eta^{1+n}, 0 < n < 1. \tag{5.9}$$

It is clear, for dimensional reasons, that (5.9) leads to distributions of the kind $P_t(x) \equiv \varrho(x, t) = x^{-1}\varphi_n(x^n/C_n t)$, which is a so-called stable distribution. In this case the inverse probability is immediately obtained from (5.6),

$$P_x(t) = \frac{x}{nt} P_t(x). \tag{5.10}$$

In this simple case $P_x(t)$ is not far from being proportional to $P_t(x)$. This is due to the simple assumptions in (5.7) and (5.9). But it is worth noting that the two probability distributions are not each others 'likelihood'.

Consider a particular choice of $n$ in (5.9). As we shall see, the case of $n = 1/2$ has particular interest. According to SSD one gets the propagator, with $C_{1/2} = C$,

$$P_t(x) = \frac{Ct}{x^{3/2}} \exp\left(-\frac{\pi C^2 t^2}{x}\right). \tag{5.11}$$

The inverse probability is found from (5.10),

$$P_x(t) = \frac{2C}{x^{1/2}} \exp\left(-\frac{\pi C^2 t^2}{x}\right). \tag{5.12}$$

Eq. (5.11) may represent the probability distribution of total energy loss $x$ for an energetic ion which passes through a foil of thickness $t$, suffering elastic collisions with atoms in the foil. The differential probability of an individual energy loss between $\eta$ and $\eta + d\eta$ is $Cdtd\eta/\eta^{3/2}$, cf. (5.9), for passage through a distance $dt$. The distribution (5.11) of total energy loss $x$ for given thickness $t$ is a peak of moderate width. If one measures a given

total energy loss and the thickness is unknown, he finds a wide probability distribution of thickness. It should be emphasized here that interpretation of inversion experiments based on (5.11), (5.12), (5.13), and (5.13′) contains many subtleties, unnecessary for the derivation in the following sections however.

The distribution (5.12) is quite familiar if the problem is turned around. Suppose one has a one-dimensional diffusion process with diffusion constant $D = 1/(4\pi C^2)$, $t$ being the numerical value of the distance from the starting-point, while $x$ is the time variable. Then the Gaussian (5.12) is the direct probability distribution of the distance $t$ for a known value of the time $x$, or of $Dx$. The inverse probability is now (5.11), giving the distribution of the time $x$, or of $Dx = \sigma^2/2$, if one measurement gives the distance $t$ from the origin.

Returning to the definite example of one particle at depth $t$ in a substance having suffered an energy loss $x$, it is quite obvious that knowledge of $t$ gives a distribution (5.11) of energy loss $x$, and knowledge of $x$ gives a distribution (5.12) of range $t$. But suppose in the former case that $x$ has a fixed unknown value, and that $\nu$ measurements are made, giving $t_1, t_2, \ldots, t_\nu$. This may be imagined to happen, somewhat oversimplified, if the track of each particle remains visible until an energy $x$ is lost, the threshold $x$ being unknown. Now, the set of $\nu$ measurements may be considered as a single measurement, and in the present case the formulae are simple if described in a $\nu$-dimensional Euclidean space. Introduce a length $T$ by $T^2 = \sum_{i=1}^{\nu} t_i^2$. The direct probability of $\bar{t}$ is a function of $\nu$ factors and may be expressed by $T$, i.e. on differential form $2(\pi^{1/2}C/x^{1/2})^\nu \exp(-\pi C^2 T^2/x) T^{\nu-1} dT/\Gamma(\nu/2)$. The usual inversion (5.6) leads to

$$P_T(x) = \frac{(\pi C^2 T^2)^{\nu/2}}{\Gamma\left(\frac{\nu}{2}\right)} \frac{1}{x^{\nu/2+1}} \exp\left(-\frac{\pi C^2 T^2}{x}\right), \tag{5.13}$$

which formula is the familiar $\chi^2$-distribution. Second, if the thickness of the substance has a fixed unknown value $t$, and energy losses $x_1, x_2, \ldots x_\nu$ are measured, a differential product probability obtains, as a function of $t$ and $\xi$, where $\xi^{-1} = \sum_{i=1}^{\nu} x_i^{-1}$. By inversion one gets from (5.6)

$$P_\xi(t) = \left(\frac{\pi C^2}{\xi}\right)^{\nu/2} \frac{2\, t^{\nu-1}}{\Gamma\left(\frac{\nu}{2}\right)} \exp\left(-\frac{\pi C^2 t^2}{\xi}\right), \tag{5.13′}$$

quite similarly to (5.13).

These results, belonging to a well-known distribution, are meant to illustrate the straightforward content of direct and inverse probabilities, as well as the combination of several measurements. Though, in principle, similar calculations may be made for other stable distributions (5.9), they are more difficult in practice.

Consider next another example with wide applicability but of particular interest in connection with discrete variables. Suppose that in (5.7)

$$g(\eta) = \frac{C}{\eta} e^{-\eta}, \tag{5.14}$$

corresponding to (5.9) in the disallowed case $n = 0$, but with an exponential cut-off. The total cross section in (5.14) is infinite, i.e. (5.8) is fulfilled. The formula (5.14) is closely analogous to the differential probability per unit time of emitting electromagnetic quanta of energy $\hbar\omega \to \eta$ by an accelerated charged particle. The desired divergence of the total cross section of (5.14) then corresponds to the so-called infrared 'catastrophe'. Replace in (5.7) the variable $x$ by $\tau$ and $Ct$ by $\mu$. The particular solution of (5.14), (5.7) which starts at the origin, i.e. the propagator, is then the gamma density

$$P_\mu(\tau) \equiv \varrho(\tau, \mu) = \frac{1}{\Gamma(\mu)} e^{-\tau} \tau^{\mu-1}, \tag{5.15}$$

with an inverse according to (5.6)

$$P_\tau(\mu) = \frac{1}{\Gamma(\mu)} \int_\tau^\infty d\tau' e^{-\tau'} \tau'^{\mu-1} \{\log \tau' - \psi(\mu)\}. \tag{5.16}$$

**Discrete variable**

As mentioned previously, the case of a discrete variable usually does not allow of a well-defined inversion of probability. There will be a latitude, but the inversion can often be bracketed rather narrowly between two probability distributions.

As a preliminary, consider the Poisson process. For definiteness, suppose that one has a radioactive specimen for which $\lambda$ is the probability of emission of an $\alpha$-particle per unit time. Therefore, $\lambda$ is a measure of the number of radioactive atoms in the specimen, being proportional to this number. Introduce $\tau = \lambda t$ as a dimensionless time variable.

There are two situations with well-defined probability distributions. First, suppose that one records the time instances at which each $\alpha$-particle is emitted. The starting-point of time is chosen to coincide with the emission labelled zero. A familiar analysis of the probability distribution of emission times, for instance by means of an equation analogous to (5.7), gives

$$\left.\begin{aligned} P_0^e(\tau) &= \delta(\tau), \\ P_m^e(\tau) &= \frac{1}{(m-1)!}\tau^{m-1}e^{-\tau}, \quad m = 1, 2, \ldots, \end{aligned}\right\} \tag{5.17}$$

i.e. the gamma distribution. The index $e$ in $P$ indicates that one is concerned with the instant of emission. The distribution (5.17) has the same composition rules as (5.15) but is confined to integers.

If one measures the time $t$ of the $n$'th emission, eq. (5.17) can give the probability distribution of $\lambda = \tau/t$. Consider an example of this kind. Suppose that one has two specimens of $\alpha$-emitters, 1 and 2, and wants to determine the unknown fractional mass $\lambda_1/(\lambda_1 + \lambda_2) = a_1$. Two time measurements are made corresponding to emission numbers $n_1$ and $n_2$, giving times $t_1$ and $t_2$. The separate and independent probability distributions of $\lambda_1$ and $\lambda_2$ are then found from (5.17), whereby the desired probability distribution of $a_1$ is obtained. Note that the two times $t_1$ and $t_2$ cannot be expected to be equal in magnitude. If they are, the quantity $a_1$ acquires the beta distribution, as it should be.

Second, the Poisson distribution results if the counter is open during a given time interval $t$, with a known value of $\lambda$, so that the dimensionless time variable, $\tau = \lambda t$, is known. One then asks about the probability of $n$ particles having been emitted during this time. The derivation is well-known and leads to

$$P_\tau(m) = \frac{1}{m!}\tau^m e^{-\tau}, \quad m = 0, 1, 2, \ldots \ldots \tag{5.18}$$

This type of measurement is the most common one, for instance with a number of specimens counted during the same time interval. It thus comprises both (2.2) and (2.1), i.e. the cases envisaged in § 2. For definiteness, let now the zero-point of the time interval $\tau = \lambda t$ in (5.18) coincide with the emission of a particle, i.e. the particle with label 0.

The noteworthy property of (5.18) is that there is not unique inversion. The reason is simply that one variable is discrete, and the lack of uniqueness has, in a sense, no connection with the fact that we are concerned with probabilities. Thus, the number $m$ in formula (5.18) means that one is somewhere in the interval $(m, m + 1)$. In fact, we have to do with one-way distributions, and thus with distributions in the interval $m \leq \mu < m + 1$ in (5.15). We can therefore introduce inversion of (5.18). The corresponding quantity will be called $\tilde{P}_m(\tau)$, where $\sim$ indicates that the function is not

uniquely defined but contains a latitude. In all estimates we get an interval of distributions

$$P_m^e(\tau) \leq \tilde{P}_m(\tau) < P_{m+1}^e(\tau), \tag{5.19}$$

where the inequalities are symbolic, meaning only that there is a latitude in the index. Thus, it holds in a straightforward sense that averages over $\tilde{P}_m(\tau)$ of increasing functions like $\tau^s$ obey inequalities,

$$\int_0^\infty P_m^e(\tau)\tau^s\,d\tau \leq \int_0^\infty \tilde{P}_m(\tau)\tau^s\,d\tau < \int_0^\infty P_{m+1}^e(\tau)\tau^s\,d\tau, \tag{5.19'}$$

because of the one-way property of the variables. It may also easily be shown that $\tilde{P}_m(\tau)$ has a simple composition rule.

**Determination of $\bar{a}$ from $N$-measurement**

Clearly, the above method allows a determination of $\tau_1$ and $\tau_2$ if $m_1$ and $m_2$ are observed. This gives in fact the inversion statement belonging to formula (2.1). I shall derive this inversion in a more direct way.

Consider a unit interval, $0 \leq \alpha \leq 1$, divided into $n$ parts of length $a_1, a_2, \ldots, a_n$, $\sum a_i = 1$. The magnitude of the $a$'s is unknown. In an $N$-measurement there will be $N$ points on the unit interval, each one with equal probability everywhere, and each one independently of the others. The probability of recording $N_1, N_2, \ldots, N_n$ points in the intervals is evidently given by (2.1). Now, disregard for a while the division in intervals and consider only the distribution of the $N$ points in the unit interval. Let the points be labelled from 1 to $N$ corresponding to increasing values of $\alpha$. If we ask for the distance between point $s$ and point $s + m$, we find that it has a probability distribution in length $P_m(\alpha)\,d\alpha$, where $\alpha$ represents $\alpha_{s+m} - \alpha_s$, and

$$P_m(\alpha)\,d\alpha = \frac{N!}{(N-m)!\,(m-1)!}(1-\alpha)^{N-m}\alpha^m\frac{d\alpha}{\alpha}, \tag{5.20}$$

the so-called beta distribution. Consider next the unknown length $a_i$ on which $N_i$ points are placed. The interval $a_i$ must be greater than the distance between the first and last points within it, i.e. $m = N_i - 1$ in (5.20) but smaller than the distance between the points just outside it, or $m = N_i + 1$ in (5.20). The uncertainty may be narrowed by switching the intervals. Thus, interchange $a_i$ and $1 - a_i$, as well as $N_i$ and $N - N_i$, so that (5.20)

applies with $m$ in the interval $(N_i, N_i + 2)$. Together, the two results imply that the original interpretation of formula (5.20) requires

$$N_i < m < N_i + 1. \tag{5.21}$$

One can in analogy to (5.20) perform a complete discussion with the $n - 1$ variables. But in fact this is not necessary, because the distribution of, say, $a_1 + a_2$ must be the same, whether we consider it as one interval with count $N_1 + N_2$ or as two intervals $a_1$ and $a_2$, afterwards integrating over one of the variables for a fixed sum. In all, we therefore obtain from (5.20) and (5.21), not a uniquely defined probability, but a distribution $\tilde{P}_{\bar{N}}(\bar{a})$ bounded by probability distributions, which may be formulated as follows

$$\left.\begin{aligned} &\tilde{P}_{\bar{N}}(\bar{a})\frac{da_1}{a_1}\cdot\ldots\cdot\frac{da_n}{a_n}\delta(\sum_i a_i - 1) = \\ &= a_1^{N_1}\cdot\ldots\cdot a_n^{N_n}\cdot\frac{da_1}{a_1}\cdot\ldots\cdot\frac{da_n}{a_n}\cdot C a_1^{\xi_1}\cdot\ldots\cdot a_n^{\xi_n}\delta(\sum_i a_i - 1), \end{aligned}\right\} \tag{5.22}$$

where $\sum_i \xi_i = 1$ and $0 < \xi_i < 1$. This formula* is applied in § 2, p. 10ff. The above-mentioned additivity of the $a_i$ is seen to be fulfilled by (5.22). This is the same additivity as is contained in the direct probability (2.1). The present description therefore does not have awkward consequences of the kind resulting from LAPLACE's rule of succession.[10)]

The above discussion of inversion is limited to one group of problems. By and large it seems not to be in disagreement with the ideas of R. A. FISHER[8)], as expressed in particular by the concepts of likelihood and fiducial probability. The proper inversion problems cover both of these concepts at the same time. On the basis of well-defined one-way distributions I have attempted to obtain quantitative statements of inversion, whereas a likelihood concept can lead to only qualitative statements, in the neighbourhood of the present ones though.

The theorem of Bayes applies when one is concerned definitely with conditional probabilities, as for dependent fields in § 4. To extend this theorem to all cases of inversion, by claiming a priori probabilities, would

* Note that the formula belongs to a total interval for which the end-points are uniquely defined; in other cases the sum $\sum_{i=1}^{n}\xi_i$ may be less than unity.

seem to confuse the issue, in principle and in practice. Thus, in practice and for continuum one-way variables it would substitute a simple unique result by indefiniteness. For discrete variables, the a priori probabilities would replace the moderate uncertainty, $w/(\prod_i a_i)$, in (2.7) and (5.22). The result would be to blow up the uncertainty if not to distort the issue completely. In other cases, an a priori probability may mask a lack of existence of probability.

**Concluding remarks**

In most of the topics and in each chapter of this paper there is an implicit, if not explicit, connection to Brownian motion. VIBEKE NIELSEN and I have studied Brownian motion of Hamiltonian systems, partly as a further elucidation of the above considerations, and partly on its own merits. We intend to publish the results in a separate paper. In connection with the present work I want to express my great indebtedness to VIBEKE NIELSEN for numerous discussions and penetrating criticism.

I am also particularly grateful to J. U. ANDERSEN, E. EILERTSEN, J. KALCKAR, P. KRISTENSEN, PH. LERVIG, and K. OLESEN, for valuable information and guidance, as well as helpful misgivings during my lectures on the subject.

I am especially indebted to SUSANN TOLDI for competent and careful preparation of this paper.

Institute of Physics,
University of Aarhus.

## References


1) TH. BAYES: An Essay towards Solving a Problem in the Doctrine of Chances. Philosophical Transactions **53**, 376 (1763), **54**, 298 (1764); Ostwald's Klassiker der exakten Wissenschaften, Nr. 169 (1908).
2) L. BRILLOUIN: Physical Entropy and Information II. J. Appl. Phys. **22**, 338 (1951).
3) H. B. G. CASIMIR: On Onsager's Principle of Microscopic Reversibility. Rev. Mod. Phys. **17**, 343 (1945).
4) S. CHANDRASEKHAR: Stochastic Problems in Physics and Astronomy. Rev. Mod. Phys. **15**, 1 (1943).
5) R. T. COX: Probability, Frequency and Reasonable Expectation. Am. J. Phys. **14**, 1 (1946).
6) H. CRAMÉR: Mathematical Methods of Statistics. Princeton University Press, (1946).
7) J. L. DOOB: Stochastic Processes. John Wiley, New York, (1953).
8) R. A. FISHER: Statistical Methods and Scientific Inference. Oliver and Boyd, Edinburgh & London, (1956); cf. also: Contributions to Mathematical Statistics, John Wiley, New York, (1950).
9) E. T. JAYNES: Information Theory and Statistical Mechanics. Page 181 *in* Statistical Physics, Vol. 3. W. A. Benjamin Inc., New York, (1963).
10) H. JEFFREYS: Theory of Probability. Clarendon Press, Oxford, (1961).
11) A. KATZ: Principles of Statistical Mechanics: The Information Theory Approach. Freeman and Co., San Francisco, (1967).
12) J. LINDHARD & VIBEKE NIELSEN: Studies in Statistical Dynamics. Mat. Fys. Medd. Dan. Vid. Selsk. **38**, No. 9 (1971). In the text, this paper is referred to as SSD.
13) J. LINDHARD: Influence of Crystal Lattice on Motion of Energetic Charged Particles. Mat. Fys. Medd. Dan. Vid. Selsk. **34**, no. 14 (1965).
14) D. V. LINDLEY: Introduction to Probability and Statistics from a Bayesian Viewpoint, I, II. Cambridge University Press, (1965).
15) L. ONSAGER: Reciprocal Relations in Irreversible Processes, I. Phys. Rev. **37**, 405 (1931); II, ibid. **38**, 2265 (1931).
16) J. S. ROWLINSON: Probability, Information and Entropy. Nature **225**, 1196 (1970).
17) C. E. SHANNON & W. WEAVER: The Mathematical Theory of Communication. University of Illinois Press, (1949).

Indleveret til Selskabet den 17. august 1973.
Færdig fra trykkeriet den 24. maj 1974.

OSKAR KLEIN

# LE PRINCIPE D'ÉQUIVALENCE D'EINSTEIN UTILISÉ POUR UNE ALTERNATIVE DE LA COSMOLOGIE RELATIVISTE EN REGARDANT LE SYSTÈME DES GALAXIES COMME LIMITÉ ET NON COMME L'UNIVERS

Det Kongelige Danske Videnskabernes Selskab
Matematisk-fysiske Meddelelser **39**, 2


Kommissionær: Munksgaard
København 1974

## Synopsis

Après l'introduction, le principe d'équivalence – étant la base de la théorie gravitationnelle d'Einstein –, est discuté en détail et illustré par le paradoxe de l'horloge. Puis il est montré que les arguments d'Einstein pour sa cosmologie sont incompatibles avec le principe d'équivalence. Aussi il est montré que la singularité de Schwarzschild, qui signifie une limite de la densité, rendra impossible la formation naturelle des cosmologies relativistes
Dans la seconde partie de l'article, l'alternative, proposée depuis longtemps par l'écrivain, est présentée, finissant par un modèle du rayonnement prédit par Alpher et Herman – mais sans le "fireball".


## Erratum

*P. 8 dernière ligne ajouter:*

« , mettant $\vartheta = 3.$ »


PRINTED IN DENMARK
BIANCO LUNOS BOGTRYKKERI A/S
ISBN 87 7304 031 2

## I. 1. Introduction

La cosmologie relativiste est actuellement en vogue parmi les chercheurs travaillant sur la théorie de la gravitation d'Einstein ainsi que parmi les astronomes, qui y voient une interprétation remarquable des grandes découvertes qui signifient non seulement une énorme expansion de la connaissance, mais aussi une expansion littérale de la multitude des galaxies, dont la vitesse est à peu près proportionnelle à leur distance.

Il faut se demander cependant si cette interprétation, qui ressemble plutôt à la physique prégaliléenne qu'à celle de nos jours, est vraiment motivée par les faits. En essayant de répondre à cette question, il est bon de commencer par la première cosmologie relativiste, celle développée par Einstein lui-même avant ces découvertes, et dont descendent les cosmologies présentes. En étudiant le chef-d'œuvre d'Einstein, où il a fondé la théorie générale de la relativité, on y trouve une vacillation entre deux points de vue, qui selon lui se soutiennent, mais qui en vérité sont contradictoires. Le premier de ceux-ci – la source principale de sa cosmologie – est la réponse à sa question: pourquoi la relativité du mouvement se limite-t-elle à des vitesses constantes en grandeur et direction? Cette question paraît bien naturelle, le mouvement étant par définition relatif. Donc, l'idée de Mach que les forces inertiales – qu'on connaît des véhicules accélérés – sont en fait une sorte de gravitation provenant de la multitude des masses dans l'univers, leur centre de gravité définissant le système de référence considéré par Newton comme l'*espace absolu*, paraît bien promettante à Einstein, quoiqu'il fallût l'adapter à la théorie de la relativité du mouvement uniforme. Tandis que ce point de vue a son origine dans des considérations philosophiques, selon lesquelles la nature doit se comporter selon nos habitudes de raisonner, l'autre point de vue Einstein l'a pris directement d'un fait expérimental, à savoir cette remarquable proportionnalité entre la masse inertiale et la masse pesante, jusque-là sans interprétation, qui s'exhibe dans l'égalité des temps de chute de tout corps tombant d'une tour haute quand la résistance de l'air peut être négligée.

**2. Le principe d'équivalence, la vraie base de la théorie générale d'Einstein**

Commençons par le dernier point de vue par lequel Einstein a créé le formalisme mathématique de sa théorie, définissant par lui les concepts qui remplacent le potentiel et le champ de la théorie ordinaire de la gravitation – ainsi que son interprétation physique. Comme une introduction Einstein a considéré certaines expériences imaginaires très simples et éclairantes – tout à fait dans la tradition des successeurs d'Archimède, qui ont établi la nouvelle physique, dont le plus connu est Galilée. Donc, à l'intérieur d'une chambre, qui tombe dans un champ gravitationnel, constant en grandeur et en direction pendant l'observation, la pesanteur est pratiquement éliminée – fait bien connu des navigateurs des satellites artificiels – parce que les objets y contenus subissent la même accélération. Inversement, si la chambre est accélérée dans une région sans gravitation, les passagers qui y sont, peuvent se croire dans un champ gravitationnel, dont la force correspond précisément à l'accélération, car un objet qu'on y lâche, est atteint par le plancher juste comme s'il tombait dans une chambre en repos.

Par un véritable trait de génie Einstein a aperçu dans ces faits, essentiellement connus depuis longtemps, un principe profond de la nature, plus tard appelé *le principe d'équivalence*, le mot équivalence se rapportant à l'identité *essentielle* des forces inertiales – produites par un mouvement non-uniforme relatif à un système de référence sans gravitation, appelé *système inertial* – et des forces gravitationnelles, produites par des masses. Et immédiatement il en a tiré des conclusions nouvelles concernant les effets de la gravitation sur la lumière: déviation d'un rayon lumineux en passant devant un corps comme le soleil, et changement de la fréquence selon le potentiel gravitationnel, ces deux effets étant vérifiés depuis.

Pour développer ces considérations en une théorie de la gravitation, qui comprend la théorie de Newton – comme la théorie électromagnétique de Maxwell comprend l'électrostatique fondée sur la loi de Coulomb – il fallait généraliser et préciser les conclusions de ces expériences imaginaires, chose plus difficile qu'on ne l'estime aujourd'hui, à cause de l'admirable simplicité du premier résultat obtenu par Einstein: à savoir que la connaissance des lois qui gouvernent un phénomène dans le cas où il n'y a aucune gravitation – *lois qui satisfont au principe de la relativité du mouvement uniforme* – suffisent pour déterminer l'effet d'un champ arbitraire de gravitation sur ce phénomène. Le premier exemple du nouveau point de vue, sans appliquer la théorie de la relativité, est que la loi de Galilée du mouvement d'un projectile

est une conséquence directe de la loi d'inertie valable dans un système de référence inertial.

Pour avancer plus loin il fallait d'abord généraliser les expériences par la remarque qu'un champ gravitationnel – sans singularité – dans une région autour d'un point en espace et en temps est de plus en plus constant quand on diminue cette région; la situation étant pareille à celle d'un petit lac, dont la courbure est négligeable. Cette situation est pratiquement réalisée par un satellite circulant autour de la terre – donc son manque de pesanteur.

La comparaison avec le lac n'est pas arbitraire. En effet, le formalisme mathématique de la théorie générale d'Einstein, y compris son interprétation de la physique, constitue une analogie très proche de la géométrie interne des surfaces courbes développée par Gauss et généralisée pour des espaces d'un nombre arbitraire de dimensions par Riemann. Comme cette géométrie est fondée sur la validité de la géométrie euclidienne dans les régions infinitésimales, la théorie d'Einstein est fondée sur la validité du principe de la relativité du mouvement uniforme dans les systèmes locaux, dit *inertiaux*, où la gravitation est éliminée.

Donc, dans la géométrie des surfaces courbes le concept de longueur est basé sur l'application du théorème de Pythagore pour exprimer l'intervalle $ds$ entre deux points voisins en coordonnées usant d'abord les coordonnées cartésiennes d'une région infinitésimale, c'est-à-dire

$$ds^2 = dx^2 + dy^2 \tag{1}$$

Similairement l'intervalle entre deux événements proches, en distance et en temps, s'exprime dans un système inertial par la formule de Minkowski

$$ds^2 = dx^2 + dy^2 + dz^2 - c^2\,dt^2 \tag{2}$$

où $c$ est la vitesse de la lumière et $t$ le temps, expression qui est invariante non seulement sous des déplacements et rotations du système des coordonnées cartésiennes, mais aussi sous des transformations de Lorentz, où la vitesse du système est changée.

Ce sont des formules pour des régions infinitésimales quand il y a de la courbure. Pour décrire une région finie il y faut introduire des coordonnées générales, deux pour une surface (comme les latitudes et les longitudes) et quatre pour l'espace et le temps, dans les champs de gravitation. Les différentielles dans les formules (1) et (2) sont alors des fonctions linéaires des différentielles des coordonnées générales, dont les coefficients sont des fonctions de ces coordonnées. Donc, on a

$$ds^2 = \sum g_{ik}\, dx^i\, dx^k \tag{3}$$

où les $x^i$ sont deux dans le cas des surfaces courbes et quatre dans la physique. Un concept de toute première importance dans les deux cas est celui de lignes géodésiques – les lignes de droiture optimale, qui sont aussi les plus courtes entre deux points d'une région univoque. Une partie infinitésimale d'une telle ligne étant droite, il est aisé de voir comment on peut les construire, quand les $g_{ik}$ sont connus – simplement en utilisant les coordonnées cartésiennes locales pas à pas, chaque pas infinitésimal ayant la même direction que le pas précédent. Leur importance dans la théorie des surfaces est évidente, définissant la route la plus courte entre deux points. Et dans la théorie de la gravitation le mouvement d'une particule – pratiquement aussi des corps macroscopiques, comme les planètes – suit une ligne géodésique en quatre dimensions.

Ici nous rencontrons une différence essentielle entre les deux cas – non pas dans les mathématiques formelles, ni dans le fait que l'interprétation va par les systèmes locaux, où la métrique, définie par les $g_{ik}$, est constante – mais dans la *signification des transformations des coordonnées*. Donc, dans la géométrie interne des surfaces on s'intéresse en premier lieu aux grandeurs invariantes – une ligne droite étant une ligne droite simplement, aussi quand on écrit son équation en coordonnées curvilignes. Ce qui compte, c'est de quelle sorte de géométrie – euclidienne ou un des différents genres de géométries non-euclidiennes – il s'agit.

Pour les transformations qui touchent seulement l'espace et non le temps, la situation est similaire dans la théorie d'Einstein, selon laquelle la géométrie est ordinairement celle de Riemann en trois dimensions. C'est dans les transformations touchant le temps que la différence se montre – en fait, comme nous avons déjà vu, dans les considérations originelles d'Einstein – car l'apparition, ou le changement, de la gravitation sont sans doute de première importance dans cette théorie.

Considérons ce cas un peu en détail – la relation d'un champ constant de gravitation et le système inertial correspondant, traité rigoureusement par C. Møller. Ici l'élément de ligne $ds$ prend la forme

$$ds^2 = d\xi^2 + d\eta^2 + d\zeta^2 - c^2\left(1 + \frac{g\zeta}{c^2}\right) d\vartheta^2 \tag{4}$$

où $\zeta$ est la cordonnée correspondant à la hauteur dans le champ de la terre, $g$ étant l'accélération produite par le champ. La transformation qui mène du

système inertial (avec les cordonnées $x$, $y$, $z$, et le temps $t$) au système en repos dans le champ (avec les coordonnées $\xi$, $\eta$, $\zeta$ et celle pour le temps $\vartheta$) peut s'écrire

$$x = \xi,\ y = \eta,\ z = \frac{c^2}{g}\left(\left(1 + \frac{g\zeta}{c^2}\right)\cosh\frac{g\vartheta}{c} - 1\right),\ t = \frac{c}{g}\left(1 + \frac{g\zeta}{c^2}\right)\sinh\frac{g\vartheta}{c}. \qquad (5)$$

Pour un projectile, lancé verticalement dans le système inertial, on a l'équation

$$z = z_0 + vt \qquad (6)$$

et en la traduisant par les relations (5) on obtient directement l'équation pour son mouvement dans le champ gravitationnel, qui en même temps est celle d'une ligne géodésique de l'élément de ligne de la métrique (4). Pour le cas non-relativiste quand $g\vartheta \ll c$ et $g\xi \ll c^2$ on a

$$\zeta = z_0 + v\vartheta - \tfrac{1}{2}g\vartheta^2 \qquad (7)$$

c'est-à-dire la loi de Galilée.

En résumant ces considérations, on peut dire que la similarité entre la théorie d'Einstein et la géométrie de Riemann correspond à celle de l'invariant de Minkowski et l'élément de ligne – selon le théorème de Pythagore de la géométrie, tandis que leur différence correspond à celle entre le temps et une cordonnée spatiale comme elle paraît déjà dans le signe négatif du carré $dt^2$. Donc, il ne faut pas oublier la différence entre la géométrie, au sens ordinaire, et la physique relativiste, ce qui est bien exprimé par le physicien hollandais Fokker par le mot *chronogéométrie*.

### 3. Le paradoxe de l'horloge et le principe d'équivalence

Comme un autre exemple du fonctionnement du principe d'équivalence, nous choisissons le paradoxe dit de l'horloge; on désigne par là la conclusion tirée par Einstein qu'une personne qui voyage aller-retour avec une vitesse comparable à celle de la lumière se trouve moins vieillie à son retour sur terre que ceux qui y sont restés, le rapport entre leurs âges étant alors égal à $\left(1 - \frac{v^2}{c^2}\right)^{1/2} : 1$, où $v$ est la vitesse moyenne du voyageur et $c$ celle de la lumière. Quoique ce rapport ait été vérifié par des expériences très précises sur la vie moyenne de particules instables, il y a encore des physiciens qui n'y croient pas, et en outre, d'autres qui débattent s'il s'agit là d'un effet de la relativité

spéciale ou de la théorie générale d'Einstein. Comme nous allons voir, cette dernière dispute est aisément résolue par le principe d'équivalence en réalisant que tous ont raison, parce que la mesure du temps est définie par des systèmes inertiaux locaux, où la théorie spéciale est valable, mais qu'un voyage aller-retour ne peut pas rester dans un seul système inertial. D'ailleurs, ceci correspond précisément à la solution du paradoxe par Einstein lui-même. Mais pour rendre les choses plus intuitives, il vaut la peine de considérer un peu en détail un tel voyage, où les conditions sont telles qu'il est impossible de fonder des doutes sur le manque de réalisme de l'entreprise.

Imaginons donc qu'un nombre de techniciens, physiciens et astronomes font un voyage aller-retour pour étudier en particulier d'autres systèmes planétaires que le nôtre en s'éloignant d'une vingtaine d'années-lumière de la terre. Leur grand vaisseau doit être fourni de toutes sortes de commodités pour le travail et le bien-être des participants, et, surtout, il faut que l'accélération du vaisseau, dirigée vers le toit, corresponde à peu près à la gravité ici sur terre – ce qui veut dire que les provisions d'aliments etc. doivent être suffisantes pour une douzaine d'années. Cette dernière supposition est la seule qui empêchera la réalisation du voyage, mais pour une raison assez triviale – le manque de carburant, dont il faudrait une quantité impossible, à savoir au moins quelques centaines de milliers de fois le poids du vaisseau même.

Il convient de diviser le voyage en quatre parties – égales au point de vue du vaisseau: accélération $g$ jusqu'à la vitesse optimale, retardation ($g$ renversé) jusqu'à la vitesse zéro, accélération $g$ vers la terre, retardation pour atterrir ($g$ renversé). Les deux moments sans gravité, où la direction de l'accélération est renversée et où le plancher et le plafond échangent leurs rôles, ne vont pas gêner les passagers.

Par un calcul simple – remplaçant l'accélération continue par des changements $g\Delta$ subits à des intervalles $\Delta$ – on obtient, par des transformations de Lorentz répétées, en allant à la limite, pour le temps $t$ du système en repos et le temps $\vartheta$ du vaisseau, la relation

$$t = \frac{c}{g} \sin h \frac{g\vartheta}{c}. \tag{8}$$

C'est, comme on voit, la formule (5) avec $\zeta = 0$, l'origine du système accéléré étant placée dans le vaisseau. Pour les passagers la durée du voyage est donc quatre fois le temps $\vartheta$ pour une des quatre parties, et pour les observateurs à terre quatre fois le temps $t$ correspondant. Pour la distance optimale, selon la terre, on obtient similairement

$$l = 2\frac{c^2}{g}\left(\cos h\frac{g\vartheta}{c} - 1\right). \tag{9}$$

Dans notre exemple nous allons prendre pour unités: l'an pour le temps et l'année lumière pour la distance, mettant $g = 1$, ce qui correspond à peu près à la gravitation ici sur terre, à savoir 950 cm/sec$^2$. Pour la durée du voyage nous obtenons donc 12 ans selon les horloges du vaisseau, mais pour les terriens à peu près 40 ans, la distance optimale étant de 18 années-lumière. Donc un des participants ayant 28 ans au départ, qui a laissé un nouveau-né à la maison, retrouvera à son retour un fils de son propre âge!

Ce calcul, où le temps $\vartheta$ est défini par la limite de la somme des éléments temporels $\Delta$ des systèmes inertiaux locaux par lesquels le vaisseau passe, donne le vrai temps, les horloges emportées étant faites pour le montrer; cela devrait suffire pour effacer tous doutes sur la réalité du paradoxe des horloges.

**4. Les arguments d'Einstein pour sa cosmologie**

Comme nous allons voir, ces arguments – le plus important d'eux étant basé sur l'hypothèse de Mach sur l'origine de l'inertie – sont étrangement contraires à son propre principe d'équivalence. Donc, Einstein a conclu que dans un univers vide il n'y aurait pas d'inertie; et il a essayé de montrer par sa théorie de la gravitation que la masse d'un corps est augmentée par la présence d'autres corps. Mais selon le principe d'équivalence la masse d'un corps est définie à l'aide d'un système inertial asymptotique exigeant des environs aussi vides que possible. Par exemple, la masse du système solaire est définie par un système de référence dans lequel le centre de gravité du soleil et ses planètes est en repos, c'est-à-dire qu'il tombe librement dans le champ gravitationnel des autres étoiles, lequel, d'ailleurs, est très faible, mais surtout extrêmement homogène dans l'étendue du système solaire. En fait, c'est ainsi qu'Einstein lui-même a défini l'énergie totale d'un système quelconque – et comme montré par lui, l'énergie totale d'un système est proportionnelle à la masse totale. L'expression mathématique due à la présence d'autres corps, représente en vérité un champ gravitationnel assez étrange, qu'on peut écarter par une transformation locale des coordonnées – donc en accord avec le principe d'équivalence.

Le système de coordonnées dans lequel le centre de gravité du système solaire est en repos, est, comme on voit, justement celui appelé par Newton *l'espace absolu*, étant très approximativement celui de Copernic, où le soleil est en repos. Il est donc erroné de croire que selon la théorie d'Einstein

la différence entre ce système et celui de Ptolémée ne soit qu'une chose de nature pratique, plutôt conventionnelle qu'essentielle. Aussi le fait que ce système est presque en repos par rapport au ciel des étoiles fixes n'est aucunement un argument en faveur de l'hypothèse de Mach, comme il est parfois énoncé. L'essentiel est qu'il est inertial.

Comme un autre argument pour sa cosmologie Einstein a considéré la circonstance que dans son univers clos on évite les conditions de limite à l'infini pour cette solution de ses équations qui remplace la loi de Newton, conditions qu'il a considérées comme contraires à l'essence de sa théorie générale, parce qu'elles ne sont pas indépendantes des coordonnées qu'on choisit. Mais, comme le montre l'exemple de la masse, selon le principe d'équivalence, de telles conditions sont nécessaires pour la définition des proprietés d'un système isolé. Et, en plus, le mot *infini* sous ce rapport est simplement une expression d'un procédé mathématique, où il s'agit des distances longues en comparaison avec les dimensions de la source du champ.

Un troisième argument pour l'univers clos a rapport au paradoxe bien connu que la gravitation dans une région où la densité de la matière en moyenne est non zéro, croît vers l'infini avec ces dimensions. Mais, sans avoir recours à cette hypothèse, ce paradoxe est évité – comme l'a montré, il y a longtemps, l'astronome suédois Charlier – si la matière est distribuée en hiérarchie, et que la densité moyenne tende vers zéro par ordre d'hiérarchie. Et, ce qui est important, cette condition est satisfaite automatiquement par ces solutions des équations d'Einstein, qui correspondent à des systèmes matériels limités, qui sont le résultat d'une accumulation graduelle de matière – comme les étoiles et les galaxies. Leur limite est donnée par l'inégalité suivante entre la masse $M$ et la densité $\mu$ du système

$$M^2\mu \leq \frac{3c^6}{32\pi G^3} = 0.73 \times 10^{83} g^3 \mathrm{cm}^{-3} \tag{10}$$

où $G$ est la constante de gravitation et $c$, comme plus haut, la vitesse de la lumière. Cette limite est loin d'être approchée pour les étoiles ordinaires et les galaxies, tandis que pour les étoiles de neutrons, récemment découvertes, elle est assez proche – et pour les solutions cosmologiques elle est dépassée.

A cette critique des arguments donnés par Einstein en faveur de sa cosmologie il faut encore remarquer que, quoiqu'il soit possible de mesurer – dans les régions qu'on peut surveiller – les propriétés du champ, qui correspondent à la courbure des surfaces, il n'est pas possible – même dans le cas où ces propriétés sont celles de la cosmologie d'Einstein – de s'assurer que

l'univers soit clos. En fait, la situation est analogue à celle qu'on connaît des discussions, menées jadis, regardant la forme de la terre, déterminée en définitive par sa circumnavigation. Il est vrai qu'on avait là, déjà tôt, une raison assez convaincante pour sa sphéricité par les éclipses de la lune. Mais sans la troisième dimension de l'espace c'eût été impossible. Et pour la cosmologie on n'a pas de dimensions supplémentaires.

Cela veut dire qu'une conclusion à cet égard serait seulement possible au moyen d'une théorie sûre et profonde. Et une telle théorie, nous ne l'avons pas. Aussi la théorie quantique de champs – qui, bien qu'encore inachevée, est la meilleure de ce genre – demande plutôt que l'univers représente l'état de moindre énergie, dont les parties où il y a une accumulation de matière, sont des fluctuations – donc, en moyenne, un vide infini.

## II. La cosmologie nouvelle et son alternative

### 1. Un modèle de la métagalaxie

Par la découverte de Hubble d'une expansion régulière du système des galaxies la cosmologie statique d'Einstein fut abandonnée et remplacée par une autre classe de ses équations découverte par le mathématicien russe Friedmann – ce qui a donné lieu, non seulement à une interprétation promettante de la loi de Hubble, mais aussi à une théorie tentante de l'origine des éléments chimiques initiée par Gamow. A ce propos ses collaborateurs Alpher et Herman ont conclu que cette théorie demande l'existence au temps présent d'un rayonnement universel et isotrope correspondant à une température de quelques degrés au-dessus du zéro absolu, étant le reste d'un rayonnement d'intensité énorme à l'état d'univers au temps de la formation des éléments. La découverte, il y a quelques ans, d'un rayonnement pareil, découverte inspirée par des physiciens – en premier lieu Wheeler et Dicke – qui n'avaient pas cessé de croire à ces idées, a contribué grandement à l'acceptation assez générale de cette cosmologie, nommée communément le «big bang» à cause du commencement violent de l'univers qu'elle suppose.

Tout de même il faut avouer que cette cosmologie, selon laquelle l'univers change avec le temps, est extrêmement éloignée – même plus que celle d'Einstein – de la physique ordinaire, dont le but est de trouver des lois de la nature de plus en plus générales et non la structure de l'univers par des considérations plus ou moins philosophiques et esthétiques.

Donc, on se demande s'il n'y a pas une manière plus naturelle d'interpréter ces deux faits – l'expansion et le rayonnement isotrope – à savoir

de regarder la multitude de galaxies, qui participent à l'expansion, comme un système régulier – une métagalaxie – bien qu'énorme, qui est limité, comme sont les étoiles et les galaxies, étant formé par contraction gravitationnelle d'un vaste nuage, extrêmement raréfié, nuage consistant de particules stables, les plus simples, protons et électrons et leurs antiparticules. C'est remplacer la cosmologie relativiste par l'étude d'un système dont les problèmes sont à peine moins difficiles que ceux qu'on a rencontrés dans l'étude des étoiles et des galaxies.

Avant d'esquisser ce qu'on a fait et ce qu'on peut attendre d'une telle étude nous allons considérer un peu un modèle – sûrement trop simplifié – de l'état présent de la métagalaxie, décrivant la loi de Hubble aussi bien que la cosmologie «big bang».

Le modèle en question est une sphère en expansion, remplie de matière, dont la densité $\mu$ est une fonction du temps, la même partout dans l'intérieur de la sphère et zéro dans l'espace extérieur. Dans l'intérieur le modèle satisfait à la solution de Friedmann usée pour le «big bang», qui à la surface est remplacée par celle de la théorie d'Einstein qui correspond à la loi de Newton. L'extrapolation en arrière, qui dans le «big bang» mène à l'état de «fire ball» (l'origine du rayonnement isotrope), est ici défendue par l'inégalité (10).

Voici quelques formules pour ceux qui s'intéressent aux détails des calculs suivants:

L'élément de ligne $ds$ est donné par

$$ds^2 = a^2\left(\frac{d\eta^2}{1+\varepsilon\eta^2} + \eta^2 d\Omega^2\right) - c^2 d\vartheta^2 \tag{11}$$

où la longueur $a$, qui est responsable de l'expansion, est une fonction du temps $\vartheta$, $\eta$ étant une coordonnée radielle et $d\Omega$ l'élément de ligne de la surface sphérique, où $\eta = 1$. Pour les solutions, qui sont en expansion vers l'infini, $\varepsilon$ est égal à $+1$, tandis que $\varepsilon = -1$ appartient aux solutions pour lesquelles l'expansion est limitée. L'intermédiare de ces deux classes correspond à $\varepsilon = 0$. Les solutions en question sont définies par les relations suivantes

$$T^{-1} = \frac{1}{a}\frac{da}{d\vartheta}, \quad \frac{8\pi}{3} G\mu T^2 = \frac{a_0}{a_0 + \varepsilon a}, \quad a_0 = \frac{8\pi}{3}\frac{G\mu a^3}{c^2} \tag{12}$$

où $T^{-1}$ est le paramètre de Hubble – la vitesse d'expansion pour des distances courtes étant donnée par la distance divisée par $T$ – et la longueur $a_0$ est constante. Comme la densité $\mu$, $T$ est une fonction du temps seul, tandis que

$$M = \frac{4\pi}{3} \mu \, a^3 \eta_l^3 \qquad (13),$$

étant la masse totale du système, est constante. Comme on voit, l'expression $\frac{8\pi}{3} G\mu T^2$ détermine la valeur de $\varepsilon(+1,0,-1)$, selon qu'elle est moins que, égale à ou plus grande que l'unité. Dans la formule (13) $\eta_l$ est la valeur de $\eta$ à la surface, la distance d'un point du centre étant égale à $a \cdot \ln((1+\eta^2)^{1/2} + \eta)$, où *ln* signifie le logarithme naturel.

Comme le montre les équations (12), la connaissance au temps présent de la densité $\mu$ et du paramètre $T$ permet de déterminer les valeurs de $a_o$ et $a$, plus ou moins réelles selon le degré de validité du modèle. Tandis que $T$ paraît être assez bien connu – 4. $10^{17}$ sec. – ce qui correspond à une vitesse de 25 kilomètres par seconde à une distance d'un million d'années-lumière, la densité $\mu$ est encore incertaine, les masses estimées variant selon le jugement concernant la quantité de masse dans l'espace entre les galaxies; la masse déduite en comptant seulement les galaxies dans un volume assez grand étant estimée à $3 \cdot 10^{-31} g\,\mathrm{cm}^{-3}$. Connaissant ce nombre, j'ai choisi, il y a quelques ans, un peu au hasard, la valeur $10^{-30} g\,\mathrm{cm}^{-3}$, correspondant à une expansion vers l'infini, la limite pour une telle expansion ($\varepsilon = 0$) étant $10^{-29} g\,\mathrm{cm}^{-3}$ avec la valeur mentionnée de $T$. Pour $a_0$ et $a$ cela donne

$$a_0 = 1.23 \times 10^{27}\,\mathrm{cm}, \quad a = 12.6 \times 10^{27}\,\mathrm{cm}.$$

Pour compléter le modèle il faut encore avoir une valeur pour $\eta_l$. Après la découverte des quasars, dont les déplacements-rouge sont les plus grands qu'on a observés, il fut naturel de penser que ces objets, qui paraissent représenter la jeunesse des galaxies, se trouvent près de la frontière de la métagalaxie, ce qui donnerait pour $\eta_l$ une valeur d'environ un. Mais depuis quelque temps on a trouvé des indications que ces objets ne sont pas tellement distants qu'on l'avait conclu par les déplacements-rouge. Et il paraît possible – même probable – que ces déplacements ont une autre cause que l'expansion.

Si on laisse de côté les quasars, le déplacement-rouge le plus grand observé correspond à un effet Doppler d'une vitesse égale à 2/5 de celle de la lumière, donnant pour $\eta_l$ une valeur de près de 0.4 – si notre galaxie se trouve dans la proximité du centre de la métagalaxie, ce qui est probable. Car, autrement, on s'attendrait à quelques effets observables de la surface dans certaines directions. Pour le lecteur qui s'intéresse aux détails de ce calcul,

voici la formule donnant $\eta$ quand on connaît le rapport $\lambda$ de la fréquence observée et de celle à la source:

$$(1+\eta^2)^{1/2}+\eta=\left(\frac{\left(1+\frac{a}{a_0}\right)^{1/2}+\left(\frac{a}{a_0}\right)^{1/2}}{\left(1+\lambda\frac{a}{a_0}\right)^{1/2}+\left(\lambda\frac{a}{a_0}\right)^{1/2}}\right)^2. \tag{14}$$

Avec les valeurs données en haut pour $a_0$ et $a$ et celle pour le plus grand déplacement-rouge (2/5 de la vitesse de la lumière, ce qui donne $\lambda=\sqrt{\frac{3}{7}}$) on obtient $\eta=0.417$.

**2. Emploi des rapports d'Eddington**

Une première indication que le rayonnement joue un rôle essentiel dans le développement de la métagalaxie fut obtenue par une tentative d'utiliser quelques rapports assez mystérieux découverts par Eddington, le grand astrophysicien, entre les dimensions de l'univers clos d'Einstein et les grandeurs atomiques, regardés par lui comme indiquant une relation profonde entre le macrocosme et le microcosme.

Il s'agit du grand nombre $N$ du rapport entre l'attraction électrique et celle de gravitation d'un proton et d'un électron, ainsi

$$N=\frac{e^2}{Gm_e m_p}=2.27\times10^{39} \tag{15}$$

où $e$ est la charge électrique élémentaire, $G$ la constante de gravitation et $m_e$ et $m_p$ les masses respectives de l'électron et du proton. Avec $d$ étant ce qu'on appelle le rayon d'électron, ces rapports sont

$$R\sim Nd,\ M\sim N^2m_p,\qquad d=\frac{e^2}{m_e c^2}=2.82\times10^{-13}\,cm \tag{16}$$

où $R$ fut le rayon de courbure et $M$ la masse de l'univers d'Einstein. Au lieu du rayon de courbure – qui est constant dans l'univers statique d'Einstein – nous allons considérer la longueur $a_0$, comparant la relation suivante

$$\frac{1}{a_0^2}=\frac{8\pi}{3}\cdot\frac{G\mu_0}{c^2} \tag{17}$$

cas spécial de (12) pour $a=a_0$, avec la relation entre le rayon de courbure et la densité dans l'univers clos, qui ne diffère de (17) que par le facteur

$4\pi$ en place de $8/3\,\pi$. La valeur de $Nd$ étant égale à $0.64 \times 10^{27}$ cm, la valeur de $a_0$ du modèle est très proche de $2Nd$, et la masse, selon (13), est très proche de $N^2 m_p \eta_l^3$. Comme la valeur de $\mu$ est bien incertaine, on n'en peut pas conclure plus qu'une concordance d'ordre de grandeur du modèle et des rapports d'Eddington, qui paraît pourtant significative.

Leur application, cependant, dépend de l'hypothèse que le rayonnement joue un rôle essentiel dans le développement de la métagalaxie, et que son action est grandement due à sa dispersion par les électrons selon la formule bien connue de J. J. Thomson, formule valable pour des fréquences dont les quanta sont petits par rapport à l'énergie $m_e c^2$.

Une condition importante pour ce rôle est que l'opacité du nuage est suffisante pour la conversion de la contraction en expansion, surtout dans l'état le plus dense du nuage, la limite de Schwarzschild, probablement près du point tournant. Définissons donc l'opacité, à cet état, $\varkappa_s$, par le rapport entre le rayon $R_s$ du nuage à ce point et le libre parcours d'un photon selon la formule de Thomson, ce qui donne

$$\varkappa_s = n_e \cdot \frac{8\pi}{3} d^2 R_s \tag{18}$$

où $n_e$ est le nombre d'électrons par unité de volume à cet état. Pour $R_s$ on a

$$R_s = \frac{2GM}{c^2} \tag{19}$$

et avec $n_p$, le nombre $\frac{\mu_s}{m_p}$ de protons dans l'unité de volume, où $\mu_s$ est la densité à la limite Schwarzschild, nous obtenons

$$R_s = \frac{1}{\varkappa_s} \cdot \frac{n_e}{n_p} \cdot Nd, \; M = \frac{1}{2\varkappa_s} \cdot \frac{n_e}{n_p} N^2 m_p. \tag{20}$$

Avec $a_0 = 2Nd$, cela nous donne pour $\varkappa_s$ la valeur $\frac{1}{2} \cdot \frac{n_e}{n_p} \eta_l^{-3}$ c'est-à-dire avec $n_e = n_p$ et $\eta_l = 0.42$, $\varkappa = 6.75$, valeur assez grande.

### 3. Quelques remarques sur le développement de la métagalaxie et sur l'origine du rayonnement isotrope

Les premiers calculs sur le développement de la métagalaxie, par Alfvén et Bonnevier et surtout par Laurent et al., bien que nécessairement très simplifiés, paraissent confirmer en grands traits l'hypothèse mentionnée

plus haut sur le rôle du rayonnement dans ce développement. Comme source primaire du rayonnement ils ont pris l'annihilation, mais dans le travail plus réaliste de Laurent a été inclus aussi l'effet Compton inverse – par lequel le rayonnement est augmenté pendant que le mouvement est freiné – et l'effet de la gravitation y est traité par la théorie d'Einstein, nécessaire dans le voisinage de la limite Schwarzschild. Dans un travail en préparation, Laurent a fait une étude approfondie de la probabilité de l'annihilation dans les circonstances en question; et il paraît qu'elle est considérablement plus grande qu'on n'avait supposé dans les travaux mentionnés.

En ce qui regarde le rôle de l'annihilation, il faut souligner l'extrême improbabilité qu'un nuage (très raréfié) contenant environ $10^{78}$ protons et électrons, n'ait pas pratiquement des quantités égales des deux espèces de matière. Ici le problème est de trouver des mécanismes vraisemblables pour leur séparation, sans laquelle toute la matière du nuage devrait être annihilée. Pour la solution de ce problème Alfvén a fait un commencement promettant, surtout par ce qu'il a appelé «l'effet Leidenfrost», la tendance d'accroissement de la séparation par l'attraction mutuelle des domaines de la même matière et la répulsion de ceux de matière opposée – causée par la pression créée par l'annihilation. Mais on ne connaît pas encore la grandeur des domaines séparés.

Ce qui suit, n'est qu'un essai préliminaire de tracer les grandes lignes d'une explication, par le modèle de la métagalaxie décrit plus haut, de ce rayonnement qu'on a considéré comme l'argument le plus fort pour la réalité de la cosmologie «big bang».

Supposons donc, qu'après une période de changements violents – pendant laquelle la contraction du nuage a été freinée, l'énergie gravitationnelle étant transformée en rayonnement et la séparation des deux espèces de matière pratiquement accomplie (les champs magnétiques y jouant un rôle décisif) – le système se trouve près de la limite Schwarzschild dans un état intermédiaire entre contraction et expansion.

Pour décrire mathématiquement cet état un peu imaginaire, nous partirons de l'état présent du modèle, dont la masse $M$ est donnée par (13), tandis que la somme $\overline{M}$ des masses de ses subsystèmes (pratiquement égale à celle de ses particules) est donnée par

$$\overline{M} = M \cdot Z(\eta_l) \tag{21}$$

où

$$Z(\eta_l) = 3\,\eta_l^{-3} \int_0^{\eta_l} \frac{x^2\,dx}{\sqrt{1+x^2}} = \tfrac{3}{2}\,\eta_l^{-3}(\eta_l(1+\eta_l^2)^{1/2} - (1+\eta_l^2) + \eta_l)). \tag{22}$$

Aussi nous supposons qu'à cet état la métrique correspond à $\varepsilon = 0$, ce qui veut dire que sa masse est égale à la somme des masses de ses particules, augmentée par celle du rayonnement $U_s/c^2$ à cet état, $U_s$ étant l'énergie correspondante.

En ce qui regarde le développement subséquent nous allons faire l'hypothèse suivante – qui n'est certainement pas exacte, mais paraît justifiée par les résultats, qu'une partie essentielle du rayonnement s'y comporte adiabatiquement, tandis que le reste, qui ne doit pas être grand, s'enfuit et, donc, ne contribue pas à la masse présente $M$. Pour $\overline{M}$ nous supposons qu'elle est pratiquement égale à cette quantité au temps présent, c'est–à–dire qu'elle est donnée par les formules (21) et (22).

Il faut encore remarquer que l'état près de la limite Schwarzschild est obtenu par une extrapolation en arrière en temps, utilisant la masse présente $M$, étant l'état le plus dense permis par elle. Il faut donc que la perte d'énergie du système, après que cet état est atteint, soit inconsidérable.

Sûrement, ces considérations, il faut les prendre avec un petit grain de sel, mais, heureusement, il y a quelques arguments à priori en leur faveur; d'abord le fait que cette solution de Friedmann, employée par Alpher et Herman dans leurs calculs regardant le rayonnement du « fire ball », est aussi valable dans notre modèle, autant qu'on peut négliger ce qui se passe à la surface; car c'est par là que le courant commence de se produire, un courant relatif aux systèmes de référence locaux. Selon cette solution l'abaissement de la température est dû au travail exercé par le rayonnement contre la force gravitationnelle, un effet renforcé, quand il y a des électrons, par l'opacité produite par eux. Et, comme on sait, à la limite Schwarzschild la gravitation seule retient entièrement le rayonnement.

De plus, comme durant le processus adiabatique il n'y a pas de courant local, et comme la propagation du courant – de la surface jusqu'au voisinage du centre – où il est en tout cas faible – est très retardée à cause de la grande distance, un tel courant à notre position (près du centre) serait, selon nos considérations, à peine observable. Nous posons maintenant, selon les hypothèses faites,

$$U_s = c^2(M - \overline{M}) = Mc^2(1 - Z(\eta_l)) \tag{23}$$

et donc pour la densité $u_s$ du rayonnement

$$u_s = \left(\frac{R}{R_s}\right)^3 (\mu c^2(1 - Z(\eta_l)) \tag{24}$$

où $R = a\eta_l$ est le rayon présent et $R_s = a_s\eta_l$ est celui à la limite Schwarz-

schild. Avec $\theta$ et $\theta_s$ étant les températures respectives présentes et à cette limite, on a, selon la loi de Stefan–Boltzmann,

$$u_s = \varrho\theta_s^4, \quad u = \varrho\theta^4 \tag{23}$$

où la constante $\varrho$ est égale à 7.65. $10^{-15}$erg (cm$^3$ degré)$^{-1}$. Et selon l'hypothèse adiabatique on a

$$\theta = \frac{R_s}{R}\theta_s \tag{24}$$

d'où nous obtenons finalement

$$\theta = \left(\frac{a_o}{a}\frac{\mu c^2}{\varrho}\eta_l^2(1 - Z(\eta_l)\right)^{1/4}. \tag{25}$$

Introduisons maintenant les nombres estimés pour $a_0$, $a$, $\mu$ et $\eta_l$ ($a_0 = 1.23 \times 10^{27}$ cm, $a = 12.6\ 10^{27}$ cm, $\mu = 10^{-30}$g cm$^{-3}$ et $\eta_l = 0.42$ nous obtenons

$$\theta = 3.15^\circ K. \tag{26}$$

Il faut accentuer que ce modèle n'est qu'un essai préliminaire. Toutefois il me paraît qu'une explication réaliste du phénomène en question se fera plûtot dans cette direction et non par le "big bang". Aussi il faut dire que la possibilité de décrire en grandes lignes l'évolution de la métagalaxie en utilisant les rapports d'Eddington ne les explique pas, ce qui demanderait une étude comparable à celle du problème analogue pour les étoiles.

Indleveret til Selskabet den 7. december 1973.
Færdig fra trykkeriet den 14. august 1974.

NILS ANDERSEN AND PETER SIGMUND

# ENERGY DISSIPATION BY HEAVY IONS IN COMPOUND TARGETS

Det Kongelige Danske Videnskabernes Selskab
Matematisk-fysiske Meddelelser **39**, 3


Kommissionær: Munksgaard
København 1974

## Synopsis

We have studied theoretically the sharing of energy among the constituents of a polyatomic medium in random atomic collision cascades initiated by heavy atomic particles. Our main interest was to estimate the significance of possible nonstoichiometric effects as they might be of interest in radiation damage and sputtering.

It is assumed that primary and recoiling particles slow down by random collisions, scattering and stopping being described according to the framework of LINDHARD, SCHARFF, and coworkers. Collision cascades are characterized quantitatively by the recoil density and the slowing-down density. The former quantity specifies the number and energy distribution of recoil atoms of the various species in a cascade and is of particular interest in radiation damage problems. The latter quantity deals with the number and energy distribution of moving atoms in a stationary state and is of particular interest in sputtering problems. Both quantities are calculated for slowing-down in an infinite medium of uniform composition. We determine explicitly the asymptotic expressions at high ion energy as compared to the recoil energy. Deviations from this asymptotic behaviour are studied, too.

We find nonstoichiometric effects in both recoil and slowing-down density, and these effects are determined not only by different binding energies of different atomic species. A key role is being played by the mutual partial stopping cross sections of the constituent atoms of the medium. It turns out that deviations from stoichiometric behaviour are independent of concentration in case of the slowing-down density, but dependent on concentration in case of the recoil density.

A preliminary account of this work has been reported at a recent conference[0]).



PRINTED IN DENMARK
BIANCO LUNOS BOGTRYKKERI A/S
ISBN 87 7304 033 9

## 1. Introduction

When an ion beam hits a solid target, the kinetic energy of the ions is dissipated among the nuclei and electrons of the medium. This energy dissipation may result in a number of observable effects such as sputtering, disordering, ionization, dissociation, etc. The theory of energy dissipation in random and crystalline media has been developed in some detail, mostly for random, monatomic targets (for a recent review see, e.g., ref. 1). One of the central problems concerns the sharing of energy between the electrons and the nuclei of the system, i.e. the relative significance of atomic displacement effects (e.g. sputtering, disordering) on the one hand, and electronic excitation effects (e.g. photon and electron emission) on the other hand. According to theoretical predictions[2], this sharing of energy depends significantly on the atomic numbers and masses of the bombarding ion and the target atoms, and on the kinetic energy of the ion. When single crystals are bombarded, the sharing also depends on orientation[3].

In the present paper we deal with the sharing of energy between the different atomic species of a polyatomic random medium, with special emphasis being laid on *binary* compounds or alloys. By analogy with the sharing of energy between electrons and nuclei, one would expect, qualitatively, that the kinetic energy of a bombarding particle is not necessarily shared stoichiometrically between the different constituents of a polyatomic medium, i.e. that the sharing does not only depend on the composition, but also on the atomic masses involved. For example, in the limiting case of Rutherford scattering, it is easily seen that energy is dissipated preferentially among the *lightest* target nuclei, although even those, in this special case, receive several orders of magnitude less energy than what is dissipated among electrons.

When energy is deposited nonstoichiometrically, preferential displacement of one particular atomic species may result, and, moreover, composi-

tion changes may occur near the surface due to preferential sputtering. Most probably *neither effect is determined by energy sharing alone*, but an understanding of energy sharing is a basic requirement for further theoretical treatment of effects connected with different binding energies and mobilities of the atomic species.

Nonstoichiometric effects have been observed in sputtering[4-10]. Their occurrence appears to be well established, whilst very little systematics has yet developed from these studies. The interpretation will almost certainly be complicated in view of the fact that the sputtering yield of a binary material, according to experimental observation, may be significantly higher or lower than the sputtering yield of either of the pure materials[10-12]. Even rather small amounts of (alloyed or implanted) impurities may influence the sputtering yield significantly in either direction, dependent on the implanted species[13]. Surface topography appears to be a particularly important factor in determining the sputtering of alloyed targets[14, 15]. Systematic nonstoichiometric effects may be observed in experiments with single crystalline targets such as GaAs[16, 17]. In view of all these competing effects the present investigation is hardly more than one step forward on a rather long way towards a comprehensive understanding of the sputtering of compound targets.

While the theory of ion ranges in polyatomic targets is well developed[18-20], the theory of energy deposition in such targets, apart from a few early investigations of Frenkel-pair production[21-23] has concentrated on the gross spatial distribution of deposited energy[20, 24] and the overall sharing of energy between nuclei and electrons[24, 25]. In view of a lack of knowledge of atomic scattering cross sections, it was not possible in the early work on Frenkel-pair production[21-23] to arrive at quantitative criteria for the importance of nonstoichiometric effects in defect production. In fact, only the influence of different displacement threshold energies was considered in detail.

In this communication, we concentrate on random collision cascades mainly in diatomic solids, with the aim of estimating the relative and, less extensively, absolute numbers of recoiling or moving constituent atoms, mostly at keV bombarding ion energies where effects of nuclear stopping are most pronounced. Both with a view on potential applications, and in order to isolate possible nonstoichiometric effects, we are in particular interested in the case of *widely different masses* of the constituent atoms. This latter attitude is somewhat complementary to that of earlier investigators[21-23] while it is similar to that of Kistemaker et.al[26] who investigated energy dissipation in organic materials qualitatively.

The basic integral equations used in the analysis (sect. 2) are equivalent to those used before[23] in similar problems. The specific results are restricted, first to a special class of cross sections (sect. 3) and, second, to binary targets (sects. 4 and 6). The ternary case is considered briefly in sect. 5. We mainly consider asymptotic solutions for high ion energy as compared to the relevant recoil energies; in sect. 7 we briefly discuss the limitations to this approximation. In sect. 8 we discuss some physical implications and the relation to experimental results.

Electronic stopping is neglected in part of the analysis. This approximation restricts the energy range under consideration, but it will be shown that mostly *absolute* rather than *relative* numbers of moving atoms are affected by this simplification.

The presentation of the basic physical model will be kept brief. The reader who is less familiar with the notation and the way of argument is referred to ref. 1 for an introduction.

## 2. Basic Equations

Consider a random, infinite medium with $N_j = \alpha_j N$ atoms of type $j$ (atomic number $Z_j$, atomic mass $M_j$) per unit volume. $\alpha_j$ $(0 \leq \alpha_j \leq 1;$ $\sum \alpha_j = 1)$ is the concentration of $j$-atoms, and $N$ the atomic density [atoms/cm$^3$]. Let an atom of type i with initial energy $E$ slow down in the medium.

For radiation damage calculations, we need the recoil density[27] $F_{ij}(E, E_0)$ which is defined as the average number of $j$-atoms *recoiling* per energy interval $(E_0, dE_0)$ in a collision cascade initiated by an $i$-atom with initial energy $E$.

For sputtering calculations we need the slowing-down density[1, 28] $G_{ij}(E, E_0)$ which is the average number of $j$-atoms *moving* per energy interval $(E_0, dE_0)$ in the stationary state, with $\psi$ [$i$-atoms/sec] slowing down from energy $E$.

Following a well-known procedure[1], the following integral equations can be derived for $F_{ij}$ and $G_{ij}$,

$$\sum_k \alpha_k \int d\sigma_{ik} \{F_{ij} - F'_{ij} - F''_{kj}\} = \alpha_j \frac{d\sigma_{ij}(E, E_0)}{dE_0} \tag{1}$$

$$\sum_k \alpha_k \int d\sigma_{ik} \{G_{ij} - G'_{ij} - G''_{kj}\} = \frac{\psi}{N v_0} \delta_{ij} \delta(E - E_0) \tag{2}$$

where $F'_{ij} = F_{ij}(E', E_0)$ and $F''_{ij} = F_{ij}(E'', E_0)$, etc. Furthermore, $E'$ and $E''$ are the energies of a scattered $i$-atom and a recoiling $k$-atom, respectively, after a collision that is governed by the differential cross section $d\sigma_{ik}(E, E', E'')$ The quantity $v_0$ is the velocity of a $j$-atom with energy $E_0$, and $d\sigma_{ij}(E, E_0)/dE_0$ stands for

$$\int_{E', E''} d\sigma_{ij}(E, E', E'')\delta(E'' - E_0).$$

The integral operators on the left-hand side of eqs. (1) and (2) are identical. However, eq. (2) has the form of an equation determining the *Green's function* of this integral operator. Hence, the functions $F_{ij}$ and $G_{ij}$ are interrelated in the following way,

$$F_{ij}(E, E_0) = \alpha_j \sum_l \int dE_1 \frac{N v_1}{\psi} G_{il}(E, E_1) \frac{d\sigma_{lj}(E_1, E_0)}{dE_0}. \tag{3}$$

Eq. (3) can be verified by insertion into eq. (1), interchanging the order of integrations, and utilizing eq. (2). Hence, once eq. (2) has been solved, $F_{ij}$ follows from $G_{ij}$ by integration according to (3). Both equations are equivalent to those used in ref. 23, although the present notation is more general. Furthermore, we use integral equations in the so-called "backward" form[29], while previous authors mostly used the forward form.

Eq. (2) will have to be solved subject to the boundary conditions

$$G_{ij}(E, E_0) = 0 \quad \text{for} \quad E < E_0. \tag{4}$$

In the special case of a *binary* medium, eq. (4) even holds for $E < E_0/\gamma_{ij}$ where

$$\gamma_{ij} = 4M_iM_j/(M_i + M_j)^2 \tag{5}$$

The following (usual) approximations will be made in order to solve eq. (2):

i) No binding energy is lost by recoiling atoms,*
ii) Electronic stopping is separated according to the scheme of LINDHARD et.al[2].

Then eq. (2) reads

$$\left.\begin{aligned} &\sum_k \alpha_k \int d\sigma_{ik}(E, T)\{G_{ij}(E, E_0) - G_{ij}(E - T, E_0) - G_{kj}(T, E_0)\} \\ &\quad + \sum_k \alpha_k S_{e,ik}(E) \frac{\partial}{\partial E} G_{ij}(E, E_0) = \frac{\psi}{N v_0} \delta_{ij} \delta(E - E_0) \end{aligned}\right\} \tag{2a}$$

* This simplification is dropped in appendix B.

where $S_{e,ik}(E)$ is the electronic stopping cross section for an $i$-atom colliding with a $k$-atom, and $T$ the recoil energy. The cross section $d\sigma_{ik}(E, T)$ is that of *elastic* collisions.

It is most often possible to define an elastic-collision region[2] $E \lesssim E_c$ where electronic stopping is relatively small, so that it can be neglected as a first approximation. In this case we shall see (sects. 3, 4 and 5) that

$$G_{ij}(E, E_0) \sim g_j(E_0) \cdot E \quad \text{for} \quad E_0 \ll E \lesssim E_c \tag{6}$$

where $g_j(E_0)$ is a well defined function. The important features of eq. (6) are i) the linear dependence on $E$ and ii) the nonoccurrence of the index i on the right-hand side.* From eqs. (2a) and (6) one verifies immediately that the following extension holds for higher energies beyond the elastic-collision region

$$G_{ij}(E, E_0) \sim g_j(E_0) \nu_i(E) \quad \text{for} \quad E_0 \ll E_c \quad \text{and} \quad E > E_c \tag{7}$$

where the $\nu_i(E)$ obey the set of equations

$$\sum_k \alpha_k \int d\sigma_{ik}(E, T) \{\nu_i(E) - \nu_i(E - T) - \nu_k(T)\} + \sum_k \alpha_k S_{e,ik}(E) \cdot \frac{d}{dE} \nu_i(E) = 0 \tag{8}$$

This is the generalization to polyatomic media of an integral equation first derived by LINDHARD et al.[2, 30]; a computer code for its solution has been worked out by WINTERBON[25]. It is obvious from eqs. (6) and (7) that, in order to determine deviations from stoichiometric energy sharing, we need the $g_j(E)$ function rather than $\nu_i(E)$. Since the former can be determined by solely considering the elastic-collision region, we shall restrict our attention to this region in the following sections. This simplifies the analysis substantially.

It may be stressed that the present argument is based on the *existence* of an elastic-collision region. For very different masses of constituent atoms, e.g. the case of a target containing very heavy atoms and *hydrogen* atoms, $E_c$ may be prohibitively small. In such a case, caution has to be applied with respect to quantitative conclusions.

* $g_j(E_0)$ does, however, depend on *all* the constituents of the medium. See, e.g., eqs. (24a, b).

## 3. Power Cross Sections

The solution of integral equations of the type of eq. (2a) is facilitated greatly by use of a power cross section of the form[31]

$$d\sigma(E, T) = CE^{-m}T^{-1-m}dT; \; 0 \leq m < 1 \tag{9}$$

This cross section describes approximately the scattering of two Thomas-Fermi atoms over a limited range of energy $E$ and recoil energy $T$. The proper value of $m$ depends essentially on the product $E \cdot T$ and on the ion-target combination[31, 20]. At present, we apply eq. (9) in the form

$$d\sigma_{ij}(E, T) = C_{ij}E^{-m_i} \; T^{-1-m_i}dT; \; 0 \leq T \leq \gamma_{ij}E \tag{10}$$

in order to allow greatest possible generality within the inherent simplicity of the power cross section.* We note that eq. (10) is somewhat more general than the cross section used in ref. 23, since it allows for a variety of energy dependences of, e.g., the stopping power. We shall see below that this generalization is significant.

In sect. 6 we shall need more specified constants $C_{ij}$. We use the two forms

$$C_{ij} = \frac{\pi}{2} \cdot \lambda_{m_i} \cdot a_{ij}^2 \left(\frac{M_i}{M_j}\right)^{m_i} \left(\frac{2Z_i Z_j e^2}{a_{ij}}\right)^{2m_i}; \; m_i > \tfrac{1}{4}, \tag{10a}$$

and

$$C_{ij} = \frac{\pi}{2} \cdot \lambda_{m_i} \cdot a_{ij}'^2 \left(\frac{M_i}{M_j}\right)^{m_i} (2A_{ij}')^{2m_i}; \qquad m_i < \tfrac{1}{4}. \tag{10b}$$

The first choice[31] corresponds to Thomas-Fermi scattering with the screening radius

$$a_{ij} = 0.8853\, a_0 (Z_1^{2/3} + Z_2^{2/3})^{-1/2} \tag{11a}$$

and[31, 20]

$$\lambda_{1/2} = 0.327; \; \lambda_{1/3} = 1.309; \tag{11b}$$

The second choice[28] corresponds to exponential interaction with[32]

* Preferably one would use exponents $m_{ij}$ instead of $m_i$; however, this would mean a substantial complication in the algebra. In fact, we have not succeeded in deriving eqs. (25) and (28) in this latter case, although the Laplace transform can be carried out easily. One might also suggest to use an index $m_j$. This would still be substantially more complicated than using $m_i$ and, more important, would be physically a less reasonable choice than the one adopted in eq. (10).

$$\left.\begin{aligned} a'_{ij} &= \text{const.} = 0.219\ \text{Å}; \\ A'_{ij} &= 52(Z_i Z_j)^{3/4} eV; \end{aligned}\right\} \quad (11c)$$

and [28)]

$$\lambda_{0.055} = 15^*; \quad \lambda_0 = 24. \quad (11d)$$

Since we need mostly the cross sections at *low* particle energy $E_0$ (in the $eV$ region) when calculating recoil and slowing-down densities[28, 34)], it is mostly the expressions (10b), (11c), and (11d) that will be used in applications. However, for low-mass ions – up to about oxygen – the Thomas-Fermi coefficients can be expected to be appropriate even in the lower $eV$-region, and will be used, therefore.

A convenient procedure of solving integral equations with a cross section like (9) has been described in detail by ROBINSON[33)] and one of the authors[1)] for the monatomic case. Straightforward generalization to the present situation is possible. Inserting $d\sigma_{ik}(E, T)$ as given by eq. (2a), setting $S_{e,ik}(E) = 0$, introducing the variables

$$E = E_0 e^u; \quad T = E_0 e^v,$$

following the procedure of ref. 1, and taking the Laplace transfrom with respect to the variable $u$ yields

$$\tilde{G}_{ij}(s) \sum_k \beta_{ik}(s)\, \varepsilon_{ik}(s) - \sum_k \beta_{ik}(s)\, \tilde{G}_{kj}(s) = \frac{\psi E_0^{2m_i - 1}}{N v_0}\, \delta_{ij} \quad (12)$$

where

$$\beta_{ik}(s) = \frac{\gamma_{ik}^{s - m_i}}{s - m_i}\, \alpha_k\, C_{ik} \quad (13a)$$

and

$$\varepsilon_{ik}(s) = \frac{s - m_i}{\gamma_{ik}^{s - m_i}} \left[ - \frac{\gamma_{ik}^{-m_i}}{m_i} - B_{\gamma_{ik}}(-m_i, s + 1) \right] \quad (13b)$$

$B_\gamma(x, y)$ is the incomplete beta function,

$$B_\gamma(x, y) = \int_0^\gamma dt\, t^{x-1} (1 - t)^{y-1} \quad (14)$$

and $\tilde{G}_{ij}(s)$ the Laplace transform

$$\tilde{G}_{ij}(s) = \int_0^\infty du\, e^{-su} G(E_0 e^u, E_0) \quad (15)$$

where use has been made of eq. (4).

* This value has been extracted from fig. 4 of ref. 28. It is rather uncertain. Note that for the high-energy portion of Born-Mayer interaction, a value about half as large was reported in ref. 28.

Eq. (12) is a system of algebraic equations that splits up into separate subsystems, one for each target element $j$. All the subsystems have the same determinant, but different inhomogeneities on the right-hand side.

In accordance with eq. (6), we are looking for solutions in the region $E \gg E_0$, i.e. large values of $u$. The procedure of determining asymptotic solutions is a generalization of the one described in detail in refs. 1,33,34. The main problem is to find the highest value of $s$, say $s = s_{ij}^{(0)}$ where $\tilde{G}_{ij}(s)$ has a single pole. Then, $G_{ij}(E, E_0)$ has the asymptotic form

$$G_{ij}(E, E_0) \sim A_{ij} \cdot (E/E_0)^{s_{ij}^{(0)}} \quad \text{for} \quad E \gg E_0 \tag{16}$$

where $A_{ij}$ is the residuum of $\tilde{G}_{ij}(s)$ at $s = s_{ij}^{(0)}$. Some properties of the asymptotic expansion will be analysed in the following in the special case of a binary target. At present we discuss, somewhat loosely, some simple consequences of eq. (12).

Poles of $\tilde{G}_{ij}(s)$ may occur at the zeros of the determinant of eq. (12) and the poles of the subdeterminants. According to (13a, b) poles of subdeterminants might occur at $s = m_i$, and at some discrete negative values of $s$. The determinant, on the other hand, is expected to have a zero at $s = 1$, just as in the monatomic case. Indeed, from (13b), it follows that

$$\varepsilon_{ik}(1) = 1. \tag{17}$$

With this, the determinant achieves the form

$$D(1) = Det\{\delta_{ik} \sum_l \beta_{il}(1) - \beta_{ik}(1)\} \tag{18}$$

which is obviously zero. Moreover, it follows from (12) that

$$G_{ij}(s) \sim \tilde{G}_{kj}(s) \quad \text{for} \quad s \sim 1 \tag{19}$$

or, from (16), $A_{ij} = A_{kj}$. This proves eq. (6). The remaining problem is to calculate $g_j(E_0)$. This will be done by evaluating determinants.

In appendix $A$ we prove that $s = s_{ij}^{(0)} = 1$ is the highest singularity for a general polyatomic target. This is not surprising from a physical point of view. It is evident already from eqs. (1) and (2) that energy conservation in binary collisions requires solutions that are asymptotically ($E \gg E_0$) linear in energy, and independent of the bombarding particle.

## 4. The Binary Case. I

With the abbreviation

$$B_j = \frac{\psi E_0^{2mj-1}}{N v_0} \tag{20}$$

the system of equations (12) has the solutions

$$\tilde{G}_{11}(s) = B_1 \frac{D_{11}^{(2)}}{D^{(2)}}; \quad \tilde{G}_{21}(s) = -B_1 \frac{D_{12}^{(2)}}{D^{(2)}} \tag{21}$$

where

$$D^{(2)} = [\beta_{11}(\varepsilon_{11} - 1) + \beta_{12}\varepsilon_{12}][\beta_{22}(\varepsilon_{22} - 1) + \beta_{21}\varepsilon_{21}] - \beta_{12}\beta_{21} \tag{22a}$$

$$D_{11}^{(2)} = \beta_{22}(\varepsilon_{22} - 1) + \beta_{21}\varepsilon_{21} \tag{22b}$$

$$D_{12}^{(2)} = -\beta_{21}. \tag{22c}$$

For $s = s_{ij}^{(0)} = 1$, and observing (17), we obtain

$$\tilde{G}_{11}(s) \sim \tilde{G}_{21}(s) \sim \frac{B_1 \beta_{21}(1)}{(s-1) D'(1)} \quad \text{for} \quad s \sim 1 \tag{23a}$$

where $D'(s) = \dfrac{d}{ds} D(s)$.*

Similarly, or by interchanging indices, we obtain

$$\tilde{G}_{22}(s) \sim \tilde{G}_{12}(s) \sim \frac{B_2 \beta_{12}(1)}{(s-1) D'(1)} \quad \text{for} \quad s \sim 1 \tag{23b}$$

Applying inverse Laplace Transform, we obtain asymptotic solutions

$$G_{11}(E) \sim G_{21}(E) \sim \frac{E}{E_0} \frac{B_1 \beta_{21}(1)}{D'(1)}; \quad \text{or} \quad g_1(E_0) = \frac{B_1 \beta_{21}(1)}{E_0 D'(1)} \tag{24a}$$

$$G_{22}(E) \sim G_{12}(E) \sim \frac{E}{E_0} \frac{B_2 \beta_{12}(1)}{D'(1)}; \quad \text{or} \quad g_2(E_0) = \frac{B_2 \beta_{12}(1)}{E_0 D'(1)}. \tag{24b}$$

These equations provide the connection with eq. (6).

* We drop the index $^{(2)}$ from $D^{(2)}$ for the rest of this section.

If we take the ratio of the fluxes of moving atoms of the two species, the determinant and the ion energy drop out, hence*

$$\left.\begin{aligned} &\frac{v_0 G_{11}(E)}{v_0 G_{12}(E)} \sim \frac{v_0 G_{21}(E)}{v_0 G_{12}(E)} \sim \frac{v_0 G_{11}(E)}{v_0 G_{22}(E)} \sim \frac{v_0 G_{21}(E)}{v_0 G_{22}(E)} \\ &\sim \frac{\alpha_1}{\alpha_2} \frac{\dfrac{\gamma_{21}^{1-m_2}}{1-m_2} C_{21} E_0^{1-2m_2}}{\dfrac{\gamma_{12}^{1-m_1}}{1-m_1} C_{12} E_0^{1-2m_1}} = \frac{\alpha_1 S_{21}(E_0)}{\alpha_2 S_{12}(E_0)} \end{aligned}\right\} \quad (25)$$

where

$$S_{ik}(E) = \int_0^{\gamma_{ik}E} T d\sigma_{ik}; \quad \beta_{ik}(1) = \alpha_k S_{ik}(E) E_0^{2m_i - 1}; \quad (26)$$

$S_{ik}(E)$ is the nuclear stopping cross section of an $i$-atom colliding with a $k$-atom.

Next, we insert eq. (24a, b) into eq. (3), and evaluate $F_{ij}$ to the highest power of $E/E_0$, i.e. the linear term. This yields, in the same notation as eq. (24),

$$F_{11}(E) \sim F_{21}(E) \sim \frac{E}{E_0^2} \frac{\beta_{21}(1)(\beta_{11}(1) + \beta_{12}(1))}{D'(1)} \quad (27a)$$

$$F_{22}(E) \sim F_{12}(E) \sim \frac{E}{E_0^2} \frac{\beta_{12}(1)(\beta_{22}(1) + \beta_{21}(1))}{D'(1)} \quad (27b)$$

From this we obtain the ratio

$$\frac{F_{11}(E)}{F_{22}(E)} \sim \frac{\alpha_1 S_{21}(E_0)}{\alpha_2 S_{12}(E_0)} \frac{\alpha_1 S_{11}(E_0) + \alpha_2 S_{12}(E_0)}{\alpha_2 S_{22}(E_0) + \alpha_1 S_{21}(E_0)} \quad (28)$$

where again eq. (26) has been used. Eqs. (25) and (28) show that in general

i) the ratio of the fluxes of moving 1-atoms to moving 2-atoms is proportional to the ratio of the respective concentrations, but not nessecarily identical with it, and

ii) an even more pronounced deviation from stoichiometry is expected in the ratio of the number of recoiling 1-atoms and recoiling 2-atoms, since the concentrations enter nonlinearly.

* We include the velocity $v_0$ in $v_0 G_{ij}(E, E_0)$ because of the index $j$ in $v_0 = \sqrt{2E_0/M_j}$. Note that both in sputtering theory[28] and in eq. (3) it is actually *this* product that is important.

## 5. The Ternary Case

We briefly mention the asymptotic solutions for the case of a ternary compound. From (12) we obtain.

$$G_{11} \sim G_{21} \sim G_{31} \sim B_1 \frac{D_{11}^{(3)}}{D^{(3)\prime}} \frac{E}{E_0} \tag{29a}$$

$$G_{12} \sim G_{22} \sim G_{32} \sim B_2 \frac{D_{22}^{(3)}}{D^{(3)\prime}} \frac{E}{E_0} \tag{29b}$$

$$G_{13} \sim G_{23} \sim G_{33} \sim B_3 \frac{D_{33}^{(3)}}{D^{(3)\prime}} \frac{E}{E_0} \tag{29c}$$

where

$$D_{11}^{(3)} = \beta_{21}\beta_{31} + \beta_{21}\beta_{32} + \beta_{23}\beta_{31} \tag{30a}$$

$$D_{22}^{(3)} = \text{cycl. perm.} \tag{30b}$$

$$D_{33}^{(3)} = \text{cycl. perm.} \tag{30c}$$

$$D^{(3)\prime} = \frac{d}{ds} D^{(3)}(s)\big|_{s=1} = (\beta_{11}\varepsilon'_{11} + \beta_{12}\varepsilon'_{12} + \beta_{13}\varepsilon'_{13}) D_{11}^{(3)} + \text{cycl. perm.}, \tag{31}$$

and the upper index (3) indicates the ternary case. Both $D_{ik}^{(3)}$, $\varepsilon'_{ik}$, and $\beta_{ik}$ are taken at $s = 1$. The $B_i$ are given in eq. (20). It is straightforward to determine *relative* magnitudes of the $G_{ik}$ from eqs. (29–31).

By applying eq. (3) to the ternary case, we readily obtain

$$F_{11} \sim F_{21} \sim F_{31} \sim \frac{E}{E_0^2} \frac{\beta_{11} D_{11}^{(3)} + \beta_{21} D_{22}^{(3)} + \beta_{31} D_{33}^{(3)}}{D^{(3)\prime}} \tag{32a}$$

$$F_{12} \sim F_{22} \sim F_{32} \sim \frac{E}{E_0^2} \frac{\beta_{12} D_{11}^{(3)} + \beta_{22} D_{22}^{(3)} + \beta_{32} D_{33}^{(3)}}{D^{(3)\prime}} \tag{32b}$$

$$F_{13} \sim F_{23} \sim F_{33} \sim \frac{E}{E_0^2} \frac{\beta_{13} D_{11}^{(3)} + \beta_{23} D_{22}^{(3)} + \beta_{33} D_{33}^{(3)}}{D^{(3)\prime}} \tag{32c}$$

Evaluation of $G_{ik}$ and $F_{ik}$ in terms of stopping powers can be made by use of eqs. (35) and (26). We shall not go into any further details with the general ternary case.

## 6. The Binary Case. II

In this section we discuss in more detail some implications of the equations derived in sect. 4 for the binary case. For illustration we have evaluated numerically the solutions in a few specific cases.

Let us first consider the ratio between the slowing-down densities. Eq. (25) may be written

$$\frac{v_0 G_1}{v_0 G_2} \sim \frac{\alpha_1}{\alpha_2} \cdot \frac{C_{21}}{C_{12}} \cdot X \cdot E_0^{2(m_1 - m_2)}, \tag{25a}$$

where the constant

$$X = \frac{1 - m_1}{1 - m_2} \gamma^{m_1 - m_2}$$

is of the order of one (In view of eq. (6), we dropped the *first* index from $G_{ij}$). For strictly stoichiometric behaviour, we would just have $\alpha_1/\alpha_2$ on the right-hand side of eq. (25a). If $m_1 \neq m_2$, the ratio (25a) depends on the energy $E_0$, and in such a way that the fraction of moving atoms of the *lighter* species increases in the *upper* parts of the energy spectrum. If $m_1 = m_2 \equiv m$, (25a) reduces to

$$\frac{v_0 G_1}{v_0 G_2} \sim \frac{\alpha_1}{\alpha_2} \cdot \frac{C_{21}}{C_{12}} = \frac{\alpha_1}{\alpha_2} \left( \frac{M_2}{M_1} \right)^{2m}, \tag{25b}$$

according to eqs. (10a, b). Then the deviation from stoichiometry does not vary over the energy spectrum (for $E_0 \ll E$) and is determined solely by the mass ratio and $m$. Since $m \geq 0$, the lighter species dominates at those energies where (25b) is valid.

The ratio between the recoil densities, eq. (28), is energy-independent even for $m_1 \neq m_2$, as may be seen by inserting

$$S_{ik}(E_0) = \frac{C_{ik}}{1 - m_i} \gamma^{1 - m_i} E_0^{1 - 2m_i}$$

into eq. (28),

$$\frac{F_1}{F_2} \sim \frac{\alpha_1}{\alpha_2} \cdot \frac{\alpha_1 \cdot \gamma^{m_1 - 1} \cdot \dfrac{C_{11}}{C_{12}} + \alpha_2}{\alpha_2 \cdot \gamma^{m_2 - 1} \cdot \dfrac{C_{22}}{C_{21}} + \alpha_1} = \frac{\alpha_1}{\alpha_2} \cdot Y \tag{28a}$$

where again the *first* index was dropped from $F_{ij}$. Here the factor $Y$ depends on concentration, and its variation with $\alpha_1$ and $\alpha_2$ determines the deviation

from stoichiometry. For small amounts of one of the constituents, (28a) reduces to

$$\frac{F_1}{F_2} \sim \frac{\alpha_1}{\alpha_2} \cdot \frac{S_{11}(E_0)}{S_{12}(E_0)} = \frac{\alpha_1}{\alpha_2} \cdot \frac{C_{11}}{C_{12}} \gamma^{m_1 - 1} (\alpha_2 \ll 1) \tag{28b}$$

$$\frac{F_1}{F_2} \sim \frac{\alpha_1}{\alpha_2} \cdot \frac{S_{21}(E_0)}{S_{22}(E_0)} = \frac{\alpha_1}{\alpha_2} \cdot \frac{C_{21}}{C_{22}} \gamma^{1 - m_2} (\alpha_1 \ll 1). \tag{28c}$$

A useful dimensionless quantity in the calculation of the average number $N_i$ of *displaced* $i$-atoms is the displacement effiency[33] $K_i$, defined by*

$$N_i = \int_{E_{d,i}}^{\infty} F_i(E, E_0)\, dE_0 = \frac{E}{E_{d,i}} \cdot \alpha_i \cdot K_i \tag{33}$$

$E_{d,i}$ is the displacement threshold energy for atoms of type $i$. In the monatomic case one obtains[27]

$$K = \frac{m}{\psi(1) - \psi(1 - m)}, \tag{34}$$

i.e. $0 \leq K \leq \dfrac{6}{\pi^2}$ for $0 \leq m \leq 1$.

For the numerical examples, we have chosen binary compounds of rather different masses : Tungsten Oxide ($\gamma = 0.295$), Uranium Carbide ($\gamma = 0.183$), and Copper-Gold ($\gamma = 0.738$). In the calculations we have used the two values of $m$, 0.055, eq. (11d) and 0.333, eq. (11b). Both choices $m_1 \neq m_2$ and $m_1 = m_2$ have been considered. In the case of different $m$-values, $m = 0.333$ has been used for the lighter element, and $m = 0.055$ for the heavier one.

According to eq. (24), the slowing-down density $G_i$ is determined by an equation of the form

$$\frac{N v_0}{\psi E} \cdot G_i = E_0^{2(m_i - 1)} \cdot A_i ; \; E_0 \ll E. \tag{35}$$

Figs. 1a and 1b show the energy dependence of this quantity for $W$ and O in $W$–O compounds, plotted for concentration 0, 1/4, 1/2, 3/4 and 1, in

* The present model for the displacement number is oversimplified, since it does not take into account replacement events. Therefore, the displacement efficiency can become greater than 0.5, contrary to the result of ref. 33. Although replacements constitute another interesting aspect of collision cascades in polyatomic targets, we refrain from including them here, since the available models seem to be even less quantitative than those for displacement. In particular, no experimental data are known to us for replacement threshold energies for any system.

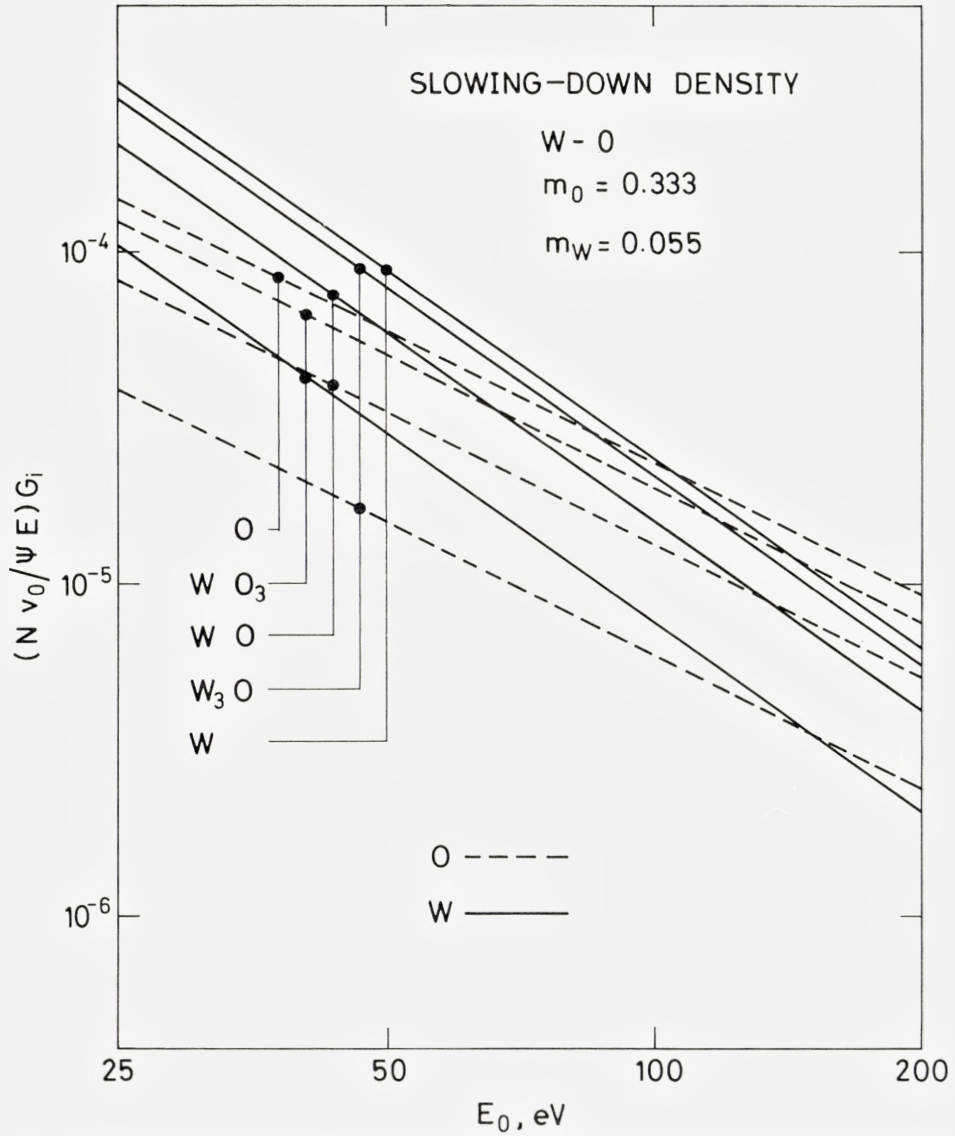


Fig. 1. Slowing-down densities of each of the two constituents of three binary compounds in relative units, eq. (35), as a function of spectral energy $E_0$. Parameters $m_O$, $m_W$, etc. refer to the scattering law, eq. (10). Note the different energy dependences of the spectra in case of $m_1 \neq m_2$. Full-drawn and stipled lines refer to the heavy and light constituent, respectively.

Fig. 1a. Tungsten oxide, $m_O > m_W$.

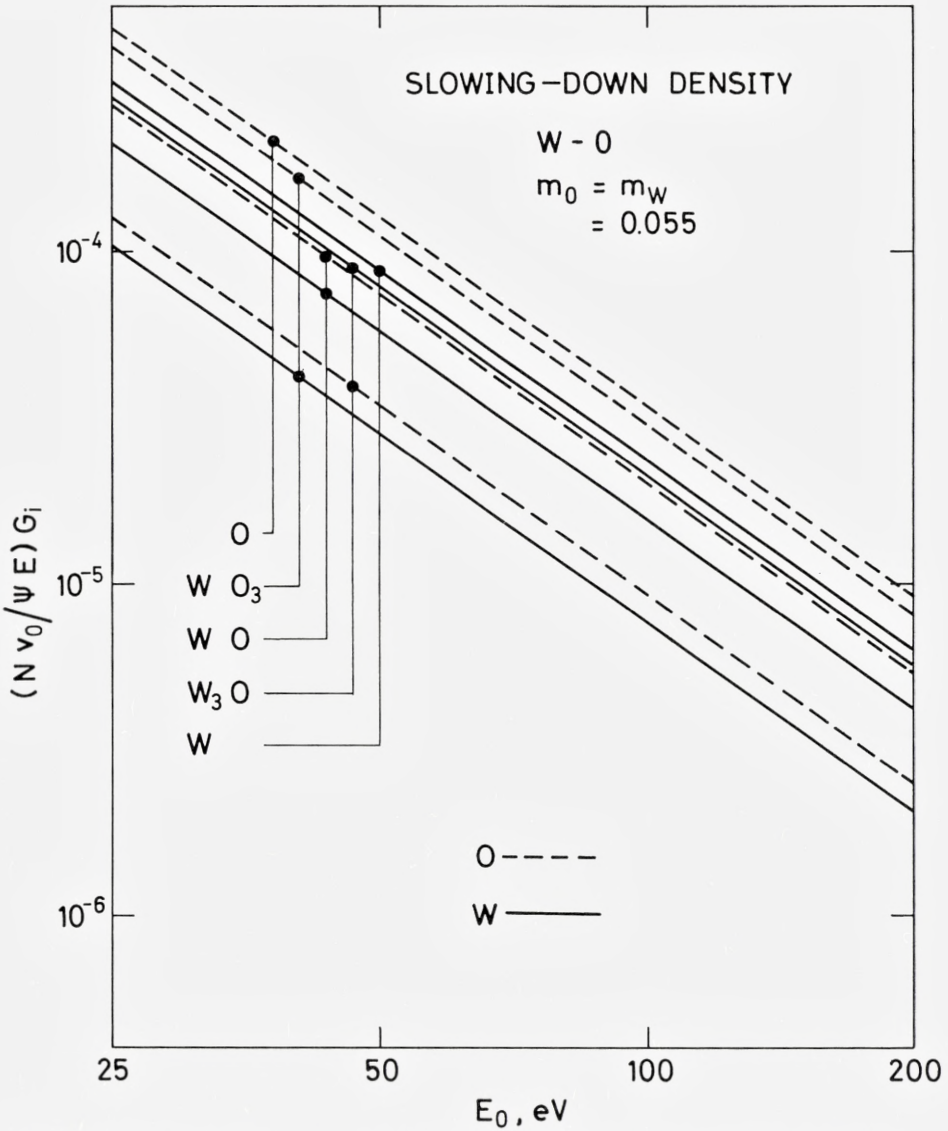


Fig. 1b. Tungsten oxide, $m_O = m_W$; this graph is presumably less realistic than fig. 1a.

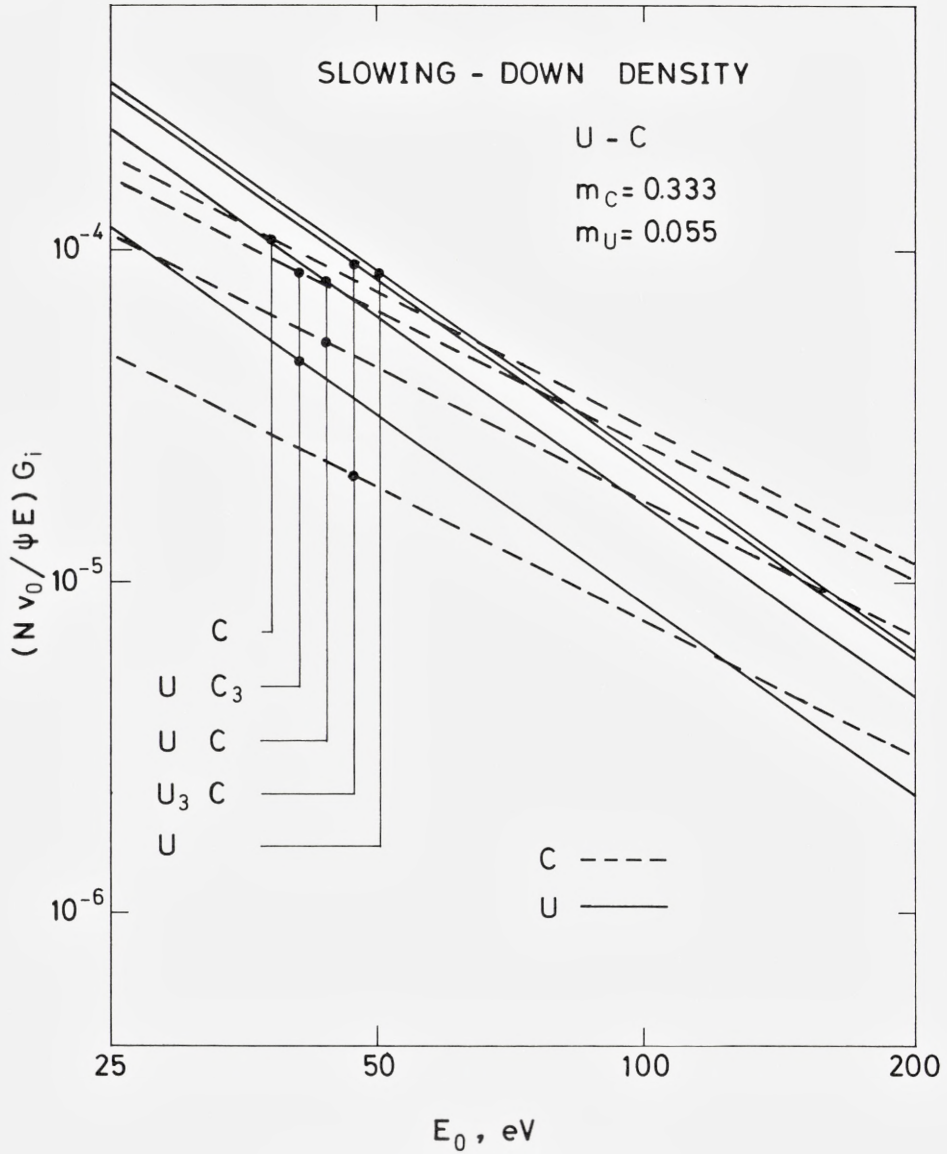


Fig. 1c. Uranium carbide, $m_C > m_U$.

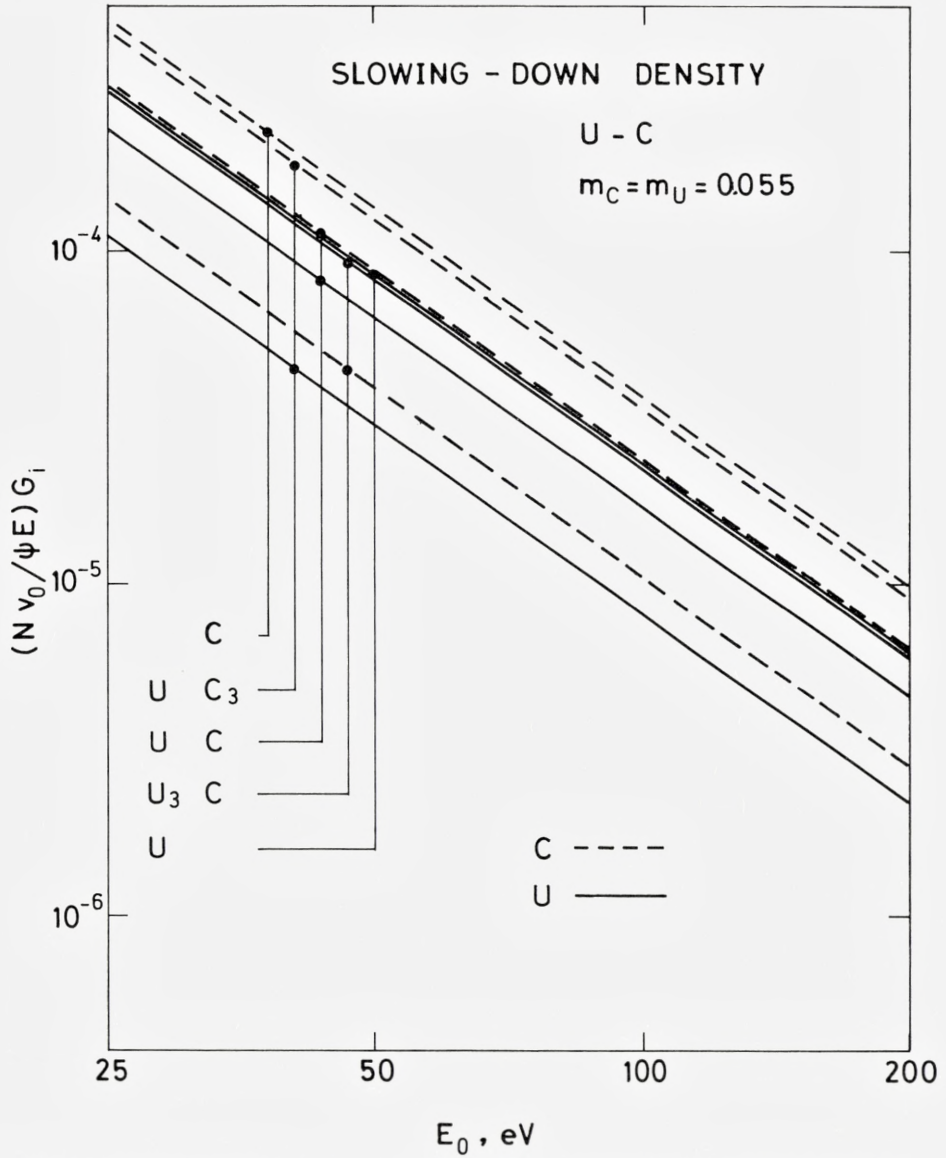


Fig. 1d. Uranium carbide, $m_C = m_U$; this graph is presumably less realistic than fig. 1c.

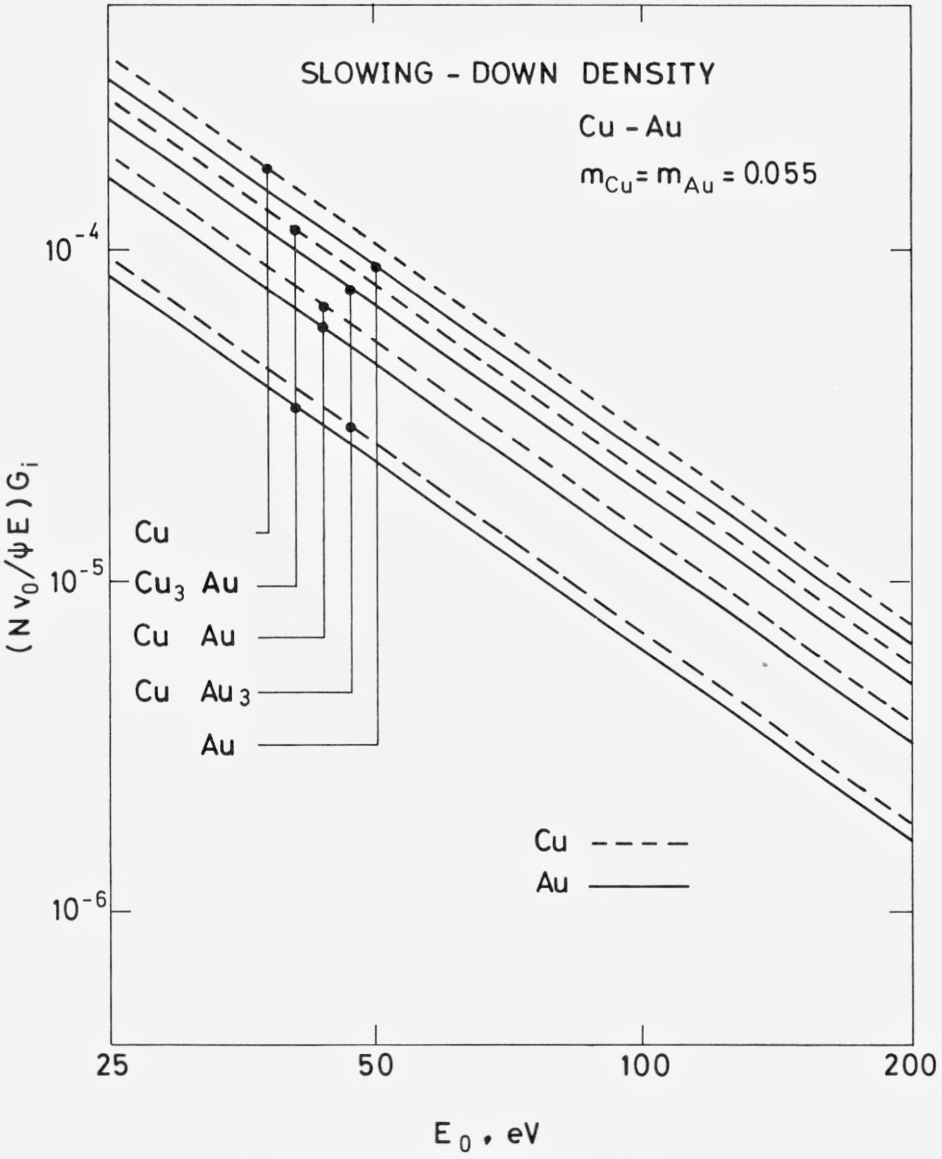


Fig. 1e. Copper-gold alloy, $m_{Cu} = m_{Au}$.

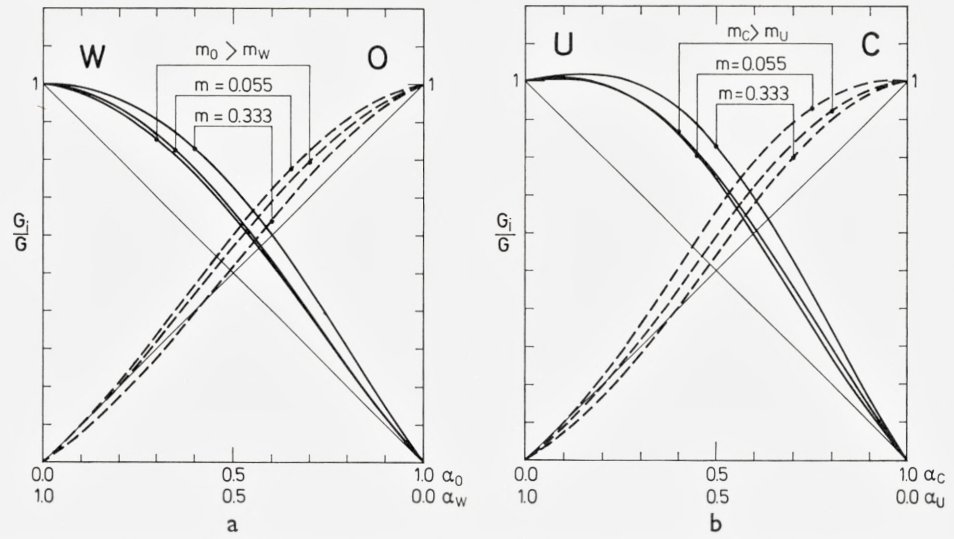


Fig. 2. Slowing-down densities $G_1$ and $G_2$ of each of the two constituents of three binary compounds, normalized to the values of the respective pure media, $G$, as a function of concentration. The ratios $G_i/G$ do not depend on spectral energy $E_0$. In addition to the two combinations of scattering parameters $m_i$ used in fig. 1, a third one with $m_1 = m_2 = 0.333$ has been included for illustration. Full-drawn and stipled lines refer to the heavy and light constituent, respectively. Apart from a constant factor given by eq. (25a) or 25b), thin fulldrawn lines refer to stoichiometric variation.

Fig. 2a. Tungsten oxide. The two curves with $m_O > m_W$ are presumed to come closest to reality.
Fig. 2b. Uranium carbide. The two curves with $m_C > m_U$ are presumed to come closest to reality.

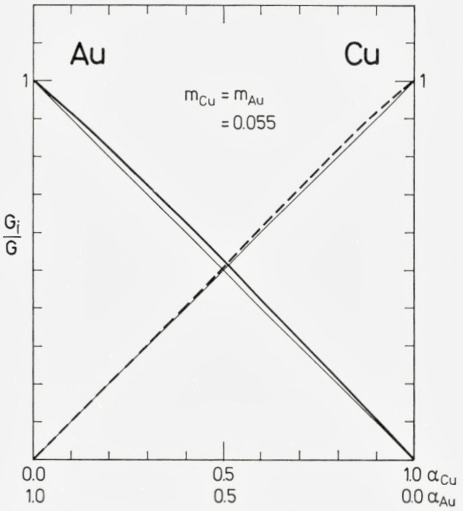


Fig. 2c. Copper-gold alloy. Only the two curves with $m_{Cu} = m_{Au}$ have been included.

case of $m_O > m_W$ and $m_O = m_W$, respectively. The variation of the expression (35) at fixed energy with composition is illustrated in fig. 2a. We notice that the variation of $G_i$ near $\alpha_i = 1$ is much weaker than the stoichiometric variation. The qualitative conclusion appears justified that the total number of moving matrix atoms in a nearly pure target is almost unaffected by alloying impurities of widely different mass.

This effect can be understood qualitatively. The slowing-down density is determined both by the number of atoms set in motion and the time for slowing-down. Alloying an impurity of very different mass causes a decrease in the former quantity (the recoil density), but an increase in the latter.

As might be expected, this effect is even more pronounced in the case of *U-C* (figs. 1c + d and 2b), and less pronounced in *Cu-Au* (figs. 1e and 2c).

The recoil density, $F_i$, is determined by eqs. (27a, b),

$$\frac{1}{E} \cdot F_i = E_0^{-2} \cdot C_i; \quad E_0 \ll E, \tag{36}$$

where $C_i = \alpha_i \cdot K_i$. The variation of the expression (36) with recoil energy $E_0$ for $W$ and $O$ in $W$–$O$ compounds is shown in figs. 3a + b for $m_O > m_W$ and $m_O = m_W$, for concentration 0, 1/4, 1/2, 3/4 and 1. For $m_O > m_W$, the *heavier* component recoils preferentially. This arises from the sensitivity of the recoil density to the steepness of the differential cross section[2, 33], the latter being greatest for the largest value of $m$ according to eq. (9).

The variation of the displacement efficiency $K_i$ with concentration is shown in fig. 4a. As one might expect, the displacement efficiency is almost independent of concentration in the vicinity of $\alpha_i = 1$. When $\alpha_i$ becomes smaller, $K_i$ drops gradually to a significantly lower value. The relatively low displacement efficiency of impurities ($\alpha \ll 1$) is due to the comparatively inefficient energy transfer in collisions with host atoms and the small chance for impurity-impurity collisions. The same features are observed for *U-C* and *Cu-Au*, see figs. 3c–e and 4b + c.

Figs. 5a–c contain the same information as fig. 4. We have plotted the factor $Y$ in eq. (28a) as a function of concentration. This factor represents the (concentration-dependent) deviation from stoichiometric behaviour of the recoil density. The upper and lower limits of $Y$ are determined by eqs. (28b, c).

To make sure that our results do not hinge heavily on the detailed assumptions concerning the displacement process, we estimated in appendix B the influence of an atomic binding energy, and especially the significance of different binding energies of the two constituents, on the slowing-down density.

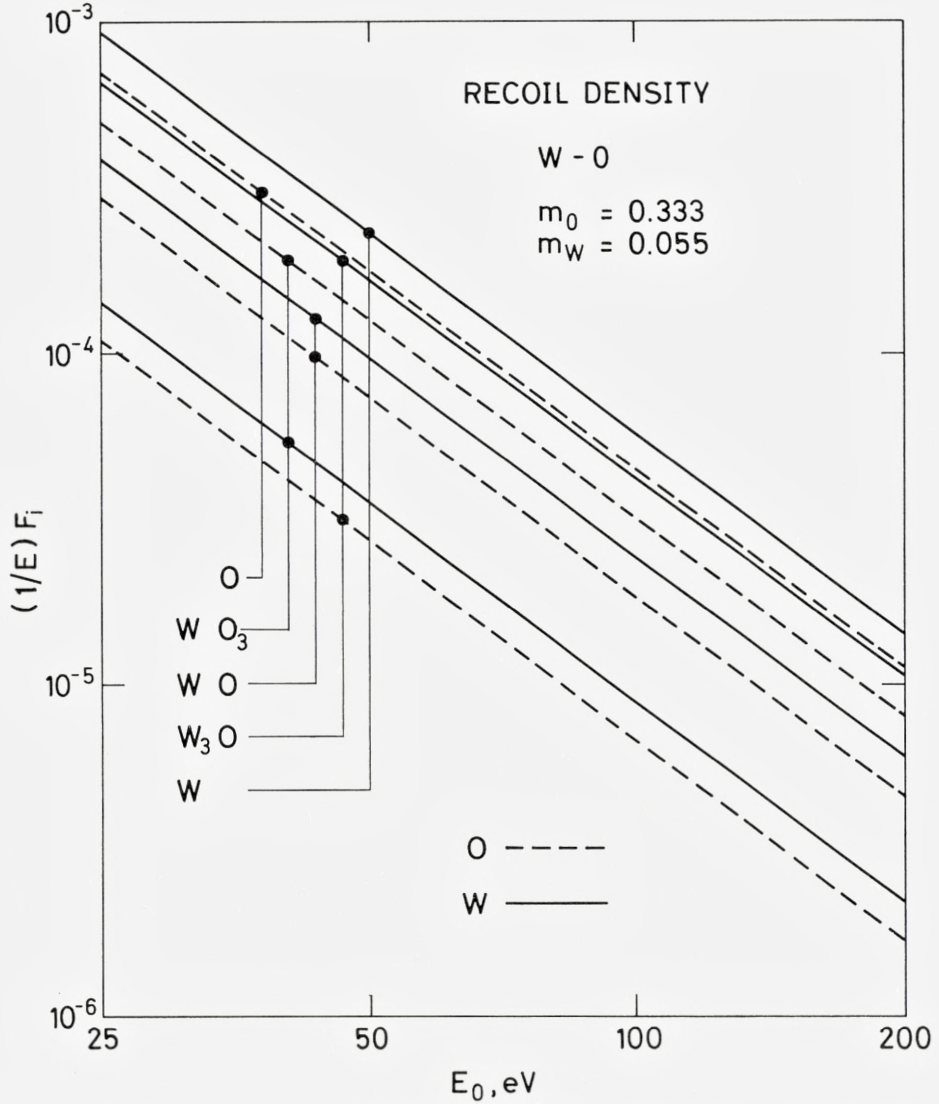


Fig. 3. Same as fig. 1 for the recoil densities, eq. (36). Note that all energy dependence goes as $E_0^{-2}$.

Fig. 3a. Tungsten oxide, $m_O > m_W$.

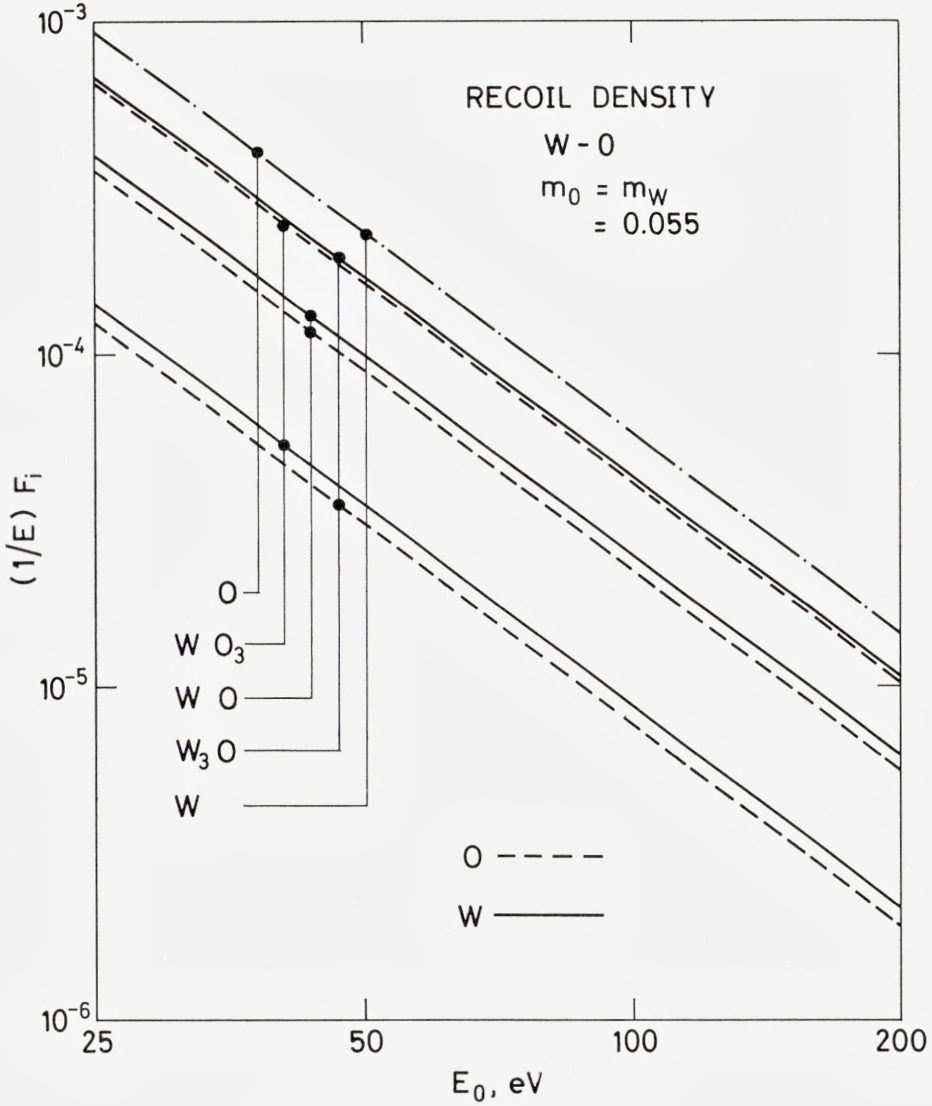


Fig. 3b. Tungsten oxide, $m_O = m_W$.

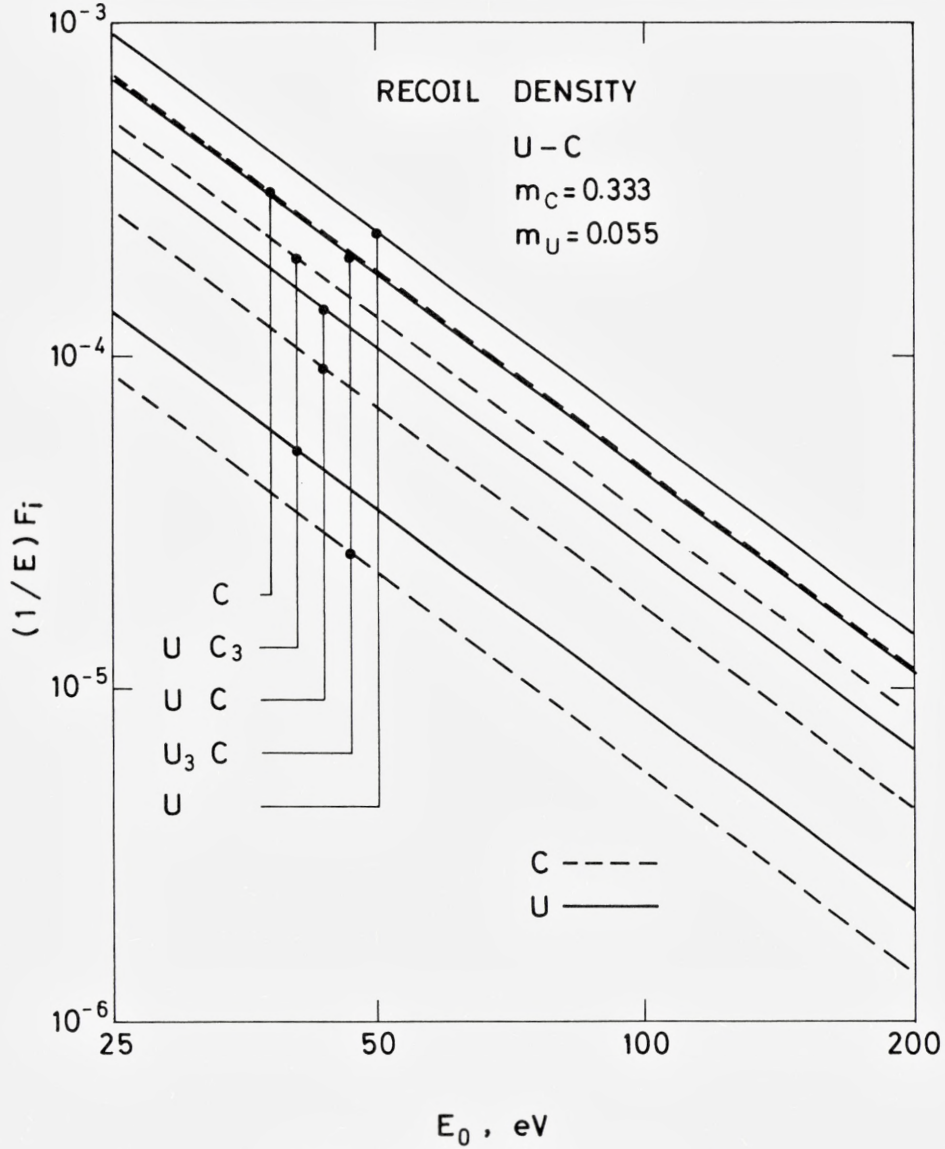


Fig. 3c. Uranium carbide, $m_C > m_U$.

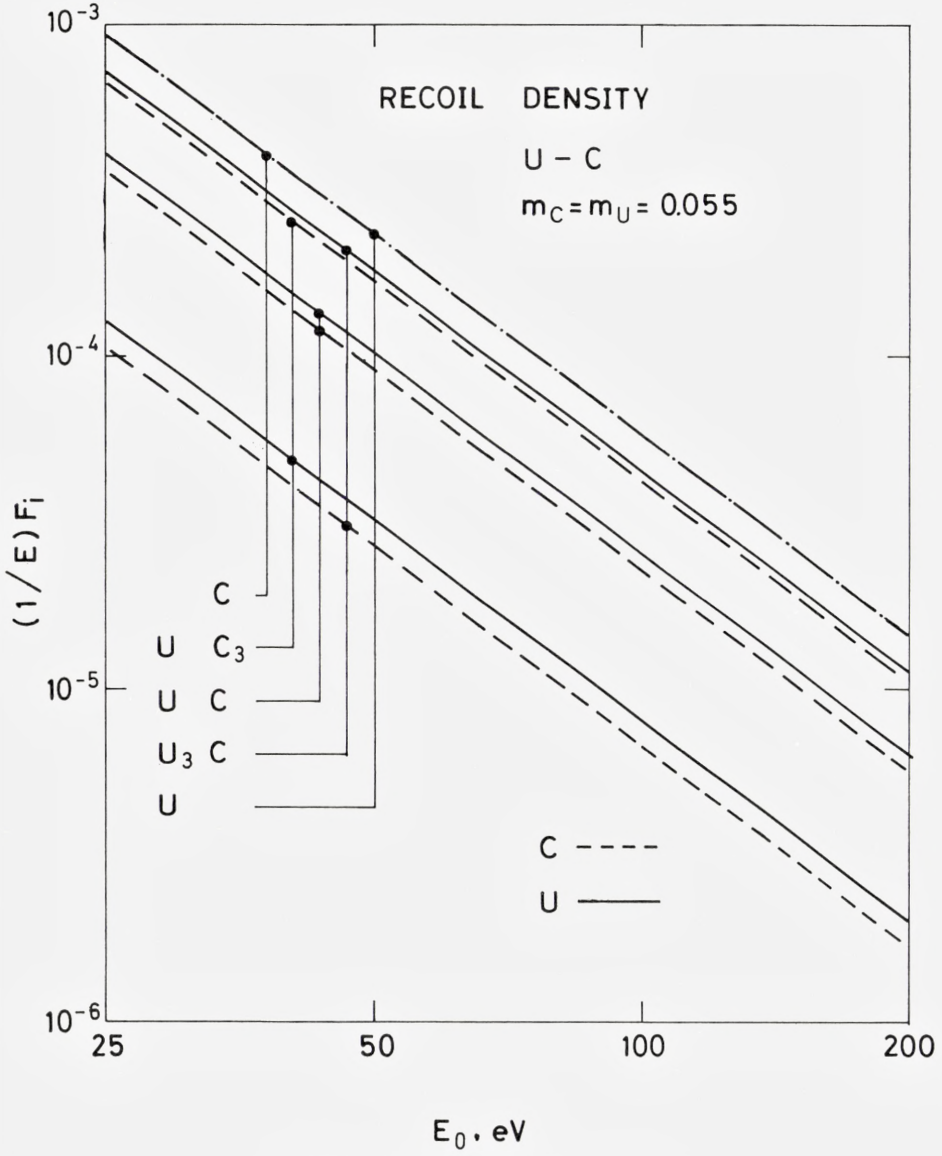


Fig. 3d. Uranium carbide, $m_C = m_U$.

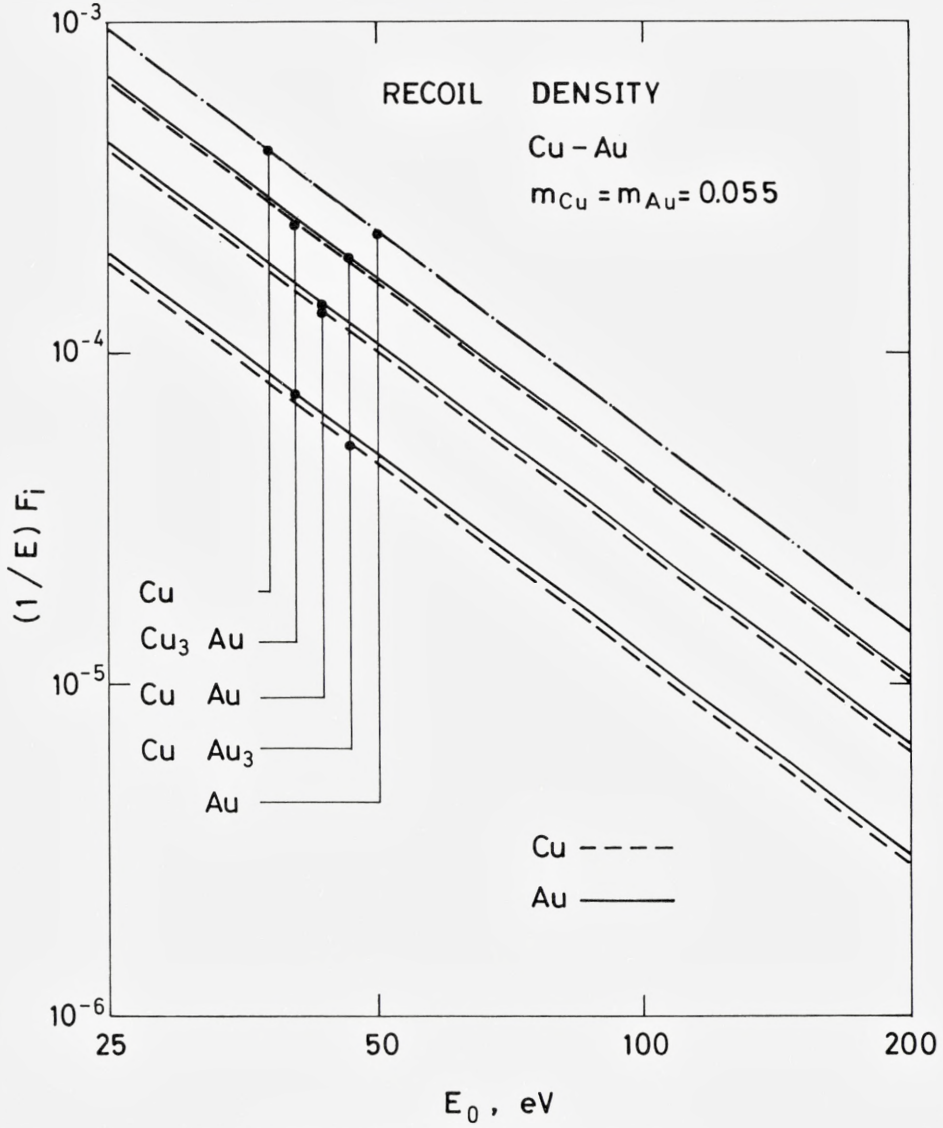


Fig. 3e. Copper-gold alloy, $m_{Cu} = m_{Au}$.

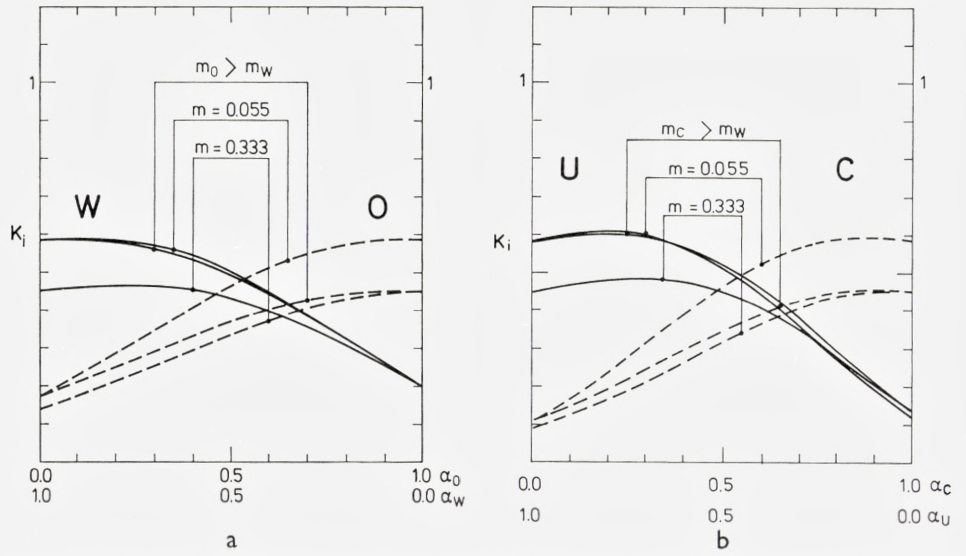


Fig. 4. Displacement efficiencies $K_1$ and $K_2$, eq. (33), of the two constituents of three binary compounds, as a function of concentration. As in fig. 2, three combinations of scattering parameters $m_1$ and $m_2$ were used. Full-drawn and stipled lines refer to the heavy and light constituent, respectively. Stoichiometric behaviour would correspond to straight horizontal lines.

Fig. 4a. Tungsten oxide. The two curves with $m_O > m_W$ are presumed to come closest to reality.
Fig. 4b. Uranium carbide. The two curves with $m_O > m_W$ are presumed to come closest to reality.

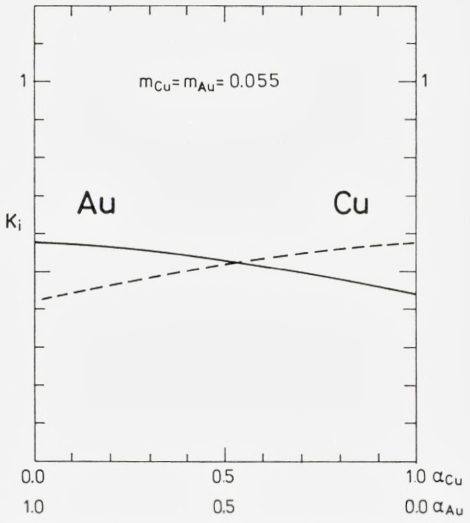


Fig. 4c. Copper-gold alloy. Only the two curves with $m_{Cu} = m_{Au}$ have been included.

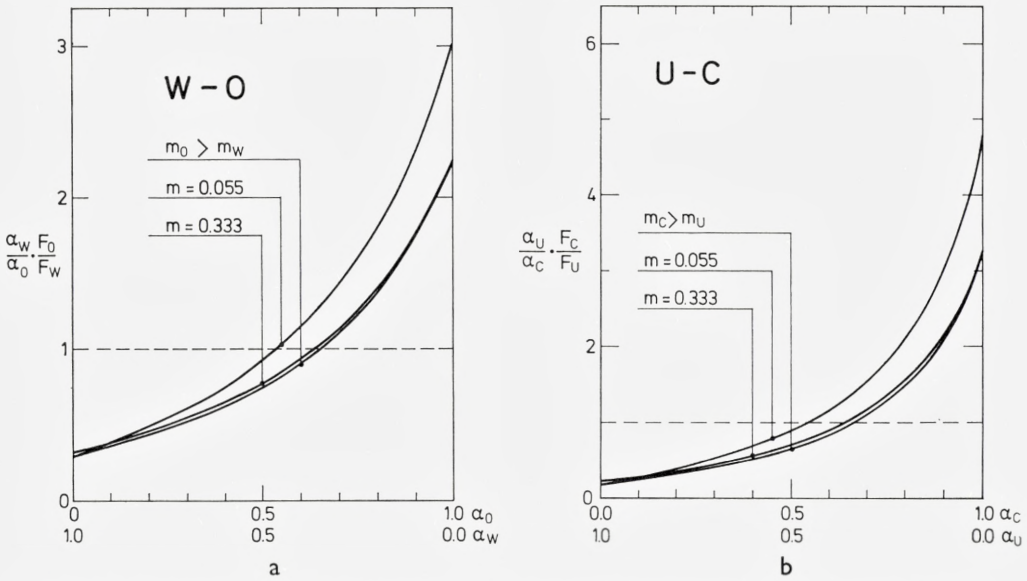


Fig. 5. Ratio of recoil densities of the constituents in three binary compounds, normalized so that stoichiometric behaviour would correspond to the dashed horizontal line. As in fig. 2, three combinations of scattering parameters $m_1$ and $m_2$ were used. Note the different scale in fig. 5b.

Fig. 5a. Tungsten oxide.
Fig. 5b. Uranium carbide.

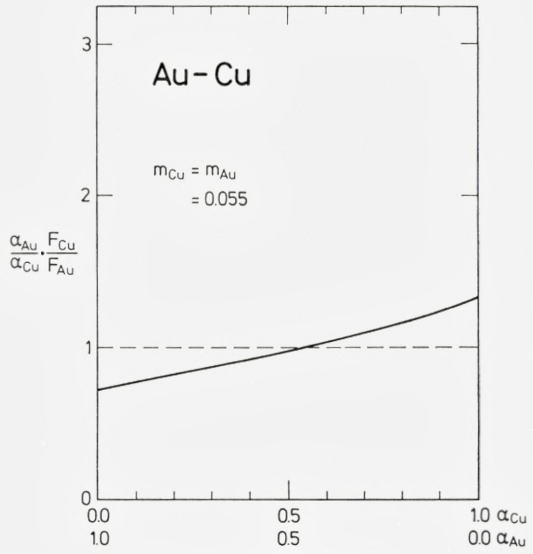


Fig. 5c. Copper-gold alloy.

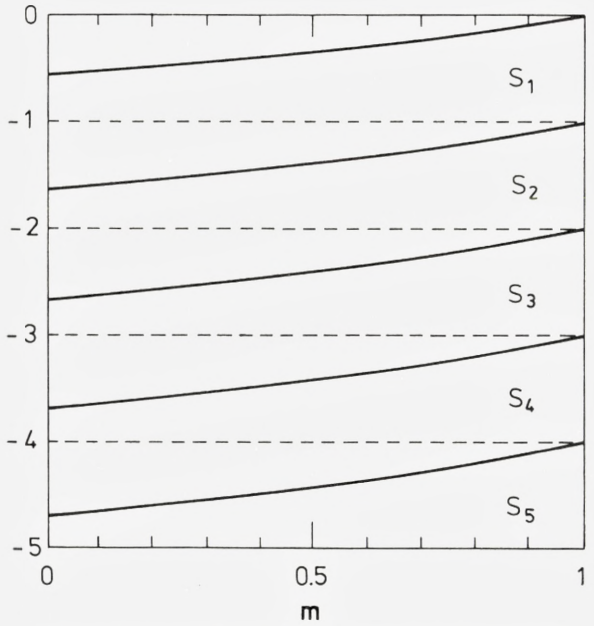


Fig. 6. The poles $s_i$ of the Laplace transform $\tilde{G}(s)$ for a monatomic medium, as a function of $m$. The principal pole at $s^{(0)} = 1$ has been omitted.

## 7. Range of Validity of the Asymptotic Solutions

We should like to estimate the range of validity of the asymptotic solutions (24) and (27). This is conveniently done by finding the correction terms in the asymptotic expansions, i.e. determining residues at subsequent poles of the Laplace Transforms, $\tilde{G}_{ij}(s)$ and $\tilde{F}_{ij}(s)$.

In the case of a monatomic target, this problem has been discussed in ref. 34, in which it is shown that the higher-order poles, $s^{(1)}, s^{(2)}, \ldots$, etc. obey the inequalities $-i + m < s^{(i)} < -i + 1$. The positions of the poles $s^{(1)}, \ldots, s^{(5)}$, in the monatomic case, for $0 < m < 1$, are plotted in fig. 6. No poles are found in the interval $0 \leq s < 1$. Therefore, for a monatomic target the asymptotic solution has a remarkably large range of validity[1)].

In the binary or polyatomic case, the situation is substantially more complicated because eq. (6) only holds for the principal term in the asymptotic expansion. The subsequent terms do not only depend on the target ($j$) but also explicitly on the projectile ($i$). For the sake of simplicity we restrict the discussion to binary targets and analyse the possibility of poles ocurring

between zero and $s = 1$. However, since eq. (6) is not generally valid we want to treat the problem for an arbitrary projectile, 3. This is conveniently done by considering a ternary target (sect. 5) with species 1, 2, 3, but $\alpha_3 = 0$. The complete set of solutions of eq. (12) is then given by :

$$\left.\begin{aligned}
\tilde{G}_{13} &= 0 \\
\tilde{G}_{23} &= 0 \\
\tilde{G}_{33} &= B_3/[\beta_{31}\varepsilon_{31} + \beta_{32}\varepsilon_{32}] \\
\tilde{G}_{12} &= B_2 \cdot \beta_{12}/D^{(2)} \\
\tilde{G}_{22} &= B_2 \cdot \{\beta_{11}(\varepsilon_{11}-1) + \beta_{12}\varepsilon_{12}\}/D^{(2)} \\
G_{32} &= B_2 \cdot \{\beta_{12}\beta_{31} + \beta_{32}[\beta_{11}(\varepsilon_{11}-1) + \beta_{12}\varepsilon_{12}]\}/\{D^{(2)}[\beta_{31}\varepsilon_{31} + \beta_{32}\varepsilon_{32}]\} \\
\tilde{G}_{11} &= B_1 \cdot \{\beta_{22}(\varepsilon_{22}-1) + \beta_{21}\varepsilon_{21}\}/D^{(2)} \\
\tilde{G}_{21} &= B_1 \cdot \beta_{21}/D^{(2)} \\
\tilde{G}_{31} &= B_1 \cdot \{\beta_{21}\beta_{32} + \beta_{31}[\beta_{22}(\varepsilon_{22}-1) + \beta_{21}\varepsilon_{21}]\}/\{D^{(2)}[\beta_{32}\varepsilon_{32} + \beta_{31}\varepsilon_{31}]\}
\end{aligned}\right\} \quad (37)$$

where we have used the notation of sect. 4. Of these equations, only the six lower ones are of interest here. Furthermore, because of symmetry we may concentrate on the lower three equations. The poles and residues of $\tilde{G}_{11}$, $\tilde{G}_{21}$ and $\tilde{G}_{31}$ determine the number of moving 1-atoms when particles of type 1, 2, or 3 impinge on a 1–2 compound. Writing $\tilde{G}_{31}$ in the form

$$\tilde{G}_{31} = \frac{\beta_{32}}{\beta_{32}\varepsilon_{32} + \beta_{31}\varepsilon_{31}}\tilde{G}_{21} + \frac{\beta_{31}}{\beta_{32}\varepsilon_{32} + \beta_{31}\varepsilon_{31}}\tilde{G}_{11} \quad (38)$$

facilitates the discussion.

From eq. (13a) it follows that $|\beta_{ik}| = \infty$ for $s = m_k$; otherwise $\beta_{ik}$ is finite and nonzero. According to (13b), the product $\beta_{ik}\varepsilon_{ik}$ is zero for $s = 0$, positive for $s > 0$ and negative for $s < 0$. Therefore, poles of $\tilde{G}_{31}$ may only occur at

(i) $s = 0$,
(ii) $s = m_1$ or $m_2$, and
(iii) the poles of $\tilde{G}_{11}$ and $\tilde{G}_{21}$.

For $s = 0$, insertion of eqs. (13a) and (13b) into (37) shows that $\tilde{G}_{11}$ and $\tilde{G}_{21}$ have finite values at this point; $\tilde{G}_{31}$ has a pole at zero because of the vanishing factor $\beta_{32}\varepsilon_{32} + \beta_{31}\varepsilon_{31}$ in the denominator.

The occurrence of poles at $s = m_1$ or $m_2$ depends on whether or not some (or all) of the parameters $m_1$, $m_2$, and $m_3$ are identical. It can happen that $\tilde{G}_{31}$ has a pole here, but not $\tilde{G}_{11}$ or $\tilde{G}_{21}$.

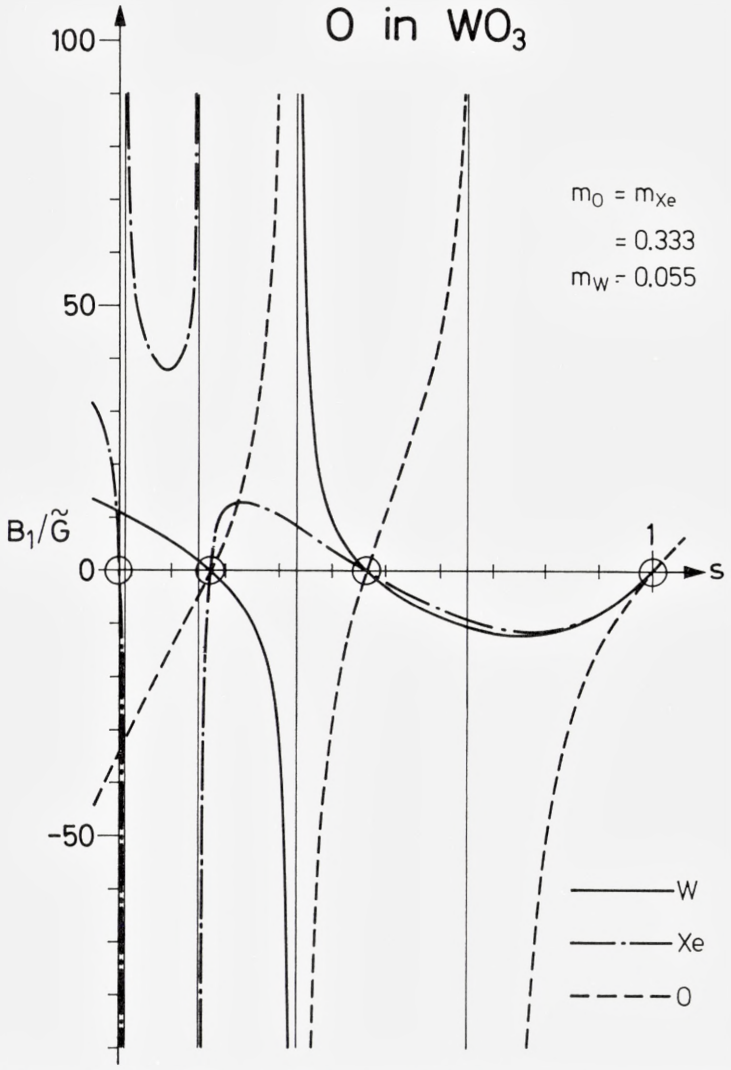


Fig. 7. Deviation of the slowing-down density $G_{ij}(E,E_0)$ from asymptotic behaviour. We plot reciprocal Laplace transforms $\tilde{G}_{11}$, $\tilde{G}_{21}$, and $\tilde{G}_{31}$ versus $s$. For details see text.

Fig. 7a. Moving oxygen atoms in $WO_3$

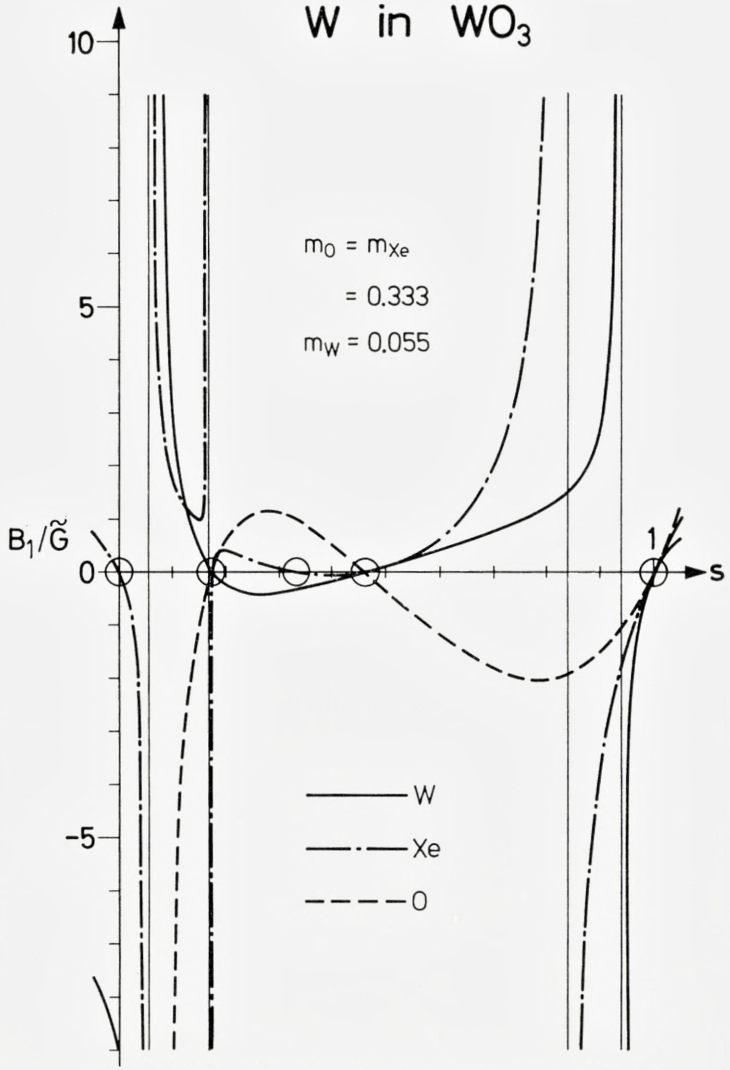


Fig. 7b. Moving tungsten atoms in $WO_3$.

The number and distribution of poles in the remaining part of the interval will depend on the parameters $\alpha_i$, $C_{ik}$, and $m_i$.

We have analysed numerically the case of a *W-O* compound bombarded with *W*, *O* and *Xe*. The positions and residues of the poles of $\tilde{G}_{11}$, $\tilde{G}_{21}$ and $\tilde{G}_{31}$ were determined, and their variation with concentration and choice of scattering parameters was investigated. Since the parameters are chosen so as to give a good description at low spectral energies, i.e. near $s = 1$, caution is required in drawing detailed physical conclusions from the correction terms to asymptotic behaviour.

An example is given in fig. 7a and b. For clarity, we have plotted the *reciprocal* values of $\tilde{G}_{11}$, $\tilde{G}_{21}$ and $\tilde{G}_{31}$ versus $s$, so that the poles of the $\tilde{G}$-functions show up as zeros, and the residues may be determined from the inverse *slope* of the $1/\tilde{G}$ – curve.

Fig. 7a shows the $1/\tilde{G}$ – functions for oxygen in a $WO_3$ target bombarded with oxygen, tungsten, or xenon, corresponding to $\tilde{G}_{11}$, $\tilde{G}_{21}$ or $\tilde{G}_{31}$, respectively. We first note that all three curves pass through $s = 1$ with identical slopes, as it should be expected from the results of sect. 3. Second, we notice that $1/\tilde{G}_{31}$ has the expected zero at $s = 0$, and the other two curves do not.

Two additional zeros occur at $s_2 \sim 0.17$ and $s_1 \sim 0.46$; these are common for all three curves. Thus, the second term in the asymptotic expansion varies approximately as $\sqrt{E/E_0}$ in all three cases. As may be seen from the figure, the residues at the second pole $s_1$ are comparable in magnitude to the residuum at $s = 1$.

Fig. 7b shows the corresponding curves for tungsten in $WO_3$, bombarded with tungsten ($\tilde{G}_{11}$), oxygen ($\tilde{G}_{21}$) or xenon ($\tilde{G}_{31}$). A very similar behaviour is observed, except that an additional zero occurs at $s = 0.333$ for $1/\tilde{G}_{31}$. Again, we observe that the second term in the expansion varies approximately as $\sqrt{E/E_0}$.

We conclude that the occurence of poles in the interval between zero and one narrows the range of validity of the asymptotic solution as compared to the monatomic case. As a rule-of-thumb the second term varies approximately as $\sqrt{E/E_0}$ as a function of energy.

## 8. Discussion

The major uncertain quantity entering the theory is the constant $C$ in the power cross section (9), in particular its value and mass dependence for $m < 1/4$, eq. (10b). Therefore, the results presented in fig. 1 for the slowing-down density can at most be considered qualitative. The other graphs, in particular figs. 2 and 4, show the slowing-down and recoil densities in a suitably normalized form so that the inherent error is minimized.

Consider the recoil density first, and its connection with the number of displaced atoms. Previous work in this field[21-23] concentrated on the *total* number of displacements created in a compound target by a primary particle. The displacement model of KINCHIN & PEASE[36] was usually adopted as well as a strongly simplified model for the scattering cross sections. BARODY[21] in particular assumed a fixed concentration, $\alpha_1 = \alpha_2 = \frac{1}{2}$. The main uncertainty was the displacement model which, for a binary target, contains at least four, perhaps six, essentially unknown parameters, i.e. two displacement thresholds, two replacement energies and, perhaps, two lattice binding energies. In most applications, the displacement and replacement energies were all set equal ($''=E_d''$), and the binding energies were either ignored or set equal $E_d$, too.

In the present calculations, we allowed for more realistic scattering cross sections, in particular for different energy dependences of the various cross sections involved. Except for appendix B we ignored binding energies, but eliminate a substantial part of the remaining uncertainty by plotting individual displacement efficiencies rather than defect numbers.

Fig. 4b shows that, for a uranium target with a few per cent alloyed carbon, the displacement efficiency of uranium atoms is six times as great as that of carbon atoms. In addition, when the carbon content increases from 0 to 40 per cent, the displacement efficiency for uranium remains essentially unchanged while the one for carbon increases by a factor of three, approximately linear with concentration. To our knowledge, such pronounced deviations from stoichiometric behaviour have not been predicted previously.

We are not aware of any experimental results that could be analysed directly in terms of a graph like fig. 4. Experiments to check these predictions (e.g. by channeling[37]) seem most promising when dealing with low, but varying concentration of one of the two species, since then the displacement threshold energies may be considered with reasonable confidence to be independent of concentration.

Obviously, fig. 4 predicts a pronounced difference in the behaviour of *dopant atoms* under irradiation between the case of bombarding electrons (where single defects dominate) and bombarding heavy ions or fast neutrons (where displacement cascades dominate).

Let us now go over to sputtering. According to ref. 28, the flux of sputtered atoms is determined by

i) the slowing-down density,
ii) the spatial distribution of deposited energy,
iii) the surface binding energy.

The two key problems in the sputtering of compound targets are

a) how is the total sputtering yield related to the sputtering yields of the respective pure targets, and
b) what is the composition of the sputtered material.

We have to note that any deviation from stoichiometric sputtering will cause a change in composition of the remaining target material, such that the target is no longer homogeneous. Homogeneity, however, is a vital assumption entering our basic equations. Thus, the present theory can at most be applied to low-dose sputtering experiments, i.e., experiments involving sputtering of, say, one monolayer of target atoms. Such experiments have been performed on pure metallic targets (e.g. ANDERSEN & BAY[13]) but, with one exception (see below) not on compound targets. The following considerations will, therefore, be kept brief and qualitative.

It is appropriate to distinguish between sputtering experiments performed at low and high bombarding energy, the former category referring to energies around or below 1 keV. Pronounced depletion of surface layers due to preferential sputtering has been reported in low-energy sputtering experiments (e.g. ASADA et al.[4]), ANDERSON[7]), TARNG et al. [9]). Because of the small penetration depth of low-energy ions, only a very shallow surface layer can be involved in the sputtering process proper. The occurrence of a massive depleted layer is, therefore, indicative of a competing migrational process. Such a process may also be a disturbing factor in high-energy sputtering experiments, and its influence needs to be checked by, e.g., variation of the target temperature during bombardment.

A number of higher-energy sputtering experiments dealt with the $Cu_3Au$ system[4–6, 8]). In high-dose experiments a gold-rich surface layer was observed[5, 6]). However, quantitative data on sputtering yields were only determined by OGAR et al.[8]). No bombardment doses were given, but since the sputtered

material was detected by neutron activation, one may assume that only few atomic layers were removed. The copper:gold sputtering ratio for $Ar^+$ and $Hg^+$ bombardment in the 10 keV region was observed to be slightly smaller than 3:1. The authors proposed preferred migration of gold atoms to the surface as an explanation. Since the observed deviation from stoichiometry is rather small ($\lesssim 10\ \%$) it does not appear feasible to make a definite statement on the actual source of nonstoichiometry. The slowing-down densities excluding bulk binding forces behave in such a way that preferential motion of copper atoms would be predicted (eq. 25b). However, inclusion of binding forces produces a shift in the right direction, the magnitude being uncertain (appendix B). Inclusion of, e.g., focused collision sequences in the sputtering mechanism would seem to enhance the contribution of copper atoms rather than decrease it. Finally, if gold atoms should migrate indeed preferentially, one might also have to consider the possibility of a lower surface binding energy of gold atoms.

Ogar et al. also determined absolute partial sputtering yields for copper and gold atoms, respectively. They report a partial sputtering yield for copper from the $Cu_3Au$ alloy that is about twice as large as the sputtering yield of pure copper under equivalent bombardment conditions. It follows from fig. 2c that such a pronounced effect cannot originate in a drastic change of the slowing-down density as compared to the pure target. Neither does it appear feasible that the surface binding energy of copper atoms differs by a factor of two from the one valid for a pure copper target. We assert the change in sputtering yield to be essentially due to the different spatial distribution of deposited energy. Indeed, alloying heavy gold atoms to a copper target causes a pronounced decrease in ion penetration due to increased importance of large-angle scattering[1, 20] and, therefore, increased energy deposition at the target surface. A quantitative evaluation is not given here since the measurements of Ogar et al. were done on $Cu_3Au$ single crystals while existing calculations refer to random targets.

Pronounced deviations are expected from stoichiometric sputtering in metallic alloys of very different masses. Figs. 2a and 2b indicate that the fluxes of both the heavy and the light constituent *increase* as compared to the pure targets, in terms of the respective concentrations. The flux of *heavy* atoms increases most pronouncedly. However, the ratio of fluxes at any given concentration behaves in a more complicated manner. Figs. 1a and 1c show that there may be different energy dependences, and comparing, e.g., figs. 1a and 1b, one may notice that preferential sputtering of the heavy constituent may be predicted from fig. 1a, and the light one from fig. 1b. In case

of $WO_3$, our preference of the choice of potential constants is such as to predict preferential sputtering of $W$. This preference is, however, not so strong as the corresponding one with the uranium carbide system.

Systematic investigations of the sputtering of oxides[10] revealed preferential sputtering of oxygen in many cases. Consistently, oxygen happened to be the lighter constituent. The analysis indicated a contribution of chemical and local-heating effects. From the point of view of the present investigation, it would be of considerable interest to have similar experimental results taken at low bombardment doses.

## Acknowledgements

We should like to thank H. H. Andersen, R. Behrisch, and J.W. Mayer for clarifying discussions, and H. Dreyer Nielsen and his crew for careful preparation of the drawings.

## Appendix A

We want to show that the determinant of the system of equations (12) has no zero for $s > 1$. First, it follows from eqs. (13) and (14) that $\beta_{ik} > 0$ and $\varepsilon_{ik} > 1$ for $s > 1$.

Now, let $\beta = (\beta_{ik})$ be an arbitrary $n \times n$ matrix with positive elements, $\beta_{ik} > 0$, and let $\varepsilon_{ik}$, where $i, k = 1, \ldots, n$ be a set of $n^2$ arbitrary elements. We define another $n \times n$ matrix $\Delta = (\Delta_{ik})$ by

$$\Delta_{ik} = \delta_{ik} \cdot \sum_j \beta_{ij} \varepsilon_{ij}$$

and will now prove the following theorem for the determinant

$$det\,(\Delta - \beta) =$$

$$= \begin{vmatrix} \beta_{11}(\varepsilon_{11} - 1) + \beta_{12}\varepsilon_{12} + \ldots + \beta_{1n}\varepsilon_{1n} & \ldots & -\beta_{1n} \\ -\beta_{21} & \beta_{22}(\varepsilon_{22} - 1) + \beta_{21}\varepsilon_{21} + \ldots + \beta_{2n}\varepsilon_{2n} \quad \ldots & -\beta_{2n} \\ \cdot & \cdot \quad \cdot & \cdot \\ \cdot & \cdot \quad \cdot & \cdot \\ \cdot & \cdot \quad \cdot & \cdot \\ -\beta_{n1} & -\beta_{n2} \ldots \beta_{nn}(\varepsilon_{nn} - 1 + \beta_{n1}\varepsilon_{n1} + \ldots + \beta_{n\,n-1}\varepsilon_{n\,n-1} \end{vmatrix}$$

*If all elements* $\varepsilon_{ik} > 1$ *then* $det\,(\Delta - \beta) > 0$.

The theorem is proved by induction, increasing the dimension of the matrix from $n$–1 to $n$.

i) The case $n = 1$ is trivial: $det(\Delta - \beta) = \beta_{11}(\varepsilon_{11} - 1)$

Since $\beta_{11} > 0$ and $\varepsilon_{11} > 1$, $det(\Delta - \beta) > 0$.

ii) The general step $n - 1 \to n$: We first note that if all $\varepsilon_{ik} = 1$ then $det(\Delta - \beta) = 0$, because the sum of the elements in each row is zero. It is, therefore, sufficient to show that for $\varepsilon_{ik} > 1$, $det(\Delta - \beta)$ is a strictly increasing function of all the $\varepsilon_{ik}$, or:

$$\frac{\partial}{\partial \varepsilon_{ik}} det(\Delta - \beta) > 0 \quad \text{for all} \quad \varepsilon_{i'k'} > 1.$$

For reasons of symmetry it is sufficient to consider the case $i = 1$. We get by differentation:

$$\frac{\partial}{\partial \varepsilon_{1k}} \begin{vmatrix} \beta_{11}(\varepsilon_{11} - 1) + \beta_{12}\varepsilon_{12} + \ldots + \beta_{1n}\varepsilon_{1n} & -\beta_{12} & \ldots & -\beta_{1n} \\ -\beta_{21} & \beta_{22}(\varepsilon_{22} - 1) + \beta_{21}\varepsilon_{21} + \ldots + \beta_{2n}\varepsilon_{2n} & \ldots & -\beta_{2n} \\ \cdot & \cdot \quad \cdot & & \cdot \\ \cdot & \cdot & & \cdot \\ \cdot & \cdot & & \cdot \\ -\beta_{n1} & -\beta_{n2} & \beta_{nn}(\varepsilon_{nn} - 1) + \beta_{n1}\varepsilon_{n1} + \ldots + \beta_{nn-1}\varepsilon_{nn-1} & \end{vmatrix}$$

$$= \begin{vmatrix} \beta_{1k} & -\beta_{12} & \ldots & -\beta_{1n} \\ 0 & \beta_{22}(\varepsilon_{22} - 1) + \beta_{21}\varepsilon_{21} + \ldots + \beta_{2n}\varepsilon_{2n} & \ldots & -\beta_{2n} \\ \cdot & \cdot \quad \cdot & & \cdot \\ \cdot & \cdot & & \cdot \\ \cdot & \cdot & & \cdot \\ 0 & -\beta_{n2} & \beta_{nn}(\varepsilon_{nn} - 1) + \beta_{n1}\varepsilon_{n1} + \ldots + \beta_{nn-1}\varepsilon_{nn-1} & \end{vmatrix}$$

$$= \beta_{1k} \begin{vmatrix} \beta_{22}(\varepsilon_{22} - 1) + \beta_{21}\varepsilon_{21} + \ldots + \beta_{2n}\varepsilon_{2n} & \ldots & -\beta_{2n} \\ \cdot & & \cdot \\ \cdot & & \cdot \\ \cdot & & \cdot \\ -\beta_{n2} & \ldots & \beta_{nn}(\varepsilon_{nn} - 1) + \beta_{n1}\varepsilon_{n1} + \ldots + \beta_{nn-1}\varepsilon_{nn-1} \end{vmatrix}$$

The last determinant is a $(n–1) \times (n–1)$ determinant, but in a form not suited for direct induction. However, the matrix can be brought into a suitable form by defining new quantities $\tilde{\varepsilon}_{ii}$ and $\tilde{\beta}_{ii}$ so that for $i = 2, \ldots, n$

1) $\beta_{ii}(\varepsilon_{ii} - 1) + \beta_{i_1}\varepsilon_{i_1} = \tilde{\beta}_{ii}(\tilde{\varepsilon}_{ii} - 1)$
2) $\tilde{\beta}_{ii} > 0$
3) $\tilde{\varepsilon}_{ii} > 1$

which is evidently possible. For $i \neq k$ we define $\tilde{\varepsilon}_{ik} = \varepsilon_{ik}$ and $\tilde{\beta}_{ik} = \beta_{ik}$. Then

$$\frac{\partial}{\partial\, \varepsilon_{1k}}\, det\, (\Delta - \beta) =$$

$$\beta_{1k} \begin{vmatrix} \tilde{\beta}_{22}(\tilde{\varepsilon}_{22}-1) + \tilde{\beta}_{23}\,\tilde{\varepsilon}_{23} + \ldots + \tilde{\beta}_{2n}\,\tilde{\varepsilon}_{2n} & \ldots & -\tilde{\beta}_{2n} \\ \cdot & \cdot & \cdot \\ \cdot & \cdot & \cdot \\ \cdot & \cdot & \cdot \\ -\tilde{\beta}_{n2} \ldots \tilde{\beta}_{nn}(\tilde{\varepsilon}_{nn} - 1) + \tilde{\beta}_{n2}\,\tilde{\varepsilon}_{n2} + & \ldots & +\tilde{\beta}_{nn-1}\,\tilde{\varepsilon}_{nn-1} \end{vmatrix}$$

Here $\beta_{1k} > 0$ and the determinant is positive too, since it is a $(n-1) \times (n-1)$-determinant of the type considered.

This proves the theorem.

## Appendix B: Effect of Atomic Binding

We want to indicate briefly the effect of atomic binding on energy dissipation. Some results of similar calculations for monatomic targets have been reported previously[1, 27, 28], yet without derivation. A detailed discussion will be given in a forthcoming paper[35], but the main steps – for a polyatomic medium – will be sketched here.

We only consider the slowing-down density $G_{ij}$. If we assume that an atom of type $i$ loses a binding energy $V_i$ upon recoiling from its rest position, the only necessary change in eq. (2a) is replacement of the recoil term $G_{kj}(T, E_0)$ by

$$G_{kj}(T - V_k, E_0), \tag{B 1}$$

while the boundary condition (4) remains unchanged.

In the evaluation for power scattering, eq. (10), the Laplace transformation is carried out conveniently by means of expansion in powers of $V_k/E_0$. Then, the recoil term $\tilde{G}_{kj}(s)$ in eq. (12) is replaced by the expression

$$\sum_{\nu=0}^{\infty} \binom{-s-1}{\nu} (V_k/E_0)^{\nu}\, \tilde{G}_{kj}(s + \nu). \tag{B 2}$$

The resulting system of equations can be solved by perturbation expansion,

$$\tilde{G}_{kj}(s) = \sum_{\nu} \tilde{G}_{kj}^{(\nu)}(s), \tag{B 3}$$

where $\tilde{G}_{kj}^{(\nu)}(s)$ contains $\nu$ factors of the set $(V_1, V_2, \ldots)$. The zero-order term $\tilde{G}_{kj}^{(0)}(s)$ is identical with the one calculated in sect. 3, and the first-order term follows from the equations

$$\left.\begin{aligned} &\tilde{G}_{ij}^{(1)}(s) \sum_k \beta_{ik}(s)\, \varepsilon_{ik}(s) - \sum_k \beta_{ik}(s)\, \tilde{G}_{kj}^{(1)}(s) = \\ &= -(s+1) \sum_k (V_k/E_0)\, \beta_{ik}(s)\, \tilde{G}_{kj}^{(0)}(s+1). \end{aligned}\right\} \tag{B 4}$$

Only the inhomogeneity on the right-hand side differs from eq. (12). In particular, the highest poles of $\tilde{G}_{ij}^{(1)}(s)$ are determined by the zeros of the determinant $D(s)$, just as those of $\tilde{G}_{ij}^{(0)}(s)$. The asymptotic solution $G_{ij}^{(1)}(E, E_0)$ for $E \gg E_0$ is, therefore, proportional to $E$, and the same is true for all higher orders $G_{ij}^{(\nu)}(E, E_0)$. Note especially that the term on the right-hand side of (B4) is regular for $s > m_i$. Then, with the notations of sect. 4, the asymptotic solutions ($s = 1$) of (B 4) in the binary case can be written in the form

$$\left.\begin{aligned} &G_{11}^{(1)}/G_{11}^{(0)} \sim G_{21}^{(1)}/G_{21}^{(0)} \sim \\ &\sim -(2/D^{(2)}(2)) \{(\beta_{11}(1) + \beta_{12}(1))(V_1/E_0) \times \\ &[(\beta_{22}(2) - 1)\beta_{22}(2) + \beta_{21}(2)\beta_{21}(2)] + (\beta_{12}(1)/\beta_{21}(1)) \times \\ &(\beta_{21}(1) + \beta_{22}(1))\,(V_2/E_0)\,\beta_{21}(2)\}, \end{aligned}\right\} \tag{B 5}$$

where $D^{(2)}(s)$, $\varepsilon_{ik}(s)$, and $\beta_{ik}(s)$ are defined in eqs. (13a, b) and (22a).

In case of a monatomic medium (i.e. either for $M_1 = M_2$ and arbitrary $\alpha_1$ or for $\alpha_1 = 1$ and arbitrary $M_2/M_1$), eq. (B5) reduces to the previously quoted result[27, 28]

$$G_{11}^{(1)}/G_{11}^{(0)} \sim -(2 - m_1)\, V_1/E_0 \qquad \text{for } M_1 = M_2 \tag{B 6}$$

as it should be.

We have evaluated eq. (B5) numerically for the tungsten-oxygen system. We write (B5) in the form

$$G_{11}^{(1)}/G_{11}^{(0)} \sim G_{21}^{(1)}/G_{21}^{(0)} \sim -R_1(V_1/E_0) - R_2(V_2/E_0) \tag{B 7}$$

and plot $R_1$ and $R_2$ in fig. 8a for oxygen and in fig. 8b for tungsten. It is seen that $R_2$ is vanishingly small in both cases. $R_1$ has its greatest value for the pure materials and drops off rapidly with increasing concentration of the alloyed impurity. This is particularly so in case of fig. 8b.

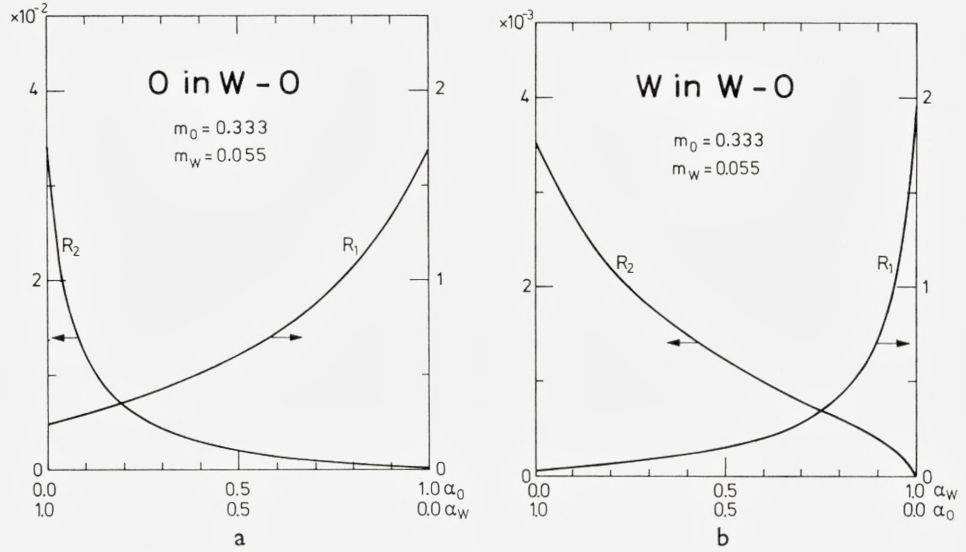


Fig. 8. First-order corrections to the slowing-down density due to atomic binding, defined in eq. (B7).

Fig. 8a. Oxygen in *W-O* compound (Index (1) refers to oxygen). Note the different scales for $R_1$ and $R_2$.

Fig. 8b. Tungsten in *W-O* compound (Index (1) refers to tungsten). Note the different scales for $R_1$ and $R_2$.

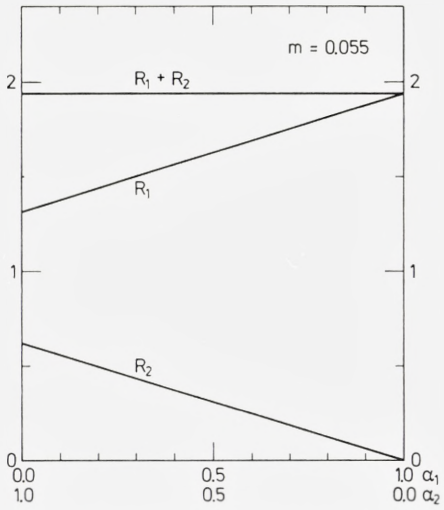


Fig. 8c. Equal-mass compound. Same scale for $R_1$ and $R_2$.

Figs. 8a and 8b indicate that the dominating contribution to eq. (B7) is due to the fact that moving atoms cannot be observed at their initial recoil energy, but at most at the recoil energy minus their respective binding energy. The loss of energy during recoiling of former generations of atoms in the cascade appears to be of minor significance for the slowing-down density.

Fig. 8c shows a similar graph for an equal-mass compound. Because of the possibility of complete exchange of energy between collision partners 1 and 2, the coefficient $R_2$ in (B7) becomes significant, though still smaller than $R_1$.

Figs. 8a–c are representative for most situations of practical interest. We conclude that the influence of atomic binding on the slowing-down density is essential only for nearly pure materials in case of very different masses, and roughly independent of concentration in case of nearly equal masses. The correction cannot exceed that of the pure material, except when the binding energies themselves undergo substantial changes due to the presence of the alloyed material.

It follows from (B7) that the influence of atomic binding is most pronounced near threshold ($E_0 \sim V_1$). In radiation damage one often meets a situation where $E_{d,i} \gg V_i$, so that the correction is unappreciable at all energies of practical interest. Therefore, we only evaluated the correction in case of the slowing-down density. In sputtering, the threshold energy of interest is the surface binding energy, which may well be comparable to $V_1$, so that a correction may be necessary in the lowest parts of the spectrum. Figs. 8a, b indicate that for the *W-O* system at intermediate concentrations, the correction is larger for oxygen than for tungsten. Since the sign is negative (eq. B7), the corrections tend to move the deviation from stoichiometric behaviour towards dominance of the *heavy* species in the particle flux.

## References


0. N. Andersen, P. Sigmund, Atomic Collisions in Solids (B. Appleton, S. Datz, & C.D. Moak, Eds.), Plenum Press, New York (1974).
1. P. Sigmund, Rev. Roum. Phys. **17**, 823, 969, 1079 (1972).
2. J. Lindhard, V. Nielsen, M. Scharff, P. V. Thomsen, Mat. Fys. Medd. Dan. Vid. Selsk. **33**, no. 10 (1963).
3. J. Lindhard, ibid. **34**, no. 14 (1965).
4. T. Asada, K. Quasebarth, Z. Phys. Chem. *A***143**, 435 (1929).
5. G. J. Ogilvie, Aust. J. Phys. **13**, 402 (1959).
6. E. Gillam, J. Phys. Chem. Sol. **11**, 55 (1959).
7. G. S. Anderson, J. Appl. Phys. **40**, 2884 (1969).
8. W. T. Ogar, N. T. Olson, H. P. Smith, J. Appl. Phys. **40**, 4997 (1969).
9. M. L. Tarng, G. K. Wehner, J. Appl. Phys. **42**, 2449 (1971); ibid. **43**, 2268 (1972).
10. R. Kelly, N. Q. Lam, Rad. Eff. **19**, 39 (1973).
11. S. D. Dahlgren, E. D. McClanahan, J. Appl. Phys. **43**, 1514 (1972).
12. L. Q. Nghi, R. Kelly, Can. J. Phys. **48**, 137 (1970).
13. H. H. Andersen, H. Bay, Rad. Eff. **13**, 67 (1972).
14. G. K. Wehner, D. J. Hajicek, J. Appl. Phys. **42**, 1145 (1971).
15. P. Sigmund, J. Mater. Sci. **8**, 1545 (1973).
16. J. Farren, W. J. Scaife, AERE Harwell Report, R5717 (1968).
17. S. P. Wolsky, E. J. Zdanuk, D. Shooter, Surf. Sci. **1**, 110 (1964).
18. H. E. Schiøtt, Can. J. Phys. **46**, 449 (1968).
19. J. B. Sanders, Can. J. Phys. **46**, 455 (1968).
20. K. B. Winterbon, P. Sigmund, J. B. Sanders, Mat. Fys. Medd. Dan. Vid. Selsk. **37**, no. 14 (1970).
21. E. M. Baroody, Phys. Rev. **112**, 1571 (1958).
22. R. M. Felder, J. Phys. Chem. Sol. **28**, 1383 (1967).
23. M. D. Kostin, J. Appl. Phys. **37**, 3801 (1966).
24. K. B. Winterbon, Rad. Eff. **13**, 215 (1972).
25. K. B. Winterbon, J. Nucl. Sci & Eng. **53**, 261 (1974).
26. J. Kistemaker, F. J. de Heer, J. Sanders, C. Snoek, *in* Radiation Research 1966; p. 68; North-Holland Publ. Comp., Amsterdam (1967).
27. P. Sigmund, Appl. Phys. Lett. **14**, 114 (1969).
28. P. Sigmund, Phys. Rev. **184**, 383 (1969).
29. J. Lindhard, V. Nielsen, Mat. Fys. Medd. Dan. Vid. Selsk. **38**, no. 9 (1971).
30. J. Lindhard, P. V. Thomsen, *in* Radiation Damage in Solids. I., IAEA, Vienna, p. 65 (1962).

31. J. Lindhard, V. Nielsen, M. Scharff, Mat. Fys. Medd. Dan. Vid. Selsk. **36**, no. 10 (1968).
32. H. H. Andersen, P. Sigmund, Nucl. Inst. Meth. **38**, 238 (1965); Danish A.E.C., Risö Report **103** (1965).
33. M. T. Robinson, Phil. Mag. **12**, 741 (1965).
34. P. Sigmund, Rad. Eff. **1**, 15 (1969).
35. P. Sigmund, Theory of Sputtering, II (to be published).
36. G. H. Kinchin, R. S. Pease, Rep. Prog. Phys. **18**, 1 (1955).
37. J. W. Mayer, L. Eriksson, J. A. Davies, Ion Implantation in Semiconductors, Academic Press, New York (1970).

*Physical Laboratory II*
*H. C. Ørsted Institute*
*DK–2100Copenhagen Ø*

Indleveret til Selskabet den 29. oktober 1973.
Færdig fra trykkeriet den 12. september 1974.

G. SIDENIUS

# SYSTEMATIC STOPPING CROSS SECTION MEASUREMENTS WITH LOW ENERGY IONS IN GASES

Det Kongelige Danske Videnskabernes Selskab
Matematisk-fysiske Meddelelser **39**, 4


Kommissionær: Munksgaard
København 1974

## Synopsis

Systematic stopping cross sections were measured in Methane ($CH_4$) for particles with atomic number $Z_1 \leq 10$. The particle energy ranged from 0.6 up to 120 keV, which involves that for heavier particles the energy loss caused by the elastic scattering (nuclear stopping) dominates over the inelastic energy losses (electronic stopping). A definition of the different stopping parameters and an analysis of the possible systematic errors caused by the multiple scattering are given. The results of the measurements are compared with the theory of LINDHARD, SCHARFF and SCHIØTT.



Printed in Denmark
Bianco Lunos Bogtrykkeri A/S
ISBN 87 7304 034 7

## 1. Introduction

Even though the penetration of atomic particles into matter now has been studied for about half a century, further experimental investigations are strongly needed in the low energy part of the range in which the energy loss due to the elastic scattering equals or exceeds the inelastic energy losses.

The stopping due to the elastic scattering (in most literature called the nuclear stopping) was discussed by BOHR[1] in 1948. The BOHR theory was further developed by LINDHARD and SCHARFF[2] and by LINDHARD, SCHARFF and SCHIØTT[3] (in the following referred to as L.S.S.). They derived a universal curve for the nuclear stopping power by using the Thomas-Fermi model of the atom to determine the screening effect from the electrons on the nuclear Coulomb interaction potential between the colliding particles. Also using the Thomas-Fermi model LINDHARD and SCHARFF[2] developed a theory for the inelastic losses (the electronic stopping power) and found these to be proportional to the particle velocity, over the energy range in which the nuclear stopping is of importance.

In figure 1 is shown the theoretical universal curve for the nuclear stopping power $(d\varepsilon/d\varrho)_n$ together with a typical electronic stopping power curve $(d\varepsilon/d\varrho)_e$ and the resulting total stopping power curve $(d\varepsilon/d\varrho)_t$. The particle energy $E$ and the range $R$ are replaced by the dimensionless parameters $\varepsilon$ and $\varrho$ as defined in L.S.S.[3].

Systematic measurements of the pure electronic stopping power at higher $\varepsilon$-values, ORMROD and DUCKWORTH[4], ORMROD et al.[5], HVELPLUND[6] and HÖGBERG[7], have shown rather strong oscillations around the theoretically predicted values due to atomic shell effects.

An experimental test of the theory of the nuclear stopping in the energy range below the crossing of the nuclear- and electronic stopping power curves, i.e. $\varepsilon < 4$, is desirable, but until now very few such measurements exist. In 1963, with a gas cell with two small openings followed by an electrostatic energy analyser, very heavy particles with $\varepsilon$-values from 0.01 to 1 was studied

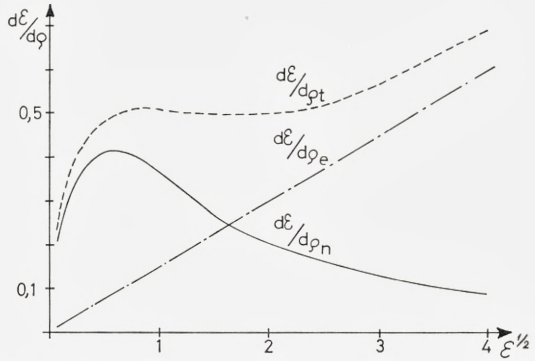


Fig. 1. Theoretical stopping power curves from LINDHARD, SCHARFF and SCHIØTT[3].

by SIDENIUS[8]. With time-of-flight method and $\alpha$-recoils the stopping in thin solid films was measured by ZAHN[9] in 1963, MARX[10] in 1966, POOLE et al.[11] in 1967 and HANCOCK et al.[12] in 1969; the method is very limited in particle- and energy range, but allows measurements with $\varepsilon$-values about 0.1. In 1971 the stopping of $3 < Z_1 < 18$ ions with 4.5 to 46 keV energy ($\varepsilon$-values from 0.7 to 21) was measured in carbon foils by HÖGBERG[7, 13].

However, in all these measurements a narrow acceptance angle of the detection system was used. The measured stopping power is therefore what we shall call the stopping power in the forward direction, which in most cases differs from the total mean stopping power. It is therefore of importance to define as clearly as possible the various stopping data found from theory and experiment and to discuss the obtainable accuracy before the description of the present experiment.

## 2. Definition and Analysis of Stopping Parameters

The different parameters observable for a beam of particles penetrating a stopping layer will first be summarized. As stopping media only gases and amorphous solids are considered. The stopping layer shown in figure 2 is homogeneous matter with the molecular density $N_m$ and plane parallel surfaces separated by the distance d. Ideally the matter consists only of atoms of one element with the atomic number $Z_2$ and the mass number $M_2$, but in practice compound molecules must also be considered.

The incident particle beam is considered to be ideal, i.e. a parallel, monoenergetic, narrow beam entering the stopping medium perpendicular to the surface. The incoming particles have atomic number $Z_1$, mass number

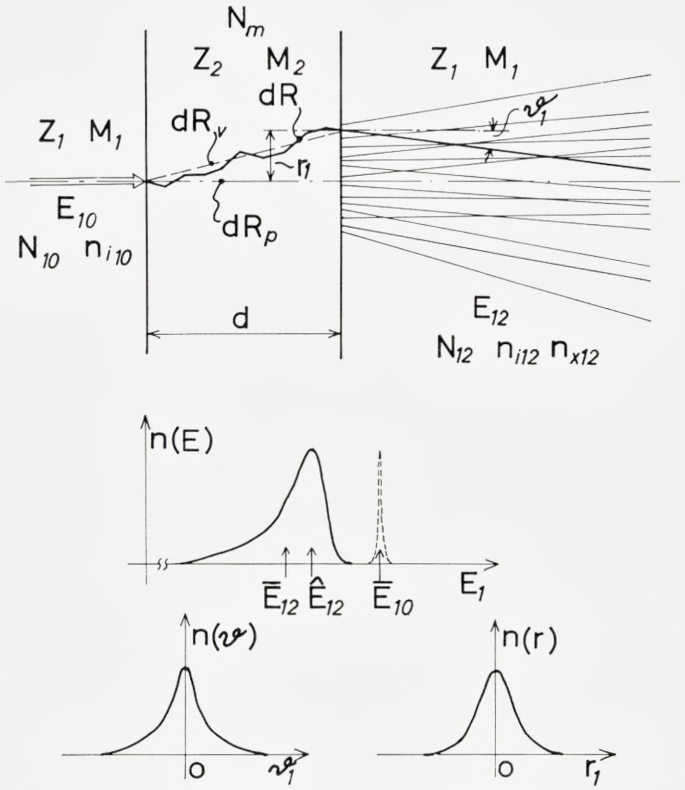


Fig. 2. Definition of stopping parameters.

$M_1$, and energy $E_{10}$, their number per unit time is $N_{10}$, and their charge state is $n_{i10}$.

The primary particles emerging from the stopping layer are well defined only in element and mass, $Z_1$ and $M_1$, and the number of particles leaving per unit time $N_{12}$, whereas the rest of the parameters are now described by distribution functions. In many cases these are non-Gaussian and non-symmetric, as shown in figure 2.

From the energy distribution $n(E_{12})$ one may derive, the mean energy $\bar{E}_{12}$, the most probable energy $\hat{E}_{12}$, and one or more parameters defining the shape of the distribution.

The multiple scattering, which is directly correlated to the nuclear stopping cross section, produces two phenomena: an angular deflection distribution $n(v_1)$ and a radial displacement distribution $n(r_1)$ in the emerging primary particles. As a rule, the radial displacement is measurable only

when the stopping element is a gas, whereas the angular deflection can be rather easily measured for a solid stopping element, but only with difficulty when the stopping element is gaseous.

Important information is contained in the relative abundances of the charges, $n_{i12}$ and excited states, $n_{x12}$ of the emerging primary particles. The study of these effects using beam foil spectroscopy[14] and beam gas spectroscopy[14] has become a growing field in the last few years.

Not shown in figure 2 is the secondary particle emission; from both the front and rear surfaces recoil target atoms and electrons will be ejected. These will be widely distributed in energy, angle, charge state, relative abundance, etc.

Important information about the slowing down process is contained in the ionization and excitation of the target atoms, effects which normally are observable only in a gaseous stopping element. For the present experimental technique the number of ionpairs created in the stopping layer per penetrating particle, $dN_i$, as well as the total number of ionpairs $N_i$ created along the whole range of the particle are especially important parameters.

Figure 2 also illustrates the definition of the different stopping lengths. $dR$ is the actual path length, $dR_v$ is the vector length defined as the linear distance between the entrance- and exit points of the particles, and $dR_p$ is the projected length as measured in the initial direction. For a plane parellel layer $dR_p$ is the same as the thickness $d$.

In the L.S.S. theory[3] the stopping power is defined as the average energy loss $dE$ per unit path length $dR$.

$$(dE/dR)_{th} = N_2 S = N_2 \int T d\sigma(T) \tag{1}$$

where $N_2$ is the number of scattering centers per unit volume and $S$ is the stopping cross section per scattering center. This is not a real cross section, but is the average energy loss per scattering center. $d\sigma(T)$ is the differential cross section for the energy transfer $T$, which may be both elastic and inelastic. Normally it is impossible to observe the path length $dR$; therefore, to define the experimental stopping power, either $dR_v$ or $dR_p$ will have to be used. $dR_p$ is the only stopping length, which can be measured for both a solid and a gaseous stopping layer. Hence the fundamental experimental stopping power is defined as

$$(dE/dR)_{tm} = \frac{dE_{tm}}{dR_p} \frac{E_{10} - \bar{E}_{12}}{dR_p} = \frac{E_{10} - \frac{1}{N_{12}} \sum_0^{N_{12}} E_{12}}{dR_p}. \tag{2}$$

This is the *total* mean stopping power, i.e. the energy analysis shall include all emerging primary particles, independent of their angle, radial displacement and charge state*.

If the energy analysis excludes some of the emerging primary particles, as hitherto always has been the case, a *fractional* mean stopping power is obtained

$$(dE/dR)_{fm} = \frac{dE_{fm}}{dR_p} = \frac{E_{10} - \frac{1}{N_f}\sum_0^{N_f} E_{12}}{Rd_p}. \qquad (3)$$

The most common fractionization is the exclusion in the energy analysis of all charge states except singly charged ions. If the stopping layer is much thicker than is needed to ensure charge equilibrium the charge fractionization should not be expected to introduce any significant error, even though ALLISON[15] has shown that there is a pronounced difference in the electronic stopping of neutral, singly or doubly charged particles.

In the case of a solid stopping layer a rather common fractionization is the exclusion of emerging particles with an angular deflection larger than a normally very small angle $\theta_{ac}$ determined by the acceptance angle of the energy analyser.

For a gaseous stopping layer the use of a small outlet opening excludes emerging particles with a radial displacement larger than the opening radius $r_0$; often a further exclusion follows due to the limited acceptance angle of the energy analyser. Here, it may be worthwhile to note that when $M_1/M_2$ is close to unity about 30 % of the nuclear stopping is caused by collisions with a deflection of the primary particle larger than 45 degrees!

If the measurement is performed in the forward direction with a small acceptance angle the measured energy loss is caused mostly by the electronic stopping. This has been utilized in measurements of the pure electronic stopping[4, 5, 6, 7]. However, for a test of the nuclear stopping theory it is an absolute requirement that the energy analysis incorporates all emerging primary particles. Only for very heavy particles stopped in a light gas ($M_1/M_2 > 100$) and a thick stopping layer is the fractionization effect negligible[8]. HÖGBERG[7, 13] has studied the influence of the target thickness and used it to determine what he calls the saturation value of the nuclear stopping, but it still is the stopping in the forward direction and all large angle scattered particles are excluded.

* More correctly, the last term should be $\frac{1}{N_{10}}\sum_0^{N_{12}} E_{12}$, since particles may be stopped completely in the layer.

Since $dR_v$ is more closely related to the path length $dR$ than is $dR_p$, a better test of the theoretically predicted stopping power would be obtained by a measurement of the total mean vector stopping power:

$$(dE/dR)_{tmv} = \frac{dE_{mv}}{dR_v} = \frac{E_{10} - \frac{1}{N_{12}} \sum_0^{N_{12}} E_{12}}{dR_v}. \tag{4}$$

(4) is the same as (2) except that $dR_v$ replaces $dR_p$, i.e. instead of a plane exit surface a sperical surface with the radius $dR_v$ is used.

In practice such measurements are possible only in a gas and only by using an outlet opening, which can be rotated around the inlet opening, thus permitting integration over all angles. A few unpublished measurements of this kind using a slight modification of the equipment described in ref.[8], confirmed the previously measured stopping power data for $^{69}_{31}$Ga in $H_2$ gas except for a correction factor of 1.1. However, the measurements still suffered from a limited acceptance angle of the energy analyser.

A search for an energy analyser for low energy heavy particles with a fractionization effect as small as possible was initiated; the resulting heavy ion detector is described in section 4. It permits measurements with very low energy particles and it has solved nearly all problems connected with the fractionization effects. It is, however, sensitive also to the recoils and their influence is therefore discussed in the following section.

## 3. The Recoil Effect

For $M_1 = M_2$ a maximum energy ($T_m$) equal to the total energy $E_1$ of the primary particle may be transferred to the secondary particle in a single collision. Since secondary and primary particles are indistinguishable, a fundamental and serious experimental problem is created. As a result of the rather slow variation of $T_m$ with $M_1/M_2$, the problem is present for a wide $M_1/M_2$ range.

Theoretically, it will be so, that if a very thin stopping layer with approximately single collision condition is placed in front of a detector with a $2\pi$ acceptance angle and the electronic stopping is negligible, all the recoil energy will be transferred to the detector. If the detector then linearly sums the energies of the primary particle and its accompanying recoil particles, the result will be a 100 $^0/_0$ error in the measurement of the elastic energy loss!

This is, however, for an ideal linear detector which gives a voltage signal proportional to the particle energy $E_p$. Fortunately the detector used in the present experiment is not ideal and the signal is a nonlinear function of the heavy particle energy. This, as will be shown, helps to decrease the error of 100 % to less than 33 %.

The detector is a low pressure proportional counter which gives a signal proportional to the number $N_i$ of ion pairs formed in it by the particle. $N_i$, however, is not proportional to the energy $E_p$ of the particle, but (see part 7 and figures 6 and 7) empirically $N_i$ was found to be approximately

$$N_i = \frac{E_p}{W_i} \simeq \frac{E_p}{\frac{k_1}{k_2 E_p} + k_1} \tag{5}$$

$W_i$ is the average energy needed to create an ion pair, which for low particle energy will be

$$W_i \sim \frac{k_w}{E_p} \tag{6}$$

and hence

$$N_i \sim \frac{E_p^2}{k_w}. \tag{7}$$

The detector is followed by an electronic analog device, which makes the output $U_d$ proportional to the particle energy

$$U_d = \sqrt{\frac{A_t}{k_w} E_p^2} = k_d E_p \tag{8}$$

$A_t$ is the total gain of the system and $k_1$, $k_2$, $k_w$, $k_d$ are constants.

Suppose $M_1 = M_2$ and hence $T_m = E_1$. With no stopping layer the signal $U_{d0}$ is

$$U_{d0} = k_d E_{10}. \tag{9}$$

With a stopping layer inserted and assuming the recoil atoms *not* to reach the detector, the signal corresponding to an energy transfer $T$ is

$$U_{d1} = \sqrt{\frac{A_t}{k_w} (E_{10} - T)^2} = k_d (E_{10} - T) \tag{10}$$

whereas if the recoil atom reaches the detector, the signal is, $k_w$ here being the same for particle and recoil atoms:

$$U_{d2} = \sqrt{\frac{A_t}{k_w}((E_{10} - T)^2 + T^2)} = k_d\sqrt{(E_{10}^2 - 2T)^2 + T^2}. \tag{11}$$

The difference between $U_{d0}$ and $U_{d1}$ is correctly proportional to the energy loss $T$

$$u_1(T) = U_{d0} - U_{d1} = k_d T \tag{12}$$

whereas the difference between $U_{d0}$ and $U_{d2}$ is

$$u_2(T) = U_{d0} - U_{d2} = k_d(E_{10} - \sqrt{E_{10}^2 + 2T^2 - 2E_{10}T}) \tag{13}$$

which may be written, introducing the ratio $r_T$:

$$r_T = \frac{T}{E_{10}} \tag{14}$$

$$u_2(T, r_T) = k_d T\frac{1 - \sqrt{1 - 2r_T + 2r_T^2}}{r_T} = u_1(T)f(r_T). \tag{15}$$

The function $f(r_T)$ is shown in figure 3 together with the relative error

$$\Delta u(T)/u_1(T) = \frac{u_1(T) - u_2(T)}{u_1(T)}. \tag{16}$$

As seen the relative error is nearly proportional to $T$.

Next we want to find the average energy loss, $dE_n$, and its error. We use the simple power law cross section from L.S.S.[3] with $s = 2$, and obtain, introducing the ratio $r_T$,

$$d\sigma(r_T) = \frac{C_2}{E_{10}r_T^{3/2}}dr_T \tag{17}$$

where the constant $C_2$ is equal to half the value of the nuclear stopping cross section, which is independent of energy.

The average voltage signal $\bar{u}_1$ for the correct measurement will be

$$\bar{u}_1 = k_d\, dR N_2 \int_0^1 E_{10} r_T \frac{C_2}{E_{10}r_T^{3/2}}dr_T = k_d\, dE_n. \tag{18}$$

According to fig. 3 $u_2(T, r_T)$ may be approximated by $u_2 = k_d E_{10} r_T (1 - r_T)$, and the average signal obtained, if recoils reach the detector, is

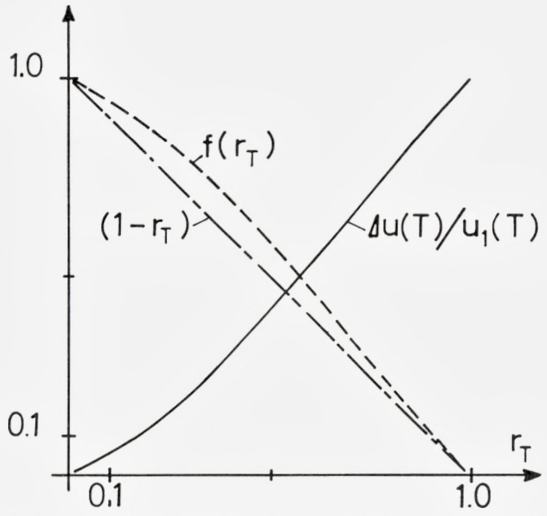


Fig. 3. The recoil influence in single collision events plotted as a function of $r_T = T/E_{10}$. The function $f(r_T) = u_2/u_1$ is the ratio between the recoil influenced signal and the correct signal and $\Delta u(T)/u_1(T)$ is the relative error.

$$\bar{u}_2 = k_d dR N_2 \int_0^1 E_{10} r_T (1 - r_T) \frac{C_2}{E_{10} r_T^{3/2}} dr_T = \tfrac{2}{3} k_d dE_n . \tag{19}$$

When $M_1/M_2$ deviates from unity, the difference $\bar{u}_1 - \bar{u}_2$ is smaller and thus the relative error in the energy loss measurement never exceeds 33 %.

This is for an assumed single collision condition, where the energy distribution of the recoils is proportional to $r_T^{-3/2}$ but in an actual stopping layer with multiple collision condition the energy distribution is expected to be proportional to $r_T^{-2}$ as has for instance been found for sputtered particles[16]. With such a distribution the relative error is reduced to less than 20 % and the angular scattering and inelastic losses will further reduce this value.

This was demonstrated by a calculation of the fraction of the total elastic energy loss, which reaches the detector volume as recoil energy. As above, the power law cross section with $s = 2$ and $M_1 = M_2$ was used, and it was assumed that the stopping consists of a part independent of energy, called the homogenenous part, caused by inelastic stopping and small angle collisions and a part caused by large angle collisions.

The results are shown in figure 4. The thickness $\Delta R$ of the stopping layer was varied, and the ratio $r_E$ between the homogeneous energy loss in $\Delta R$ and the primary particle energy $E_1$, is used as a parameter. $dE_n$ is the

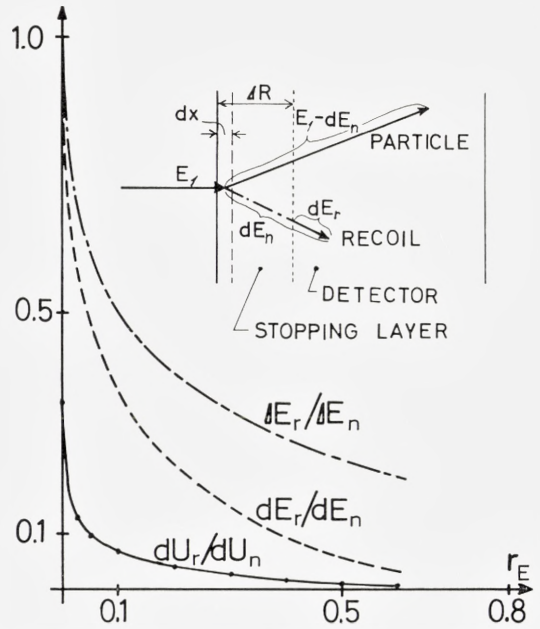


Fig. 4. Fraction of the elastic energy loss transported by recoils into the detector from $dx$, ($dE_r/dE_n$), and from $\Delta R$, ($\Delta E_r/\Delta E_n$) and the relative error, $dU_r/dU_n$, on the detector signal plotted as functions of the parameter $r_E$ (see text). A single event is shown very schematically.

total elastic energy loss in a thin layer $dx$ next to the entrance surface. $dE_r$ is the part of $dE_n$ which is transported through the stopping layer $\Delta R$ to the detector. $\Delta E_r$ and $\Delta E_n$ corresponds to the whole stopping layer.

Especially $dE_r/dE_n$ is strongly affected by the total stopping layer thickness. This leads to the conclusion that the best method in stopping power measurements is to add stopping layers in increments of $dx$, adjust the primary particle energy for each step with an energy increment $dE$ so that the average detector signal stays constant and in this way obtain a $dE/dx$ value. Hereby it is obtained, that in the layer between the $dx$ layer and the detector volume the particle energy and the recoil balance is nearly unchanged and the error is caused only by the recoils from $dx$ and hence, as seen from figure 4, decreases rapidly with increasing thickness of the total stopping layer.

If the reduction effect of the detector nonliniarity is also taken into consideration, the resulting relative error on the detector signal, $dU_r/dU_n$, shown in figure 4 is obtained. Thus the error is very small, except for the first few steps in a measurement.

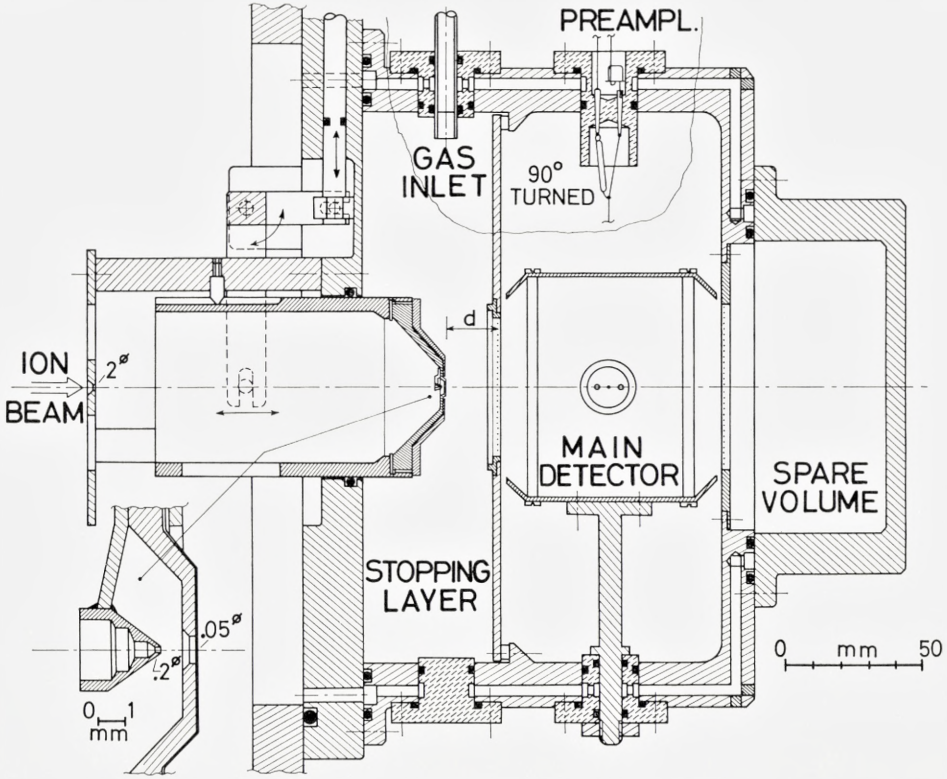


Fig. 5. The mechanical design of the detector system.

## 4. Experimental Apparatus

The fundamental problem of obtaining full transmission from the stopping layer to the energy analyser is solved by using a low pressure proportional counter as the energy detector and through the use of the same gas in the stopping layer and in the detector thus permitting the use of a high transmission grid between them.

In figure 5 is shown a somewhat simplified drawing of the system. The ion beam which is precollimated by a 2 mm diameter aperture enters the gas through a 0.05 mm diameter opening in a 0.05 mm thick stainless steel foil.

When a gas target is used, the beam inlet opening presents a problem, because of the difficulty in defining the exact boundary between the vacuum

and the gas. With the present small opening, the vacuum in the accelerator is hardly affected. The gas molecules are therefore streaming out with a mean free path of the order of many centimeters and a density which drops off with distance so fast that the addition to the gas layer caused by the outstreaming gas, when converted to the pressure inside the chamber, is smaller than the diameter of the opening, and therefore negligible.

Since the ion beam outside the opening easily contains up to $10^6$ times more particles than the number, which enters the chamber (normally about $10^3$ per second), the scattering in the outstreaming gas is not negligible. An antiscatter aperture, shown in fig. 5 in larger scale, reduces the number of scattered primary particles and recoil atoms, which otherwise would give rise to a low energy background in the detector, to a nearly nondetectable level.

The beam inlet opening is placed on a cylinder movable along the axial direction, so that the distance $d$ to the grid can be varied, from zero to 40 mm. $d$ is measured with a micrometer to an accuracy of $\pm$ 0.02 mm. By means of a linear potentiometer mechanically connected to the cylinder an electric signal indicating the position is obtained. The cylinder is insulated to allow the use of a bias voltage.

The central wire in the detector is a 0.11 mm diameter $W$-wire; the outer detector walls are 80 mm apart and have a length of 200 mm. By means of an $\alpha$-source with a 3° collimation, the electron collection efficiency and the gas amplification were tested and found to be constant to better than 1 % over the whole volume where ion pairs are formed by the primary particles.

The entrance opening to the detector has a diameter of 50 mm and is covered by a grid, formed by 0.05 mm diameter $N_i$-wires spaced 0.5 mm.

To minimize disturbing effects from ionization of impurity atoms by metastable states of the detector gas atoms (Penning effect) the highest purity of the gas is essential. Double $O$-ring seals were used everywhere in the apparatus and in the gas inlet system. The volume between any pair of $O$-rings was connected to high vacuum and thus no impurities could leak into the gas, which was taken from high pressure bottles with an impurity content less than 0.01 %. The gas pressure, which ranged from 3 to 15 Torr, is stabilized to better than 1 part in $10^3$ over periods of several hours by a special oilmanometer system[17] with both optical and electrical read-out of the oil level, and an electronically controlled leak valve[18]. The system is held at 22° C $\pm$ 0°.1 C.

The detector electronic system is standard equipment for pulsehandling except for two special modules. One is the inlet control box, which ensures that there is the same field strenght but in opposite directions on the two

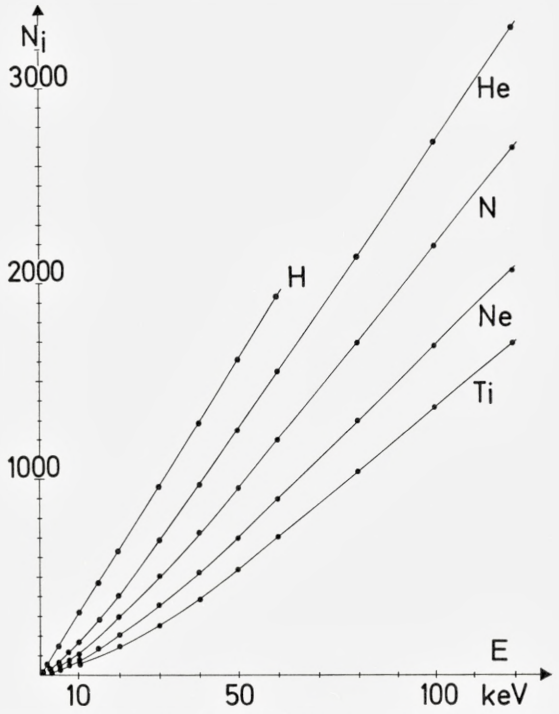


Fig. 6. Number of ion pairs formed in Methane by five different particles plotted as functions of the particle energy.

sides of the entrance grid of the detector for all positions of the inlet system, wherefore electrons formed outside the detector volume are not collected on the detector wire.

A 512 channel pulse height analyser is used to analyse the pulse height distributions. But since the energy distribution often is unsymmetric, and since a quick determination of the mean energy is essential, a special electronic unit, the C.M.C.[19], was designed and connected to the pulse height analyser. It permits a calculation of the center of mass channel number to be made in less than 10 seconds and displayed on a scaler with an accuracy of 0.1 channel.

## 5. The Energy Detector

With $CH_4$ as the detector gas the number of ion pairs $N_i$ as a function of the particle energy $E$ was investigated in the energy range 10–120 keV for particles with $Z_1 \leq 22$ by Macdonald and Sidenius[20]. Figure 6 shows some

typical examples of $N_i = f(E)$ curves. Figure 7 gives the $N_i$ dependency on $Z_1$ for fixed energies and, as seen, the oscillations found in the measurements of the pure electronic stopping[4, 5, 6, 7] also show up here.

This complex relation between $N_i$, $E$, $Z_1$, which itself gives important information about the slowing down of low energy heavy particles, involves that, for the proper use, the detector must be calibrated for each particle-gas combination.

As seen in figure 7, the number of ion pairs formed by the very low energy heavy particles is of the order of 10 to 100 and consequently the resolution of the detector is primarily determined by the statistical fluctuations in these low numbers. At higher energies, the fluctuations in the different energy loss processes will set the limit in resolution. The best resolution obtained has been about 5 % F.W.H.M. for 50 keV $H^+$ in $CH_4$.

The electronic noise from the preamplifier is almost without influence on the resolution, but sets the limit for the lowest energy, which can be detected. To allow the detector to work with the lowest gas amplification, which gives the most stable condition, a low noise preamplifier with a F.W.H.M. noise of about 250 ion pairs is used. With a gas amplification of about 200 the pulse height distributions from a mean value of 10 primary ion pairs are completely resolved from the noise.

With $CH_4$ as detector gas the gain stability is better than 0.2 % for several hours, whereas other gases require the use of a gain stabilizer to give the same stability.

## 6. Measuring Methods and Procedure

Two methods of stopping measurements are possible. In the variable pulse height method (V.P.H.) the incident particle energy $E_{10}$ is kept constant and the shift in the average energy $E_{12}$ of the emerging particles is observed as a function of the stopping layer thickness $d$. In the constant pulse height method (C.P.H.) the incident particle energy $E_{10}$ is adjusted as a function of the stopping layer $d$ so that the average energy $E_{12}$ of the emerging particles is kept constant.

In principle the two methods should yield the same results, but they differ in their sensitivity to the multiple scattering effects, the V.P.H. method being the more sensitive. Furthermore, the data analysis is much more difficult for the V.P.H. method because the pulse height data must be converted into energy data via the calibration curve; this introduces unnecessary errors. The V.P.H. method was therefore disregarded except for a few

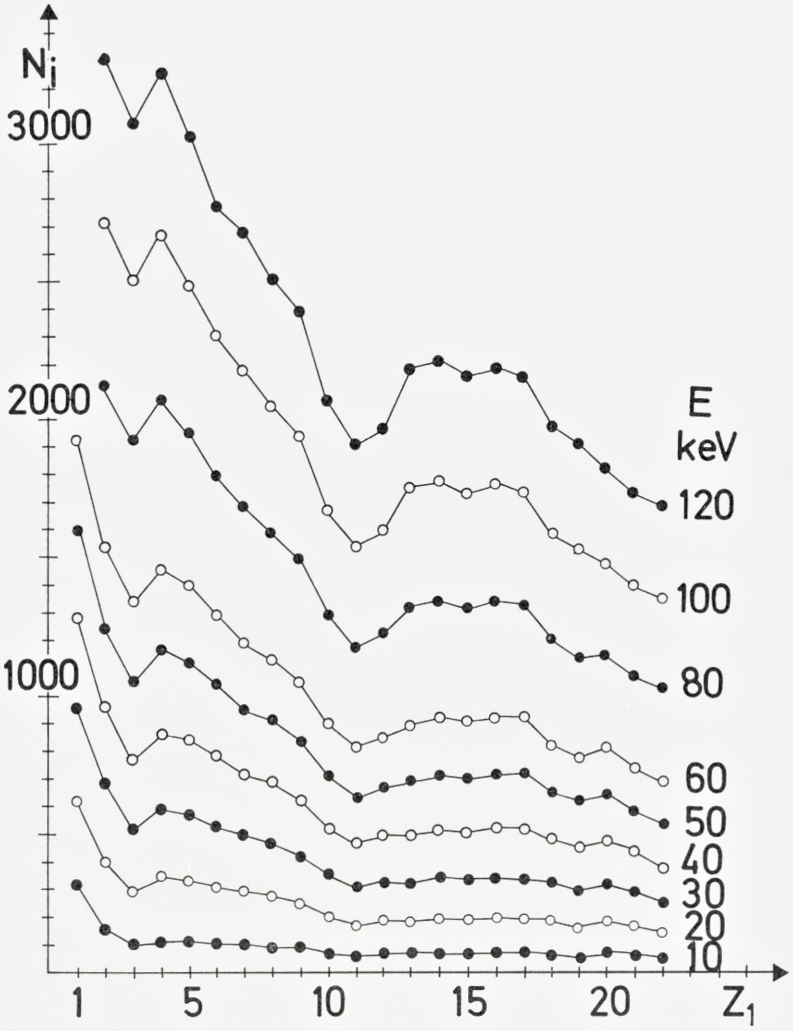


Fig. 7. Number of ion pairs formed in Methane plotted as functions of the atomic number $Z_1$ of the incoming particle and with the energy as parameter.

measurements with protons for which the calibration curve is linear and for which the V.P.H. method can be used to a somewhat lower energy than can the C.P.H. method.

The particles are produced by the reconstructed, 30 year old Copenhagen isotope separator[21]; now used as a modern universal range ion accelerator and separator (URIAS)[22]. The ions are mass analysed at a fixed energy

and afterwards either retarded or post accelerated. Thereby it is possible to obtain singly charged particles of continuously variable energy from less than 1 keV up to 60 keV. For higher energies doubly or triply charged ions are used.

The ions are produced in a high temperature universal ion source[23] with an energy spread of less than than one electron volt. The energy of the ions is measured with a digital voltmeter to an accuracy of $\pm$ 0.1 %.

After a suitable target gas pressure is set with $d = 0$, the particle energy is set to the lowest value $E_{10}$, and the center of mass value $N_{CM0}$ for the impulse height distribution is found using the C.M.C. The inlet system is then displaced one millimeter and the particle energy adjusted until $N_{CM1}$ read approximately the same as $N_{CM0}$, and both $d$, $E_{11}$ and $N_{CM1}$ are recorded.

This procedure is repeated for increasing distances until the $E_{12}$ distribution becomes so broad that the low energy tail extends down to the noise. $d$ is then turned back to zero and the stability of the system checked through the measurement of $N_{CM0}$ at energy $E_{10}$.

A new value of $E_{10}$ is then chosen, well inside the energy range covered in the first run, and the measurements are repeated.

The $E_1$ data are corrected for the small difference between $N_{CM0}$ and $N_{CMn}$

$$E'_{1n} = E_{1n} + E_{10}\left(1 - \frac{N_{CMn}}{N_{CM0}}\right) \tag{20}$$

the $dE/dx$ for each 1 mm step increment is found as

$$dE/dx = \frac{E'_{1\,(n+1)} - E'_{1n}}{dx} \tag{21}$$

and the data are normalized for different pressures etc. by converting them into the molecular stopping cross section $S_x$, the average energy loss per stopping molecule.

The statistical fluctuations in $S_x$ from these small values of $dx$ and $dE$ is normally rather large, up to $\pm$ 10 %, but they are useful for an estimate of the quality of the measurements. Another test of the quality of the measurements is obtained by the requirement that the various ($E'_1$, $d$) curves corresponding to different $E_{10}$ starting values must accurately fit together to form a smooth curve. Figure 8 shows, as an example, curves for Nitrogen stopped in Methane. Not all the single curves used to obtain the final curve are shown. The points from the different measurements are scattered less than 1 % in the

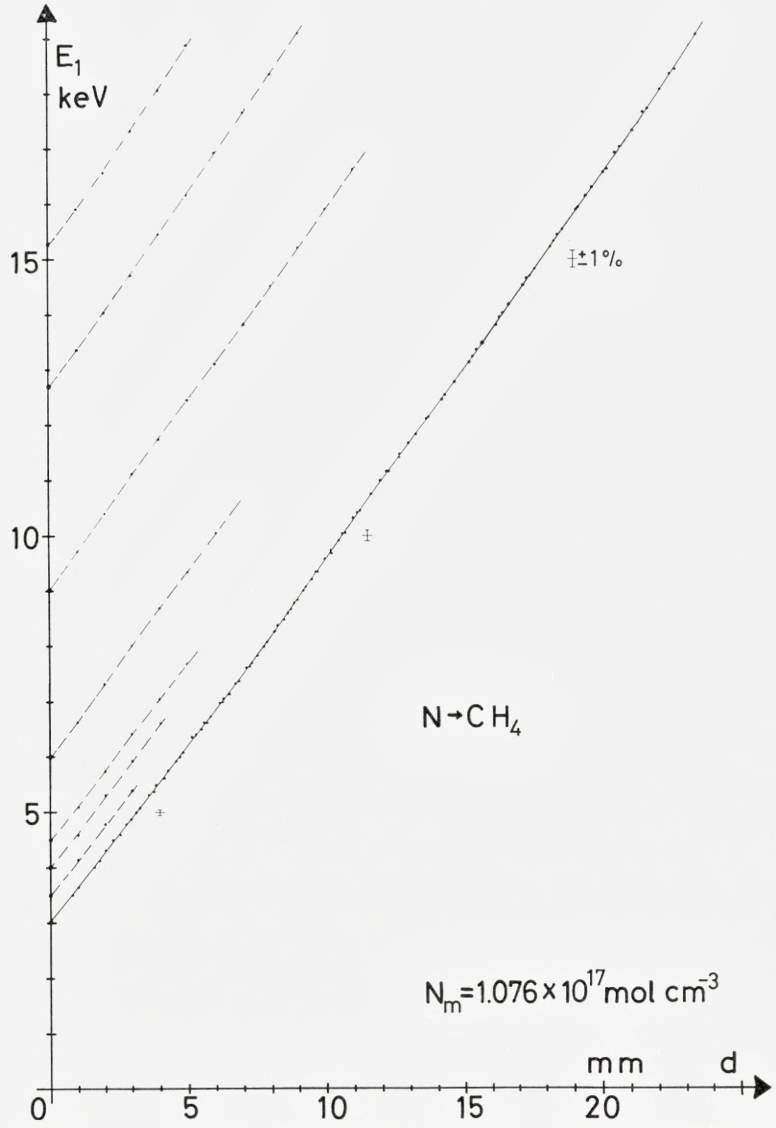


Fig. 8. Primary energy, $E_1'$, plotted as function of distance, $d$, for constant mean energy after the stopping layer. The curves corresponding to different starting values (dotted lines) are fitted together to form the final energy-range curve (full line) for Nitrogen stopped in Methane.

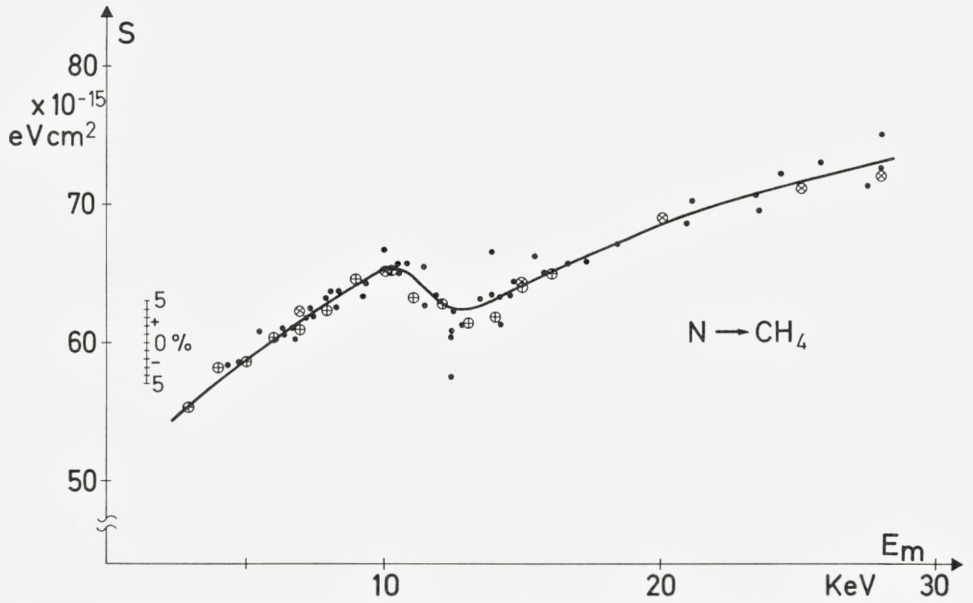


Fig. 9. Low energy part of the stopping cross section curve for Nitrogen stopped in Methane. Points are from the data analysis described in the text, crosses are from a differentiation of the final curve in figure 8.

low energy range and less than $^1/_2$ % in the high energy range. Points from two sets of measurements with pressures of 3.20 and 6.40 Torr are shown.

Figure 9 shows the low energy part of the stopping cross section curve for Nitrogen slowed down in $CH_4$. A rather narrow structure, at approximately 10 keV, is seen. The points are from the data analysis described, but using values of $dx$ from 3 to 6 mm, and the average spread around the smooth curve is about $\pm$ 2.5 %. As a comparison a differentiation of the final energy-range curve in figure 8 yielded results shown as circled crosses; there is satisfactory agreement between the results found by the two different analysing methods.

## 7. Systematic and Statistical Errors

In the C.P.H. method a calibration curve is, in principle, not needed, but due to the nonlinear pulse height-energy relation a systematic error is introduced. With increasing stopping layer thickness the energy distribution becomes wider due to the straggling and if two distribution curves having the same center of mass but different widths are each folded with the same non-

linear function the resulting curves will not have the same center of mass. Therefore to the main pulse height amplifier was added a variable nonlinear stage, which served to straighten the pulse height-energy curve to a linear curve without any loss in the overall stability.

As previously shown, a systematic error arises from recoils reaching the main detector. However, the detector reduction effect and the use of the C.P.H. method reduce this error to less than 5 to 10 % of the elastic stopping except for the first one or two mm stopping layer.

Any possible systematic error will be strongly dependent on the stopping layer thickness. The best estimate of their influence is obtained by measurements of $dE/dR$ data for the same mean energy but measured with different layer thicknesses and at different distances from the grid.

As shown in figure 8 and 9, except for the first one or two mm of stopping layer such differences in stopping data were found to be smaller than the statistical uncertainties. For the present measurements in $CH_4$, it is estimated that in the region from 3 to 10 keV the systematic error is less than $-5$ to $+15$ %, from 10 to 30 keV less than $-3$ to $+10$ %, and from 30 up to 120 keV less than $-2$ to $+4$ %.

The statistical fluctuation in the mean value of the $E_{12}$ distribution varies from $\pm 0.5$ % at low energies to $\pm 0.2$ % at high energies. Since $dE$ is determined as the difference between two nearly equal numbers, ($dE$ is normally less than 10 % of $E_{12}$ except at low energies) the fluctuation in $dE$ and therefore in the stopping power ranges from $\pm 2.5$ % to $\pm 7$ % depending on the magnitude of $dE$ and $E_{12}$.

All the present stopping cross section curves are results of many repeated measurements carried out with different pressures.

## 8. Results and Discussion

There are several reasons for choosing the most simple hydrocarbon, $CH_4$, as stopping gas. Firstly it is found to give optimum stability of the detector, secondly the content of the light $H$-atoms decreases the scattering and recoil effects, and finally the slowing-down of particles in hydrocarbons has great interest for the application of the stopping data in health physics and radiation damage theory, J. A. Dennis[24, 25].

As particles the first ten elements in the periodic system were used. The energy ranged from 0.6 keV up to 110 keV.

The data obtained are the total mean stopping power for the projected path given by formula (2) and they are not directly comparable with the

theory, which refers to the mean stopping along the actual path, as given by formula (1). Since no theoretical calculation of the total mean stopping for the projected path is available, no attempt was made to correct neither the experimental nor the theoretical data. But a correction of the theoretical curve would in all cases have resulted in an increase in the stopping cross section especially at low energy. Still, the theoretical curves, calculated from L.S.S.[3], will be of interest for comparison and they are therefore in all cases shown together with the experimental results.

For protons the stopping cross section curve from 0.6 up to 60 keV is shown in figure 10, together with other experimental results and the theoretical curve which is only valid up to about 15 keV. The agreement between the present results and those of Reynolds et al.[26] and Park and Zimmerman[27] is excellent, whereas a systematic disagreement exists with the measurements of Hughes[28]. The explanation seems to be that Hughes has used an ion source giving a high output of $H_2^+$ instead of $H^+$ and he has not used an analysing magnet. Much better agreement would be obtained if his energy scale was divided by two!

The stopping cross section for Helium ions was measured in the energy interval from 3 to 60 keV and is shown in figure 10. The theoretical curves for Helium and for the heavier particles to be discussed later were calculated as the sum of the nuclear and electronic stopping cross sections of the Carbon atom and the four Hydrogen atoms.

$$S_t = S_{nC} + S_{eC} + 4S_{nH} + 4S_{eH}. \tag{22}$$

The agreement between the present results and the theory and the results of J. T. Park[29] could have been better, but at least the slope is about the same. Park has used a very small analyser acceptance angle and this may be the reason for the discrepancy between the two experimental results.

At low energies, two interesting effects are observed. One is the bump in the curve at about 10 keV which seems to indicate some kind of resonance effect in the losses. Secondly, in disagreement with theory, the experimental curve does not level out below 5 keV.

That the latter is not a result of a systematic error is proved by the fact that no such effect is found for the two Lithium isotopes, as shown in figure 11. The agreement with the point of Teplova et al.[30] is reasonably good. The magnitudes of the experimental and theoretical values differ strongly, but this may be explained by difference in the electronic stopping. More important, the general behaviour of the two sets of curves is the same; note especially the crossing caused by the isotope effect.

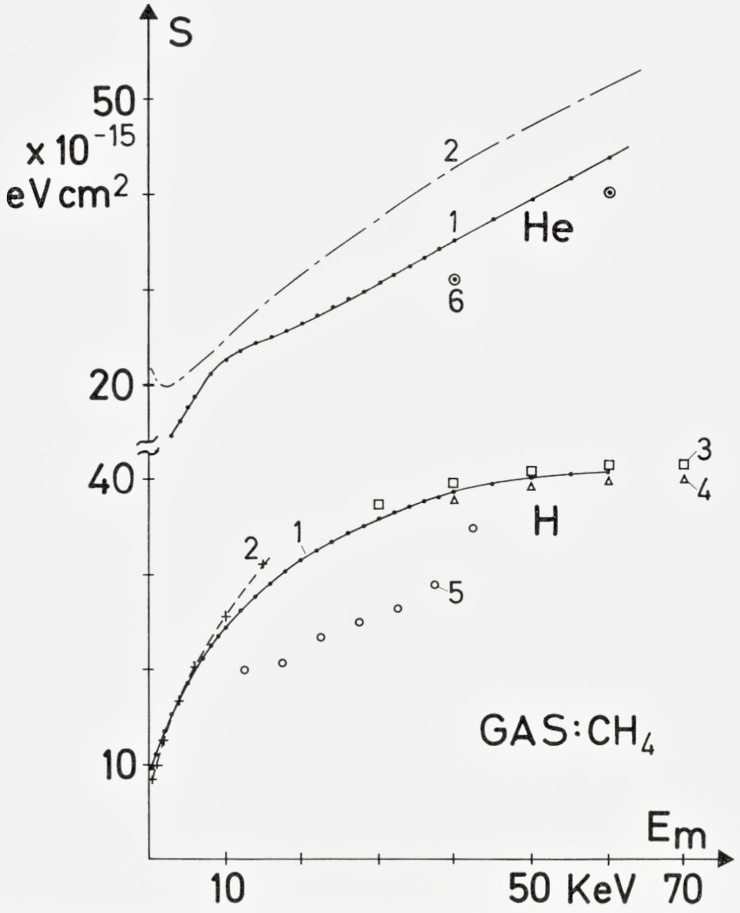


Fig. 10. Stopping cross sections for Hydrogen and Helium stopped in Methane. The curves marked 1 give the results of the present experimental investigations whereas 2 are the theoretical estimates. Other experimental results are: 3, REYNOLDS et al.[26], 4, PARK and ZIMMERMANN[27], 5, S. HUGHES[28], and 6, J. T. PARK[29].

Results for particles ranging from Beryllium to Neon are shown in figure 12 and 13. For all the particles the experimental stopping cross section at low energy is much lower than the theoretically predicted. A most striking feature is the pronounced structure in the curves for Nitrogen and for Carbon. If this structure is caused by the nuclear stopping one should expect a similar structure to appear for the neighbouring elements more pronounced than is the case; therefore the electronic stopping must be responsible for the structure. The broader structure of the Fluorine and the Neon curves rather seems to belong to the same type as the Helium curve.

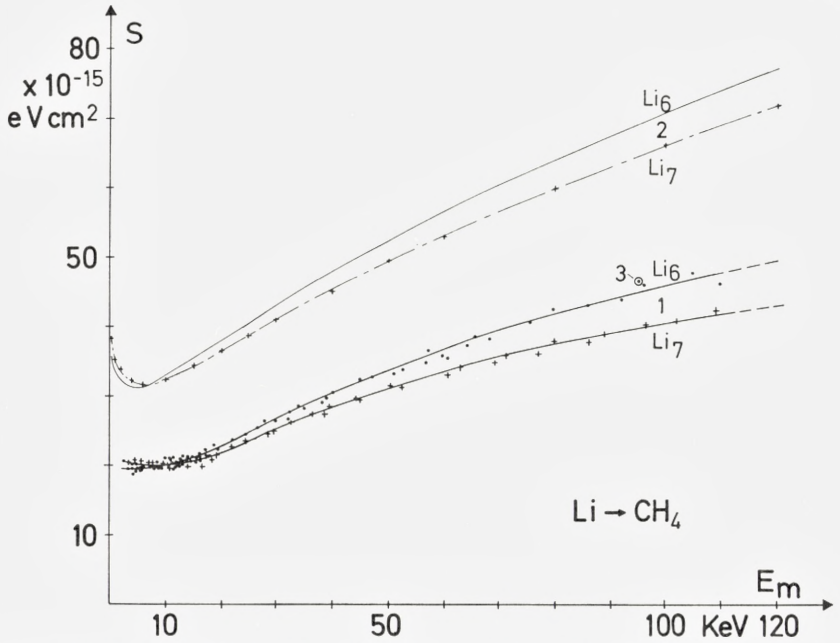


Fig. 11. Stopping cross sections for the two Lithium isotopes stopped in Methane. Curve set 1 gives the results of the present experiments whereas curve set 2 represents the theory. Point 3 is the experimental result by TEPLOVA et al.[30].

The agreement with the data of TEPLOVA et al. for Boron could have been better, whereas for Nitrogen there is surprisingly good agreement with the data of HUGHES, though these might have been expected, like for hydrogen, to be in error due to a dominating beam of doubly charged ions.

In figure 14 all the experimental results are shown together.

## 9. Deduction of the Electronic Stopping Cross Section

In the present investigations experimental values for the total stopping cross section were obtained. If we take the values for the various particles at a selected common velocity and subtract the corresponding theoretical values from L.S.S.[3] of the nuclear stopping cross section, values for the electronic stopping cross section Se may be obtained.

The resulting values of $S_e$ for particles with the velocity $v = 0.5\ v_0 = 1.09 \cdot 10^8$ cm $s^{-1}$ are plotted in figure 15 together with the theoretical estimates of $S_e$ by L.S.S.[3]. Contrary to the smooth shape of the latter, the experimental values exhibit an oscillatory variation, for which the magnitudes of the

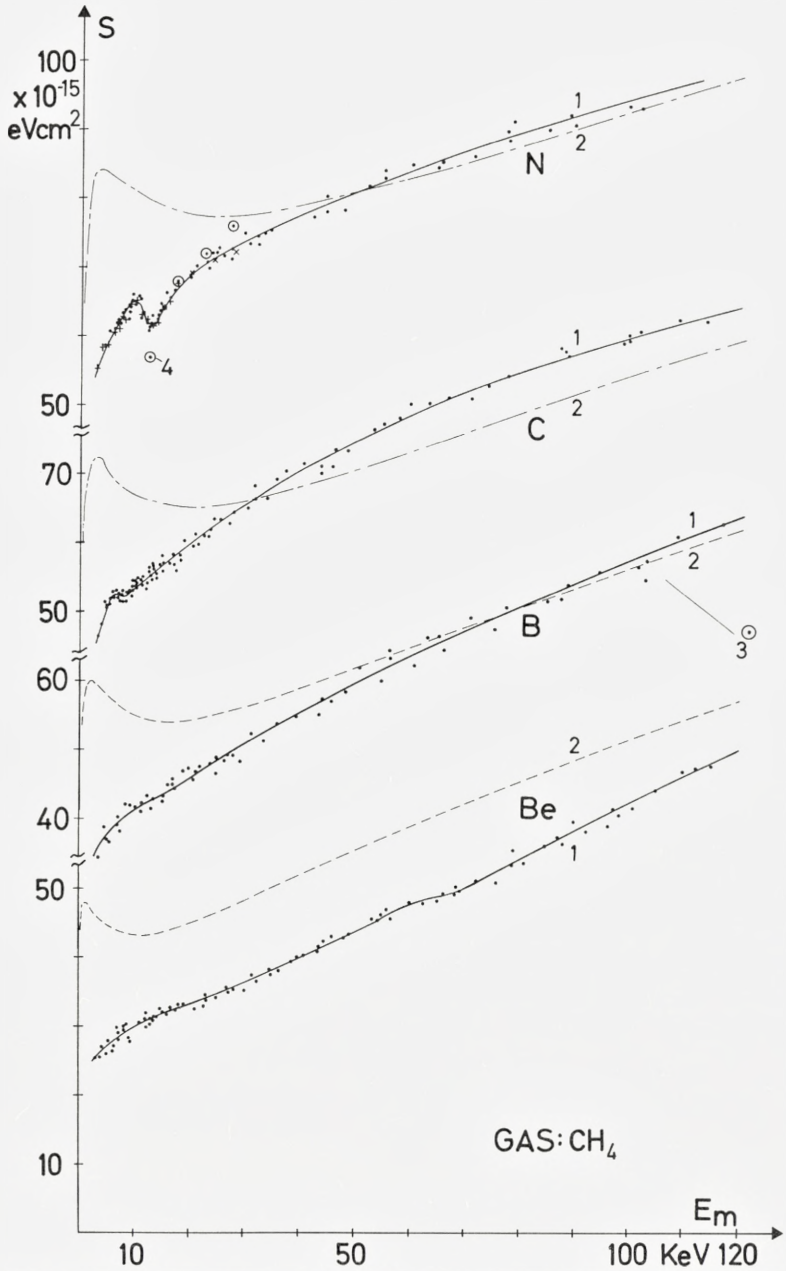


Fig. 12. Stopping cross sections for Berylium, Boron, Carbon and Nitrogen stopped in Methane. The curves marked 1 give the results of the present experiments, 2, are the theoretical estimates. Other experimental results are: 3, TEPLOVA et al.[30] and 4, S. HUGHES[28].

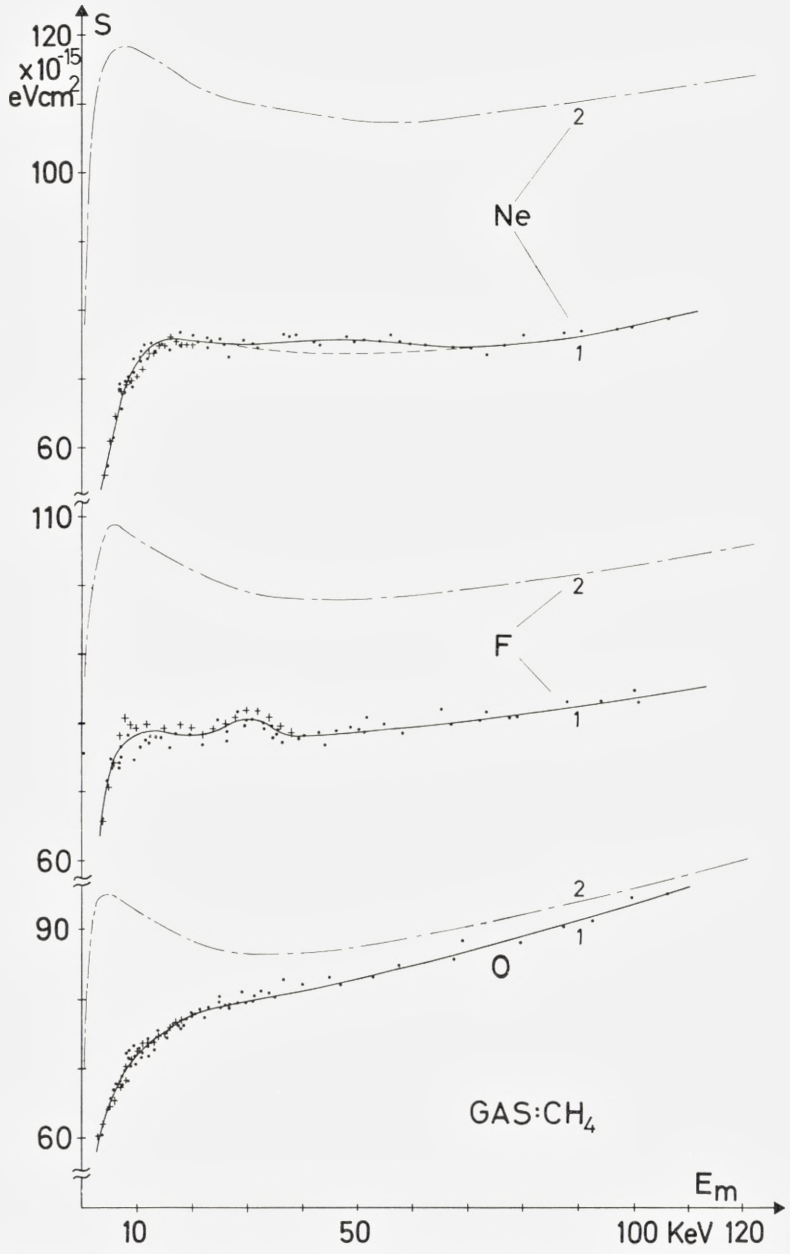


Fig. 13. Stopping cross sections for Oxygen, Fluorine and Neon stopped in Methane. The curves marked 1 give the results of the present experiments and 2 are the theoretical estimates.

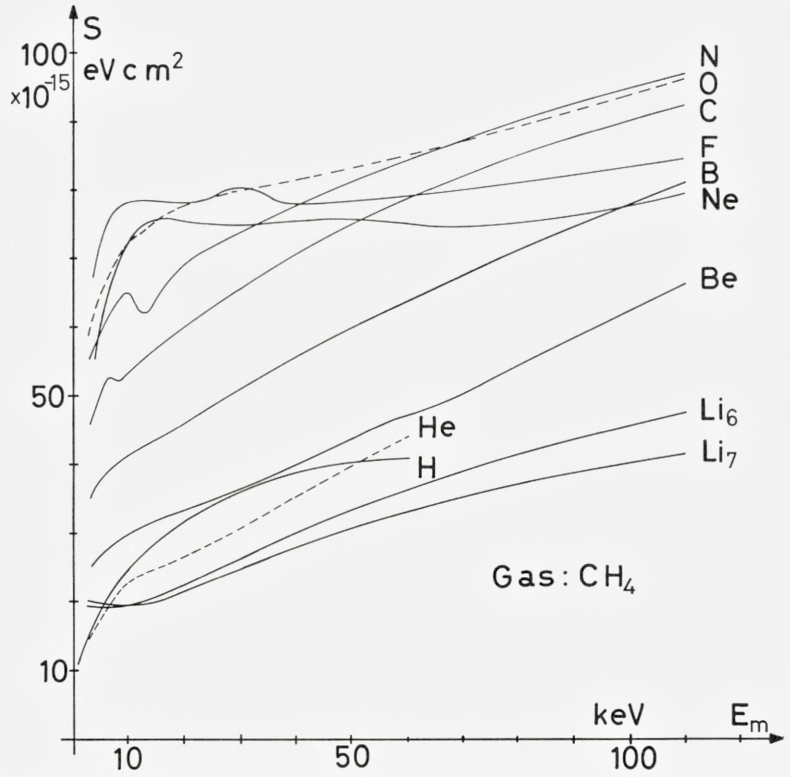


Fig. 14. Experimental total mean stopping cross sections for the first ten elements stopped in Methane.

maxima and minima are in good agreement with measurements in other gases by HVELPLUND[6].

At the selected velocity the theoretical nuclear stopping ranges, for the light particles from 10 % of the total experimental stopping up to 50 % for the heavy particles. Since the nuclear stopping seems to be overestimated by the theory (se next chapter) the deduced values for $S_e$ are probably too low especially for the heavy particles. On the other hand the theoretical value refer to the actual path of the particle and the experimental value refer to the projected path, this causing the obtained values for $S_e$ to be too high. The uncertainties in the values of $S_e$ will therefore be of the order of $\pm$ 10 % for the light particles up to $\pm$ 30 % for the heavy particles.

## 10. The Nuclear Stopping Cross Section

The ultimate aim of the present experiment is to obtain information on the nuclear stopping. Since the nuclear stopping is most dominating in the stopping of the heavist particles, Neon shall be used as example in the following analysis. To learn about the nuclear stopping we might use the reverse of the procedure for deducing the electronic stopping, i.e. we might assume the theoretical value of the electronic stopping to be correct and subtract it from the experimental values of the total stopping. However since for Neon the experimental value of $S_e$ in all measurements has been found to be much smaller than the theoretical estimate, the use of the latter without correction is not reasonable. Instead, two different values, $S_{e1}$ and $S_{e2}$ of the electronic stopping stopping cross section have been tried. $S_{e1}$ is the theoretical value from L.S.S.[3], multiplied by the ratio between the present measured value and the theoretical value for the total stopping cross section at 120 keV. $S_{e2}$ is the theoretical value multiplied by a factor obtained from measurements of the stopping of Neon in Air, HVELPLUND[6], and the stopping of Neon in Nitrogen, ORMROD[31]. Their measurements lead to almost the same ratio between the experimental and the theoretical values for the total stopping.

In figure 16 the resulting curves are shown. The choise between $S_{e1}$ and $S_{e2}$ is seen to be of importance for the experimental value of $S_n$ at high energy, but rather unimportant for the position and magnitude of the maxima. Judging from the curves at high energies, where the slope of $S_{n2}$ too quickly approaches zero, $S_{e1}$ is a better choice than $S_{e2}$. The general shapes of the two curves $S_{n1}$ and $S_{nt}$ (curves 7 and 3) are in reasonable agreement, but the magnitudes and positions of the maxima differ.

Table 1 gives the ratios between the maximum values of the experimental and theoretical nuclear stopping cross sections, $r_{\hat{S}} = \hat{S}_{n1}/\hat{S}_{nt}$, and the ratios of the energies corresponding to these maxima, $r_{\hat{E}} = \hat{E}_{n1}/\hat{E}_{nt}$, for the six

TABLE 1.

| $Z_1$ | $r_{\hat{S}} = S_{n1}/S_{nt}$ | $r_{\hat{E}} = \hat{E}_{n1}/\hat{E}_{nt}$ |
|---|---|---|
| Boron | 0.46 | 2.5 |
| Carbon | 0.55 | 2.3 |
| Nitrogen | 0.59 | 2.8 |
| Oxygen | 0.61 | 3.0 |
| Fluorin | 0.66 | 1.7 |
| Neon | 0.61 | 2.7 |

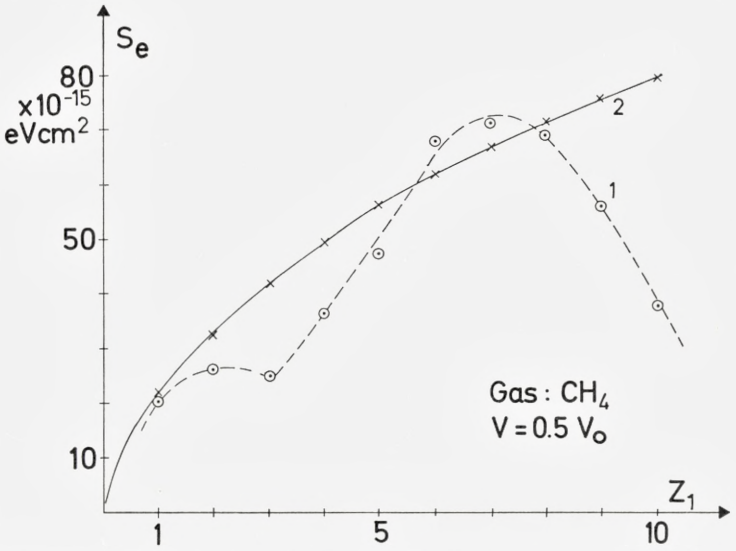


Fig. 15. Electronic stopping cross sections. 1 are the present experimental results and 2 the theoretical value from L.S.S.[3].

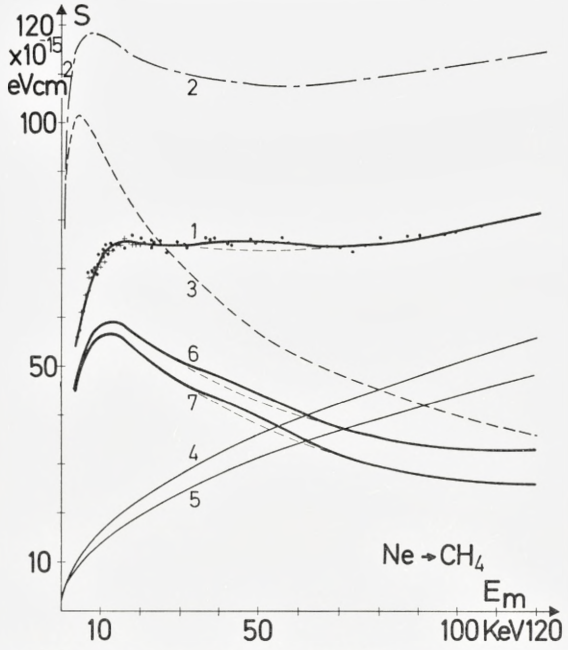


Fig. 16. Deduction of the pure nuclear stopping cross section. The curves are: 1, experimental total stopping $S_x$; 2, theoretical total stopping $S_t$, 3, theoretical nuclear stopping $S_{nt}$ from L.S.S.[3]; 4 and 5, reduced theoretical electronic stopping curves $S_{e_1}$ and $S_{e_2}$, respectively; 6 and 7, experimental nuclear stopping curves $S_{n_2}$ and $S_{n_1}$, obtained from curve 1 by subtracting $S_{e_2}$ and $S_{e_1}$, respectively.

heaviest elements, which were measured. The experimental maximum values of $S_n$ are about half the theoretically predicted, and the maxima are experimentally found to lie at energies from two to three times higher than theoretically predicted.

To take into account possible systematic errors, the uncertainty in the $S_e$-value and in determining the exact position of the maximum, we estimate uncertainties of the order of $\pm 30\ ^0/_0$ for $r_{\hat{S}}$ and $r_{\hat{E}}$.

No correction for the difference between the projected range and the actual path length was applied. It should be pointed out, that therefore the difference between the theoretical and the measured values of the stopping cross sections, especially in the low energy range, may be expected to be even larger.

In the paper preceding L.S.S.[3] (Notes on Atomic Collisions I)[32] stopping cross section curves for three screened Coulomb potentials were given. In addition to the curve corresponding to the THOMAS-FERMI potential, which was chosen in the further development of the stopping theory, curves corresponding to a LENZ-JENSEN potential and a BOHR potential were given, (figure 7, Ref. 32). Comparing them to the THOMAS-FERMI curve, in the same way as the experimental results, they are both found to have $r_{\hat{S}}$ values of about 0.88, and the LENZ-JENSEN curve has $r_{\hat{E}} = 1.6$ and the BOHR curve has $r_{\hat{E}} = 2.5$.

Unpublished stopping power measurements by HVELPLUND[33] and recent range measurements by NEILSON et al[34] in the $\varepsilon$-range in which the nuclear stopping is dominating, also suggest that the nuclear stopping is overestimated by L.S.S.[3] and that the application of an other potential will give a better agreement between theory and experiment.

## 11. Conclusion

By applying the proportional detector technique, stopping cross section measurements were extended to very low energies and nearly all the problems connected with the fractionization effects and partly the problem connected with the recoil effect were solved.

The obtained complex results show that an extension of the measurements would be highly interesting, especially by using noble gases as stopping media and heavier ions as particles.

## Acknowledgements

I would like to thank first of all FIN HANSEN, who, with great skill and care, has operated the accelerator and the equipment. Furthermore J. R. MACDONNALD and E. STRØMBERG for their help with the testing and the calibration of the detector. I am much indebted to J. LINDHARD and K. O. NIELSEN for inspiring discussions and to P. SIGMUND for valuable comments.

*The Niels Bohr Institute*
*University of Copenhagen*
*Copenhagen, Denmark*

Indleveret til Selskabet den 24. oktober 1973.
Færdig fra trykkeriet den 2. juli 1974.

## References


1 N. Bohr, Mat-fys. Medd. Dan. Vid. Selsk. **18**, 8, (1948).
2 J. Lindhard and M. Scharff, Phys. Rev. **124**, 128, (1961).
3 J. Lindhard, M. Scharff and H. E. Schiøtt, Mat.-fys. Medd. Dan. Vid. Selsk. **33**, 14, (1963).
4 J. H. Ormrod and H. E. Duckworth, Can. J. Phys., **41**, 1424, (1963).
5 J. H. Ormrod, J. R. Macdonald and H. E. Duckworth, Can. J. Phys., **43**, 275, (1965).
6 P. Hvelplund, Mat-fys. Medd. Dan. Vid. Selsk. **38**, 4, (1971).
7 G. Högberg, Phys. Stat. Sol. (b), **48**, 829, (1971).
8 G. Sidenius, Proc. 3rd Conf. Physics of Electr. and Atomic Collisions, London 1963, p. 709.
9 P. Zahn, Z. Physik, **172**, 85, (1963).
10 D. Marx, Z. Physik, **195**, 26, (1966).
11 D. H. Poole, A. G. Warner, R. Hancock and R. L. Woolley, Journ. Physics D, **1**, 309, (1968).
12 R. Hancock, A. G. Warner and R. Woolley, Journ. Physics D, **2**, 991, (1969).
13 G. Högberg, Phys. Letters, **35**A, 327, (1971).
14 Proc. Second Int. Conf. on Beam Foil Spectroscopy, Nucl. Instr. and Meth., **90**, (1970).
15 S. K. Allison, J. Cuevas and M. Garcia-Munos, Phys. Rev. **127**, 792, (1962).
16 M. W. Thomson, Phil. Mag., **18**, 377, (1968).
17 G. Sidenius, Journ. Physics E, **2**, 657, (1968).
18 G. Sidenius, Journ. Physics E, **4**, 771, (1971).
19 G. Sidenius, Nucl. Instr. and Meth., **96**, 1, (1971).
20 J. R. Macdonald and G. Sidenius, Phys. Let., **28**A, 543, (1969).
21 K. O. Nielsen and O. Skilbreid, Nucl. Instr. and Meth., **2**, 15, (1958).
22 G. Sidenius and O. Holck, Proc. 8th Int. Conf. Low Energy Ion Acc. and Mass Separators, Sweden, 1973.
23 G. Sidenius, Proc. Int. Conf. Electromagnetic Isotope Separators., Marburg 1970, p. 423.
24 J. A. Dennis, Radiation Effects, **8**, 87, (1971).
25 J. A. Dennis, A.E.R.E.-Report – M – 2346.
26 H. K. Reynolds, D. N. F. Dunbar, W. A. Wenzel and W. Whaling, Phys. Rev. **92**, 742, (1953).
27 J. T. Park and E. J. Zimmerman, Phys. Rev. **131**, 1611, (1963).
28 S. Hughes, Phys. Med. Biol., **12**, 565, (1967).
29 J. T. Park, Phys. Rev. **138**, A1317, (1965).
30 Y. A. Teplova, V. S. Niclaev, I. S. Dmitriev and L. N. Fateeva, Sov. Phys. JETP, **15**, 31, (1962).
31 J. H. Ormrod, Can. J. Phys. **46**, 497, (1968).
32 J. Lindhard, V. Nielsen and M. Scharff, Mat-fys. Medd. Dan. Vid. Selsk. **36**, 10, (1968).
33 P. Hvelplund, private communications.
34 G. W. Neilson, B. W. Farmery and M. W. Thompson, Phys. Let., **46**A, 45, (1973).

GERT KJÆRGÅRD PEDERSEN

# BOREL STRUCTURE IN OPERATOR ALGEBRAS

Det Kongelige Danske Videnskabernes Selskab
Matematisk-fysiske Meddelelser **39**, 5


Kommissionær: Munksgaard
København 1974

## Synopsis

Abstract measure theory is often described as the study of the two classes $C(X)$ and $\mathscr{B}(X)$ consisting, respectively, of the continuous and the Borel measurable functions on a locally compact space $X$. A measure $\mu$ on $X$ is a functional on $C(X)$ and it can be extended to $\mathscr{B}(X)$, thus giving rise to various normed spaces, in particular $L^1_\mu(X)$ and $L^\infty_\mu(X)$.

This paper is concerned with certain aspects of non-commutative measure theory. In that version $C(X)$ is replaced by a non-commutative C*-algebra $\mathscr{A}$, and the Borel algebra $\mathscr{B}$ associated with $\mathscr{A}$ replaces $\mathscr{B}(X)$. Instead of $L^\infty_\mu(X)$ one must now accept any von Neumann algebra $\mathscr{M}$ for which there is a representation $\pi$ of $\mathscr{A}$ into $\mathscr{M}$ such that $\pi(\mathscr{B}) = \mathscr{M}$. In a certain sense it can be said that $\pi$ replaces $\mu$.

It is shown that for each locally compact group $G$ of automorphisms of a von Neumann algebra $\mathscr{M}$ there is an essentially unique C*-algebra $\mathscr{A}$ with Borel algebra $\mathscr{B}$ and a representation $\pi$ with $\pi(\mathscr{B}) = \mathscr{M}$, such that $G$ can be realized as a Borel group of automorphisms of $\mathscr{B}$. This generalizes classical lifting theorems by J. von Neumann and G. W. Mackey.

The problem arises (in connection with model quantum field theory) whether a group $G$ of automorphisms of $\mathscr{M}$ can be lifted to the Borel algebra $\mathscr{B}$ of an arbitrary C*-algebra $\mathscr{A}$ with a representation $\pi$ such that $\pi(\mathscr{B}) = \mathscr{M}$. This is answered in the affirmative when $G$ is countable or has uniformly continuous action on $\mathscr{M}$.

PRINTED IN DENMARK
BIANCO LUNOS BOGTRYKKERI A/S
ISBN 87 7304 036 3

## 1. Introduction

This paper is concerned with the generalization of certain results from the theory of standard Borel spaces to the theory of (non-commutative) operator algebras. With each separable C*-algebra $\mathscr{A}$ is associated a C*-algebra $\mathscr{B}$ – the Borel algebra. In the commutative case $\mathscr{A}$ is isomorphic to the algebra of continuous functions vanishing at infinity on some separable locally compact Hausdorff space $X$ and $\mathscr{B}$ is then the algebra of bounded Borel functions on the standard Borel space $X$. In the non-commutative case the Borel algebra $\mathscr{B}$ serves as an analogue of the bounded Borel functious. For example the central disintegration of representations of $\mathscr{A}$ is uniquely determined by standard measures on the spectrum of the center of $\mathscr{B}$ (see [4] and [13]).

In theoretical quantum physics the symmetries or the time evolution of a physical system is often given by a group of unitaries $G$ on a Hilbert space $H$ on which the observables, or rather the C*-algebra $\mathscr{A}$ they generate, have a faithful representation $\pi$. A recurrent problem is that the group $G$ does not leave the algebra $\pi(\mathscr{A})$ invariant although it induces automorphisms of the von Neumann algebra $\pi(\mathscr{A})''$ generated by the observables. This could be explained as the effect of a wrong choice of "local algebras" (as defined in [5]), but it might also be an inherent obstacle in the model. Certainly there are many purely mathematical examples where the modular group corresponding to a cyclic and separating vector for $\pi(\mathscr{A})''$ does not give automorphisms of $\pi(\mathscr{A})$. As pointed out by E. B. Davies a natural approach (from a commutative point of view) would be to show that the automorphisms of $\pi(\mathscr{A})''$ induced by $G$ can be lifted to a group of automorphisms of the Borel algebra $\mathscr{B}$ of $\mathscr{A}$. Then one would have a global (i.e. space free) description of $G$ but of course at the expense of dealing now with the considerably larger algebra $\mathscr{B}$ of "measurable observables". The present paper evolved from an attempt to solve the mathematical problems involved in such a lifting.

Our point of departure is a non-commutative version of von Neumann's classical theorem on point realizations of isomorphisms between $L^\infty$-spaces, which constitute section 3 of the paper. In section 4 we show that each

separable locally compact $\sigma$-weakly continuous group of automorphisms of a von Neumann algebra on a separable Hilbert space can be lifted to a group of automorphisms of an essentially unique Borel algebra. The result is an exact analogue of a result about transformation groups of standard spaces proved by G. W. Mackey in [8]. In section 5 we show that each separable uniformly continuous group (in particular each countable group) of automorphisms of a von Neumann algebra quotient of a Borel algebra $\mathscr{B}$ can be lifted to a uniformly continuous group of automorphisms of $\mathscr{B}$. Finally, in section 6 we comment on the equivalence problem for Borel algebras.

## 2. Notation and preliminaries

Let $\mathscr{A}$ be a separable C*-algebra and consider $\mathscr{A}$ in its universal representation so that the enveloping von Neumann algebra $\mathscr{A}''$ is isomorphic (as a Banach space) to the second dual of $\mathscr{A}$ (see [3, § 12]). For each subset $\mathscr{S}$ of $\mathscr{A}''$ let $\mathscr{S}_{sa}$ denote the self-adjoint part of $\mathscr{S}$. Let $\mathscr{B}_{sa}$ be the smallest class of operators in $\mathscr{A}''_{sa}$ which contains $\mathscr{A}_{sa}$ and is closed under the process of taking limits of bounded monotone (increasing or decreasing) sequences from the class. The *Borel algebra* associated with $\mathscr{A}$ is the C*-algebra $\mathscr{B} = \mathscr{B}_{sa} + i\mathscr{B}_{sa}$ (see [6, p. 316] and [11, Theorem 1]). Each representation $\pi$ of $\mathscr{A}$ on a Hilbert space $H$ extends uniquely to a normal representation (again denoted by $\pi$) of $\mathscr{A}''$ onto the von Neumann algebra generated by $\pi(\mathscr{A})$. The restriction of $\pi$ to $\mathscr{B}$ maps $\mathscr{B}_{sa}$ onto the monotone sequential closure of $\pi(\mathscr{A})_{sa}$ (by [10, Proposition 4.2]) and if $H$ is separable, $\pi(\mathscr{B})$ is the von Neumann algebra generated by $\pi(\mathscr{A})$ (by [6, p. 322] or [12, Theorem 1]). The fact that the atomic representation of $\mathscr{A}$ extends to a faithful representation of $\mathscr{B}$ ([13, Corollary 3.9]) allows us to regard $\mathscr{B}$ as the non-commutative analogue of the bounded Borel functions on a standard Borel space.

## 3. A theorem of von Neumann

A classical result of J. von Neumann asserts that if $\mu_1$ and $\mu_2$ are probability measures on standard Borel spaces $X_1$ and $X_2$, respectively, such that $L^\infty_{\mu_1}(X_1)$ is isomorphic to $L^\infty_{\mu_2}(X_2)$, then the isomorphism can be lifted to a Borel isomorphism of $X_1 \setminus N_1$ onto $X_2 \setminus N_2$ where $\mu_1(N_1) = \mu_2(N_2) = 0$ (see [9]). The theorem below is the non-commutative analogue of von Neumann's result and yields a reasonably simple proof of it upon specialization to commutative C*-algebras.

*Theorem* 1. Let $\mathscr{A}_1$ and $\mathscr{A}_2$ be separable C*-algebras with Borel algebras $\mathscr{B}_1$ and $\mathscr{B}_2$, respectively. If for each $i = 1, 2$, $\pi_i$ is a representation of $\mathscr{A}_i$ on a separable Hilbert space and $\varrho$ is an isomorphism between the von Neumann algebras $\pi_1(\mathscr{B}_1)$ and $\pi_2(\mathscr{B}_2)$ then there are central projections $e_i$ in $\mathscr{B}_i$ with $\pi_i(1-e_i) = 0$ and an isomorphism $\lambda$ of $e_1\mathscr{B}_1$ onto $e_2\mathscr{B}_2$ such that $\varrho\,\pi_1(x) = \pi_2\,\lambda(x)$ for each $x$ in $e_1\mathscr{B}_1$.

*Proof.* Since each quotient of a separable C*-algebra $\mathscr{A}$ has a Borel algebra isomorphic to a direct summand in $\mathscr{B}$ (see section 6, Proposition 3) we may assume that the representations $\pi_1$ and $\pi_2$ are faithful on $\mathscr{A}_1$ and $\mathscr{A}_2$.

Let $\mathscr{A}_3$ (resp. $\mathscr{A}_4$) denote the separable C*-algebra generated by $\pi_1(\mathscr{A}_1)$ and $\varrho^{-1}\pi_2(\mathscr{A}_2)$ (resp. $\pi_2(\mathscr{A}_2)$ and $\varrho\pi_1(\mathscr{A}_1)$). Then $\varrho(\mathscr{A}_3) = \mathscr{A}_4$. Choose separable C*-algebras $\mathscr{D}_i$ in $\mathscr{B}_i$ containing $\mathscr{A}_i$ such that $\pi_i(\mathscr{D}_i) \supset \mathscr{A}_{i+2}$. There are then central projections $z_i$ in $\mathscr{B}_i$ such that $\pi_i(1-z_i) = 0$ and $\pi_i$ is injective on $z_i\mathscr{D}_i$ (take $1-z_i$ to be the support projection of the separable set $\ker \pi_i \cap \mathscr{D}_i$).

For each $x$ i $\mathscr{A}_1$ define $\Phi_0(x)$ as the unique element in $z_2\mathscr{D}_2$ satisfying $\pi_2\Phi_0(x) = \varrho\pi_1(x)$. Then $\Phi_0$ is a morphism of $\mathscr{A}_1$ into $\mathscr{B}_2$ (even an isometry). Since $\mathscr{B}_2$ is a Borel algebra there is a unique extension $\Phi_1$ of $\Phi_0$ to a $\sigma$-normal morphism of $\mathscr{B}_1$ into $\mathscr{B}_2$. As $\pi_2\Phi_1(x) = \varrho\pi_1(x)$ for each $x$ in $\mathscr{A}_1$ the same is true for any $x$ in $\mathscr{B}_1$. In the same manner we obtain a $\sigma$-normal morphism $\Phi_2$ of $\mathscr{B}_2$ into $\mathscr{B}_1$ satisfying $\pi_1\Phi_2(x) = \varrho^{-1}\pi_2(x)$ for each $x$ in $\mathscr{B}_2$.

Put $\Psi = \Phi_2\Phi_1$. Then for each $x$ in $\mathscr{B}_1$

$$\pi_1\,\Psi(x) = \pi_1\,\Phi_2\Phi_1(x) = \varrho^{-1}\pi_2\,\Phi_1(x) = \varrho^{-1}\varrho\,\pi_1(x) = \pi_1(x).$$

Let $(x_n)$ be a norm dense sequence in $\mathscr{A}_1$ and for each $n$ let $y_n$ be the central projection supporting $x_n - \Psi(x_n)$. Then $\pi_1(y_n) = 0$, whence $\pi_1(y) = 0$ where $y = \bigvee y_n$; and $(1-y)\,(x_n - \Psi(x_n)) = 0$ for all $n$. Since $(x_n)$ is a generating sequence for $\mathscr{B}_1$ we have $(1-y)\,(x - \Psi(x)) = 0$ for all $x$ in $\mathscr{B}_1$. Define $f_1 = \bigwedge \Psi^n(1-y)$. Then

$$\pi_1(f_1) = \bigwedge \pi_1\,\Psi^n(1-y) = \pi_1(1-y) = 1,$$

so that $\pi_1(1-f_1) = 0$. We have $f_1(x - \Psi(x)) = 0$ for all $x$ in $\mathscr{B}_1$; in particular $f_1(f_1 - \Psi(f_1)) = 0$ so that $f_1 \leq \Psi(f_1)$. In the same manner we obtain a central projection $f_2$ in $\mathscr{B}_2$ with $\pi_2(1-f_2) = 0$ and $f_2 \leq \Phi_1\Phi_2(f_2)$ such that $f_2(x - \Phi_1\Phi_2\,(x)) = 0$ for all $x$ in $\mathscr{B}_2$.

Define $e_1 = f_1\,\Phi_2(f_2)$ and $e_2 = f_2\,\Phi_1(f_1)$. Then

$$\Phi_2(e_2) = \Phi_2(f_2)\,\Phi_2\Phi_1(f_1) \geq \Phi_2(f_2)\,f_1 = e_1,$$

and similarly $\Phi_1(e_1) \geq e_2$. Define $\lambda$ on $e_1\mathscr{B}_1$ by $\lambda(x) = e_2\,\Phi_1(x)$ and $\mu$ on $e_2\mathscr{B}_2$ by $\mu(x) = e_1\,\Phi_2(x)$. If $x \in e_1\mathscr{B}_1$ then

$$\mu\lambda(x) = e_1\,\Phi_2(e_2\,\Phi_1(x)) = e_1\,\Phi_2(e_2)\,\Psi(x) = e_1\,\Psi(x) = e_1\,x = x,$$

and similarly $\lambda\mu(x) = x$ for each $x$ in $e_2\mathscr{B}_2$. Thus $\lambda$ is an isomorphism of $e_1\mathscr{B}_1$ onto $e_2\mathscr{B}_2$ and it is clear that $\pi_2\lambda(x) = \varrho\pi_1(x)$ for each $x$ in $e_1\mathscr{B}_1$.

## 4. The Borel G-algebra associated with an automorphism group of a von Neumann algebra

Let $\mathscr{A}$ be a separable C*-algebra and $G$ a separable locally compact group of automorphisms of $\mathscr{A}$ such that each function $g \to g(x)$, $x \in \mathscr{A}$ is continuous from $G$ to $\mathscr{A}$. By double transposition we may extend $G$ uniquely to a group of automorphisms of $\mathscr{A}''$. The Borel algebra $\mathscr{B}$ of $\mathscr{A}$ is a subset of $\mathscr{A}''$, and since the class of self-adjoint operators $x$ for which $g(x) \in \mathscr{B}$ for all $g$ in $G$ is monotone sequentially closed and contains $\mathscr{A}_{sa}$, it contains $\mathscr{B}_{sa}$. Thus we may regard $G$ as a group of automorphisms of $\mathscr{B}$. We shall refer to this situation by saying that $\mathscr{B}$ is a *Borel G-algebra*.

*Lemma* 1. If $\mathscr{B}$ is a Borel $G$-algebra and $\varphi$ is a bounded functional on $\mathscr{A}$ then for each $x$ in $\mathscr{B}$ the function $g \to \langle g(x), \varphi\rangle$ is Borel measurable on $G$. Moreover, for each $\xi$ in $L^1(G)$ (with respect to a left Haar measure) the element $\xi(x)$ in $\mathscr{A}''$ given by

$$\langle \xi(x), \varphi\rangle = \int_G \langle g(x), \varphi\rangle\, \xi(g)dg$$

belongs to $\mathscr{B}$.

*Proof.* If $x \in \mathscr{A}$ then each function $g \to \langle g(x), \varphi\rangle$ is continuous on $G$ and the element $\xi(x)$ belongs to $\mathscr{A}$. Since the class of self-adjoint operators which satisfy the two conditions in the lemma is monotone sequentially closed and contains $\mathscr{A}_{sa}$, it also contains $\mathscr{B}_{sa}$.

The following result is known (see [1, 3.2 Satz]). For completeness we indicate a proof.

*Lemma* 2. Let $G$ be a separable locally compact group of automorphisms of a von Neumann algebra $\mathscr{M}$ on a separable Hilbert space $H$. If for each $x$ in $\mathscr{M}$ and each pair $\xi, \eta$ in $H$ the function $g \to (g(x)\,\xi|\eta)$ is Borel measurable on $G$ then there is a faithful normal representation $\varrho$ of $\mathscr{M}$ on a separable Hilbert space $K$ and a strongly continuous unitary representation $g \to u_g$ of $G$ on $K$ such that $\varrho(g(x)) = u_g\,\varrho(x)\,u_g^*$. In particular, $G$ is $\sigma$-weakly continuous on $\mathscr{M}$.

*Proof.* Let $K$ be the separable Hilbert space of square integrable functions $\xi$ from $G$ to $H$ with the inner product

$$(\xi|\,\eta) = \int_G (\xi(h)|\,\eta(h))\,dh.$$

Define a strongly continuous unitary representation of $G$ on $K$ by $(u_g\xi)\,(h) = \xi(g^{-1}h)$. By assumption each function $g \to g(x)\xi$, $x \in \mathscr{M}$, $\xi \in H$ is weakly Borel measurable and bounded so that if $\xi \in K$ we may define $\varrho(x)\xi$ in $K$ by $(\varrho(x)\xi)\,(h) = h^{-1}(x)\xi(h)$. It only requires a mildly routine argument to show that $\varrho$ is a faithful normal representation of $\mathscr{M}$ (since $H$ is separable it is enough to check the normality of $\varrho$ on increasing sequences from $\mathscr{M}$, where Lebesgues monotone convergence theorem applies) and that $\varrho(g(x)) = u_g\varrho(x)u_g^*$ for all $x$ in $\mathscr{M}$ and $g$ in $G$.

A $\sigma$-normal representation $\pi$ of a Borel $G$-algebra $\mathscr{B}$ is called *$G$-invariant* if the kernel of $\pi$ is a $G$-invariant ideal in $\mathscr{B}$. The next result characterizes the $G$-invariant representations of $\mathscr{B}$. The equivalence of conditions (iii) and (iv) is due to H. J. Borchers in a more general setting (see [1, 2.3. Theorem]).

*Proposition* 1. Let $\mathscr{A}$ be a separable C*-algebra with Borel algebra $\mathscr{B}$, and $G$ a separable locally compact group for which $\mathscr{B}$ is a Borel $G$-algebra. The following conditions on a representation $\pi$ of $\mathscr{A}$ on a separable Hilbert space are equivalent:

(i) $\pi$ extends to a $G$-invariant representation of $\mathscr{B}$.

(ii) The kernel of $\pi$ in $\mathscr{A}$ is $G$-invariant and the elements in the representation of $G$ as automorphisms of $\pi(\mathscr{A})$ are all extendable to automorphisms of $\pi(\mathscr{B})$.

(iii) The transposed action of $G$ on the dual of $\mathscr{A}$ leaves the predual of $\pi(\mathscr{B})$ invariant (as a subset of the dual of $\mathscr{A}$) and for each $\varphi$ in the predual of $\pi(\mathscr{B})$ the function $g \to g^t(\varphi)$ is norm continuous.

(iv) $\pi$ is quasi-equivalent to a representation $\varrho$ of $\mathscr{A}$ on a separable Hilbert space in which $G$ has a strongly continuous unitary representation $g \to u_g$ such that $\varrho(g(x)) = u_g\,\varrho(x)u_g^*$.

*Proof.* The implications (iv) $\Rightarrow$ (iii) $\Rightarrow$ (ii) are immediate.

To prove (ii) $\Rightarrow$ (i) note first that an automorphism $g$ of $\pi(\mathscr{A})$ is extendable to an automorphism $\bar{g}$ of $\pi(\mathscr{B})$ if and only if $g$ is $\sigma$-weakly continuous on $\pi(\mathscr{A})$. Let $g \to \bar{g}$ denote the representation of $G$ as automorphisms

of $\pi(\mathscr{B})$. Since by assumption $\pi(g(x)) = \bar{g}(\pi(x))$ for all $x$ in $\mathscr{A}_{sa}$ the same is true for all $x$ in the monotone sequential closure $\mathscr{B}_{sa}$ of $\mathscr{A}_{sa}$, which shows that the kernel of $\pi$ in $\mathscr{B}$ is $G$-invariant.

The implication (i) $\Rightarrow$ (iv) follows from Lemma 2 since $G$ acts on $\pi(\mathscr{B})$ as a Borel group by Lemma 1.

For every topological group $G$ of automorphisms of a C*-algebra $\mathscr{A}$ let $\mathscr{A}_c$ denote the C*-subalgebra of $\mathscr{A}$ consisting of those elements $x$ for which the function $g \to g(x)$ is continuous.

*Lemma* 3. Let $\mathscr{M}$ be a von Neumann algebra on a separable Hilbert space and $G$ a separable locally compact group of automorphisms of $\mathscr{M}$ which is $\sigma$-weakly continuous. Then there is a separable $G$-invariant C*-algebra of $\mathscr{M}_c$ which is weakly dense in $\mathscr{M}$.

*Proof.* If $x \in \mathscr{M}$ and $\xi \in L^1(G)$ then the element

$$\xi(x) = \int g(x)\ \xi(g)dg$$

(defined as a weak integral on the pre-dual of $\mathscr{M}$) belongs to $\mathscr{M}$; and if $\xi$ runs through an approximate unit for $L^1(G)$ then $\xi(x)$ converges $\sigma$-weakly to $x$ because $G$ is $\sigma$-weakly continuous. However,

$$g(\xi(x)) = \int h(x)\ \xi(g^{-1}h)\ dh$$

so that

$$\|g(\xi(x)) - \xi(x)\| \leq \|x\| \int |\ \xi(g^{-1}h) - \xi(h)\ |\ dh \to 0$$

as $g$ tends to the identity of $G$. It follows that $\xi(x) \in \mathscr{M}_c$ for each $x$ in $\mathscr{M}$, which shows that $\mathscr{M}_c$ is weakly dense in $\mathscr{M}$.

Choose a separable weakly dense C*-algebra $\mathscr{A}_0$ of $\mathscr{M}_c$. If $(g_k)$ is a countable dense subgroup of $G$ let $\mathscr{A}$ be the C*-algebra generated by $\cup\, g_k(\mathscr{A}_0)$. Clearly $\mathscr{A}$ is separable and weakly dense in $\mathscr{M}$, but since $\mathscr{M}_c$ is $G$-invariant, $\mathscr{A} \subset \mathscr{M}_c$ so that for each $x$ in $\mathscr{A}$ the set $\{g_k(x)\}$ is norm dense in the orbit $G(x)$; whence $G(x) \subset \mathscr{A}$ so that $\mathscr{A}$ is $G$-invariant.

*Theorem* 2. (cf. [8, Theorems 1 and 2]). Let $G$ be a separable locally compact $\sigma$-weakly continuous group of automorphisms of a von Neumann algebra $\mathscr{M}$ on a separable Hilbert space. There is a separable C*-algebra $\mathscr{A}_1$ whose Borel algebra $\mathscr{B}_1$ is a Borel $G$-algebra and a $G$-invariant representation $\pi_1$ such that $\pi_1(\mathscr{B}_1) = \mathscr{M}$.

If $\mathscr{A}_2$, $\mathscr{B}_2$ and $\pi_2$ satisfy the same conditions then there are central $G$-invariant projections $e_1$ and $e_2$ with $\pi_1(1 - e_1) = \pi_2(1 - e_2) = 0$ and an iso-

morphism $\lambda$ of the $e_1\mathscr{B}_1$ onto $e_2\mathscr{B}_2$ which commutes with $G$ and satisfies $\pi_1 = \pi_2\,\lambda$.

*Proof.* The existence of $\mathscr{A}_1$, $\mathscr{B}_1$ and $\pi_1$ follows immediately from Lemma 3. To prove the essential uniqueness we shall repeat the constructions from the proof of Theorem 1 with minor adjustments arising from the action of $G$.

Note first that if $x \in \mathscr{M}_c$ and $(\xi_n)$ is an approximate unit for $L^1(G)$ then $\| x - \xi_n(x) \| \to 0$. Thus for $i = 1, 2$, if $b_i \in \mathscr{B}_i$ with $\pi_i(b_i) = x$ then $\xi_n(b_i) \in \mathscr{B}_i$ by Lemma 1 and as in the proof of Lemma 3 we see that $\xi_n(b_i) \in \mathscr{B}_{ic}$. Since $\pi_i(\xi_n(b_i)) = \xi_n(x)$ we have shown that $\pi_i(\mathscr{B}_{ic}) = \mathscr{M}_c$.

With this in mind we can choose the C*-algebras $\mathscr{D}_i$ as subalgebras of $\mathscr{B}_{ic}$. (The notation is as in the proof of Theorem 1). We may assume that the $\mathscr{D}_i$'s are $G$-invariant, replacing them otherwise with the C*-algebras generated by $\cup\, g_k(\mathscr{D}_i)$, where $(g_k)$ is a countable dense subgroup of $G$. This implies that the support projection $1 - z_i$ of the set $\ker \pi_i \cap \mathscr{D}_i$ is $G$-invariant, thus $z_i\mathscr{D}_i \subset \mathscr{B}_{ic}$. Therefore the morphism $\Phi_1$ of $\mathscr{B}_1$ into $\mathscr{B}_2$ will satisfy $\Phi_1(\mathscr{A}_1) \subset \mathscr{B}_{2c}$. Moreover, since $z_2\mathscr{D}_2$ is $G$-invariant, $\Phi_1(g(x)) = g(\Phi_1(x))$ for each $x$ in $\mathscr{A}_1$ and consequently for all $x$ in $\mathscr{B}_1$. Since a similar statement is true for $\Phi_2$, the endomorphism $\Psi = \Phi_2\Phi_1$ of $\mathscr{B}_1$ will be $G$-invariant. In particular, $\| \Psi(x) - g(\Psi(x)) \| \leq \| x - g(x)) \|$, which shows that $\Psi(\mathscr{B}_{1c}) \subset \mathscr{B}_{1c}$.

Since therefore $x_n - \Psi(x_n) \in \mathscr{B}_{1c}$, the central projection $y_n$ is the limit of an increasing sequence of positive elements from $\mathscr{B}_{1c}$. (With $a_n = |x_n - \Psi(x_n)|$ and $(u_j)$ a dense sequence of unitaries in $\mathscr{A}_1$, put $b_{nk} = \Sigma_{j=1}^{k} u_j^* a_n u_j$. Then $\left(\frac{1}{k} + b_{nk}\right)^{-1} b_{nk} \nearrow y_n$). Replace $y_n$ by $y_n' = \bigvee g_k(y_n)$. Then $y_n'$ is $G$-invariant. In fact, if $g$ is a limit point of $(g_k)$ then for each state $\varphi$ of $\mathscr{A}_1$,

$$\langle g(y_n), \varphi\rangle \leq \liminf \langle g_k(y_n), \varphi\rangle \leq \langle y_n', \varphi\rangle,$$

since $g \to \langle (y_n), \varphi\rangle$ is a lower semi-continuous function on $G$. It follows that $g(y_n') \leq y_n'$, whence $g(y_n') = y_n'$.

We still have $\pi_1(y_n') = 0$ and the construction from the proof of Theorem 1 can now be completed without further alterations. The resulting projections $e_1$ and $e_2$ will be $G$-invariant and since $\Psi$ is already $G$-invariant, so is the isomorphism $\lambda$ from $e_1\mathscr{B}_1$ to $e_2\mathscr{B}_2$.

Simple commutative examples (e.g. rational translations in $L^\infty(\mathbf{R})$) show that even if $G$ is ergodic on $\mathscr{M}$ it may not be possible to find a Borel $G$-algebra $\mathscr{B}$ and a $G$-invariant representation of $\mathscr{B}$ on $\mathscr{M}$ such that $G$ is ergodic on $\mathscr{B}$ (in the strict sense). However, as the next result shows, the

other possibility is excluded. If $G$ is ergodic on $\mathscr{B}$, then it is ergodic in each $G$-invariant representation of $\mathscr{B}$.

*Proposition* 2 (cf. [8, Theorem 3]). Let $\mathscr{B}$ be a Borel $G$-algebra and $\pi$ a $G$-invariant representation on a separable Hilbert space. If $x \in \mathscr{B}$ and $\pi(x)$ is $G$-invariant in $\pi(\mathscr{B})$ then there is a $G$-invariant element $y$ in $\mathscr{B}$ such that $\pi(y) = \pi(x)$.

*Proof.* If $a = \pi(x)$ let $\mathscr{A}_1$ be the separable $G$-invariant C*–algebra generated by $\pi(\mathscr{A})$ and $a$. Since $a \in \pi(\mathscr{B})_c$ we have $\mathscr{A}_1 \subset \pi(\mathscr{B})_c$ so that $G$ is pointwise norm continuous on $\mathscr{A}_1$. With $\mathscr{B}_1$ as the Borel algebra of $\mathscr{A}_1$ we see that $\mathscr{B}_1$ is a Borel $G$-algebra, and the identical representation of $\mathscr{A}_1$ extends to a $G$-invariant representation $\pi_1$ of $\mathscr{B}_1$. By Theorem 2 we can find central $G$-invariant projections $e$ and $e_1$ with $\pi(1-e) = \pi_1(1-e_1) = 0$ and a $G$-invariant isomorphism $\lambda$ of $e_1\mathscr{B}_1$ onto $e\mathscr{B}$ such that $\pi_1 = \pi\lambda$. Set $y = \lambda(e_2 a)$. Then $y$ is $G$-invariant since $e_2 a$ is $G$-invariant and $\pi(y) = \pi_1(e_2 a) = \pi(x)$, as desired.

## 5. Lifting automorphisms from von Neumann algebras

Let again $\mathscr{A}$ be a separable C*-algebra with Borel algebra $\mathscr{B}$. If $\pi$ is a representation of $\mathscr{A}$ on a separable Hilbert space and $G$ is a group of automorphisms of the von Neumann algebra $\pi(\mathscr{B})$ is it then possible to lift $G$ to a group of automorphisms of $\mathscr{B}$ such that $G\pi = \pi G$?

If $\mathscr{A}$ is commutative and $G$ is separable, locally compact and $\sigma$-weakly continuous then this problem has a positive solution. We sketch the argument: The atomic part of $\pi(\mathscr{B})$ is $G$-invariant and corresponds to a direct summand in $\mathscr{B}$. The lifting in this case presents no problems and we assume therefore that $\pi(\mathscr{B})$ contains no minimal projections. By Theorem 2 there is a commutative separable C*-algebra $\mathscr{A}_1$ such that its Borel algebra $\mathscr{B}_1$ is a Borel $G$-algebra, and a $G$-invariant representation $\pi_1$ such that $\pi_1(\mathscr{B}_1) = \pi(\mathscr{B})$. By Theorem 1 there are projections $e$ and $e_1$ with $\pi(1-e) = \pi_1(1-e) = 0$ and an isomorphism $\lambda$ of $e\mathscr{B}$ onto $e_1\mathscr{B}_1$ such that $\pi = \pi_1\lambda$. We have $\mathscr{B} = \mathscr{B}(X)$ and $\mathscr{B}_1 = \mathscr{B}(X_1)$, where $X$ and $X_1$ are standard Borel spaces which are uncountable (hence Borel isomorphic to $\mathbf{R}$) since $\pi(\mathscr{B})$ has no minimal projections. We may identify $1-e$ and $1-e_1$ with Borel subsets $N$ and $N_1$ of $X$ and $X_1$, respectively; and we may assume that they are both uncountable, replacing otherwise $e$ and $e_1$ with slightly smaller projections. Then $N$ and $N_1$ are Borel isomorphic so there is an isomorphism $\lambda_0$ of $(1-e)\mathscr{B}$ onto $(1-e_1)\mathscr{B}_1$. Combining $\lambda$ and $\lambda_0$ we obtain an isomorphism $\lambda_1$ of $\mathscr{B}$ onto $\mathscr{B}_1$

such that $\pi = \pi_1\lambda_1$. Since $\mathscr{B}_1$ is a Borel $G$-algebra we can define $\bar{G} = \lambda_1^{-1}G\lambda_1$ on $\mathscr{B}$ and this gives a lifting of $G$ from $\pi(\mathscr{B})$ to $\mathscr{B}$.

In the general case the problem remains open even when $G$ is a $\sigma$-weakly continuous one-parameter group of automorphisms of $\pi(\mathscr{B})$. We have a positive solution, however, if $G$ is uniformly continuous on $\pi(\mathscr{B})$.

*Theorem* 3. Let $\mathscr{A}$ be a separable C*-algebra with Borel algebra $\mathscr{B}$. If $\pi$ is a representation of $\mathscr{A}$ on a separable Hilbert space and $G$ is a separable uniformly continuous group of automorphisms of the von Neumann algebra $\pi(\mathscr{B})$ then $G$ can be lifted to a uniformly continuous group of automorphisms of $\mathscr{B}$.

*Proof.* Choose a separable C*-algebra $\mathscr{A}_1$ in $\pi(\mathscr{B})$ which is weakly dense. We may assume that $\mathscr{A}_1$ is $G$-invariant, replacing it otherwise with the C*-algebra generated by $\cup\, g_k(\mathscr{A})$, where $(g_k)$ is a countable dense subgroup of $G$. Then $G$ is a uniformly continuous group of automorphisms of $\mathscr{A}_1$, hence by double transposition extends to a uniformly continuous group of automorphisms of $\mathscr{A}_1''$. By restriction we may regard $G$ as a uniformly continuous group of automorphisms of the Borel algebra $\mathscr{B}_1$ of $\mathscr{A}_1$.

By Theorem 1 there are central projections $e$ and $e_1$ with $\pi(1-e) = \pi_1(1-e_1) = 0$ and an isomorphism $\lambda$ of $e\mathscr{B}$ onto $e_1\mathscr{B}_1$ such that $\pi = \pi_1\lambda$. With $(g_k)$ a countable dense subgroup of $G$ define $p_1 = \wedge\, g_k(e_1)$ and $p = \lambda^{-1}(p_1)$. Then $p_1$ is $G$-invariant; for if $g$ is a limit point of $(g_n)$ then

$$g\, g_k(e_1) = \lim g_n g_k(e_1) \geq p_1,$$

whence $g(p_1) \geq p_1$ and since this holds for all $g$ in $G$ we have $g(p_1) = p_1$.

For each $g$ in $G$ and $x$ in $\mathscr{B}$ define

$$\bar{g}(x) = \lambda^{-1}g\lambda(px) + (1-p)\,x.$$

This gives a faithful representation of $G$ as a uniformly continuous group of automorphisms of $\mathscr{B}$, and since for each $x$ in $\mathscr{B}$

$$\pi\bar{g}(x) = \pi\lambda^{-1}g\lambda(px) = \pi_1 g\lambda(px) = g\pi_1\lambda(px) = g\pi(x),$$

this representation is a lifting of $G$.

*Corollary.* If $\pi$ is a representation of $\mathscr{A}$ on a separable Hilbert space and $G$ is a countable group of automorphisms of the Neumann algebra $\pi(\mathscr{B})$, then $G$ can be lifted to a group of automorphisms of $\mathscr{B}$.

## 6. The isomorphism problem

One enormous simplification in the theory of standard spaces is that there are only countably many Borel isomorphism classes and that the cardinality is a complete invariant for each class. In the non-commutative situation very little is known about C*-algebras having isomorphic Borel algebras. But with uncountably many different von Neumann factors around it seems improbable that there should be only a countable number of isomorphism classes of Borel algebras.

The type I situation is completely known. If $H_n$ is an $n$-dimensional Hilbert space, $1 \leq n \leq \infty$, and $X_n$ is a standard Borel space let $\mathscr{B}(X_n, B(H_n))$ denote the algebra of bounded weakly Borel measurable functions from $X_n$ to $B(H_n)$. If $\mathscr{A}$ is a separable C*-algebra of type I then its Borel algebra is isomorphic to an algebra $\Sigma^{\oplus} \mathscr{B}(X_n, B(H_n))$ by [11, Proposition 7] (see also [2, Theorem 4.5]). Each isomorphism class is therefore determined by a sequence of standard spaces, one from each dimension. In particular there are only countably many isomorphism classes in each dimension.

It is evidently a problem of great interest to determine when two C*-algebras have isomorphic Borel algebras. If so they have the same representations, and these representations can be decomposed in the same manner. Moreover, there is an affine Borel isomorphism between their state spaces. The isomorphism classes are much more unstable in the non-commutative theory than usual. For example, by adjoining a unit to a C*-algebra one may obtain a C*-algebra which is not Borel equivalent to the former; simply because the latter has a one-dimensional representation while the former may have none. The next result provides us with some examples of non-isomorphic C*-algebras whose Borel algebras are isomorphic.

*Proposition* 3. Let $\mathscr{A}$ be a separable C*-algebra and $\mathscr{I}$ a closed ideal of $\mathscr{A}$. Then the Borel algebra of $\mathscr{A}$ is isomorphic to that of $\mathscr{I} \oplus \mathscr{A}/\mathscr{I}$.

*Proof.* Let $z$ be the central projection in the Borel algebra $\mathscr{B}$ of $\mathscr{A}$ obtained as the supremum of any approximate unit for $\mathscr{I}$. Then $\mathscr{I} = z\mathscr{B} \cap \mathscr{A}$ and $\mathscr{A}/\mathscr{I} = (1-z)\mathscr{A}$; and if $H$ is the universal Hilbert space for $\mathscr{A}$ then $zH$ and $(1-z)H$ are the universal Hilbert spaces for $\mathscr{I}$ and $\mathscr{A}/\mathscr{I}$, respectively. It follows that the Borel algebra of $\mathscr{I}$ is $z\mathscr{B}$ and the Borel algebra of $\mathscr{A}/\mathscr{I}$ is $(1-z)\mathscr{B}$, and this completes the proof.

*Problem.* Do all hyperfinite C*-algebras have isomorphic Borel algebras.

## References


[1] H. J. Borchers, Über C*-Algebren mit lokalkompakten Symmetriegruppen. Nachr. Göttinger Akad. 1973 Nr. 1.

[2] E. B. Davies, On the Borel structure of C*-algebras. Commun. math. Phys., **8** (1968), 147–163.

[3] J. Dixmier, Les C*algèbres et leurs représentations. Gauthier-Villars, Paris, 1964.

[4] E. G. Effros, The canonical measures for a separable C*-algebra. Amer. J. Math., **92** (1970), 56–60.

[5] R. Haag, R. V. Kadison and D. Kastler, Nets of C*-algebras and Classification of States. Commun. math. Phys. **16** (1970), 81–104.

[6] R. V. Kadison, Unitary invariants for representations of operator algebras. Ann. of Math., **66** (1957), 304–379.

[7] G. W. Mackey, Borel structure in groups and their duals. Trans. Amer. Math. Soc., **85** (1957), 134–165.

[8] G. W. Mackey, Point realizations of transformation groups. Illinois J. Math., **6** (1962), 327–335.

[9] J. von Neumann, Einige Sätze über messbare Abbildungen. Ann. of Math., **33** (1932), 574–586.

[10] G. K. Pedersen, Measure theory for C*-algebras III. Math. Scand. **25** (1969), 71–93.

[11] G. K. Pedersen, On weak and monotone $\sigma$-closures of C*-algebras. Commun. math. Phys., **11** (1969), 221–226.

[12] G. K. Pedersen, Monotone closures in operator algebras. Amer. J. Math., **94** (1972), 955–962.

[13] G. K. Pedersen, Applications of weak* semicontinuity in C*-algebra theory. Duke Math. J., **39** (1972), 431–450.


Indleveret til Selskabet den 23. april 1974.
Færdig fra trykkeriet den 14. oktober 1974.

JØRGEN KALCKAR AND OLE ULFBECK

# ON THE PROBLEM OF GRAVITATIONAL RADIATION

Det Kongelige Danske Videnskabernes Selskab
Matematisk-fysiske Meddelelser **39**, 6


Kommissionær: Munksgaard
København 1974

## Synopsis

The problem of gravitational radiation is discussed. First, from classical electrodynamics those basic principles are isolated, the joint validity of which implies the occurrence of electromagnetic radiation, and it is investigated to what extent conclusions regarding gravitational radiation can be based solely on the same premises. Next, the consequences are explored of introducing new features, which – like the Equivalence Principle – distinguish between gravitational and electromagnetic interactions.



PRINTED IN DENMARK
BIANCO LUNOS BOGTRYKKERI A/S
ISBN 87 7304 040 1

In spite of the far reaching formal completeness of the General Theory of Relativity, the inherent conceptual and mathematical difficulties of the scheme, together with the absence of conclusive empirical evidence, has sustained the discussion of the problem of gravitational radiation, ever since the original work of Einstein* on the energy loss from a spinning rod.

In this situation it may be of interest to isolate from classical electrodynamics those basic principles, the joint validity of which implies the occurrence of electromagnetic radiation, and investigate to what extent conclusions regarding gravitational radiation can be based solely on the same premises. Having clarified this problem, one may then as a next step explore the consequences of the introduction of new features, which – like the Equivalence Principle – distinguish between gravitational and electromagnetic interactions.

The clue to the radiation problem is to be found in the limitations in the possibility of accounting for the instantaneous energy balance for a system of interacting particles solely in terms of the particle degrees of freedom. Clearly, no such limitations exist in the purely static case, and consequently, from this point of view, the impartion of energy to a static field must be regarded as a matter of convention. Quite a different situation is met with in the case of time varying charge and current distributions. Due to the retardation of physical actions, the field now represents independent degrees of freedom of the total system, which can only be ignored or eliminated at the expense of giving up the notion of instantaneous energy momentum balance.**

To illustrate this interrelationship in the case of electrodynamics, we consider two particles of charge $Q$ — originally at rest at a relative distance

* A. Einstein, Sitzungsberichte der Preuss. Akad., Berlin, p. 688 (1916); p. 154 (1918).

** A comprehensive discussion of these problems is given in a treatise shortly to appear in Kgl. Vid. Selsk. Med.

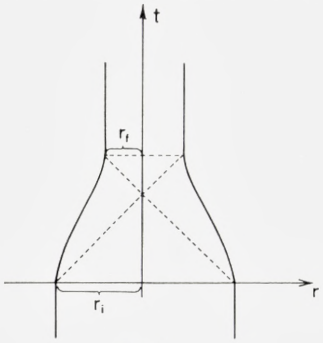


Fig. 1

$2r_i$ —, which are moved simultaneously and symmetrically towards each other to a relative distance $2r_f$ ($r_f < r_i$), where they stay at rest (see figure 1). If the process is carried out adiabatically, the external work performed equals the change in potential energy

$$W_{ad} = \frac{Q^2}{2r_f} - \frac{Q^2}{2r_i}. \tag{1}$$

If, however, the process is carried out in a finite time, the work required will in general, as a consequence of the retardation, differ from $W_{ad}$.

Suppose that the duration of the process, $\Delta t$, is chosen so that

$$r_i - r_f < c\Delta t \leq r_i + r_f, \tag{2}$$

which implies that the electromagnetic force on each particle due to the other one during the entire motion is given by the original static Coulomb field. In this case, the work required to overcome the electrostatic repulsion only amounts to

$$2\left(\frac{Q^2}{r_i + r_f} - \frac{Q^2}{2r_i}\right). \tag{3}$$

The very fact that this work differs from the change in potential energy (1) faces us with the choice of either giving up the customary idea of energy conservation, or recognizing the existence of some non-conservative force acting on each particle independently of the motion of the other since during the process considered no communication is possible between the particles. Within the customary mechanical framework the non-conservative character of this "damping force" is interpreted as a manifestation of an

independent set of degrees of freedom with which the particles may interact and exchange energy, the damping force being just a phenomenological way of taking this interaction into account.

Reconsidering now the above process in this extended framework, we notice that the external work, $W_D$, required to overcome the damping force on each particle during the displacement must, for symmetry reasons, be the same for both particles and, according to its definition, independent of the motion of the other. Thus the total energy to be supplied is not given by eq. (3) but by the relation

$$W = 2\left(\frac{Q^2}{r_i + r_f} - \frac{Q^2}{2r_i} + W_D\right), \tag{4}$$

where $W_D$ is related to the hypothetical "radiation energy" $\mathscr{E}_R$ by the requirement of energy balance

$$\mathscr{E}_R + \frac{Q^2}{2r_f} = W + \frac{Q^2}{2r_i}. \tag{5}$$

Hence:

$$2W_D - \mathscr{E}_R = Q^2 \frac{(r_i - r_f)^2}{2r_i r_f (r_i + r_f)}. \tag{6}$$

Whereas this expression is still compatible with a complete absence of radiation, corresponding to $\mathscr{E}_R = 0$, evidently, $\mathscr{E}_R$ and $W_D$ cannot *both* vanish. Furthermore, the fact that, according to the initial conditions, $\mathscr{E}_R \geqq 0$, implies that $W_D$ is positive definite, reflecting the irreversible character of the process of radiation emission.

Consider now in particular the case in which the equality sign in eq. (2) holds, i.e.

$$c\Delta t = r_i + r_f \tag{7}$$

and assume for simplicity that

$$\Delta r \equiv r_i - r_f \ll c\Delta t. \tag{8}$$

Then, eq. (6) may be rewritten in the suggestive form

$$2W_D - \mathscr{E}_R = 2\frac{Q^2}{c^3}\left(\frac{\Delta r}{(\Delta t)^2}\right)^2 \Delta t. \tag{9}$$

So far we cannot draw any conclusions as to the individual value of $W_D$ and $\mathscr{E}_R$. However, since $W_D$, as already noticed, is independent of the

motion of the other particle, it may be determined by considering another process, in which only one of the particles is displaced along the same world line as before, whereas the other is kept fixed. Denoting by $E_R$ the energy transferred to the radiation field during this process, the energy balance now yields the relation:

$$E_R + \frac{Q^2}{r_i + r_f} = \tfrac{1}{2} W + \frac{Q^2}{2 r_i}, \tag{10}$$

where $W$ is given by eq. (4) as before. Hence it follows that

$$E_R = W_D. \tag{11}$$

Since the role of the fixed charge in this process is purely auxiliary, we may conclude, that whenever a charge, $Q$, is displaced a distance $\Delta r$ during a time $\Delta t$, being at rest outside this time interval, a positive net external work equal to $W_D$ has to be performed. In view of the relation (11), it is immediately clear that eq. (6) simply expresses the amount of interference in the radiation process considered. Combined with simple invariance requirements, this fact fixes, as we shall now see, the absolute rate of radiative energy loss from the individual particle.

For the following discussion it is convenient to generalize the above experiment to include arbitrary but small displacements of the two charges. Introducing the change in dipolemoment

$$\Delta \vec{d}_1 = Q_1 \Delta \vec{x}_1, \; \Delta \vec{d}_2 = Q_2 \Delta \vec{x}_2, \tag{12}$$

the equation (9) is now easily seen to be replaced by

$$\mathscr{E}_R - E_R^{(1)} - E_R^{(2)} = - \frac{\Delta \vec{d}_1 \cdot \Delta \vec{d}_2 - 3(\Delta \vec{d}_1 \cdot \hat{e})(\Delta \vec{d}_2 \cdot \hat{e})}{(c \Delta t)^3} \tag{13}$$

where $\hat{e}$ denotes the unit vector along the line of connection of the particles.

As far as the energy loss from the displacement of a single particle is concerned, the demand that the rate contains $Q^2$ as a factor, requires it for dimensional reasons to be proportional to $1/c^3$ times the square of the acceleration.* Furthermore, due to the assumption of rotational invariance, the square of the acceleration $\ddot{\vec{x}}$ can only occur in the combinations $\ddot{\vec{x}}^2$ and

* The product $(\dddot{\vec{x}} \cdot \dot{\vec{x}})$ is rejected by the demand that the rate be proportional to the square of a field of the proper dimension decreasing like $1/r$.

$(\ddot{\vec{x}} \cdot \hat{n})^2$, where $\hat{n}$ defines the direction of observation, or equivalently, in spherical components*

$$\left| \sum_{\mu} \ddot{x}_{\mu}^{*} \mathscr{D}^{1}_{\mu h}(\hat{n}) \right|^2, \qquad h = 0, \pm 1 \tag{14}$$

$\mathscr{D}^{j}_{mm'}$ denoting the well-known rotation matrices. Finally, the fact that we are dealing with a transverse vector field excludes the case $h = 0$. Since the invariants corresponding to $h = 1$ and $h = -1$ are identical, the rate of energy loss must then be of the form

$$\frac{d^2 E_R}{d\Omega dt} = \alpha \frac{1}{c^3} \left| \sum_{\mu} \ddot{d}_{\mu}^{*}(t_{\text{ret}}) \mathscr{D}^{1}_{\mu 1}(\hat{n}) \right|^2, \tag{15}$$

where $\vec{d} = Q\vec{x}$ and $\alpha$ is a numerical constant.

To determine the unknown constant $\alpha$, we apply the general expression (15) to calculate, in the case of the experiment discussed above, the amount of interference also given by eq. (13). According to eq. (15) the total energy loss, $\mathscr{E}_R$, from the two particles amounts to

$$\mathscr{E}_R = \frac{\alpha}{c^3} \int\int d\Omega dt \left| \sum_{\mu} \{ \ddot{d}_{\mu}^{(1)*}(t_{\text{ret}}^{(1)}) + \ddot{d}_{\mu}^{(2)*}(t_{\text{ret}}^{(2)}) \} \mathscr{D}^{1}_{\mu 1}(\hat{n}) \right|^2, \tag{16}$$

where the relation between the time and angle variables is evident from figure 2. In fact, since the displacement of the individual particle is assumed to be small compared to their mutual distance $c\Delta t$, we have

$$\left.\begin{aligned} t_{\text{ret}}^{(1)} &= t - R_1/c \simeq t - R/c - \frac{\Delta t}{2}\cos\theta \\ t_{\text{ret}}^{(2)} &= t - R_2/c \simeq t - R/c + \frac{\Delta t}{2}\cos\theta . \end{aligned}\right\} \tag{17}$$

From eq. (16) we immediately get the interference term

$$\mathscr{E}_R - E_R^{(1)} - E_R^{(2)} = \frac{2\alpha}{c^3} \int\int d\Omega dt \, Re\{ \sum_{\mu\mu'} \ddot{d}_{\mu}^{(1)*} \ddot{d}_{\mu'}^{(2)} \mathscr{D}^{1}_{\mu 1}(\hat{n}) \mathscr{D}^{1}_{\mu' 1}{}^{*}(\hat{n}) \}, \tag{18}$$

* Since the use of spherical tensors greatly facilitates the computations in the gravitational case, we employ also here the same technique.

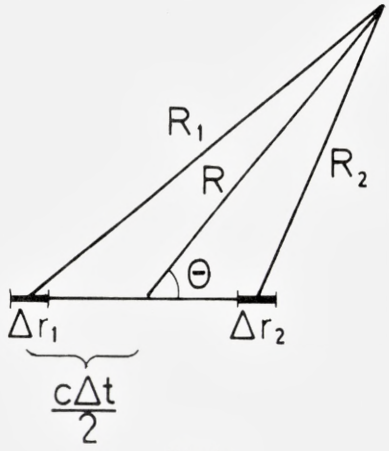


Fig. 2

where the axial symmetry around the $z$-axis, chosen along the line of connection between the particles, restricts the summation to the terms with $\mu = \mu'$.

Now, coupling the $\mathscr{D}$-functions, in the usual manner, by means of Clebsch-Gordan coefficients, we obtain*

$$\left.\begin{aligned} &\mathscr{E}_R - E_R^{(1)} - E_R^{(2)} = \\ &\frac{2\alpha}{c^3}\sum_{\lambda}(-)^{h=1}\langle 11\ 1\ -1\,|\,\lambda 0\rangle \int\int d\Omega dt\,(\ddot{d}^{(1)}\ddot{d}^{(2)})_{11;\lambda 0}\mathscr{D}^{\lambda}_{00}(\hat{n}). \end{aligned}\right\} \tag{19}$$

Replacing through the relation (17) the variables $t$ and $\cos\theta$ by $t_1 \equiv t_{\text{ret}}^{(1)}$ and $t_2 \equiv t_{\text{ret}}^{(2)}$, the eq. (19) takes the form

$$\left.\begin{aligned} &\mathscr{E}_R - E_R^{(1)} - E_R^{(2)} = \\ &-\frac{4\pi\alpha}{c^3}\sum_{\lambda}\langle 11\ 1\ -1\,|\,\lambda 0\rangle \int_0^{\Delta t}\int_0^{\Delta t}\frac{dt_1\,dt_2}{\Delta t}(\ddot{d}^{(1)}(t_1)\ddot{d}^{(2)}(t_2))_{11;\lambda 0}\mathscr{D}^{\lambda}_{00}\left(\frac{t_2 - t_1}{\Delta t}\right). \end{aligned}\right\} \tag{20}$$

Finally, integrating by part once in each variable, we note that only the term with $\lambda = 2$ survives, and we are left with

* We are here taking advantage of a notation for the coupling of spherical tensors, so convincingly recommended for its flexibility in a recent booklet on Nuclear Structure by A. Bohr and B. Mottelson:

$$(d^{(1)}d^{(2)})_{11;\lambda\mu} \equiv \sum_{\mu'\mu''}\langle 1\mu'\,1\mu''\,|\,\lambda\mu\rangle\, d^{(1)}_{\mu'}\,d^{(2)}_{\mu''}.$$

The phase conventions employed in the present paper are identical to those of the mentioned authors.

$$\left.\begin{aligned} \mathscr{E}_R - E_R^{(1)} - E_R^{(2)} &= -\frac{4\pi\alpha}{c^3}\langle 11\,1\,-1|20\rangle \frac{1}{\Delta t}(\Delta d^{(1)}\Delta d^{(2)})_{11;\,20}\cdot\frac{(-3)}{(\Delta t)^2} \\ &= 2\pi\alpha\sqrt{6}\,\frac{(\Delta d^{(1)}\Delta d^{(2)})_{11;\,20}}{(c\Delta t)^3}. \end{aligned}\right\} \tag{21}$$

Comparing this result with eq. (13), rewritten in spherical components:

$$\mathscr{E}_R - E_R^{(1)} - E_R^{(2)} = \sqrt{6}\,\frac{(\Delta d^{(1)}\Delta d^{(2)})_{11;\,20}}{(c\Delta t)^3}, \tag{13'}$$

we conclude that

$$\alpha = \frac{1}{2\pi}. \tag{22}$$

It needs hardly be emphasized that the argumentation has not aimed at the determination *per se* of the numerical value of the constant $\alpha$, but at the elucidation of the assumptions which are crucial for such a determination. On the one hand, the existence of radiation is implied by the equations (6) and (11), which in turn rest solely on the principles of energy conservation and retardation. The answer to the further question as to the amount of radiation, emitted in a given process, demanded on the other hand explicit assumptions regarding the tensorial character of the field.

In the spirit of the above discussion, we shall commence the analysis of the gravitational case by exploring the consequences immediately to be deduced from the form of the static interaction (Newton's law), the requirement of energy balance and retardation. To exhibit most clearly the interplay of the various assumptions, it is essential to employ a sufficiently general formalism.

With the purpose of deriving relations analogous to eqs. (9) and (11), let us consider the gravitational interaction energy between two bodies which are widely separated compared to their dimensions (see figure 3).
Denoting by $\vec{r}$ the vector joining two fixed points, situated inside the bodies, the interaction energy becomes*

$$\mathscr{U} = -G\int d\vec{r}_1 d\vec{r}_2 \frac{\sigma_1(\vec{r}_1)\,\sigma_2(\vec{r}_2)}{|\vec{r}+\vec{r}_1-\vec{r}_2|}, \tag{23}$$

* The question of the interaction energy associated with the mass currents in the two bodies is not touched upon here. Accordingly, the following discussion is restricted to gravitational radiation of the "electric multipole" type.

where $\sigma$ denotes the gravitational charge density, $G$ the gravitational constant and the integration variables $\vec{r}_1$ and $\vec{r}_2$ are measured from the two fixed points mentioned. It is immediately clear, that the expansion of the rotational invariant $1/|\vec{r} + \vec{r}_1 - \vec{r}_2|$ must have the form*


Fig. 3

$$\left.\begin{aligned} &\frac{1}{|\vec{r} + \vec{r}_1 - \vec{r}_2|} = \\ &\sqrt{4\pi} \sum_{\lambda_1 \lambda_2 \lambda} (-)^{\lambda} A(\lambda, \lambda_1, \lambda_2) \frac{r_1^{\lambda_1} r_2^{\lambda_2}}{r^{\lambda+1}} (Y_{\lambda_1}(\hat{r}_1) Y_{\lambda_2}(\hat{r}_2) Y_{\lambda}(\hat{r}))_{(\lambda_1\lambda_2)\lambda\lambda;\,00} \end{aligned}\right\} \tag{24}$$

where the subscript again specifies the coupling scheme. For dimensional reasons the summation must be restricted to terms for which $\lambda = \lambda_1 + \lambda_2$, and by considering the special case, where $\vec{r}_1$, $\vec{r}_2$ and $\vec{r}$ are all parallel, the coefficients $A(\lambda, \lambda_1, \lambda_2)$ are easily found to be

$$A(\lambda, \lambda_1, \lambda_2) = (-1)^{\lambda_1} \delta(\lambda_1 + \lambda_2 - \lambda) 4\pi \sqrt{\frac{(2\lambda_1 + 2\lambda_2)!}{(2\lambda_1 + 1)!(2\lambda_2 + 1)!}}. \tag{25}$$

Introducing the gravitational charge multipole moments for the first body,

$$Q^{(1)}_{\lambda\mu} = \int d\vec{r}_1 \sigma(\vec{r}_1) r_1^{\lambda} Y_{\lambda\mu}(\hat{r}_1), \tag{26}$$

and analogously for the second, the expansion of the interaction energy thus takes the form

$$\mathcal{U} = -G \sum_{\lambda_1 \lambda_2 \lambda} \sqrt{4\pi} (-1)^{\lambda} A(\lambda, \lambda_1, \lambda_2) \frac{(Q^{(1)}_{\lambda_1} Q^{(2)}_{\lambda_2} Y_{\lambda}(\hat{r}))_{(\lambda_1\lambda_2)\,\lambda\lambda;\,00}}{r^{\lambda+1}}. \tag{27}$$

Choosing the $z$-axis in the direction $\hat{r}$, eq. (27) reduces to

$$\mathcal{U} = -G \sum_{\lambda_1 \lambda_2 \lambda} A(\lambda, \lambda_1, \lambda_2) \frac{(Q^{(1)}_{\lambda_1} Q^{(2)}_{\lambda_2})_{\lambda_1\lambda_2;\,\lambda 0}}{r^{\lambda+1}}. \tag{28}$$

* See also K. Alder and Aa. Winther, Nuclear Physics A132 (1969) 1.

Let us consider rigid motions of the two bodies, assuming for simplicity the displacement of any point of the bodies to be small, compared to their mutual distance. For an adiabatic process, the external work performed equals the change in the potential energy (28). However, if the process is carried out in a finite time, $\Delta t$, the external work, $W$, required, will — owing to the dependence of the interaction energy on the mutual orientation of the bodies — differ from its adiabatic value, when the retardation is taken into account. Considering, as before, the case* $c\Delta t = r$, the work $W$ is given by

$$W = -G\sum_{\lambda_1\lambda_2\lambda} A(\lambda, \lambda_1, \lambda_2) \frac{[Q^{(1)}_{\lambda_1}(0)\Delta Q^{(2)}_{\lambda_2} + \Delta Q^{(1)}_{\lambda_1} Q^{(2)}_{\lambda_2}(0)]_{\lambda_1\lambda_2;\,\lambda 0}}{(c\Delta t)^{\lambda+1}} + W_D^{(1)} + W_D^{(2)}, \quad (29)$$

where $Q(0)$ refers to the initial value of the multipole moment in question and $\Delta Q$ to its change. Thus, the first term in eq. (29) is obtained as the external work required to change the multipole moment of the second body in the original multipole field of the first, and vice versa, whereas $W_D^{(1)}$ and $W_D^{(2)}$ denotes the externally supplied energy to overcome the damping force. Clearly, just as in the electromagnetic case, the damping force acting on each body is independent of the motion of the other.

As a next step energy conservation is invoked in a form which leaves room for a possible gravitational "radiation energy", $\mathscr{E}_R$:

$$\mathscr{U}(t = 0) + W = \mathscr{U}(t = \Delta t) + \mathscr{E}_R \quad (30)$$

or — by means of eqs. (28) and (29) —

$$\mathscr{E}_R - W_D^{(1)} - W_D^{(2)} = G \sum_{\lambda_1\lambda_2\lambda} A(\lambda, \lambda_1, \lambda_2) \frac{(\Delta Q^{(1)}_{\lambda_1} \Delta Q^{(2)}_{\lambda_2})_{\lambda_1\lambda_2;\,\lambda 0}}{(c\Delta t)^{\lambda+1}}. \quad (31)$$

Again, considering a process in which only the first body is moved, the second being kept fixed, one concludes, in analogy to eq. (11), that $W_D^{(1)}$ equals the radiative energy loss, $E_R^{(1)}$, suffered by the first body under these circumstances. Specializing for the sake of simplicity to the case where only a single multipole moment, of order $\lambda$, is changed in each body, one obtains

* The choice of the velocity $c$ in the present context does not amount to assuming that gravity propagates with the velocity of light, but merely that the propagation velocity does not exceed the light velocity.

in strict analogy* to eq. (13′)

$$\mathscr{E}_R - W_D^{(1)} - W_D^{(2)} = GA(2\lambda, \lambda, \lambda) \frac{(\Delta Q_\lambda^{(1)} \Delta Q_\lambda^{(2)})_{\lambda\lambda;\, 2\lambda\, 0}}{(c\Delta t)^{2\lambda+1}}. \tag{32}$$

Having thus obtained the interference term, we proceed to determine the general form of the radiative energy loss from a time varying multipole moment of order $\lambda$. Again, from dimensional arguments and rotational invariance (cf. also footnote on page 6), the rate can only depend on the invariants

$$\frac{G}{c^{2\lambda+1}} \left| \sum_\mu {}^{(\lambda+1)}Q^*_{\lambda\mu}\, \mathscr{D}^\lambda_{\mu h}(\hat{n}) \right|^2, \quad h = \lambda, \lambda-1, \ldots, 0, \tag{33}$$

where $\hat{n}$ defines the direction of observation and ${}^{(\lambda+1)}Q_{\lambda\mu}$ denotes the $(\lambda+1)$-fold time derivative of $Q_{\lambda\mu}$. Clearly, the $(\lambda+1)$ invariants (33) correspond in terms of cartesian components to the possible quadratic invariants formed of a symmetric, traceless tensor of rank $\lambda$ and the vector $\hat{n}$.

Relying on the analogy to the case of electromagnetism, the idea suggests itself, that the rate of energy loss can only depend on such a combination of the invariants, which can be interpreted as a quadratic rotational invariant formed from some tensor field describing a definite spin $s$. Any such field can be expanded in terms of tensor spherical harmonics

$$\mathscr{D}^\lambda_{\mu h}(\hat{n})\, \varepsilon^s_h(\hat{n}) \qquad \begin{array}{l} \lambda = s, s+1, \ldots \infty \\ \mu = \lambda, \lambda-1, \ldots -\lambda;\ h = s, s-1, \ldots -s, \end{array}$$

where the $2s+1$ unit polarization tensors $\varepsilon^s_h$ (each of which of course carries the appropriate cartesian indices) necessarily become orthogonal to each other for different values of $h$, if they are defined so as to transform irreducibly into each other according to the unitary representation $\mathscr{D}^s$. Thus, each of the invariants (33) has the form of the square of a tensor spherical harmonic with definite $h$ and definite amplitude.

Although the question of the propagation velocity of gravity has been left open in the argumentation so far, nevertheless the form of Newton's

* By the comparison of (32) and (13′) it must be borne in mind that the definition of the electric dipole moment, $d_\mu$, differs from the corresponding mass moment (26) by a factor:

$$d_\mu = \sqrt{\frac{4\pi}{3}} \int d\vec{r}\; r\varrho(\vec{r})\, Y_{1\mu}(\hat{r}).$$

Furthermore, there is an overall change of sign, due to the difference in sign of the basic interactions.

law suggests that gravity propagates with the velocity of light, and thus it is expected that only the two "helicity" amplitudes corresponding to $h = \pm s$ are present in the expansion of the free field. Hence the rate of gravitational radiative energy loss of multipole order $\lambda (\geqslant s)$ must have the general form

$$\frac{d^2E_R}{d\Omega dt} = \alpha_\lambda \frac{G}{c^{2\lambda+1}} \left| \sum_\mu {}^{(\lambda+1)}Q^*_{\lambda\mu} \mathscr{D}^\lambda_{\mu h=s}(\hat{n}) \right|^2, \tag{34}$$

where $\alpha_\lambda$ is a numerical constant.

To determine this constant, we apply the general expression (34) to calculate, in the case of the experiment discussed above, the amount of interference, also given by eq. (32). According to eq. (34), the total energy loss, $\mathscr{E}_R$, from the two bodies amounts to

$$\mathscr{E}_R = \frac{\alpha_\lambda G}{c^{2\lambda+1}} \int\int d\Omega dt \left| \sum_\mu \left\{ {}^{(\lambda+1)}Q^{(1)}_{\lambda\mu}(t^{(1)}_{\text{ret}}) + {}^{(\lambda+1)}Q^{(2)}_{\lambda\mu}(t^{(2)}_{\text{ret}}) \right\} \mathscr{D}^{\lambda *}_{\mu s}(\hat{n}) \right|^2 \tag{35}$$

where $t^{(1)}_{\text{ret}}$ and $t^{(2)}_{\text{ret}}$ are again given by eq. (17). Hence, by steps strictly analogous to those leading to eq. (20), one obtains the interference term

$$\left.\begin{aligned} \mathscr{E}_R - E^{(1)}_R - E^{(2)}_R &= \frac{4\pi\alpha_\lambda G}{c^{2\lambda+1}} \sum_{\lambda'} (-1)^s \langle \lambda s \; \lambda \; -s | \lambda' 0 \rangle \cdot \\ \cdot \int_0^{\Delta t} \int_0^{\Delta t} \frac{dt_1 dt_2}{\Delta t} \Big[ {}^{(\lambda+1)}Q^{(1)}_\lambda(t_1) \; {}^{(\lambda+1)}Q^{(2)}_\lambda(t_2) \Big]_{\lambda\lambda;\lambda' 0} \mathscr{D}^{\lambda'}_{00}\left( \frac{t_2 - t_1}{\Delta t} \right), & \end{aligned}\right\} \tag{36}$$

where it is again understood that the $z$-axis is chosen along the line of connection of the two bodies.

Integrating by part $\lambda$ times in each variable, we note that only the term with $\lambda' = 2\lambda$ survives, and since, moreover, the coefficient to the highest power of $\dfrac{t_2 - t_1}{\Delta t}$ in $\mathscr{D}^{2\lambda}_{00}$ is

$$\frac{(4\lambda)!}{2^{2\lambda}((2\lambda)!)^2},$$

one is left with

$$\left.\begin{aligned} &\mathscr{E}_R - E_R^{(1)} - E_R^{(2)} = \\ &4\pi\alpha_\lambda G(-)^s\langle\lambda s\ \lambda\ -s|2\lambda\ 0\rangle\frac{(\Delta Q_\lambda^{(1)}\,\Delta Q_\lambda^{(2)})_{\lambda\lambda;\,2\lambda\,0}}{(c\Delta t)^{2\lambda+1}}(-)^\lambda(2\lambda)!\,\frac{(4\lambda)!}{2^{2\lambda}((2\lambda)!)^2}\cdot \end{aligned}\right\} \quad (37)$$

Comparing this result with eq. (32), and inserting the value for $A(2\lambda, \lambda, \lambda)$ given by eq. (25), one obtains

$$\alpha_\lambda = (-)^s\frac{2^{2\lambda}}{(2\lambda+1)!\sqrt{(4\lambda)!}}\cdot\frac{1}{\langle\lambda s\ \lambda\ -s|2\lambda\ 0\rangle}. \quad (38)$$

Since the Clebsch-Gordan coefficient is positive for all $s \leq \lambda$, the demand that $\alpha_\lambda$ be positive requires the rank $s$ to be even. If the basic interaction had been repulsive, as in electrodynamics, the interference term had changed sign, and the conslusion had been that $s$ were odd.

More specific conclusions regarding the possible spin values, $s$, can be drawn by noticing that the relation (32) definitely predicts the occurrence of multipole radiation of any order unless some principle forbids the change of one or more multipole moments for an isolated system. Thus, in the case of electromagnetism, where the smallest possible value of $s$ is one, the necessary prohibition of a change in the monopole moment is expressed by the principle of charge conservation. In the case of gravity, where the empirically established equivalence between gravitational and inertial mass requires the gravitational charge density to be identified with the energy density, the conservation laws for energy and momentum prohibit the change of both monopole and dipole moments, at least in the limit where an unambiguous distinction between source and field is possible. Barring *ad hoc* assumptions to exclude the change of higher multipole moments, the spin of the gravitational field can therefore only be zero or two* Clearly, only the value $s = 2$ is immediately compatible with the fact that the energy density is a component of a four-tensor.

Returning to eq. (38) , we obtain for $\alpha_\lambda$ in the case $s = 2$

$$\alpha_\lambda = (2\lambda+1)\left\{\frac{1}{[(2\lambda+1)!!]^2}\cdot\frac{\lambda+1}{\lambda}\right\}\cdot\frac{\lambda+2}{\lambda-1}. \quad (39)$$

which only differs from the well-known result of electromagnetism by the ratio

* If, for instance, the value of $s$ had been four, some mechanism had to be in operation to ensure conservation of the quadrupole and octupole moments appearing in eq. (32).

$$\frac{\langle \lambda 1 \; \lambda -1 | 2\lambda \, 0 \rangle}{\langle \lambda 2 \; \lambda -2 | 2\lambda \, 0 \rangle} = \frac{\lambda + 2}{\lambda - 1}. \tag{40}$$

For the case of special interest, $\lambda = 2$, eq. (34) then reads

$$\frac{d^2 E_R}{d\Omega dt} = \frac{2}{15} \frac{G}{c^5} \left| \sum_{\mu} \ddot{Q}^*_{2\mu} \mathscr{D}^2_{\mu 2}(\hat{n}) \right|^2, \tag{41}$$

which, in terms of the cartesian components of the mass quadrupole moment tensor

$$Q_{ik} = \int d\vec{x} \, \sigma(\vec{x}) [3 x_i x_k - \delta_{ik} \vec{x}^2], \tag{42}$$

takes the familiar form*

$$\frac{d^2 E_R}{d\Omega dt} = \frac{G}{36 \pi c^5} [\tfrac{1}{4} (\dddot{Q}_{ik} n_i n_k)^2 + \tfrac{1}{2} \ddot{Q}^2_{ik} - \ddot{Q}_{ik} \dddot{Q}_{kl} n_i n_l]. \tag{43}$$

---

In so far as the assumptions underlying the present analysis are intimately related to those on which the General Theory of Relativity is based, it is hardly surprising that the result (43) is identical to the one originally derived by Einstein. Accordingly, the emphasis in the above discussion has been placed on the elucidation of the interplay between those basic principles the joint validity of which implies the mentioned conclusions. In particular, it seems noteworthy that not only the existence of the gravitational radiation, but even its quantitative expression and spin character, can be so directly related to these simple premises. Of course, the price for this simplicity in the derivation has been a resignation with respect to that far reaching unification of the fundamental principles which is so remarkably achieved by the General Theory of Relativity.

* See f.i. C. Møller: Theory of Relativity (3. ed.), Oxford Univ. Press 1972. L. D. Landau and E. M. Lifshitz: The Classical Theory of Fields, Pergamon Press (3. ed.) 1971.

---

## Acknowledgement

We take this opportunity to thank friends and colleagues at the Institutes in Copenhagen and Aarhus for many enjoyable conversations. One of us (O. U.) gratefully acknowledges the grant of a Nordita fellowship; the other one (J. K.) wishes to thank professor P. Kabir, University of Virginia, for his kind hospitality and for interesting discussions. Last but not least both of us feel it a special pleasure to express our gratitude to professor Jens Lindhard for his critical attention to our work and much friendly advice.

JØRGEN KALCKAR
*The Niels Bohr Institute, University of Copenhagen,*
*DK–2100 Copenhagen Ø, Denmark*

OLE ULFBECK
*NORDITA, Blegdamsvej 17,*
*DK–2100 Copenhagen Ø, Denmark*

Indleveret til Selskabet den 13. maj 1974.
Færdig fra trykkeriet den 3. januar 1975.

C. MØLLER

# A STUDY IN GRAVITATIONAL COLLAPSE

Det Kongelige Danske Videnskabernes Selskab
Matematisk-fysiske Meddelelser **39**, 7


Kommissionær: Munksgaard
København 1975

## CONTENTS




### Synopsis

In order to study the nature of the essentiel singularities occurring in Einstein's theory of gravitation the collapse of an arbitrary spherical distribution of incoherent matter is investigated in detail. The treatment is characterized by the use of one global Gaussian system of coordinates in which the matter is constantly at rest and which is free of coordinate singularities both inside and outside the matter. These coordinates have a simple physical interpretation and in the empty space outside the matter they represent a substitute for the rather formal Kruskal coordinates. The metric tensor is expressable in terms of simple well-known functions of the coordinates and the radial motion of light signals and the line shift of spectral lines are given by simple formulae.



Printed in Denmark by Bianco Lunos Bogtrykkeri. ISBN 87 7304 045 2

## Introduction

One of the most surprising and disturbing discoveries in later years is that of the occurrence of essential singularities in the solutions of Einstein's gravitational field equations. Unlike the "coordinate singularities", as for instance the well-known Schwarzschild singularity in empty space, essential singularities cannot be removed by any change of coordinates. The occurrence of non-trivial singularities in a physical theory may generally be taken as a sign that the theory has been applied to a phenomenon that lies outside the domain of applicability of the theory. Thus in the gravitational case one would be inclined to conclude that Einstein's theory breaks down in regions of space-time close to the singularities i.e. for extremely strong gravitational fields – a thought that was not unfamiliar to Einstein himself.[1]

The most general proofs of the inevitability of singularities in Einstein's theory were given by PENROSE (1965), GEROCH (1966) and by HAWKING and ELLIS (1968),[2] who showed that this phenomenon is independent of the special form of the energy-momentum tensor of the matter provided the equation of state is such that

$$\mu^0 c^2 + p > 0 \qquad \text{I}$$

everywhere inside the matter. Here $\mu^\circ$ is the proper mass density regarded as a scalar, $p$ is the pressure and $c$ is the usual universal constant.

In order to study the nature of the singularities a little more closely we shall in this paper reconsider the simple problem treated by OPPENHEIMER and SNYDER in 1939.[3] These authors considered a model consisting of a spherical distribution of incoherent matter which initially (at $t = 0$) is at rest and fills a sphere of finite radius with constant density. Due to the mutual gravitational attraction the matter will start contracting and after some time the appropriate solutions of Einstein's field equations develop singularities both inside and outside the matter. We shall here consider the somewhat more general case where the proper mass density initially is an arbitrarily given function of the distance from the centre. Of course, this does not make the model much more realistic, but the justification for treating this model in more detail is that the solution of the field equations, also in this more general case, can be expressed by simple well-known mathematical functions

and that the Hawking-Penrose condition I obviously is satisfied in this case, since $p = 0$ for incoherent matter and $\mu^\circ$ is positive. Thus the case considered represents the simplest imaginable illustration of the general theorems.

## 1. A Global System of Comoving Gaussian Coordinates

Since the physical system considered is spherically symmetric we can introduce a system of coordinates

$$x^i = \{r, \theta, \varphi, t\} \tag{1.1}$$

in which the line element in 4-space

$$ds^2 = g_{ik} dx^i dx^k \tag{1.2}$$

is of the form*

$$\left.\begin{aligned} ds^2 &= a(r,t)\, dr^2 + R(r,t)^2 d\Omega^2 - b(r,t) dt^2 \\ d\Omega^2 &= d\theta + \sin^2\theta\, d\varphi^2 . \end{aligned}\right\} \tag{1.3}$$

The functions $a$, $R$ and $b$ are determined by Einstein's field equations

$$G_i^k = -\varkappa T_i^k \tag{1.4}$$

which have the "conservation laws"

$$T^k_{i;\,k} = 0 \tag{1.5}$$

as a consequence.

For incoherent matter $T_i^k$ has the form

$$T_i^k = h^0 U_i U^k = \mu^0 c^2 U_i U^k \tag{1.6}$$

where $U^i$ is the four-velocity of the matter (divided by $c$) and the scalar function

$$h^0 = \mu^0 c^2 \tag{1.7}$$

is the proper energy density as measured in a local rest system of inertia. From (1.6) and (1.5) we obtain the law of conservation of proper energy in the form**

$$(h^0 U^k)_{;k} = \frac{1}{\sqrt{-g}} (\sqrt{-g}\, h^0 U^k)_{,k} = 0 . \tag{1.8}$$

In our case $h^0(r, t)$ and $U^i(r, t)$ are functions of $r$ and $t$ only, and the determinant $g$ is (by 1.3)

*) In this paper the variables $t$, $T$, $\tau$, $\tau_0$ etc, denote time variables multiplied by the universal constant c.

**) Semicolon and comma denote covariant and usual partial derivatives respectively.

$$g = -abR^4\sin^2\theta . \tag{1.9}$$

Since $g$ must be negative in any physically meaningful case we must have

$$ab > 0 . \tag{1.10}$$

In order to secure a simple and unique physical interpretation of the solutions of the field equations we shall in this paper preferably use coordinates (1.1) for which $a$ and $b$ are positive:

$$a > 0, \qquad b > 0. \tag{1.11}$$

Only in this case does the system $S$ of coordinates in 4-space correspond to a uniquely defined system of reference $R$ in the 3-dimensional physical space with reference points $(r, \theta, \varphi)$ = (constants) that are moving with subluminar velocities, so that real measuring instruments can be attached to the reference points. The distance $\sigma$ between two reference points $p_1$ and $p_2$ on the same "radius vector", as measured by means of standard measuring sticks at rest in $R$, is then at the time $t$ given by

$$\sigma = \int_{r_1}^{r_2} \sqrt{a(r, t)}\, dr. \tag{1.12}$$

Similarly, the time $\tau_0$ between two events $P_1$ and $P_2$ at a fixed reference point $p$, as measured by a standard clock at rest in $p$, is

$$\tau_0 = \int_{t_1}^{t_2} \sqrt{b(r, t)}\, dt . \tag{1.13}$$

In their treatment of the problem OPPENHEIMER and SNYDER used different systems of coordinates (and corresponding different systems of reference) inside and outside the matter. Inside the matter sphere they used a *comoving* system of reference of the type first introduced by TOLMAN, relative to which each matter particle is constantly at rest. Since the particles of incoherent matter are freely falling in the gravitational field, it follows that $b$ is a function of $t$ only; for the acceleration of a free particle momentarily at rest is quite generally proportional to $b' \equiv \dfrac{\partial b}{\partial r}$. Therefore $b'$ must be zero in a comoving system of coordinates, and by a suitable transformation of the time variable it is then always possible to make

$$b = 1 . \tag{1.14}$$

In a comoving "Gaussian" system of coordinates of this type the components of the four-velocity are

$$U^i = \delta_{i4}, \qquad U_i = -\delta_{i4} \tag{1.15}$$

and the matter tensor (1.6) has only one non-vanishing component:

$$T_i^k = -h^0(r,t)\,\delta_{i4}\delta_{k4}. \tag{1.16}$$

In this case the conservation law (1.8) reduces to

$$(\sqrt{-g}\,h^0)_{,4} = 0. \tag{1.17}$$

In the empty space outside the matter OPPENHEIMER and SNYDER used so called "curvature coordinates"

$$X^i = \{R,\ \theta,\ \varphi,\ T\} \tag{1.18}$$

in which the line element is of the form

$$ds^2 = A\,dR^2 + R^2 d\Omega^2 - B dT^2. \tag{1.19}$$

As shown first by BIRKHOFF the metric is in these coordinates outside matter in arbitrary radial motion given by the static Schwarzschild metric. Thus

$$A = \frac{1}{1-\alpha/R}, \qquad B = 1 - \alpha/R. \tag{1.20}$$

where $\alpha$ is the Schwarzschild constant

$$\alpha = \frac{\varkappa M c^2}{4\pi} = \frac{\varkappa H}{4\pi}, \tag{1.21}$$

$M$ is the total gravitational mass of the system and $H = Mc^2$ is the total energy of matter plus gravitational field.

By matching the internal and external expressions for the metric at the boundary of the matter one then obtains the motion of the boundary relative to the static system of reference of the system of curvature coordinates. However, the line element (1.19), (1.20) in the latter coordinates has the well-known drawback that the quantities $A$ and $B$ are singular for $R = \alpha$ and that the conditions (1.11) are violated for $R < \alpha$. This makes the physical interpretation of the solution somewhat obscure for $R < \alpha$, and as we shall see it may easily lead to a wrong physical picture of the contraction process. On the other hand we cannot simply exclude the region $R \leq \alpha$; for the determinant (1.9) is here $g = -R^4 \sin^2\theta$, i.e. it remains finite and negative in the whole domain $R > 0$. In fact the Schwarzschild singularity is only a

coordinate singularity which can be removed by suitable coordinate transformations. This was shown already in 1933 by LEMAITRE[4] who introduced a Gaussian system of coordinates which has a singularity at $R = 0$ only. Contrary to the Schwarzschild system the Lemaitre system of coordinates is not stationary. It has even been shown by SERINI and by EINSTEIN and PAULI[5] that no non-singular solutions of the field equations for empty space exist that are stationary and for which $g_{44} \to -1 + \alpha/r$ for $r \to \infty$.

Now one could think of repeating the Oppenheimer-Snyder considerations with the curvature coordinates replaced by the Lemaître coordinates in the outer space, in which case the reference points would be moving like freely falling particles both in the external and in the internal system of reference. Still this would not be quite practical; for the initial velocities of the reference points in the Lemaître system are not adapted to the initial conditions of our problem. Therefore we shall now try to introduce one global system of coordinates in which the matter is constantly at rest and where $b$ is given by (1.14) throughout space-time.

The initial distribution of matter at $t = 0$ is described by

$$h^0(r, 0) = \mu^0(r, 0)c^2 \tag{1.22}$$

which may be regarded as a given function of $r$ that vanishes for large values of $r$. Since the matter is initially at rest we have for $t = 0$ and arbitrary $r$

$$\dot{h}^0(r, 0) \equiv \frac{\partial h^0}{\partial t}(r, 0) = 0. \tag{1.23}$$

In our system of coordinates the metric (1.3) is throughout of the form

$$ds^2 = a(r, t)\, dr^2 + R(r, t)^2 d\Omega^2 - dt^2. \tag{1.24}$$

The reference points $(r, \theta, \varphi) = (\text{constants})$ are moving as freely falling particles and inside the matter the numbers $(r, \theta, \varphi)$ are simply fixed labels of the different matter particles, $r = 0$ corresponding to the centre of the matter. According to (1.13) with $b = 1$ the time variable $t$ is equal to the time $\tau_0$ of standard clocks at rest in the reference points, and inside the matter $t$ is simply equal to the proper time of the matter particles. The form (1.24) of the metric is unchanged under arbitrary transformations

$$\bar{r} = f(r) \tag{1.25}$$

of the radial coordinate.

The matter tensor $T_i^k$ is again of the form (1.16) and the field equations (1.4) consist of three independent equations only:

$$G_1^4 = 0, \quad G_1^1 = 0, \quad G_4^4 = \varkappa h^0. \tag{1.26}$$

For given initial conditions they are just sufficient to determine the three unknown functions $a(r, t)$, $R(r, t)$ and $h^\circ(r, t)$. In view of (1.23) we are looking for solutions $a$ and $R$ that are stationary at $t = 0$, i.e. for which the partial time derivatives of first order are zero at $t = 0$. In particular we require

$$\dot{R}(r, 0) = 0. \tag{1.27}$$

By a suitable transformation of the type (1.25) we can always arrange it so that

$$R(r, 0) = r \tag{1.28}$$

i.e.

$$R'(r, 0) = 1. \tag{1.29}$$

With the expressions for $G_{ik}$ following from (1.24) the field equations (1.26) are

$$-G_1^4 \equiv \frac{2\dot{R}'}{R} - \frac{R'}{R}\frac{\dot{a}}{a} = 0 \tag{1.30}$$

$$G_1^1 \equiv \frac{1}{R^2}\left(2R\ddot{R} + \dot{R}^2 + 1 - \frac{R'^2}{a}\right) = 0 \tag{1.31}$$

$$G_4^4 \equiv -\frac{1}{aR^2}\left(2RR'' + R'^2 - \frac{a'RR'}{a}\right) + \frac{1}{R^2} + \frac{1}{R^2}\left(\dot{R}^2 + \frac{\dot{a}R\dot{R}}{a}\right) = \varkappa h^0, \tag{1.32}$$

where dot and dash denote partial derivatives with respect to $t$ and $r$ respectively.

Multiplication of (1.30) by $RR'/a$ yields

$$\frac{\partial}{\partial t}(R'^2/a) = 0 \tag{1.33}$$

which shows that $R'^2/a$ is a function of $r$ only. If we denote this function of integration by $1 - \psi(r)$ we obtain

$$a = \frac{R'^2}{1 - \psi(r)}. \tag{1.34}$$

Introduction of this expression for $a$ into (1.31) gives

$$2R\ddot{R} + \dot{R}^2 + \psi(r) = 0. \tag{1.35}$$

Thus

$$\frac{\partial}{\partial t}\left\{R\left[\dot{R}^2 - \psi\left(\frac{r}{R} - 1\right)\right]\right\} = \dot{R}[2R\ddot{R} + \dot{R}^2 + \psi(r)] = 0$$

which shows that $R\left[\dot{R}^2 - \psi\left(\frac{r}{R} - 1\right)\right]$ is a function of $r$ only; but this function must be zero for all $r$ on account of the initial conditions (1.27), (1.28). Hence

$$\dot{R}^2 + \psi = r\psi/R \tag{1.36}$$

and from (1.35)

$$\ddot{R} = -r\psi/2R^2. \tag{1.37}$$

By means of (1.34) and (1.36) the field equation (1.32) may be written

$$G_4^4 \equiv \frac{[R(\psi + \dot{R}^2)]'}{R^2R'} = \frac{(r\psi)'}{R^2R'} = \varkappa h^0(r, t). \tag{1.38}$$

Since $(r\psi)'$ is time-independent it follows from this equation that $\varkappa h^0(r, t)R^2R'$ is a function of $r$ only, say

$$\varkappa h^0(r, t)\, R^2R' = 3r^2\lambda(r). \tag{1.39}$$

This is in accordance with the conservation equation (1.17) since

$$\sqrt{-g} = R^2\sqrt{ab}\sin\theta = R^2R'\sin\theta/\sqrt{1 - \psi(r)} \tag{1.40}$$

from (1.24) and (1.34). The function $\lambda(r)$ is obtained by putting $t = 0$ in (1.39) and by using the initial conditions (1.28), (1.29) which gives

$$\lambda(r) = \frac{\varkappa h^0(r, 0)}{3}, \tag{1.41}$$

Thus $\lambda(r)$ may be regarded as a known function of $r$ given by the initial distribution of matter. The energy density $h^0(r, t)$ at any time is, by (1.39) and (1.41),

$$h^0(r, t) = \frac{3r^2\lambda(r)}{\varkappa R^2R'} = \frac{r^2h^0(r, 0)}{R^2R'} = \mu^0(r, t)c^2. \tag{1.42}$$

If we introduce (1.39) into (1.38) we get the following differential equation for the function $\psi(r)$:

$$(r\psi)' = 3r^2\lambda(r), \tag{1.43}$$

From (1.10), (1.14) and (1.34) it follows that $\psi(r)$ in any physically meaningful case must lie in the interval

$$\psi(r) < 1 . \tag{1.44}$$

Thus $r\psi = 0$ for $r = 0$ and by solving (1.43) we obtain

$$\psi(r) = \frac{3}{r}\int_0^r r^2\lambda(r)\,dr = r^2\lambda(r) - \frac{1}{r}\int_0^r r^3\lambda'(r)\,dr \tag{1.45}$$

which determines $\psi(r)$ uniquely for a given initial distribution of matter.

When $\psi(r)$ has been determined by (1.45) we can solve the differential equation (1.36) for $R(r, t)$. It is easily verified that the solution corresponding to the initial condition (1.28) is given by

$$R(r, t) = rC(u) \tag{1.46}$$

$$u = t\sqrt{\psi/r^2} \tag{1.47}$$

where the function $C(u)$ of the variable $u$ is a solution of the differentiel equation

$$\left(\frac{dC}{du}\right)^2 \equiv C'(u)^2 = \frac{1}{C(u)} - 1 \tag{1.48}$$

with

$$C(0) = 1 . \tag{1.49}$$

From (1.48) we obtain

$$C'(u) = \pm\sqrt{\frac{1 - C(u)}{C(u)}} \tag{1.50}$$

and by differentiation

$$C''(u) = -\frac{1}{2C(u)^2} . \tag{1.51}$$

The solutions of (1.50), (1.49) are

$$\mp u = -\int_1^C \sqrt{\frac{C}{1 - C}}\,dC = \sqrt{C(1 - C)} + \tan^{-1}\sqrt{\frac{1 - C}{C}} \tag{1.52}$$

or

$$\mp u = \sqrt{C(1 - C)} + \cos^{-1}\sqrt{C} = \sqrt{C(1 - C)} + \frac{\pi}{2} - \sin^{-1}\sqrt{C} , \tag{1.53}$$

where the signs here correspond to the signs in (1.50).

The graphical picture of the function $C(u)$ of $u$ is a cycloid with the parametric representation

$$C = \tfrac{1}{2}(1 + \cos\eta), \quad u = \tfrac{1}{2}(\eta + \sin\eta). \tag{1.54}$$

We have now obtained the complete solution of our problem in a global system of coordinates $S_M$ that is Gaussian and in which all parts of the matter are constantly at rest in the corresponding system of reference $R_M$. In $S_M$ the metric in 4-space is

$$ds^2 = \frac{R'(r, t)^2}{1 - \psi(r)}\, dr^2 + R(r, t)^2 d\Omega^2 - dt^2. \tag{1.55}$$

Here $\psi(r)$ is determined by the given initial distribution of the matter through (1.45) and $R(r, t)$ is given by (1.46) – (1.54). Thus

$$\left.\begin{aligned} &R = rC(u), \quad u(r, t) = t\sqrt{\psi}/r, \quad \dot{u} = \sqrt{\psi}/r, \\ &u' = \frac{u}{r}\frac{(r\psi)' - 3\psi}{2\psi} = \frac{3u}{2r^2\psi}\int_0^r r^3\lambda'(r)\, dr, \\ &\dot{R} = r\, C'(u)\dot{u} = \sqrt{\psi}\, C'(u), \\ &R' = C(u) + rC'(u)u'. \end{aligned}\right\} \tag{1.56}$$

For simplicity we shall assume that $\lambda(r)$ is a never increasing function of $r$. Then

$$\int_0^r r^3\lambda'(r)\, dr < 0 \quad \text{and} \quad R' > 0. \tag{1.57}$$

The matter density at any time is given by (1.42), and the naturally measured distance from the centre of a fixed point in the matter is from (1.12)

$$\sigma(r, t) = \int_0^r \frac{R'(r, t)}{\sqrt{1 - \psi(r)}}\, dr. \tag{1.58}$$

## 2. Discussion of the Solution

In a contraction process starting from a state of rest at $t = 0$ the solution (1.55) is regular everywhere in a region of $r$ and $t$ for which $u$ in (1.56) lies in the interval

$$0 \leq u < \frac{\pi}{2}. \tag{2.1}$$

The corresponding values of the parameter $\eta$ in (1.54) and of $C(u)$ lie in the intervals

$$0 \leq \eta < \pi, \quad 1 \geqslant C(u) > 0. \tag{2.2}$$

In this region

$$C'(u) = -\sqrt{\frac{1 - C}{C}} \tag{2.3}$$

and we have to use the lower signs in (1.52), (1.53). Further

$$R'(r, t) > 0, \quad \dot{R} \leq 0 \tag{2.4}$$

from (1.56) and (1.57), and

$$R = rC \leq r. \tag{2.5}$$

However for $u \to \frac{\pi}{2}$ we have

$$C(u) \to 0, \quad C'(u) \to -\infty, \quad R \to 0. \tag{2.6}$$

Thus for any fixed value of $r$ in the interval $0 \leq r < \infty$ the metric becomes singular after a finite time $t_s(r)$ measured on a standard clock at rest in $R_M$. This time is given by

$$u(r, t_s) = \frac{\pi}{2} \tag{2.7}$$

or from (1.47)

$$t_s(r) = \frac{\pi r}{2\sqrt{\psi(r)}} \tag{2.8}$$

which goes to infinity for $r \to \infty$ (comp. (2.13)). According to (1.40) the quantity $\sqrt{-g}$ is proportional to $R^2R'$ and from (1.56), (1.57) and (2.3) we have

$$R^2R' = r^2\left[C^3 + C\sqrt{C(1 - C)}\frac{3u}{2r\psi}\left(-\int_0^r r^3\lambda'(r)dr\right)\right], \tag{2.9}$$

which shows that $\sqrt{-g}$ goes to zero as $C^{3/2}$ for $u \to \frac{\pi}{2}$. Therefore we are

dealing with essential singularities in this limit, and it has no physical meaning to extend space-time beyond the region defined by (2.1). From (1.42) it follows that the proper mass density at any point inside the matter with constant $r$ goes to infinity for $t \to t_s(r)$. This is accompanied by a singularity in the metric that spreads outward into the empty space outside the matter according to the equation

$$u(r, t) = \sqrt{\psi}\, t/r = \frac{\pi}{2} \tag{2.10}$$

or

$$R(r, t) = 0\,. \tag{2.11}$$

By differentiation of (2.10) we get for the velocity with which the singularity propagates

$$V_s = \left.\frac{dr}{dt}\right|_{u=\frac{\pi}{2}} = -\frac{\dot{u}}{u'} = \frac{4r\psi^{3/2}}{3\pi} \Big/ \left( -\int_0^r r^3 \lambda'(r) dr \right) > 0 \tag{2.12}$$

from (1.56) and 1(1.57). $V_s \to 0$ for $r \to \infty$ (comp. (2.21)). At any time $t < t_s(r)$ the metric is regular for all $r$. There are no coordinate singularities in $S_M$.

For an insular system of the type considered here the function $h^0(r, 0)$ or $\lambda(r)$ is zero in the empty space outside the matter, say for $r \geq r_b$. In this region we get from (1.45) and (1.41)

$$\psi(r) = \alpha/r \tag{2.13}$$

where

$$\alpha = 3\int_0^\infty r^2 \lambda(r) dr = \frac{\varkappa}{4\pi} \iiint h^0(r, 0) r^2 \sin\theta dr d\theta d\varphi \tag{2.14}$$

is a constant which has a simple physical meaning. For a real physical system we must have

$$r_b < \alpha \tag{2.15}$$

on account of (1.44). The naturally measured spatial volume element is

$$dV = \sqrt{\gamma}\, dr d\theta d\varphi = \sqrt{ab}\, R^2 \sin\theta\, dr d\theta d\varphi = \frac{R^2 R' \sin\theta}{\sqrt{1 - \psi(r)}} dr d\theta d\varphi \tag{2.16}$$

which for constant $(r, \theta, \varphi)$ and $(dr, d\theta, d\varphi)$ goes to zero for $t \to t_s$. However, from (1.42) the total proper matter energy is

$$H^0 = \iiint h^0(r, t) dV = \iiint \frac{h^0(r, 0)}{\sqrt{1 - \psi(r)}} r^2 \sin\theta dr d\theta d\varphi \tag{2.17}$$

which is constant in time. As we shall see now the constant $\alpha$, which also may be written

$$\alpha = \frac{\varkappa}{4\pi} \iiint h^0(r, t) \sqrt{1 - \psi(r)}\, dV, \tag{2.18}$$

represents the total energy of the system, i.e. the total energy of matter plus gravitational field.

In any asymptotically Lorentzian system of coordinates the total four-momentum $P_i$ of an insular system is given by[6]

$$P_i = \lim_{r \to \infty} \frac{1}{c} \int_f \psi_i^{4\lambda} n_\lambda r^2 \sin\theta \, d\theta d\varphi \tag{2.19}$$

where the integration is extended over a large sphere $f$ of radius $r_0$. $n_2$ is a normal unit vector in the outward direction and $\psi_i^{kl}$ is the $v$. Freud superpotential.[7] For $r \geq r_b$ we get from (1.56), (2.13), (2.3)

$$\left.\begin{aligned} R &= r\,C(u), \quad u = t\sqrt{\alpha/r^3}, \quad \dot{u} = \sqrt{\alpha/r^3} \\ u' &= -3u/2r, \quad R' = C(u) + \frac{3u}{2}\sqrt{\frac{1-C}{C}}, \\ \dot{R} &= -\sqrt{\alpha/r}\sqrt{\frac{1}{C} - 1} = -\sqrt{(\alpha/R) - \alpha/r} \end{aligned}\right\} \tag{2.20}$$

and from (2.12)

$$V_s = -\dot{u}/u' = \frac{2}{3u}\sqrt{\alpha/r} = \frac{4}{3\pi}\sqrt{\alpha/r}. \tag{2.21}$$

It is seen that $u \to 0$ in the limit $r \to \infty$ for any constant $t$, and a Taylor expansion of the function $C(u)$ for small $u$ gives by (1.49)—(1.51)

$$\left.\begin{aligned} C(u) &= 1 - \tfrac{1}{4}u^2 + O(u^4) \\ R'(u) &= 1 + \tfrac{1}{2}u^2 + O(u^4). \end{aligned}\right\} \tag{2.22}$$

In calculating $P_i$ in (2.19) we shall only need the asymptotic expression of $g_{ik}$ entering in $\psi_i^{4\lambda}$ in which terms of order $u^2 = t^2\alpha/r^3$ can be neglected. In this approximation we have $C = R' = 1$, $R = r$ and we get for the symptotic form of (1.55)

$$ds^2 = \frac{dr^2}{1 - \alpha/r} + r^2 d\Omega^2 - dt^2 \tag{2.23}$$

which is time-independent. For $r \to \infty$ this goes over into the Minhowski line element written in polar coordinates. Therefore introducing spatial coordinates $(x, y, z)$ that are connected with $(r, \theta, \varphi)$ in the same way as Cartesian and polar coordinates in a Euclidian space, we obtain an asymptotically Lorentzian system of space-time coordinates

$$x^i = \{x, y, z, t\} \tag{2.24}$$

in which the expression (2.19) can be safely applied. In these coordinates the metric tensor of the line element (2.23) takes the form

$$g_{ik} = \eta_{ik} + \frac{\alpha}{r} n_i n_k + O\left(\frac{1}{r^2}\right) \tag{2.25}$$

where $\eta_{ik}$ is the Minhowski tensor and

$$n_i = \frac{\partial r}{\partial x^i} = \{n_\iota, 0\}. \tag{2.26}$$

$O(1/r^2)$ is a term of order $1/r^2$ which does not give any contribution to the integral (2.19) in the limit $r \to \infty$.

With $g_{ik}$ given by (2.25) the superpotential is easily calculated. Neglecting terms of order $1/r^3$ we obtain

$$\psi_i^{4\lambda} = -\delta_{i4} \frac{\alpha}{\varkappa r^2} n_\lambda \tag{2.27}$$

and from (2.19)

$$P_i = -\delta_{i4} \frac{4\pi\alpha}{\varkappa c} = \{\boldsymbol{P}, -H/c\}. \tag{2.28}$$

Thus the total momentum $\boldsymbol{P}$ of the system is zero and the total energy $H$ is

$$H = \frac{4\pi\alpha}{\varkappa} = Mc^2 \tag{2.29}$$

A comparison of this equation with (1.21) shows that the constant $\alpha$ in (2.13), (2.14) or (2.18) is identical with the Schwarzschild constant.

So far we have not made any assumption about the initial distribution of the matter, except that $\lambda'(r) \leq 0$ and $\lambda(r) = 0$ for $r \geq r_b$. Let us now consider the case where $\lambda(r)$ is equal to a constant $\lambda_0$ for $r \leq r_c < r_b$, i.e.

$$\lambda(r) = \begin{cases} \lambda_0 & \text{for} \quad 0 \leq r \leq r_c \\ 0 & \text{for} \quad r \geq r_b \end{cases}. \tag{2.30}$$

In the inner region $r \leq r_c$ we obtain from (1.45), (1.56)

$$\left.\begin{aligned} &\psi = \lambda_0 r^2, \quad R = rS(t), \quad S(t) = C(u), \\ &u = \sqrt{\lambda_0}\, t, \quad \dot{u} = \sqrt{\lambda_0}, \quad u' = 0, \\ &\dot{S} = \sqrt{\lambda_0}\, C' = -\sqrt{\lambda_0}\sqrt{\frac{1}{S} - 1}, \quad \dot{R} = r\dot{S}, \quad R' = C(u) = S(t) \end{aligned}\right\} \tag{2.31}$$

and the line element (1.55) takes the simple form

$$ds^2 = S(t)^2\left[\frac{dr^2}{1-\lambda_0 r^2} + r^2 d\Omega^2\right] - dt^2. \tag{2.32}$$

In the same region we get from (1.42)

$$h^0(r, t) = \frac{3r^2\lambda_0}{\varkappa r^2 S^3} = \frac{h^0(r, 0)}{S(t)^3} \tag{2.33}$$

and the singularity occurs simultaneously at all points inside $r_c$ at the time

$$t_s = \pi/2\sqrt{\lambda_0}. \tag{2.34}$$

From (1.58) we get for the naturally measured distance

$$\sigma(r, t) = S(t)\int_0^r \frac{dr}{\sqrt{1-\lambda_0 r^2}} = \frac{C\left(\sqrt{\lambda_0}\, t\right)}{\sqrt{\lambda_0}} \sin^{-1}\left(\sqrt{\lambda_0}\, r\right). \tag{2.35}$$

For constant $r$ this distance decreases steadily in our case to the value zero for $t \to t_s$, which shows that we have contraction of the matter when $C'(u)$ is negative.

If we make the transition from the constant value $\lambda_0$ of $\lambda(r)$ for $r \leq r_c$ to the value $\lambda(r) = 0$ for $r \geq r_b$ sufficiently smooth in the interval $r_c \leq r \leq r_b$, the components of the metric tensor in (1.55) will be continuous and differentiable in the whole region of space-time with $t < t_s(r)$, even if $r_b - r_c$ is very small. However, it should be remarked that in the limit $r_c \to r_b$, where $\lambda(r)$ is a step function at $r = r_b$ and therefore

$$\lambda_0 r_b^2 = \alpha/r_b, \tag{2.36}$$

the quantities $u'$ in (1.56) and hence $R'$ and $a$ in (1.34) are discontinuous at $r = r_b$. According to (1.38) this is directly connected with the discontinuity of $h^\circ$ at this point. The relation (2.36) between $\lambda_0$ and $r_b$ is a good approximation also for finite $r_b - r_c$ provided that

$$(r_b - r_c)/r_b \ll 1. \tag{2.37}$$

## 3. Curvature Coordinates

According to (1.55) the area of a sphere of constant $r$ and $t$ is equal to $4\pi R^2$ and the "curvature radius" $R$ is a function of $r$ and $t$ given by

$$R = R(r, t) = r\, C(u) = r\, C\left(t\sqrt{\psi/r^2}\right). \tag{3.1}$$

We are now looking for a system $S_c$ of curvature coordinates

$$X^i = \{R, \theta, \varphi, T\} \tag{3.2}$$

in which $ds^2$ is of the form (1.19):

$$ds^2 = AdR^2 + R^2 d\Omega^2 - BdT^2. \tag{3.3}$$

To this end we have to find a transformation

$$T = \varphi(r, t) \tag{3.4}$$

which together with (3.1) brings (1.55) into the form (3.3). This is brought about by choosing $\varphi(r, t)$ as a solution of the partial differential equation

$$(1 - \psi(r))\varphi'(r, t) - \dot{R}R'\dot{\varphi}(r, t) = 0. \tag{3.5}$$

In fact, from (3.1) and (3.4) we obtain by differentiation and by solving for $dr$ and $dt$

$$\left.\begin{aligned} dr &= (\dot{\varphi}dR - \dot{R}dT) \,/\, (R'\dot{\varphi} - \dot{R}\varphi') \\ dt &= (R'dT - \varphi' dR) \,/\, (R'\dot{\varphi} - \dot{R}\varphi'). \end{aligned}\right\} \tag{3.6}$$

When this is introduced into (1.55) it is seen that the terms containing $dRdT$ cancel, on account of (3.5), and $ds^2$ takes the form (3.3) with

$$\left.\begin{aligned} A &= \frac{R'^2\dot{\varphi}^2 - \varphi'^2(1 - \psi)}{(1 - \psi)(R'\dot{\varphi} - \dot{R}\varphi')^2} \\ B &= \frac{R'^2(1 - \psi - \dot{R}^2)}{(1 - \psi)(R'\dot{\varphi} - \dot{R}\varphi')^2}. \end{aligned}\right\} \tag{3.7}$$

Eliminating $\varphi'$ by means of (3.5) and using (1.36) we obtain

$$A = \frac{1}{1 - r\psi/R}, \qquad B = \frac{1 - \psi}{\dot{\varphi}^2(1 - r\psi/R)}. \tag{3.8}$$

In the system $S_c$ the metric tensor is more singular than in the system $S_M$ of section 1 and 2. Besides for

$$R = 0 \tag{3.9}$$

which is the essential singularity (2.11), $A$ and $B$ are singular also at

$$R = r\psi \tag{3.10}$$

and for $R < r\psi$, the conditions (1.11) are violated since

$$A < 0, \quad B < 0. \tag{3.11}$$

In empty space, where (2.13) holds, the singularity (3.10) is identical with the Schwarzschild singularity at

$$R = \alpha. \tag{3.12}$$

From the form (3.3) of $ds^2$ in $S_e$ one would be inclined to draw the wrong conclusion that the essential singularity (3.9) occurs at the centre of the matter only. It is true that $R = 0$ at the centre $r = 0$; but from (1.46) it follows that $R$ is also zero for $r \neq 0$ whenever $C(u) = 0$, i.e. along the whole curve (2.7) which also concerns points outside the matter. If we put $t = 0$ in (3.5) we obtain by (1.27)

$$\varphi'(r, 0) = 0 \tag{3.13}$$

or

$$\varphi(r, 0) = \text{constant}$$

It is convenient to choose the value of this constant equal to zero, i.e.

$$\varphi(r, 0) = 0 \tag{3.14}$$

for then the time variable $T$ in the system $S_e$ is zero for all events at $t = 0$ the time coordinates $T$ and $t$ coincide at the origin $T = t = 0$.

In the empty space outside the matter, where $\psi = \alpha/r$, the solution of the differential equation (3.5) with the initial condition (3.14) is given by

$$\left.\begin{aligned} \varphi(r, t) = t\sqrt{1 - \alpha/r} + 2\sqrt{\alpha(r - \alpha)}\tan^{-1}\sqrt{\frac{r - R}{R}} \\ + 2\alpha\log\frac{\sqrt{R(r - \alpha)} + \sqrt{\alpha(r - R)}}{\sqrt{r\,|R - \alpha|}} \end{aligned}\right\} \tag{3.15}$$

where $R(r, t)$ is the function of $r$ and $t$ given by (3.1) and $|R - \alpha|$ is the absolute value of $R - \alpha$, i.e.

$$|R - \alpha| = \begin{cases} R - \alpha & \text{for} \quad R > \alpha \\ \alpha - R & \text{for} \quad R < \alpha. \end{cases} \tag{3.16}$$

Partial differentiation of (3.15) with respect to $t$ and $r$ gives after a somewhat lengthy calculation using (2.20) and (1.52)

$$\dot{\varphi} = \frac{\sqrt{1-\alpha/r}}{1-\alpha/R}, \quad \varphi' = \frac{\dot{R}R'}{\sqrt{1-\alpha/r}(1-\alpha/R)} \tag{3.17}$$

which shows that (3.15) is a solution of (3.5) with $\psi = \alpha/r$. Further since $R = r$ for $t = 0$ it also satisfies the initial condition (3.14). Since $r \geq r_b > \alpha$ in the outer space and $R \leq r$ the function $T = \varphi(r, t)$ is real and positive for $t > 0$ and arbitrary $r$. For $R \to \alpha$ this function diverges logarithmically. It is this singularity in the time transformation (3.4) that causes the coordinate singularity of the metric in $S_c$ at $R = \alpha$.

With $\dot{\varphi}$ given by (3.17) and $r\psi = \alpha$ the quantities $A$ and $B$ in (3.8) reduce to the Schwarzschild expressions

$$B = \frac{1}{A} = 1 - \alpha/R \tag{3.18}$$

in accordance with Birkhoff's theorem. In a region of space-time where $R > \alpha$ and $A$ and $B$ positive, the system $S_c$ furnishes the simplest and most convenient description of the motion of particles and light signals. This is above all due to the fact that the system of reference $R_c$ corresponding to $S_c$ is rigid. According to (1.12) the naturally measured radial distance $\sigma$ is

$$\sigma = \int_{R_1}^{R_2} \frac{dR}{\sqrt{1-\alpha/R}} \tag{3.19}$$

which is time independent and by (1.13) the time $\tau_0$ of a standard clock at a fixed reference point in $R_c$ is

$$\tau_0 = T\sqrt{1-\alpha/R}. \tag{3.20}$$

However in a region where $R < \alpha$ the expressions (3.19), (3.20) have no physical meaning. The reason for this becomes clear when we consider the motion of a point of constant $(R, \theta, \varphi)$ relative to the 'rest system' $S_M$ of the matter which is described by the equation (3.1) with constant $R$. Thus it moves radially outward with the velocity

$$\left.\frac{dr}{dt}\right|_R = -\frac{\dot{R}}{R'} = \frac{\sqrt{(r\psi/R)-\psi}}{R'} = \frac{\sqrt{(\alpha/R)-\alpha/r}}{R'} \tag{3.21}$$

on account of (1.56) and (2.20). On the other hand we get from (1.55) for an outward moving light signal for which $ds^2 = 0$

$$\left(\frac{dr}{dt}\right)_L = \frac{\sqrt{1-\psi}}{R'} = \frac{\sqrt{1-\alpha/r}}{R'} \tag{3.22}$$

which is smaller than $\left.\frac{dr}{dt}\right|_R$ for $R < \alpha$. Thus in the region $R < \alpha$ the reference points of $R_c$ are moving with super light velocities so that it is impossible to attach real measuring instruments to these points. This explains why the expressions (3.19), (3.20) are meaningless in this domain. On the other hand, if $r$ is very large compared with $\alpha$ the quantity $u^2 = t^2\alpha/r^3$ will during a long period of time be small compared with 1. In this region

$$\alpha/r \ll 1, \qquad u^2 = t^2\alpha/r^3 \ll 1 \tag{3.23}$$

and we have according to (2.20), (2.22) and (3.21)

$$C = R' = 1, \qquad R = r \gg \alpha, \qquad \left.\frac{dr}{dt}\right|_R \ll 1. \tag{3.24}$$

Thus, in the region of space-time (3.23) which covers the larger part of the outer space during a long time the systems of reference $R_c$ and $R_M$ coincide.

## 4. Radial Motion of Free Particles and Light Signals

On account of the just mentioned "unphysical" motion of the system of reference $R_c$ for $R < \alpha$ it is preferable to describe the motion of free particles and light signals in the system $S_M$ with the metric (1.55). The simplest solution of the equations of motion for a free particle is given by

$$(r, \theta, \varphi) = (\text{constants}) . \tag{4.1}$$

In terms of the radial curvature coordinate the motion is described by (1.46) with constant $r$:

$$R = r\,C(u) = r\,C\left(t\sqrt{\psi/r^2}\right). \tag{4.2}$$

Thus, $R$ is a steadily decreasing function of the time $t$ measured on a standard clock following the particle. For $dr = 0$ we get from (3.1) and (3.4)

$$dR = \dot{R}dt, \qquad dT = \dot{\varphi}dt. \tag{4.3}$$

In empty space this gives by (2.20) and (3.17)

$$dR = -\sqrt{(\alpha/R) - \alpha/r}\,dt, \qquad dT = \frac{\sqrt{1-\alpha/r}}{1-\alpha/R}\,dt, \tag{4.4}$$

$$\frac{dR}{dT} = -\frac{\sqrt{(\alpha/R) - \alpha/r}}{\sqrt{1 - \alpha/r}} \cdot (1 - \alpha/R). \tag{4.5}$$

Thus, the "velocity" $dR/dT$ of the particle in $S_c$ is positive for $R < \alpha$ in spite of the fact that $R$ is steadily decreasing. This is due to the circumstance that $T$ is decreasing along the time-track of the particle for $R < \alpha$ as is seen from (4.4). Further since $T \to \infty$ for $R \to \alpha$ observers in $S_c$ might come to the conclusion that the value $R = \alpha$ never can be reached if $R$ initially is larger than $\alpha$, although we know that this happens in a finite time measured on the standard clocks.

For $r = r_b$ where $\psi = \alpha/r_b$ we get from (4.2)

$$R_b = r_b\, C(u_b) = r_b C\left(t\sqrt{\alpha/r_b^3}\right) \tag{4.6}$$

which describes the motion of the boundary of the matter. $R_b$ decreases from the value $r_b > \alpha$ at $t = 0$ to the value $R_b = \alpha$ in a finite time $t_\alpha(r_b)$ determined by the equation

$$C\left(t_\alpha(r_b)\sqrt{\alpha/r_b^3}\right) = \alpha/r_b. \tag{4.7}$$

Introducing this value for $C$ into (1.53) we get for this time

$$t_\alpha(r_b) = r_b\sqrt{1 - \alpha/r_b} + r_b\sqrt{r_b/\alpha}\left(\frac{\pi}{2} - \sin^{-1}\sqrt{\alpha/r_b}\right). \tag{4.8}$$

Somewhat later at the time

$$t_s(r_s) = r_b\sqrt{r_b/\alpha}\,\frac{\pi}{2} \tag{4.9}$$

where $C = 0$ the surface of the matter runs into the singularity (2.11) which then spreads into the outer space with the velocity (2.21). The time interval $t_{\alpha s}$ in which $R_b$ of the surface decreases from the Schwarzschild value $\alpha$ to the value zero is

$$t_{\alpha s} = t_s(r_s) - t_\alpha(r_s) = r_b\sqrt{r_b/\alpha}\sin^{-1}\left(\sqrt{\alpha/r_b}\right) - r_b\sqrt{1 - \alpha/r_b}. \tag{4.10}$$

As an example we consider a spherical system of incoherent matter with the mass and radius of a typical galaxy, say $M = 10^{45} gm$ and $r_b = 10^{23}$ $cm$. Then $\alpha \simeq 10^{17}$ $cm$ from (1.21). According to (4.8) such a system would collapse through the Schwarzschild radius after a time

$$t_\alpha(r_b)/c \simeq \tfrac{1}{2}\, 10^{16} \text{ sec} \approx 160 \text{ million years}. \tag{4.11}$$

At this time the individual stars in the galaxy would still be far from touching each other, so that the approximation of incoherent matter would seem not

to be too unrealistic. Provided the galaxy is non-rotating this phenomenon should actually occur after the comparatively short time (4.11). After a further very short time $t_{\alpha s}/c$ our model predicts a total collapse of the matter into the singularity. For $\alpha/r_b \ll 1$ (4.10) reduces to

$$t_{\alpha s}/c = \alpha/2c \approx 19 \text{ days} \tag{4.12}$$

in our case; but in the later part of this process the assumption of zero pressure is of course highly unrealistic. During the first 10 million years of the contraction process the quantity $u^2 = t^2\alpha/r_b^3$ is only about 0.01. Thus, we are in the region (3.23), where the systems $R_c$ and $R_M$ coincide for the whole outside space $r > r_b$. During the time interval

$$t_\alpha(r_b) < t < t_s(r_b) \tag{4.13}$$

the system represents a "black hole", i.e. no information can be transferred from the surface of the matter to regions of space-time where $R > \alpha$. In order to study this phenomenon a little more closely we need only to consider the motion of light signals through empty space; for no real signal can move faster than light. From (1.55) and (2.13) we obtain for the radial velocity of light, since $ds^2 = 0$ for such signals,

$$\left(\frac{dr}{dt}\right)_L^2 = \frac{1 - \alpha/r}{R'^2} \tag{4.14}$$

with $R'$ given by (2.20). Hence

$$\left(\frac{dr}{dt}\right)_L = \pm \frac{\sqrt{1 - \alpha/r}}{R'} \tag{4.15}$$

where the upper and lower signs hold for signals that are moving in the outward and inward directions, respectively, relative to $S_M$, i.e. relative to the matter. The changes of the curvature coordinates $R$ and T along the time-tracks of the signals are by (4.15), (3.4) and (3.17)

$$\frac{dR}{dt} = R'\left(\frac{dr}{dt}\right)_L + \dot{R} = \pm\sqrt{1 - \alpha/r} + \dot{R} \tag{4.16}$$

$$\frac{dT}{dt} = \varphi'\left(\frac{dr}{dt}\right)_L + \dot{\varphi} = \left(\pm\dot{R} + \sqrt{1 - \alpha/r}\right)/(1 - \alpha/R), \tag{4.17}$$

or using (2.20)

$$\frac{dR}{dt} = \pm\sqrt{1 - \alpha/r} - \sqrt{(\alpha/R) - \alpha/r} \tag{4.18}$$

$$\frac{dT}{dt} = \left(\sqrt{1 - \alpha/r} \mp \sqrt{(\alpha/R) - \alpha/r}\right)/(1 - \alpha/R). \tag{4.19}$$

The solutions of the two differential equations (4.15) are given implicitly by the equations

$$F_{\pm}(r, t) = C_{\pm} \tag{4.20}$$

where $C_+$ and $C_-$ are constants of integration and $F_+$ and $F_-$ are the following functions of $r$ and $t$:

$$F_{\pm}(r, t) = \pm \varphi(r, t) - R - \alpha \log \frac{|R - \alpha|}{\alpha}. \tag{4.21}$$

In fact, by differentiation of these functions we get

$$\frac{dF_{\pm}}{dt} = F'_{\pm}\left(\frac{dr}{dt}\right)_L + \dot{F}_{\pm}(r, t) = \pm \frac{\sqrt{1 - \alpha/r}}{R'} F'_{\pm} + \dot{F}_{\pm} \tag{4.22}$$

and by (3.17)

$$\left.\begin{aligned} F'_{\pm} &= \pm \varphi' - \left(1 + \frac{\alpha}{R - \alpha}\right) R' = \frac{R'}{\sqrt{1 - \alpha/r}} \frac{\pm \dot{R} - \sqrt{1 - \alpha/r}}{1 - \alpha/R} \\ \dot{F}_{\pm} &= \pm \dot{\varphi} - \frac{\dot{R}}{1 - \alpha/R} = \frac{\pm \sqrt{1 - \alpha/r} - \dot{R}}{1 - \alpha/R}. \end{aligned}\right\} \tag{4.23}$$

Hence

$$\frac{dF_{\pm}}{dt} = \frac{\dot{R} \mp \sqrt{1 - \alpha/r}}{1 - \alpha/R} + \frac{\pm \sqrt{1 - \alpha/r} - \dot{R}}{1 - \alpha/R} = 0,$$

which shows that the functions $F_{\pm}(r, t)$ are integrals of the motion of the light signals.

When the signals start at the point $r_0$ at the time $t_0$ the motion of the outward and inward going signals are described by the two equations

$$F_{\pm}(r, t) = F_{\pm}(r_0, t_0) \tag{4.24}$$

that also may be written

$$\pm (T - T_0) - (R - R_0) - \alpha \log \frac{|R - \alpha|}{|R_0 - \alpha|} = 0 \tag{4.25}$$

from (4.21) and (3.4). Two signals starting at the times $t_0/c$ and $(t_0 + dt_0)/c$ from the point $r_0$ will arrive in the fixed point $r$ at the times $t/c$ and $(t + dt)/c$ respectively, where the relation between $dt$ and $dt_0$ is obtained by differentiation of (4.24):

$$\dot{F}_{\pm}(r, t)dt = \dot{F}_{\pm}(r_0, t_0)dt_0. \tag{4.26}$$

If the light at the start from $r_0$ has the (standard) frequency $\nu_0$ and the wave length $\lambda_0 = c/\nu_0$, the interval $dt_0$ between the emission of successvie wave crests is $dt_0 = c/\nu_0 = \lambda_0$ and the corresponding interval for their arrival in $r$ is $dt = c/\nu = \lambda$ where $\lambda$ is the observed wave length at $r$.
Then, we obtain the relative shift of the spectral lines

$$z = \frac{\lambda - \lambda_0}{\lambda_0} = \frac{\lambda}{\lambda_0} - 1 \tag{4.27}$$

from (4.26) and (4.23) which give

$$\lambda/\lambda_0 = \frac{\dot{F}_{\pm}(r_0, t_0)}{\dot{F}_{\pm}(r, t)} = \frac{\pm\sqrt{1 - \alpha/r_0} - \dot{R}_0}{1 - \alpha/R_0} \cdot \frac{1 - \alpha/R}{\pm\sqrt{1 - \alpha/r} - \dot{R}} \tag{4.28}$$

The function $F_+$ given by (4.21) and (3.15) contains a term $-2\alpha \log \frac{|R - \alpha|}{\alpha}$ so that

$$F_+ \to \infty \quad \text{for} \quad R \to \alpha \tag{4.29}$$

while $F_-$ remains finite in this limit, since the logarithmic terms in $F_-$ cancel.

Let us now first consider the case of an outward moving signal, where the upper signs hold in the preceding formulae. If $t_0$ lies in the interval (4.13) and $r_0$ is equal to $r_b$ we have $R_0 = R(r_0, t_0) < \alpha$ and $F_+(r_0, t_0)$ is a finite constant. Then it follows from (4.24) and (4.29) that $R$ can never become equal to $\alpha$ during the motion, i.e. the signal can never penetrate into a region where $R > 0$. At the first moment this is somewhat surprising, since $\left(\frac{dr}{dt}\right)_L$ according to (4.15) with the plus sign never becomes negative. However the outward velocity is zero for $R' = \infty$ which happens when $u = t\sqrt{\alpha/r^3} = \pi/2$. Thus the signal does not stop before it runs into the singularity (2.7) where $r$ and $t$ have values $(r^*, t^*)$ connected by the equation

$$u^* = t^*\sqrt{\alpha/r^{*3}} = \pi/2. \tag{4.30}$$

For these values also

$$R^* = R(r^*, t^*) = 0 \tag{4.31}$$

which shows that $R$ must decrease along the time-track of the signal from the value $R_0$ to the value zero while $r$ increases from $r_0$ to $r^*$. This is in accordance with (4.18) since $dR/dt$ is negative all the time for $R < \alpha$. Also it follows from (4.19) that $dT/dt > 0$ in this case, i.e. $T$ increases from the value $T_0$ to the value

$$T^* = \varphi(r^*, t^*) = t^* \sqrt{1 - \alpha/r^*} + \pi \sqrt{\alpha(r^* - \alpha)} \tag{4.32}$$

obtained from (3.15) by putting $R = R^* = 0$. Further we have by (4.25) with $R = R^* = 0$

$$T^* = T_0 - R_0 + \alpha \log \frac{\alpha}{\alpha - R_0} \tag{4.33}$$

which is indeed larger than $T_0$ for $R_0 < \alpha$. The equations (4.30) and (4.33) with (4.32) determine the place $r^*$ and the time $t^*$ at which the light ray runs into the singularity.

For $r_0 = r_b$ and $t_0 < t_\alpha(r_b)$ we have $R_0 > \alpha$ and the outward going light signal will proceed to arbitrarily large values of $r$ and of $R = r\, C(t\sqrt{\alpha/r^3})$. This follows at once from (4.18) and (4.15) which show that $dR/dt$ and $(dr/dt)_L$ are positive all the way. An observer sitting at a point with

$$r \gg \alpha, \quad R \gg \alpha. \tag{4.34}$$

will observe a line shift given by (4.28). With the value for $\dot{R}$ given by (2.20) and with (4.34) we obtain

$$\lambda/\lambda_0 = \frac{\sqrt{1 - \alpha/r_0} + \sqrt{(\alpha/R_0) - \alpha/r_0}}{1 - \alpha/R_0}. \tag{4.35}$$

The light is shifted towards the red. For $t_0 \ll t_\alpha(r_b)$ so that $u_0^2 = t_0^2 \alpha/r_0^3 \ll 1$, i.e. in the region (3.23) we have from (3.24) $C_0 = 1$, $R_0 = r_0$ and the formula reduces to the well-known red shift formula

$$\lambda = \lambda_0/\sqrt{1 - \alpha/R_0} \tag{4.36}$$

for a source at rest in the Schwarzschild system of coordinates. In general $\lambda > \lambda_0 \sqrt{1 - \alpha/r_0}/(1 - \alpha/R_0) > \lambda_0/\sqrt{1 - \alpha/R_0}$ which shows that the light is always redshifted in this case.

Let us now consider the case of ingoing light where we have to use the lower signs in the equations (4.17)–(4.28). Since $F_-$ is regular everywhere in the physical region $t < t_s(r)$, there is nothing to stop the signal from going from a place with $R_0 > \alpha$ right through to the surface of the matter sphere even if $R_b$ is smaller than $\alpha$ at the time of arrival. This is also seen from (4.18) which shows $dR/dt < 0$ for all $R$ in this case. Thus the Schwarzschild wall $R = \alpha$ separates space-time into two regions I and II with $R < \alpha$ and $R > \alpha$ respectively. While information can pass freely from II to I, no information about happenings in I can ever reach the region II.

Now consider an observer on the boundary of the sphere $r = r_b$ which

at the time $t < t_s(r_b)$ receives light from a distant star with $r_0 \gg \alpha$ and $R_0 \gg \alpha$. Then we get from (4.28) and (2.20)

$$\frac{\lambda}{\lambda_0} = \frac{1 - \alpha/R_b}{\sqrt{1 - \alpha/r_b} - \sqrt{(\alpha/R_b) - \alpha/r_b}} \tag{4.37}$$

where $R_b$ is the value of $R$ at the time $t$ of reception at $r_b$. When this time is small compared with $t_\alpha(r_b)$ in (4.8), i.e. in the region (3.23), we have $R_b = r_b$ and (4.37) reduces to

$$\lambda = \lambda_0 \sqrt{1 - \alpha/R_b}, \tag{4.38}$$

the light is shifted towards blue. In the limit $t \to t_\alpha(r_b)$ where $R_b \to \alpha$ we get from (4.37)

$$\lambda \to 2\lambda_0 \sqrt{1 - \alpha/r_b}. \tag{4.39}$$

For $\alpha/r_b \ll 1$, as in the example on p. 21, this corresponds to a redshift. Under the same assumption we have for $t_\alpha(r_b) < t < t_s(r_b)$, where $R_b < \alpha$, the redshift formula

$$\lambda = \lambda_0 \frac{\alpha/R_b - 1}{\sqrt{\alpha/R_b} - 1} = \lambda_0 \left(1 + \sqrt{\alpha/R_b}\right). \tag{4.40}$$

## 5. Continuation of the Solution of Section 1 to $t < 0$

In the preceding sections we have considered a contraction process starting from a state of rest at $t = 0$ corresponding to the initial conditions (1.23), (1.27). However, it is clear that (1.55) with (1.56) is a regular solution of Einstein's field equations in the whole region

$$-t_s(r) < t < t_s(r) \tag{5.1}$$

with $t_s(r)$ given by (2.8). In this region the parameters $u$ and $\eta$ in (1.54) take on all values in the intervals

$$-\frac{\pi}{2} < u < \frac{\pi}{2}, \qquad -\pi < \eta < \eta. \tag{5.2}$$

During the time interval

$$-t_s(r) < t \leq 0 \tag{5.3}$$

the quantity

$$u = t' \sqrt{\varphi/r^2} \tag{5.4}$$

goes from $-\pi/2$ to 0 and $C(u)$ increases from 0 to 1. Thus in the interval (5.3) we have instead of (2.3)

$$C'(u) = \sqrt{\frac{1-C}{C}} \tag{5.5}$$

corresponding to an expansion process. From (1.56), (5.5) it follows that $R'$ is still positive in the interval (5.3), but

$$\dot{R} \geq 0 \tag{5.6}$$

in contrast with (2.4). More precisely we have

$$\left.\begin{aligned} R(r, -t) &= R(r, t), \quad R'(r, -t) = R'(r, t) \\ \dot{R}(r, -t) &= -\dot{R}(r, t). \end{aligned}\right\} \tag{5.7}$$

In empty space we have in particular from (5.7) and (2.20)

$$\dot{R}(r, t) = \sqrt{(\alpha/R) - \alpha/r} \tag{5.8}$$

for $t$ in the interval (5.3).

The system described by this solution corresponds to a spherical distribution of incoherent matter which jumps out of a singularity at $t = -t_s(r)$ for which $u = -\pi/2$, $R = 0$ and expands with decreasing speed until it comes to rest at $t = 0$, after which it performs the contraction process described in the preceding sections.

For $t > 0$ the function $\varphi(r, t)$ was defined by (3.15). We extend the definition to negative $t$ by requiring that $\varphi(r, t)$ is an uneven function of $t$, i.e.

$$\varphi(r, -t) = -\varphi(r, t). \tag{5.9}$$

Since $R$ is an even function of $t$ this gives

$$\left.\begin{aligned} \varphi(r, t) = t\sqrt{1 - \alpha/r} - 2\sqrt{\alpha(r-\alpha)}\tan^{-1}\sqrt{\frac{r-R}{R}} \\ - 2\alpha \log \frac{\sqrt{R(r-\alpha)} + \sqrt{\alpha(r-R}}{\sqrt{r\,|R-\alpha|}} \end{aligned}\right\} \tag{5.10}$$

for $t$ in the interval (5.3). From (5.9) we obtain

$$\dot{\varphi}(r, -t) = \varphi(r, t), \quad \varphi'(r, -t) = -\varphi'(r, t). \tag{5.11}$$

Since also $\dot{R}$ is an uneven function of $t$ it follows that the expressions (3.17) are valid also for negative $t$. Therefore, in empty space the transition to curvature coordinates is also in the region (5.3) effected by the transforma-

tions (3.1, (3.4) with $\varphi$ given by (5.10), and the metric in $S_e$ is the same as in (3.3) (3.18). Since $T \geq 0$ for $t \geq 0$ and arbitrary $r$ we have $T \leq 0$ for $t \leq 0$ from (5.9).

All the considerations performed in the preceding sections for $t > 0$ can now be repeated for the region (5.3). The motion of the boundary relative to $S_e$ is again given by (4.6) with negative $t$. It starts at $t = -t_s(r_b)$ with $R_b = 0$ and increases to the value $R_b = \alpha$ for $t = -t_s(r_b)$ after which it increases further to the value $R_b = r_b$ at $t = 0$.

The motions of outward and inward going light signals are still determined by (4.15) and (4.16), but in view of (5.8) we have instead of (4.18)

$$\frac{dR}{dt} = \pm\sqrt{1 - \alpha/r} + \sqrt{(\alpha/R) - \alpha/r} \tag{5.12}$$

for $t < 0$. The solutions of the equations (4.15) are again given by (4.24), (4.25) where the functions $F_{\pm}(r, t)$ are determined by (4.21) and (5.10) for $t < 0$, but in this region $F_{+}(r, t)$ is everywhere regular, while

$$F_{-} \to \infty \quad \text{for} \quad R \to \alpha \tag{5.13}$$

Therefore, light emitted from a point $r_0 = r_b$ on the surface of the matter sphere at the time $t_0 < 0$ can freely move to the outside region with $R > \alpha$ even if $R_b < \alpha$ at the time of emission $t_0$. This also follows from (5.12) with the upper sign since $dR \,/\, dt$ is positive for all $R$. On the other hand, ingoing light starting at an event point $(r_0, t_0)$ with $R_0 > \alpha$, where $F_{-}(r_0, t_0)$ has a finite value, can never penetrate into a region where $R < \alpha$ on account of (5.13). This is also seen from (5.12) with the lower sign, since $dR \,/\, dt = 0$ for $R = \alpha$ and $dR \,/\, dt > 0$ for $R < \alpha$.

Thus, during the time interval

$$-t_s(r_b) < t < -t_\alpha(r_b) \tag{5.14}$$

where $R_b < \alpha$, the system is a "white hole". It can emit light into the outside world, where $r$ and $R$ are large compared with $\alpha$, but an observer on the sphere cannot during the period (5.14) receive any light from a distant star with $r_0 \gg \alpha$, $R_0 \gg \alpha$. On the other hand for $t > -t_\alpha(r_b)$ an observer on the sphere can receive any message from the outside world since $R > \alpha$ and $dR/dt < 0$ all the way along the time-tracks of ingoing light signals.

The relative line shift $z$ is in the whole region (5.1) given by (4.27), (4.28), but for negative $t$ the quantity $\dot{R}$ in (4.28), as given by (5.8), has the opposite sign of the expression in (2.20) valid for $t > 0$. Therefore, light

of wave length $\lambda_0$ emitted at $r_0 = r_b$ at a time $t_0$ in the interval (5.3) will be observed by a distant observer at $r \approx R \gg \alpha$ with the frequency $\lambda$ given by

$$\frac{\lambda}{\lambda_0} = \frac{\sqrt{1 - \alpha/r_0} - \sqrt{(\alpha/R_0) - \alpha/r_0}}{1 - \alpha/R_0} \tag{5.15}$$

which is the reciprocal of (4.37). Thus, if the light received at a place $r = r_b$ at a time $t > 0$ from a distant star is redshifted, the light emitted from the time-inversed point $(r_b, -t)$ as observed by a distant observer will be blueshifted and vice versa.

Similarly, for light from a distant star with $r_0 \approx R_0 \gg \alpha$ that is received at a point $r = r_b$ at a time in the interval

$$-t_\alpha(r_b) < t < 0 \tag{5.16}$$

where $R_b > \alpha$, we have

$$\frac{\lambda}{\lambda_0} = \frac{1 - \alpha/R_b}{\sqrt{1 - \alpha/r_b} + \sqrt{(\alpha/R_b) - \alpha/r_b}}. \tag{5.17}$$

This expression is the reciprocal of (4.35), i.e. the light received from a distant star at the surface of the sphere is blueshifted.

If the matter inside the sphere is uniformly distributed, the metric is given by (2.32) for $r < r_c$, which is identical with the Friedman solution for a spatially closed universe with constant positive curvature. According to the conventional cosmological ideas there is nothing outside this closed world, but the question now arises if the observable part of the universe in reality could be the inner part of a "meta galaxy" immersed in a much larger closed or open universe. In this respect the usually assumed values for the radius and average mass density of the universe are strangely suggestive. For a model of the type considered in this section with a radius of $10^{10}$ light years and density $10^{-29}\,\mathrm{gm/cm^3}$ the Schwarzschild constant would be of the order of magnitude of the radius, and it is conceivable that the observable universe at the present time is a "white hole", so that no information from distant stars outside the meta galaxy can penetrate into the interior. However, we shall not enlarge upon this picture here.

## Conclusion

In this paper we have reconsidered in more detail the problem of the collapse of incoherent matter under the influence of its own gravitational field. It serves as a simple illustration of the general theorem of Hawking and Penrose according to which singularities will develop both inside and outside the matter after a comparatively short time as measured on standard clocks at rest in a system $S_M$ in which the matter is constantly at rest (compare the example mentioned on p. 21). Not only does the density of matter go to infinity, as would be the case also in Newton's theory of gravitation, but in Einstein's theory the metric of space-time itself becomes singular at the finite time $t_s(r)$. In section 2 it was shown that the coefficients of $dr^2$ and $d\Omega^2$ in $ds^2$ in general have the following limiting values for $t \to t_s(r)$ and constant $r$:

$$a \to \infty, \quad R^2 \to 0$$

and for the determinant $g$ we found

$$g \to 0 \text{ for } t \to t_s(r).$$

The singularities in question are essential singularities that cannot be removed by any coordinate transformation.

In section 1 it was emphasized that the determinant $g$ must be negative in any case which has a physical meaning. Thus the occurrence of the just mentioned essential singularities means that the system according to Einstein's theory after a finite time runs into an unphysical state — a kind af nirvana where the time stops and the notions of space and time lose their meaning. It is hard for a physicist to accept this and one would rather conclude that Einstein's theory, which so admirably accounts for all phenomena in the case of normal gravitational fields, breaks down in cases where the components of the curvature tensor of space-time are extremely large.

## References


1. See ALBERT EINSTEIN, The Meaning of Relativity, Princeton University Press, Princeton 1953, p. 129.
2. R. PENROSE, Phys. Rev. Lett. **14,** 57 (1965).
   R. GEROCH, Phys. Rev. Lett. **17,** 455 (1966).
   S. HAWKING and G. ELLIS, Ap. J. **152,** 25 (1968).
3. J. R. OPPENHEIMER and H. SNYDER, Phys. Rev. **56,** 455 (1939).
4. G. E. LEMAÎTRE, Ann. Soc. Scient. Bruxelles, Ser. A. **53,** (51), (1933).
5. R. SERINI, Atti Acad. Lincei (5), **27,** 235 (1918).
   A. EINSTEIN, Revista (Univ. Nac. Tucuman) A. **2,** 11 (1941).
   A. EINSTEIN and W. PAULI, Ann. of Math. **44,** 131 (1943).
6. C. MØLLER, The Theory of Relativity, 2. Edition, Clarendon Press, Oxford 1972. Eq. (11.183).
7. See reference 6, Eqs. (11.179), (11.180).



Indleveret til Selskabet den 4. marts 1975.
Færdig fra trykkeriet den 5. september 1975.

F. HYNNE

# A CLASS OF MOLECULAR CORRELATION FUNCTIONS RELATED TO URSELL FUNCTIONS

Det Kongelige Danske Videnskabernes Selskab
Matematisk-fysiske Meddelelser **39,** 8


Kommissionær: Munksgaard
København 1975

## Synopsis

We study a class of intermolecular correlation functions $\mathscr{Y}_{[p]}$ appearing in refractive index theory. An explicit expression for $\mathscr{Y}_{[p]}$ in terms of Ursell functions and a recurrence relation in terms of distribution functions are derived. The function $\mathscr{Y}_{[p]}$ is shown to be invariant under permutations of the variables belonging to the dihedral group $D_p$. The results are applied to a problem of refractive index theory.


Printed in Denmark by Bianco Lunos Bogtrykkeri A/S. ISBN 87 7304 046 0

## Introduction

Intermolecular positional correlation forms the core of a description of fluid structure (see e.g. FRISCH and LEBOWITZ 1964, FISHER 1964, RICE and GRAY 1965, COLE 1967, EGELSTAFF 1967, and, for experimental data, FRISCH and SALSBURG 1968). The response of a molecular fluid to light is largely[1] determined by the response of an isolated molecule and by the equilibrium structure of the unperturbed fluid. It can therefore be described in terms of molecular correlation. Molecular refractive index theory results in a perturbation series for the refractive index $m$, which can be interpreted as describing a series of elementary scattering processes (YVON 1937, MAZUR 1958, BULLOUGH 1968, BULLOUGH, e.a. 1968, to be referred to as I, HYNNE 1970, to be referred to as II). A general term of such series involving $p$ molecules, contains a $(p-1)$-fold integral having a particular $p$-body correlation function[2] as a weight factor. This correlation function gauges the contribution to the refractive index of a multiple scattering process with $p$ scattering events from $p$ molecules in given configuration. Clearly, the character of the many-body response (as condensed in $m$) depends decisively on the set of correlation functions.

In this paper we consider correlation functions $\mathscr{Y}_{[p]}$ that appear as weight factors in a theory of the refractive index of a molecular fluid formulated in terms of a 'screened' intermolecular interaction (II). Although entirely microscopic[3], the screened theory has interesting macroscopic consequences: from the theory we have derived (HYNNE and BULLOUGH 1972, to be referred to as III) a generalized form of a dispersion relation, previously obtained by ONSAGER (1936) and BÖTTCHER (1942) by purely macroscopic

[1] Namely in the approximations of a quasistatic linear response theory and the polarization diagram approximation (I).

[2] We use the term 'correlation function' to denote an arbitrary combination of distribution functions (compare e.g. HILL 1958). We deviate from the terminology in our previous papers on refractive index theory which did not distinguish distribution functions from other correlation functions.

[3] The screened theory is initially completely equivalent to the fundamental unscreened theory (BULLOUGH 1968, I, II) but the 'bulk approximation' (see II) is required to reach the final, translationally invariant form.

arguments. We have also obtained (HYNNE 1974) an expression for absorption lines, at variance with simple two-body results, but agreeing with linewidths from coupled oscillator theory (HOLTSMARK 1925). The physical significance of these results shows that the screened formulation is physically very natural and motivates a study of the $\mathscr{Y}$ functions. A more concrete incentive is the necessity of knowing the asymptotic behaviour of the $\mathscr{Y}$ functions for a proof of convergence in the refractive index theory.

Correlation of $p$ molecules can be expressed by the $p$-body (reduced) molecular distribution function, which gives the probability density of configurations of any subset of $p$ molecules. (See e.g. HILL 1958, FRISCH and LEBOWITZ 1964; compare also section 2 of this paper). The $p$-body correlation function

$$\mathscr{Y}_{[p]} = \mathscr{Y}_{123\,\ldots\,p} = \mathscr{Y}_p\,(\boldsymbol{x}_1,\ \boldsymbol{x}_2,\ \boldsymbol{x}_3,\ \ldots,\ \boldsymbol{x}_p) \tag{1.1}$$

considered here is a function of the $p$ points in space $\boldsymbol{x}_1,\ \boldsymbol{x}_2,\ \ldots,\ \boldsymbol{x}_p$, and can be expressed as a combination of distribution functions of orders $q \leq p$. Although the set of distribution functions is perhaps the most natural choice other sets of functions, notably the set of Ursell functions,[4] may serve equally well as basis for a description of intermolecular correlation. It is the purpose of this paper to characterize the set of $\mathscr{Y}$ functions in relation to the two fundamental sets of functions, the set of distribution functions and the set of Ursell functions.

In the following section we introduce generalized correlation functions and define $\mathscr{Y}$ functions by an equation emerging from the refractive index theory (II). The most important part of the paper is a derivation in section 3 of an explicit expression (2.12) for the $\mathscr{Y}$ functions in terms of generalized Ursell functions and a recurrence relation (2.11) in terms of generalized distribution functions. Section 4 contains a discussion of some properties of $\mathscr{Y}$ functions, and section 5 an application of the result (2.12) to the original physical problem. The short section 6 summarizes the results.

[4] The Ursell functions can be defined without reference to distribution functions. For this and for a more general discussion of Ursell functions see in particular PERCUS 1964; see also the brief review in section 2 below. Notice, however, that there exists a different usage of the term 'Ursell function'; see e.g. FISHER 1964 and UHLENBECK and FORD 1962 and compare the original paper by URSELL (1927).

## 2. Definition of $\mathscr{Y}$ functions

Rather than using ordinary distribution functions we shall work in terms of generalized distribution functions

$$\mathscr{G}_{[p]} = \mathscr{G}_{123\ldots p} = \langle \varrho(\boldsymbol{x}_1)\, \varrho(\boldsymbol{x}_2)\, \varrho(\boldsymbol{x}_3) \ldots \varrho(\boldsymbol{x}_p) \rangle_{\mathrm{av}} \tag{2.1}$$

which are averages of products of the 'instantaneous' density of molecules

$$\varrho(\boldsymbol{x}) = \sum_j \delta(\boldsymbol{x} - \boldsymbol{x}_j^{\mathrm{in}}), \tag{2.2}$$

taken at different points. The instantaneous density $\varrho(\boldsymbol{x})$ depends on the configuration of molecules[5] (specified by the positions $\boldsymbol{x}_j$) of a member of the grand canonical ensemble. The system is homogeneous, and the average density $n = \langle \varrho(\boldsymbol{x}) \rangle_{\mathrm{av}}$ is independent of $\boldsymbol{x}$. In equation (2.1) and below we use subscript indices to denote position variables.

The $\mathscr{G}$ functions generalize the ordinary distribution functions of statistical mechanics (see e.g. HILL, 1956) to include self-correlations, and the first few functions are (see e.g. LEBOWITZ and PERCUS 1963; $\mathscr{G}_{1234}$ is exhibited in HYNNE 1974, p. 452)

$$\left.\begin{aligned} \mathscr{G}_1 &= n \\ \mathscr{G}_{12} &= n^2 g_{12} + n\delta_{12} \\ \mathscr{G}_{123} &= n^3 g_{123} + n^2(\delta_{12} g_{23} + \delta_{23} g_{31} + \delta_{31} g_{12}) + n\delta_{12}\delta_{23} \end{aligned}\right\} \tag{2.3}$$

In equation (2.3) $n^p g_{[p]}$ is the ordinary $p$-body distribution function and $\delta_{ij} = \delta(\boldsymbol{x}_i - \boldsymbol{x}_j)$ denotes a delta function representing a self-correlation.

Although ordinary correlation functions are perhaps appropriate for most applications, generalized functions are in many ways simpler than ordinary ones. In many-body optics it is possible to exploit the simplicity of the generalized functions to great advantage by formally expressing radiation reaction in terms of self-correlations (I). This definition is made initially in the (more fundamental) 'unscreened theory' (I), but it is carried over, with new significance, into the screened theory. (See II and, in particular, III). The $\mathscr{Y}$ functions therefore emerge from the screened theory with all self-correlations included, and it is natural to express them in terms of the generalized distribution functions.

[5] The refractive index theory (I, II) applies only to optically isotropic molecules for which orientational correlation is irrelevant.

The function $\mathscr{Y}_{[p]}$ is the average value of the instantaneous (configurational dependent) function $\mathscr{Y}^{\text{in}}_{[p]}$, recursively defined by the relation

$$\left.\begin{aligned} \mathscr{Y}^{\text{in}}_{1} &= \varrho_1 = \varrho(\boldsymbol{x}_1) \\ \mathscr{Y}^{\text{in}}_{123\,\cdots\,p} &= \mathscr{Y}^{\text{in}}_{123\,\cdots\,p-1}\,\varrho_p - \sum_{q=1}^{p-1} \mathscr{Y}^{\text{in}}_{123\,\cdots\,q}\,\mathscr{Y}_{q+1\,\cdots\,p}, \end{aligned}\right\} \tag{2.4}$$

which emerges from an integral equation in the refraction index theory (equation (2.6) of III).

We easily find the first few $\mathscr{Y}$ functions directly from the definition (2.4):

$$\left.\begin{aligned} \mathscr{Y}_1 &= \mathscr{G}_1 \\ \mathscr{Y}_{12} &= \mathscr{G}_{12} - \mathscr{G}_1\,\mathscr{G}_2 \\ \mathscr{Y}_{123} &= \mathscr{G}_{123} - \mathscr{G}_{12}\,\mathscr{G}_3 - \mathscr{G}_{23}\,\mathscr{G}_1 - \mathscr{G}_{31}\,\mathscr{G}_2 + 2\,\mathscr{G}_1\,\mathscr{G}_2\,\mathscr{G}_3 \end{aligned}\right\} \tag{2.5}$$

It is remarkable that these $\mathscr{Y}$ functions are identical with the corresponding generalized Ursell functions, which can be defined as (I, Stell 1964, Lebowitz and Percus 1963)

$$\mathscr{G}_{[p]} = \sum_{\pi \in \mathscr{P}_p} \prod_{Q \in \pi} \mathscr{U}_Q . \tag{2.6}$$

In equation (2.6) the sum is taken over the collection $\mathscr{P}_p$ of all partitions of the set of indices $[p] = (1, 2, 3, \ldots, p)$.[6]

The generalized Ursell functions may be obtained from a simpler recurrence relation, derivable from equation (2.6) (compare Percus 1964):

$$\mathscr{G}_{[p]} = \sum_{Q} \mathscr{U}_Q\,\mathscr{G}_{[p]-Q}, \quad 1 \in Q \tag{2.7}$$

in which the sum is taken over all subsets $Q$ of $[p]$ containing 1, and $[p]-Q$ denotes a set difference with ordered elements (compare footnote 6 and below). The $p$-body Ursell function[7] can be characterized (Percus 1964) as the part of the correlation between $p$ particles not contained in lower order functions. This characterization is natural in view of the definition (2.6), and it manifests itself in the asymptotic properties of the Ursell functions. Let the variables of $\mathscr{U}_{[p]}$ be partitioned into two sets with indices $Q$ and $R = [p] - Q$ and let $d_{QR}$ denote the minimum distance between the two sets:

[6] Below we shall take sets of indices like $[p]$ and $Q$ to denote ordered sets. Here, the ordering is immaterial because both $\mathscr{G}_{[p]}$ and $\mathscr{U}_{[p]}$ are symmetric in all their variables.

[7] Here and below 'Ursell functions' and 'distribution functions' denote generalized functions unless the contrary is expressly stated.

$$d_{QR} = \min |\boldsymbol{x}_i - \boldsymbol{x}_j|, \quad i \in Q, \; j \in R. \tag{2.8}$$

For any such partition the Ursell function $\mathcal{U}_{[p]}$ satisfies

$$\mathcal{U}_{[p]} \to 0 \quad \text{for} \quad d_{QR} \to \infty. \tag{2.9}$$

This is the cluster property of the Ursell function (compare UHLENBECK and FORD 1962), which follows (compare KAHN and UHLENBECK 1938) from equation (2.6) and the factorization of distribution functions

$$\mathcal{G}_{[p]} \to \mathcal{G}_Q \mathcal{G}_R \quad \text{for} \quad d_{QR} \to \infty.$$

The asymptotic behaviour (2.9) makes the Ursell functions very suitable for discussion of convergence of integrals, a property we exploit in section 5.

However, direct evaluation shows that

$$\mathcal{Y}_{1234} = \mathcal{U}_{1234} + \mathcal{U}_{13}\mathcal{U}_{24}; \tag{2.10}$$

so despite the striking coincidence at the lowest orders, the class of $\mathcal{Y}$ functions differs from the class of Ursell functions. Nevertheless, the results (2.5) and (2.10) suggest that the two classes of functions are simply related.

Whereas it is relatively easy to obtain expressions for lower order $\mathcal{Y}$ functions directly from (2.4), several features of the defining relation (2.4) complicate the derivation of a general expression for $\mathcal{Y}_{[p]}$, whether in terms of distribution functions or in terms of Ursell functions: Equation (2.4) is a non-linear many-terms mixed recurrence relation in the instantaneous functions $\mathcal{Y}^{\text{in}}$ involving the averaging operation in addition to arithmetic operations.

In the next section we shall solve this problem by deriving the following two relations

$$\mathcal{G}_{[p]} = \sum_{\sigma \in \mathcal{S}_p} \prod_{S \in \sigma} \mathcal{Y}_S \tag{2.11}$$

$$\mathcal{Y}_{[p]} = \sum_{\gamma \in \mathcal{C}_p} \prod_{C \in \gamma} \mathcal{U}_C \tag{2.12}$$

which independently determine $\mathcal{Y}_{[p]}$: equation (2.11) is a pure recurrence relation for $\mathcal{Y}_{[p]}$ in terms of distribution functions whereas equation (2.12) is an explicit expression for $\mathcal{Y}_{[p]}$ in terms of Ursell-functions.[8] The sums in equations (2.11) and (2.12) are taken over certain sets of partitions of the index set $[p] = (1, 2, 3, \ldots, p)$ defined in the following section. Indeed, the

[8] The result (2.12) has been quoted in II: here we present the derivation of the result.

core of the derivation involves essentially just manipulations with partitions of index sets, and it would be a futile notational complication to formulate the derivation in terms of the functions. We therefore base the derivation on two lemmas on 'ordered partitions' which we derive in the following section. Since this arrangement may obscure the motivation for the various steps of the derivation, we start with a brief outline of the argument.

## 3. Derivation of Equations (2.11) and (2.12)

To derive (2.11) we first obtain an expression for a product of functions $\varrho(\boldsymbol{x})$ (compare equation (2.1)) which upon averaging yields equation (2.11). The structure of the terms of the sum in equation (2.11) can be ascertained by scrutinizing equation (2.4). Here, we prove the result by induction. For this proof we use equation (2.4) and a lemma showing how the set $\mathscr{S}_{p+1}$ of partitions of $[p+1]$ can be generated from the set $\mathscr{S}_p$ of partitions of $[p]$. From equation (2.11) we obtain (2.12) by comparison of equations (2.6) and (2.11) using another lemma which states that any partition of $[p]$ can be uniquely decomposed into a certain subpartition of a partition belonging to $\mathscr{S}p$. We first derive the lemmas.

We consider partitions of the set

$$[p] = (1, 2, 3, \ldots, p) \tag{3.1}$$

of the first $p$ positive integers. The relevant partitions are all characterized with reference to the numerical order of the integers.[9] We shall also need to consider ordered subsets of $[p]$ as well as partitions of such subsets. We therefore take $[p]$ to denote the naturally ordered set, and we shall understand that any set of integers (whether it is element of a partition or not) is ordered according to magnitude unless the contrary is stated. By an ordered partition of an ordered set we simply mean a partition in which the elements are ordered within each set of the partition, whereas the sets of the partition are not ordered among themselves. (Nevertheless, the ordering induces a relation among the sets, which we exploit below).

It is very helpful to represent partitions by diagrams. Let the elements $1, 2, 3, \ldots, p$ of the basic index set $[p]$ be represented by consecutive vertices of a regular polygon of $p$ sides. A partition of $[p]$ is then represented by a collection of polygons (which may include points and lines as degenerate

[9] The ordering arises from a chronological ordering of scattering events in the refractive index theory (II).

cases), each having the representative points of a set of the partition as vertices. The sides of a set-polygon connect vertices corresponding to cyclically consecutive elements of a set. Figure 1 c exemplifies the diagram representation by showing the representation of the partition

$$\{(1, 4, 7), (2, 8), (3), (5, 6)\} \tag{3.2}$$

of the set [8].

From any partition of $[p]$ containing a set $Q$ with more than one element we obtain a particular subpartition by dividing $Q$ into a non-empty, proper,

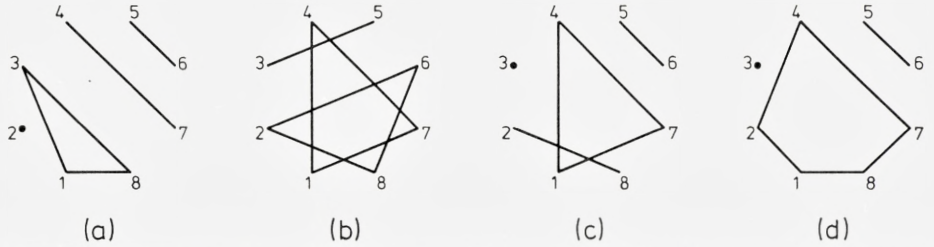


Figure 1. Diagrammatic representations of partitions exemplifying the various types of partitions:

(a) The *s*-partition (3.3)
(b) The *c*-partition (3.5)
(c) The composite partition (3.2)
(d) The basis (3.4) of the composite partition (c).

The composite partition (c) is neither an *s*-partition nor a *c*-partition; but it can be obtained from the *s*-partition (d) which is its basis by replacing the sets of (d) by definite c-partitions of these. This representation of the composite partition (3.2) as a subpartition of its basis is the *sc*-decomposition of the partition.

ordered subset of *consecutive* elements from $Q$ and the ordered subset of the remaining elements from $Q$. We call this special subpartitioning an s-process (where *s* stands for 'sequence'). We define an *s*-partition of $[p]$ as any partition that can be obtained from $[p]$ by repeated use of *s*-processes. By definition, $[p]$ is itself an *s*-partition.[10] The diagram representation permits an especially simple characterization: A partition is an *s*-partition if and only if it is represented by a diagram in which sides of different polygons do not intersect. This is a direct consequence of the definition of *s*-partitions. Figure 1 a illustrates the property for the *s*-partition

$$\{(1, 3, 8), (2), (4, 7), (5, 6)\}. \tag{3.3}$$

The diagram representation shows that we may replace the term 'consecutive' by 'cyclically consecutive' in the definition of the *s*-process.

[10] We shall not distinguish between the one-set partition $\{[p]\}$ and the set $[p]$ itself.

We denote by $\mathscr{S}_p$ the collection of all $s$-partitions $\sigma_p$ of $[p]$, and by $\mathscr{S}_p^0$ the subset of $\mathscr{S}_p$ consisting of the partitions $\sigma_p^0$ in which the integers 1 and $p$ belong to the same set. We obtain a mapping $f_p$ from $\mathscr{S}_p$ into the set $\mathscr{P}_{p+1}$ of all partitions of $[p+1]$ by defining the image $f_p(\sigma_p)$ of a partition $\sigma_p \in \mathscr{S}_p$ as the partition obtained from $\sigma_p$ by adjoining $p+1$ to the set in $\sigma_p$ containing the integer 1. Since 1 and $p+1$ are cyclic neighbours in $[p+1]$, and since $\sigma_p \in \mathscr{S}_p$, $f_p(\sigma_p)$ belongs to $\mathscr{S}_{p+1}$ and hence to $\mathscr{S}_{p+1}^0$. Conversely, for each $\sigma_{p+1}^0 \in \mathscr{S}_{p+1}^0$ there is a unique original element under $f_p$ obtained simply by removing the integer $p+1$ from $\sigma_{p+1}^0$. Thus, $f_p$ establishes a one-to-one correspondence between $\mathscr{S}_p$ and $\mathscr{S}_{p+1}^0$.

We now find a prescription for generating the whole collection $\mathscr{S}_{p+1}$ from $\mathscr{S}_{p+1}^0$ and hence (by $f_p$) from $\mathscr{S}_p$. We obtain $\mathscr{S}_{p+1}$ as the collection of the partitions in $\mathscr{S}_{p+1}^0$ and the partitions obtained from each of these partitions by employing one $s$-process in all possible different ways giving partitions in which 1 and $p+1$ belong to different sets. All the partitions obtained this way belong to $\mathscr{S}_{p+1}$ by construction, and each element $\sigma_{p+1}$ of $\mathscr{S}_{p+1}$ is generated exactly once. If $\sigma_{p+1} \in \mathscr{S}_{p+1}^0$, this is obvious. If $\sigma_{p+1} \notin \mathscr{S}_{p+1}^0$, it arises precisely once from the unique partition obtained from $\sigma_{p+1}$ by uniting the sets containing the elements 1 and $p+1$: The resulting partition is indeed contained in $\mathscr{S}_{p+1}^0$ since 1 and $p+1$ are cyclic neighbours in $[p+1]$. We refer to the rule for obtaining $\mathscr{S}_{p+1}$ from $\mathscr{S}_p$ as lemma 1.

Consider diagrams of partitions as two-dimensional point sets. We say that two sets of an ordered partition are connected if the diagram of the partition contains a continuous curve joining points of the polygons that represent the two sets.[11]

Clearly, connectivity is an equivalence relation and hence gives rise to a classification of the sets of a partition. From an arbitrary partion $\pi$ we obtain another partition $\sigma_\pi$ which we call the basis of $\pi$, by replacing each connectivity class by the union of all sets in the class. The basis of a partition has a diagram in which no polygon-sides intersect: it is an $s$-partition. For example, the basis of the partition (3.2) (exhibited in figure 1 c) is

$$\{(1, 2, 4, 7, 8), (3), (5, 6)\} \tag{3.4}$$

which is an $s$-partition as figure 1 d clearly shows. An $s$-partition is its own basis.

A partition in which all sets are connected is said to be connected and

[11] 'Connectivity' is not used in the graph-theoretical sense: the diagrams are not graphs in the narrow sense of this term (compare e.g. BERGE 1962).

is called a $c$-partition. Compare the diagram in figure 1b which represents the $c$-partition,

$$\{(1, 4, 7), (2, 6, 8), (3, 5)\} \tag{3.5}$$

of the set [8]. The set of all $c$-partitions of $[p]$ is denoted $\mathscr{C}_p$. The basis of a $c$-partition of $[p]$ is $[p]$ itself (compare footnote 10).

Any partition determines its basis uniquely and can be recovered from this by a unique, partitioning of the sets of the basis into connected partitions. Therefore, any partition can be uniquely decomposed into a $c$-subpartition of an $s$-partition. We refer to this result as lemma 2. It shows that $c$-partitions are in a sense complementary to $s$-partitions.

The sets $\mathscr{S}_p$ and $\mathscr{C}_p$ appearing in equation (2.11) and (2.12) are now well defined, and we procede to prove these relations. Assume[12]

$$\varrho_1 \varrho_2 \varrho_3 \cdots \varrho_p = \sum_{\sigma \in \mathscr{S}_p} \mathscr{Y}^{\text{in}}_{S_1} \prod_{j>1} \mathscr{Y}_{S_j} \tag{3.6}$$

where the sum is taken over all partitions $\sigma = \{S_1, S_2, \ldots\} \in \mathscr{S}_p$, and $S_1$ is the set containing the integer 1. Multiply both sides of equation (3.6) by $\varrho_{p+1}$ and eliminate all products $\mathscr{Y}^{\text{in}}_{S_1} \varrho_{p+1}$ by equation (2.4). By employing lemma 1 we then find that the resulting expression has the form (3.6) with $p$ replaced by $p+1$, and the validity of equation (3.6) follows by induction. From equation (3.6) we obtain the recurrence relation (2.11) by taking the average value.

Consider now equation (2.6). By lemma 2 we can write the sum over $\mathscr{P}_p$ in this equation as the sum over $\mathscr{S}_p$ of the sum over all $c$-subpartitions: The existence of the $sc$-decomposition of an arbitrary partition guarantees that all terms of (2.6) are included in the double sum, and the uniqueness of the decomposition ensures that each term is included only once. All terms of (2.6) having a given basis $\sigma \in \mathscr{S}_p$ factorize alike, corresponding to the sets $S$ of $\sigma$. We can therefore rewrite equation (2.6)

$$\mathscr{G}_{[p]} = \sum_{\sigma \in \mathscr{S}_p} \prod_{S \in \sigma} \sum_{\gamma \in \mathscr{C}(S)} \prod_{C \in \gamma} \mathscr{U}_C \tag{3.7}$$

in which $\mathscr{C}(S)$ denotes the collection of all connected partitions of the ordered set $S$.

To prove the expression (2.12) equate the right hand sides of equations (2.11) and (3.7) and assume equation (2.12) to be valid for all orders smaller than $p$. All terms in the sums over $\mathscr{S}_p$ except those corresponding to $\sigma = [p]$ then cancel[10] leaving the expression (2.12) at order $p$, and the general validity of equation (2.12) follows by induction.

[12] We simplify the notation when no confusion can arise.

## 4. Discussion of Results

The derivation of equation (2.12) in the preceding section reveals that the two equations, (2.11) and (2.12), are in a sense complementary with respect to equation (2.6). The $\mathscr{Y}$ functions may therefore be naturally characterized as being intermediate between the distribution functions and the Ursell functions. Both equations have a form comparable to that of equation (2.6), but in equation (2.11) the $\mathscr{Y}$ functions appear similar to Ursell functions, whereas in equation (2.12) they appear similar to distribution functions.

Equation (2.12) is an explicit expression for the $\mathscr{Y}$ functions. It shows that these are sums of products of Ursell functions. To illustrate the structure of the $\mathscr{Y}$ functions we have displayed these up to order six, in figure 2, using a diagram notation related to the one used for partitions: A diagram with dashed lines represents a product of Ursell functions, and a polygon covering a set of vertices corresponding to an index set $Q$ indicates the presence of a factor $\mathscr{U}_Q$. The terms of the sum for $\mathscr{Y}_{[p]}$ appear in classes within which the terms only differ by cyclic permutations or by complete reversal followed by cyclic permutations of the indices. (Compare the discussion of symmetry below). For clearity and to save space we therefore represent the terms of a class by just one diagram with unnumbered vertices, and indicate the number of terms in a class by a coefficient to the diagram. For example, there are six terms in two classes at order five, namely

$$\left.\begin{aligned}\mathscr{Y}_{12345} = {} & \mathscr{U}_{12345} + \mathscr{U}_{135}\mathscr{U}_{24} + \mathscr{U}_{124}\mathscr{U}_{35} \\ & + \mathscr{U}_{235}\mathscr{U}_{14} + \mathscr{U}_{134}\mathscr{U}_{25} + \mathscr{U}_{245}\mathscr{U}_{13}.\end{aligned}\right\} \tag{4.1}$$

Equation (2.11) gives the $\mathscr{Y}$-functions in terms of distribution functions only implicitly. A simpler recurrence relation is readily obtained from equation (2.11):

$$\mathscr{G}_{[p]} = \sum_Q \mathscr{Y}_Q \prod_j \mathscr{G}_{Q_j}, \quad 1 \in Q. \tag{4.2}$$

Here the sum is taken over all subsets $Q$ of $[p]$ containing 1, and $\{Q, Q_1, Q_2, \ldots\}$ is the smallest[13] partition of $[p]$ in which each set $Q_j$ consists of a single chain of consecutive integers. Evidently, the partition is determined uniquely by $Q$.

Equation (4.2) is directly comparable to equation (2.7). The only difference of form is that the single function $\mathscr{G}_{[p]-Q}$ in the equation with Ursell

[13] That is, the partition with the least number of sets.

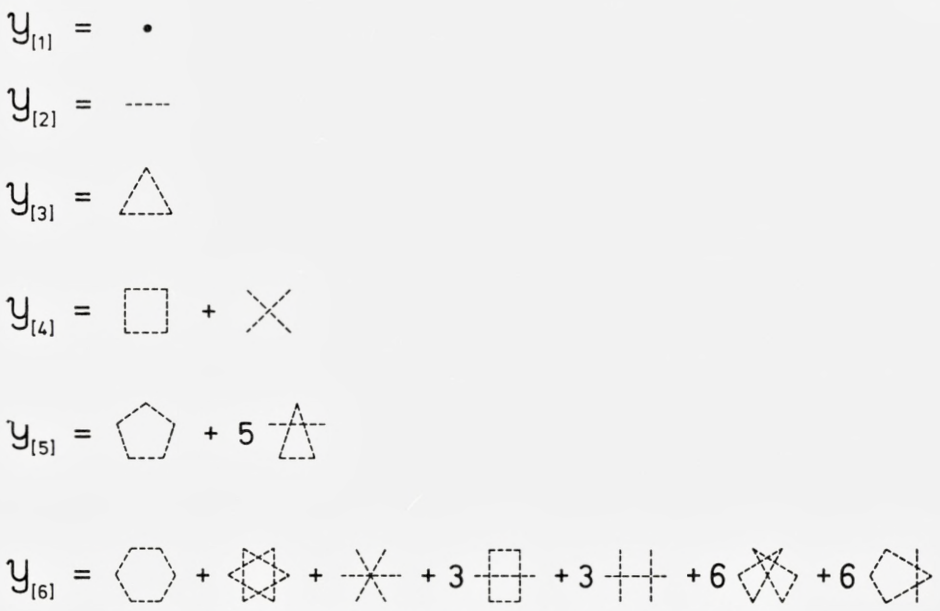


Figure 2. Diagrammatic representations of the first six $\mathcal{Y}$ functions.

functions is replaced by a product of $\mathcal{G}$ functions covering the set $[p]-Q$ in the equation with $\mathcal{Y}$ functions.

It is plain from equation (4.2) that the explicit expression for $\mathcal{Y}_{[p]}$ in terms of distribution functions must have the form

$$\mathcal{Y}_{[p]} = \sum_{\sigma \in \mathcal{S}_p} c_\sigma \prod_{S \in \sigma} \mathcal{G}_S \tag{4.3}$$

The coefficients $c_\sigma$ can be obtained from equation (4.2). This is easy for partitions with few sets. In particular, the coefficient $c_\zeta$ to the constant term $\mathcal{G}_1 \mathcal{G}_2 \ldots \mathcal{G}_p = n^p$ of $\mathcal{Y}_{[p]}$ (corresponding to $\zeta = \{(1), (2), \ldots, (p)\}$) is found to be $c_\zeta = (-1)^{p-1}(p)_{p-1}/p!$, which (apart from sign) is known as a Catalan number (Sloane 1973). The constant terms of the $\mathcal{Y}$ functions are of special interest in the refractive index theory (II) where they give rise to contributions which produce the 'cavity field factor' of the dispersion relation (see section 2 of III). But the general coefficient $c_\sigma$ depends on the detailed structure of the partition $\sigma$ in a rather complicated way,[14] and this fact detracts from the usefulness of the explicit form (4.3). The simple

[14] In the corresponding expression for the Ursell functions, the coefficients are $(-1)^{q-1}(q-1)!$, determined solely by the number $q$ of sets in the correponding partition.

expression (2.12) in terms of Ursell functions is the natural representation of $\mathscr{Y}_{[p]}$.

Both distribution functions and Ursell functions are symmetric in all variables, i.e. $\mathscr{G}_{[p]}$ and $\mathscr{U}_{[p]}$ are invariant under all permutations of $[p]$. In contrast, for $p > 3$ $\mathscr{Y}_{[p]}$ is only invariant under permutations belonging to the dihedral group $D_p$, a proper subgroup of order $2p$ of the symmetric group of degree $p$ (and order $p!$). The group $D_p$ consists of all cyclic permutations of $[p]$ and of these followed by complete reversal of order (which e.g. takes $(1, 2, \ldots, p-1, p)$ into $(p, p-1, \ldots, 2, 1)$). The elements in $D_p$ are precisely the permutations that carry the polygon representing $[p]$ into itself (except for the numbering). It is clear from the explicit form (2.12) that $\mathscr{Y}_{[p]}$ is invariant under permutations from $D_p$: These map the set of connected partitions onto itself (except for ordering) and hence just cause a rearrangement of the terms in the sum on the right hand side of equation (2.12). (The Ursell functions are symmetric in all variables). On the other hand, there can be no forther symmetry: For any permuation $\mathrm{P} \notin D_p$ of $[p]$ there exists at least one pair $(i, j)$ of not cyclically consecutive integers which is mapped by P into consecutive integers. Therefore, P maps the $c$-partition $\{(i, j), [p] - (i, j)\}$ into an $s$-partition, and consequently, there exists at least one term in the sum on the right hand side of equation (2.12) which transforms under P into a term not contained in the original sum (and not cancelled by other terms).

A consequence of the incomplete symmetry of $\mathscr{Y}_{[p]}$ is that the asymptotic behaviour of $\mathscr{Y}_{[p]}$ depends on the limit considered. Let the variables of $\mathscr{Y}_{[p]}$ be divided into two sets as discussed above equation (2.8), define $d_{QR}$ by equation (2.8), and define

$$d_Q = \max |\boldsymbol{x}_i - \boldsymbol{x}_j|, \; i, j \in Q. \tag{4.4}$$

Equations (2.9) and (2.12) then show that

$$\mathscr{Y}_{[p]} \to 0 \quad \text{for} \quad d_{QR} \to \infty, \, d_Q, d_R < \infty, \tag{4.5}$$

if and only if[15] $Q$ consists of cyclically consecutive integers of $[p]$. In particular, $\mathscr{Y}_{[p]} \to 0$, when the distance from one point to all the other points goes to infinity. These asymptotic properties of $\mathscr{Y}$ functions are important in refractive index theory as we shall see in the following section.

In closing this section we note a straightforward extension of the results.

[15] The 'only if' part of the statement disregards possible accidental zeros for special configurations within the two sets of points.

The $\mathscr{Y}$ functions are generalized correlation functions in the sense that they include all self-correlations. By simply omitting these self-correlations we obtain a corresponding set of 'ordinary' functions which evidently satifies equations analogous to (2.11), (2.12) with the $\mathscr{G}$ and $\mathscr{U}$ functions replaced by ordinary distribution functions and Ursell functions. Obviously, the ordinary functions also share the symmetry and the asymptotic behaviour (4.5) with the $\mathscr{Y}$ functions.

## 5. $\mathscr{Y}$ functions in Refractive Index Theory

We now analyse a problem of convergence arising in refractive index thory, in which the special structure of the $\mathscr{Y}$ functions plays a peculiar role.

In microscopic refractive index theory (e.g. Yvon 1937, Bullough 1967, I) the macroscopic response of a many-body system to an external electromagnetic field is naturally described in terms of elementary scattering processes taking place in vacuum. In this theory, the response related to bulk porperties is mixed at all orders in multiple scattering with irrelevant surface effects associated with molecular description of reflection and diffraction (I). Mathematically, the surface effect appears through integrals over a finite region, which diverge when taken over all space.

We have systematically eliminated the surface effect to all orders in multiple scattering and obtained a translationally invariant theory, the screened theory (II), by a reformulation of the theory in which the elementary scattering processes take place in the medium (compare Bullough 1965, 1967). This elimination involves extension of integrations to all space, a procedure that demands a proof of convergence. It is this problem we consider here.

A typical integral to be analysed (from the term at order $p$ in multiple scattering) is

$$\int\int \ldots \int \tilde{\mathbf{F}}_{12} \cdot \tilde{\mathbf{F}}_{23} \ldots \tilde{\mathbf{F}}_{(p-1)\,p} \exp(\mathrm{i}m\,\boldsymbol{k}_0 \cdot (\boldsymbol{x}_p - \boldsymbol{x}_1))\,\mathscr{Y}_{123\ldots p}\, d\boldsymbol{x}_2\, d\boldsymbol{x}_3 \ldots d\boldsymbol{x}_p \qquad (5.1)$$

in which $\boldsymbol{k}_0$ is a fixed vector of length $k_0$, and the refractive index $m$ is taken to be real.[16] The tensor $\tilde{\mathbf{F}}_{jk} = \tilde{\mathbf{F}}(\boldsymbol{x}_j, \boldsymbol{x}_k; \omega)$ is given by

[16] The choice $\mathrm{Im}\,(m) = 0$ is consistent with translational invariance, but means neglect of external scattering. This is a logically necessary but unphysical feature of a translationally invariant theory. But the final equation (of which (5.1) is a part) admits of no purely real solution for $m$ (compare especially Hynne 1974). Thus, the translationally invariant form of the screened theory contains a logical inconsistency (compare Bullough 1965, 1967). We shall not discuss this question further here, however.

$$\tilde{\mathbf{F}}(\boldsymbol{x}, \boldsymbol{x}'; \omega) = (\nabla\nabla + m^2 k_0^2 \mathbf{U})\left(\frac{\exp(\mathrm{i}m k_0 r)}{m^2 r}\right), \quad r = |\boldsymbol{x} - \boldsymbol{x}'| \tag{5.2}$$

where $\mathbf{U}$ is the unit tensor. It describes the propagation of radiation from a dipole in a medium of refractive index $m$. It has the asymtotic form

$$\tilde{\mathbf{F}}(\boldsymbol{x}, \boldsymbol{x}'; \omega) \sim k_0^2(\mathbf{U} - \hat{\boldsymbol{r}}\hat{\boldsymbol{r}})\frac{\exp(\mathrm{i}m k_0 r)}{r}, \quad k_0 r \gg 1, \tag{5.3}$$

where $\hat{\boldsymbol{r}} = (\boldsymbol{x} - \boldsymbol{x}')/r$.

For $m$ real, $\tilde{\mathbf{F}}$ is long range, and the convergence of the multiple integral (5.1) is ensured neither by the $\tilde{\mathbf{F}}$ tensors alone nor by the $\mathscr{Y}$ functions alone. (Compare the discussion of the asymptotic behaviour of the $\mathscr{Y}$ functions in the preceding section). It is through the special *combination* of Ursell functions and $\tilde{\mathbf{F}}$ tensors the integrals converge. As we shall see, the convergence is only just secured, however.

Express $\mathscr{Y}_{[p]}$ by equation (2.12) as a sum of products of Ursell functions, and consider a typical term. The structure of such a term is best visualized by the diagram for the product of Ursell functions in which the $\tilde{\mathbf{F}}$ tensors are indicated by heavy lines; a coincidence of a dashed and a heavy line is indicated by adding a cross to the heavy line (compare figure 3 a). Because of the short range of the Ursell functions, we can integrate first over the relative coordinates of each cluster (set of particles covered by one Ursell function) with one particle of the cluster held fixed. Hereby we are left with integrations over relative positions of clusters. We can assume that the $\tilde{\mathbf{F}}$ tensors that connect particles in different clusters can be replaced by $\tilde{\mathbf{F}}$ tensors connecting the fixed particles of the clusters. (This approximation is good when the clusters are far apart, and certainly proper for discussion of convergence). The crucial point now is, that every cluster is connected with

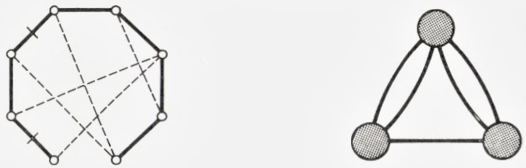


Figure 3. (a) Diagram representing an integral of the type shown in equation (5.1) for $p = 8$ with $\mathscr{Y}_{[8]}$ replaced by a typical term $\mathscr{U}_{126}\mathscr{U}_{348}\mathscr{U}_{57}$ of its expansion (2.12). (b) A schematic representation of the same term exposing its structure of clusters (represented by shaded circles in (b) and by dashed polygons in (a)) connected by 'external' $\tilde{\mathbf{F}}$ tensors (represented by heavy lines).

every other cluster by at least three independent chains of $\tilde{\mathbf{F}}$ tensors. This fact is illustrated in figure 3 b for the term shown in figure 3 a. Here, clusters are indicated by large shaded circles, and $\tilde{\mathbf{F}}$ tensors going between clusters are shown whilst $\tilde{\mathbf{F}}$ tensors going inside a cluster are omitted. Any two of the three clusters in figure 3 b are connected by precisely three independent chains of $\tilde{\mathbf{F}}$ tensors. (This exemplifies the 'worst case': in the term corresponding to the partition exhibited in figure 1 b, e.g., which also has three clusters, there are four independent chains between any pair).

An immediate consequence of this structure of multiply connected sets of clusters is that the integral over all positions of any one cluster with all the remaining clusters fixed in arbitrary configuration, converges. This almost proves the convergence of the multiple integral (5.1). The remaining step of a complete and rigerous proof is complicated by the fact that the individual integrals are not in general absolute convergent. This means that the process of integration over all space must be specified, for example as a limit of integration over a finite region; it is then still necessary to specify the passage to that limit. Such a proof is outside the scope of this paper.

As conclusion we may say that the result (2.12) forms an excellent basis for analysis of convergence of the multiple integral (5.1). This analysis strongly suggests that the multiple integral does converge although the convergence is shown to be conditional and extremely slow. Certainly, the transformation to the translationally invariant screened theory has eliminated all the manifestly divergent integrals that appear in the unscreened theory when the integrations are extended to all space.

## 6. Summary of Results

The $p$-body correlation function

$$\mathscr{Y}_{[p]} = \mathscr{Y}_{123\,\ldots\,p} = \mathscr{Y}_p(\boldsymbol{x}_1, \boldsymbol{x}_2, \boldsymbol{x}_3, \ldots, \boldsymbol{x}_p) \tag{6.1}$$

is a function of $p$ variables (points in space). It is symmetric in the variables corresponding to the dihedral permutation group $D_p$, i.e. it is invariant under cyclic permutations of the variables as well as under complete reversal of the order of the variables. It is a generalized correlation function in the sense that it includes all self-correlations, but all results can be reinterpreted in terms of ordinary functions.

The set of $\mathscr{Y}$ functions is related to the set of generalized distribution functions on the one hand, and to the set of generalized Ursell functions on the other hand, by the pair of equations (2.11), (2.12), the main result of

this paper. This pair of equations shows that the $\mathscr{Y}$ functions can be said to be intermediate between distribution functions and Ursell functions. Each of the two equations independently determine the $\mathscr{Y}$ functions: equation (2.11) is a recurrence relation for the $\mathscr{Y}$ functions in terms of generalized distribution functions, and (2.12) is an explicit expression in terms of generalized Ursell functions. The two equations involve sums over either of two distinct sets of partitions of the index set $[p]$ that marks the variables of the functions. These partitions are defined in section 3, and the derivation of equation (2.11) and (2.12) is based on an analysis of 'ordered partitions' resulting in a theorem (lemma 2, stated below equation (3.5)) on decomposition of partitions. The $\mathscr{Y}$ functions of orders up to six are displayed in figure 2 in a diagram notation explained in section 4. The first three $\mathscr{Y}$ functions are identical to the corresponding Ursell functions.

The explicit expression (2.12) is utilized to prove (with qualifications) that characteristic asymptotic properties of the $\mathscr{Y}$ functions just secure convergence of integrals appearing in refractive index theory.

*Chemistry Laboratory III*
*H. C. Orsted Institute*
*Universitetsparken 5*
*DK 2100 Copenhagen O*
*Denmark*

## References


Berge, C., 1962. *The Theory of Graphs*, Methuen, London.

Bullough, R. K., 1965. Phil. Trans. Roy. Soc. (London) **A 258**, 387.

Bullough, R. K., 1967. *Proc. Second Interdiciplinary Conf. Electromagnetic Scattering*, p. 537–77, Gordon and Breach, New York.

Bullough, R. K., 1968. J. Phys. A: Gen. Phys. **1**, 409.

Bullough, R. K., Obada, A.-S. F., Thompson, B. V. and Hynne, F., 1968, Chem. Phys. Lett. **2**, 293. (Referred to as I).

Böttcher, C. J. F., 1942. Physica **9**, 937.

Cole, G. H. A., 1967. *An Introduction to the Statistical Theory of Classical Simple Dense Fluids*, Pergamon, Oxford.

Egelstaff, P. A., 1967. *An Introduction to the Liquid State*, Academic Press, New York.

Fisher, I. Z., 1964. *Statistical Theory of Liquids*, University of Chicago Press, Chicago.

Frisch, H. L. and Lebowitz, J. L., 1964. *The Equilibrium Theory of Classical Fluids*, Benjamin, New York.

Frisch, H. L. and Salsburg, Z. W., 1968. *Simple Dense Fluids*, Academic Press, New York.

Hill, T. L., 1956. *Statistical Mechanics*, McGraw-Hill, New York.

Holtsmark, J., 1925. Z. Physik **34**, 722.

Hynne, F., 1970. J. Phys. A: Gen. Phys. **3**, L 24. (Referred to as II).

Hynne, F., 1974. J. Quant. Spectrosc. Radiat. Transfer **14**, 437.

Hynne, F. and Bullough, R. K., 1972. J. Phys. A: Gen. Phys. **5**, 1272 (Referred to as III).

Kahn, B. and Uhlenbeck, G. E., 1938. Physica **5**, 399.

Lebowitz, J. L. and Percus, J. K., 1963. J. Math. Phys. **4**, 116.

Mazur, P.,1958. *Advances in Chemical Physics* vol. 1, p. 309. Interscience, New York.

Onsager, L., 1936. J. Am. Chem. Soc. **58**, 1486.

Percus, J. K., 1964. in *The Equilibrium Theory of Classical Fluids*, p. II–33, eds. Frisch and Lebowitz, Benjamin, New York.

Rice, S. A. and Gray, P., 1965. *The Statistical Mechanics of Simple Liquids*, Interscience, New York.

Sloane, N. J. A., 1973. *A Handbook of Integer Sequences*, Academic Press, New York.

Stell, G., 1964. in *The Equilibrium Theory of Classical Fluids*, p. II–171, eds. Frisch and Lebowitz, Benjamin, New York.

Uhlenbeck, G. E. and Ford, G. W., 1962. in *Studies in Statistical Mechanics*, vol. 1 p. 119, eds. de Boer and Uhlenbeck, North-Holland, Amsterdam.

Ursell, H. D., 1927. Proc. Cambridge Phil. Soc. **23**, 685.

Yvon, J., 1937. Actualites Scientifiques et Industrielles No. 543.


Indleveret til Selskabet den 29. september 1974.
Færdig fra trykkeriet den 10. oktober 1975.

JØRGEN KALCKAR AND OLE ULFBECK

# STUDIES IN CLASSICAL ELECTRON THEORY I

## Radiation Damping and Differential Conservation Laws

Det Kongelige Danske Videnskabernes Selskab
Matematisk-fysiske Meddelelser **39**, 9


Kommissionær: Munksgaard
København 1976

## Synopsis

The present study is the first in a series of three attempting a critical assessment of the status of classical electron theory.

By means of a simple idealized experiment the relationship is exhibited between the retardation of physical actions and the requirement of energy conservation on the one hand and the occurrence of radiation damping on the other. From this example it emerges, that radiation phenomena are characterized by a certain feature of wholeness, even within the domain of classical physics.

The mechanism of radiation reaction is further analysed within the context of the classical Maxwell theory, where the phenomenon of damping – like that of electromagnetic inertia – naturally originates in the mutual interaction between the various infinitesimal constituents making up any finite change. On this background the interplay between the various assumptions, underlying the attempts initiated by Dirac of incorporating the notion of an "ideal point charge" into the foundation of classical electrodynamics, is critically examined.

In the "point electron description" the phenomenon of damping has no natural place, although the proponents of this description have offered several arguments leading to the well-known expression for the damping. Closer scrutiny reveals, however, that these arguments are at variance with the proper Maxwell theory and must be regarded as *ad hoc* assumptions carefully chosen so as to achieve the desired result. In this connection it is emphasized that the problem of "acausalities" associated with the Lorentz-Dirac equation are by no means inherent difficulties in classical electron theory, but are procured only through the postulate that this equation represents the *exact* equation of motion for a point electron.


Printed in Denmark by Bianco Lunos Bogtrykkeri AS. ISBN 87 7304 047 9

## § 1. Introduction

In Classical Electron Theory, as based on the pioneering work of ABRAHAM and LORENTZ, the electron is conceived of as a minute spherical distribution of an in principle infinite number of infinitesimal electrified constituents. From the very beginning it was, of course, realized that an explanation of the *stability* of such a system was outside the purview of the Maxwell theory, but nevertheless the hope was entertained that once the stability was taken for granted, a consistent scheme could be developed in which empirically well established phenomena like emission of radiation, the presence of radiation damping and — perhaps — even the inertia of the electron were unambiguous consequences of the mutual interaction of the constituent corpuscles. Thus, fundamentally the classical electron is to be regarded as a system of infinitely many mechanical degrees of freedom (in addition to the degrees of freedom of the field).

Within the framework of a non-relativistic description the reduction of the number of mechanical degrees of freedom to six, characterizing the mechanical phase of a single charged particle, presents no difficulties, amounting merely to the introduction of appropriate assumptions regarding the rigidity of the charge distribution. However, within a proper relativistic scheme this situation is radically different owing to the finite propagation velocity of all physical actions, referred to as "retardation". Indeed, within the framework of the Maxwell theory, any charge distribution — however limited its spatial extension — retains the full complexity associated with a system of infinitely many degrees of freedom*. This circumstance is especially conspicuous in the formulation of the detailed energy-momentum balance, where the energy-momentum tensor, not only of the electromagnetic field but of the "mechanical" part of the system as well, presents the natural tool.

An attempt to formulate a relativistic description of a point electron, characterized exhaustively by the parameters fixing its mechanical phase,

* A similar feature appears in quantum electrodynamics. Here the infinitely many degrees of freedom manifest themselves through excitations of the "electron field".

was initiated by DIRAC[1] in his well-known treatise "Classical Theory of Radiating Electrons", which was followed by several other contributions, notably by FEYNMAN and WHEELER[2] and by ROHRLICH[3]. Basic to these departures from the conventional scheme are the endeavours to express the equation of motion as well as the conservation laws as four-vector relations involving only the momentary velocity, acceleration (and higher derivatives) of the particle besides its phenomenologically introduced mass and the external force. Within such a scheme, however, the phenomenon of damping now poses a problem and can, in fact, only be treated at all on the basis of recipes specially concocted for that very purpose.

Surveying the numerous discussions in the litterature, it is hard to overlook the presence of a certain confusion arising primarily from a lack of sufficient care in distinguishing between the rigorous consequences of the Maxwell theory on the one hand, and the conclusions — e.g. concerning acausalities in the equation of motion — reached by Dirac and his followers by transcending this framework, on the other.

The series of studies here undertaken represents an attempt to arrive at a clearer understanding in this respect. Part I, presented on the following pages, is concerned with the energy-momentum balance in processes where radiative phenomena are important, whereas part II, soon to be published, deals with the "mechanical" or "adiabatic" approximation and analyses from various angles the question of the transformation properties of electromagnetic energy and momentum. Finally, part III is intended to illustrate some of the general principles through the specific example of a charge in hyperbolic motion.

Although the discussion of consistency problems is an essential aspect of the present study, we have not followed the axiomatic approach, preferred by some workers, starting with rigorous definitions of concepts like radiation. Notwithstanding the intrinsic interest of such attempts, they appear to convey an unwarranted impression of freedom in the choice and definition of concepts on which to base our description of nature. Thus, we have preferred to proceed by analysing some idealized examples which are simple enough to allow of a detailed analytical treatment and still sufficiently general to demonstrate typical features in the mechanism of the energy-momentum balance in radiation processes. This attitude towards the consistency problem was greatly influenced by the general lesson of quantum theory, which entailed a serious warning against a priori definitions of physical concepts.

## § 2. Energy-Momentum Balance for Corpuscular Systems in Closed Processes

The concept of a field, possessing independent dynamical degrees of freedom and acting as mediator of interactions between material bodies, springs naturally from the attempt of basing the description of this interaction on customary mechanical ideas, even under circumstances when the retardation of all physical actions plays an essential role. Thus, in electrodynamics, where such a program has met with a far-reaching success, the notion of propagating fields, carrying a well-defined amount of energy, has found a domain of unambiguous applicability, whereas in the General Theory of Relativity, which entails a certain renunciation with respect to the applicability of the usual mechanical concept of force, the attribution of energy to the gravitational field is in general ambiguous. Nevertheless, to the extent that ordinary mechanical ideas may also here serve as a point of departure, the field concept has the same status as in electrodynamics[4].

For historical reasons, the field concept is often related to the rejection of the idea of forces acting at a distance. This view implies that also static electric or magnetic fields are considered as proper dynamical systems in which a well-defined amount of energy is localized, even though they have, of course, no independent dynamical role in the account of the energy-momentum balance. This situation is essentially different, when time-varying fields are considered, since the question at issue now concerns the possibility of upholding the customary idea of conservation of energy and momentum, rather than a more or less justified prejudice against "action-at-a-distance".

*

As a point of departure, let us recall the familiar account of the energy balance in electrostatic systems. Consider a charge $Q$, which is divided into a very large number, $N$, of small charge elements $\delta q_a$, situated at the positions $\vec{r}_a$. The total energy of the system, defined as the external work required to build it up adiabatically, is then given by

$$W = \tfrac{1}{2} \sum_{a \neq b}^{N} \frac{\delta q_a \, \delta q_b}{|\vec{r}_a - \vec{r}_b|}. \tag{1}$$

The feature to be noticed in this expression is the absence of the self-energy of the constituents. In fact, for increasing $N$, the self-interaction of the constituents decreases relative to their mutual interaction and vanishes in the limit of a continuous charge distribution. Indeed, this feature is merely the

formal expression of the observation, already alluded to in the Introduction, that the atomicity of charge is a foreign element in the classical Maxwell theory. Within this framework, properties like electromagnetic self-mass or self-angular-momentum originates in the mutual interactions between the infinitesimal constituents of the system in question, whereas the constituents themselves, according to their very definition, possess no self-energy, self-angular-momentum or similar properties. It is essential to realize that this line of argumentation does not imply any resignation as regards the scope and domain of applicability of the classical Maxwell theory, but rather serves to remind us about the conceptual framework within which any consistent use of the theory must remain.

Rewritten in continuum language the expression (1) takes the familiar form

$$W = \tfrac{1}{2} \int d\vec{x}\, \varrho(\vec{x})\, \varphi(\vec{x}), \tag{2}$$

where $\varrho(\vec{x})$ is the charge density and $\varphi(\vec{x})$ the potential, or expressed in terms of the electric field $\vec{E}(x)$:

$$W = \frac{1}{8\pi} \int d\vec{x}\, \vec{E}^2(\vec{x}). \tag{3}$$

Although the relation (3), in agreement with Pointings theorem, may be formally interpreted as the integral over an energy density, the derivation provides no basis for conclusions regarding the possibilities for an ascertainment of the presence of energy localized in the field. On the contrary, eq. (3) must so far be regarded merely as a recipe for evaluating the total electromagnetic energy of the system.

As an illustration consider the contrivance recently discussed by Møller[5], consisting of a small condensor suitably charged so as to cancel a given external electric field within the spatial domain between the plates. This example might convey the impression that, since the electrostatic field energy within the domain considered in this manner can be converted into mechanical energy without noticeable influence on the field outside the condensor, it has indeed been demonstrated that the energy in question was localized in the domain covered by the condensor. However, as must be evident from the beginning, electrodynamics provides no basis for such a conclusion.

Imagine for definiteness a small uncharged condensor which is slowly carried from infinity and placed at a distance $R$ from a charge $Q$, assuming $R$ to be large compared to the dimensions of the condensor, so that the

Coulomb field from the charge $Q$ within the plates may be approximated by a homogeneous electric field. Under these conditions the displacement of the uncharged condensor from infinity to the distance $R$ does not require external work.

Next, in order to neutralize the Coulomb field inside the condensor, the plates are connected by a conducting wire, and since the two plates coinside with different potential surfaces, a current will flow through the wire until the appropriate charge has been carried from one plate to the other. The current may be utilized to drive a mechanical device, thereby converting the electric field energy into mechanical work.

The charge, $q$, on the condensor, after the compensation of the field, is given by

$$4\pi \frac{q}{A} = \frac{Q}{R^2}, \tag{4}$$

$A$ denoting the area of the plates, and the total energy gained is thus

$$\Delta U = \frac{1}{8\pi} A d \frac{Q^2}{R^4}, \tag{5}$$

where $d$ signifies the distance between the plates.

Suppose now that it is possible to neglect the field modification outside the condensor. Then, after having cut the conducting wire, one may remove the charge $Q$ to infinity without performing external work, being in the end left with a charged condensor, from which the energy (5) could once more be gained. Thus, it is clearly necessary to take into account that after the original charging up of the condensor, the outside field is modified. In fact, the condensor behaves as a small dipole bound in the Coulomb field from the charge $Q$. The binding energy $\Delta\varphi$ can be estimated as

$$-\Delta\varphi = -\frac{qQ}{R} + \frac{qQ}{R+d} \simeq -qQ\frac{d}{R^2}, \tag{6}$$

or by means of eqs. (4) and(5)

$$\Delta\varphi = 2\Delta U. \tag{7}$$

Instead of cutting the conducting wire before the removal of the charge $Q$, the connection between the plates could have been maintained, whereby the field between the plates would have been cancelled at each instance, implying the relation (4) to hold for every $r$ during this process. When the charge has been removed to infinity, the condensor is discharged and the total energy gained is now given by eq. (5). Correspondingly, the force on $Q$ now varies as

$$K(r) = \frac{qQ}{r^2} - \frac{qQ}{(r+d)^2} \simeq \frac{2Q^2}{r^5}\frac{Ad}{4\pi}, \tag{8}$$

since

$$q = \frac{A}{4\pi}\frac{Q^2}{r^2}.$$

Thus, as expected, the total mechanical work amounts to:

$$W = \int_R^\infty K(r)\, dr = \frac{1}{8\pi}\frac{Q^2}{R^4} Ad. \tag{9}$$

This example illustrates how the energy balance for electrostatic systems can be exhaustively accounted for in terms of the customary mechanical concept of potential energy without any reference to the field. Quite generally, within the framework of electrodynamics the impartation of energy to a static field is purely conventional in so far as the energy in question may alternatively be expressed in terms of the co-ordinates of the charged particles.

* *

Quite a different situation is met with in the case of time-varying charge and current distributions. Due to the retardation of physical actions, the field now represents independent degrees of freedom of the total system, which can only be ignored or eliminated at the expense of giving up the notion of energy-momentum balance. As a simple illustration* consider two particles of charge $Q$ — originally at rest at a relative distance $2r_i$ —, which are moved simultaneously and symmetrically towards each other** to a relative distance $2r_f$ ($r_f < r_i$), where they stay at rest (see figure 1). If the process is carried out adiabatically, the external work performed equals the change in potential energy

$$W_{ad} = \frac{Q^2}{2r_f} - \frac{Q^2}{2r_i}. \tag{10}$$

If, however, the process is carried out in a finite time, the work required will, as a consequence of the retardation, differ from $W_{ad}$.

Suppose that the duration of the process, $\Delta t$, is chosen so that

$$r_i - r_f < c\Delta t \leq r_i + r_f, \tag{11}$$

* The following example was already discussed in reference 4. Since, however, it shall be utilized here for other purposes, it is reproduced for the convenience of the reader.

** Since the entire discussion is carried out within the framework of special relativity, the freedom to invoke the actions of arbitrary external forces is exploited throughout.

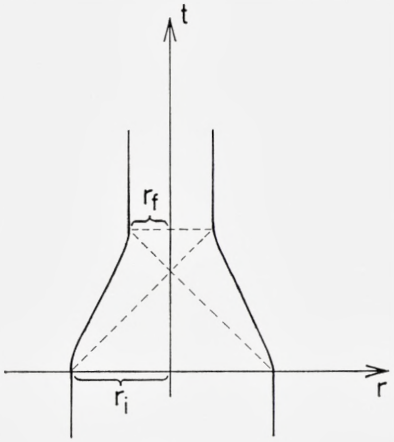


Fig. 1.

which implies that the electromagnetic force on each particle due to the other one during the entire motion is given by the original static Coulomb field. In this case the work required to overcome the electrostatic repulsion only amounts to*

$$2\left(\frac{Q^2}{r_i + r_f} - \frac{Q^2}{2r_i}\right). \tag{12}$$

The very fact that this work differs from the change in potential energy (10) faces us with the choice of either giving up the customary idea of energy conservation, or recognizing the existence of some non-conservative force acting on each particle, independently of the motion of the other since during the process considered no communication is possible between the particles. Within the customary mechanical framework the non-conservative character of this so-called "damping force" is interpreted as a manifestation of an independent set of degrees of freedom, with which the particles may interact and exchange energy, the damping force being just a phenomenological way of taking this interaction into account.

Reconsidering now the above process in this extended framework, we notice that the external work, $W_D$, required to overcome the damping force on each particle during the displacement must, for symmetry reasons, be the same for both particles and, according to its definition, independent of the motion of the other. Thus the total energy to be supplied is not given by eq. (12) but by the relation

* If the retarded interaction were replaced by a time-symmetric interaction, clearly, the work performed would also in this case equal $W_{ad}$.

$$W = 2\left(\frac{Q^2}{r_i + r_f} - \frac{Q^2}{2r_i} + W_D\right), \tag{13}$$

where $W_D$ is related to the hypothetical "radiation energy" $\mathscr{E}_R$ by the requirement of energy balance

$$\mathscr{E}_R + \frac{Q^2}{2r_f} = W + \frac{Q^2}{2r_i}. \tag{14}$$

Hence:

$$2W_D - \mathscr{E}_R = Q^2 \frac{(r_i - r_f)^2}{2r_i r_f (r_i + r_f)}. \tag{15}$$

Whereas this expression is still compatible with a complete absence of radiation, corresponding to $\mathscr{E}_R = 0$, evidently, $\mathscr{E}_R$ and $W_D$ cannot *both* vanish. Furthermore, the fact that, according to the initial conditions, $\mathscr{E}_R \geqslant 0$, implies that $W_D$ is positive definite, reflecting the irreversible character of the process of radiation emission.

Face now the particular case in which the equality sign in eq. (11) holds, i.e.

$$c\Delta t = r_i + r_f \tag{16}$$

and introduce the average velocity $v$ and average acceleration $g$ through the relations

$$\left.\begin{aligned} v &= \frac{\Delta r}{\Delta t} = c\frac{r_i - r_f}{r_i + r_f} \\ g &= \frac{\Delta r}{(\Delta t)^2} = c^2 \frac{r_i - r_f}{(r_i + r_f)^2}. \end{aligned}\right\} \tag{17}$$

Then eq. (15) may be rewritten in the suggestive form

$$2W_D - \mathscr{E}_R = 2\frac{Q^2}{c^3}\frac{g^2}{1 - v^2/c^2}\Delta t. \tag{18}$$

So far no conclusions as to the individual value of $W_D$ and $\mathscr{E}_R$ can be drawn. However, since $W_D$, as already noticed, is independent of the motion of the other particle, it may be determined by considering another process, in which only one of the particles is displaced along the same world line as before, whereas the other is kept fixed. Denoting by $E_R$ the energy transferred to the radiation field during this process, the energy balance now yields the relation:

$$E_R + \frac{Q^2}{r_i + r_f} = \tfrac{1}{2}W + \frac{Q^2}{2r_i}, \tag{19}$$

where $W$ is given by eq. (13) as before. Hence it follows that

$$E_R = W_D. \tag{20}$$

Since the role of the fixed charge in this process is purely auxiliary, we may conclude that whenever a charge, $Q$, is displaced a distance $\Delta r$ during a time $\Delta t$, being at rest outside this time interval, a net external work equal to $W_D$ has to be performed*.

Furthermore, it follows from eq. (18) that**

$$E_R = W_D \geqslant \frac{Q^2}{c^3} \frac{g^2}{1 - v^2/c^2} \Delta t. \tag{21}$$

The above example is well suited to exhibit the futility of attempts to achieve a pictorial representation of the energy transfer to the radiation field as an emission process localized in space and time***. In fact, such a picture would entail that since a single charge during the displacement (the other being kept fixed) emits the amount of energy $E_R = W_D$, — which, as far as the particle degrees of freedom are concerned, is irreversibly lost once the particle comes to rest again — it would emit the same amount of energy, even if the second particle were simultaneously displaced, since the first particle could only recognize this displacement after the completion of its own act of emission. Thus, the conclusion would be — in conflict with the result (15) — that the total amount of energy emitted equaled $2W_D$, and furthermore, provided the original distance $2r_i$ is chosen larger than $2c\,\Delta t$, that this energy, immediately after the particles had come to rest, were localized within two non-overlapping spherical shells.

Thus a proper account of the energy balance in the process considered cannot be given within the picture indicated but must start from the recognition that a radiation process, far from having the character of a localized event, manifests a modification of the field as a whole. Although at the

* Since only the Coulomb potential enters into the above example, it may appear puzzling how to carry through the argumentation in the Coulomb Gauge. The solution to this conundrum was confided to us by JENS LINDHARD.

** In the non-relativistic limit minimization of the integral $(2Q^2/3c^3)\int_0^{\Delta t} \ddot{x}^2\,dt$, subject to the appropriate boundary conditions, actually gives 8 times the value (21). However, considering more cunning contrivances involving several charges, it is easy to increase the lower bound of the inequality (21).

*** For a detailed exposition of such attempts, see ref. 3 & 6.

termination of the displacement of a particular charge, a definite amount of work has been performed on this charge independently of a possible displacement of the other, still the fraction of this supplied energy, ultimately to appear in the radiation field, is at this moment to a certain extent indeterminate, being dependent on whether or not the second particle is actually displaced.

* * *

The preceding analysis has demonstrated how the combined requirements of energy conservation and retardation entails the existence of the phenomenon of damping for a single finite charge. Thus, a detailed account of the energy balance associated with the mutual interaction between the infinitesimal constituents of the charge, each of which suffers no damping, must necessarily substantiate this conclusion. Furthermore, the analysis suggests that the total damping acting on the charge may be pictorially represented as the accumulated effect of the continual lack of "adjustment" of action and reaction in the mutual forces between the corpuscles, brought about by the impossibility of instantaneous communication between them.

To trace the problem further back is clearly impossible within the framework of the Maxwell theory, since it would amount to deducing the retarded, as opposed to the advanced, character of the electromagnetic interaction, a program, the very formulation of which would involve a contradiction in terms within a scheme which implicitly assumes the freedom to influence the behaviour of the charges or charge elements in question*.

With the purpose of obtaining a quantitative expression** for the damping, let us evaluate the total four-momentum to be supplied to constrain a system of electrified corpusles with a given total charge, to perform a cyclic process, where in the initial and final state the corpuscles are at rest in a given configuration. Since an adiabatic process is of no consequence for the problem at issue, we may for simplicity assume that this configuration is originally built up by adiabatically assembling the corpuscles from rest at infinity, and finally adiabatically decomposed by removing the corpuscles back to infinity.

The fact that a finite amount of energy-momentum has to be supplied at all in a cyclic process clearly reflects the limitations in the usual form of the law of action and reaction in situations where the retardation must be

* See in this connection the further remarks on page 32 ff.

** In the following $x$ denotes the four-vector $(\vec{x}, it)$ and a similar notation is employed for other four-vectors, the scale of length being chosen as the distance travelled by a light signal per unit of time. Also, for the sake of clarity all tensor indices have been suppressed, since it will be clear from the context whether matrix multiplication or scalar products are implied. Where ambiguities may occur, scalar products are indicated by a dot.

taken explicitly into account. Indeed, the total four-momentum $P_R^{(1,2)}$ which a corpuscle 2 via its retarded field communicates to another corpuscle 1 during the process considered does *not* equal minus the four-momentum $P_R^{(2,1)}$ which the first corpuscle via its retarded field communicates to the second. Instead, the generalized law of action and reaction may for a closed, cyclic process be expressed as

$$P_R^{(1,2)} + P_A^{(2,1)} = 0 \tag{22}$$

where $P_A^{(2,1)}$ signifies the four-momentum communicated to the second corpuscle via the *advanced* field of the first.

To demonstrate this symmetry, consider a single pair of corpuscles. The four-momentum $P_R^{(1,2)}$ communicated during the process to the first corpuscle via the retarded field of the second is given by

$$P_R^{(1,2)} = \oint dx \mathscr{F}_R^{(2)}(x) s_1(x), \tag{23}$$

where $\mathscr{F}_R^{(2)}(x)$ denotes the field tensor corresponding to the retarded electromagnetic field generated by the second corpuscle, and

$$s_1(x) = \delta q_1 \int d\tau_1 \delta^{(4)}(x - x_1(\tau_1)) U_1(\tau_1) \tag{24}$$

the charge current density associated with the motion of corpuscle one along its world line $x_1(\tau_1)$; $U_1 = \dfrac{dx_1}{d\tau_1}$. Similarly

$$P_A^{(2,1)}(x) = \oint dx \mathscr{F}_A^{(1)}(x) s_2(x), \tag{25}$$

where $\mathscr{F}_A^{(1)}(x)$ denotes the advanced electromagnetic field generated by the first corpuscle.

Expressing $\mathscr{F}_R^{(2)}$ and $\mathscr{F}_A^{(1)}$ in terms of the currents $s_2(x)$ and $s_1(x)$ by means of the retarded and advanced Green's functions $\mathscr{D}_R(x)$ and $\mathscr{D}_A(x)$, and remembering that $\mathscr{D}_R(x) = \mathscr{D}_A(-x)$, one obtains*:

$$\left.\begin{aligned} P_R^{(1,2)} + P_A^{(2,1)} &= 4\pi \oint dxdy \{[\partial_x \mathscr{D}_R(x-y) \wedge s_2(y)]\, s_1(x) + [\partial_y \mathscr{D}_A(y-x) \wedge s_1(x)] s_2(y)\} \\ &= 4\pi \oint dxdy \{[\partial_x \mathscr{D}_R(x-y) \wedge s_2(y)] s_1(x) + [s_1(x) \wedge \partial_x \mathscr{D}_R(x-y)] s_2(y)\} \\ &= -4\pi \oint dxdy [s_2(y) \wedge s_1(x)] \partial_x \mathscr{D}_R(x-y), \end{aligned}\right\} \tag{26}$$

where the last equality follows from the identity

* For the antisymmetric tensor $a_i b_j - a_j b_i$ constructed from two four-vectors $a$ and $b$, we employ the customary notation $a \wedge b$.

$$[a \wedge b]\, c + [c \wedge a]\, b + [b \wedge c]\, a = 0 \tag{27}$$

valid for any three four-vectors, $a$, $b$, $c$. Finally, taking advantage of the continuity equation for the currents, the expression (26) is immediately transformed to a surface integral, which vanishes by virtue of the boundary conditions*

$$\left.\begin{aligned} &P_R^{(1,2)} + P_A^{(2,1)} = \\ &\quad - 4\pi \oint dxdy \{s_2(y)\partial_x \cdot (s_1(x)\mathscr{D}_R(x-y)) + s_1(x)\partial_y \cdot (s_2(y)\mathscr{D}_R(x-y))\} = 0. \end{aligned}\right\} \tag{28}$$

It may be remarked in passing that this result may also be immediately obtained by variation of the translational invariant quantity

$$\int_{-\infty}^{+\infty}\int d\tau_1 d\tau_2 \mathscr{D}_R(x_1(\tau_1) - x_2(\tau_2)) U_1(\tau_1) \cdot U_2(\tau_2). \tag{29}$$

Continuing the evaluation of the damping, it is next noticed that, since according to their very definition, the corpuscles suffer no damping, the equations of motion for two constituents are

$$\left.\begin{aligned} \delta m_1 g_1 &= F_1^{(\mathrm{el})} + K_1^{(\mathrm{ext})} \\ \delta m_2 g_2 &= F_2^{(\mathrm{el})} + K_2^{(\mathrm{ext})}, \end{aligned}\right\} \tag{30}$$

where $F_1^{(\mathrm{el})}$ ($F_2^{(\mathrm{el})}$) denotes the electromagnetic four-force generated by the second (first) corpuscle, whereas $K_1^{(\mathrm{ext})}$ ($K_2^{(\mathrm{ext})}$) stands for the external force required to constrain the corpuscles in question to perform the prescribed cyclic motion. Hence the total four-momentum $P$ supplied during the process, amounts to

$$\left.\begin{aligned} P &= \oint \{K_1^{(\mathrm{ext})} d\tau_1 + K_2^{(\mathrm{ext})} d\tau_2\} \\ &= - \oint \{F_1^{(\mathrm{el})} d\tau_1 + F_2^{(\mathrm{el})} d\tau_2\} \\ &= - (P_R^{(1,2)} + P_R^{(2,1)}) \end{aligned}\right\} \tag{31}$$

where $P_R^{(1,2)}$ ($P_R^{(2,1)}$) is given by eq. (23). Now utilizing the generalized relationship (22) between action and reaction, the expression for $P$ may be rewritten as

$$\left.\begin{aligned} P &= - P_R^{(1,2)} + P_A^{(1,2)} \\ &= - \oint dx [\mathscr{F}_R^{(2)}(x) - \mathscr{F}_A^{(2)}(x)] s_1(x). \end{aligned}\right\} \tag{32}$$

It should be emphasized that neither this result, nor the relation (22) on which it is based, is valid differentially, but only holds for the entire cyclic process.

* A similar result is obtained by FEYNMAN and WHEELER (loc. cit), who, however, attempt to interpret the relation differentially, in stead of maintaining the integral form.

Finally, summing the contributions from the infinitely many charged constituents of the system, and remembering that the importance of the "self-terms" is negligible compared to the interaction terms, one obtains for the total expenditure of four-momentum during the process

$$\left.\begin{aligned} \mathscr{P} &= -\tfrac{1}{2}\sum_{a\neq b}\oint dx[\mathscr{F}_R^{(b)}(x) - \mathscr{F}_A^{(b)}(x)]s_a(x) \\ &= -\tfrac{1}{2}\oint dx[\mathscr{F}_R(x) - \mathscr{F}_A(x)]s(x), \end{aligned}\right\} \tag{33}$$

where $s(x)$ now signifies the total four-current density, and $\mathscr{F}_{R,A}(x)$ the total electromagnetic field.

This result, which is valid for an arbitrary finite charge distribution, represents a rigorous consequence of the conventional Maxwell theory, and the appearance in the integrand of the advanced fields raises no problem of interpretation. Indeed, it is clear that the derivation provides no basis for attributing to the difference $\mathscr{F}_R(x) - \mathscr{F}_A(x)$ the status of a measurable field; the occurrence of this difference is merely dependent on the formal artifice of exploiting the symmetry between the retarded and advanced Green's functions so as to combine in a special way the contributions in eq. (31) from the mutual interactions to the net energy-momentum expenditure.

The general expression (33) may in particular be applied to the case of a charge distribution so limited in spatial extension, that the difference $\mathscr{F}_R(x) - \mathscr{F}_A(x)$ (which is regular even in the point limit on the world line of the source) may be expanded in terms of the dimensions of the system. The well-known result*, first derived by DIRAC, for the difference $\mathscr{F}_R^{(a)}(x) - \mathscr{F}_A^{(a)}(x)$, in the immediate vicinity of the world-line of the $a$'th corpuscle, is

$$\mathscr{F}_R^{(a)}(x) - \mathscr{F}_A^{(a)}(x) \simeq \tfrac{4}{3}\delta q_a[U_a \wedge \dot{g}_a], \tag{34}$$

where the terms neglected vanish as the point $x$ approaches the world-line. Inserting this relation into equation (33), and using the expression (24) for the current density, one finds for the total four-momentum expenditure in the limit when all the world-lines of the corpuscles become identical

$$\mathscr{P} = \tfrac{2}{3}Q^2\oint\{g^2U - \dot{g}\}d\tau \tag{35}$$

(the second term in the integrand does of course not contribute in a cyclic process).

* * *

* For completeness a slightly simplified version of Dirac's derivation is given in appendix A.

Since the previous considerations were solely concerned with cyclic processes, the entire energy-momentum expenditure was of course of irreversible character. For the following discussion it is essential to generalize the considerations so as to embrace instances in which the energy and momentum of the system also suffer a reversible change. Thus, consider a process, in which a pair of corpuscles is brought from rest at infinite separation along arbitrary world-lines to a state of common uniform motion. From the equations of motion (30) the total energy and momentum to be supplied is now given by

$$\left.\begin{aligned} \Delta P(T) &= \int_{-\infty}^{T} K_1^{(\mathrm{ext})}\, d\tau_1 + \int_{-\infty}^{T} K_2^{(\mathrm{ext})}\, d\tau_2 \\ &= (\delta m_1 + \delta m_2)\Delta U - \int_{-\infty}^{T} dx \left\{ \mathscr{F}_R^{(2)}(x) s_1(x) + \mathscr{F}_R^{(1)}(x) s_2(x) \right\}, \end{aligned}\right\} \tag{36}$$

where $\Delta U$ denotes the change in the four-velocity. The integral is evaluated in appendix B, and the ensuing result for $P = P_{\mathrm{initial}} + \Delta P$ is

$$\left.\begin{aligned} P(T) &= (\delta m_1 + \delta m_2) U \\ &+ \frac{\delta q_1 \delta q_2}{\varepsilon} U + \frac{\delta q_1 \delta q_2}{\varepsilon^3} \left( \frac{l_4}{i\gamma} \right) l - \int_{-\infty}^{t_{12}} dx [\mathscr{F}_R^{(2)}(x) - \mathscr{F}_A^{(2)}(x)] s_1(x), \end{aligned}\right\} \tag{37}$$

where it is understood that the final state of common uniform motion has been reached at least a time $2\gamma\varepsilon$ prior to $T$, $\varepsilon$ being the rest-distance between the corpuscles. Furthermore $l$ denotes the four-vector of length $\varepsilon$ joining the two world lines, perpendicularly to the common four-velocity $U$, and $t_{12}$ is defined such that a light signal emitted from the first corpuscle at that time will reach the second corpuscle at time $T$ (see figure 2). Finally, $i\gamma = U_4$.

Provided the system becomes isolated at time $T$ in the laboratory by simultaneous removal of the external constraining forces, the energy and momentum of the system is given by the expression (37). Clearly the non-covariant appearance of the third term in this formula is associated with the fact that the plane $T = \text{constant}$ is not intrinsically related to the world lines. In the present case of common uniform motion, however, the plane perpendicular to the four-velocity is evidently singled out, and it can therefore be expected, that if in the integration leading to equation (37) the plane $T = \text{constant}$, is replaced by the plane $\mathring{T} = \text{constant}$ (corresponding to removal of the external forces simultaneously in the rest-frame) the resulting expression $P_{(\mathring{T})}$ would "appear more covariant". Indeed, it is evident (see figure 2) that

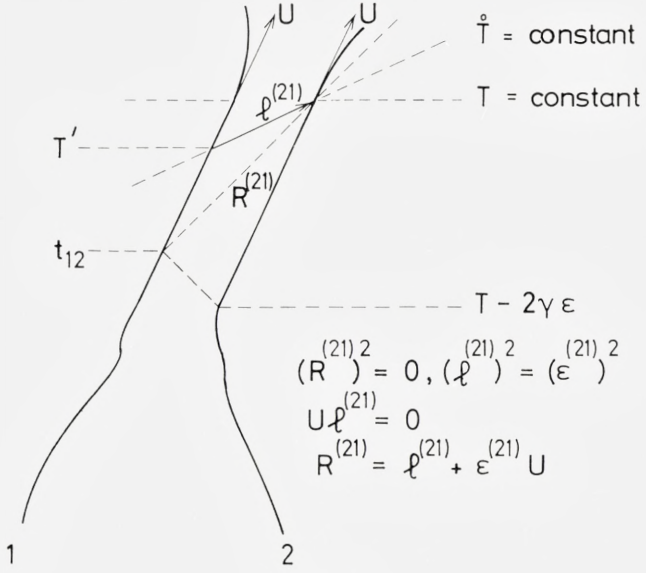


Fig. 2.

$$\left.\begin{aligned} \Delta P_{(\mathring{T})} &= \int_{-\infty}^{T'} K_1^{(\mathrm{ext})}\, d\tau_1 + \int_{-\infty}^{T} K_2^{(\mathrm{ext})}\, d\tau_2 \\ &= \Delta P(T) + \delta q_1 \int_{T'}^{T} \mathscr{F}_R^{(2)}(x_1(\tau))\, U_1(\tau)\, d\tau \\ &= \Delta P(T) + \delta q_1 \delta q_2 \left(\frac{-l_4}{i\gamma}\right) \frac{[U \wedge l]}{\varepsilon^3}\, U, \end{aligned}\right\} \quad (38)$$

where the last step is justified since the motion in the time interval concerned is uniform. Hence, $P_{(\mathring{T})} = P_{\mathrm{initial}} + \Delta P_{(\mathring{T})}$ is given by

$$P_{(T)} = (\delta m_1 + \delta m_2)\, U_{(\mathring{T})} + \frac{\delta q_1\, \delta q_2}{\varepsilon}\, U_{(\mathring{T})} - \int_{-\infty}^{t_{12}} dx\, [\mathscr{F}_R^{(2)}(x) - \mathscr{F}_A^{(2)}(x)]\, s_1(x). \quad (39)$$

It is important to realize that equation (39) should not be construed as a re-definition of the energy and momentum of the original system, but that it represents the true energy and momentum of a *different* system, namely one prepared by removing the constraining agents at different instances $T'$ and $T$ (as judged from the laboratory system) for the two corpuscles. Thus, the symbol $U_{(\mathring{T})}$ is meant to indicate that the four-velocity $U$ is achieved by the two corpuscles at times $T'$ and $T$, respectively.

Extending the above considerations to the case of a large number of corpuscles of identical charge, uniformly distributed on an infinitesimal spherical shell of radius $\varepsilon$ in the common rest-frame, one obtains in the continuum limit in place of eq. (37):

$$\left.\begin{aligned} \mathscr{P}(T) &= \tfrac{1}{2}\sum_{a\neq b}\Big\{(\delta m_a+\delta m_b)\,U+\frac{\delta q_a\,\delta q_b}{\varepsilon_{ab}}U \\ &+\frac{\delta q_a\,\delta q_b}{\varepsilon_{ab}^3}\left(\frac{l_4^{(ab)}}{i\gamma}\right)l^{(ab)}-\int_{-\infty}^{t_{ab}}dx[\mathscr{F}_R^{(b)}(x)-\mathscr{F}_A^{(b)}(x)]s_a(x)\Big\} \\ &= MU+\frac{Q^2}{2\varepsilon}\gamma\left(\tfrac{4}{3}\vec{v},\, i(1+\tfrac{1}{3}v^2)\right)+\tfrac{2}{3}Q^2\int_{-\infty}^{\tau(T)}g^2U d\tau, \end{aligned}\right\} \tag{40}$$

where we have used the relation (34) and where $M=\sum\delta m$.
Similarly eq. (39) is replaced by

$$\mathscr{P}_{(\mathring{T})}=MU_{(\mathring{T})}+\frac{Q^2}{2\varepsilon}U_{(\mathring{T})}+\tfrac{2}{3}Q^2\int_{-\infty}^{\tau}g^2U\,d\tau. \tag{41}$$

Defining the electromagnetic energy-momentum tensor for the system of electrified corpuscles

$$\mathscr{T}_{ik}=\sum_{a\neq b}\frac{1}{4\pi}\{\mathscr{F}_{im}^{(a)}\mathscr{F}_{mk}^{(b)}-\tfrac{1}{4}\delta_{ik}(\mathscr{F}^{(a)}\mathscr{F}^{(b)})\} \tag{42}$$

(where of course in the continuum limit the restriction on the summation may be dropped), the four-momentum $\mathscr{P}(T)$ may alternatively be expressed as*

$$\mathscr{P}(T)=MU-\sum_{a\neq b}\int^{T}dx\mathscr{F}_R^{(b)}(x)s_a(x)=MU-\int^{T}dx\;\partial_x\cdot\mathscr{T}(x) \tag{43}$$

or

$$\mathscr{P}(T)=MU+\int_{T=\text{const.}}\mathscr{T}\cdot d\Gamma, \tag{44}$$

where $d\Gamma_4=id\vec{x}$.
Similarly, the expression (41) for the four-momentum $\mathscr{P}_{(\mathring{T})}$ may be written

$$\mathscr{P}_{(\mathring{T})}=MU_{(\mathring{T})}+\int_{\mathring{T}=\text{const.}}\mathscr{T}\cdot d\Omega. \tag{45}$$

* Actually, the ensuing expressions (44) and (45) are slightly more general than the corresponding expression (40) and (41), since the former do not presuppose the corpuscles to be in uniform motion at the moment considered.

Of course, once the system, prepared according to the prescription (45), has become isolated, it is possible to replace the plane $\mathring{T}$ = constant with the plane $T$ = constant without changing the value of the constant four-vector $\mathscr{P}_{(\mathring{T})}$ However, on the plane $T$ = constant the corpuscles would in general *not* move with the common velocity $U_{(\mathring{T})}$ and the value of the electromagnetic energy-momentum tensor would have changed accordingly. Thus, it is important to bear in mind that even in the point limit, when the charge is concentrated within a vanishingly small spatial domain, the two quantities $\mathscr{P}(T)$ and $\mathscr{P}_{(\mathring{T})}$ remain quite distinct in value as well as in physical content*.

## § 3. Differential Energy-Momentum Balance and Equations of Motion for a Point Charge

In accordance with the plan outlined in the Introduction, we now proceed to the contraposition of the conclusions arrived at in the previous paragraph, based on the conventional Maxwell theory, with the endeavours initiated by DIRAC[1] to develop a classical description of an ideal point electron. Although the inference drawn in the earlier discussion regarding the occurrence of damping acting on the individual charge remains valid, the question as to the origin of this phenomenon now requires a new answer. Indeed, since the mentioned inference did only depend on the principles of retardation and energy conservation, it is clear that — unless at least one of these general principles is abandoned** — the introduction of the notion of an ideal point charge immediately creates the need for the concoction of a recipe to account for the damping, a direct analysis being excluded by the very quality of this notion. Needless to say, there is a considerable freedom in selecting the way in which the classical electron theory is adapted to this new concept.

To exhibit most clearly the essential differences between the theory proposed by DIRAC and the conventional description, it is advantageous not to follow directly the path trodden by him, but to proceed in a manner which at every step permits of a comparison between the two different schemes. Hence, the plan of action for the ensuing section is as follows:

Imagine that in each of the momentary rest systems corresponding to the motion of the electron, the point charge is surrounded by a sphere of

* A thorough discussion of this aspect of the problem will be found in Studies in Classical Electron Theory II.

** Cf. the later remarks on the work by FEYNMAN & WHEELER[2].

vanishingly small radius $\varepsilon$, and evaluate in the momentary rest-frame the total electromagnetic momentum and energy $(\overset{\circ}{\vec{\mathscr{P}}}_{\Omega}, \overset{\circ}{\mathscr{E}}_{\Omega})$ formally associated with the region, $\Omega$, exterior to this tiny sphere. Follow next Dirac and his school in — explicitly or implicitly — exploiting the freedom gained through the introduction of the notion of a "point charge" to re-define the electromagnetic energy and momentum of the system so as to transform as a four-vector, namely that four-vector whose components in the momentary rest-frame are given by $(\overset{\circ}{\vec{\mathscr{P}}}_{\Omega}, i\overset{\circ}{\mathscr{E}}_{\Omega})$ just introduced. Finally, contemplate for comparison the similar problem, within the conventional scheme, of evaluating the electromagnetic momentum and energy $(\vec{\mathscr{P}}_{\Gamma}, \mathscr{E}_{\Gamma})$ associated with the domain $\Gamma$ exterior to the Heaviside ellipsoid corresponding to a sphere of radius $\varepsilon$ in the momentary rest-frame. Of course, the quantity $(\vec{\mathscr{P}}_{\Gamma}, i\mathscr{E}_{\Gamma})$ is not a four-vector, as is evident from the fact that the electromagnetic energy-momentum tensor is not separately divergence-free.

*

To carry into effect this plan, consider the motion of a charged particle interacting with an incoming external source-free electromagnetic field, $\mathscr{F}_{(in)}$ and focus the attention on that part of the total electromagnetic field, which is causally connected to a definite segment of the particle trajectory, corresponding to two successive positions of the particle $\vec{x}(t_1)$ and $\vec{x}(t_2)$ at times $t_1$ and $t_2$. Remarkably enough, it is possible to evaluate explicitly the total momentum and energy formally associated with the mentioned part of the field, which is of course confined to the region $\Xi$ (see fig. 3) between two consecutive light spheres centred at the two points $\vec{x}(t_1)$ and $\vec{x}(t_2)$ respectively. Although the momentum and energy of this part of the field has no direct physical significance, the formal expressions obtained are of some interest in themselves and will provide a useful intermediate step for the evaluation of the corresponding quantities associated with the domains of proper interest, $\Omega$ and $\Gamma$.

The total field may be written as

$$\left.\begin{aligned} \vec{E}(t) &= \vec{E}_R(t) + \vec{E}_{in}(t) \\ \vec{H}(t) &= \vec{H}_R(t) + \vec{H}_{in}(t), \end{aligned}\right\} \tag{46}$$

where the retarded Liénard-Wichert fields $\vec{E}_R$ and $\vec{H}_R$ are given by the familiar expressions

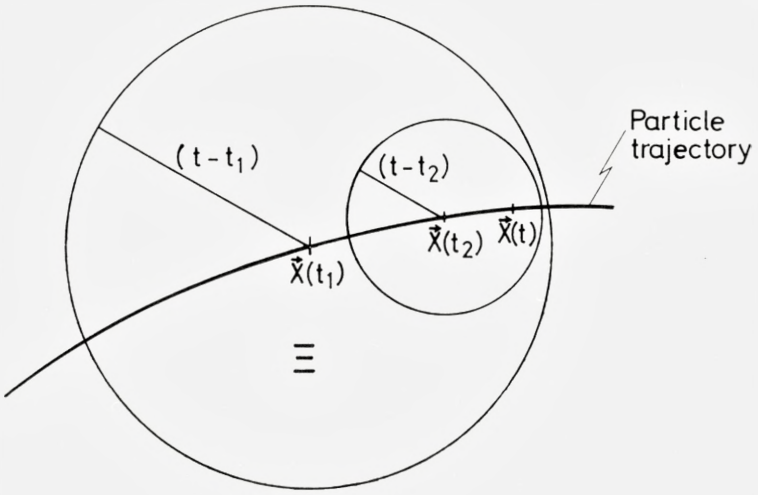


Fig. 3.

$$\left.\begin{aligned} \vec{E}_R(t) &\equiv \vec{E}_{\mathrm{I}}(t) + \vec{E}_{\mathrm{II}}(t) \\ &= \frac{Q}{\gamma^2(1-\vec{v}\cdot\hat{n})^3}\frac{n-\vec{v}}{(t-t_R)^2} + \frac{Q}{(1-\vec{v}\cdot\hat{n})^3}\frac{\hat{n}\times[(\hat{n}-\vec{v})\times\vec{g}]}{(t-t_R)} \\ \vec{H}_R(t) &\equiv \vec{H}_{\mathrm{I}} + \vec{H}_{\mathrm{II}}(t) = \hat{n}\times\vec{E}_{\mathrm{I}} + \hat{n}\times\vec{E}_{\mathrm{II}}, \end{aligned}\right\} \quad (47)$$

the abbreviations $\vec{E}_{\mathrm{I}}$ and $\vec{E}_{\mathrm{II}}$ referring to the first and second term of $\vec{E}_R$ respectively and correspondingly for $\vec{H}_R$. Furthermore $\hat{n}$ denotes the unit vector from the retarded position to the field point and the velocity $\vec{v}$ as well as the acceleration $\vec{g}$ are to be evaluated at the retarded time $t_R$; as usual $\gamma^{-2} = 1 - v^2$. The straightforward but cumbersome evaluation of the integrals

$$\left.\begin{aligned} \mathscr{E}_{\Xi} &= \frac{1}{8\pi}\int_{\Xi}\{(\vec{E}_{\mathrm{I}} + \vec{E}_{\mathrm{II}} + \vec{E}_{in})^2 + (\vec{H}_{\mathrm{I}} + \vec{H}_{\mathrm{II}} + \vec{H}_{in})^2\}dV \\ \vec{\mathscr{P}}_{\Xi} &= \frac{1}{4\pi}\int_{\Xi}\{(\vec{E}_{\mathrm{I}} + \vec{E}_{\mathrm{II}} + \vec{E}_{in})\times(\vec{H}_{\mathrm{I}} + \vec{H}_{\mathrm{II}} + \vec{H}_{in})\}dV \end{aligned}\right\} \quad (48)$$

is deferred to appendix C, but for the purpose of reference the results are quoted here term by term:*

* It is noteworthy that the expressions (49a) and (50a) depend only on the instantaneous velocity of the particle, in spite of the fact that the integrands depend on the entire preceding trajectory.

$$
\left.\begin{aligned}
&\frac{1}{8\pi}\int_{\Xi}\{\vec{E}_{\mathrm{I}}^2+2\vec{E}_{\mathrm{I}}\vec{E}_{\mathrm{II}}+\vec{H}_{\mathrm{I}}^2+2\vec{H}_{\mathrm{I}}\vec{H}_{\mathrm{II}}\}\,dV\\
&\quad=\frac{Q^2}{3}\left[\frac{4\gamma^2(t_2)-1}{2(t-t_2)}-\frac{4\gamma^2(t_1)-1}{2(t-t_1)}\right] && \text{(a)}\\
&\frac{1}{8\pi}\int_{\Xi}\{\vec{E}_{\mathrm{II}}^2+\vec{H}_{\mathrm{II}}^2\}\,dV=\tfrac{2}{3}Q^2\int_{t_1}^{t_2}\frac{\vec{g}^2-(\vec{g}\times\vec{v})^2}{(1-v^2)^3}\,dt && \text{(b)}\\
&\frac{1}{8\pi}\int_{\substack{\text{all}\\ \text{space}}}\{\vec{E}_{in}^2+\vec{H}_{in}^2\}\,dV\equiv\mathscr{E}_{in}=\text{constant} && \text{(c)}\\
&\frac{1}{8\pi}\int_{\substack{\text{all}\\ \text{space}}}\{2\vec{E}_R\vec{E}_{in}+2\vec{H}_R\vec{H}_{in}\}\,dV=-\int_{-\infty}^{t}\vec{E}_{in}\vec{v}\,dt. && \text{(d)}
\end{aligned}\right\}\quad(49)
$$

Similarly

$$
\left.\begin{aligned}
&\frac{1}{4\pi}\int_{\Xi}\{\vec{E}_{\mathrm{I}}\times\vec{H}_{\mathrm{I}}+\vec{E}_{\mathrm{I}}\times\vec{H}_{\mathrm{II}}+\vec{E}_{\mathrm{II}}\times\vec{H}_{\mathrm{I}}\}\,dV\\
&\quad=\tfrac{2}{3}Q^2\left[\frac{\gamma^2(t_2)}{t-t_2}\vec{v}\,(t_2)-\frac{\gamma^2(t_1)}{t-t_1}\vec{v}\,(t_1)\right] && \text{(a)}\\
&\frac{1}{4\pi}\int_{\Xi}\{\vec{E}_{\mathrm{II}}\times\vec{H}_{\mathrm{II}}\}\,dV=\tfrac{2}{3}Q^2\int_{t_1}^{t_2}\frac{\vec{g}^2-(\vec{g}\times\vec{v})^2}{(1-v^2)^3}\vec{v}\,dt && \text{(b)}\\
&\frac{1}{4\pi}\int_{\substack{\text{all}\\ \text{space}}}\{\vec{E}_{in}\times\vec{H}_{in}\}\,dV=\vec{\mathscr{P}}_{in}=\text{constant}. && \text{(c)}\\
&\frac{1}{4\pi}\int_{\substack{\text{all}\\ \text{space}}}\{\vec{E}_R\times\vec{H}_{in}+\vec{E}_{in}\times\vec{H}_R\}\,dV=-Q\int_{-\infty}^{t}\{\vec{E}_{in}+\vec{v}\times\vec{H}_{in}\}dt. && \text{(d)}
\end{aligned}\right\}\quad(50)
$$

The constancy of $\mathscr{E}_{in}$ and $\vec{\mathscr{P}}_{in}$ simply expresses that the incoming field $\vec{E}_{in}$, $\vec{H}_{in}$, according to its definition, at all times develops as a free field, independent of the presence of the charge. Thus the fact that the incoming field may nevertheless transfer energy and momentum to the particle, is reflected through the occurrence of interference between this field and the retarded field generated by the charge (cf. equations (49 d) and (50 d)).

Although the structure of the right-hand side of equations (49b) and (50b), in view of the expression (35), may invite an interpretation of $\vec{E}_{II}$ and $\vec{H}_{II}$ as "the radiation field" carrying at any time the "total radiated four-momentum", it must be clearly recognized that such an interpretation is purely *formal*, already because the quantities $\vec{E}_{II}$ and $\vec{H}_{II}$ do not by themselves satisfy the Maxwell equations. As far as equations (49a) and (50a) are concerned, the curious form of the right-hand sides is clearly connected to the fact, that the boundaries of the region $\Xi$ are spheres whose centres are displaced relative to the instantaneous position of the particle.

Collecting the terms in eqs. (49) and (50), letting $t_1 \to -\infty$ and (in the regular terms) $t_2 \to t$ one obtains*

$$\left.\begin{aligned}
\mathscr{E}_{\Xi}(t) &= \tfrac{1}{3} Q^2 \frac{4\gamma^2(t_2) - 1}{2(t - t_2)} - Q \int_{-\infty}^{t} \vec{v} \cdot \vec{E}_{in}\, dt \\
&\quad + \tfrac{2}{3} Q^2 \int_{-\infty}^{t} \frac{\vec{g}^2 - (\vec{g} \times \vec{v})^2}{(1 - v^2)^3}\, dt + \mathscr{E}_{in} \\
\vec{\mathscr{P}}_{\Xi}(t) &= \tfrac{2}{3} Q^2 \frac{\gamma^2(t_2)}{(t - t_2)} \vec{v}(t_2) - Q \int_{-\infty}^{t} \{\vec{E}_{in} + \vec{v} \times \vec{H}_{in}\}\, dt \\
&\quad + \tfrac{2}{3} Q^2 \int_{-\infty}^{t} \frac{\vec{g}^2 - (\vec{g} \times \vec{v})^2}{(1 - v^2)^3} \vec{v}\, dt + \vec{\mathscr{P}}_{in}.
\end{aligned}\right\} \quad (51)$$

From this result it is not difficult (see appendix C) to arrive at the desired expressions for the energy and momentum corresponding to the regions $\Omega$ and $\Gamma$:

$$\left.\begin{aligned}
\overset{\circ}{\mathscr{E}}_{\Omega} &= \frac{Q^2}{2\varepsilon} - Q \int_{-\infty}^{t} \vec{v} \cdot \vec{E}_{in}\, dt + \tfrac{2}{3} Q^2 \int_{-\infty}^{t} \frac{\vec{g}^2 - (\vec{g} \times \vec{v})^2}{(1 - v^2)^3}\, dt + \mathscr{E}_{in} \\
\overset{\circ}{\vec{\mathscr{P}}}_{\Omega} &= -\tfrac{2}{3} Q^2 \vec{g}(t) - Q \int_{-\infty}^{t} \{\vec{E}_{in} + \vec{v} \times \vec{H}_{in}\}\, dt \\
&\quad + \tfrac{2}{3} Q^2 \int_{-\infty}^{t} \frac{\vec{g}^2 - (\vec{g} \times \vec{v})^2}{(1 - v^2)^3} \vec{v}\, dt + \vec{\mathscr{P}}_{in}
\end{aligned}\right\} \quad (52)$$

and

* Of course we assume that $\gamma^2(t_1)/t_1 \to 0$ for $t_1 \to -\infty$ thus excluding cases like the ideal hyperbolic motion.

$$
\left.
\begin{aligned}
\mathscr{E}_\Gamma &= \frac{Q^2}{2\varepsilon}\gamma(t)\left(1+\tfrac{1}{3}v^2(t)\right) - Q\int_{-\infty}^{t}\vec{v}\cdot\vec{E}_{in}\,dt \\
&\quad + \tfrac{2}{3}Q^2\int_{-\infty}^{t}\frac{\vec{g}^2-(\vec{g}\times\vec{v})^2}{(1-v^2)^3}\,dt + \mathscr{E}_{in} \\
\vec{\mathscr{P}}_\Gamma &= \tfrac{4}{3}\frac{Q^2}{2\varepsilon}\gamma(t)\vec{v}(t) - Q\int_{-\infty}^{t}\{\vec{E}_{in}+\vec{v}\times\vec{H}_{in}\}dt \\
&\quad + \tfrac{2}{3}Q^2\int_{-\infty}^{t}\frac{\vec{g}^2-(\vec{g}\times\vec{v})^2}{(1-v^2)^3}\vec{v}\,dt + \vec{\mathscr{P}}_{in},
\end{aligned}
\right\} \qquad (53)
$$

where, in the latter case, the expansion of $\mathscr{E}_\Gamma$ and $\vec{\mathscr{P}}_\Gamma$ in powers of $\varepsilon$ has been restricted to the leading-order term (proportional to $Q^2/2\varepsilon$) which for dimensional reasons is independent of the acceleration.

Thus, in comparing eq. (52) with eg. (53) written down in the momentary restframe, it should be borne in mind, that in the derivation of eq. (53) from eq. (51) a zeroth-order term in $\varepsilon$, corresponding to a term which, again for dimensional reasons, must be linear in the acceleration, has been neglected.

In passing, it may provoke some reflexion that the Lagrangian density corresponding to the retarded field, $\frac{1}{8\pi}(E_R^2 - H_R^2)$, integrated over the regions $\Xi(t_1 \to -\infty)$ and $\Gamma$, respectively, yields the simple results:

$$
\frac{1}{8\pi}\int_{\Xi}(E_R^2 - H_R^2)\,dV = \frac{Q^2}{2(t-t_2)} \qquad (54)
$$

$$
\frac{1}{8\pi}\int_{\Gamma}(E_R^2 - H_R^2)\,dV = \frac{Q^2}{2\varepsilon}\frac{1}{\gamma(t)}. \qquad (55)
$$

To complete the provisional plan agreed on, it only remains to declare the electromagnetic energy and momentum of the system to be given by that four-vector $\mathscr{P}_\Omega(\tau) = (\vec{\mathscr{P}}_\Omega(\tau),\ i\mathscr{E}_\Omega(\tau))$ which in the momentary rest-frame reduces to $(\mathring{\vec{\mathscr{P}}}_\Omega,\ i\mathring{\mathscr{E}}_\Omega)$ given by eq. (52). Thus

$$
\left.
\begin{aligned}
\mathscr{P}_\Omega(\tau) &= \frac{Q^2}{2\varepsilon}U - \tfrac{2}{3}Q^2 g + \tfrac{2}{3}Q^2\int_{-\infty}^{\tau} g^2 U\,d\tau - Q\int_{-\infty}^{\tau}\mathscr{F}_{(in)}U\,d\tau + \mathscr{P}_{in} \\
&= \int_{-\infty}^{\tau}\left\{\frac{Q^2}{2\varepsilon}g - \tfrac{2}{3}Q^2(\dot{g}-g^2U) - Q\mathscr{F}_{(in)}U\right\}d\tau + \mathscr{P}_{in} \\
&= \int_{\Omega}\mathscr{T}\cdot d\Omega,
\end{aligned}
\right\} \qquad (56)
$$

where $\mathscr{T}$ denotes the total electromagnetic energy-momentum tensor, and where the symbol below the integral sign is meant to indicate that the integration is extended over the domain $\Omega$, i.e. that part of the three dimensional hyperplane orthogonal to the momentary four-velocity, which is exterior to a sphere of radius $\varepsilon$ centred at the momentary position of the charge. The last step in eq. (56) is justified by noting that in the momentary rest-frame

$$\int_{\Omega} \mathscr{T} \cdot d\Omega \Big|_{\text{rest}} = \left( \frac{1}{4\pi} \int_{\Omega} (\vec{E} \times \vec{H}) \, dV, \quad \frac{i}{8\pi} \int_{\Omega} (\vec{E}^2 + \vec{H}^2) \, dV \right) \tag{57}$$

the right-hand side being given by eq. (52).

Compare now eq. (56) with the corresponding expression (not four-vector) within the conventional scheme:

$$(\vec{\mathscr{P}}_\Gamma(t), \; i\mathscr{E}_\Gamma(t)) = \int_{\Gamma} \mathscr{T} \cdot d\Gamma = i \int_{\Gamma} \mathscr{T}_{i4} \, dV, \quad (d\Gamma_4 = i dV) \tag{58}$$

where the symbol below the integral sign is now meant to indicate that the integration is extended over the domain $\Gamma$ at constant laboratory time $T$. Clearly, the important feature to notice is that since in eq. (56) contributions from various spatial regions are added corresponding to simultaneity in the rest-frame (as opposed to eq. (58)), the definition (56) of $\mathscr{P}_\Omega(\tau)$ is tantamount to abandoning the idea that the electromagnetic energy and momentum at a given moment is carried by the field at that moment. In this connection it is essential to realize that even though the energy-momentum tensor is divergence-free through all space outside the charge, it is not possible to tilt the cut hyperplane, over which the integral in eq. (56) extends, without changing the value of $\mathscr{P}_\Omega(\tau)$. This fact is already manifest from a comparison of the expressions (56) and (53) in the special case where the acceleration actually vanishes at the moment considered.

Although the appearance of the expressions (56) for $\mathscr{P}_\Omega(\tau)$ and (53), (58) for $(\mathscr{P}_\Gamma, \mathscr{E}_\Gamma)$ naturally invites comparison with the expressions (41), (45) for $\mathscr{P}_{(\mathring{T})}$ and (40), (44) for $\mathscr{P}(T)$, respectively, it should be borne in mind that, whereas the latter quantities simply refer to different electrified systems, the former ones are competing candidates for the role as the electromagnetic energy and momentum for one definite system, consisting of a point charge interacting with an external field. As a matter of fact, even if DIRAC and his school claim to consider the electron strictly as a point charge, nevertheless their exploitation of the conventional Maxwell theory presupposes an under-

lying picture of the "point electron" as the limit of a tiny charged spherical shell. A further dissimilarity to bear in mind, when comparing the mentioned expressions, arises from the different attitudes towards the stability problem in the two models. In fact, in accordance with the classical Lorentz theory, the stability of the corpuscular system poses no specific problem, once definite assumptions regarding the stabilizing forces are agreed on. In contrast, the very idea behind the endeavours of the proponents of the "point electron" is precisely to avoid any reference to non-electromagnetic forces as stabilizing agents. In this situation the non-vanishing divergence of the electromagnetic energy-momentum tensor becomes an obstacle, which is only circumvented by re-introducing the non-electromagnetic forces well hidden in the disguise of "mass renormalization".

* *

On the background thus acquired it is particularly easy to display the essence of the attempts initiated by DIRAC of constructing a renormalized equation of motion for a classical point charge. Indeed, once it has been agreed that the electromagnetic energy and momentum is given by the four-vector eq. (56), the gist of these endeavours amounts — in one way or another — to the assertion of the existence of a conservation law of the form

$$m_b U(\tau) + \mathscr{P}_\Omega(\tau) = \text{constant}, \tag{59}$$

where $m_b$ denotes the "bare" mass of the particle. Inserting $\mathscr{P}_\Omega(\tau)$ from eq. (56) and differentiating with respect to $\tau$, one immediately arrives at the familiar Lorentz-Dirac equation

$$mg = \tfrac{2}{3} Q^2 [\dot{g} - g^2 U] + Q \mathscr{F}_{(in)} U, \tag{60}$$

where $m$ denotes the "renormalized" mass

$$m = m_b + \frac{Q^2}{2\varepsilon}. \tag{61}$$

Even though the eq. (60) is, of course, known to be approximately valid in many instances, the claim that it represents the exact equation of motion for a classical point charge is unwarranted, in so far as no physical arguments can be adduced neither to justify the identification of the electromagnetic energy and momentum with the components of the four-vector $\mathscr{P}_\Omega(\tau)$, (56), nor to support the conservation law (59).

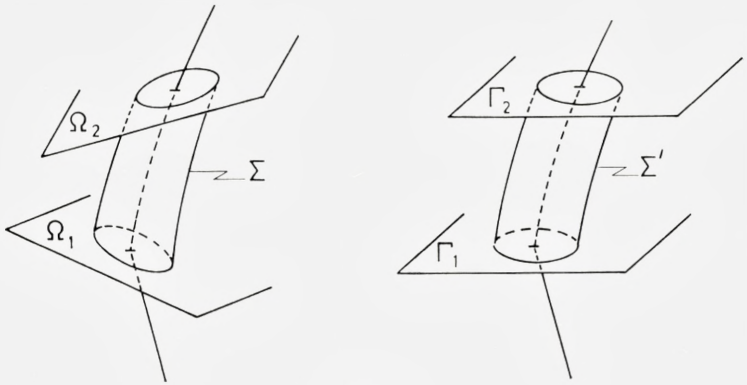


Fig. 4.

After this adumbration of the essential features in the reasoning leading Dirac and others to the "one-body" equation of motion (60), the remainder of this paragraph is devoted to a more careful analysis of the assumptions by which the conventional scheme must be supplemented to allow the deduction of a result, which could not be justified within this frame.

Let us first notice that the difference $\mathscr{P}_Q(\tau_2) - \mathscr{P}_Q(\tau_1)$ with $\mathscr{P}_Q(\tau)$ given by eq. (56), may — by applying Gauss' theorem — be written as

$$\left.\begin{aligned} \mathscr{P}_Q(\tau_2) - \mathscr{P}_Q(\tau_1) &= \int_{\Omega_2} \mathscr{T} \cdot d\Omega_2 - \int_{\Omega_1} \mathscr{T} \cdot d\Omega_1 = \int_{\Sigma} \mathscr{T} \cdot d\Sigma \qquad \text{(a)} \\ \int_{\Sigma} \mathscr{T} \cdot d\Sigma &= \int_{\tau_1}^{\tau_2} d\tau \left\{ \frac{Q^2}{2\varepsilon} g - \tfrac{2}{3} Q^2 (\dot{g} - g^2 U) - Q \mathscr{F}_{(in)} U \right\}, \qquad \text{(b)} \end{aligned}\right\} \tag{62}$$

where $\Sigma$ denotes a 3-dimensional tube surrounding the world line bound by the two cut planes $\Omega_1$ and $\Omega_2$ and where the intersection between the tube and the mentioned planes is the two-dimensional spherical surface of radius $\varepsilon$ (see figure 4). The identity (62 b), which forms the basis for Dirac's discussion is derived by him through direct expansion of the energy-momentum tensor in powers of $\varepsilon$.

A critical step in Dirac's analysis is his identification of the left hand side of eq. (62) as "the difference in energy (or momentum) residing within the tube at the two ends...". Indeed, implicitly relying on the assumption that the energy and momentum within the tube at the two ends constitute a four-vector, Dirac demands that this four-vector at any given point $x(\tau)$ of the world line be expressible as some universal function $B$ of the particle variables $(U, \dot{U}, \ddot{U}, \ldots)$ at that point. Consequently, it is required that

$$B(U(\tau_2), \dot{U}(\tau_2), \ldots) - B(U(\tau_1), \dot{U}(\tau_1), \ldots) = \int_{\Sigma} \mathscr{T} \cdot d\Sigma. \tag{63}$$

Clearly, the integral (62 b) extended along an arbitrary world line would not in general possess this remarkable property, which, of course, amounts to requiring that the integrand in eq. (62 b) be equal to $\dot{B}$, i.e., the differential of the universal function $B$. Hence, the demand (63) is but a recipe for the selection of the set of *permissible* world lines, and thus — for each choice of $B$ — it is equivalent to *prescribing* the equations of motion for the particle.

Returning to the above-mentioned crucial interpretation of the left-hand side of eq. (62), we have just seen that the four-vector character of this integral necessitates the assumption that the energy and momentum within the tube constitute a four-vector. However, since the energy and momentum within the tube regarded as integrals over appropriate densities at definite laboratory time do not form a four-vector, Dirac's identification amounts to a re-definition of these quantities, analogous to that discussed above for the energy and momentum "outside" the tube*. In particular, combining the eqs. (62 a) and (63), we see that the conservation of the total four-momentum is expressed** as

$$\mathscr{P}_{\Omega}(\tau) - B(\tau) = \text{constant}. \tag{64}$$

In contrast to what is the case in the conventional scheme, this equation implies that the conserved four-momentum for the total closed system can be decomposed into a sum of four-momenta referring to the interacting subsystems.

It is instructive to paraphrase the above "deductions" within the conventional scheme. Here the difference in electromagnetic energy and momentum "outside" the tube at two successive instances $T_1$ and $T_2$, referred to one and same system of inertia, is given by:

$$\left.\begin{aligned} &(\vec{\mathscr{P}}_{\Gamma}(T_2), i\mathscr{E}_{\Gamma}(T_2)) - (\vec{\mathscr{P}}_{\Gamma}(T_1), i\mathscr{E}_{\Gamma}(T_1)) \\ &= \int_{\overline{\Gamma_2}} \mathscr{T} \cdot d\Gamma_2 - \int_{\overline{\Gamma_1}} \mathscr{T} \cdot d\Gamma_1 = \int_{\Sigma'} \mathscr{T} \cdot d\Sigma' \end{aligned}\right\} \text{(a)} \tag{65}$$

* This remark is further substantiated by the observation that the integral over the surface $\Sigma$, referred to by Dirac as the flow of energy and momentum through the tube, cannot in general – when the end-surfaces $\Omega_1$ and $\Omega_2$ are tilted relative to each other – be interpreted as the flux through a moving surface during a *definite* time interval.

** Dirac remarks that the simplest choice for $B$ would be $B = -m_b U$ in which case the conservation laws (64) and (59) become identical.

$$\left.\begin{aligned}\int_{\Sigma'} \mathscr{T}\cdot d\Sigma' &= \frac{Q^2}{2\varepsilon}\gamma(T_2)\left(\tfrac{4}{3}\vec{v}(T_2),\, i(1+\tfrac{1}{3}\vec{v}^2(T_2))\right)\\ &\quad -\frac{Q^2}{2\varepsilon}\gamma(T_1)\left(\tfrac{4}{3}\vec{v}(T_1),\, i(1+\tfrac{1}{3}\vec{v}^2(T_1))\right)\\ &\quad -\int_{T_1}^{T_2} d\tau\left\{-\tfrac{2}{3}Q^2g^2U+Q\mathscr{F}_{(in)}U\right\},\end{aligned}\right\}\ \text{(b)} \qquad (65)$$

where $\Gamma_1$ and $\Gamma_2$ denote the cut hyperplanes $T_1 = \text{const.}$ and $T_2 = \text{const.}$, respectively, and where $\Sigma'$ refers to the surface of the tube between $\Gamma_1$ and $\Gamma_2$, the intersection between the tube and the planes $\Gamma_1$ and $\Gamma_2$ being Heaviside ellipsoids (see figure 4). Furthermore, we have used eq. (53) neglecting again in the expressions for $\mathscr{E}_\Gamma$ and $\vec{\mathscr{P}}_\Gamma$ a term linear in the acceleration*. Insisting that the permissible world lines are selected according to the requirement that the left-hand side of eq. (65b) be expressible as the difference in values taken by some universal function $B' = (\vec{B}'(T), iB_0'(T))$ (not four-vector) of the particle variables at times $T_2$ and $T_1$, we have now in place of eq. (63)

$$B'(\vec{v}(T_2), \vec{g}(T_2), \ldots) - B'(\vec{v}(T_1), \vec{g}(T_1), \ldots) = \int_{\Sigma'} \mathscr{T}\cdot d\Sigma', \qquad (66)$$

which combined with eq. (65a) leads to conservation law (analogous to eq. (64))

$$(\vec{\mathscr{P}}_\Gamma(T), \mathscr{E}_\Gamma(T)) - (\vec{B}'(T), B_0'(T)) = \text{constant}. \qquad (67)$$

In this case, the energy and momentum of the subsystems, adding up to the total conserved four-momentum, do not themselves constitute the components of four-vectors. Nevertheles, it is still possible to perform a mass renormalization, and the form of eq. (53) immediately suggests that the most alluring** choice of $B'$ would be

$$(\vec{B}', iB_0') = -m_b U + \frac{Q^2}{2\varepsilon}\gamma\left(\tfrac{1}{3}\vec{v}, i\tfrac{1}{3}v^2\right) + \tfrac{2}{3}Q^2 g \qquad (68)$$

where $m_b$ again denotes the bare mass. Indeed, combining the eqs. (53), (67) and (68), one arrives once more at the conservation law

* It is easy to verify that the difference between the right-hand sides of eqs. (62b) and (65b) just equals the flux of $\mathscr{T}$ through the tiny sections of the tube between the planes $\Omega_1$ and $\Gamma_1$, and $\Omega_2$, and $\Gamma_2$.

** It should be noted, that the four functions $B'$ cannot be chosen completely independently of each other, since we are dealing with only three independent equations of motion. Thus, the choice of the first two members on the right hand side of eq. (68) immediately implies the need for a third term to ensure the mutual compatibility of the resulting equations of motion, and it is easily seen, that $\frac{2}{3}Q^2g$ represents the simplest possible choice for this additional term.

$$mU(\tau) - \int_{-\infty}^{\tau} d\tau \left\{ \tfrac{2}{3} Q^2 (\dot{g} - g^2 U) + Q \mathscr{F}_{(in)} U \right\} = \text{constant}, \tag{69}$$

where the renormalized mass $m$ is again defined by eq. (61). Differentiation of eq. (69) immediately gives back the equations of motion (60).

From the above "deductions" it emerges that the most prominent departure by DIRAC and his followers from the conventional scheme — namely, the re-definition of the electromagnetic energy and momentum so as to transform like a four-vector — surprisingly enough turns out to be unessential, at least in so far as the resulting equation of motion does not depend on this assumption. Instead, the pivot, on which the entire argumentation turns, is seen to be the much less conspicuous step of taking for granted that the energy and momentum "residing within the tube at the two ends" should be a state function expressible solely in terms of the particle variables*. It is through the insistence that this demand on the integral (62) be the guiding principle for the selection of the permissible world lines that the ground of classical electrodynamics is left behind. Indeed, this "principle" merely conceals a postulate of the desired equation of motion.

## § 4. Concluding Remarks

As emphasized in the preceding discussion, Classical Electron Theory does provide a well-defined framework within which any question, concerning the behaviour of electrified bodies, which may at all be formulated in terms of classical physical ideas, can in principle be answered, irrespectively of the magnitude of the charge and mass of the bodies concerned. In contrast, as analysed in the previous paragraph, the attempts by DIRAC, ROHRLICH and others to implement the scheme of classical electrodynamics have not resulted in a systematic description in which the notion of a point charge is harmoniously incorporated into the ordinary Maxwell theory for extended charge distributions. Furthermore, the physical interpretation of the new scheme is hampered by the well-known difficulties associated with the appearance of "advanced effects" or "acausalities" in the solutions of the Lorentz-Dirac equation. From the conventional standpoint these difficulties may be explained simply as the result of an unwarranted extrapolation of conclusions drawn on the basis of an *approximate* equation of motion. How-

* It is even more misleading when some authors profess to "derive" this property by arguing that the integral (62) is independent of the shape of the *tube*. Of course, the question at issue concerns a variation of the world line.

ever, since in the "point electron theory" the Lorentz-Dirac equation is considered an *exact* equation of motion, the "acausalities" acquire a fundamental status thereby creating the need for a comprehensive revision of the conceptual framework. Indeed, it seems that the prediction of "advanced effects" in the theory represents a contradiction in terms unless it is explicitly assumed that – for some reason or another – the freedom, commonly assumed, of external agents or "observers" to intervene in the system under consideration is limited. As long as this feature is not reflected in the formal description itself – in the way the reciprocal measuring limitations are built into the foundations of quantum theory –, the description remains logically incomplete and the question as to its observable consequences cannot even be formulated, much less answered*.

It needs hardly be added that a solution to the logical dilemma represented by the prediction of "acausalities" cannot be achieved by reference to the empirical limitations of the classical description itself. Indeed, in any comparison between the "point electron theory" and the conventional scheme, it is of course essential as clearly as possible to distinguish between the problem of internal consistency of the description on the one hand, and the question of its range of empirical validity on the other. In the present context, reference to empirical evidence merely serves to emphasize that since quantum phenomena become important already when probing into regions of extension far bigger than the classical electron radius, there is – empirically speaking – no room for unambiguous application of a "point electron theory" within classical physics.

Another aspect of the problems discussed is associated with the consequent use of the concept of "radiation" within the classical description. In § 2 a simple example was analysed, which exhibited the inadequacy of attempts to picture the act of radiation emission as a continuous process localized in space and time, and it was concluded that the radiation process entailed a modification of the electromagnetic field as a whole. Thus, the fact that the field strength in a given space-time domain is causally connected to the motion of the source particle at a definite segment of the world line, does not provide a physical basis for the notion that the field energy associated with the domain considered has been "emitted" by the charge on the corresponding segment.

Clearly, the above conclusions bring in relief the arbitrariness, discussed

* It has been suggested (ROHRLICH, loc. cit.), that detection of radiation from a uniformly accelerated electron should provide direct evidence for an acausal equation of motion. It will be clear from part III of these studies that this idea cannot be upheld.

in § 3, in the interpretation of the formal expressions for the "energy-momentum flux" through the tube surrounding the world line of the charge. Particularly misleading in this context is the occasional reference in the literature to an analogy with "photons", since the very definition of this concept excludes any well-defined application of the field picture, on which the entire discussion is based.

Thus, in dealing with radiation phenomena, we are presented with a feature of wholeness, familiar in quantal processes, but less so within the domain of classical physics. This feature receives a particular emphasis in the "action-at-a-distance" formulation of classical electrodynamics by FEYNMAN and WHEELER[2], who, however, by completely eliminating the degrees of freedom associated with the field, are led to give up the notion of instantaneous energy-momentum balance, at least in its customary form.

Among the attempts to formulate a classical theory of a "point electron" the work of FEYNMAN and WHEELER is distinguished by its inner consequence. As already discussed, in a "point electron" theory the presence of damping poses a problem without counterpart in the conventional scheme. In fact, within the former description the damping must either be considered the result of the action of the self-field on the particle, through a mechanism which, however, by the very idea of a point charge remains unanalysible, thus reducing the problem at issue to being a matter of composing a recipe for evaluating the effect. Or, more consequently relative to the premises, the possibility of self-interactions is denied altogether, in conformity with the conception of "charge" as an elementary property of the particle, expressing its ability to influence other similar particles according to a definite set of rules. Thus, in this case the presence of the damping acting on an individual particle can only be related to the interaction with other distant particles outside the system under consideration, and this interaction cannot possibly be retarded, even if only an approximate simultaneity between the motion and the damping of the particle is insisted upon.

A solution to this problem was achieved by FEYNMAN and WHEELER through the introduction of an allegedly "fundamental" time symmetric interaction, which, on the one hand, makes possible the description of the damping acting on the individual particle as the advanced effect of the polarization induced in the "distant absorbers" by the retarded interaction generated by the particle, and which, on the other hand — through a subtle interference between the advanced fields of the absorber and the charge, eliminating all advanced effects prior to the motion of the source — guarantees the repro-

duction of the usual "effectively" retarded field as generated by the charge in question.

Notwithstanding the lesson conveyed by the very possibility of constructing a coherent description of electrodynamics so far beyond immediate conceptions, it remains a delicate question to what extent the scheme admits of the intervention of external irreversible devices, not necessarily of electromagnetic origin. Indeed, in the absence of absorbers the time symmetric scheme is clearly incompatible with the presence of irreversibly functioning contrivances capable of distinguishing future from past and hence also of making a non-predictable choice as to whether or not to prevent the occurrence of an event, which in the description is held responsible for actions already completed. Such paradoxes are avoided by the introduction of the distant absorbers, which, as already indicated, causes the interaction to become "effectively" retarded. However, in spite of the apparent formal unimpeachability achieved through the above-mentioned destructive interference between the advanced fields, crucial for the compatibility of the time symmetric scheme and the possibility of influencing the future, there seems to be an inherent ambiguity in the notion of an advanced field — existing at all times prior to the future event to which it is correlated — which again becomes especially conspicuous if the occurrence of the mentioned event is made dependent on the outcome of a process which is unpredictable in principle.

As is evident from these considerations, not only the need but also the room for transcending classical electrodynamics, as proposed by FEYNMAN and WHEELER, is procured just by the new element added to it, namely the idea of an indivisible point charge. In fact, as far as observable consequences are concerned, the new scheme reduces, in the case of complete absorption, identically to the conventional electrodynamics, if this concept is abandoned, the damping becoming again an expression for the mutual interaction between the infinitesimal constituents of the "point charge".

**Acknowledgement**

We take this opportunity to thank friends and colleagues at the Institutes in Copenhagen and Aarhus for many enjoyable conversations. One of us (O. U.) gratefully acknowledges the grant of a Nordita fellowship as well as economic support from the Danish Research Council. — During the long time in which we have been engaged in the present studies, we have enjoyed the favour of frequent consultations with JENS LINDHARD. It is a special pleasure for us here to express our gratitude for the encouragement and inspiration we have derived from these conversations.

JØRGEN KALCKAR
*The Niels Bohr Institute, University of Copenhagen,*
*DK–2100 Copenhagen Ø, Denmark*

OLE ULFBECK
*NORDITA, Blegdamsvej 17,*
*DK–2100 Copenhagen Ø, Denmark*

## Appendix A

*Evaluation of the difference $\mathscr{F}_R(x) - \mathscr{F}_A(x)$ in the vicinity of the world line.*

The difference between the retarded and advanced Lienard-Wiechert potentials at a fixed space-time point $x$ is given by

$$A_R(x) - A_A(x) = -\delta q \left\{ \frac{U(\tau)}{(x - x(\tau))U(\tau)}\bigg|_{\tau_R} + \frac{U(\tau)}{(x - x(\tau))U(\tau)}\bigg|_{\tau_A} \right\}, \tag{A1}$$

where $\tau_A > \tau_R$ denote the two roots of the equation $(x - x(\tau))^2 = 0$. Expanding the function $(x - x(\tau))^2$ around its extremal value $\varepsilon^2$, which for convenience is taken to occur for $\tau = 0$, introducing the abreviation $l = x - x(0)$, and agreeing that all quantities $U$, $g$, $\dot{g}$ etc. written without argument, refer to the value $\tau = 0$, one has

$$\left.\begin{aligned} (x - x(\tau))^2 &= \varepsilon^2 - (1 + gl)\tau^2 - \tfrac{1}{3}(\dot{g}l)\tau^3 - \tfrac{1}{12}g^2\tau^4 + \ldots \\ (x - x(\tau))\,U(\tau) &= (1 + gl)\tau + \tfrac{1}{2}(\dot{g}l)\tau^2 + \tfrac{1}{6}g^2\tau^3 + \ldots \end{aligned}\right\} \tag{A2}$$

Hence to the accuracy required, the sum and the product of the roots of the equation $(x - x(\tau))^2 = 0$ are given by

$$\tau_R + \tau_A \simeq -\tfrac{1}{3}(\dot{g}l)\varepsilon^2, \qquad \tau_R\tau_A \simeq -\varepsilon^2. \tag{A3}$$

Next, expand the difference (A1) in the form

$$\left.\begin{aligned} A_R(x) - A_A(x) &= \delta q \left\{ \left( \frac{a_{-1}}{\tau_R} + a_0 + a_1\tau_R + \ldots \right) + \left( \frac{a_{-1}}{\tau_A} + a_0 + a_1\tau_A + \right) \right\} \\ &= \delta q \left\{ a_{-1}\frac{\tau_R + \tau_A}{\tau_R\tau_A} + 2a_0 \right\} + o(\varepsilon^2), \end{aligned}\right\} \tag{A4}$$

where the constant vectors $a_1$, and $a_0$ are seen to be determined by

$$a_{-1} = \frac{U}{1 + gl}, \quad a_0 = \frac{d}{d\tau}\frac{\tau U(\tau)}{(x - x(\tau))U(\tau)}\bigg|_{\tau = 0} = \frac{g}{1 + gl} - \tfrac{1}{2}(\dot{g}l)U. \tag{A5}$$

Finally, remembering that $U$, $g$, $\dot{g}$ etc. depend implicitly on $x$, one has

$$\left.\begin{aligned} A_R(x) - A_A(x) &= -\delta q \left\{ \frac{2g}{1 + gl} - \tfrac{2}{3}(\dot{g}l)\,U \right\} + o(\varepsilon^2) \\ &= -\delta q \left\{ \tfrac{4}{3}(\dot{g}l)\,U + 2\partial_x ln(1 + gl) \right\} + o(\varepsilon^2). \end{aligned}\right\} \tag{A6}$$

Whence the field tensor, correct to zeroth order in $\varepsilon$, is obtained as

$$\mathscr{F}_R(x) - \mathscr{F}_A(x) = \partial_x \wedge (A_R(x) - A_A(x)) \simeq -\tfrac{4}{3}\delta q\, \partial \wedge (\dot{g}l)\, U \simeq \tfrac{4}{3}\delta q\, U \wedge \dot{g}, \quad \text{(A7)}$$

where it has been observed, that a change $\delta x$ in $x$ causes a change $\delta l = \delta x + (U\delta x)\, U$ in $l$.

## Appendix B

*Evaluation of energy-momentum expenditure to bring two electrified corpuscles from rest at infinite separation along arbitrary world-lines to a state of common uniform motion.*

To evaluate the integral $\mathscr{I}$ in eq. (36), introduce the retarded Green's function $\mathscr{D}_R(x)$:

$$\left.\begin{aligned} \mathscr{I} &= \int^T dx \{\mathscr{F}_R^{(2)}(x) s_1(x) + \mathscr{F}_R^{(1)}(x) s_2(x)\} \\ &= \iint^T dx dy \{[\partial_x \mathscr{D}_R(x-y) \wedge s_2(y)] s_1(x) + [\partial_x \mathscr{D}_R(x-y) \wedge s_1(y)] s_2(x)\} \\ &\equiv \mathscr{I}_1 + \mathscr{I}_2 + \mathscr{I}_3, \end{aligned}\right\} \quad \text{(B1)}$$

where

$$\left.\begin{aligned} \mathscr{I}_1 &= \iint^T dx dy (\partial_x \mathscr{D}_R(x-y)) s_2(y) \cdot s_1(x) \\ \mathscr{I}_2 &= \iint^T dx dy (\partial_x \mathscr{D}_R(x-y)) s_1(y) \cdot s_2(x) \\ \mathscr{I}_3 &= -\iint^T dx dy \{(s_1(x) \cdot \partial_x \mathscr{D}_R(x-y)) s_2(y) + (s_2(x) \cdot \partial_x \mathscr{D}_R(x-y)) s_1(y)\}. \end{aligned}\right\} \quad \text{(B2)}$$

The integral $\mathscr{I}_3$ is immediately evaluated by partial integration and application of the equation of continuity for the current densities. Taking into account the boundary conditions at $t = -\infty$ one obtains

$$\mathscr{I}_3 = -\delta q_1 A_R^{(2)}(\vec{x}_1(T), T) - \delta q_2 A_R^{(1)}(\vec{x}_2(T), T) = -2\frac{\delta q_1\, \delta q_2}{\varepsilon} U, \quad \text{(B3)}$$

where the last equality is justified by the assumption stated in the text, that the motion has been uniform for at least a time $2\gamma\varepsilon$ prior to $T$.

Consider next the term $\mathscr{I}_2$, remembering the symmetry relation $\mathscr{D}_R(x) = \mathscr{D}_A(-x)$:

$$\left.\begin{aligned}
\mathscr{I}_2 &= \int\int dx dy\, \Theta(T-t_x)(\partial_x \mathscr{D}_R(x-y)) s_1(y)\cdot s_2(x) \\
&= -\int\int dx dy\, \Theta(T-t_x)(\partial_y \mathscr{D}_A(y-x)) s_2(x)\cdot s_1(y) \\
&= -\int dy \Big[\partial_y \int dx\, \Theta(T-t_x)\mathscr{D}_A(y-x) s_2(x)\Big] s_1(y) \\
&= -\int dy \Big[\partial_y \Theta(T-t_y-|\vec{x}_2(T)-\vec{y}|) A_A^{(2)}(y)\Big] s_1(y),
\end{aligned}\right\} \quad \text{(B4)}$$

where $\Theta(t)$ denotes the step function

$$\left.\Theta(t) = \begin{cases} 1 & \text{for} \quad t > 0 \\ 0 & \text{for} \quad t < 0 \end{cases}\right\} \quad \text{(B5)}$$

obeing the relation

$$\partial_x \Theta(t-|\vec{x}|) = -2\Theta(t)\delta(x^2)x. \quad \text{(B6)}$$

Thus one obtains

$$\left.\begin{aligned}
\mathscr{I}_2 &= -\int dy\, \Theta(T-t_y-|\vec{x}_2(T)-\vec{y}|)[\partial_y A_A^{(2)}(y)] s_1(y) \\
&\quad -\int dy\, 2\Theta(T-t_y)\delta((x_2-y)^2)(A_A^{(2)}(y)\cdot s_1(y))(x_2-y) \\
&= -\int^{t_{12}} dy [\partial_y A_A^{(2)}(y)] s_1(y) + \frac{\delta q_1\, \delta q_2}{\varepsilon^2} R^{(21)},
\end{aligned}\right\} \quad \text{(B7)}$$

where $x_2 = (\vec{x}_2(T), iT)$ and where $t_{12}$ and the light-vector $R^{(21)}$ are defined on figure 2 of the text.

From the results (B1), (B2), (B3) and (B7) one finds:

$$\left.\begin{aligned}
\mathscr{I} &= \int^{t_{12}} dx [\partial_x (A_R^{(2)} - A_A^{(2)})] s_1(x) + \frac{\delta q_1\, \delta q_2}{\varepsilon^2} l^{(21)} - \frac{\delta q_1\, \delta q_2}{\varepsilon} U \\
&\quad + \int_{t_{12}}^{T} dx [\partial_x A_R^{(2)}(x)] s_1(x).
\end{aligned}\right\} \quad \text{(B8)}$$

Remembering that for the time interval over which the last integral extends

$$A_R^{(2)}(x_1(\tau)) = \delta q_2 \frac{U}{\varepsilon} \quad \text{and} \quad \partial_x \varepsilon = -\frac{l^{(21)}}{\varepsilon},$$

the last integral in eq. (B8) is evaluated to yield

$$-\frac{\delta q_1\, \delta q_2}{\varepsilon^3} l^{(21)} \frac{(T-t_{12})}{\gamma}, \quad \text{(B9)}$$

where

$$T - t_{12} = \frac{1}{i} R_4^{(21)} = \frac{1}{i}(l_4^{(21)} + i\varepsilon\gamma).$$

Subtracting finally the quantity

$$\int^{t_{12}} dx s_1(x) \cdot \partial_x [A_R^{(2)}(x) - A_A^{(2)}(x)] = \int^{t_{12}} dx \partial_x \cdot [s_1(x)(A_R^{(2)} - A_A^{(2)})] = 0$$

(remembering that $A_R = A_A$ for the final rectilinear sections of the world lines) one obtains

$$\mathscr{I} = \int^{t_{12}} dx [\partial_x \wedge (A_R^{(2)} - A_A^{(2)})] s_1(x) - \frac{\delta q_1 \delta q_2}{\varepsilon} U - \frac{\delta q_1 \delta q_2}{\varepsilon^3} \left( \frac{l_4^{(21)}}{i\gamma} \right) l^{(21)}. \tag{B10}$$

## Appendix C

*Explicit evaluation of the energy and momentum associated with the domains $\Xi$, $\Gamma$ and $\Omega$.*

By means of the expression for $\vec{E}_{\mathrm{I}}$, $\vec{H}_{\mathrm{I}}$, $\vec{E}_{\mathrm{II}}$, $\vec{H}_{\mathrm{II}}$ as defined by eq. (47) one finds

$$\left.\begin{aligned} &\frac{1}{8\pi} \int_{\Xi} dV [\vec{E}_{\mathrm{I}}^2 + 2\vec{E}_{\mathrm{I}} \cdot \vec{E}_{\mathrm{II}} + \vec{H}_{\mathrm{I}}^2 + 2\vec{H}_{\mathrm{I}} \cdot \vec{H}_{\mathrm{II}}] = \\ &\frac{1}{8\pi} \int_{\Xi} dV \left\{ \frac{(1-v^2)^4}{(t-t_R)^4} \frac{1 + v^2 - (\vec{v} \cdot \hat{n})^2 - 2\vec{v} \cdot \hat{n}}{(1 - \vec{v} \cdot \hat{n})^6} \right. \\ &\qquad \left. + 4 \frac{(1-v^2)}{(t-t_R)^3} \left[ \frac{\vec{v} \cdot \vec{g}}{(1 - \vec{v} \cdot \hat{n})^5} - \frac{(\hat{n} \cdot \vec{v})(\hat{n} \cdot \vec{g})}{(1 - \vec{v} \cdot \hat{n})^6} + \frac{\hat{n} \cdot \vec{g}}{(1 - \vec{v} \cdot \hat{n})^6} v^2 \right] \right\}. \end{aligned}\right\} \tag{C1}$$

$$\left.\begin{aligned} &\frac{1}{8\pi} \int_{\Xi} dV [\vec{E}_{\mathrm{II}}^2 + \vec{H}_{\mathrm{II}}^2] = \\ &\frac{1}{8\pi} \int_{\Xi} dV \left\{ \frac{g^2}{(1 - \vec{v} \cdot \hat{n})^4} + \frac{(v^2 - 1)(\hat{n} \cdot g)^2}{(1 - \vec{v} \cdot \hat{n})^6} + \frac{2(\hat{n} \cdot \vec{g})(\vec{v} \cdot \vec{g})}{(1 - \vec{v} \cdot \hat{n})^5} \right\} \frac{1}{(t - t_R)^2} \end{aligned}\right\} \tag{C2}$$

$$\left.\begin{aligned} &\frac{1}{4\pi} \int_{\Xi} dV [\vec{E}_{\mathrm{I}} \times \vec{H}_{\mathrm{I}} + \vec{E}_{\mathrm{I}} \times \vec{H}_{\mathrm{II}} + \vec{E}_{\mathrm{II}} \times \vec{H}_{\mathrm{I}}] = \\ &\frac{1}{4\pi} \int_{\Xi} dV \left\{ \left[ \frac{1 - v^2}{(1 - \vec{v} \cdot \hat{n})^6} \frac{1 + v^2 - 2\vec{v} \cdot \hat{n}}{(t - t_R)^4} \right. \right. \end{aligned}\right\} \tag{C3}$$

$$+\frac{2}{(t-t_R)^2}\frac{1-v^2}{(1-\vec{v}\cdot\hat{n})^6}[(\vec{v}\cdot\vec{g})(1-\vec{v}\cdot\hat{n})-(\hat{n}\cdot\vec{v})(n\cdot\vec{g})+v^2\hat{n}\cdot\vec{g}]\Big]\hat{n}$$

$$-\frac{(1-v^2)}{(t-t_R)^2(1-\vec{v}\cdot\hat{n})^2}\left[\frac{1-v^2}{(1-\vec{v}\cdot\hat{n})^3}\frac{\hat{n}-\vec{v}}{(t-t_R)^2}+\frac{(\hat{n}\cdot\vec{g})(\hat{n}-\vec{v})-(1-\hat{n}\cdot\vec{v})\vec{g}}{(1-\vec{v}\cdot\hat{n})^3(t-t_R)}\right]\Bigg\}. \tag{C3}$$

$$\frac{1}{4\pi}\int_{\Xi}dV(\vec{E}_{II}\times\vec{H}_{II}) =$$

$$\frac{1}{4\pi}\int_{\Xi}dV\left\{\frac{\vec{g}^2}{(1-\hat{n}\cdot\vec{v})^4}+\frac{(v^2-1)(\hat{n}\cdot\vec{g})^2}{(1-\vec{v}\cdot\hat{n})^6}+\frac{2(\hat{n}\cdot\vec{g})(\vec{v}\cdot\vec{g})}{(1-\vec{v}\cdot\hat{n})^5}\right\}\frac{\hat{n}}{(t-t_R)^2}. \tag{C4}$$

To find the value of these integrals at time $t$, each point $\vec{x}$ in the domain $\Xi$ is parametrized by the corresponding retarded point $\vec{x}_R(t_R)$ on the particle trajectory. In terms of the variables $\hat{n}=\bar{x}-\bar{x}_R/|\bar{x}-\bar{x}_R|$ and $t-t_R$, the volume element is easily seen to be given by*

$$dV=(1-\vec{v}_R\cdot\hat{n})(t-t_R)^2dt_R\,d\Omega \tag{C5}$$

and the outer (inner) boundary of $\Xi$ to be determined by $t_R=t_1(t_R=t_2)$. Differentiating the identities

$$\int\frac{d\Omega}{4\pi}\frac{1}{(1-\vec{v}\cdot\hat{n})^2}=\frac{1}{1-v^2}\quad\text{and}\quad\int\frac{d\Omega}{4\pi}\frac{1}{(1-\vec{v}\cdot\hat{n})^3}=\frac{1}{(1-v^2)^2}$$

the appropriate number of times with respect to the components of $\vec{v}$, the necessary angular integrals are immediately obtained:

$$\int\frac{d\Omega}{4\pi}\frac{n_\iota}{(1-\vec{v}\cdot\hat{n})^3}=\frac{v_\iota}{(1-v^2)^3}\qquad\int\frac{d\Omega}{4\pi}\frac{n_\iota}{(1-\vec{v}\cdot\hat{n})^4}=\tfrac{4}{3}\frac{v_\iota}{(1-v^2)^3}$$

$$\int\frac{d\Omega}{4\pi}\frac{n_\iota n_\varkappa}{(1-\vec{v}\cdot\hat{n})^4}=\tfrac{4}{3}\frac{v_\iota v_\varkappa}{(1-v^2)^3}+\tfrac{1}{3}\frac{\delta_{\iota\varkappa}}{(1-v^2)^2}$$

$$\int\frac{d\Omega}{4\pi}\frac{n_\iota n_\varkappa}{(1-\vec{v}\cdot\hat{n})^5}=2\frac{v_\iota v_\varkappa}{(1-v^2)^4}+\tfrac{1}{3}\frac{\delta_{\iota\varkappa}}{(1-v^2)^3}$$

$$\int\frac{d\Omega}{4\pi}\frac{n_\iota n_\varkappa n_\lambda}{(1-\vec{v}\cdot\hat{n})^5}=2\frac{v_\iota v_\varkappa v_\lambda}{(1-v^2)^4}+\tfrac{1}{3}\frac{v_\iota\delta_{\varkappa\lambda}+v_\lambda\delta_{\iota\varkappa}+v_\varkappa\delta_{\lambda\iota}}{(1-v^2)^3}.$$

* The use of the standard notation $d\Omega$ for the surface element on the unit sphere should here cause no confusion with the volume element on the hyperplane $\Omega$ used elsewhere.

Inserting these integrals and the volume element into eqs. (C1)–(C4), one finds the results (49a, b) and (50a, b) of the text:

$$\left.\begin{aligned} &\frac{1}{8\pi}\int_{\Xi}[\vec{E}_{\mathrm{I}}^{2}+2\vec{E}_{\mathrm{I}}\cdot\vec{E}_{\mathrm{II}}+\vec{H}_{\mathrm{I}}^{2}+2\vec{H}_{\mathrm{I}}\cdot\vec{H}_{\mathrm{II}}]\,dV \\ &=\frac{Q^{2}}{2}\int_{t_1}^{t_2}dt_R\left\{\frac{1}{(t-t_R)^{2}}\frac{1+v^{2}/3}{1-v^{2}}+\tfrac{8}{3}\frac{1}{(t-t_R)}\frac{\vec{v}\cdot\vec{g}}{(1-v^{2})}\right\} \\ &=\frac{Q^{2}}{3}\left\{\frac{4\gamma^{2}(t_2)-1}{2(t-t_2)}-\frac{4\gamma^{2}(t_1)-1}{2(t-t_1)}\right\} \end{aligned}\right\} \tag{49a}$$

$$\frac{1}{8\pi}\int_{\Xi}[\vec{E}_{\mathrm{II}}^{2}+\vec{H}_{\mathrm{II}}^{2}]\,dV=\tfrac{2}{3}Q^{2}\int_{t_1}^{t_2}dt_R\frac{\vec{g}^{2}-(\vec{g}\times\vec{v})^{2}}{(1-v^{2})^{3}} \tag{49b}$$

$$\left.\begin{aligned} &\frac{1}{4\pi}\int_{\Xi}[\vec{E}_{\mathrm{I}}\times\vec{H}_{\mathrm{I}}+\vec{E}_{\mathrm{I}}\times\vec{H}_{\mathrm{II}}+\vec{E}_{\mathrm{II}}\times\vec{H}_{\mathrm{I}}]\,dV \\ &=Q^{2}\int_{t_1}^{t_2}dt_R\left\{\tfrac{2}{3}\frac{\vec{v}}{(1-v^{2})(t-t_R)^{2}}+\tfrac{2}{3}\frac{\vec{g}}{(t-t_R)(1-v^{2})}+\tfrac{4}{3}\frac{(\vec{g}\cdot\vec{v})\vec{v}}{(t-t_R)(1-v^{2})^{2}}\right\} \\ &=\tfrac{2}{3}Q^{2}\left\{\frac{\gamma^{2}(t_2)}{(t-t_2)}\vec{v}(t_2)-\frac{\gamma^{2}(t_1)}{(t-t_1)}\vec{v}(t_1)\right\}. \end{aligned}\right\} \tag{50a}$$

$$\frac{1}{4\pi}\int_{\Xi}[\vec{E}_{\mathrm{II}}\times\vec{H}_{\mathrm{II}}]\,dV=\tfrac{2}{3}Q^{2}\int_{t_1}^{t_2}dt_R\frac{\vec{g}^{2}-(\vec{g}\times\vec{v})^{2}}{(1-v^{2})^{3}}\vec{v}. \tag{50b}$$

* * *

To derive the equation (50d), notice, that $\vec{E}_R$, $\vec{H}_R$ satisfy the Maxwell equations with the currents $[\vec{j}(\vec{x}),\, i\varrho(\vec{x})]=\delta(\vec{x}-\vec{x}(t))\,[\vec{v},\, i]$, whereas $\vec{E}_{in}$, $\vec{H}_{in}$ satisfy the free Maxwell equations. Thus

$$\begin{aligned} Q\int_{-\infty}^{t}dt[E_{in}(\vec{x}(t))+\vec{v}\times\vec{H}_{in}(\vec{x}(t))] &=\int_{-\infty}^{t}dt\int dV[\vec{E}_{in}(\vec{x})\varrho(\vec{x})+\vec{j}(\vec{x})\times\vec{H}_{in}(\vec{x})] \\ &=\frac{1}{4\pi}\int_{-\infty}^{t}dt\int dV\left[\vec{E}_{in}\,\mathrm{div}\,\vec{E}_R-\vec{H}_{in}\times\mathrm{rot}\,\vec{H}_R+\vec{H}_{in}\times\frac{\partial\vec{E}_R}{\partial t}\right]. \end{aligned}$$

From the identity

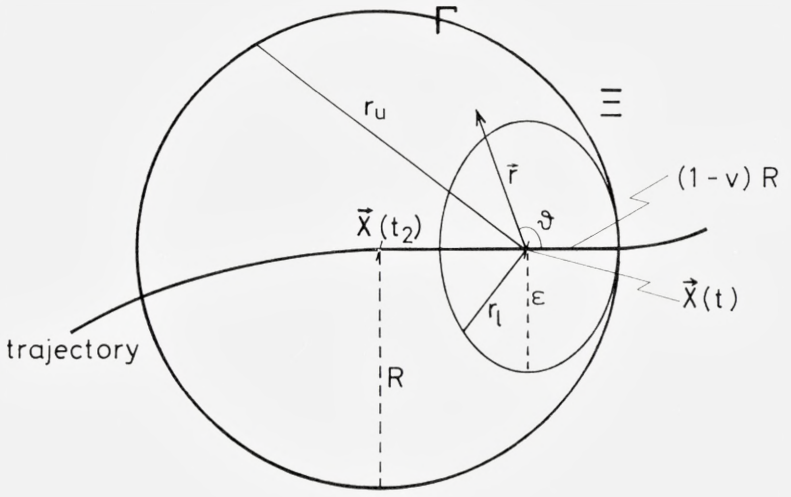


Fig. 5.

$(\vec{A}\ \mathrm{div}\ \vec{B} + \vec{B}\ \mathrm{div}\ \vec{A})_\iota = (\vec{A} \times \mathrm{rot}\ \vec{B} + \vec{B} \times \mathrm{rot}\ \vec{A})_\iota + \partial_\varkappa (A_\iota B_\varkappa + A_\varkappa B_\iota - \delta_{\iota\varkappa} \vec{A} \cdot \vec{B})$

valid for any two vector fields $\vec{A}$ and $\vec{B}$, we find with $\vec{A} = \vec{E}_{in}$ and $\vec{B} = \vec{E}_R$ that

$$\vec{E}_{in}\ \mathrm{div}\ \vec{E}_R = \vec{E}_{in} \times \mathrm{rot}\ \vec{E}_R + \vec{E}_R \times \mathrm{rot}\ \vec{E}_{in} + \text{surface terms.}$$

Similarly the identity reduces for $\vec{A} = \vec{H}_{in}$ and $\vec{B} = \vec{H}_R$ to

$$\vec{0} = \vec{H}_{in} \times \mathrm{rot}\ \vec{H}_R + \vec{H}_R \times \mathrm{rot}\ \vec{H}_{in} + \text{surface terms.}$$

Hence, by combining these results with the Maxwell equations and assuming that the product of $\mathscr{F}_{(in)}$ and $\mathscr{F}_R$ vanishes sufficiently rapidly at spatial infinity, one arrives at the equation (50 d):

$$Q \int_{-\infty}^{t} dt [\vec{E}_{in}(\vec{x}(t)) + \vec{v} \times \vec{H}_{in}(\vec{x}(t))]$$

$$= \frac{1}{4\pi} \int_{-\infty}^{t} dt \int dV \left\{ \vec{E}_{in} \times \mathrm{rot}\ \vec{E}_R + \vec{E}_R \times \mathrm{rot}\ \vec{E}_{in} + \vec{H}_R \times \mathrm{rot}\ \vec{E}_{in} + \vec{H}_{in} \times \frac{\partial \vec{E}_R}{\partial t} \right\}$$

$$= -\frac{1}{4\pi} \int_{-\infty}^{t} dt \int dV \left\{ \vec{E}_{in} \times \frac{\partial \vec{H}_R}{\partial t} + \vec{E}_R \times \frac{\partial \vec{H}_{in}}{\partial t} + \frac{\partial \vec{E}_{in}}{\partial t} \times \vec{H}_R + \frac{\partial \vec{E}_R}{\partial t} \times \vec{H}_{in} \right\}$$

$$= -\frac{1}{4\pi} \int dV \{ \vec{E}_{in} \times \vec{H}_R + \vec{E}_R \times \vec{H}_{in} \}.$$

Similarly, equation (49d) is immediately obtained by integration of the identity

$$\frac{2}{8\pi}\frac{\partial}{\partial t}\{\vec{E}_{in}\cdot\vec{E}_R+\vec{H}_{in}\cdot\vec{H}_R\}=\frac{1}{4\pi}\operatorname{div}(\vec{E}_{in}\times\vec{H}_R+\vec{E}_R\times\vec{H}_{in})-\vec{j}\cdot\vec{E}_{in}.$$

* * *

To evaluate the leading-order term in the energy and momentum associated with the domain $\Gamma$, the Heaviside ellipsoide — with semi-major axis $\varepsilon$ — centred at the instantaneous position $\vec{x}(t)$ of the charge, is enclosed in the smallest possible lightsphere centred at the retarded position $\vec{x}(t_2)$. Since the terms proportional to $Q^2/2\varepsilon$ are independent of the acceleration, the motion may be assumed to be uniform between $t_2$ and $t$. Then, as is evident from the figure, the radius $R=t-t_2$ is related to $\varepsilon$ and $v$ by $R=\varepsilon\dfrac{\sqrt{1-v^2}}{1-v}$. Furthermore the surface of the ellipsoide and the lightsphere is described by the relations

$$\left.\begin{aligned}\frac{1}{r_l}&=\frac{1}{\varepsilon\sqrt{1-v^2}}\sqrt{1-v^2\sin^2\vartheta}\\ \frac{1}{r_u}&=\frac{1}{R(1-v^2)}\left[v\cos\vartheta+\sqrt{1-v^2\sin^2\vartheta}\right],\end{aligned}\right\}$$

where $r_l$ and $r_u$ are defined on figure 5.

Since by assumption the field at time $t$ between the two surfaces in question corresponds to that of a uniformly moving charge, the integral over the appropriate densities are easily evaluated to yield

$$\left.\begin{aligned}\Delta\mathscr{E}_{\Gamma-\Xi}&=\frac{1}{8\pi}\int\limits_{\Gamma-\Xi}dV[\vec{E}^2+\vec{H}^2]_{\text{uniform}}\\ &=\frac{1}{8\pi}\int\limits_{\Gamma-\Xi}dV\frac{Q^2}{r^4}\frac{(1-v^2)^2}{(1-v^2\sin^2\vartheta)^3}(1+v^2\sin^2\vartheta)=\frac{Q^2}{2\varepsilon}\frac{v}{1+v}\left(1+\frac{v^2}{3}\right)\gamma\\ \Delta\vec{\mathscr{P}}_{\Gamma-\Xi}&=\frac{1}{4\pi}\int\limits_{\Gamma-\Xi}dV[\vec{E}\times\vec{H}]_{\text{uniform}}\\ &=\frac{\vec{v}}{4\pi}\int\limits_{\Gamma-\Xi}dV\frac{Q^2}{r^4}\frac{(1-v^2)^2}{(1-v^2\sin^2\vartheta)^3}\sin^2\vartheta=\frac{Q^2}{2\varepsilon}\frac{\frac{4}{3}v}{1+v}\gamma\vec{v}.\end{aligned}\right\}$$

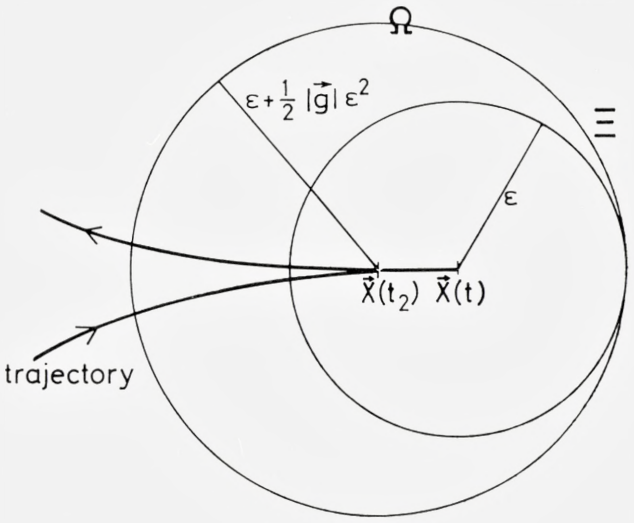


Fig. 6.

Hence, remembering that $t - t_2 = R$, one obtains the eq. (53) by means of the relation:

$$(\vec{\mathscr{P}}_\Gamma(t), \mathscr{E}_\Gamma(t) = (\vec{\mathscr{P}}_\Xi(t)), \vec{\mathscr{E}}_\Xi(t)) + (\Delta\vec{\mathscr{P}}_{\Gamma-\Xi}, \Delta\mathscr{E}_{\Gamma-\Xi}),$$

where $(\vec{\mathscr{P}}_\Xi(t), \mathscr{E}_\Xi(t))$ is given by eq. (51).

* * *

Finally, to evaluate the energy and momentum associated with the volume $\Omega$, the sphere of radius $\varepsilon$ centred at the instantaneous position $\vec{x}(t)$ is enclosed in the smallest possible lightsphere (i.e. of radius $t - t_2 \sim \varepsilon + \frac{1}{2}|\vec{g}|\varepsilon^2$, remembering $\vec{v}(t) = 0$) centred at the retarded position $\vec{x}(t_2)$ (see figure 6).

Since $|\vec{x}(t_2) - \vec{x}(t)| \sim \frac{1}{2}|\vec{g}|\varepsilon^2$, the volume $\Omega - \Xi$ between the two spheres is of the order of magnitude $|\vec{g}|\varepsilon^4$, and hence there is a finite amount of energy, $\Delta\mathscr{E}_{\Omega-\Xi}$, associated with this volume even in the limit of vanishing $\varepsilon$. To the appropriate accuracy it is evident that (cf. the footnote on page 39)

$$\Delta\mathscr{E}_{\Omega-\Xi} = \frac{1}{8\pi}\int_{\Omega-\Xi}\frac{Q^2}{r^4}\,dV = \frac{Q^2}{\varepsilon^4}\int\frac{d\Omega}{8\pi}\varepsilon^2\tfrac{1}{2}|\vec{g}|\varepsilon^2(1-\cos\vartheta) = \frac{Q^2}{4}|\vec{g}|.$$

Whence, inserting $t - t_2 = \varepsilon + \frac{1}{2}|\vec{g}|\varepsilon^2$ into the expression for $\mathscr{E}_\Xi$ as given by eq. (51), one obtains the first of the eqs. (52): $\mathring{\mathscr{E}}_\Omega = \mathscr{E}_\Xi + \Delta\mathscr{E}_{\Omega-\Xi}$. Since

the momentum density associated with the volume in question is of order $Q^2|\vec{g}|/\varepsilon^3$, the corresponding momentum vanishes with $\varepsilon$. Thus the value of $\overset{\circ}{\vec{\mathscr{P}}}_{\Omega}$ may be immediately obtained by substituting $\vec{v}(t_2) \sim -\vec{g}(t)(t-t_2)$ into the expression (51) for $\vec{\mathscr{P}}_{\Xi}(t)$.

## References


1) P. A. M. Dirac: Classical Theory of Radiating Electrons, Proc. Roy. Soc. (London) **A 167**, 148 (1938).
R. Haag: Die Selbstwechselwirkung des Elektrons, Z. Naturforschg. **10**a, 752, 1955.
2) R. P. Feynman and J. A. Wheeler: Interaction with the Absorber as the Mechanism of Radiation, Rev. Mod. Phys. **17**, 157 (1945).
Classical Electrodynamics in Terms of Direct Interparticle Action, Rev. Mod. Phys. **21**, 425 (1949).
3) F. Rohrlich: The Definition of Electromagnetic Radiation, Il Nuovo Cimento **XXI,** 811 (1961).
Classical Charged Particles (Addison-Wesley, Reading, Mass. 1965).
4) J. Kalckar and O. Ulfbeck: On the Problem of Gravitational Radiation, Mat. Fys. Medd. Dan. Vid. Selsk. **39** no. 6 (1974).
5) C. Møller: The Theory of Relativity, 2 ed. p. 458, (Clarendon Press, Oxford 1972).
6) C. Teitelboim: Splitting of the Maxwell Tensor: Radiation Reaction without Advanced Fields.
Phys. Rev. **D 1**, 1572 (1970).
Erratum, Phys. Rev. **D 2**, 1763 (1970).
Splitting of the Maxwell Tensor II. Sources, Phys. Rev. **D 3**, 297 (1971).
Radiation Reaction as a Retarded Self-Interaction, Phys. Rev. **D 4**, 345 (1971).


Indleveret til Selskabet den 14. april 1975.
Færdig fra trykkeriet den 30. april 1976.

J. U. ANDERSEN, S. KJÆR ANDERSEN
AND W. M. AUGUSTYNIAK

# CHANNELING OF ELECTRONS AND POSITRONS

## Correspondence between Classical and Quantal Descriptions

Det Kongelige Danske Videnskabernes Selskab
Matematisk-fysiske Meddelelser **39**, 10


Kommissionær: Munksgaard
København 1977

## Synopsis

Channeling of 700-keV electrons in silicon has been investigated by measurements of the large-angle scattering yield from thin single crystals as a function of incidence direction. The peaks in yield for incidence parallel to low-index planes and axes are compared mainly to calculations based upon the dynamical theory of electron diffraction. This description is reviewed in a formulation emphasizing similarity to the classical theory of channeling. The relationship between the two descriptions is discussed, and correspondence in the limit of large quantum numbers is illustrated, partly by the example of a harmonic oscillator, partly by analytical results for a simple model, derived within the WKB approximation. Estimates of the magnitude of the quantum numbers associated with the transverse motion of channeled particles are derived semiclassically from the available phase space for bound states in the transverse continuum potential, and the importance of distinguishing between axes and planes and between positive and negative particles, is pointed out. These qualitative considerations are supplemented with results of numerical calculations, based upon the classical channeling theory and the dynamical theory of electron diffraction, respectively. This comparison illustrates the transition to the classical limit for increasing projectile mass and provides a quantitative test of the correspondence criteria based on semiclassical estimates.



Printed in Denmark by Bianco Lunos Bogtrykkeri A/S. ISBN 87-7304-084-3

## List of Contents

## Introduction

This study of electron and positron channeling may be seen as part of a general investigation of the channeling of light particles which, during the last decade, has been performed partly at the University of Aarhus, partly at Bell Telephone Laboratories. Motivated by the strong channeling effects found for heavy particles (protons, $\alpha$ particles, etc.)[1,2], attemps were made to look for similar phenomena for electrons penetrating single crystals[3]. The basic features of the channeling effect for both positrons and electrons were first established by Uggerhøj in a beautiful experiment[4], where the angular distribution of electrons and positrons, emitted by $^{64}$Cu embedded in a copper single crystal, were studied simultaneously. The observation of an axial dip in yield for positrons, and a peak for electrons, was in qualitative agreement with expectations based upon the theory[5] of heavy-particle channeling. The measurement was continued in order to obtain more quantitative data, and the results were found to be in fair agreement with estimates based upon classical mechanics[6].

A basic difficulty in such emission experiments is the damage due to implantation of the radioactive atoms. To avoid this problem, experiments with external beams of electrons and positrons were initiated. A measurement of the large-angle scattering yield as a function of direction for an external beam is, in principle, equivalent to a determination of the angular distribution of particles emitted from lattice sites (reversibility[5] or reciprocity[7]).

Positron channeling in gold[8] and silicon[9] was studied with an external beam. The general result was that positron channeling is adequately described by the channeling theory based upon classical mechanics, although for planar channeling some fine structure due to Bragg interference was observed.

For electrons the situation is somewhat different[10]. Owing to their negative charge, electrons penetrate readily to the atomic scattering centers in the

rows and planes. Incoherent multiple scattering will therefore be stronger than for positive particles. Furthermore, it may be seen from semiclassical phase-space estimates that the number of bound states in the transverse potential is quite large in most cases for channeled positrons, while for electrons it is considerably larger than unity only at relativistic energies.

The possibility of electron motion in bound states along rows of atoms, describable to some extent by classical mechanics, was first studied theoretically by LINDHARD[11]. In an experimental study of electron channeling in gold by UGGERHØJ et al.[12], the interest was focussed on classical aspects of axial channeling and on predictions from the classical treatment. Later the measurements have been extended[13] to higher energies and to include also planar effects and a detailed comparison to many-beam calculations. Parallel to these investigations, the measurements to be reported here of the channeling of 700-keV electrons in silicon were undertaken. Results on axial channeling were included in the discussion by UGGERHØJ et al.[12,13].

Electron channeling was approached independently on the basis of the well-established theory for the phenomena observed in electron microscopy[14]. Angular variations of the electron-backscattering yield for incidence close to a planar direction were predicted by HIRSCH et al.[15] and found experimentally by DUNCOMB[16]. In the study by HALL[17] of the effect of lattice structure on the yield of characteristic x rays, the main emphasis was on a detailed description of the thickness dependence due to inelastic scattering. Later HOWIE et al.[18] studied the emission of electrons from neutron-activated thin crystals and compared to both classical calculations and calculations based upon diffraction theory. It is a common feature of these experiments that only planar channeling has been investigated. From the point of view of diffraction theory, an axis is basically an intersection of a set of planes, and nothing much but unnecessary complications is gained by studying channeling close to an axial direction[19]. In LINDHARD's theoretical work on channeling, however, the axial case is qualitatively different from the planar case. For heavy positive particles, axial effects are stronger than planar effects and therefore, from most points of view, more interesting. Also, for electrons and positrons, the quantum numbers associated with axial effects are larger than for planar effects, and classical concepts may therefore more readily be applied to the axial case.

The attempts[4,6] mentioned earlier to relate the channeling phenomena for electrons and positrons to classical channeling theory for heavy particles were met with strong criticism. The possibility of understanding electron and positron channeling on the basis of electron-diffraction theory was first

pointed out by HOWIE[20] and later argued strongly by DE WAMES et al. in a series of publications[21]. The resulting, at times rather heated, discussion greatly stimulated the interest in channeling of light particles and, more specifically, in the problem of correspondence between classical and quantal calculations related to channeling [22–25]. For fairly recent reviews of the field, and discussions of correspondence from different points of view, we may refer to Refs. 26–28.

Correspondence between classical and quantal treatment of channeling phenomena is the main theme of the present study. It is composed of four parts. The first is a report on an experimental investigation of electron channeling in silicon, performed at Bell Telephone Laboratories in 1968. The main emphasis is on measurements of axial and planar peaks in yield of large-angle scattering. While electron microscopy is based on wave interference observed in transmission, the most interesting and useful phenomenon associated with classical channeling is the strong angular dependence of the yield of processes which require a close encounter between projectiles and target atoms.

The experimental results are compared mainly to calculations based upon the dynamical theory of electron diffraction. This theoretical description is in the second part reviewed briefly in a formulation which emphasizes similarity to the classical description of channeling. Problems related to incoherent scattering are discussed qualitatively, and examples are given of the treatment in terms of an imaginary potential and scattering into plane-wave states.

Correspondence with the classical treatment is discussed in the third part and illustrated partly by an analysis of the example of a harmonic oscillator, partly by some simple calculations based upon the WKB approximation. This general analysis is followed in the fourth part by a derivation from semiclassical phase-space arguments of estimates of the number of bound states in the transverse motion of channeled particles, leading to simple criteria for the applicability of a classical description. Differences between positive and negative particles, and also between the axial and planar cases, are discussed on the basis of two examples. The transition to the classical limit is then investigated quantitatively by a comparison of classical and quantal calculations for different electron and positron energies. At high energy, where the number of bound states becomes large owing to the increase in relativistic projectile mass, the quantal results approach the classical predictions. These are for the planar case obtained from the formalism developed for heavy positive particles[29]. For negative particles,

the axial case presents special problems, in particular concerning the applicability of results obtained from the assumption of statistical equilibrium in the transverse motion. These problems are discussed in the appendix, which contains the derivation of a classical estimate of the axial peak in yield for negative particles, based on statistical equilibrium.

## I. Experimental Study of Electron Channeling in Silicon

### *I.1. Experimental procedure*

*Setup.* A sketch of the experimental arrangement is shown in Fig. I.1. The electron beam, with an initial energy of 800 keV, is scattered by a 30-$\mu$m gold foil. The current of electrons transmitted through the foil into the Faraday cup is used to monitor the beam intensity. The electrons scattered by 90° lose on the average ~ 100 keV in the gold foil, leading to a final beam energy of ~ 700 keV, with a measured spread of 85-keV FWHM. The angular spread of 0.05° full width is defined by a 1-mm collimator placed immediately in front of the gold foil and a 0.4-mm collimator at the entrance to the scattering chamber.

The beam is incident on a thin silicon crystal, mounted in a goniometer with two perpendicular rotations. The scattering chamber contains three different detection systems:

(i) Annular detector for electrons scattered through ~ 10–20° by the crystal.
(ii) Movable detector ('forward detector') to scan the intensity distribution in the forward direction. Both detectors are silicon surface-barrier detectors.
(iii) Film to record photographically the angular intensity distribution in the forward direction.

*Crystals.* The thin crystals were prepared by etching 0.15-mm thick silicon wafers, cut perpendicular to a ⟨110⟩ direction. A thicker ring was left at the edge for support. The crystals were mounted by sandwiching them between aluminum and lucite plates with a 5-mm hole in the center. Mounting the thinner crystals was a delicate operation, after which a careful examination for wrinkles was necessary.

Results for two thicknesses are reported. From an $\alpha$-particle, energy loss measurement, the thicker crystal was estimated to be 2.8 $\mu$m thick. Unfortunately the thinner crystal was broken before a similar meassurement

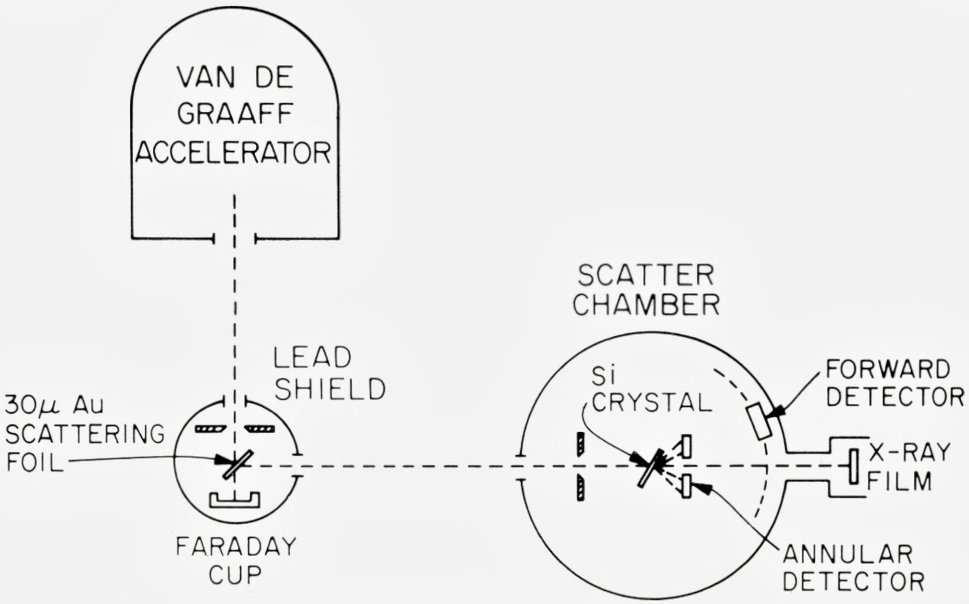


Fig. I.1: Experimental arrangement.

could be made, but from the relative electron-scattering yield, its thickness was estimated to be 0.2–0.3 $\mu$m.

*Measuring procedure.* The orientation of the crystal was determined by the standard technique known from proton channeling[30]. The planes were identified by an increase in yield of the scattering into the annular detector. A stereogram was constructed, and thus the rotation parameters corresponding to various planar and axial directions could be determined.

Angular scans through major planes and axes were performed by measuring the yield of scattering into the annular detector for a fixed accumulated charge in the Faraday cup. In preliminary experiments, the "forward detector" was used, positioned at some large angle to the beam direction. Strong asymmetries of the peaks in yield were observed, however, and these asymmetries turned out to be dependent on the position of the detector. Such effects are known also for proton channeling and are usually ascribed to "blocking" of the scattered particles. In this case, however, the solid angle subtended by the detector was very large compared to the widths of the channeling peaks. Also asymmetries were seen, depending only on the detector being 'to the left' or 'to the right' of the beam direction. Rather than investigate these phenomena in detail, it was decided to use an annular

counter which is axially symmetric and averages over a very large solid angle.

The forward detector was then used to scan angular distribution of the beam after its passage through the crystal. Because of the small distance from the crystal, the angular resolution was not very good. A better resolution was obtained in the photographic exposures.

*I.2. Results*

Results from measurements on two samples of thickness 0.2–0.3 $\mu$m and 2.8 $\mu$m, respectively, are reported. The thickness may be compared to the mean-free path for scattering, defined as $l = (N\sigma)^{-1}$, where $\sigma$ is the total atomic scattering cross section and N the density of atoms, $N = 5 \times 10^{22}$ cm$^{-3}$ for Si. A simple estimate of $\sigma$ is obtained in the Born approximation for an exponentially screened Coulomb potential,

$$\sigma = \pi a^2 \varkappa^2, \tag{I.1}$$

where a is the screening parameter and $\varkappa$ is defined as

$$\varkappa = \frac{2|Z_1|Z_2 e^2}{\hbar v}. \tag{I,2}$$

Here, $Z_1 e$ and $Z_2 e$ are the charges of the particle and the scattering nucleus, and $v$ is the particle velocity. While for $\varkappa > 1$, the collision may be described by classical mechanics[31], the Born approximation is valid in the limit of $\varkappa < 1$. In the present case, we have $\varkappa^2 \simeq 0.05$. For the screening parameter $a$, we way may insert the Thomas-Fermi screening radius, $a = 0.8853\, Z_2^{-1/3}\, a_0$, where $a_0$ is the Bohr radius, $a_0 = 0.53$ Å. This leads to a cross section of $\sigma \simeq 5 \times 10^{-3}$ Å$^2$ and a mean-free path for scattering, $l \simeq 4000$ Å. More accurate calculations indicate that such a simple estimate is probably not far off[32]. According to Eq. (I,1), $l$ depends on $Z_2$ approximately as $l \propto Z_2^{-4/3}$ for fixed electron energy. The scattering length in gold will then be roughly ten times shorter, in good agreement with the measured value of $l \simeq 400$ Å for 1-MeV electrons[12].

Thus the thickness of the thinner sample is comparable to the scattering length, whereas the thickness of the thicker sample corresponds to about $7l$. The angular distributions of the transmitted electrons were in qualitative agreement with these estimates. For the thinner sample, the distribution consisted of an unscattered, central peak with tails due to single (or plural) scattering, whereas for the thicker sample, no central peak was observed.

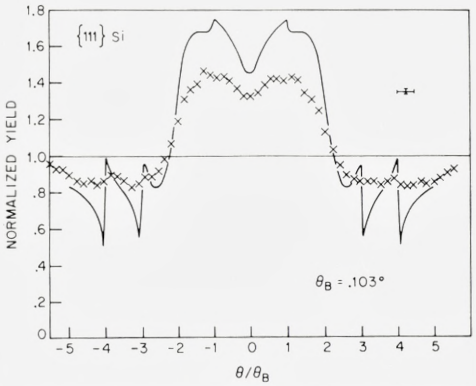


Fig. I.2: Scan through {111} plane for the 0.2–0.3-$\mu$m sample. The crosses are experimental points, and the fully drawn curve is the result of a nine-beam calculation for a static lattice. Bragg reflections of order up to ± 4 are included (9 beams).

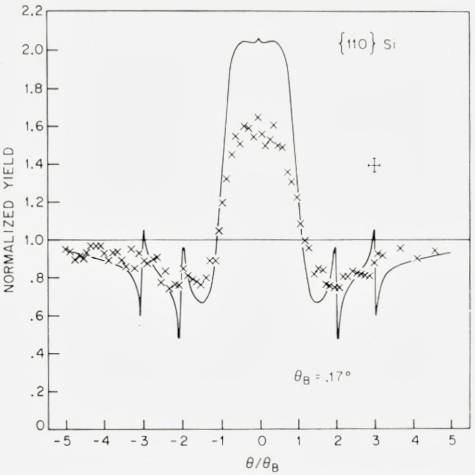


Fig. I.3: Scan through {110} plane for the 0.2–0.3-$\mu$m sample. This calculation includes reflections of order up to ± 3 (7 beams). The error flag on the upper right-hand side indicates beam divergence and statistical uncertainty of the measurements.

As mentioned above, the angular resolution in scans with the forward detector was too poor for quantitative measurements. More direct information on the scattering and its variation with incidence direction is obtained from the yield of large-angle scattering into the annular detector.

*0.2–0.3 $\mu$m crystal.* Scans through the three major planes, {111}, {110}, and {100} are shown in Figs. I.2–I.4. The measured yields are normalized to the yield in a "random" (nonsymmetry) direction. The angle with the plane is given in units of the Bragg angle, $\theta_B = \lambda/(2d_p)$, where $\lambda$ is the electron wavelength and $d_p$ the planar spacing. We shall discuss the calculations in more detail in the following chapter. Inelastic scattering is not included, and thus the discrepancy in peak height, due to attenuation with depth, is to be expected. If, for simplicity, exponential damping with depth is assumed, the measurements indicate that the length corresponding to a reduction by $1/e$ is approximately equal to the crystal thickness (cf. also Sec. II.7).

The general peak shapes are rather well reproduced by the calculations. For the {110} and {100} planes, the width is twice the Bragg angle, whereas for the strongest plane, the {111}, the width is 4 to 5 times $\theta_B$. The peculiar shape of the {111} peak is due to the diamond structure of silicon. Each {111} atomic plane is split into two planes with a separation of $d_p/4$. The

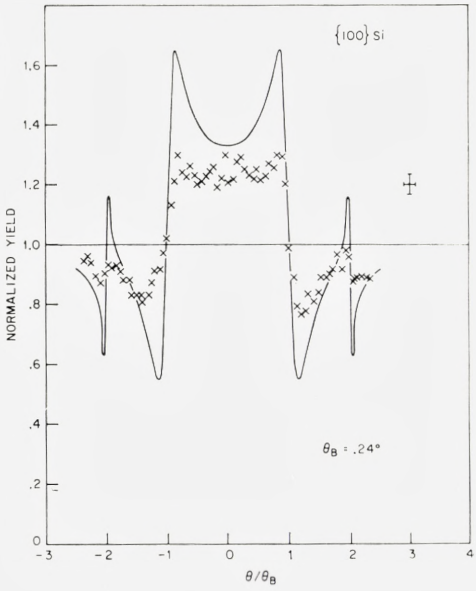


Fig. I.4: Scan through {100} plane for the 0.2–0.3-$\mu$m sample compared with five-beam calculation. The error flag on the upper right-hand side indicates beam divergence and statistical uncertainty of the measurements.

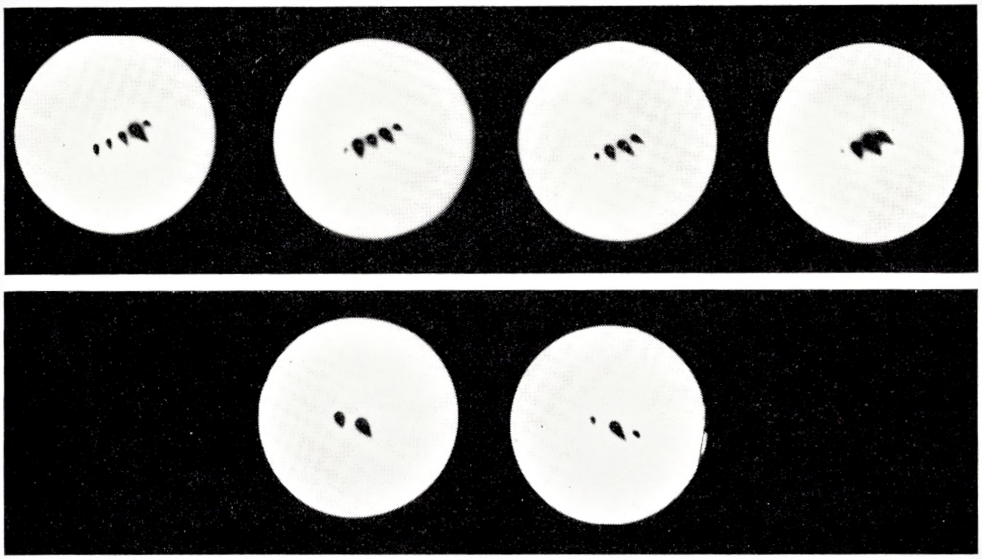

Fig. I.5: Film exposures of the forward beam for the 0.2–0.3 $\mu$m sample. The upper series of four exposures corresponds to the incidence angles of $3\theta_B$, $2\theta_B$, and $\theta_B$, and 0 with respect to a {111} plane. The lower two exposures correspond to incidence angles of $\theta_B$ and 0 with respect to a {110} plane.

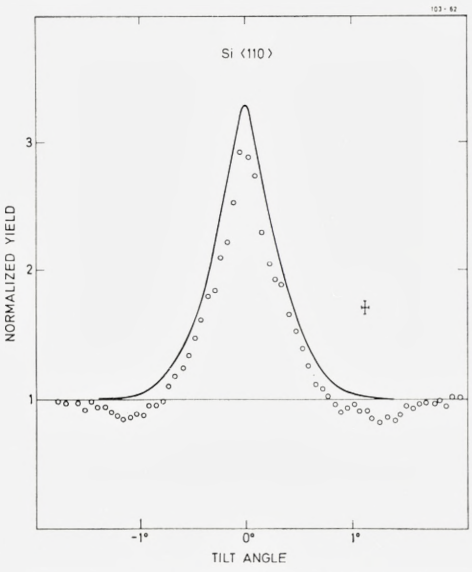


Fig. I.6: Scan through the ⟨110⟩ axis for the 0.2–0.3-$\mu$m sample. The experimental results are compared to the classical formula derived in the Appendix. The calculated excess yield has been multiplied by 0.5 to account approximately for inelastic scattering. The error flag on the upper right-hand side indicates beam divergence and statistical uncertainty of the measurements.

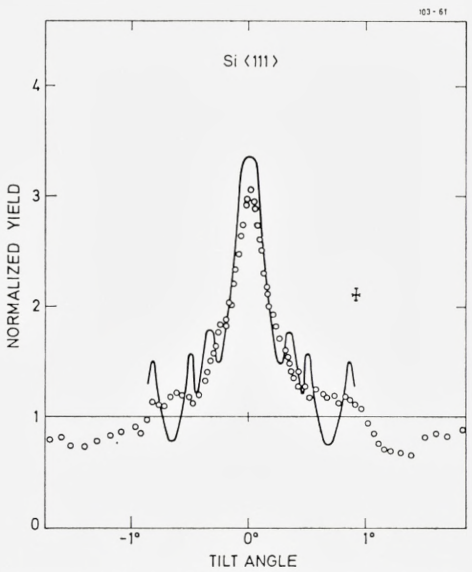


Fig. I.7: Scan through a ⟨111⟩ axis for the 0.2–0.3-$\mu$m sample. The experimental results are compared to the peak in yield obtained from a 49-beam calculation. Effects of thermal vibrations are included, but inelastic scattering is not. Instead, the calculated increase in yield has been multiplied by 0.5 as in the previous figure (cf. also Fig. II.4).

{110} and {100} planes are regularly spaced. Finally, we note that the beam collimation was not sufficient to resolve the "wiggles" at high-order Bragg-reflection positions. There are, however, slight indications of these wiggles, especially in the {100} scan.

For selected directions of indicence, photographic exposures of the transmitted beam were taken. Two series of exposures are shown in Fig. I.5. The upper four exposures correspond to beam incidence at angles $3\theta_B$, $2\theta_B$, $\theta_B$, and 0 (left to right) relative to a {111} plane. In this case, the Bragg angle is $\theta_B \simeq 0.1°$, and the distance between the spots is $2\theta_B \simeq 0.2°$. The spot corresponding to the incidence direction is the most intense one (second from the right). Below are two exposures for beam incidence at an angle of $\theta_B \simeq 0.17°$ and parallel to a {110} plane, respectively. All spots in the figure

have a pronounced tail. This corresponds to a low-energy tail of the beam-energy distribution since electrons of lower energies are deflected slightly more by the earth magnetic field.

Scans through the ⟨110⟩ and ⟨111⟩ axes are shown in Figs. I.6 and I.7. The peaks are much stronger than the planar ones, rising by about a factor of three over normal yield. The ⟨110⟩ peak is compared to the classical prediction derived in the Appendix. The theoretical curve is multiplied by a factor of 0.5. The width and shape of the peak are then quite well reproduced. Since the attenuation with depth is expected to be stronger than for planes, also the absolute agreement is reasonable.

The peak along the weaker ⟨111⟩ axis is compared to a many-beam calculation, multiplied also by a factor of 0.5, to correct roughly for inelastic scattering (cf. Sec. II.7). The widths are in good agreement and significantly narrower than predicted by a classical estimate. This qualitative difference between the two axes is also apparent in the diffraction patterns discussed below.

Film exposures of the transmitted beam for incidence close to an axis are shown in Fig. I.8. The exposures in the upper series are taken at tilts of 0.6°, 0.4°, 0.2°, and 0° from the ⟨111⟩ direction. The series below corresponds to incidence angles of 0.75°, 0.50°, 0.25°, and 0° relative to a ⟨110⟩ direction (from left to right). The strongest spot, corresponding to the incidence direction, is fairly easy to identify in the upper series. In the lower series, the spots are very poorly resolved, but it is evident that quite a large number of reflections are excited. Especially at the larger tilt angles to the ⟨110⟩ axis, the scattering is clearly seen to be confined to a ring around the axis, corresponding to conservation of transverse energy[5]. In the terminology of the theory of electron diffraction, the observed pattern is denoted the zero-order Laue zone and corresponds to the intersection of the Ewald sphere with a plane in the reciprocal lattice[14].

2.8-$\mu m$ *crystal.* Angular scans through the three major planes, {111}, {110}, and {100}, are shown in Figs. I.9–I.11. The peaks are much smaller than those for the thinner crystal, indicating a strong depth dependence. Once again, we may estimate the thickness corresponding to a reduction by $1/e$, assuming exponential attenuation. In this case it turns out to be $\sim 0.4\ \mu$m, in reasonable agreement with the estimate based on the thin-crystal result. The assumption of exponential damping is obviously very crude. The peak shapes are now quite different. The dips are relatively more pronounced, and the widths are narrower, especially for the {111} plane. (cf. the discussion in Sec. II.7).

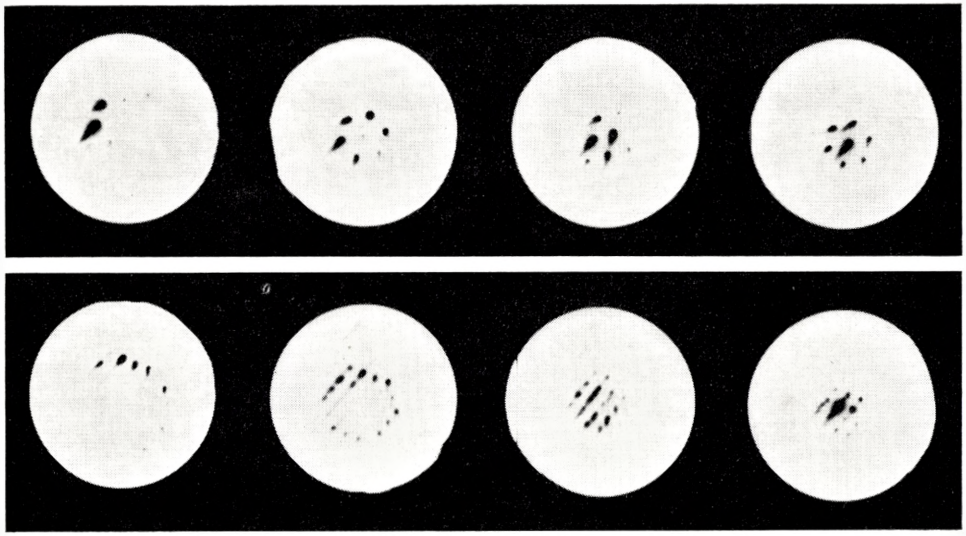

Fig. I.8: Film exposures of the forward beam for the 0.2–0.3 $\mu$m sample. The upper series corresponds to incidence angles of 0.6°, 0.4°, 0.2°, and 0°, relative to a $\langle 111 \rangle$ axis, the lower series to incidence angles of 0.75°, 0.50°, 0,25°, and 0°, relative to a $\langle 110 \rangle$ axis.

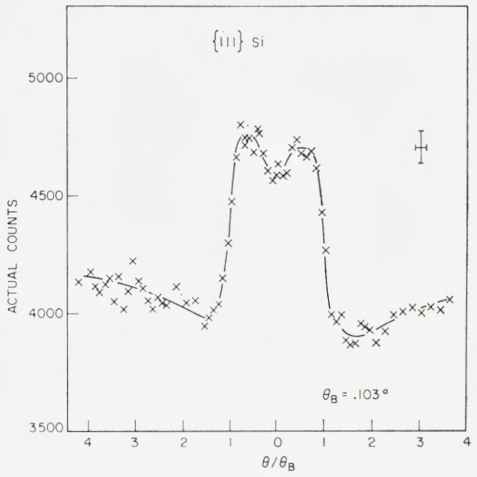


Fig. I.9: Scan through {111} plane for the 2.8-$\mu$m sample. The error flag on the upper right-hand side indicates beam divergence and statistical uncertainty of the measurements.

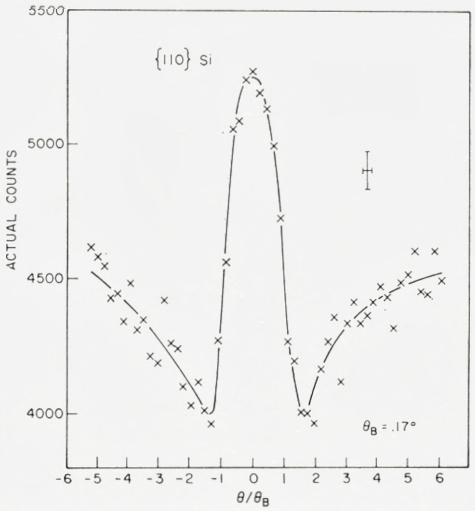


Fig. I.10: Scan through {110} plane for the 2.8-$\mu$m sample. The error flag on the upper right-hand side indicates beam divergence and statistical uncertainty of the measurements.

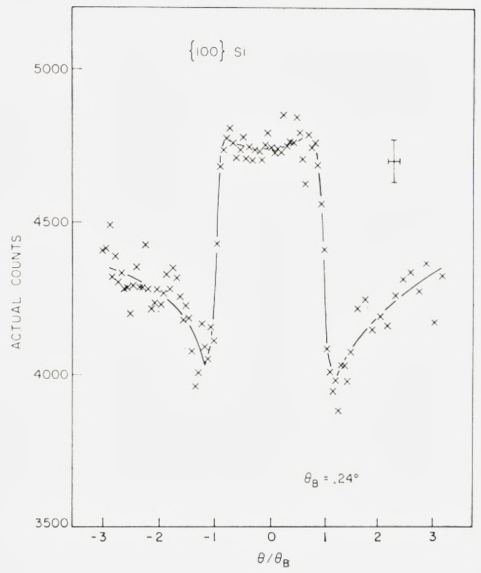


Fig. I.11: Scan through {100} plane for the 2.8-$\mu$m sample. The error flag on the upper right-hand side indicates beam divergence and statistical uncertainty of the measurements.

Scans through the ⟨111⟩ and ⟨110⟩ axes are shown in Figs. I.12 and I.13. The peak heights are strongly reduced, and a lot of fine structure has developed. An angular width is difficult to define, but it is obvious that the peaks are much broader than for the thinner crystal. No attempt has been made to check the suggested conservation of the peak volume[11,12]. To calculate this, it would have been necessary to assume azimuthal symmetry of the peak which, for the present measurements, would have been altogether too bold. The decrease in peak height is certainly to some extent counteracted by a broadening of the peak. This is qualitatively different from the planar case, which can be related to the fact that at least from classical estimates, the compensation of the peak for planes is concentrated in a narrow, negative shoulder, whereas for an axis the compensation is shallow and stretches out to angles of order $2a/d$. In the present cases, $2a/d \simeq 4°$.

Film exposures of the transmitted beam are shown in Fig. I.14 for incidence parallel to the two axes ⟨111⟩ and ⟨110⟩ and the three planes {100}, {110}, and {111}. The quality of the pictures is very poor compared to the beautiful Kikuchi patterns obtainable in electron microscopy, where a wealth of lines are resolved[33]. It does, however, suffice to demonstrate two qualitative features: (i) In contrast to Fig. I.5, the angular distribution of the electrons after their passage through a 2.8-$\mu$m crystal is determined by multiple (inelastic) scattering. (ii) In analogy to the star patterns observed for

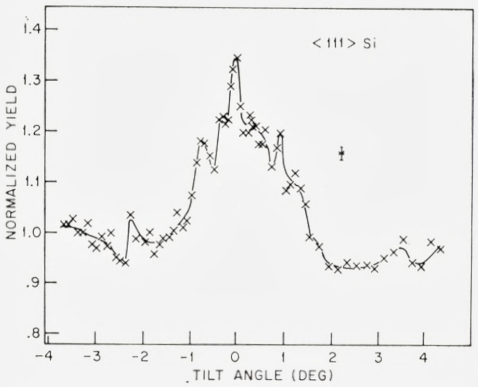


Fig. I.12: Scan through ⟨111⟩ axis for the 2.8-$\mu$m sample. The error flag on the upper right-hand side indicates beam divergence and statistical uncertainty of the measurements.

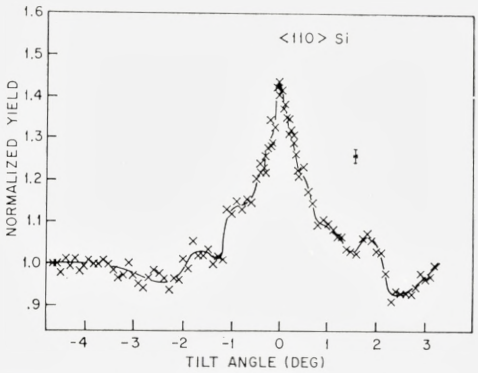


Fig. I.13: Scan through ⟨110⟩ axis for the 2.8-$\mu$m sample. The error flag on the upper right-hand side indicates beam divergence and statistical uncertainty of the measurements.

protons transmitted through thin single crystals[27], there are minima in the intensity at angles associated with a high large-angle scattering yield and, conversely, there are maxima at angles associated with a low yield.

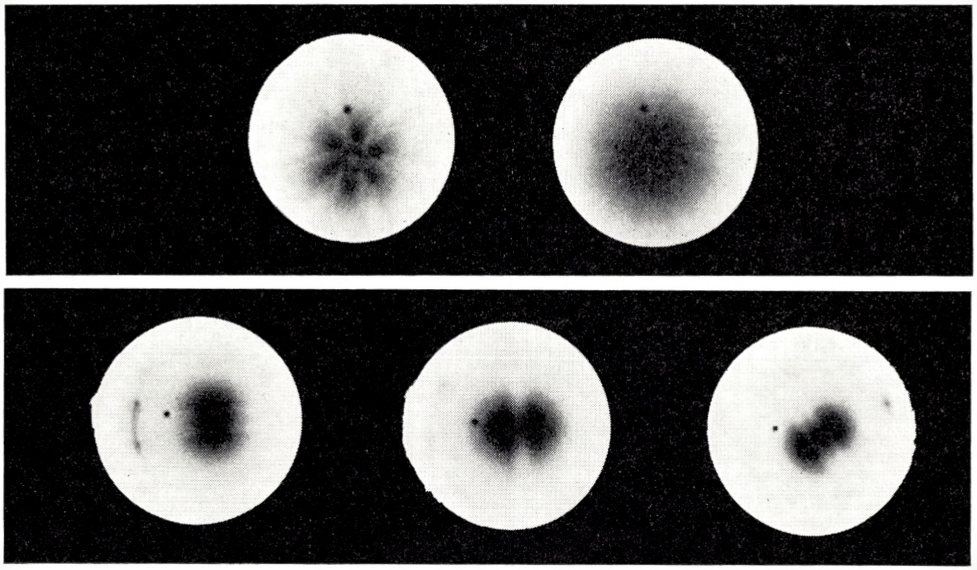

Fig. I.14: Film exposures of the beam transmitted through the 2.8 $\mu$m crystal. The upper two exposures correspond to beam incidence parallel to a ⟨111⟩ axis and a ⟨110⟩ axis. The lower three exposures correspond to incidence along {100}, {110}, and {111} planes. The small intense spot visible in all exposure is due to x rays produced in the gold scattering foil.

## II. Wave-Mechanical Description

The calculations leading to the theoretical curves in some of the preceding figures (I.2–I.4 and I.7) are based upon the dynamical theory of electron diffraction[14]. Similar calculation have been published by several authors[13, 18–21]. A brief description was also given in connection with the measurements on positron channeling[8, 9]. The following presentation is intended to serve as a basis for the discussion of correspondence in the following chapter and therefore emphasizes the analogy with the classical description of directional effects[5] and uses the notation belonging to that description. This is in accordance with the quantal treatment by LERVIG et al.[10], and we shall at first follow their development and discuss the derivation of the two-dimensional wave equation from the three-dimensional Klein-Gordon equation. In this context, the 'many-beam' formulation of the dynamical theory of electron diffraction then appears as an approximation procedure for solving by Fourier expansion the equation of motion in the continuum approximation.

### *II.1. Basic wave equation*

First, we derive the basic wave equation for the transverse motion, following the procedure of LERVIG et al. Suppose the interaction between particle and lattice can be described by a potential,

$$V(\bar{R}) = V(z, \bar{r}) = \sum_i V_a(\bar{R} - \bar{R}_i), \tag{II.1}$$

where $\bar{R} = (x, y, z)$ is the position of the particle and $\bar{r} = (x, y)$, while the $\bar{R}_i$'s are atomic positions and $V_a$ the atomic potential. The $z$ axis is parallel to an axis or plane, and the particle is assumed to move nearly parallel to it. Since we are concerned with particles at relativistic velocities, we base the discussion on the Klein-Gordon equation for a particle of total energy $E$ and rest mass $M_0$,

$$\{(\hbar c)^2 \Delta_{\bar{R}} + [(E - V(z,\bar{r}))^2 - M_0^2 c^4]\}\psi(\bar{R}) = 0. \tag{II.2}$$

By describing the interaction with the crystal by a potential (Eq. (II.1)) and disregarding the degrees of freedom belonging to atoms, we have at first neglected inelastic scattering by electrons and phonons, which leads to incoherence of the particle wave function. Furthermore, when the description is based upon the Klein-Gordon equation rather than the Dirac equation, spin-dependent terms in the Hamiltonian are neglected.

The incident particle may be represented by a plane wave,

$$\psi_0(\bar{R}) = e^{i\bar{k}\cdot\bar{R}}, \quad E^2 = (\hbar c)^2 k^2 + M_0^2 c^4. \tag{II.3}$$

Since the scattering at high particle energies is strongly forward-peaked, the interaction with the lattice only leads to transfer of rather small momenta in the $x$ and $y$ directions, the momentum in the $z$ dirsction being approximately conserved. The motion may therefore be separated into a transverse motion in the $x$–$y$ plane and a longitudinal motion in the $z$ direction with constant velocity $v_z \simeq v = \hbar k/M$, where $M$ is the relativistic mass, $M = E/c^2$. For the transverse motion it is then natural to introduce time, $t = z/v$, as a parameter. The wave function is written as

$$\psi(\bar{R}) = e^{ikz} \cdot u(z,\bar{r}). \tag{II.4}$$

When this is inserted into Eq. (II.2) and we neglect a term $V^2$ compared to $2EV$ and $\partial^2/\partial z^2$ compared to $2k\partial/\partial z$, corresponding to scattering by small angles only, an equation of a type of a time-dependent, non-relativistic Schrödinger equation for the transverse motion is obtained,

$$\left.\begin{aligned} i\hbar \frac{\partial}{\partial t} u(t,\bar{r}) &= Hu(t,\bar{r}) \\ H &= -\frac{\hbar^2}{2M}\Delta_{\bar{r}} + V(t,\bar{r}). \end{aligned}\right\} \tag{II.5}$$

For a discussion of the corrections to the approximations leading to Eq. (II.5), the reader is referred to Lervig et al.[10].

*II.2. Continuum approximation*

Let the crystal surface correspond to $z = vt = 0$. For $t < 0$, the potential is zero, and according to Eqs. (II.3) and (II.4), the transverse wave function is then

$$\left.\begin{aligned} u(t,\bar{r}) &= \exp\{i\bar{k}\cdot\bar{R} - ikz\} \simeq \exp\{i\bar{k}_\perp\cdot\bar{r} - iE_\perp t/\hbar\} \\ E_\perp &= \frac{\hbar^2 k_\perp^2}{2M} \simeq E - [(\hbar c)^2 k_z^2 + M_0^2 c^4]^{1/2} \\ \bar{k} &= (\bar{k}_\perp, k_z) = (k_x, k_y, k_z). \end{aligned}\right\} \quad \text{(II.6)}$$

At time $t = 0$, the potential changes suddenly. In the axial case, it is for $t > 0$ a periodic function of $t$, with period $\tau = d/v$, where $d$ is the spacing of atoms in the strings. In the continuum approximation, this time-dependent potential is replaced by its time average,

$$V(\bar{r}) = \frac{1}{\tau}\int_t^{t+\tau} V(t,\bar{r})\,dt, \quad t > 0. \qquad \text{(II.7A)}$$

The question of the validity of this approximation was studied in detail by Lervig et al. Also in the classical treatment of directional effects, this question is crucial. For the axial case, the accuracy of the continuum description may be assessed by the more accurate halfway-plane treatment[5, 10]. It turns out that the continuum picture is obtained in the limit of high particle velocities where the time interval $\tau$ between collisions becomes short.

In the planar case, the continuum approximation is obtained by averaging the potential along both the $z$ axis ('time average') and the transverse coordinate $y$ parallel to the plane,

$$V(x) = \frac{1}{A}\int_A dy\,d(vt)\,V(t,\bar{r}). \qquad \text{(II.7B)}$$

The accuracy of this approximation has not been studied by a systematic approximation procedure like the halfway-plane treatment of the axial case. In the classical description[5], the continuum approximation was seen to break down at distances from a plane of order a, the Thomas-Fermi screening distance, even for very large particle velocities.

In the dynamical theory of electron diffraction, the continuum approximation corresponds to a Fourier expansion of the lattice potential in one or two dimensions, for the planar and axial case, respectively. It is argued[14] that for high-energy electrons incident at a small angle to a plane (or an axis), only reciprocal lattice points on a line (or a plane) perpendicular to the plane (or axis) are close enough to the Ewald sphere for the corresponding reflections to be appreciably excited. The important question remains, whether scattering processes leading to nonconservation of transverse energy

are weak enough to be treated as a perturbation. Such processes may be either inelastic scattering, or elastic scattering corresponding to reciprocal lattice points off the line (or plane) perpendicular to the plane (or axis). For the axial case, the importance of the latter type was assessed in Ref. 10.

We shall base our discussion of correspondence in the following chapter on the continuum picture, mainly because this leads to rather simple results in both classical and quantal treatments. In so far as the main difference between the results consists of fine structure due to wave interference, the difference may be reduced by inelastic scattering leading to incoherence of the wavefunction.

*II.3. Solution of wave equation*

In order to solve Eq. (II.5) for $t > 0$, we consider the stationary wave equation corresponding to well-defined transverse energy $E_\perp$. For simplicity, we restrict ourselves to the planar case,

$$\left.\begin{aligned} \left[-\frac{\hbar^2}{2M}\frac{\partial^2}{\partial x^2} + V(x)\right] u^j(x) &= E_\perp^j u^j(x), \\ u^j(t,x) &= u^j(x)\, e^{-iE_\perp^j t/\hbar}, \end{aligned}\right\} \quad \text{(II.8)}$$

where $u^j(x)$ is the eigenfunction belonging to the eigenvalue $E_\perp^j$. The Hamiltonian is invariant under transformations $x \to x + nd_p$, where $n$ is an integer and, consequently, $u^j(x)$ can be written as a Bloch wave,

$$u^j(x) = e^{ik_\perp x}\omega^j(x), \quad \text{(II.9)}$$

where $\omega^j(x)$ is a periodic function, $\omega^j(x + nd_p) = \omega^j(x)$. In order to find solutions (II.9) to (II.8), we expand the potential as well as the wave function in a Fourier series,

$$V(x) = \sum_n V_n e^{ingx} \quad \text{(II.10)}$$

$$\omega^j(x) = \sum_m C_m^j e^{imgx} \quad \text{(II.11)}$$

where $g$ is the length of the reciprocal lattice vector corresponding to the distance $d_p$ between neighbouring planes, $g = 2\pi/d_p$.

If we insert (II.10) and (II.11) in (II.8), and identify terms with the same exponential factor, we obtain for the coefficients $C_n^j$

$$\frac{\hbar^2}{2M}(k_\perp + ng)^2 C_n^j + \sum_m C_m^j V_{n-m} = E_\perp^j C_n^j. \quad \text{(II.12)}$$

This system of equations leads to approximate eigenfunctions when only a finite number of terms in (II.10) and (II.11) are included. In the terminology of diffraction therory, the term in (II.11) with $n = 0$ is the primary beam, whereas terms with $n \neq 0$ correspond to diffracted beams. A calculation including $N$ terms in the expansions (II.10) and (II.11) is therefore denoted an $N$-beam calculation. The system of equations (II.12) then reduces to an eigenvalue problem for an $N \times N$ matrix $\tilde{A}$ given by

$$\left.\begin{aligned} A_{nm} &= V_{n-m}, \quad n \neq m \\ A_{nn} &= \frac{\hbar^2}{2M}(k_\perp + ng)^2 + V_0. \end{aligned}\right\} \quad \text{(II.13)}$$

In an $N$-beam calculation there are for fixed $k_\perp$ $N$ eigenvalues $E_\perp^j$ corresponding to $N$ orthogonal wave functions $u^j(x)$ given by (II.9) and (II.11). The dependence of the exact eigenvalues and eigenfunctions on $k_\perp$ is periodic with period $g$. For the solutions of a truncated matrix (II.13), this periodicity will only hold approximately within a limited range of $k_\perp$ values. In practice, the number of beams is chosen to be large enough for this range to comprise the interesting range of incidence angles.

### *II.4. Scattering yield*

At first we estimate the atomic scattering yield relative to the random case, corresponding to an eigenfunction $u^j(x)$. For large-angle scattering, the contributions from different atoms are incoherent due to the recoil. Classically large-angle scattering of energetic particles corresponds to collisions with very small impact parameter, and the yield will therefore be proportional to the particle flux at atomic positions. The classical picture applies when the quantity $\varkappa$, defined in Eq. (I.2), is large compared to unity. In the opposite limit of small $\varkappa$ values, the scattering by a single atom may be calculated in the Born approximation. The yield is then proportional to the square of the matrix element $\langle u^l | V_a | u^j \rangle$, where $u^j$ and $u^l$ are the initial and final states of the projectile and $V_a$ is the atomic potential. For large-angle-scattering corresponding to a transfer of a large transverse momentum $\hbar \Delta k$, the matrix element receives its major contribution from distances $\leqslant 1/\Delta k$ from the the center of the atom. If the initial wave function does not vary significantly over distances $\sim 1/\Delta k$, the yield will then also in this limit be proportional to the intensity $|u^j|^2$ at the position of the atom. This result is therefore obtained as a direct consequence of our basic assumption of predominance of

small-angle scattering, which implies that in the matrix (Eq. (II.13)), only Fourier components corresponding to $ng \ll \Delta k$ need be included.

If the intensity distribution $|u^j(x)|^2$ varies only little over a distance $\sim \varrho$, the R.M.S. vibrational amplitude perpendicular to the plane, the yield $\pi_j$ is given approximately by the intensity at the equilibrium position,

$$\pi_j = |u^j(0)|^2 = (\sum_n C_n^j)^2. \tag{II.14}$$

Here, and in the following, we assume the coefficients $C_n^j$ to be real, which may always be achieved if the crystal has reflection symmetry. Also, for simplicity, we have assumed that $x = 0$ corresponds to the position of the atomic plane. The two assumptions are not always compatible as, e.g., they are not for a {111} plane in a diamond lattice (cf. Fig. I.2 and the corresponding comment in the text). In such cases, the appropriate phase factor must be included in Eq. (II.14), which is modified to

$$\pi_j = \sum_{n,m} C_n^j C_m^j e^{i(n-m)gx_0}, \tag{II.14a}$$

when the atomic plane is at $x = x_0$.

As in the classical description[29], the most important correction for thermal vibrations is the modification of the yield $\pi_j$ due to displacements of the scattering centers from the plane. When the intensity is averaged over a Gaussian distribution of displacements, Eq. (II.14) is modified into

$$\pi_j = \sum_{m,n} C_n^j C_m^j D_{nm}, \tag{II.15}$$

where $D_{nm}$ are factors of Debye-Waller type,

$$D_{nm} = \exp\{-\tfrac{1}{2}(n-m)^2 g^2 \varrho^2\}. \tag{II.16}$$

A less significant effect of thermal vibrations is the modification of the lattice potential. Incoherence due to atomic recoil reduces the coherent scattering, and this may be taken into account by multiplying the Fourier components of the potential by a Debye-Waller factor,

$$V_n \to V_n D_{no}, \tag{II.17}$$

where $D_{no}$ is given by Eq. (II.16). The corresponding reduction of large Fourier components may alternatively be interpreted as being due to the smearing of the planar potential which results from a convolution with the Gaussian probability distribution for the position of atoms relative to the plane.

The corrections (II.15) and (II.17) only become important when the wave function contains Fourier components corresponding to transverse wave vectors $ng \gtrsim 1/\varrho$. Since $d_p/\varrho \gtrsim 30$ this will only be the case when at least 5–10 beams have to be included in the calculation.

*II.5. Surface transmission*

The wave function for $t > 0$ may be expanded in terms of eigenfunctions,

$$u(t,x) = \sum_j \alpha_j u^j(x) e^{-iE_\perp^j t/\hbar} = e^{ik_\perp x} \sum_j \alpha_j e^{-iE_\perp^j t/\hbar} \sum_n C_n^j e^{ingx}, \qquad \text{(II.18)}$$

where we have utilized that matching at the surface ($t = 0$) to the incoming plane wave requires all eigenfunctions in Eq. (II.18) to correspond to the value of $k_\perp$ determined by Eq. (II.6). Also the coefficients $\alpha_j$ are determined by this matching, and we obtain

$$\sum_j \alpha_j C_n^j = \delta_{no}. \qquad \text{(II.19)}$$

If the eigenfunctions are normalized,

$$\sum_n C_n^j C_n^k = \delta_{jk}, \qquad \text{(II.20)}$$

it is easily seen that

$$\alpha_j = C_o^j. \qquad \text{(II.21)}$$

Neglecting at first thermal vibrations, we then obtain for the yield $P$ of large-angle scattering, combining (II.14) with (II.21),

$$P = \sum_j (C_o^j)^2 \pi_j = \sum_j (C_o^j \sum_n C_n^j)^2. \qquad \text{(II.22)}$$

If thermal vibrations are taken into account, Eq. (II.14) is replaced by (II.15), and we obtain

$$P = \sum_j (C_o^j)^2 \sum_{m,n} C_n^j C_m^j D_{nm}. \qquad \text{(II.23)}$$

In Eqs. (II.22) and (II.23) we have added the contribution from different eigenfunctions incoherently. The results therefore apply to measurements which are averages over a thickness large enough to correspond to large variations of the relative phase of different eigenfunctions. This assumption of random relative phases is analogous to the assumption of statistical equilibrium in the classical treatment.

The yield of large-angle scattering is determined by the spatial intensity distribution of the channeled particles. By a transmission measurement of the intensity of different Bragg spots, one may determine the distribution in momentum space[34]. The corresponding formulae may easily be derived, but we shall instead turn to the problem of incoherent scattering which, in the theory of electron diffraction, plays a role very similar to that of dechanneling by multiple scattering in the classical theory of channeling.

*II.6. Incoherent scattering*

An order-of-magnitude estimate of the total cross section for scattering by atoms in a random medium was given in the previous chapter (Eq. (I.1)). For a wave function with high intensity at the atomic sites, there will be a strong increase in scattering. On the other hand, for small scattering angles, the intensity is mainly concentrated in the coherent Bragg peaks. A cursory estimate of the corresponding reduction of in coherent scattering may be obtained from the scattering law applied in the previous estimates,

$$d\sigma(\theta) \propto \frac{d(\theta^2)}{(\theta^2 + \theta_0^2)}. \tag{II.24}$$

Here, $\theta_0$ is given by the ratio of the electron wavelength $\lambda\!\!\!^{-}$ to the screening radius $a$, $\theta_0 = \lambda\!\!\!^{-}/a$. Since the incoherent scattering is proportional to a factor $[1 - \exp(-\varrho^2\theta^2/\lambda\!\!\!^{-2})]$, a rough estimate of the incoherent fraction is

$$\frac{\sigma_{\text{inc}}}{\sigma_{\text{tot}}} \simeq \frac{1}{\sigma_{\text{tot}}} \int d\sigma(\theta) \Big|_{\varrho^2\theta^2/\lambda\!\!\!^{-2} > 1} = [1 + a^2/\varrho^2]^{-1}. \tag{II.25}$$

In silicon this estimate leads to a rather small incoherent fraction, $\simeq 1/6$. In view of the rough approximations made in the calculation, this number should be considered only as an indication of the importance of corrections for coherent scattering to the inelastic scattering cross section. If the atomic scattering is strongly reduced, inelastic scattering by electrons may play a significant role especially for low $Z_2$. It should be noted, however, that the enhancement of incoherent scattering (anomalous absorption) corresponding to the increase in large angle scattering yield will be much stronger for thermal scattering than for electronic scattering.

A considerable amount of work has been devoted to the problem of estimating inelastic scattering in connection with electron microscopy. Recently, a review was given by Howie and Stern[35], which also may be

consulted for further references. Usually, inelastic scattering is taken into account by adding an imaginary part to the potential. Such a simple treatment will probably not suffice in the present connection. Since the inelastically scattered electrons also contribute to the large-angle scattering yield, we are concerned not only with the effect of inelastic scattering on the initial, coherent wave function – absorption – but also with the properties of the final states. Thus it may be complicated to introduce inelastic scattering even in the comparatively simple two-beam case[17]. As a first approximation, the final states may be assumed to be plane waves[36]. For the thermal scattering, which involves rather large momentum transfers, this assumption may not be too bad. Since, however, for scattering by electrons, the cross section is strongly peaked at small momentum transfers, the wavefunction may not change its symmetry even after several plasmon excitations[14, 35].

In the axial case, the problem of incoherent scattering is particularly severe. The strong potential minimum should lead to fairly localized states and a large peak in scattering yield. Such states will be highly unstable, and the incoherent scattering cannot be treated as a small perturbation. A treatment in terms of statistical concepts may then be more appropriate[11, 37].

*II.7. Numerical evaluation and comparison to experiment*

When only a small number of Fourier components (beams) are included, the many-beam formalism lends itself readily to numerical evaluation. Planar peaks in scattering yield for 700-keV electrons along {111} and {110} planes in silicon are shown in Figs. II.1 and II.2. A fairly rapid convergence with increasing number of beams is indicated. The number of beams necessary in such a calculation depends on the strength of the planar potential and the relativistic particle mass. In the present case, 7–9 beams are sufficient for the most closely packed plane, the {111} plane, whereas for the weaker {110} and {100} planes, only 5–7 and 3–5 beams, respectively, are needed.

The relative excitation of different Bragg-reflected beams can be directly observed in the photographic exposures of the transmitted beam (Fig. I.5). For the {111} plane, both second – and third-order reflections are quite important, and of the order of five beams are strongly excited. It may be noted that due to the already mentioned split of the {111} plane in a diamond-type lattice, the second-order Fourier component of the {111} planar potential vanishes. Thus the second-order beam can only be excited indirectly, and the very strong excitation indicated in Fig. I.5 shows the importance of

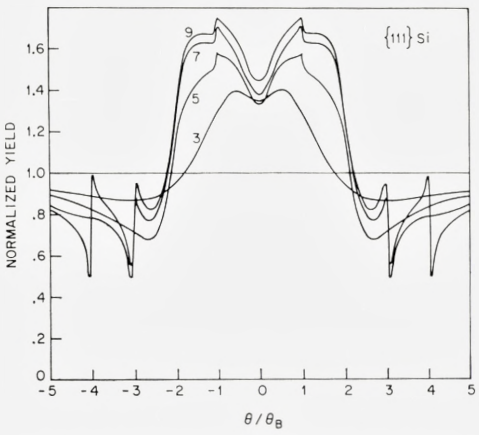


Fig. II.1: Many-beam calculations of the {111} peak for 0.7-MeV e⁻ on Si, including 3, 5, 7, and 9 beams, respectively (static lattice).

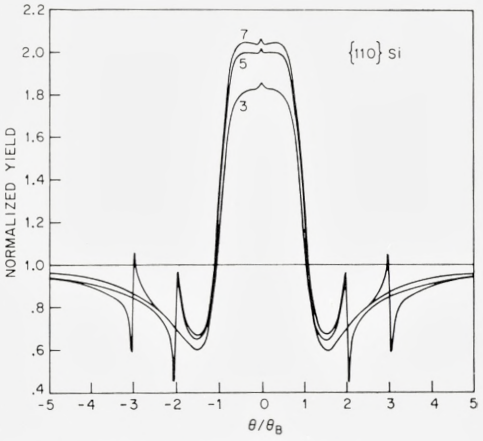


Fig. II.2: Many-beam calculations of the {110} peak for 0.7-MeV e⁻ on Si, including 3, 5, and 7 beams, respectively (static lattice).

dynamical effects. The two exposures for the {110} plane indicate that for this somewhat weaker plane, fewer beams are excited.

In the axial cases, a much larger number of beams are excited simulataeously, as may be appreciated by looking at the Bragg spot patterns in Fig. I.8. For the ⟨111⟩ axis, the number of spots is still fairly small, and a calculation analogous to those for planar cases was therefore attempted (see Fig. I.7). The convergence with number of beams is illustrated in Fig. II.3. For the ⟨110⟩ axis, the spot pattern in Fig. I.8 contains many, fairly weak,

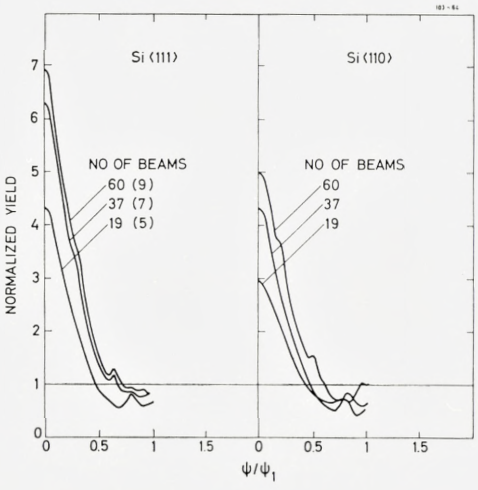


Fig. II.3: Convergence of axial many-beam calculations for 0.7-MeV e⁻ on Si. The number of beams included is indicated in the figure. For the ⟨111⟩ axis, the equivalent number of beams for a {110} planar calculation is given in parentheses. In contrast to the calculations shown in the previous figures, the most important reflections were selected independently for each angle of incidence. Incoherent scattering is neglected, but other effects of thermal vibrations are included (cf. Eqs. (II.15) and II.17)). The values of the characteristic angle $\psi_1$ for classical channeling are 0.75° and 0.92° for the ⟨111⟩ axis and the ⟨110⟩ axis, respectively.

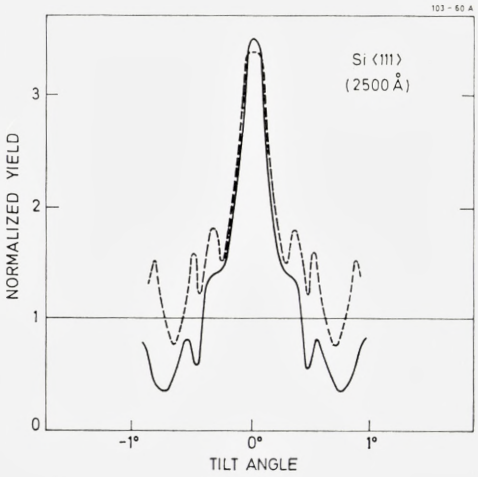


Fig. II.4: Axial peak in large-angle scattering yield for 0.7-MeV $e^-$, derived from a 49-beam calculation (cf. Fig. II.3). The influence of incoherent scattering has been estimated by including an imaginary component in the potential and assuming scattering into plane-wave states. The magnitude of the imaginary Fourier components of the potential has been evaluated from an approximation to the results given in Ref. 38. The peak derived from this calculation is compared to that obtained without absorption, multiplied by 0.5, corresponding to the correction for inelastic scattering applied in Figs. I.6 and I.7 (dashed curve).

reflections. This may be related to the complicated transverse arrangement of ⟨110⟩ strings and explain the apparent lack of convergence in the many-beam calculations for this case (see Fig. II.3). Also, the ⟨110⟩ axis is somewhat stronger than the ⟨111⟩ axis, and the experimental results were therefore compared (in Fig. I.6) to a classical calculation. It is clear that for a strong, narrow potential, two-dimensional Fourier expansion is basically a very inefficient method.

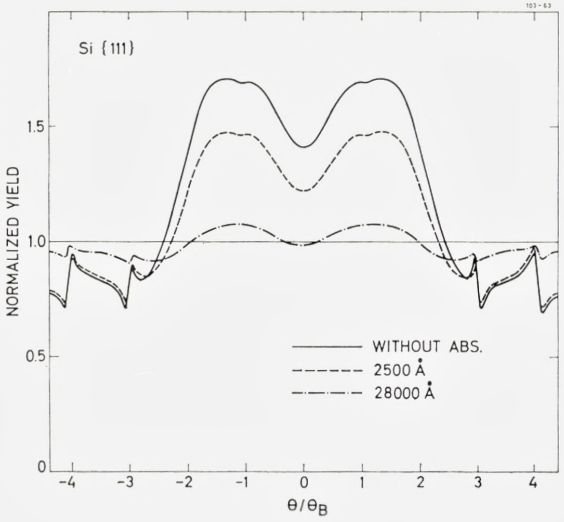


Fig. II.5: 20-beam planar calculation for $e^-$ on Si. Effects of thermal vibration are included according to Eqs. (II.15) and (II.17), and the influence of incoherent scattering has been estimated as described for the previous figure.

As mentioned in the previous section, inelastic scattering is normally in electron microscopy taken into account by adding an imaginary component to the potential, and this treatment may be applied to measurements of large-angle scattering if the final states are assumed to be plane waves. Examples of results from such a procedure are given in Figs. II.4 and II.5 for the $\langle 111 \rangle$ axis and the $\{111\}$ plane, respectively. For the axis, the calculation supports the simple estimate of a reduction by a factor of two, which was applied in Figs. I.6 and I.7. Also for the plane, the result for the thinner crystal is in fair agreement with measurement, but for the thicker crystal, the calculation does not lead to the narrowing of the peak observed experimentally (Fig. I.9). It would seem that measurements of the type described here could serve as a useful tool to test the description of inelastic scattering.

The main conclusion of the comparison between calculations and experiments is, however, that for small depths, the dynamical theory of electron diffraction yields results in good agreement with experiments, at least for planes and weaker axes. A similar conclusion was reached for experiments with positrons[8, 9], and we may therefore in the following investigate the relation to channeling of heavy particles by studying the relationship of this theoretical description with classical channeling theory.

## III. Correspondence

III.1. *General considerations*

The main objective of this investigation of electron and positron channeling has been to study the limits for applicability of classical mechanics in the description of channeling phenomena for light particles, and in particular the relation between the theory of electron diffraction, as formulated in Chapter II, and classical channeling theory. In the papers by LINDHARD[5] and LERVIG et al.[10], the validity of classical orbital pictures in the description of collisions with an isolated string was studied in detail with emphasis on the case of heavy particles (protons, $\alpha$ paticles, etc.). For this case it was concluded that in the limit of high particle velocities, a collision with a string of atoms remains classical although classical mechanics does not apply to scattering by a single atom since the quantity $\varkappa$, defined in Eq. (I.2), becomes small compared to unity.

For channeling of light particles (positrons and electrons), an analysis of the interaction with the lattice in terms of scattering of a wave packet by isolated strings or planes may not be appropriate, as the requirements of localization in space and angular spread smaller than a characteristic angle, which for axial channeling is of order[10]

$$\psi_1 = \left(\frac{4Z_1 Z_2 e^2}{pvd}\right)^{1/2}, \tag{III.1}$$

may be mutually exclusive.

Decisive for this question is the magnitude of the number of bound states in the transverse potential minimum. Semiclassically this number may be obtained from the available phase space for transverse energy below the potential barrier. If there are no bound states the scattering is determined by simultaneous interaction with many strings or planes, and no similarity with classical results can be expected. In the limit of many bound states, on the other hand, the classical picture is approached.

In the case of axial channeling, positively charged particles with transverse energy below the barrier for penetration through strings are not bound to one channel but may move freely between strings except at very low transverse energy ('proper channeling'). Still, the number of states per unit cell in the transverse plane (or per string), with transverse energy below the barrier for penetration into strings, is an important quantity. Qualitatively it may be seen from the fact that many states per unit cell are required to form a wave packet which is well localized within this area. More directly, it follows from the quantal treatment in Ch. II. The stationary wave equation (two-dimensional analogue of Eq. (II.8)) may be reduced to one unit cell with periodic boundary conditions, and the conclusions reached in the following concerning the behaviour of the solutions of this equation may therefore be expected also to apply to the axial case for positive particles, with the definition given above for 'the number of bound states'.

At this point it may be appropriate to discuss the special quantal phenomena caused by the lattice periodicity. Indeed the strong diffraction phenomena observed for electrons and positrons constitute the most striking deviation from classical behaviour. The interference due to transverse periodicity with period $d_p$ may be described as a quantization of transverse momentum transfers in bits of $\delta p_\perp = 2\pi\hbar/d_p$, corresponding to an angular deflection of twice the Bragg angle. This quantization was explicitly disregarded by LERVIG et al. on the ground that for particles heavy compared to the electron, $\delta p_\perp$ is very small. In point of fact, for $p_\perp = p\psi_1$, we have[10]

$$\left(\frac{\delta p_\perp}{p_\perp}\right) = \pi\left(\frac{a_0}{d_p}\right)^{1/2}\left(\frac{m_0}{M}\right)^{1/2}(Z_1 Z_2)^{1/2} \ll 1 \quad \text{for} \quad M \gg m_0, \tag{III.2}$$

where $M$ and $Z_1$ are the mass and charge of the incident particles.

Should we not then, as the essential criterion for classical behaviour, require that the transverse momentum quantum $\delta p_\perp$ be small compared to the transverse momentum corresponding to the potential barier $E_b$, $p_\perp = (2ME_b)^{1/2}$? Although this is a necessary condition, it is not sufficient. Also the width of the potential minimum is important since, together with the barrier height, it determines the number of bound states.

The interference structure may be smeared by incoherent scattering or poor collimation. This, however, only leads to classical results if the phase-space criterion is fulfilled such that the quantal description leads to a classical envelope with fine structure due to diffraction. In this transition region, deviations from classical results due to tunneling may also be expected.

Channeled positive particles are prevented from penetrating into the center of atoms by the transverse potential barrier. The probability of close encounters with atoms is thereby strongly reduced for incidence parallel to an axis or plane, and the magnitude of this reduction may be sensitive to the probability of tunneling into the classically forbidden regions. Cursory estimates of tunneling probabilities for strings and planes, based upon the WKB approximation, were given in Ref. 10.

We may conclude these general remarks by considering some characteristic lengths, the relative magnitude of which governs the approach towards the classical picture of channeling. The transverse wavelength $\lambda_\perp^b$, which corresponds to a transverse kinetic energy equal to the potential barrier $E_b$, is given by $2\pi\hbar/(2ME_b)^{1/2}$, where $M$ is the relativistic mass of the particle. This length may first be compared to the width of the potential minimum which, for electrons, is a few times the Thomas-Fermi screening distance $a$ and for positrons is of the order of $d$, the lattice spacing. When $\lambda_\perp^b$ is small compared to the width, the phase space is large, there will be many bound states, and the quantization of transverse energy may be disregarded.

Second, the importance of the quantization of transverse momentum depends on the relative magnitude of $\lambda_\perp^b$ and the characteristic lengths for lattice periodicity, which again is of order $d$. If the phase-space criterion is fulfilled, $\lambda_\perp^b$ will be small compared to $d$, and we may expect interference due to periodicity to lead to fine structure only.

Third, penetration into potential barriers is small if the width of the barrier is large compared to $\lambda_\perp^b$. For positive particles, the barrier widths are of order $a$ or a few times $a$. Tunneling may therefore lead to important modifications of classical results, even if the phase space is relatively large. In Ref. 8 it was concluded, however, that the influence of tunneling is strongly reduced by the smearing of the distribution of atoms, due to thermal vibrations.

### *III.2. Analogy between quantal and classical descriptions*

In the following we shall try to describe in some detail how the quantal description of channeling approaches the classical description and illustrate the importance of the phase-space criterion. In this connection it is important to specify the type of measurement we are considering. We shall be concerned only with predictions of the dependence on incidence direction of the yield of a close-encounter process such as large-angle scattering or inner-shell excitation. This simplifies the problem considerably since we need not

consider in detail the validity of classical orbital pictures in describing particle trajectories[25] but only the ability of classical mechanics to predict the distribution of particles in the transverse direction or plane. A quantal treatment was discussed in the previous chapter and for the classical description, we may refer to Lindhard's original treatment[5]. Numerical estimates based upon the two formulations are compared in Ch. IV. In the Appendix, an example is given of an analytical calculation based upon the classical description.

The physical situation we are concerned with is an external beam of particles incident on a single crystal at an angle $\psi$ to a major plane (or axis), and we ask for the probability $P(\psi)$ for particles to come close to the center of crystal atoms, as manifested in the yield of a close-encounter reaction. Many similarities are apparent between the classical and the quantal treatments of this problem. Owing to the predominance of forward scattering, the motion of the particles may be separated into a longitudinal motion with nearly constant velocity and a transverse component, which may be described as motion in an averaged potential with approximate conservation of the transverse energy $E_\perp$ ('continuum approximation'). The probability $P(\psi)$ is then determined in two steps:

First, the probability $\pi(E_\perp)$ for a particle with transverse energy $E_\perp$ to have a close encounter with an atom is calculated. In the classical treatment, this involves finding the probability distribution in transverse space as a function of $E_\perp$, based on statistical arguments. In the quantal treatment, $E_\perp$ is quantized. The eigenfunction $u^j(x)$ belonging to an eigenvalue $E_\perp^j$ may be calculated from Eqs. (II.8), (II.9), (II.11), and (II.12). The probability density in transverse space is given by the square of this eigenfunction. In both cases, the reaction yield is assumed to be proportional to the density at atomic positions.

Second, the population of transverse-energy levels is determined by surface transmission. Classically, a particle hitting the crystal at a distance $x$ from a plane acquires a potential energy $V(x)$, leading to a total transverse energy

$$E_\perp = E\psi^2 + V(x). \tag{III.3}$$

Since the intensity of the beam is uniform over the crystal surface, the distribution in transverse energy is then given by

$$W(E)_\perp \propto \int dx \delta(E_\perp - E\psi^2 - V(x)) = \sum_i \left| \frac{\partial V}{\partial x} \right|^{-1}_{x = x_i} \tag{III.4}$$

where the $x_i$'s are solutions to Eq. (III.3). Formulae analogous to (III.3) and (III.4) hold for the axial case.

In the wave-mechanical formulation, the population of energy levels is determined by a matching of the total wave function at the crystal surface to the incident plane wave, which yields the coefficients (Eq. (II.21)) of different eigenfunctions. In the expressions for the total probablility density in the transverse plane, interference between different eigenfunctions is neglected. In the planar case, this corresponds to the assumption of statistical equilibrium in the classical calculation and should be valid for not too small thicknesses. Problems related to the assumption of statistical equilibrium for axial channeling are discussed in Ch. IV and, in more detail, in the Appendix. Deviations from equilibrium close to the surface have been studied extensively for heavy-particle channeling[27] and recently also for electron channeling[37, 39].

In the following we shall analyze both of these steps in detail for the one-dimensional case. In the quantal treatment in Ch. II, the problem of determining eigenfunctions for the transverse Hamiltonian was reduced to solving the Schrödinger equation (II.8) in a finite interval $[0,d_p]$, with periodic boundary conditions according to Eq. (II.9). In order to gain insight into the properties of such solutions, we consider a simpler analogous problem where the particle is confined by infinite potential walls. For the general qualitative conclusions concerning the importance of the magnitude of quantum numbers, the difference in boundary conditions should not be of any importance and, furthermore, the boundary conditions are for strongly bound states determined by the local potential minimum and not by periodicity (cf. also Sec. IV.2).

### *III.3. Harmonic oscillator*

First, we treat the familiar example of a harmonic oscillator. For many physical problems, this is a basic example, which may be solved by analytical methods. In fact, the spatial probability density for a particle bound in a harmonic potential is used as a standard textbook illustration of correspondence with classical mechanics in the limit of large quantum numbers[40]. According to the general discussion above, evaluation of this density is the first task to be performed.

*Spatial density.* With the potential $V(x) = \frac{1}{2} M\omega^2 x^2$, the eigenvalue equation becomes

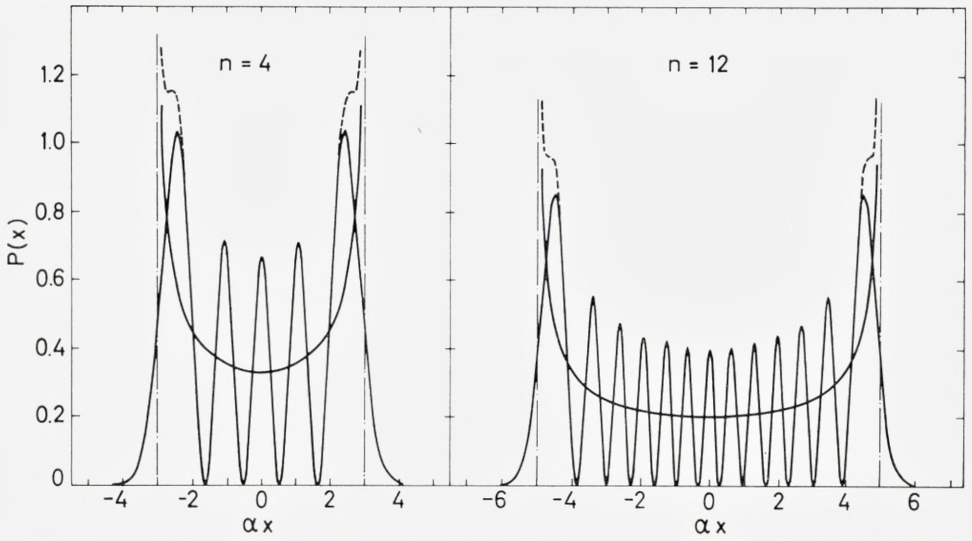


Fig. III.1: Spatial density for harmonic-oscillator eigenfunctions corresponding to n = 4 and n = 12, respectively. The classical turning points are indicated by dot-and-dash lines, and the classical spatial probability (Eq. (III.9)) is given by the smooth solid curve. The oscillating solid curve corresponds to the exact distribution $|u_n(x)|^2$ (Eq. (III.7)) and the dashed curve to the density obtained from the WKB approximation (Eq. (III.22)).

$$\left[-\frac{\hbar^2}{2M}\frac{\partial^2}{\partial x^2}+\tfrac{1}{2}M\omega^2x^2\right]u(x) = Eu(x). \tag{III.5}$$

Here, and in the following, the transverse energy is denoted simply by $E$. This equation has the well-known solutions

$$E_n = \hbar\omega(n+\tfrac{1}{2}), \tag{III.6}$$

and

$$u_n(x) = N_nH_n(\alpha x)e^{-1/2\,\alpha^2x^2}, \tag{III.7}$$

where $\alpha^2 = M\omega/\hbar$, $H_n$ is the n'th Hermite polynomial, and $N_n$ is a normalization constant,

$$N_n = \sqrt{\alpha}/(\sqrt{\pi}2^n n!)^{1/2}. \tag{III.8}$$

The probability density, $|u(x)|^2$, is in Fig. III.1 compared to the classical distribution,

$$\varrho(x) = \left(\frac{M\omega^2}{2\pi^2}\right)^{1/2}(E-\tfrac{1}{2}M\omega^2x^2)^{-1/2}, \tag{III.9}$$

for two values of $n$. For moderately high $n$, the distributions are very similar except for the rapid oscillations of the quantal density.

*Surface transmission.* Corresponding to the case where particles are incident on a crystal at an angle $\varphi$ to a major plane, we now ask for the population of the harmonic-oscillator eigenstates for $\psi(x,\ t=0) = e^{ikx}$, where $\hbar k$ denotes the transverse momentum, related to the total momentum $p$ by $\hbar k = p\varphi$. The classical result is

$$W(E) = 2\left(\frac{\partial V}{\partial x}\right)^{-1}\Bigg|_{V=E-\hbar^2k^2/(2M)} = \left(\frac{2}{M\omega^2}\right)^{1/2}\left(E-\frac{\hbar^2k^2}{2M}\right)^{-1/2}. \qquad \text{(III.10)}$$

In order to find the quantal distribution, we have to evaluate the matrix element

$$\langle u_n \,|\, e^{ikx}\rangle = N_n \int_{-\infty}^{\infty} dx H_n(\alpha x)\, e^{-1/2\,\alpha^2x^2} e^{ikx}. \qquad \text{(III.11)}$$

This integral may be evaluated by repeated partial integration when the following represention of the Hermite polynomial is used,

$$H_n(x) = (-1)^n e^{x^2}\frac{\partial^n}{\partial x^n} e^{-x^2}, \qquad \text{(III.12)}$$

and the result is

$$\langle u_n \,|\, e^{ikx}\rangle = \frac{1}{\alpha} N_n \sqrt{2\pi}\,(-i)^n\, e^{-k^2/(2\alpha^2)} H_n(k/\alpha). \qquad \text{(III.13)}$$

Since Eq. (III.11) is essentially the momentum representation of the n'th state, this result, except for a phase factor, also follows directly from the symmetry between $x$ and $\dfrac{\partial}{\partial x}$ in the Hamiltonian.

The population of the n'th energy level is given by the square of this matrix element,

$$P(E_n) = \left(\frac{2\pi\hbar}{M\omega}\right)\cdot N_n^2 \cdot e^{-k^2/\alpha^2} H_n^2(k/\alpha). \qquad \text{(III.14)}$$

When this expression is divided by the spacing of levels, $h\omega$, the relation to the classical energy distribution (III.10) is the same as the relation between the quantal and classical spatial densities except for the fact that the expressions are now compared as functions of $E$ (cf. Fig. III.3).

Since the main purpose of these considerations is to illustrate the correspondence qualitatively, we shall only for a special case prove that the quantal result approaches the classical one in the limit of large quantum numbers. Consider the energy distribution (III.14) for $k = 0$, corresponding

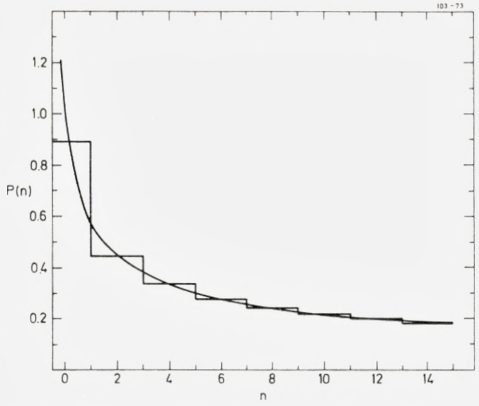


Fig. III.2: Comparison of quantal (Eq. (III.5)) and classical (Eq. (III.10)) energy distributions for $k = 0$, corresponding to incidence parallel to a plane. The two distributions have been multiplied by $1/2(M\omega^2\hbar\omega)^{1/2}$. Here $n$ denotes the level number, i.e., $E_n = (n+1/2)\hbar\omega$, and the staircase distribution gives the population for $n$ even.

for the channeling case to zero angle of incidence with a plane. Only states with even parity are then populated, and we may compare the classical density (Eq. (III.10)) to $P(E_{2n})/(2\hbar\omega)$. Using the relation $H_{2n}(0) = (-1)^n(2n)!/n!$ we obtain

$$P(E_{2n})/(2\hbar\omega) = \left(\frac{2}{M\omega^2}\right)^{1/2} \cdot \frac{1}{(\hbar\omega)^{1/2}} \cdot \left(\frac{\pi}{2}\right)^{1/2} \cdot \frac{(2n)!}{2^{2n}(n!)^2}. \qquad \text{(III.15)}$$

For large $n$, we may evaluate the factorials by Stirling's formula,

$$n! \simeq \sqrt{2\pi n} \cdot e^{-n} \cdot n^n \qquad \text{(III.16)}$$

and obtain

$$P(E_{2n})/(2\hbar\omega) \simeq \left(\frac{2}{M\omega^2}\right)^{1/2} \cdot \frac{1}{(2n\hbar\omega)^{1/2}}. \qquad \text{(III.17)}$$

This result is essentially identical to Eq. (III.10) for $k = 0$. The distributions (III.10) and (III.15) are compared in Fig. III.2.

### *III.4. WKB approximation*

The general approach to the classical description for large quantum numbers may be seen more directly in the WKB approximation. This semiclassical description offers a convenient stepping stone from a quantal formulation to the classical treatment (cf. also Ref. 25).

*Spatial density.* A stationary solution to the Schrödinger equation with a potential $V(x)$ may be written

$$\psi(x,t) = C\exp\{i(s(x) - Et)/\hbar\}, \qquad \text{(III.18)}$$

where the phase function $s(x)$ satisfies

$$\frac{1}{2M}\left(\frac{\partial}{\partial x}s\right)^2 - [E - V(x)] - \frac{i\hbar}{2M}\frac{\partial^2}{\partial x^2}s = 0. \tag{III.19}$$

The WKB approximation obtains the first two terms of a formal expansion of $s$ in powers of $\hbar$. In classically allowed regions, $(E > V(x))$, the general solution in this approximation is[40]

$$\left.\begin{aligned} u_E(x) = Ak(x)^{-1/2}\exp\left\{i\int_{x_0}^{x} k(x')\,dx'\right\} + \\ + Bk(x)^{-1/2}\exp\left\{-i\int_{x_0}^{x} k(x')\,dx'\right\}. \end{aligned}\right\} \tag{III.20}$$

where we have introduced the local wave vector

$$k(x) = \frac{1}{\hbar}(2M(E - V(x)))^{1/2}. \tag{III.21}$$

Apart from oscillations due to interference between the two amplitudes corresponding to opposite directions of the particle velocity, we have $|u(x)|^2 \propto \propto (E - V(x))^{-1/2}$ as for the classical spatial distribution (cf. Eq. (III.9)). The condition for the validity of the WKB approximation is that the fractional change in wavelength be small over a distance of one wavelength. Except for the regions close to the classical turning points ($V(x) \simeq E$), this is in the case of a potential minimum equivalent to a demand for many nodes in the wave function or a large quantum number $n$.

*Surface transmission.* Consider for simplicity a symmetric potential $V(x) = V(-x)$ increasing monotonically to infinity for $x \to \infty$ with $V'(x) \neq 0$ for $x \neq 0$. When the solution (Eq. (III.20)) for $V < E$ is matched to the WKB solutions in the classically forbidden regions ($V > E$), the wave function becomes[40]

$$u_E(x) = Ak(x)^{-1/2}\cos\left(\int_{-a}^{x} k(x')\,dx' - \frac{\pi}{4}\right). \tag{III.22}$$

Matching to the solution for $V > E$ at the turning points, $x = \pm a$, leads to quantization of the energy, determined by[40]

$$\int_{-a}^{a} k(x)\,dx = (n + \tfrac{1}{2})\pi, \qquad n = 0,1,2,\ldots \tag{III.23}$$

In order to determine the population of eigenstates corresponding to an initial wave function $\psi(x, t = 0) = e^{ik_0 x}$, we consider again the matrix element

$$\langle u_E(x) | e^{ik_0 x} \rangle = A \int k(x)^{-1/2} \cos\left( \int_{-a}^{x} k(x')\, dx' - \frac{\pi}{4} \right) e^{ik_0 x}\, dx. \quad \text{(III.24)}$$

This integral we may evaluate by the stationary-phase method. First, the wave function $u_E(x)$ may be written as a sum of two amplitudes corresponding to opposite directions of the velocity (cf. Eq. (III.20)). A stationary phase, determined by

$$\frac{d}{dx}\left( \pm \int_{-a}^{x} k(x')\, dx' \pm \frac{\pi}{4} + k_0 x \right) = 0, \quad \text{(III.25)}$$

is obtained only for the amplitude corresponding to the velocity direction given by the sign of $k_0$. For $0 < k_0 < k(0)$, Eq. (III.25) is fulfilled for two values of $x$, $x = \pm x_k$, determined by

$$k(\pm x_k) = k_0. \quad \text{(III.26)}$$

The contributions from the two $x$ values are then approximately given by the expression

$$\left.\begin{aligned} &\frac{A}{2} k(x_k)^{-1/2} \exp\left\{ -i \int_{-a}^{\pm x_k} k(x)\, dx \pm i k_0 x_k - \frac{i\pi}{4} \right\} \times \\ &\qquad \times \int dx \exp\left\{ i \frac{MV'(\pm x_k)}{2\hbar k_0} x^2 \right\}, \end{aligned}\right\} \quad \text{(III.27)}$$

in which the phase has been expanded to second order around the points $x = \pm x_k$. When the result ($c > 0$)

$$\int_{-\infty}^{\infty} \exp(\pm i c x^2)\, dx = \sqrt{\frac{\pi}{2c}}\,(1 \pm i) \quad \text{(III.28)}$$

is applied, the magnitude of the two contributions may be evaluated, and we obtain

$$P(E) = |\langle u_E(x) | e^{ik_0 x} \rangle|^2 = \frac{2\pi\hbar}{MV'(x_k)} A^2 \cos^2\left( \int_0^{x_k} (k(x) - k_0)\, dx - \frac{\pi}{4} \right), \quad \text{(III.29)}$$

where the argument of the cosine corresponds to half the relative phase of the contributions from $x = \pm x_k$. As for the harmonic oscillator we obtain an energy population which oscillates as a function of energy, and we have

now seen that this behaviour is caused by interference between the amplitudes corresponding to the two points $x = \pm x_k$, at which the velocity of a particle with energy $E$ matches the well-defined velocity for $t = o$, $v = \hbar k_0/M$.

In order to compare with the classical energy population,

$$W(E)dE = 2V'(x_k)^{-1}dE, \tag{III.30}$$

we must evaluate the normalization constant $A$ and furthermore divide $P(E)$ by the splitting $\Delta E$ between eigenstates. The normalization is determined by,

$$A^2 \int_{-a}^{a} k(x)^{-1} \cos^2\left(\int_{-a}^{x} k(x')\,dx' - \frac{\pi}{4}\right) dx = 1. \tag{III.31}$$

If the condition for the WKB approximation is fulfilled, the potential varies only little over one wavelength, and we have approximately

$$A^2 \simeq 2\hbar \left\{\int_{-a}^{a} k(x)^{-1}\,dx\right\}^{-1}. \tag{III.32}$$

The quantization of energy is given by Eq. (III.23). At high quantum numbers, we may evaluate the splitting $\Delta E$ from

$$\Delta E \frac{d}{dE}\left(\int_{-a}^{a} k(x)\,dx\right) \simeq \pi. \tag{III.33}$$

With the definition (III.21) of $k(x)$, this leads to

$$\Delta E \simeq \frac{\pi\hbar^2}{M}\left\{\int_{-a}^{a} k(x)^{-1}\,dx\right\}^{-1}. \tag{III.34}$$

Combining Eqs. (III.32) and (III.34) with Eq. (III.29), we obtain

$$P(E)/\Delta E \simeq (4/V'(x_k))\cos^2\left(\int_{0}^{x_k} (k(x) - k_0)\,dx - \frac{\pi}{4}\right). \tag{III.35}$$

When averaged over the oscillations, this expression is idential to the classical result in Eq. (III.30).

It should be noted that the method of evaluation used here is limited to energies somewhat larger than classical minimum energy, $E = V(0) + \hbar^2k^2/(2M)$. Also, for large values of $E$, the method breaks down because the stationary points $\pm x_k$ are too close to the classical turning points, where the expression (III.22) for the wave function cannot be applied. In these regions, we way instead expand the potential to first order around $x = \pm a$

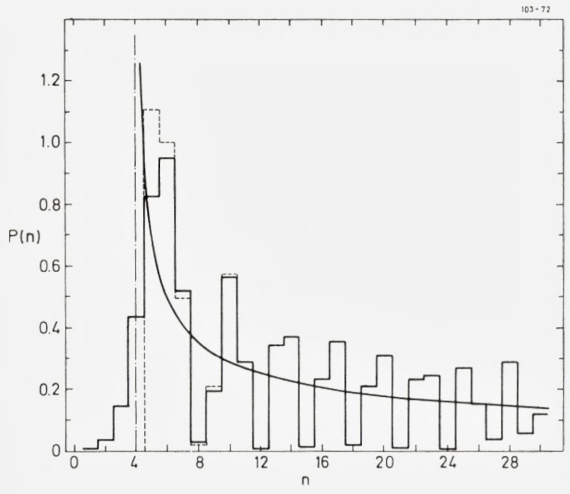


Fig. III.3: Population of levels in harmonic oscillator for $\psi(x, t = 0) = \exp(ikx)$, with a value of $k$ corresponding to $(\hbar k)^2/(2M) = 4.5\ \hbar\omega$. This lower limit for the classical energy population is indicated by a dot-and-dash line, and the classical distribution (Eq.(III.10)) is given by the smooth solid curve. The solid staircase distribution corresponds to the exact population (Eq. (III.14) divided by $\hbar\omega$), while the result obtained from the WKB approximation (Eq. (III.35)) is indicated by the dashed lines. Normalization and notation as for Fig. III.2.

and represent the wave function by an Airy function. For $k = 0$, a result analogous to Eq. (III.35) is then easily obtained, with the cosine replaced by 0 or 1 for odd and even parity, respectively.

We shall not go into the details of such estimates since the main purpose of this chapter is to provide some general insight into the correspondence between classical and quantal results. Such insight is more readily gained from analytical treatments of simple examples than from more realistic numerical calculations, as presented in Ch. IV. For this purpose, the WKB approximation is particularly helpful, yielding basically classical results modulated by oscillations due to interference between different amplitudes.

We conclude this chapter by an assessment of the accuracy of the WKB approximation for the harmonic oscillator, which was treated exactly in the previous section. Figure III.3 shows the population of different energy levels for a plane wave with a $k$ value corresponding to $(\hbar k)^2/2M = 4.5\hbar\omega$. The smooth curve is the classical energy distribution given by Eq. (III.10), while the staircase distributions correspond to the exact quantal result (Eq. (III.14), fully drawn) and the WKB approximation (Eq. (III.35), dashed). Only close to the minimum energy do the two distributions differ enough to be drawn separately. It should be noted that for the harmonic oscillator, Eq. (III.23) reproduces the exact energy quantization. For the spatial density distribution, shown in Fig. III.1, the accuracy of the WKB approximation is similar, and appreciable deviations from the exact results occur only close to the classical turning points. For small values of $\alpha x$, the distributions deviate by less than one percent.

## IV. Applicability of Classical Calculations to Electron and Positron Channeling

In this chapter, we first apply the general quantative results of the previous chapter to obtain approximate criteria for the applicability of classical concepts to channeling of electrons and positrons from estimates of the number of bound states in the transverse continuum potential According to Eq. (III.23), this number may be obtained approximately as the available phase space divided by Planck's constant $h$ (or by $h^2$ in two dimensions).

Second, the transition to the classical limit at high quantum numbers is studied quantitatively by a comparison of classical results for the directional dependence of the large-angle-scattering yield with results obtained from the many-beam description reviewed in Ch. II. The calculations also provide a check of the formulas for the number of bound states derived from semiclassical estimates.

### *IV.1. Number of bound states*

The following estimates correspond closely to those given in previous work[8–13]. Also in the review by GEMMEL[27], such estimates were given. For the planar case, our results are essentially in agreement, apart from a trivial mistake by a factor of two in his formulas. For axial channeling of negative particles, there is a more important difference in method as well as result.

*Planes.* The planar potential is illustrated in Fig. IV.1 for positive particles. We base the estimates of the phase space upon Lindhard's standard potential, which for a particle with one positive charge, leads to the planar potential.

$$V(x) = 2\pi Z_2 e^2 N d_p [(x^2 + C^2 a^2)^{1/2} - x], \tag{IV.1}$$

where $Nd_p$ is the density of atoms in the planes, $d_p$ being the planar spacing. The width of the potential maximum is approximately $3Ca$, where a is the Thomas-Fermi screening distance and $C$ a potential parameter, $C \sim \sqrt{3}$.

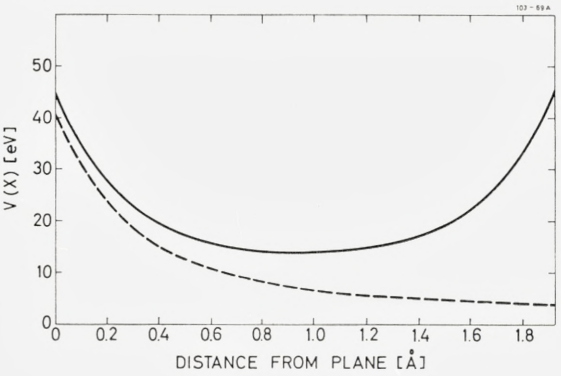


Fig. IV.1: Si {110} planar potential for positrons. The potential from a single plane is represented by the dashed curve (Eq. (IV.1)), while the solid curve is obtained by adding the potential from the neighbouring plane. The phase-space estimates are based on the latter potential.

The number of bound states in the potential is given by

$$\nu_p \simeq \frac{1}{\pi\hbar}\int_0^{d_p}(2M(V_{\max}-V))^{1/2}dx, \tag{IV.2}$$

where $M$ is the relativistic particle mass.

From a numerical integration of (IV.2), we obtain for negative particles a result corresponding approximately to a square-well potential with depth $V(0)$ given by Eq. (IV.1), and width $\sim 3Ca$,

$$\nu_p^- \simeq \left(\frac{M}{m_0}\right)^{1/2}\left(\frac{4a_0}{d_p}\right)[Nd_p^3]^{1/2}, \tag{IV.3}$$

where $m_0$ is the electron rest mass and $a_0$ the Bohr radius, $a_0 = 0.53$ Å. For positive particles, the potential minimum is wider by a factor of $\approx d_p/(3Ca)$, and Eq. (IV.2) leads to

$$\nu_p^+ \simeq Z_2^{1/3}\left(\frac{M}{m_0}\right)^{1/2}[Nd_p^3]^{1/2}. \tag{IV.4}$$

The ratio of these two numbers is approximately

$$\nu_p^+/\nu_p^- \simeq Z_2^{1/3}. \tag{IV.5}$$

Even for strong planes, the estimate (IV.3) leads to a number of bound states of the order of unity, $\nu_p^- \sim 1$ for electrons of not too high energy. In contrast, for positrons, the potential minimum between planes may often contain quite a few bound states. We shall return to a more detailed comparison of negative and positive particles below.

*Strings.* For negative particles, the number of bound states in a string potential is given by

$$\nu_s^- \simeq \frac{1}{4\pi^2\hbar^2}\int d^2\bar{r}\int d^2\bar{p}_\perp\Big|_{E_\perp<0}, \tag{IV.6}$$

where $E_\perp = p_\perp^2/(2M) + U(\bar{r})$, and we have assumed that the continuum potential vanishes far from strings. Performing the integration over transverse momentum, we obtain

$$\nu_s^- \simeq \frac{M}{2\pi\hbar^2}\int d^2\bar{r}\,|U(\bar{r})|. \tag{IV.7}$$

Again we may introduce the standard potential, which for strings leads to

$$U(r) \simeq -\frac{Z_2e^2}{d}\log\left(\left(\frac{Ca}{r}\right)^2+1\right), \tag{IV.8}$$

where $d$ denotes the spacing of the atoms in the string. This corresponds to a rotationally symmetric potential inside the area, $\pi r_0^2 = (Nd)^{-1}$, belonging to one string. Subtracting the value $U(r_0)$ from Eq. (IV.8), we obtain from Eq. (IV.7)

$$\nu_s^- \simeq \frac{M}{2\hbar^2}\cdot\frac{Z_2e^2}{d}(Ca)^2\log\left(\frac{r_0}{Ca}\right)^2. \tag{IV.9}$$

Since normally the log term in (IV.9) is of order 3–4, we obtain[11]

$$\nu_s^- \simeq \left(\frac{4a_0}{d}\right)\cdot\left(\frac{M}{m_0}\right)Z_2^{1/3}. \tag{IV.10}$$

By partial integration, the formula (IV.7) may also be expressed in terms of the average square radius of the atoms,

$$\langle R^2\rangle = Z_2^{-1}\int_0^\infty 4\pi R^4\varrho(R)\,dR, \tag{IV.11}$$

where $\varrho(R)$ is the electron density belonging to one atom. The result is

$$\nu_s^- = \frac{M}{2\hbar^2}\cdot\frac{Z_2e^2}{d}\cdot\tfrac{2}{3}\langle R^2\rangle. \tag{IV.12}$$

For the somewhat more realistic Lenz-Jensen potential, the average-square radius becomes[5] $\langle R^2\rangle \simeq 15a^2$, which again leads to (IV.10). For 1-MeV electrons, this formula gives a number of bound states $\nu_s^- \sim 4$–$10$ for a major axis.

For positive particles, the accessible area per string is $\sim \pi r_0^2$. If the effective transverse-energy barrier is $\sim \frac{1}{2} pv\psi_1^2$, corresponding to a critical angle[10],

$$\psi_1 = \left(\frac{4Z_2 e^2}{pvd}\right)^{1/2}, \tag{IV.13}$$

we obtain for the number of bound states (or rather states per string with energy below the barrier, cf. sec. III.1).

$$\nu_s^+ \simeq \frac{1}{\pi}\left(\frac{d}{a_0}\right)\left(\frac{M}{m_0}\right) Z_2 (Nd^3)^{-1}. \tag{IV.14}$$

This number is normally quite large, $\nu_s^+ \sim 10^2$ for 1-MeV positrons.

*Comparison of different cases.* The relationship between the four estimates, Eqs. (IV.3), (IV.4), (IV.10), and (IV.14) is illustrated in Table IV.1 for 1-MeV electrons and positrons along a {110} plane and a ⟨110⟩ axis, respectively, in silicon and gold.

Table IV.1.
Number of bound states for 1-Mev $e^+$, $e^-$ in Si and Au.

| | Silicon | | Gold | |
|---|---|---|---|---|
| | $e^+$ | $e^-$ | $e^+$ | $e^-$ |
| ⟨110⟩ | 34 | 4 | 286 | 9 |
| {110} | 2.5 | 1.1 | 9 | 1.5 |

These examples clearly indicate the importance of distinguishing between positive and negative particles as well as between axial and planar cases. The difference in magnitude of the number of bound states for axes and planes is, to a large extent, due to the fact that the axial potential is two-dimensional, while the planar potential is one-dimensional. It might therefore be argued that the number of bound states in the planar potential should be compared to the square root of the corresponding number for strings. This, however, would not change the qualitative conclusion drawn from Table IV.1, that classical concepts may be applied more readily to axial than to planar motion. This difference is strongest for high values of $Z_2$ where also the difference between electrons and positrons is most pronounced.

*IV.2. Comparison of classical and quantal calculations*

Although the approach towards a classical description is basically governed by the magnitude of quantum numbers, as derived semiclassically above, it must be borne in mind that the validity of classical estimates may depend strongly on the specific phenomenon under observation. In this section, we shall compare directly quantal and classical calculations of the directional dependence of close-encounter yields[34]. The quantal calculations are based on the many-beam description, reviewed in Ch. II, which was seen to describe the experimental results fairly well, at least for planes. From such calculations, also the transverse energy levels are determined, and first we shall compare the number of bound states with the semiclassical estimates.

*Bound states.* The transverse energy levels for electrons and positrons moving along a {110} plane in silicon are shown in Fig. IV.2, as functions of projectile energy. Zero on the ordinate scale corresponds to a transverse energy equal to the potential maximum (cf. Fig. IV.1). The levels are shown for incidence parallel to the plane as well as for an indidence angle equal to the Bragg angle. For negative transverse energy, corresponding to a bound state, the levels become independent of incidence angle because the components of the wave function belonging to different planar channels no longer communicate. Owing to the difference in shape of the potentials (cf. Fig. IV.1), this happens more rapidly with decreasing transverse energy for electrons than for positrons.

In Fig. IV.3, the number of bound states is shown compared to the estimates, Eqs. (IV.3) and (IV.4), derived in the previous section. Also shown in the figure are results obtained for electrons moving along a ⟨111⟩ axis, compared to the estimate in Eq. (IV.10). For this axis, the many-beam calculations were in Sec. II.7 shown to converge reasonably well with number of beams for an electron energy of 0.7 MeV, but for higher energies, the convergence is more doubtful, and the number of bound states may be slightly underestimated. In any case, the agreement is quite good for the axial as well as for the planar cases, considering the approximate nature of the semiclassical estimates. In particular, the predicted differences in both absolute magnitude and energy dependence are clearly confirmed.

*Close-encounter yield.* For the comparison between calculations of the yield of a close-encounter process such as large-angle scattering, we concentrate on the planar case. First, the many-beam calculation is technically simpler and more reliable in this case, owing to the rapid convergence with

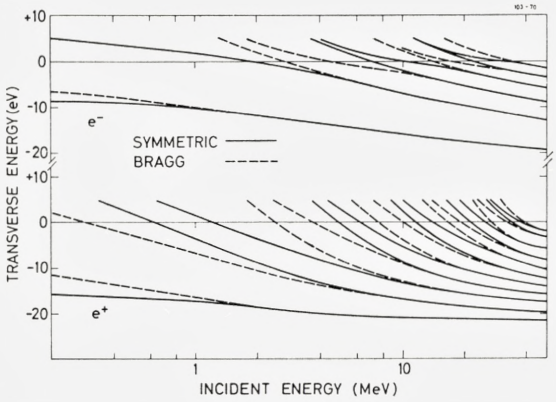


Fig. IV.2: Transverse energy levels for $e-$ and $e+$ incident along a $\{110\}$ plane in Si, as a function of projectile energy. The results are obtained from 20-beam calculations with a thermally averaged (Eq. (III.17)) Molière potential[41]. The levels indicated by solid and dashed curves are obtained for projectile incidence parallel to the plane and at the Bragg angle, respectively. Zero on the ordinate scales corresponds to the maximum of the Molière planar potentials (similar to the potential shown in Fig. IV.1).

number of beams. Second, the classical limit is less well-defined in the axial case, at least for electrons. The classical result derived in the Appendix is based on statistical equilibrium on an energy shell in transverse phase space. In the planar case, this assumption simply leads to results corresponding to an average over depth of penetration, and it is equivalent to the assumption in the quantal calculation of random relative phases of eigenfunctions. For axial channeling, the assumption is based on more subtle arguments, as discussed in the Appendix.

Results for planar channeling of electrons and positrons along a $\{110\}$ plane in silicon are shown in Figs. IV.4 and IV.5. A rapid convergence towards the classical result is indicated, but in contrast to the expectation based on the number of bound states shown in Fig. IV.3, the classical results seem to be somewhat more accurate for electrons than for positrons. In particular is the interference structure at Bragg angles considerably stronger for positrons. This may, however, not be so surprising when we consider the

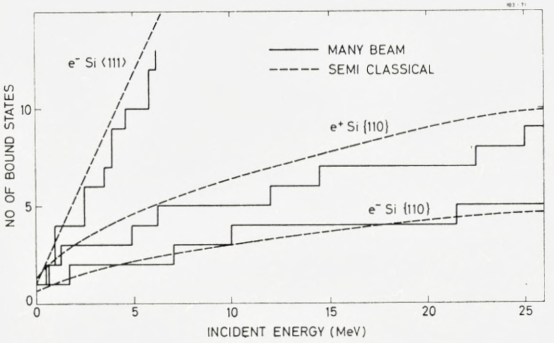


Fig. IV.3: Comparison of the number of bound states derived from Fig. IV.2 with the semiclassical estimates (Eqs. (IV.3) and (IV.4). Also shown are results for a $\langle 111 \rangle$ axis derived from a 60-beam calculation and compared to Eq. (IV.10).

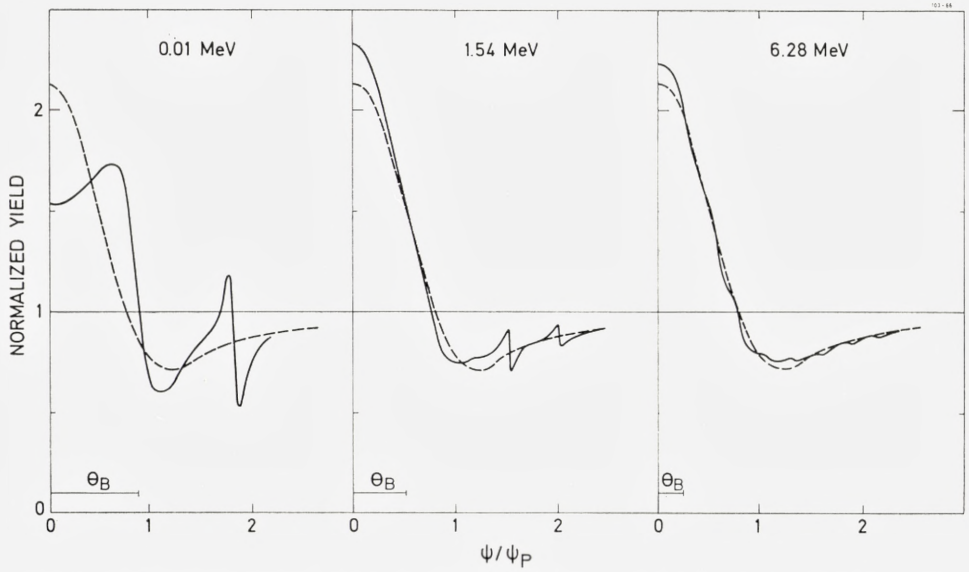


Fig. IV.4: Comparison of classical and quantal calculations of the peak in large-angle-scattering yield for electrons incident on Si along a {110} plane. The classical yield is derived from formulas analogous to those given in Ref. 29 for positive particles, with a thermally averaged Molière planar potential[41], including the contributions from the neighbouring plane (cf. Fig. IV.1). The quantal result is obtained from a 20-beam calculation (Eq. (II.23)), also with the Molière potential and including effects of thermal vibrations (Eqs. (II.15) and (II.17)). The classical result scales with the planar characteristic angle $\psi_p = \psi_1(\mathrm{Ca}/d)^{1/2}$, where $d$ is defined through $Nd^2dp = 1$ (Ref. 29). For each projectile energy, the magnitude of the Bragg angle $\theta_B$ is indicated (classical calculations: dashed curves; quantal calculations: solid curves).

fact that the close-encounter yield is proportional to the intensity of the transverse wave function at the atomic positions. For negative projectiles, lattice atoms are situated in a potential minimum, while for positive particles they are at potential maximum. In the latter case, the results therefore depend on the intensity of wave functions close to or inside classically forbidden regions, where the strongest deviations from classical behaviour occur. (Note also that for silicon, the difference in number of bound states between $e^+$ and $e^-$ is small (cf. Table IV.I).

In spite of the difficulties for axes mentioned above, it may be of interest to compare the quantal and classical calculations also for this case. A set of calculations for electrons incident along a ⟨111⟩ axis is shown in Fig. IV.6. At the higher energies, the agreement is, in fact, rather good. It should be noted that neither of the calculations need correspond very closely to reality. The neglect of inelastic scattering is for axial channeling of negative par-

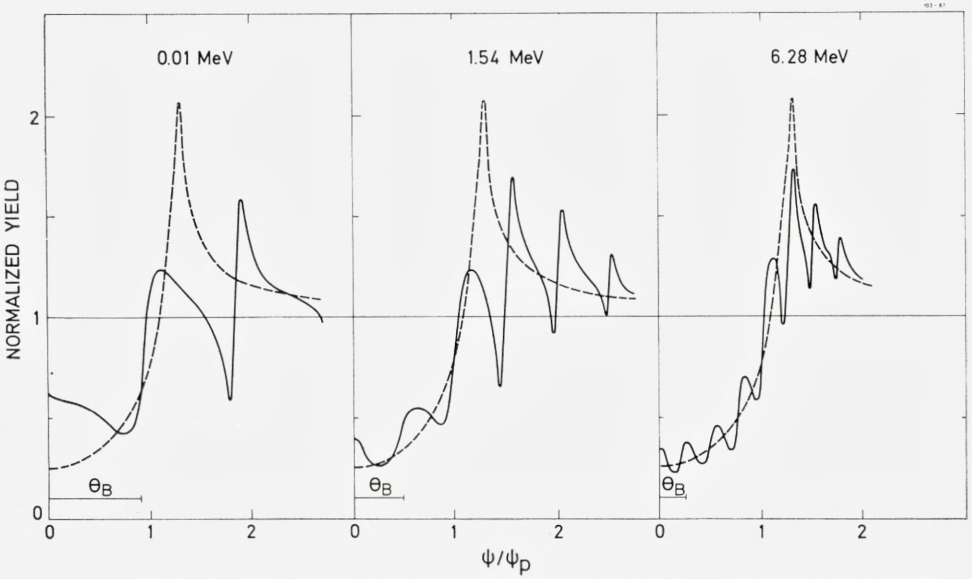


Fig. IV.5: Comparison of quantal (solid curves) and classical (dashed curves) results for positronss incident along {110} plane in Si. For details of the calculations, see Fig. IV.4.

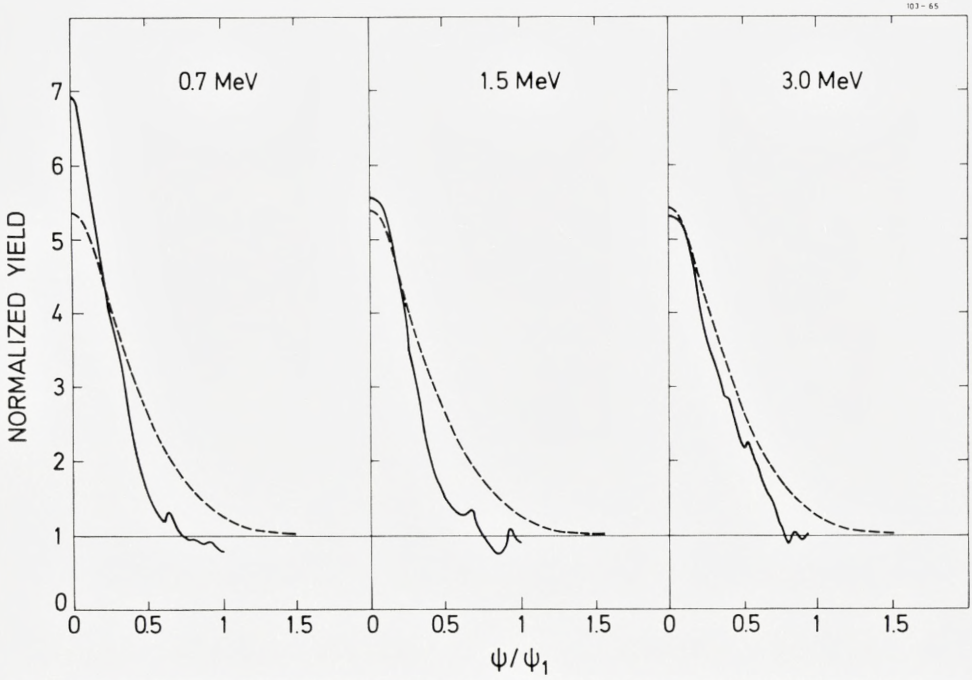


Fig. IV.6: Axial peaks in large-angle-scattering yield for elctrons incident along a ⟨111⟩ direction in Si. Quantal results obtained from 60-beam calculations with Molière potential (formula analogous to Eq. (II.23)) (solid curves). Classical results derived in the Appendix (Eq. (A21)), with the standard potential (Eq. (IV.8)) (dashed curves).

ticles hardly justified even at rather shallow depths since the collisional broadening of closely bound states will be very large. But a statistical treatment is obviously much simplified if classical concepts may be applied, and this should be justified when the volume in phase-space available to bound particles is large enough to correspond to many quantum states.

Finally, for axial channeling of positive particles, the number of "bound" states is very large (cf. Eq. (IV.14) and Table IV.1), and therefore the number of beams needed in a many-beam calculation becomes prohibitively large. However, a comparison of experimental results for positrons and protons indicates[8, 9] that for this case, a classical treatment should be justified.

*Acknowledgements*

For inspiration and guidance through many discussions, we would like to express our gratitude to J. Lindhard. Also the collaboration and discussions with E. Bonderup, A. Howie, and E. Uggerhøj, on problems related to the present work, have been of great value. A special thank to W. L. Brown for providing excellent working conditions in his laboratory during the time when the experimental part of this work was completed.

## Appendix: Classical Estimate for Axial Electron Channeling

In this appendix we shall derive the expression for the axial peak in yield for negative particles, which was used in Chapter IV for comparison with results from "many-beam" calculations. The calculation is based on a classical description of the particle motion. The transverse energy of the particles is assumed to be conserved, and for fixed transverse energy, their trajectories are assumed to fill out the transverse four-dimensional phase-space uniformly. We shall not discuss the validity of these assumptions in detail, but to put the results in perspective it may be useful to review briefly the situation for channeling of positive particles, which has been studied much more thoroughly.

Conservation of transverse energy for channeled particles is the basis of the channeling phenomenon and was discussed in detail by LINDHARD[5]. At large depths of penetration, the distribution in transverse energy is modified due to multiple scattering by electrons and by the small lattice irregularities introduced by the thermal motion of lattice atoms. The effect of these "dechanneling" processes may be calculated with reasonable accuracy from a diffusion equation[5, 42, 43].

Statistical equilibrium, on the other hand, will be established only after a finite depth of penetration. The trend towards equilibrium was studied by LINDHARD[5]. It was shown that when strings are assumed to be randomly distributed in the transverse plane, scattering of the channeled particles by these strings leads to a rapid approach towards equilibrium in transverse-momentum space, the characteristic length being much shorter than that corresponding to dechanneling. At smaller depths, results based on equilibrium may often be interpreted as corresponding to simple averages over azimuthal angle of incidence with respect to a string, and averages over oscillations with depth. As emphasized mainly by BARRETT[44, 45], such an interpretation may not hold in special cases, for example, for the yield of close-encounter reactions for incidence parallel to a string, which at small

depths is higher than estimated from equilibrium by an average factor of 2 to 3. This is a consequence of the regular lattice arrangement of strings, which introduces additional approximately conserved quantities, namely transverse energy with respect to planes (or strings of strings[5]). This will hinder the approach towards equilibrium. A treatment in terms of equilibrium in restricted regions of phase space seems, however, straightforward but has not yet been carried out in detail[46].

Thus for positive particles, the approximations of conservation of transverse energy and statistical equilibrium are consistent and provide a good starting point for a treatment of channeling phenomena. Deviations from these assumptions may then be treated as corrections to the basic picture. For negative particles, however, the situation is less clear. First, multiple scattering is stronger than for positive particles since the atomic scattering centers are situated at a minimum of the transverse potential. Second, the peak in yield is largely due to particles bound in an axial-potential minimum. Such particles interact with only one string, and since the potential is nearly symmetric around the string, angular momentum with respect to this string will be approximately conserved (Rosette motion[47]). Multiple scattering may, however, be strong enough to provide a trend towards equilibrium. In fact, the scattering is strong enough to make the description of the most strongly bound states somewhat uncertain. In the following we disregard these problems and base our treatment upon conservation of transverse energy and statistical equilibrium. The calculations can at least serve as an illustration of the classical treatment, which was discussed in Sec. III.2 and may, as for positive particles, provide a useful standard for comparison, also of experimental results[6, 13] (see also Fig. I.6).

*Emission*

The derivation is analogous to that in Ref. 5 of the dip in yield for positive particles in the continuum approximation. We use the same notation and also consider emission of particles from a lattice atom, i.e., blocking rather than channeling. The two cases are related by reversibility[5] or reciprocity[7]. If electrons with momentum $p$ and velocity $v$ are emitted isotropically from an atom at a distance $r$ from a string, their distribution in transverse energy, $E_\perp$, is given by

$$\pi(E_\perp, r) = \int d(E\varphi^2)\,\delta(E_\perp - U(r) - E\varphi^2) = \begin{cases} 1 \text{ for } E_\perp > U(r) \\ 0 \text{ for } E_\perp < U(r) \end{cases}. \qquad \text{(A1)}$$

Here, $E = 1/2\ pv = 1/2\ Mv^2$, where $M$ is the relativistic mass (cf. Ch. II). The angle with the string is denoted $\varphi$ so that $E\varphi^2$ is the transverse kinetic energy. The transverse potential energy is determined by the average string potential $U(r)$. In the following calculations, we once more apply LINDHARD's standard potential,

$$U(r) = -\tfrac{1}{2}E\psi_1^2 \log\left(\left(\frac{Ca}{r}\right)^2 + 1\right), \tag{A2}$$

where $\psi_1$ is the characteristic angle for axial channeling (Eq. (IV.13)), a the screening distance, and $C \simeq \sqrt{3}$.

The probability of different displacements $r$ is determined by thermal vibrations and denoted $dP(r)$. For the distribution in transverse energy averaged over displacements, we obtain

$$\pi(E_\perp) = \int dP(r) \int d(E\varphi^2)\delta(E_\perp - U(r) - E\varphi^2) = \int dP(r)\Big|_{U(r)<E_\perp}. \tag{A3}$$

By inserting into this formula the standard potential and a Gaussian displacement distribution, LINDHARD obtained a simple analytical estimate of the dip in yield for positive particles.

*Surface transmission*

When the emitted particles pass the crystal surface, the transverse potential energy is lost and the angle $\psi$ with the string after transmission is determined by $E\psi^2 = E_\perp - U(r)$. For the distribution in angle outside the crystal, we may write

$$P(E\psi^2) = \int dE_\perp T(E_\perp, E\psi^2)\pi(E_\perp), \tag{A4}$$

where $T(E_\perp, E\psi^2)d(E\psi^2)$ is the probability for a particle with transverse energy $E_\perp$ in the crystal to leave the surface at an angle $\psi$ to the string. This probability is determined by the spatial probability density of particles with transverse energy $E_\perp$. In statistical equilibrium, the density in two dimensions is uniform in the allowed area, and we obtain

$$T(E_\perp, E\psi^2) = \int_0^{r_0^2} \frac{d(r^2)}{\hat{r}^2(E_\perp)}\,\delta(E\psi^2 - E_\perp + U(r)). \tag{A5}$$

Here we have, as usual, approximated the area per string in the transverse plane by a circular disc of radius $r_0$, related to the spacing $d$ of atoms in the string through $\pi r_0^2 = (Nd)^{-1}$, where $N$ is the density of atoms in the crystal. The radius $\hat{r}$ of the accessible area is given by

$$\left.\begin{aligned} U(\hat{r}) &= E_\perp \quad \text{for} \quad E_\perp < U(r_0) \\ \hat{r} &= r_0 \quad \text{for} \quad E_\perp > U(r_0) \end{aligned}\right\} \tag{A6}$$

By combining (A4) and (A5), we obtain

$$P(E\psi^2) = \int_0^{r_0^2} \frac{d(r^2)}{\hat{r}^2(E\psi^2 + U(r))}\, \pi(E\psi^2 + U(r)). \tag{A7}$$

While for positive particles the difference between the distributions $P(E\psi^2)$ and $\pi(E_\perp)$ implied by (A7) is important for $E\psi^2 \sim 0$ only[29], the surface transmission is of major importance for negative particles. The two distributions are completely different. The function $\pi(E_\perp)$ defined by (A3) is below unity for all values of $E_\perp$ and has a tail stretching to $E_\perp \to -\infty$, while $P$ is only defined for $E\psi^2 > 0$ and has a strong increase above unity at $E\psi^2 \simeq 0$. This peak contains the particles which inside the crystal have negative transverse energy, i.e., which are bound in the string potential.

Inserting into (A7) the emission distribution (A3), we obtain

$$\left.\begin{aligned} P(E\psi^2) &= \int_0^{r_0^2} \frac{d(r^2)}{\hat{r}^2(E\psi^2 + U(r))} \int dP(r') \Big|_{U(r') < E\psi^2 + U(r)} = \\ &= \int_0^{r_0^2} \frac{d(r^2)}{r_0^2} \frac{r_0^2}{\hat{r}^2(E\psi^2 + U(r))} \int_0^{\hat{r}} dP(r'). \end{aligned}\right\} \tag{A8}$$

From this expression it is seen that $P \geq 1$. Thus the peak in yield at small angles $\psi$ is not compensated for by a descrease below unity at larger angles. This lack of compensation is a characteristic feature of the continuum string approximation[5]. In the refined treatment by halfway planes, negative 'shoulders' stretching out to angles $\sim 2a/d$ compensate for the excess yield at small angles.

*Peak height*

From formula (A8), we may calculate the peak height $P(0)$,

$$P(0) = \int_0^{r_0^2} \frac{d(r^2)}{r^2} \int_0^{r} dP(r'). \tag{A9}$$

By inserting a Gaussian distribution,

$$dP(r') = e^{-r'^2/\varrho^2} \frac{d(r'^2)}{\varrho^2}, \quad \varrho \ll r_0, \tag{A10}$$

we obtain by partial integration

$$P(0) \simeq \int_0^{r_0^2} e^{-r^2/\varrho^2} \log\left(\frac{r_0^2}{r^2}\right) \frac{d(r^2)}{\varrho^2} = \log\left(\gamma \frac{r_0^2}{\varrho^2}\right), \tag{A11}$$

where $\gamma$ is Euler's constant, $\gamma = 1.78$. This estimate may be compared to the corresponding estimate in Ref. 11 for the standard potential with a cut-off,

$$U(r) = \begin{cases} -E\psi_1^2 \log \dfrac{Ca}{r}, & r < Ca \\ 0 \quad , & r > Ca \end{cases}, \tag{A12}$$

leading to

$$P(0) \simeq 1 + \log\left(\frac{(Ca)^2\gamma}{\varrho^2}\right) \quad \text{for} \quad Ca \gg \varrho. \tag{A13}$$

While (A11) leads to $P(0) \sim 5$–$6$, formula (A13) predicts a value of $P(0) \sim 2$–$3$. Since the potential decreases very rapidly and is essentially flat at large distances, the implicit assumption in the derivation of (A11) of an attractive potential at all distances $r$ may not be valid at distances $r \sim r_0$. The cut-off at $r = Ca$ in the potential (A12), however, is probably at too small a distance Thus the two values may reasonably be regarded as upper and lower limits, respectively.

*Angular dependence*

With the potential (A12) it is easily seen that the excess yield in (A13) is multiplied by a factor $\exp(-2E\psi^2/E\psi_1^2)$ for particles incident at an angle $\psi$ to the string,

$$P(E\psi^2) \simeq 1 + e^{-2E\psi^2/(E\psi_1^2)} \log\left(\frac{(Ca)^2\gamma}{\varrho^2}\right) \quad \text{for} \quad Ca \gg \varrho \tag{A14}$$

as given in Ref. 11.

In order to obtain a reasonably simple analytical estimate with the standard potential (A2), we replace the Gaussian displacement distribution (A10) by

$$dP(r') = \begin{cases} \dfrac{d(r'^2)}{\varrho_0^2}, & r' < \varrho_0 \\ 0 \quad , & r' > \varrho_0 \end{cases}. \tag{A15}$$

Inserting this distribution into (A9), we obtain for the peak height

$$P(0) = 1 + \log \frac{r_0^2}{\varrho_0^2}. \tag{A16}$$

In order to reproduce the result (A11), we choose

$$\varrho_0^2 = \varrho^2 \cdot \frac{e}{\gamma} = 1.53\varrho^2. \tag{A17}$$

With the distribution (A15), the integration in (A8) is straightforward,

$$P(E\psi^2) = \int_0^{r_1^2} \frac{d(r^2)}{\varrho_0^2} + \int_{r_1^2}^{r_2^2} \frac{d(r^2)}{\hat{r}^2(E\psi^2 + U(r))} + \int_{r_2^2}^{r_0^2} \frac{d(r^2)}{r_0^2}. \tag{A18}$$

where $r_1$ and $r_2$ are determined by

$$\left.\begin{aligned} U(r_1) &= U(\varrho_0) - E\psi^2 \\ U(r_2) &= U(r_0) - E\psi^2. \end{aligned}\right\} \tag{A19}$$

The two first terms correspond to bound particles with a maximum distance to the string not exceeding $\varrho_0$ and $r_0$, respectively, while the third term corresponds to unbound particles. All integrations are elementary, and we obtain,

$$P(E\psi^2) = 1 + e^{-2\psi^2/\psi_1^2} \log(r_2^2/r_1^2) \tag{A20}$$

or inserting the value (A19) for $r_1$ and $r_2$,

$$P(E\psi^2) = 1 + e^{-2\psi^2/\psi_1^2} \log \left\{ (r_0^2/\varrho_0^2) \frac{[(Ca)^2 + \varrho_0^2]\, e^{2\psi^2/\psi_1^2} - \varrho_0^2}{[(Ca)^2 + r_0^2]\, e^{2\psi^2/\psi_1^2} - r_0^2} \right\}. \tag{A21}$$

This formula is rather similar to (A14) for not too small angles. As might be expected, however, the inclusion of the outer shallow part of the potential leads to a steep increase in yield at small angles. In fact, the peak height is larger by a factor of $\sim 2$, and the full width at half maximum is therefore significantly smaller than the value $\Delta\psi = \sqrt{2 \log 2}\ \psi_1$ derived from Eq. (A14).

## References


1) E. Bøgh, J. A. Davies, and K. O. Nielsen, Phys. Letters **12**, 129 (1964).
2) B. Domeij and K. Björkqvist, Phys. Letters **14**, 127 (1965).
3) G. Astner, I. Bergström, B. Domeij, L. Eriksson, and A. Persson, Phys. Letters, **14**, 308 (1965).
4) E. Uggerhøj, Phys. Letters **22**, 382 (1966).
5) J. Lindhard, Mat.-Fys. Medd. Dan. Vid. Selsk. **34**, No 14 (1965).
6) E. Uggerhøj and J. U. Andersen, Can. J. Phys. **46**, 543 (1968).
7) M. von Laue, Materiewellen und Ihre Interferenzen (Akademische Verlagsgesellschaft, Leipzig, 1948).
8) J. U. Andersen, W. M. Augustyniak, and E. Uggerhøj, Phys. Rev. **B3**, 705 (1971).
9) M. J. Pedersen, J. U. Andersen, and W. M. Augustyniak, Rad. Effects **12**, 47 (1972).
10) P. Lervig, J. Lindhard, and V. Nielsen, Nucl. Phys. **A96**, 481 (1967).
11) J. Lindhard, Atomic Collision Phenomena in Solids (North Holland Publishing Co., Amsterdam, 1970), p. 1.
12) E. Uggerhøj and F. Frandsen, Phys. Rev. **B2**, 582 (1970).
13) S. Kjær Andersen, F. Bell, F. Frandsen, and E. Uggerhøj, Phys. Rev. **B8**, 4913 (1973).
14) P. B. Hirsch, A. Howie, R. B. Nicholson, D. W. Pashley, and M. J. Whelan, Electron Microscopy of Thin Crystals (Butterworths, 1965); se also A. Howie in *Modern Diffraction and Imaging Tcehniques in Materials Science* (North-Holland, Amsterdam 1970), p. 295.
15) P. B. Hirsch, A. Howie, and M. J. Whelan, Phil. Mag. **7**, 2095 (1962).
16) P. Duncomb, Phil. Mag. **7**, 2101 (1962).
17) C. R. Hall, Proc. Roy. Soc. **A295**, 140 (1966).
18) A. Howie, M. S. Spring, and P. N. Tomlinson, Atomic Collision Phenomena in Solids (North Holland Publishing Company, Amsterdam, 1970), p. 34; see also P. N. Tomlinson and A. Howie, Phys. Letters **27 A**, 491 (1968).
19) M. J. Whelan, Atomic Collision Phenomena in Solids (North-Holland Publishing Company, Amsterdam, 1970), p. 3.
20) A. Howie, Phil. Mag. **14** 223 (1966), and Brookhaven National Laboratory, Report No 50083, Solid State Physics with Accelerators (1967) p. 15.
21) R. E. De Wames and W. F. Hall, Acta Cryst. **A24**, 206 (1968).
22) R. E. De Wames, W. F. Hall, and G. W. Lehmann, Phys. Rev. **174**, 392 (1968).
23) L. T. Chadderton, Phil. Mag. **18**, 1017 (1968).

24) L. T. Chadderton, J. Appl. Cryst. **3**, 429 (1970).
25) M. V. Berry, J. Phys. **C 4**, 697 (1971).
26) M. V. Berry, Rad. Effects **27**, 1 (1973).
27) D. S. Gemmel, Rev. Mod. Phys. **46**, 129 (1974).
28) L. T. Chadderton in *Channeling*, ed. D. V. Morgan (Wiley, N. Y. 1973).
29) J. U. Andersen, Mat. Fys. Medd. Dan. Vid. Selsk. **36** No. 7 (1967), J. U. Andersen and L. C. Feldman, Phys. Rev. **B1**, 2063 (1970).
30) J. U. Andersen, J. A. Davies, K. O. Nielsen, and S. L. Andersen, Nucl. Instr. Methods **38**, 210 (1965).
31) N. Bohr, Mat.-Fys. Medd. Dan. Vid. Selsk. **18** No 8 (1948).
32) E. Keil, E. Zeitler, and W. Zinn, Z. Naturforsch. **15a**, 1031 (1960).
33) F. Fujimoto, S. Takagi, K. Komaki, H. Koike, and Y. Uchida, Rad. Effects **12**, 153 (1972).
34) S. Kjær Andersen, Thesis, University of Aarhus (1974).
35) A. Howie and R. M. Stern, Z. Naturforschung **27a**, 382 (1972).
36) J. P. Spencer, C. J. Humphreys, and P. B. Hirsch, Phil. Mag. **26**, 193 (1972).
37) Y. Kagan and Y. V. Kononets, Zh. Edsp. Teor. Fiz. **58**, 226 (1970). [Sov. Phys. -JETP **31**, 124 (1970)].
38) C. J. Humphreys and P. B. Hirsch, Phil. Mag. **18**, 115 (1968).
39) D. Cherns, A. Howie, and M. H. Jacobs, Z. Naturforsch. **28a**, 565 (1973).
40) D. Bohm, *Quantum Theory* (Prentice-Hall, N. Y. 1951)
41) B. R. Appleton, C. Erginsoy, and W. M. Gibson, Phys. Rev. **161**, 330 (1967).
42) E. Bonderup, H. Esbensen, J. U. Andersen, and H. E. Schiøtt, Rad. Effects **12**, 261 (1972).
43) H. E. Schiøtt, E. Bonderup, J. U. Andersen, H. Esbensen, M. J. Pedersen, D. J. Elliott, and E. Lægsgaard, in Proc. 5th Conf. on Atomic Collisions in Solids, Gatlinburg, Tenn., Vol. 2, p. 843 (1973).
44) J. H. Barrett, Phys. Rev. **166**, 219 (1968).
45) J. H. Barrett, Phys. Rev. Letters **31**, 1542 (1973).
46) J. A. Golovchenko, Phys. Rev. **B 13**, 4672 (1976).
47) H. Kumm, F. Bell, R. Sizmann. and H. J. Kreiner, Rad. Effects **12**, 53 (1972).

Indleveret til Selskabet august 1976.
Færdig fra trykkeriet september 1977.

PETER SIGMUND

# CLASSICAL SCATTERING OF CHARGED PARTICLES BY MOLECULES

*Single and Multiple Collisions at Small Angles*

Det Kongelige Danske Videnskabernes Selskab
Matematisk-fysiske Meddelelser **39**, 11


Kommissionær: Munksgaard
København 1977

## Table of Contents



### Synopsis


The effect of *molecular geometry* on *single and multiple scattering of charged particles* off molecules is investigated theoretically. The treatment is based on *classical scattering* theory and is valid at small scattering angles. Two limiting cases are identified; a short-range limit where atoms within a molecule act as separate scattering centers, and a long-range limit, where a molecule acts as one scattering center. The transition region is shown to fall into the range of impact parameters corresponding to moderately screened Coulomb scattering, i.e., the typical *Thomas-Fermi scattering* region. General expressions are derived for single-collision cross sections valid in each limit and in the transition region, and for the half-widths of angular and lateral multiple-scattering distributions. Comments are made upon the behaviour of the shape of multiple-scattering profiles. Quantitative results are based on the *power approximation* to the Thomas-Fermi and Lenz-Jensen interaction. Comparison with recent experimental results on multiple-scattering half-widths for the $Pb^{+}-N_2$ system shows excellent agreement. Even more pronounced effects are predicted for polyatomic molecules.




Printed in Denmark by Bianco Lunos Bogtrykkeri A/S. ISBN 87-7304-080-0

## 1. Introduction

When asked to describe the interaction between an energetic particle and a molecule, you will most likely choose one of two simplifications as your starting point. Either you consider the molecule as one target particle, with a suitably simplified shape (spherical, linear, etc.), or you treat it as being composed of independent atoms. Which of the two simplifications you will judge to be the more appropriate one depends on the effective range of interaction. In typical molecular-beam experiments, at *eV* energies or below, collision partners interact at distances well up to, and greater than, internuclear distances in molecules, hence the first description is likely to be preferred. Conversely, *MeV* or more energetic particles have their most violent encounters at very small internuclear distances, whence the second description might seem more appropriate. Indeed, a very customary approach to penetration problems in molecular solid or gaseous targets is to ignore molecular structure altogether, and to consider instead a mixture of randomly distributed atoms of the right overall density and composition.

There must be an intermediate situation where neither description is appropriate. As an example, let the typical interaction distance be of the order of one half the internuclear distance in a binary target molecule, and let the target be a dilute gas of such binary molecules. Then, every collision of the projectile with one target atom is accompanied by another collision with the other atom in the molecule. While the impact parameter specifying the first collision is distributed at random, the corresponding quantity for the second collision is obviously correlated. Whereas in an atomic gas of equal composition all collisions would obey a random distribution of impact parameters, only half of them do so in the molecular gas. Thus, molecular geometry has an influence on the spectral distribution of energy loss, deflection angles, and excitation phenomena. It is the purpose of this paper to investigate the influence of molecular geometry on small-angle single and multiple scattering of a beam of charged particles penetrating a molecular gas. In a related paper, the corresponding problem of energy loss is treated[1]. A short note reporting some conclusions of the present work as well as experimental results on multiple scattering by molecules has appeared recently[2].

The geometric effects discussed in this paper are characteristic of such scattering processes where the trajectory of the scattered particle as well as the location of the scatterer are well-defined in terms of a classical-orbit picture. There is a broad range of heavy-particle scattering processes, initial energies, and scattering angles where the scattering cross sections derived from classical dynamics can be applied in the analysis. These include the scattering of *MeV* fission fragments in solids or gases at the one end, and the scattering of *keV* or even *eV* helium and hydrogen ions in dilute gas targets at the other end. Criteria for the validity of a classical-orbital picture have been established[3,4], and are fulfilled in those cases where numerical results are given in this paper. Experimental work has been reviewed recently[5,6].

The present analysis has been developed in close analogy and simultaneously with related work on energy loss[1], and the outline of this paper has been deliberately chosen to be that of a follow-up. Although the presentation is hopefully self-contained, you may find it advantageous to first have a look at the simpler, 1-dimensional problem of energy loss.

## 2. General Description

Let a charged particle (usually an energetic ion) pass by a molecule (Fig. 1) at a vector distance $\mathbf{p}$ from some point $Q$ that specifies the position of the molecule. Throughout this paper, we only consider situations where the deflection of the projectile at the molecule (and at its constituent atoms) is so small that the trajectory can be approximated by a straight line over the range of interaction with the molecule. This implies high velocity and/or large impact parameter $p(= |\mathbf{p}|)$. Within the region of validity of classical scattering, the ion is scattered by some angle

$$\varphi = \varphi(\mathbf{p}, \Omega),$$

where $\Omega$ stands for three or two angles that specify the orientation of the target molecule with respect to the direction of motion of the projectile. We shall assume that $\varphi$ is also small in an absolute sense, such that the direction of motion of a scattered ion is determined by a small increment

$$\boldsymbol{\varphi} = \boldsymbol{\varphi}(\mathbf{p}, \Omega) \tag{1}$$

to be added (and perpendicular to) the unit vector along the initial direction (Fig. 1). With that direction representing a polar axis, we can introduce an "impact plane" perpendicular to it; this plane contains the 2-dimensional

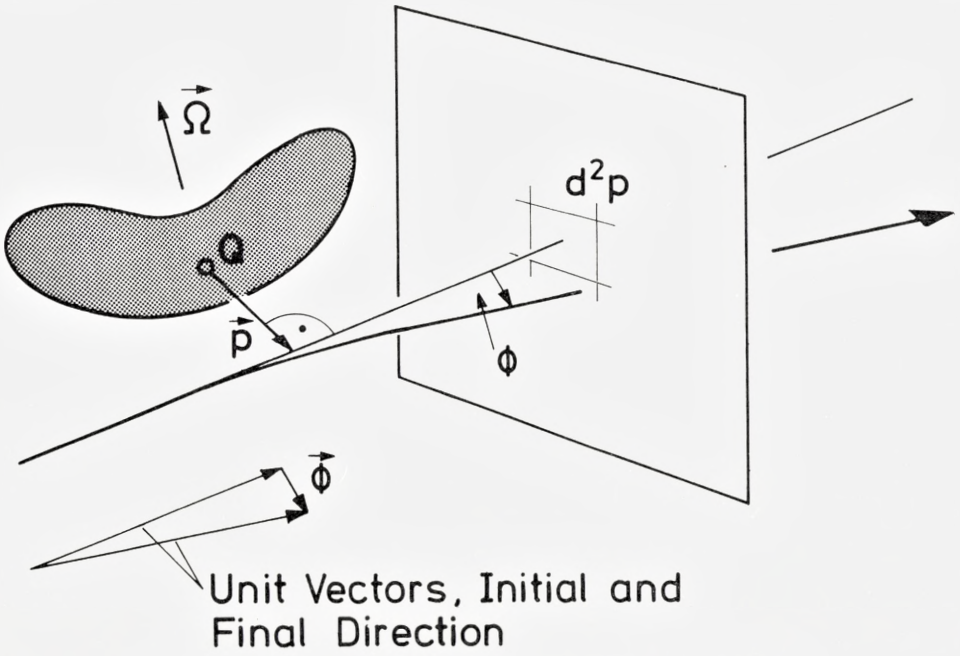


Fig. 1. Geometry of charged-particle scattering on a molecule.

vectors $\mathbf{p}$ and $\varphi$. In accordance with the conventional concept of a cross section we denote the quantity

$$d\sigma \equiv K(\varphi)d^2\varphi = d^2\varphi \int d^2\mathbf{p}\,\delta(\varphi - \varphi(\mathbf{p},\Omega)) \tag{2}$$

the differential cross section for scattering into the solid angle $d^2\varphi$ at $\varphi$, where $\delta$ is the Dirac delta funtion in two dimensions, and $d^2\mathbf{p}$ an element of the impact plane (Fig. 1).

Eq. (2) applies to a polarized gas, i.e. where all target molecules have the same orientation $\Omega$. For random orientation, we generalize (2) so that

$$K(\varphi) = \int d^2\mathbf{p} \langle \delta(\varphi - \varphi(\mathbf{p},\Omega)) \rangle_\Omega \,, \tag{2'}$$

where $\langle \ldots \rangle_\Omega$ indicates an average over all orientations.

It will be convenient in the following to carry on the analysis in the Fourier space conjugate to $\varphi$. In order to avoid the complications of a possible divergency at $\varphi = 0$, we consider the transport cross section

$$\sigma(\mathbf{k}) = \int d^2\varphi K(\varphi)(1 - e^{i\mathbf{k}\cdot\varphi}) = \int d^2\mathbf{p} \langle (1 - e^{i\mathbf{k}\cdot\varphi(\mathbf{p},\Omega)}) \rangle_\Omega \,, \tag{3}$$

from which the differential cross section can be recovered[7] by inverse Fourier transformation,

$$K(\varphi) = -\frac{1}{(2\pi)^2}\int d^2k\ \sigma(\mathbf{k})e^{-i\mathbf{k}\cdot\varphi} \qquad \text{for} \qquad \varphi \neq 0. \tag{4}$$

### 3. Binary Molecules. General

Let us first consider a binary target molecule. The total deflection $\varphi$ is then composed of two parts,

$$\varphi = \varphi_1 + \varphi_2, \tag{5}$$

i.e., the respective (vectorial) scattering angles belonging to the constituent atoms 1 and 2 of the molecule. Such a division is straight forward in case of a hypothetical molecule consisting of two nonoverlapping target atoms. In real molecules, the region of overlapping electron shells is occupied by valence electrons; these contribute to scattering only in a certain class of (very soft) collisions. In cases where this is important, scattering regions for atoms 1 and 2 may have to be defined. In case of a minor contribution of valence electrons to the scattering potential, the above picture of a molecule consisting of two unperturbed target atoms appears acceptable. This implies that the *individual* scattering vectors in (5) exhibit radial symmetry,

$$\varphi_i = \varphi_i(\mathbf{p}_i) = \varphi_i(p_i)\mathbf{p}_i/p_i, \qquad i = 1, 2. \tag{6}$$

where $\mathbf{p}_1$ and $\mathbf{p}_2$ are distance vectors from the two target nuclei to the trajectory (Fig. 2), and $p_i = |\mathbf{p}_i|$ the individual impact parameters.

Eq. (3) can now be written in the form

$$\sigma(\mathbf{k}) = \langle\int d^2\mathbf{p}(1 - e^{i\mathbf{k}\cdot(\varphi_1(\mathbf{p}_1)+\varphi_2(\mathbf{p}_2))}\rangle_\Omega\,, \tag{7'}$$

which can be rearranged in the form

$$\sigma(\mathbf{k}) = \sigma_1(\mathbf{k}) + \sigma_2(\mathbf{k}) + \delta\sigma(\mathbf{k}). \tag{7}$$

Here,

$$\sigma_i(\mathbf{k}) = \langle\int d^2\mathbf{p}(1 - e^{i\mathbf{k}\cdot\varphi_i(\mathbf{p}_i)})\rangle_\Omega \equiv \int d\sigma_i(1 - e^{i\mathbf{k}\cdot\varphi}); \qquad i = 1, 2, \tag{8}$$

with $d\sigma_i(\varphi)$ being the differential cross section of atom $i$; because of (6), the rotational average has no effect on eq. (8). The following interference term remains,

$$\delta\sigma(\mathbf{k}) = -\langle\int d^2p(1 - e^{i\mathbf{k}\cdot\varphi_1(\mathbf{p}_1)})(1 - e^{i\mathbf{k}\cdot\varphi_2(\mathbf{p}_2)})\rangle_\Omega\,; \tag{9}$$

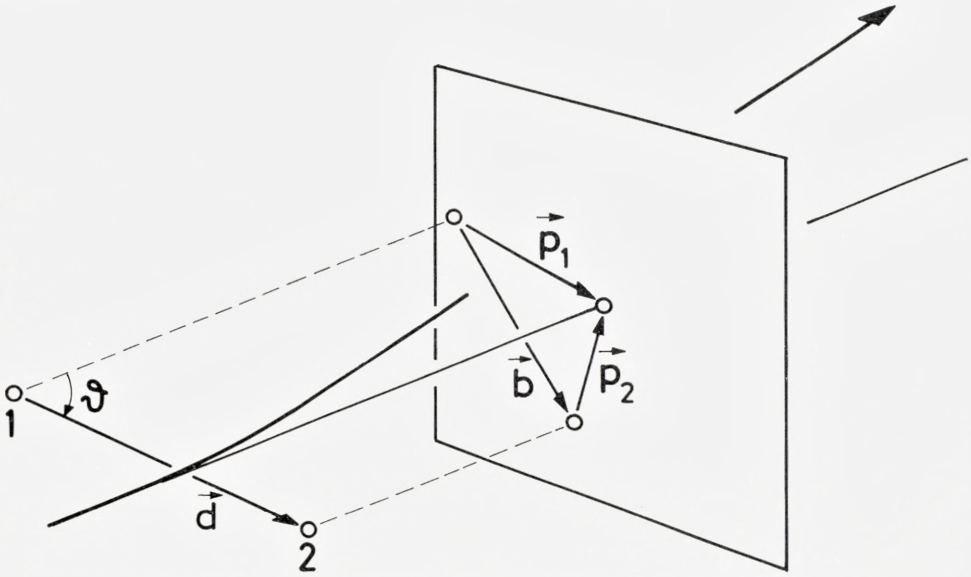


Fig. 2. Geometry of charged-particle scattering on a diatomic molecule.

this term is nonpositive, and composed of contributions from those impact parameters $p_1$ and $p_2$, and orientations $\Omega$, where both $\varphi_1$ and $\varphi_2$ are nonzero. (The orientational dependence ($\Omega$) is implicit in $\mathbf{p}_1$ and $\mathbf{p}_2$).

## 4. Binary Molecules. Evaluation of the Transport Cross Section

Let the internuclear distance vector in the molecule be $\mathbf{d}$, and its projection on the impact plane be $\mathbf{b}$. Then (Fig. 2),

$$\mathbf{b} = \mathbf{p}_1 - \mathbf{p}_2, \tag{10}$$

and

$$\delta\sigma(\mathbf{k}) = -\int d^2\mathbf{p}_1(1 - e^{i\mathbf{k}\cdot\varphi_1(\mathbf{p}_1)})\int d^2\mathbf{p}_2(1 - e^{i\mathbf{k}\cdot\varphi_2(\mathbf{p}_2)})\cdot\langle\delta(\mathbf{p}_1 - \mathbf{p}_2 - \mathbf{b})\rangle_\Omega. \tag{11}$$

The last factor in the integral has been evaluated previously[1]; it is easily found to be

$$\langle\delta(\mathbf{p}_1 - \mathbf{p}_2 - \mathbf{b})\rangle_\Omega = \frac{1}{2\pi d^2}(1 - (\mathbf{p}_1 - \mathbf{p}_2)^2/d^2)^{-1/2} \tag{12}$$

for $|\mathbf{p}_1 - \mathbf{p}_2| \leq d = |\mathbf{d}|$, and zero otherwise. In those situations where the integral (11) is made up mainly of contributions from impact parameters $|\mathbf{p}_1 - \mathbf{p}_2| \ll d$, we obtain from (11) and (12) the asymptotic relationship

$$\delta\sigma(\mathbf{k}) \sim -\frac{\sigma_1(\mathbf{k})\,\sigma_2(\mathbf{k})}{2\pi d^2}, \tag{13}$$

by means of eq. 8. Therefore, eq. 7 reads*

$$\sigma(k) = \sigma_1(k) + \sigma_2(k) - \frac{\sigma_1(k)\,\sigma_2(k)}{2\pi d^2} \ldots \text{ for "large } d\text{"} \tag{14}$$

In the opposite limit of a large interaction range ($\rangle\rangle\, d$), Taylor expansion of the delta function in (11) yields

$$\langle \delta(\mathbf{p}_1 - \mathbf{p}_2 - \mathbf{b})\rangle_\Omega = \delta(\mathbf{p}_1 - \mathbf{p}_2) + \frac{d^2}{6}\nabla^2_{\mathbf{p}_1}\delta(\mathbf{p}_1 - \mathbf{p}_2)\ldots$$

and, by direct evaluation of eq. (7′),

$$\sigma(\mathbf{k}) = \int d^2\mathbf{p}(1 - e^{i\mathbf{k}\cdot(\varphi_1+\varphi_2)}) - \frac{d^2}{6}\int d^2\mathbf{p} e^{i\mathbf{k}\cdot\varphi_2}\nabla^2_{\mathbf{p}}\, e^{i\mathbf{k}\cdot\varphi_1} \ldots \text{ for "small } d\text{"} \tag{15}$$

where $\varphi_i$ now stands for $\varphi_i(\mathbf{p})$.

## 5. Power Scattering

The integrals that appeared in the previous section offer themselves for convenient evaluation in the particular case of power scattering

$$\varphi_i(p) = \frac{C_i}{p^s}; \qquad i = 1, 2 \tag{16}$$

with a positive parameter $s$. It is known[3–5] that within the small-angle approximation, (16) represents the scattering law for a repulsive interaction potential $\propto R^{-s}$ where $R$ is the distance from the scattering center. The quantity $C_i$ contains atomic parameters and is inversely proportional to the energy. Thus, at any given impact parameter $p$, the small-angle assumption can always be fulfilled by choice of a sufficiently high ion energy.

* *Note added in proof:* Eq. (14) is formally very similar to an expression derived by Glauber[18] for the forward scattering amplitude in GeV nucleon-deuteron scattering. The underlying physical effect in that case is a mutual shadowing of two independent scatterers. This shadowing effect has the same origin as the correlation effects considered in the present work as well as in previous work on energy loss[1], i.e., the geometric structure of the target particle, but it is otherwise different because of the rather different scattering mechanism. In particular, Glauber's treatment of diffraction scattering yields an interference term corresponding to (13) that is a factor of two smaller. I am grateful to N. Andersen for drawing my attention to a note referring to Glauber's work.

It is known that by proper choice of the power $s$, an accurate representation can be found for repulsive atomic interaction potentials[3], cross sections for screened-Coulomb scattering[4], and multiple-scattering profiles[8]. For the present purpose, the assumption of *one* exponent $s$ applying to *both* atoms ($i = 1, 2$) is an important mathematical simplification. Except in case of very different masses of the constituent atoms, this assumption is not a severe physical limitation.

Inserting (16) into (8), we obtain[7]

$$\sigma_i(k) = A_i k^{2m} \tag{17}$$

with

$$A_i = \pi \frac{\Gamma(1 - m)}{\Gamma(1 + m)} (C_i/2)^{2m} \tag{17a}$$

and

$$m = 1/s \tag{17b}$$

Moreover, (15) reads

$$\sigma(k) = Ak^{2m} + Bd^2 + \ldots \tag{18}$$

with

$$A = (A_1{}^{s/2} + A_2{}^{s/2})^{2m} \tag{18a}$$

and

$$B = \frac{\pi}{3}(s - m) \frac{C_1 C_2}{(C_1 + C_2)^2}. \tag{18b}$$

## 6. Single Scattering. Differential and Incomplete Total Cross Section

After inserting (14) into (4), and observing (17) we obtain the following expression for the single-collision cross section of a diatomic molecule in the power approximation, in the limit of short-range interaction,

$$K(\varphi) = K_1(\varphi) + K_2(\varphi) - \frac{R(m)}{m} \cdot \frac{K_1(\varphi) K_2(\varphi) \varphi^2}{d^2} \ldots \tag{19'}$$

where

$$K_1(\varphi) = \frac{A_1 m}{\pi} \varphi^{-2-2m} \frac{2^{2m} \Gamma(1 + m)}{\Gamma(1 - m)} \tag{20}$$

and

$$R(m) = \frac{\Gamma(1 + 2m) \Gamma(1 - m)^2}{\Gamma(1 - 2m)\, \Gamma(1 + m)^2} \tag{21}$$

$R(m)$ has been plotted in fig. 3.

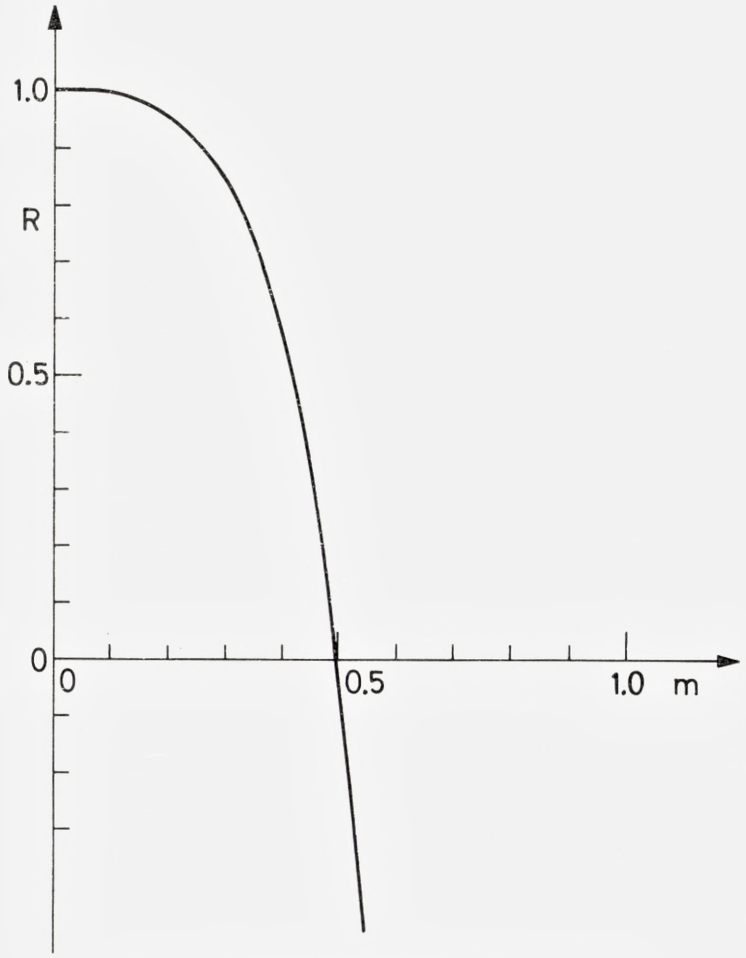


Fig. 3. The quantity $R$ defined by (21), versus m.

In the (more familiar) notation

$$d\sigma \equiv K(\varphi)d^2\varphi \equiv \frac{d\sigma}{d\varphi}\,d\varphi, \tag{22}$$

(19') reads

$$\frac{d\sigma}{d\varphi} = \frac{d\sigma_1}{d\varphi} + \frac{d\sigma_2}{d\varphi} - \frac{R(m)}{m}\,\frac{\varphi}{2\pi d^2}\,\frac{d\sigma_1}{d\varphi}\,\frac{d\sigma_2}{d\varphi} + \ldots; \tag{19}$$

the subsequent term in the series would be proportional to $d^{-4}$. In the opposite limit of long-range interaction, eq. (18) yields

$$\left.\begin{aligned} K(\varphi) &= \frac{m}{\pi} \cdot A \cdot \varphi^{-2-2m} \frac{2^{2m}\Gamma(1+m)}{\Gamma(1-m)} + \ldots \\ &= [(K_1(\varphi))^{s/2} + (K_2(\varphi))^{s/2}]^{2m} + \ldots , \end{aligned}\right\} \tag{23}$$

and the subsequent term in the series would behave like $d^2 \cdot \delta(\varphi)$; it has to be dropped, according to eq. (4).

In small-angle single-scattering experiments, it is most often the incomplete total cross section

$$\sigma_{\text{tot}} = \int_{\varphi_c}^{\pi} d\varphi \frac{d\sigma}{d\varphi} \tag{24}$$

which is the measured quantity. Here, $\varphi_c$ is a (very small) limiting angle defined by the geometry of the apparatus. From eqs. (19) and (23) we obtain by integration

$$\sigma_{\text{tot}} = \sigma_{1,\text{tot}} + \sigma_{2,\text{tot}} - R(m) \frac{\sigma_{1,\text{tot}}\,\sigma_{2,\text{tot}}}{2\pi d^2} \ldots \tag{25}$$

for large $d$ (short-range limit), and

$$\sigma_{\text{tot}} = [(\sigma_{1,\text{tot}})^{s/2} + (\sigma_{2,\text{tot}})^{s/2}]^{2m} + \ldots \tag{26}$$

for small $d$ (long-range limit). Alternatively, (25) is a high-energy, and (26) a low-energy expansion.

Take, as an example, the case of a homonuclear binary molecule. Then, eqs. (19′), (19), and (25) represent the limit of a molecule consisting of two independent, identical scattering centers, and the apparent cross section is twice the cross section of a single atom (for $d \to \infty$). Conversely, eqs. (23) and (26) represent the case of a molecule acting as one target particle, the apparent cross section (averaged over all orientations) being $2^{2m}$ times the cross section of a single atom. This value is smaller (larger) than the former one provided that $m$ is smaller (larger) than 1/2. The behaviour of the numerical factor $R(m)$ in (19′), (19), and (25) is consistent herewith: $R(m) \gtrless 0$ for $m \lessgtr 1/2$. Therefore, so long as the inter-atomic potential itself is reasonably close to a power potential, we can expect that the two limiting expansions, with some possible interpolation, describe the small-angle single-scattering cross section of a molecule satisfactorily. As will be shown in the following section, the short range limit (19) is appropriate in existing differential measurements, while it is not normally reached in measurements of the incomplete total cross section.

## 7. Application: Thomas-Fermi Scattering for Homonuclear Diatomic Target Molecule

Lindhard et al.[4] have given a very compact description of the elastic scattering between heavy atomic particles on the basis of a Thomas-Fermi (TF) interatomic potential. Their description hinges on the power-like behaviour of the TF potential over a moderately wide range of interaction energies. In their description[4],

$$d\sigma = \pi a^2 \frac{d\eta}{\eta^2} f(\eta) \tag{27}$$

where $a$ is the screening radius of the interaction, and*

$$\eta = \varepsilon \sin \theta/2 \tag{28}$$

with $\theta$ the center-of-mass scattering angle, and $\varepsilon$ the center-of-mass energy in units of $Z_1 Z_2 e^2/a$, $Z_1$ and $Z_2$ being atomic numbers of ion and target *atom*. $f(\eta)$ is some (given) universal function that can be approximated as

$$f(\eta) = \lambda \eta^{1-2m} \tag{29}$$

over limited regions of $\eta$, with $\lambda$ a dimensionless constant depending on $m$, and $m$ ranging from slightly greater than 0 to 1. $m = 1$ refers to Rutherford scattering.

In the small angle approximation, (28′) can be written in the form

$$\eta = \frac{E}{Z_1 Z_2 e^2/a} \cdot \frac{\varphi}{2} \equiv \tilde{\varphi}, \tag{28′}$$

where $E$ is the laboratory energy, and the last part defines the scaled laboratory scattering angle $\tilde{\varphi}$. (21) reads, then

$$\frac{d\sigma}{d\tilde{\varphi}} = \frac{\pi a^2}{\tilde{\varphi}^2} f(\tilde{\varphi}) \quad \text{for} \quad \varphi \ll 1. \tag{27′}$$

The TF description is valid mostly at comparatively small interaction distances ($\lesssim a_0 = 0.529\,\text{Å}$). Therefore, the TF cross section for a diatomic homonuclear molecule is to be found primarily from eq. (19) which reads, by means of (27′)

* The notation $t^{1/2}$ is frequently found in the literature for $\eta$.

$$\left.\begin{aligned}\frac{d\sigma}{d\tilde{\varphi}} &= 2\frac{d\sigma_1}{d\tilde{\varphi}} - \frac{R(m)}{m}\frac{\tilde{\varphi}}{2\pi d^2}\left(\frac{d\sigma_1}{d\tilde{\varphi}}\right)^2 \cdots \\ &= \frac{2\pi a^2}{\tilde{\varphi}^2} f(\tilde{\varphi})\left[1 - \frac{R(m)}{4m}\cdot\frac{a^2}{d^2}\frac{f(\tilde{\varphi})}{\tilde{\varphi}} \cdots\right].\end{aligned}\right\} \quad (29')$$

In the limit of large $E$, i.e. large $\tilde{\varphi}$, the expression in brackets is small, and the molecule acts like two independent atoms. The case of strict Rutherford scattering ($m = 1$) has to be excluded, however, since the expansion (19) is not applicable in that case ($R(m = 1) = -\infty$). Pronounced deviations from the independent-atom picture occur at small values of $\tilde{\varphi}$, i.e. at low energies and/or small angles. In that case, ($\tilde{\varphi} \lesssim 0.1$) the TF interaction is described well by (29) with[9]

$$m = 1/3; \qquad \lambda = 1.309, \quad (30)$$

and the factor in the brackets of (29) reads, then,

$$1 - 0.761\frac{a^2}{d^2}\tilde{\varphi}^{-2/3} \qquad \text{(TF)} \quad (31)$$

since $R(1/3) = 0.775$. For medium-mass collision partners we have[3, 4] $a \cong 0.885\, a_0(Z_1^{2/3} + Z_2^{2/3})^{-1/2} \sim 10^{-1}$ Å, i.e. $a^2/d^2 \sim 10^{-2}$. Hence, measurable deviations from 1 occur for $\tilde{\varphi} \lesssim 0.1$, and the expansion breaks down above $\tilde{\varphi} \sim 10^{-3}$. In fact, the low-energy limit (23) yields

$$d\sigma/d\tilde{\varphi} \to 2^{2/3}\, d\sigma_1/d\tilde{\varphi}; \quad (32)$$

this value is reached, according to (31), at

$$\tilde{\varphi} \approx 7\frac{a^3}{d^3},$$

i.e. around $\tilde{\varphi} \sim 10^{-2}$. Thus, the following qualitative picture arises for the small-angle scattering on molecular targets.

i) At scattering angles corresponding to $\tilde{\varphi} = \eta > 1$, a molecule behaves with high accuracy (better than 1 pct.) like two independent atoms.
ii) In the region $10^{-2} \lesssim \tilde{\varphi} \lesssim 1$ the cross section of a molecule becomes measurably smaller than that of two independent atoms.
iii) In the region $\tilde{\varphi} \lesssim 10^{-2}$ the cross section approaches the long-range limit.

Now, conventional small-angle scattering experiments that have been performed on molecular gas targets[5, 10] (in the $\sigma_{tot}$-geometry) dealt with impact parameters in the Born-Mayer region, where $\tilde{\varphi} < 10^{-3}$, and thus refer to the long-range limit. The analysis of those experiments has been based on a molecular picture. The present analysis confirms this picture but adds little new to it. In fact, it is oversimplified in this respect since valence electrons are important there, but are not taken into account explicitly.

Conversely, differential cross section measurements tend to deal with large enough angles and/or energies so that $\tilde{\varphi} > 1$, and the short-range limit should apply. A notable exception is Loftager's setup[11] where differential cross sections have been determined in the genuine TF region ($10^{-3} \lesssim \tilde{\varphi} < 10$), i.e. including the transition region between the long- and short-range limit. So far, mainly experiments with noble-gas targets have been performed, but pronounced molecular effects would be expected. Since, in that work, the atomic interaction appeared to be closer to a Lenz-Jensen (LJ) potential as characterized by (29) with[12]

$$m = 0.191; \qquad \lambda = 2.92 \tag{33}$$

at small values of $\eta$, we also quote the expression corresponding to (31) for LJ interaction,

$$1 - 3.68 \frac{a^2}{d^2} \tilde{\varphi}^{-0.382}; \tag{34}$$

the long-range limit $d\sigma/d\tilde{\varphi} \to 2^{0.382}\, d\sigma_1/d\tilde{\varphi}$ is reached around $\tilde{\varphi} = 500\,(a/d)^5 \sim 1/2 \cdot 10^{-2}$, i.e. at a similar value as in the TF case*.

## 8. Multiple Scattering. Angular and Lateral Distributions

In typical multiple-scattering experiments, either an angular distribution $F(x,\alpha)d\Omega$ of an initially collimated beam, or a lateral distribution $G(x,\varrho)d^2\rho$ is observed (fig. 4), where $x$ is the travelled distance in the target. In the small-angle approximation, the angular distribution is given by Bothe's formula[7]

$$F(x,\alpha) = \frac{1}{2\pi} \int_0^\infty dk\, k\, J_0(k\alpha) e^{-N' x \sigma(k)}, \tag{35}$$

* Since the Lenz-Jensen interaction potential, contrary to the TF potential, does not approach power form at large inter-atomic distances, eqs. (29) and (33) approximate the LJ scattering law less accurately than eqs. (29) and (30) approximate the TF seattering law. In an accurate analysis of molecular scattering measurements, it may thus be necessary to explicitly include a dependence $m = m(\tilde{\varphi})$ in $R = R(m)$.

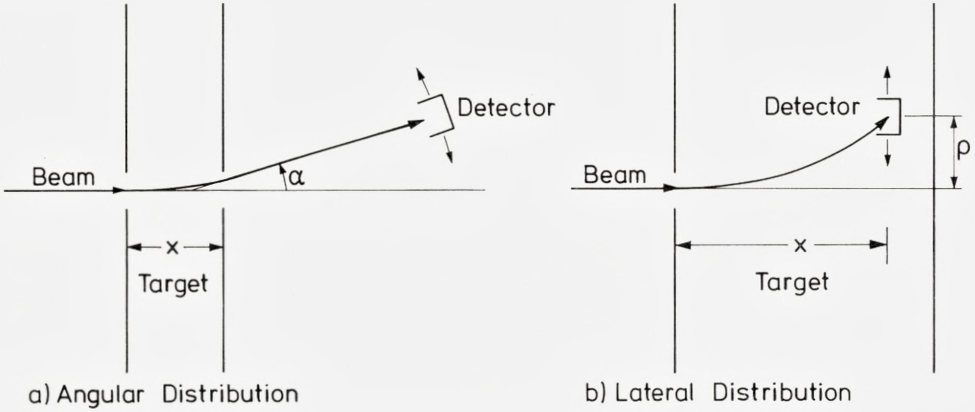


Fig. 4. Geometry of typical multiple-scattering experiments with gas targets.

where $N'$ is the density of scattering centers and $\sigma(k)$ the transport cross section (3). Similarly[8],

$$G(x,\varrho) = \frac{1}{2\pi}\int_0^\infty \varkappa d\varkappa\, J_0(\varkappa\varrho)\exp\left(-N'\int_0^x dx'\sigma(\varkappa x')\right). \tag{39}$$

The two distributions are formally very similar and contain equivalent information. In addition, somewhat surprisingly, the two distributions scale very accurately even rather far out into the tails, as has been shown both theoretically[8] and experimentally[13]. It was found recently[8] that the power approximation for the transport cross section, as exemplified by eq. (17), serves as a very accurate basis for multiple-scattering theory in the screened-Coulomb region; it seems, in fact, more accurate than the actual underlying power potential and single-scattering cross section. The following considerations, therefore, have been based on the power approximation (17).

Let us apply eqs. (35) and (36) to *atomic* systems first. From (17) and (35), we find that $k$ scales like $(N'x)^{-\frac{1}{2m}}/C_i$ and $\alpha$ like $k^{-1}$, i.e. $(N'x)^{\frac{1}{2m}}C_i$. In particular, the half-width $\alpha_{1/2}$ of $F(x,\alpha)$ must behave like

$$\alpha_{1/2} \propto (N'x)^{\frac{1}{2m}}/E, \tag{37}$$

since $C_i \propto 1/E$.

Similarly, from (17) and (36),

$$\varrho_{1/2} \propto (N'x)^{\frac{1}{2m}} \cdot \frac{x}{E}. \tag{38}$$

These variations have been checked experimentally in considerable detail. With regard to the present analysis, experiments with gases have been most convincing[13–15].

Let us, now, consider a diatomic gas, and let us assume, as in sect. 5, that one and the same power $m$ governs collisions with both types of constituent atoms.

In the following, our reference standard is the completely dissociated gas of $N' = N/2$ atoms of type 1 and 2; $N$ is the density of *atoms*. In that state, the exponent in the exponential function in (35) reads

$$-\frac{N}{2}x(\sigma_1 + \sigma_2) = -\frac{N}{2}x(A_1 + A_2)k^{2m} \tag{39}$$

$A_1$ and $A_2$ being defined in (17a).

In the long-range limit, (18a) yields instead,

$$-\frac{N}{2}x(A_1^{\frac{1}{2m}} + A_2^{\frac{1}{2m}})^{2m}k^{2m};$$

The latter expression takes on the form (39) if an apparent target thickness

$$x' = \frac{(C_1 + C_2)^{2m}}{C_1^{2m} + C_2^{2m}}\,x \tag{40a}$$

is introduced. Eq. (37) provides then the following relationship for the angular half-widths,

$$\frac{(\alpha_{1/2})_{\text{mol}}}{(\alpha_{1/2})_{\text{dissoc}}} = \left(\frac{x'}{x}\right)^{\frac{1}{2m}} \to \frac{C_1 + C_2}{(C_1^{2m} + C_2^{2m})^{\frac{1}{2m}}} \tag{41}$$

in the long-range limit. In particular, for homonuclear atoms, $C_1 = C_2$, (41) yields $2^{1-1/2m}$.

The same argument applied to (36) yields another apparent thickness

$$\left(\frac{x''}{x}\right)^{2m+1} = \frac{(C_1 + C_2)^{2m}}{C_1^{2m} + C_2^{2m}}. \tag{40b}$$

This, together with (38), provides a relationship between the lateral half-widths

$$\frac{(\varrho_{1/2})_{\text{mol}}}{(\varrho_{1/2})_{\text{dissoc}}} = \left(\frac{x'}{x}\right)^{1+\frac{1}{2m}} = \left(\left(\frac{x'}{x}\right)^{1+2m}\right)^{\frac{1}{2m}} = \frac{C_1 + C_2}{(C_1^{2m} + C_2^{2m})^{1/2m}} \tag{42}$$

i.e. exactly the same ratio as (41) in the short-range limit. In particular, this ratio becomes $2^{1-\frac{1}{2m}}$ for a homonuclear molecule. The angular and lateral half-widths $(\alpha_{1/2})_{\text{dissoc}}$ and $(\varrho_{1/2})_{\text{dissoc}}$ are comparable to atomic quantities that are known experimentally for a wide selection of ions and targets. The present argument makes use only of the scaling properties of the power cross section, i.e. of the experimental fact that the relations (37) and (38) are satisfied. The parameter $m$ occurring in (41) and (42), in particular in the homonuclear case, is thus to be understood as the one extracted from measurements on the corresponding *atomic* systems.

The transition between the short- and long-range limit is harder to find. The argument has been outlined briefly in ref. 2. We note first that straight insertion of (14) into (35) or (36) with $\sigma_i(k)$ according to (17), would yield a spurious divergence at $k = \infty$, since the correction term $\delta\sigma(k)$ would be applied outside the region where it is small. Instead, a perturbation approach is taken.

Let us, first, insert (14) and (17) into (35). The exponent of the exponential function can be written in the form

$$\left.\begin{aligned} &- N'x(A_1 + A_2)k^{2m}\left[1 - \frac{A_1A_2}{A_1 + A_2} \cdot k^{2m}/2\pi d^2\right] \\ \approx\ &- N'x(A_1 + A_2)k^{2m}\left[1 - \frac{A_1A_2}{A_1 + A_2} \cdot k_0^{2m}/2\pi d^2\right] \end{aligned}\right\} \tag{43}$$

where $k_0$ is some representative value of $k$ that will be specified below. This approximation is appropriate so long as the term in the brackets does not differ substantially from 1. It is also vital that $k^{2m}$ varies slowly. (In the subsequent example, $m \approx 0.2$). Eq. (43) reduces the molecular correction to the independent-atom limit to an apparent target thickness $x_1'$,

$$x_1' \simeq x\left(1 - \frac{A_1A_2}{A_1 + A_2}\frac{k_0^{2m}}{2\pi d^2}\right),$$

and thus, by means of (37)

$$\frac{(\alpha_{1/2})_{\text{mol}}}{(\alpha_{1/2})_{\text{dissoc}}} = \left(\frac{x_1'}{x}\right)^{\frac{1}{2m}} \simeq 1 - \frac{1}{2m}\frac{A_1A_2}{A_1 + A_2}\frac{k_0^{2m}}{2\pi d^2}. \tag{44}$$

Similarly, the exponent in (36) reads

$$\approx -N'(A_1+A_2)\varkappa^{2m}\frac{x^{2m+1}}{2m+1}\left\{1-\frac{2m+1}{4m+1}\frac{A_1A_2}{A_1+A_2}\frac{\varkappa_0^{2m}x^{2m}}{2\pi d^2}\right\} \tag{45}$$

with $\varkappa_0$ same representative value of $\varkappa$. Again, the molecular correction can be described by an apparent thickness $x_1''$ with

$$(x_1'')^{2m+1} = x^{2m+1}\left(1-\frac{2m+1}{4m+1}\frac{A_1A_2}{A_1+A_2}\frac{\varkappa_0^{2m}x^{2m}}{2\pi d^2}\right),$$

from which the lateral half-width can be found by means of (38)

$$\frac{(\varrho_{1/2})_{\mathrm{mol}}}{(\varrho_{1/2})_{\mathrm{dissoc}}} = \left(\frac{x_1''}{x}\right)^{1+\frac{1}{2m}} \simeq 1-\frac{1}{2m}\frac{2m+1}{4m+1}\frac{A_1A_2}{A_1+A_2}\frac{\varkappa_0^{2m}x^{2m}}{2\pi d^2}. \tag{46}$$

The values of $k_0$ and $\varkappa_0$ need to be determined from the *unperturbed* integrals, i.e. the multiple-scattering distributions for the dissociated gas. According to (43), $k_0^{2m}$ must scale like $[N'x(A_1+A_2)]^{-1}$; correspondingly (45) requires $\varkappa_0^{2m}$ to scale like $(2m+1)/[N'(A_1+A_2)x^{2m+1}]$. Therefore, (44) and (46) read

$$\frac{(\alpha_{1/2})_{\mathrm{mol}}}{(\alpha_{1/2})_{\mathrm{dissoc}}} \simeq 1-\mathrm{const}\frac{1}{2m}\frac{1}{2\pi d^2N'x}\frac{A_1A_2}{(A_1+A_2)^2} \tag{44'}$$

$$\frac{(\varrho_{1/2})_{\mathrm{mol}}}{(\varrho_{1/2})_{\mathrm{dissoc}}} \simeq 1-\mathrm{const}'\frac{1}{2m}\frac{(2m+1)^2}{4m+1}\frac{1}{2\pi d^2N'x}\frac{A_1A_2}{(A_1+A_2)^2} \tag{46'}$$

The values of the dimensionless constants in (44′) and (46′) depend on the precise definition of $k_0$ and $\varkappa_0$. Since the integrands in (35) and (36) are normally far from narrow, symmetric distributions, a choice based on extrema or zeros appears inappropriate. Instead, the median values have been chosen; moreover, for simplicity, we take median values at $\alpha = 0$, and $\varrho = 0$, respectively. The latter choice is justified because of the qualitative similarity of the contributions to the profile at any angle (or lateral spread) within the half-width.

It is easily shown (and specified in appendix A) that this choice yields

$$\mathrm{const} = \mathrm{const}' = g(m) \tag{47}$$

where $g$ is the solution of the equation

$$\int_0^g dt\, t^{\frac{1}{m}-1}e^{-t} = \tfrac{1}{2}\int_0^\infty dt\, t^{\frac{1}{m}-1}e^{-t}. \tag{47a}$$

TABLE I. The quantity $g$ as defined by eq. (47a), versus $m$.

| $m$ | $g$ | $m$ | $g$ | $m$ | $g$ |
|---|---|---|---|---|---|
| 1.000 | 0.694 | 0.250 | 3.671 | 0.143 | 6.671 |
| 0.667 | 1.184 | 0.222 | 4.170 | 0.133 | 7.171 |
| 0.500 | 1.678 | 0.200 | 4.672 | 0.125 | 7.669 |
| 0.400 | 2.175 | 0.182 | 5.170 | 0.118 | 8.171 |
| 0.333 | 2.675 | 0.167 | 5.673 | 0.111 | 8.669 |
| 0.286 | 3.174 | 0.154 | 6.170 | 0.105 | 9.167 |

The function $g(m)$ has been tabulated in table I.

The present discussion referred to the half-width of multiple scattering distributions rather than the full profile. The perturbation approach used precluded the consideration of a possible influence on the *shape* of the distributions by the molecular structure. A qualitative argument suggests that there is indeed such an influence. Take, as an example, the angular distribution $F(x,\alpha)$, and consider first the range of angles up to the half-width $\alpha_{1/2}$. The integral (35) receives, then, essential contributions from a certain range of $k$-values around the median value $k_0$. Now, with $\alpha$ increasing, the important range of $k$ shifts towards smaller values because of the Bessel function, $J_0(k\alpha)$; consequently, the molecular correction becomes less important (cf. eq. (43)). Thus, at sufficiently large values of $\alpha$ the multiple-scattering profile for a molecular gas will approach the independent-atom solution, even though the half-width may be close to or within the long-range limit. This result is consistent with what has been found in the single-collision case, e.g., eq. (29′). A more quantitative consideration is sketched in appendix B.

## 9. Application: Multiple Scattering on Diatomic Homonuclear Molecules

Just as in sect. 7, the description can be simplified substantially in case of homonuclear molecules by the introduction of TF variables. These are well established in multiple-scattering theory (cf., e.g., refs. 7 and 8). We have

$$\tau = \pi a^2 N x \tag{48a}$$

$$\tilde{\alpha} = \frac{Ea}{2Z_1 Z_2 e^2}\,\alpha \tag{48b}$$

$$\tilde{\varrho} = \pi a^2 N \cdot \frac{Ea}{2Z_1 Z_2 e^2}\,\varrho \tag{48c}$$

where $a$ is the Thomas-Fermi radius and $N = 2N'$ the number of atoms per unit volume. The latter choice has been made because it fits best to the dissociated gas as a reference standard. Inserting these definitions into (44′) and (46′), and regarding that $A_1 = A_2$ for homonuclear molecules, we finally obtain

$$\frac{(\tilde{\alpha}_{1/2})_{\mathrm{mol}}}{(\tilde{\alpha}_{1/2})_{\mathrm{dissoc}}} = \begin{cases} 1 - \dfrac{1}{2m}\left(\dfrac{a}{2d}\right)^2 \cdot \dfrac{g}{\tau} & \text{large } \tau \\ \text{for} & \\ 2^{1-\frac{1}{2m}} & \text{small } \tau \end{cases} \tag{49}$$

and

$$\frac{(\tilde{\varrho}_{1/2})_{\mathrm{mol}}}{(\tilde{\varrho}_{1/2})_{\mathrm{dissoc}}} = \begin{cases} 1 - \dfrac{1}{2m}\,\dfrac{(2m+1)^2}{4m+1}\left(\dfrac{a}{2d}\right)^2 \cdot \dfrac{g}{\tau} & \text{large } \tau \\ \text{for} & \\ 2^{1-\frac{1}{2m}} & \text{small } \tau \end{cases} \tag{50}$$

The upper relationships in (49) and (50) refer to the independent-atom or short-range limit. The lower values refer to the long-range limit. It is obvious that the relevant variable is the thickness parameter $\tau$ that also controls the half-widths[7, 8] $\tilde{\alpha}_{1/2}$ and $\tilde{\varrho}_{1/2}$: At large $\tau$ (large half-width) the short-range limit is appropriate, and the reverse is true at small $\tau$.

The upper parts of eqs. (49) and (50) were already mentioned in a short note[2], where the notation

$$h(m) = \frac{2m+1}{4m+1}\, g(m) \tag{51}$$

was employed. Moreover, as was shown in ref. 8, the parameter $m$, which determines the interatomic potential, can be related in a definite way to the thickness parameter $\tau$, eq. (48a), such that a function $m = m(\tau)$ can be defined for a given screened-Coulomb interaction potential. By means of these relationships for TF and Lenz-Jensen (LJ) interaction, one can relate $g$ and $h$ to $\tau$ directly (Fig. 5).

Fig. 6 shows experimental results of lateral half-widths measured with lead ions scattered on nitrogen and neon at the same density of atoms[2]. The TF screening radii are determined essentially by the heavy lead ions, so that from the point of view of comparison, neon ions should be an accurate substitute for nitrogen. The two full-drawn theoretical curves refer to eq. (50), with $m = 0.2 = \mathrm{const}$. This value is very close to the LJ value

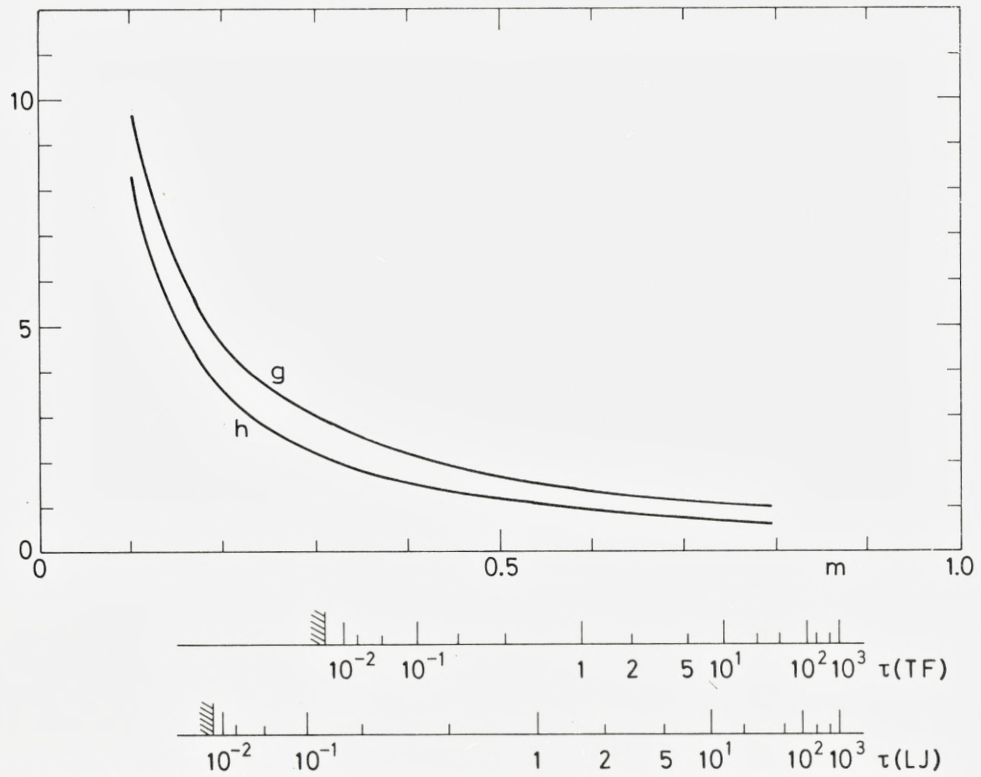


Fig. 5. The quantities $g$ and $h$ defined by eqs. (47a) and (51), respectively, versus power $m$. Scales of $\tau$ (48a) have been included by means of the relations derived in ref. 8.

0.191; it was chosen as the one extracted from measurements of the lateral half-width $\tilde{\varrho}_{1/2}$ on noble-gas targets[14] in the critical $\tau$ range $10^{-2} - 10^{-1}$. The TF curve has been included for comparison. Both the general trend, the region of the drop-off, and in particular the long-range limit are described quite well by the theoretical curve for $m = 0.2$. At the low $\tau$ values it is clearly superior to the TF-curve. Neither of them, however, explains the peculiar behaviour of the experimental points that is observed between $\tau = 1$ and 5.

## 10. Polyatomic Molecules

By application of the same physical model to a polyatomic molecule consisting of $z$ atoms 1, 2, ... $z$, eqs. (7′) and (7) can be readily generalized,

$$\sigma(\mathbf{k}) = < \int d^2\mathbf{p}(1 - e^{i\mathbf{k}\cdot\sum_{i=1}^{z}\varphi_i(\mathbf{p}_i)}) \qquad (52')$$

and

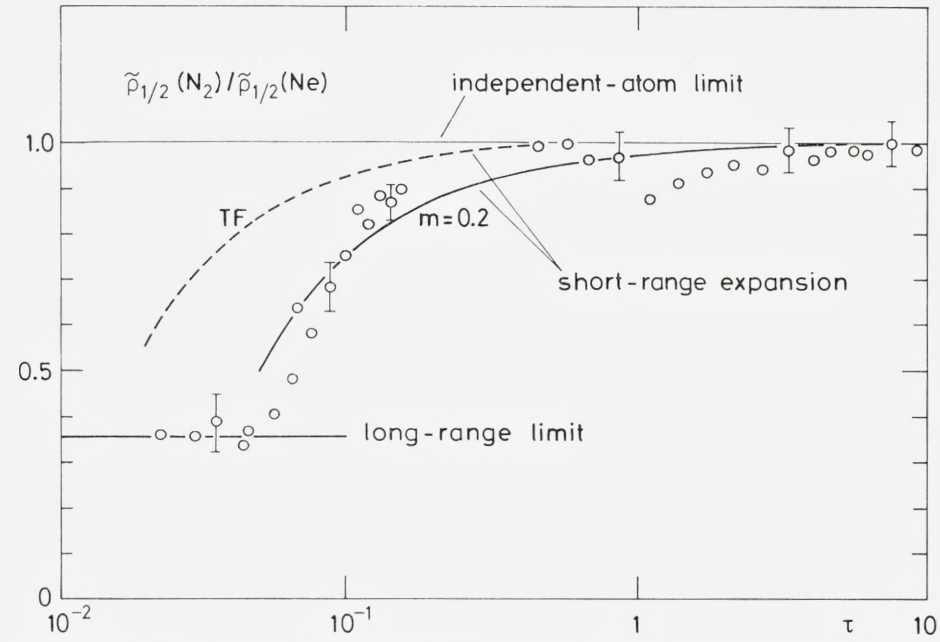


Fig. 6. Experimental ratio of lateral half-widths, $\tilde{\varrho}_{1/2}$ (nitrogen)/$\tilde{\varrho}_{1/2}$ (neon), versus thickness parameter $\tau$ (48a) from ref. 2. Fulldrawn curves: Eq. (50) for power $m = 0.2$ (Lenz-Jensen) at all $\tau$. Dashed curve: Eq. (50) for Thomas-Fermi interaction.

$$\left.\begin{aligned}\sigma(\mathbf{k}) = \sum_i \sigma_i(k) - \sum_{i<j} \delta\sigma_{ij}(\mathbf{k}) + \sum_{i<j<k} \delta\sigma_{ijl}(\mathbf{k}) \ldots \\ \ldots + (-)^{z+1} \delta\sigma_{12\ldots z}(\mathbf{k})\end{aligned}\right\} \quad (52)$$

with $\sigma_i(\mathbf{k})$ defined by eq. (8) for $i = 1, 2, \ldots z$, and

$$\delta\sigma_{ij\ldots}(\mathbf{k}) = \langle \int d^2\mathbf{p}(1 - e^{i\mathbf{k}\cdot\varphi_i(\mathbf{p}_i)})(1 - e^{i\mathbf{k}\cdot\varphi_j(\mathbf{p}_j)}) \ldots \rangle; \quad (53a)$$

$\mathbf{p}_i$ is the (vectorial) impact parameter with atom $i$. The long-range limit is readily found from eq. (52′). Indeed, the leading term for small interatomic distances reads

$$\sigma(\mathbf{k}) \sim \int d^2\mathbf{p}(1 - e^{i\mathbf{k}\cdot\Sigma\varphi_i(\mathbf{p})}) \quad (53)$$

or, for power scattering, by means of (16) and (17),

$$\sigma(\mathbf{k}) \sim \left(\sum_1^z A_i^{\frac{1}{2m}}\right)^{2m} k^{2m}, \quad (54)$$

of which (18a) is a special case. In the short-range limit, eq. (52) yields

$$\sigma(\mathbf{k}) \sim \sum_i \sigma_i(\mathbf{k}) - \sum_{i<j} \frac{\sigma_i(k)\,\sigma_j(k)}{2\pi d_{ij}^2} + \sum_{i<j<k} \delta\sigma_{ijk}(k) \ldots \quad (55)$$

where $d_{ij}$ is the distance between atoms $i$ and $j$. The term $\delta\sigma_{ij}(\mathbf{k})$, according to its definition (53a), is equivalent with (9) for $i = 1$, $j = 2$, and is, therefore, identical with (13) for $1 = i$, $2 = j$. It will now be shown that except for a very small number of special cases, the subsequent terms in (55), from $\delta\sigma_{ijk}$ on, are of higher than second order in the inverse interatomic distance, and therefore have to be dropped.

Take the term $\delta\sigma_{123}$ as given by

$$\left.\begin{aligned}\delta\sigma_{123} &= \langle \int d^2\mathbf{p}(1 - e^{i\mathbf{k}\cdot\varphi_1(\mathbf{p}_1)})(1 - e^{i\mathbf{k}\cdot\varphi_2(\mathbf{p}_2)})(1 - e^{i\mathbf{k}\cdot\varphi_3(\mathbf{p}_3)})\rangle_\Omega \\ &= \prod_{i=1} \left\{\int d^2\mathbf{p}_i(1 - e^{i\mathbf{k}\cdot\varphi_i(\mathbf{p}_i)})\right\} \cdot \langle \delta(\mathbf{p}_1 - \mathbf{p}_2 - \mathbf{b}_{12})\delta(\mathbf{p}_1 - \mathbf{p}_3 - \mathbf{b}_{13})\rangle_\Omega \ ,\end{aligned}\right\} \tag{56}$$

where $\mathbf{b}_{ij}$ is the projection of the interatomic distance vector $\mathbf{d}_{ij}$ on the impact plane. Since only the leading term for large interatomic distances is of interest, we can simplify the rotational average

$$\langle \delta(\mathbf{p}_1 - \mathbf{p}_2 - \mathbf{b}_{12})\delta(\mathbf{p}_1 - \mathbf{p}_3 - \mathbf{b}_{13})\rangle_\Omega \sim \delta\langle(\mathbf{b}_{12})\delta(\mathbf{b}_{13})\rangle_\Omega \ . \tag{57'}$$

The operation $\langle \ldots \rangle_\Omega$ includes an integration over all orientations of an arbitrary rotational axis (here taken to be $\mathbf{d}_{12}$) and over the azimuthal angle of an arbitrary point within the molecule (here taken to be atom 3) with respect to that axis.

The azimuthal average is evaluated first. The factor $\delta(\mathbf{b}_{12})$ is not affected by this operation, but it ensures (by $\mathbf{b}_{12} = 0$) that the rotational axis is identical with the polar axis of the system. Therefore,

$$\langle \delta(\mathbf{b}_{12})\delta(\mathbf{b}_{13})\rangle_\Omega = \langle \delta(\mathbf{b}_{12}) \cdot \frac{\delta(b_{13})}{\pi b_{13}}\rangle = \frac{\delta(d_{13}\sin\varphi_{23})}{\pi d_{13}\sin\varphi_{23}}\langle \delta(\mathbf{b}_{12})\rangle .$$

Here, $\varphi_{23}$ is the angle between $\mathbf{d}_{13}$ and $\mathbf{d}_{12}$, i.e. a fixed angle within the molecule, so that $b_{13} = d_{13}\sin\varphi_{23}$.

The average over the rotational axis reduces then to

$$\langle \delta(\mathbf{b}_{12})\rangle = \frac{1}{2\pi {d_{12}}^2}$$

a result which is identical with (12) for $\mathbf{p}_1 - \mathbf{p}_2 = 0$. Therefore,

$$\langle \delta(\mathbf{b}_{12}) \cdot \delta(\mathbf{b}_{13})\rangle_\Omega = \frac{\delta(\sin\varphi_{23})}{2\pi^2 {d_{12}}^2 {d_{13}}^2 \sin\varphi_{23}}, \tag{57}$$

and, from (56)

$$\delta\sigma_{123} \sim \frac{\sigma_1(k)\sigma_2(k)\sigma_3(k)}{2\pi^2 {d_{12}}^2 {d_{13}}^2} \cdot \frac{\delta(\sin\varphi_{23})}{\sin\varphi_{23}} . \tag{58}$$

Thus, for $\sin\varphi_{23} \neq 0$, we have $\delta\sigma_{123} = 0$ to order ${d_{12}}^{-2}\,{d_{13}}^{-2}$.

For a *linear* molecule, $\varphi_{23} = 0$, (58) becomes strongly divergent. In a real molecule, this divergence will be smeared out by molecular vibrations. Let, for example, $\varphi_{23}$ be distributed according to a gaussian distribution

$$g(\varphi_{23})d^2\varphi_{23} = \frac{1}{2\pi\varphi_0{}^2}\, e^{-\frac{\varphi_{23}^2}{2\varphi_0{}^2}}\, 2\pi\varphi_{23}d\varphi_{23} \tag{59}$$

with a width $\varphi_0 \ll 1$, then $\langle \delta(\sin\varphi_{23})/\sin\varphi_{23}\rangle_g = \dfrac{1}{2\varphi_0{}^2}$, and

$$\langle \delta\sigma_{123}\rangle_g \sim \frac{\sigma_1\sigma_2\sigma_3}{(2\pi)^2 d_{12}{}^2 d_{13}{}^2\varphi_0{}^2}. \tag{60}$$

This expression is negligible in comparison with, e.g., $\delta\sigma_{12}$, if

$$2\pi d_{13}{}^2\varphi_0{}^2 \gg \sigma_3 \tag{61}$$

The factor $\varphi_0{}^2$ makes this a rather strong requirement that will often not be fulfilled in cases of practical interest.

Therefore, the linear molecule needs to be treated separately, once more, and starting from (56). In such a molecule, we have, e.g.,

$$\mathbf{d}_{13} = \lambda\mathbf{d}_{12} \quad \text{with } \lambda \neq 0, \neq 1 \tag{62}$$

and hence

$$\mathbf{b}_{13} = \lambda\mathbf{b}_{12} \tag{62a}$$

Thus, the rotational average in (56) can be written

$$\left.\begin{aligned} \langle \delta(\mathbf{p}_1 - \mathbf{p}_2 - \mathbf{b}_{12})\delta(\mathbf{p}_1 - \mathbf{p}_3 - \mathbf{b}_{13})\rangle_\Omega &= \delta(\mathbf{p}_1 - \mathbf{p}_3 - \lambda(\mathbf{p}_1 - \mathbf{p}_2))\cdot \\ \cdot\langle \delta(\mathbf{p}_1 - \mathbf{p}_2 - \mathbf{b}_{12})\rangle_\Omega &\sim \delta(\mathbf{p}_1 - \mathbf{p}_3 - \lambda(\mathbf{p}_1 - \mathbf{p}_2))\cdot \frac{1}{2\pi d_{12}{}^2}. \end{aligned}\right\} \tag{63}$$

If this is inserted into (56), it becomes obvious that $\delta\sigma_{123} \propto d_{12}{}^{-2}$, i.e. of the same order as the $\delta\sigma_{ij}$ and therefore not negligible in general, for a linear molecule. The resulting expression

$$\left.\begin{aligned} \delta\sigma_{123} \sim \frac{1}{2\pi d_{12}{}^2}\int d^2\mathbf{p}_1(1 - e^{i\mathbf{k}\cdot\varphi_1(\mathbf{p}_1)})\int d^2\mathbf{p}_2(1 - e^{i\mathbf{k}\cdot\varphi_2(\mathbf{p}_2)})\cdot \\ \cdot(1 - e^{i\mathbf{k}\cdot\varphi_3(\mathbf{p}_1\cdot(1-\lambda)+\mathbf{p}_2\cdot\lambda)}) \end{aligned}\right\} \tag{64}$$

is a 2-center integral that can be evaluated by means of an expansion in Bessel functions, if needed. At present, we consider two limiting cases by means of a simple estimate.

We first note that the integrand in the expression

$$\sigma_i(k) = \int d^2\mathbf{p}(1 - e^{i\mathbf{k}\cdot\varphi_i(\mathbf{p})})$$

can be represented as a step function,

$$1 - e^{i\mathbf{k}\cdot\varphi_i(\mathbf{p})} \approx \left.\begin{aligned} &1 \;\ldots\ldots\ldots\; p \lesssim p_{0i}(k) \\ &0 \;\ldots\ldots\ldots\; p \gtrsim p_{0i}(k) \end{aligned}\right\} \tag{65}$$

since for small $p$, $\varphi_i$ is large, and the exponential rapidly oscillating. By comparison with (17) and (17a) we find

$$p_{0i}(k) = \gamma_m (kC_i)^m \tag{65a}$$

with a well defined constant $\gamma_m$.

The following considerations refer, more or less explicitly, to a triatomic molecule. Take first the case where $p_{03}(k)$ is greater than $p_{01}(k)$ and $p_{02}(k)$, i.e., $C_3 > C_1, C_2$. Then, the integration region in (64) is determined essentially by $p_{01}$ and $p_{02}$, and the last factor is 1 in that region. Then,

$$\delta\sigma_{123} \sim \frac{1}{2\pi {d_{12}}^2} \sigma_1\sigma_2 \sim \delta\sigma_{12};\ C_1, C_2 < C_3. \tag{66a}$$

In the opposite case, where $p_{03}$ is substantially smaller than $p_{01}$ and $p_{02}$, a similar consideration yields

$$\delta\sigma_{123} \ll \frac{\sigma_1\sigma_2}{2\pi {d_{12}}^2};\qquad C_1, C_2 \gg C_3. \tag{66b}$$

Now, $C_i$ increases with increasing atomic number of the target atom. Therefore, the two limiting cases refer to molecules where one heavy atom (3) is surrounded by two light ones, and one light atom (3) surrounded by two heavy ones, respectively. For a triatomic molecule (55) yields

$$\sigma \sim \sigma_1 + \sigma_2 + \sigma_3 - \frac{\sigma_1\sigma_3}{2\pi {d_{13}}^2} - \frac{\sigma_2\sigma_3}{2\pi {d_{23}}^2} \qquad \text{(atom 3 heavy)} \tag{67a}$$

and

$$\sigma \sim \sigma_1 + \sigma_2 + \sigma_3 - \frac{\sigma_1\sigma_2}{2\pi {d_{12}}^2} - \frac{\sigma_1\sigma_3}{2\pi {d_{13}}^2} - \frac{\sigma_2\sigma_3}{2\pi {d_{23}}^2} \qquad \text{(atom 3 light)} \tag{67b}$$

The latter result does not differ from what would be expected for a nonlinear triatomic molecule. And the former result (67a) could just as well have been derived by means of the fact that the term $\delta\sigma_{12} \sim \frac{\sigma_1\sigma_2}{2\pi {d_{12}}^2}$ would be smaller than $\delta\sigma_{13}$ and $\delta\sigma_{23}$, both because $\sigma_1, \sigma_2 \ll \sigma_3$ and $d_{12} > d_{13}, d_{23}$. It thus appears that the only case where some uncertainty prevails is that of a linear molecule with 3 roughly equal constituents. In that case, we have

$$\frac{\sigma_1\sigma_3}{2\pi {d_{13}}^2} \approx \frac{\sigma_2\sigma_3}{2\pi {d_{23}}^2} \approx 4\frac{\sigma_1\sigma_2}{2\pi {d_{12}}^2} \tag{68}$$

if 1 and 2 are the outer atoms. Thus, the uncertainty due to lack of knowledge of the accurate value of the sum $-\delta\sigma_{12} + \delta\sigma_{123}$ is $\sim$ 12 pct. of $\delta\sigma_{13} + \delta\sigma_{23}$, i.e. a 12 pct. error in a correction. This must most often be an acceptable uncertainty.

It, occurs therefore, that at least for triatomic molecules, the expression

$$\sigma(k) \sim \sum_{i=1}^{z} \sigma_i(k) - \sum_{i<j} \frac{\sigma_i(k)\sigma_j(k)}{2\pi d_{ij}^2} \tag{69}$$

gives a satisfactory estimate of the transport cross section in the short-range limit, independent of the detailed geometry of the molecule.

In atoms containing more than three molecules, similar considerations would have to be applied to terms of the type $\delta\sigma_{1234}$ etc. The type of argument would be the same as what was applied in this section, and the results would be similar. A case where caution would have to be applied is that of long chain molecules ("strings"). Other types of processes[16] that are outside the scope of this paper would have to be considered there.

## 11. Polyatomic Molecules: Single Scattering

Single-scattering cross sections for polyatomic molecules are established readily be means of eqs. (54) and (69) from eq. (4). The results are straight generalizations of those quoted in sect. 6 for diatomic molecules. They read

$$\frac{d\sigma}{d\varphi} = \sum_i \frac{d\sigma_i}{d\varphi} - \frac{R(m)}{m} \sum_{i<j} \frac{\varphi}{2\pi d_{ij}^2} \frac{d\sigma_i}{d\varphi} \cdot \frac{d\sigma_j}{d\varphi} \cdots \tag{70a}$$

for small interaction distance, and

$$\frac{d\sigma}{d\varphi} = \left( \sum_i \left( \frac{d\sigma_i}{d\varphi} \right)^{\frac{1}{2m}} \right)^{2m} \cdots \tag{70b}$$

in the long-range limit. $R(m)$ is defied by eq. (21) and plotted in fig. 3. Both equations show that the relative magnitude of molecular corrections in comparison with the independent-atom limit ($d_{ij} = \infty$) increases with increasing number of atoms per molecule. The conclusions made in sect. 6 remain otherwise unchanged.

If the molecule is built up of $z$ atoms with similar atomic numbers and masses, we can ignore the differences between the constituents, and write eqs. (70) in the form

$$\frac{d\sigma}{d\varphi} \simeq z \frac{d\sigma_1}{d\varphi} - \frac{R(m)}{m} \varphi \left( \frac{d\sigma_1}{d\varphi} \right)^2 \sum_{i<j} \frac{1}{2\pi d_{ij}^2} \cdots \tag{70a'}$$

$$\frac{d\sigma}{d\varphi} = z^{2m} \frac{d\sigma_1}{d\varphi} \cdots \tag{70b'}$$

Thus, the two limiting cases differ by a factor of $z^{2m-1}$; since the long-range limit applies mainly to collisions where $m \lesssim 0.2$ (LJ), this ratio decreases substantially with increasing $z$. When the sum in (70a') is written in the form

$$\sum_{i<j} \frac{1}{2\pi d_{ij}^2} = < \frac{1}{2\pi d_{ij}^2} > \tfrac{1}{2} z(z-1), \tag{71}$$

it becomes evident that the molecular correction to the independent-atom limit increases like $z-1$ on a relative scale for small molecules ($z \lesssim 5$), but more slowly for larger ones.

These relations can easily be written in terms of TF variables (28). However, TF variables provide a substantial simplification only for homonuclear (or approximately homonuclear) molecules.

## 12. Polyatomic Molecules: Multiple Scattering

The generalization to polyatomic molecules of the relations derived in sect. 8 for multiple scattering starts also with eqs. (54) and (69), and eqs. (35) and (36). Instead of (41) and (42), we obtain

$$\frac{(\alpha_{1/2})_{\text{mol}}}{(\alpha_{1/2})_{\text{dissoc}}} = \frac{(\varrho_{1/2})_{\text{mol}}}{(\varrho_{1/2})_{\text{dissoc}}} = \frac{\sum_i C_i}{(\sum_i C_i^{2m})^{1/2m}} \tag{72}$$

in the long-range limit. This approaches $z^{1-1/2m}$ for homonuclear molecules.

For nearly independent atoms, we obtain the following relations instead of (44′) and (46′),

$$\frac{(\alpha_{1/2})_{\text{mol}}}{(\alpha_{1/2})_{\text{dissoc}}} \simeq 1 - \frac{g}{2m} \cdot \frac{1}{(\sum_i A_i)^2} \sum_{i<j} \frac{A_i A_j}{2\pi d_{ij}^2 N' x} \tag{73a}$$

$$\frac{(\varrho_{1/2})_{\text{mol}}}{(\varrho_{1/2})_{\text{dissoc}}} \simeq 1 - \frac{g}{2m} \frac{(2m+1)^2}{4m+1} \frac{1}{(\sum_i A_i)^2} \sum_{i<j} \frac{A_i A_j}{2\pi d_{ij}^2 N' x} \tag{73b}$$

where $A_i$ and $g$ are given by (17a) and table I, respectively.

In case of (approximately) homonuclear target molecules, (73a) reads

$$\frac{(\alpha_{1/2})_{\text{mol}}}{(\alpha_{1/2})_{\text{dissoc}}} \simeq 1 - \frac{g}{2m} \frac{1}{z^2} \sum_{i<j} \frac{1}{2\pi d_{ij}^2 N' x} = 1 - \frac{g}{2m} \cdot \frac{z-1}{2} < \frac{1}{2\pi d_{ij}^2 N x} > \tag{73a′}$$

where $N = zN'$ is the number of atoms per unit volume. Obviously, the molecular correction to the independent-atom limit increases with increasing $z$ in much the same way as was found in case of the single-scattering cross section. The corresponding relations for $\varrho_{1/2}$, and the equations for TF-scaled quantities (in the homonuclear case) are easily found.

## 13. Summary

1. In the classical small-angle scattering of charged particles by molecules it is convenient to define three regions; a long-range limit, where the interaction takes place at a sufficiently large distance so that the molecule acts as one target particle; a short-range limit where the interaction takes place at sufficiently small distances so that each constituent atom (if close enough to the orbit) acts as one target particle; and a transition region.

2. In single scattering, the long-range limit is reached at low energies and/or small scattering angles. The reverse is true for the short-range limit. The transition region covers the range $10^{-2} \lesssim \eta (= t^{1/2}) \lesssim 1$ in Thomas Fermi variables. This corresponds to moderate screening of the Coulomb interaction. Typical measurements of incomplete total cross sections trace the region of excessive screening ($\eta \ll 10^{-2}$); the long-range limit applies to those situations.

3. In multiple scattering, the long-range limit applies to small values of the thickness parameter $\tau = \tau a^2 N x$, and large ones for the short-range limit. The transition region covers the range $10^{-2} \lesssim \tau \lesssim 1$.

4. The short-range limit can be realized experimentally by means of a dissociated gas target, or a noble-gas target with similar atomic number. The single-collision cross section of the molecular gas (differential or total) is smaller by up to a factor of the order of $\sim z^{2m-1} \approx z^{-0.6}$ than the corresponding quantity for the dissociated gas, where $z$ is the number of atoms in the molecule. Multiple-scattering half-widths (angular or lateral) are smaller by up to a factor of $\sim z^{1-1/2m} \approx z^{-3/2}$.

5. The calculations presented here are based on the simplifying assumption of a target molecule composed of undisturbed, spherically symmetric atoms that are arranged in some geometric configuration; i.e., valence effects are ignored. Since the transition region between the long- and short-range limit lies entirely in the Thomas-Fermi region of the scattering diagram where valence effects are unimportant, this simplifying assumption only affects the detailed behaviour *within* the long-range limit. The quantitative results presented in this paper refer to the deviations from an independent-atom picture, i.e. the short-range limit and the transition region; these results are insensitive to valence effects.

6. For essentially the same reason, the exclusive use of a classical-orbit picture of the scattering process is not a severe limitation.

7. Experimental data on single scattering off molecules in the transition region do not appear to be available. One recently published set of multiple-scattering half-widths on nitrogen is in excellent agreement with the theoretical prediction, both in the long-range limit and the transition region, provided that the scattering law for individual atoms is chosen in accordance with the experimentally found multiple-scattering half-widths on noble gases. This scattering law corresponds much closer to Lenz-Jensen than to Thomas-Fermi screening. The multiple-scattering half-width in the transition region is quite sensitive to the scattering law for individual atoms. Therefore, the molecular effect described in this paper serves as an additional probe for interatomic potentials in the moderately-screened Coulomb region.

8. With respect to practical applications in accelerator physics, it may be useful to recall that regardless of the nature of the target molecule, target pressure, and ion type and energy, the multiple-scattering distribution is narrower for the molecular than for the dissociated gas, so long as the small-angle approximation applies.

## Acknowledgements

This work was stimulated by Georg Sidenius' insistence that a molecule is not just the sum of its atoms. A major incitament was the close cooperation with the experimental groups in Copenhagen, N. Andersen and G. Sidenius, and in Aarhus, F. Besenbacher, J. Heinemeier, P. Hvelplund, and H. Knudsen. Special thanks are due to J. Schou for checking some of the integrals, and to N. Andersen for numerous discussions. A. Russek made valuable comments on the manuscript.

## Appendix A

This appendix serves to specify the median values $k_0$ and $\varkappa_0$ as representative values of $k$ and $\varkappa$ in Bothe's formula (35) and its modification (36) for lateral profiles. Consider (35) first and define $k_0$ by the relation

$$\frac{1}{2\pi}\int_0^{k_0} dk\, k J_0(k\alpha)\, e^{-N' x \sigma(k)} = \frac{1}{2\pi}\int_{k_0}^{\infty} dk\, k J_0(k\alpha)\, e^{-N' x \sigma(k)}, \qquad \text{(A1)}$$

i.e., $k_0$ divides up the integration into two equal parts. For values of $\alpha$ within the half-width $\alpha_{1/2}$, one may set $\alpha = 0$ without making a serious error. Then, $k_0$ becomes independent of $\alpha$, and (A1) has a unique solution.

(A1) is rewritten by means of (18).

$$\int_0^{k_0} dk\, k e^{-N' x A k^{2m}} = \tfrac{1}{2} \int_0^{\infty} dk\, k e^{-N' x A k^{2m}} \tag{A2}$$

or, after introduction of the variable

$$t = N' x A k^{2m}, \tag{A3}$$

$$\int_0^{g} dt\, t^{\frac{1}{m}-1} e^{-t} = \tfrac{1}{2} \int_0^{\infty} dt\, t^{\frac{1}{m}-1} e^{-t}, \tag{A4}$$

where

$$g = N' x A k_0^{2m}; \tag{A5}$$

In terms of an incomplete gamma function[17], (A4) reads

$$P\left(\frac{1}{m}, g\right) = \tfrac{1}{2}; \tag{A6}$$

This determines $g = g(m)$. Table I shows $g$ as evaluated from the tables in ref. 17. Insertion of (A5) into (44) with $A = A_1 + A_2$ yields (44′) and (47).

By applying the same argument to the lateral distribution (36), the equation that corresponds to (A2) reads

$$\int_0^{\varkappa_0} d\varkappa\, \varkappa e^{-N' \frac{x^{2m+1}}{2m+1} A \varkappa^{2m}} = \tfrac{1}{2} \int_0^{\infty} d\varkappa\, \varkappa e^{-N' \frac{x^{2m+1}}{2m+1} A \varkappa^{2m}}. \tag{A7}$$

The proper variable is now

$$t = N' \frac{x^{2m+1}}{2m+1} A \varkappa^{2m} \tag{A8}$$

and

$$g = N' \frac{x^{2m+1}}{2m+1} a \varkappa_0^{2m} \tag{A9}$$

with $g$ being a solution of (A6). (A9) inserted into (46) yields (46′) and (47).

## Appendix B

It is the purpose of this appendix to provide a somewhat more quantative argument for the claim that a molecular multiple-scattering profile approaches the independent-atom profile at larger scattering angles. Only the angular profile $F(x,\alpha)$ will be considered. The procedure is a generalization of the perturbation approach taken in sect. 8.

Take eq. (35) and insert (14),

$$F(x,\alpha) \simeq \frac{1}{2\pi}\int_0^\infty k dk J_0(k\alpha)\, e^{-N'x\left(\sigma_1(k)+\sigma_2(k)-\frac{\sigma_1(k)\,\sigma_2(k)}{2\pi d^2}\right)} \tag{B1}$$

for $x$ sufficiently large so that the molecular correction is small. Within the perturbation approach, we can write

$$F(x,\alpha) \approx e^{N'x\frac{\sigma_1(k_1)\sigma_2(k_1)}{2\pi d^2}} \cdot \frac{1}{2\pi}\int_0^\infty k dk J_0(k\alpha)\, e^{-N'x(\sigma_1(k)+\sigma_2(k))}, \tag{B2}$$

where

$$k_1 = k_1(\alpha) \tag{B3}$$

is the median value of the integral (B2). Therefore, (B2) can be written in the form

$$F(x,\alpha) \simeq S(\alpha)\cdot F_{at}(x,\alpha) \tag{B4}$$

where $F_{at}(x,\alpha)$ is the independent-atom distribution, and

$$S(\alpha) = e^{N'x\frac{\sigma_1(k_1)\sigma_2(k_1)}{2\pi d^2}} \tag{B5}$$

This function is greater than 1 for $\alpha = 0$, and decreases towards 1 with increasing $\alpha$, since $k_1(\alpha)$ decreases. An approximate expression for $k_1(\alpha)$ is found by series expansion,

$$J_0(k\alpha) \approx 1 - k^2\alpha^2/4\,; \tag{B6}$$

$$k_1(\alpha) \approx k_0 - r_0\alpha^2 \tag{B7}$$

where $k_0$ is defined by eq. (A2). The requirement of $k_1(\alpha)$ being a median value yields, then, to first order in $\alpha^2$, the following expression for $r_0$,

$$\left.\begin{aligned} r_0 = \frac{e^{N'x[\sigma_1(k_0)+\sigma_2(k_0)]}}{8k_0}\Bigg\{&\int_0^\infty dk\, k^3 e^{-N'x(\sigma_1(k)+\sigma_2(k))} \\ &- 2\int_0^{k_0} dk\, k^3 e^{-N'x(\sigma_1(k)+\sigma_2(k))}\Bigg\}; \end{aligned}\right\} \tag{B8}$$

In the notation of appendix $A$, this can be written

$$r_0 = \Gamma(2/m)(1 - 2P(2/m,g))\frac{e^g}{16m}\cdot k_0^{-1}\cdot(N'xA)^{-2/m}. \tag{B9}$$

From this, and (B7), we obtain

$$S(\alpha) \simeq 1 + \frac{g^2 A_1 A_2}{2\pi d^2 N' x (A_1 + A_2)^2} \left[ 1 - B(m) \left( \frac{\alpha}{2[gN' x (A_1 + A_2)]^{1/2m}} \right)^2 \right] \qquad \text{(B10)}$$

where

$$B(m) = \Gamma(2/m)\,(1 - 2P(2/m,g))e^g \qquad \text{(B11)}$$

(B10) shows that the zero-angle scattering intensity is greater than its independent-atom value by an amount that corresponds to the decrease in half-width (44′) due to the molecular correction. With increasing angle, this enhancement approaches zero.

## References


1. P. Sigmund, Phys. Rev. A. **14**, 996 (1976).
2. G. Sidenius, N. Andersen, P. Sigmund, F. Besenbacher, J. Heinemeier, P. Hvelplund, and H. Knudsen, Nucl. Inst. Meth. **134**, 597 (1976).
3. N. Bohr, Mat. Fys. Medd. Dan. Vid. Selsk. **18**, no. 8 (1948).
4. J. Lindhard, V. Nielsen, and M. Scharff, ibid. **36**, no. 10 (1968).
5. U. Buck, Rev. Mod. Phys. **46**, 369 (1974).
6. P. Sigmund, *in* Physics of Ionized Gases, M. Kurepa, editor, Institute of Physics, Belgrade, p. 137 (1972).
7. P. Sigmund and K. B. Winterbon, Nucl. Inst. Meth. **119**, 541 (1974); ibid. **125**, 491 (1975).
8. A. D. Marwick and P. Sigmund, Nucl. Inst. Meth. **126**, 317 (1975).
9. K. B. Winterbon, P. Sigmund, and J. B. Sanders, Mat. Fys. Medd. Dan. Vid. Selsk. **37**, no. 14 (1970).
10. H. van Dop, A. J. H. Boerboom, and J. Los, Physica **61**, 626 (1972).
11. P. Loftager and G. Claussen, Proc. Int. Conf. Electronic and Atomic Collisions, Boston, Mass. (1969), p. 518.
12. K. B. Winterbon, Rad. Effects **13**, 215 (1972).
13. G. Sidenius and N. Andersen, Nucl. Inst. Meth. **128**, 271 (1975); ibid. **131**, 387 (1975).
14. F. Besenbacher, J. Heinemeier, P. Hvelplund, and H. Knudsen, Phys. Rev. A. **13**, 2095 (1976).
15. B. Efken, D. Hahn, D. Hilscher, and G. Wüstefeld, Nucl. Instr. Meth. **129**, 227 (1975)
16. J. Lindhard, Mat. Fys. Medd. Dan. Vid. Selsk. **34**, no. 14 (1965).
17. M. Abramowitz and I. Stegun, Handbook of Mathematical Functions, Dover Publ. Inc., New York (1964).
18. R. J. Glauber, Phys. Rev. **100,** 242 (1955).


*Peter Sigmund*
*Physical Laboratory II*
*H. C. Ørsted Institute*
*DK–2100 Copenhagen Ø.*

Indleveret til Selskabet oktober 1976.
Færdig fra trykkeriet juni 1977.

JENS PEDER DAHL

# THE SPINNING ELECTRON

Det Kongelige Danske Videnskabernes Selskab
Matematisk-fysiske Meddelelser **39**, 12


Kommissionær: Munksgaard
København 1977

*Dedicated to Professor Per-Olov Löwdin*
*on the Occasion of his 60th Birthday*


**Synopsis**

The properties of the *quantum mechanical rotor* are reviewed, and the conditions studied under which its dynamics is in accordance with the invariance requirements of the inhomogeneous Lorentz group. It is shown that these requirements select the *spin* $^1/_2$ quantum states as the only permissible ones, and that the motion of the rotor must be governed by the *Dirac equation*. The properties of this equation and its solutions are then reconsidered in the new perspective, with special emphasis on the symmetry of the problem. A simple interpretation is given of the *PCT operation*, and Wigner's *time reversal* operation is shown to be composed of two more elementary operations.




Printed in Denmark by Bianco Lunos Bogtrykkeri A/S. ISBN 87-7304-076-2

## Introduction

The idea that the electron is a spinning top was introduced by UHLENBECK and GOUDSMIT (1925) fifty years ago and has been touched upon at numerous occasions ever since. DIRAC (1928) found "a great deal of truth in the spinning electron model, at least as a first approximation", but he did not make any attempts to interpret the "other dynamical variables" required "besides the co-ordinates and momenta of the electron". Instead, he created a purely mathematical model of the electron, in which these variables are represented by $4\times4$ matrices. The resulting equation leads to complete agreement with experiment and is, therefore, the equation of motion for the electron.

Several authors have felt the need of some type of interpretation of the internal variables in DIRAC's theory, and have explored the quantum theory of rotating systems with this in mind. Thus, BOPP and HAAG (1950) drew attention to the fact, that the differential operators describing the angular momentum of a two particle system admit eigenfunctions with half-integral quantum numbers. Yet, they found that no associated Schrödinger equation could make use of these through its regular solutions.

These findings, together with the generally accepted view that it is impossible to formulate a satisfactory relativistic description of a 3-dimensional rotor, have led to the consideration of more complex models with added degrees of freedom. At the same time, the scope has been widened by extending the group of particle characteristics to be described to include e.g. isospin and hypercharge. ALLCOCK (1961), in his investigations, considers a particle model based on two 3-dimensional rotors rotating with respect to each other. Other authors (VAN WINTER, 1957; HILLION ET VIGIÉR, 1958; BOHM, HILLION and VIGIÉR, 1960) consider instead a 4-dimensional space-time rotor. A comprehensive list of the many diverse classical and quantum mechanical papers in the field is presented in the monograph by CORBEN (1968).

A study of the various sophisticated models does admittedly leave one with the impression, that the whole field has acquired a somewhat metaphysical character. It is at least fair to say that no simple alternative to DIRAC's purely mathematical model af the electron has emerged.

The alternative does exist, however, as we show in the present paper. It is in fact nothing but the elementary 3-dimensional rotor governed by relativistic quantum mechanics. The dynamics of the rotor is in all respects identical with the dynamics of a DIRAC particle, and hence it gives us new and equally exact ways of visualizing the sometimes rather complex behaviour of electrons.

To make the following presentation reasonably self-contained we summarize the most relevant properties of a 3-dimensional rotor in section 2. Section 3 discusses the relativistic description of a spinless particle; the extension to the relativistic rotor as a model of a particle with spin is considered in section 4, and the possible forms of a local Hamiltonian are derived in section 5. In agreement with DIRAC's conclusions, it is found that only for $s = \frac{1}{2}$ can one construct a local relativistic Hamiltonian (the DIRAC Hamiltonian), and the rotor is in this case an asymmetric top. The DIRAC equation and its solutions are then discussed in sections 6–12 in the light of the preceding sections. The invariance group of the problem is described, and detailed expressions are given for all symmetry operations of this group. Throughout the paper we operate with an unassigned indicator, reflecting the fact that the basic commutator relations may be written in two ways, either with an $i$ or a-$i$.

## 2. The quantum mechanical rotor

Consider a right handed Cartesian coordinate system $S_0$, with axes $X$, $Y$, $Z$ and origin $O$. Two points

$$\boldsymbol{r}_1 = (x_1, y_1, z_1), \qquad \boldsymbol{r}_2 = (x_2, y_2, z_2) \tag{1}$$

define a second right handed system $S$ with origin $O$ and axes specified by the unit vectors

$$\left.\begin{aligned} \boldsymbol{e}_1 &= \frac{1}{2\sin\frac{u}{2}}\left(\frac{\boldsymbol{r}_1}{r_1} - \frac{\boldsymbol{r}_2}{r_2}\right), \\ \boldsymbol{e}_2 &= \frac{1}{2\cos\frac{u}{2}}\left(\frac{\boldsymbol{r}_1}{r_1} + \frac{\boldsymbol{r}_2}{r_2}\right), \\ \boldsymbol{e}_3 &= \frac{1}{r_1 r_2 \sin u}\,\boldsymbol{r}_1 \times \boldsymbol{r}_2 \equiv \boldsymbol{e}_1 \times \boldsymbol{e}_2, \end{aligned}\right\} \tag{2}$$

where $u$ is the angle between $\boldsymbol{r}_1$ and $\boldsymbol{r}_2$. The orientation of $S$ with respect to $S_0$ may be specified by three Euler angles $\alpha$, $\beta$, $\gamma$ such that (ROSE 1957) $S$ is obtained from $S_0$ by

1) a rotation about the $Z$-axis through the angle $\alpha$,
2) a rotation about the new $Y$-axis through the angle $\beta$,
3) a rotation about the new $Z$-axis through the angle $\gamma$.

The following relations are then valid:

$$\left.\begin{aligned} x_1 &= -r_1\left[\cos\alpha\cos\beta\sin\left(\gamma-\frac{u}{2}\right)+\sin\alpha\cos\left(\gamma-\frac{u}{2}\right)\right], \\ y_1 &= -r_1\left[\sin\alpha\cos\beta\sin\left(\gamma-\frac{u}{2}\right)-\cos\alpha\cos\left(\gamma-\frac{u}{2}\right)\right], \\ z_1 &= r_1\sin\beta\sin\left(\gamma-\frac{u}{2}\right), \end{aligned}\right\} \tag{3}$$

$$\left.\begin{aligned} x_2 &= -r_2\left[\cos\alpha\cos\beta\sin\left(\gamma+\frac{u}{2}\right)+\sin\alpha\cos\left(\gamma+\frac{u}{2}\right)\right], \\ y_2 &= -r_2\left[\sin\alpha\cos\beta\sin\left(\gamma+\frac{u}{2}\right)-\cos\alpha\cos\left(\gamma+\frac{u}{2}\right)\right], \\ z_2 &= r_2\sin\beta\sin\left(\gamma+\frac{u}{2}\right). \end{aligned}\right\} \tag{4}$$

The components $s_1$, $s_2$, $s_3$ of the vector operator

$$\boldsymbol{s} = -\iota\hbar\left[\boldsymbol{r}_1\times\nabla_1+\boldsymbol{r}_2\times\nabla_2\right] \tag{5}$$

are the generators for rotations of $S$ about the $X$, $Y$, $Z$ axes, respectively. A finite rotation through an angle $\varepsilon$ about a unit vector $\boldsymbol{n}$ is effected by the operator

$$Q(\boldsymbol{n},\varepsilon) = \exp(-\iota\varepsilon\boldsymbol{n}\cdot\boldsymbol{s}/\hbar). \tag{6}$$

The "indicator" $\iota$ is either $i$ or $-i$, with i being the ordinary imaginary unit. Obviously, $Q(\boldsymbol{n}, \varepsilon)$ is independent of the value assigned to the indicator.

Substitution of (3) and (4) into (5) gives:

$$\left.\begin{aligned} s_1 &= \iota\hbar\left(\sin\alpha\frac{\partial}{\partial\beta}+\cot\beta\cos\alpha\frac{\partial}{\partial\alpha}-\frac{\cos\alpha}{\sin\beta}\frac{\partial}{\partial\gamma}\right),\\ s_2 &= \iota\hbar\left(-\cos\alpha\frac{\partial}{\partial\beta}+\cot\beta\sin\alpha\frac{\partial}{\partial\alpha}-\frac{\sin\alpha}{\sin\beta}\frac{\partial}{\partial\gamma}\right),\\ s_3 &= -\iota\hbar\frac{\partial}{\partial\alpha}. \end{aligned}\right\} \tag{7}$$

The operators

$$\zeta_1 = \boldsymbol{s}\cdot\boldsymbol{e}_1, \qquad \zeta_2 = \boldsymbol{s}\cdot\boldsymbol{e}_2, \qquad \zeta_3 = \boldsymbol{s}\cdot\boldsymbol{e}_3 \tag{8}$$

commute with every component of $\boldsymbol{s}$ and have the form:

$$\left.\begin{aligned} \zeta_1 &= \iota\hbar\left(-\sin\gamma\frac{\partial}{\partial\beta}-\cot\beta\cos\gamma\frac{\partial}{\partial\gamma}+\frac{\cos\gamma}{\sin\beta}\frac{\partial}{\partial\alpha}\right),\\ \zeta_2 &= \iota\hbar\left(-\cos\gamma\frac{\partial}{\partial\beta}+\cot\beta\sin\gamma\frac{\partial}{\partial\gamma}-\frac{\sin\gamma}{\sin\beta}\frac{\partial}{\partial\alpha}\right),\\ \zeta_3 &= -\iota\hbar\frac{\partial}{\partial\gamma}. \end{aligned}\right\} \tag{9}$$

They satisfy the "anomalous" commutator relations

$$[\zeta_i,\zeta_j] = -\iota\hbar\varepsilon_{ijk}\zeta_k, \tag{10}$$

whereas the operators $s_1$, $s_2$, $s_3$ satisfy the "normal" relations

$$[s_i,s_j] = \iota\hbar\varepsilon_{ijk}s_k. \tag{11}$$

$\varepsilon_{ijk}$ is the Levi-Civita symbol, antisymmetric in all three indices ($\varepsilon_{123}=1$), and the convention of summing over repeated indices is understood.

We also note, that

$$s^2 = -\hbar^2\left[\frac{1}{\sin\beta}\frac{\partial}{\partial\beta}\left(\sin\beta\frac{\partial}{\partial\beta}\right)+\frac{1}{\sin^2\beta}\left(\frac{\partial^2}{\partial\alpha^2}+\frac{\partial^2}{\partial\gamma^2}\right)-\frac{2\cos\beta}{\sin^2\beta}\frac{\partial^2}{\partial\alpha\partial\gamma}\right], \tag{12}$$

where

$$s^2 = s_is_i = \zeta_i\zeta_i. \tag{13}$$

The expressions (5) – (12) are, of course, well known. They are reproduced here for the sake of reference and in order to stress, that the $s_i$ and $\zeta_i$ operate directly on the "dreibein" defined by $\boldsymbol{e}_1$, $\boldsymbol{e}_2$ and $\boldsymbol{e}_3$, or equivalently, on functions depending on the orientation of the dreibein through $\alpha$, $\beta$ and $\gamma$. Thus, we do not consider $\boldsymbol{r}_1$ and $\boldsymbol{r}_2$ as coordinates of particles, they

are merely mathematical points by means of which the dreibein may be defined. $r_1$, $r_2$ and $u$ are, in accordance with this, dummy coordinates which drop out of the description as soon as the Euler angles are introduced. It is in this way that it becomes possible to separate the fact that a system may have an orientation, from more or less arbitrary speculations concerning an internal distribution of matter. That such a separation can be made is, of course, the basic assumption behind most efforts mentioned in the Introduction — with the work of BOPP and HAAG as an exception.

The vector $\boldsymbol{r}_1$ and $\boldsymbol{r}_2$ may play a very different role in other contexts, as in the theory of two-electron atoms (HYLLERAAS, 1929; BREIT, 1930) where they do represent particle coordinates. $r_1$, $r_2$ and $u$ are then actual internal variables, of the greatest importance for the character of the atomic states. The construction of internal coordinate systems similar to ours has consequently been studied by several authors. A review is due to BHATIA and TEMKIN (1964).

Let us now assume that the dreibein discussed above describes the orientation of an elementary particle with respect to $S_0$. The probability amplitude for this orientation is then a wavefunction built over the simultaneous eigenfunctions $D^s_{mn}(\alpha, \beta, \gamma)$ of the commuting operators $s^2$, $s_3$ and $\zeta_3$. These eigenfunctions have been known since the early days of quantum mechanics, and up-to-date presentations of their properties, as well as the various phase conventions introduced in the course of time, may be found in the books by BOHR and MOTTELSON (1969) and JUDD (1975). They satisfy the relations:

$$\left.\begin{aligned} s^2 D^s_{mn} &= s(s+1)\hbar^2 D^s_{mn} && (s = 0, \tfrac{1}{2}, 1 \ldots), \\ s_3 D^s_{mn} &= m\hbar D^s_{mn} && (m = s, s-1, \ldots, -s), \\ \zeta_3 D^s_{mn} &= n\hbar D^s_{mn} && (n = s, s-1, \ldots, -s). \end{aligned}\right\} \quad (14)$$

For each value of $s$ they define a linear function space $\Omega_s$ of dimension $(2s+1)^2$. Properly normalized they satisfy the orthonormality condition:

$$\left.\begin{aligned} \langle D^s_{mn} \mid D^{s'}_{m'n'} \rangle &= \int_0^{2\pi} d\alpha \int_0^{\pi} \sin\beta d\beta \int_0^{4\pi} d\gamma D^s_{mn}(\alpha,\beta,\gamma)\, {}^*D^{s'}_{m'n'}(\alpha,\beta,\gamma) \\ &= \delta_{ss'}\delta_{mm'}\delta_{nn'}, \end{aligned}\right\} \quad (15)$$

and the phases may be chosen such that

$$\left.\begin{aligned} (s_1 \pm \imath s_2) D^s_{mn} &= \hbar\left[(s \mp m)(s \pm m + 1)\right]^{1/2} D^s_{m\pm 1, n}, \\ (\zeta_1 \mp \imath \zeta_2) D^s_{mn} &= \hbar\left[(s \mp n)(s \pm n + 1)\right]^{1/2} D^s_{m, n\pm 1}. \end{aligned}\right\} \quad (16)$$

Thus we have, for $s = \frac{1}{2}$:

$$\left.\begin{aligned}
\theta_1 &= D^{1/2}_{1/2,\,1/2} = (8\pi^2)^{-1/2}\cos\frac{\beta}{2}\,e^{\iota\alpha/2}\,e^{\iota\gamma/2},\\
\theta_2 &= D^{1/2}_{-1/2,\,1/2} = (8\pi^2)^{-1/2}\sin\frac{\beta}{2}\,e^{-\iota\alpha/2}\,e^{\iota\gamma/2},\\
\theta_3 &= D^{1/2}_{1/2\,-1/2} = -(8\pi^2)^{-1/2}\sin\frac{\beta}{2}\,e^{\iota\alpha/2}\,e^{-\iota\gamma/2},\\
\theta_4 &= D^{1/2}_{-1/2,\,-1/2} = (8\pi^2)^{-1/2}\cos\frac{\beta}{2}\,e^{-\iota\alpha/2}\,e^{-\iota\gamma/2}.
\end{aligned}\right\} \tag{17}$$

It was shown by EULER, in his pioneer work on the motion of rigid bodies two hundred years ago, that the configuration space for a 3-dimensional rotor is the 4-dimensional unit sphere (see, e.g. WHITTAKER, 1904), each orientation of the rotor corresponding to two points on the sphere. The functions $D^s_{mn}$ may accordingly be viewed as 4-dimensional spherical harmonics (HUND, 1928), and $\Omega_s$ is an irreducible function space under the operations of $O(4)$, the 4-dimensional orthogonal group. The operators $s_i$ and $\zeta_i$ represent the generators of $O(4)$. It is for certain purposes convenient to replace them by the operators

$$\left.\begin{aligned}
\lambda_i &= s_i - \zeta_i,\\
\chi_i &= s_i + \zeta_i,
\end{aligned}\right\} \tag{18}$$

which obey the commutator relations:

$$\left.\begin{aligned}
[\lambda_i, \lambda_j] &= \iota\hbar\varepsilon_{ijk}\lambda_k,\\
[\lambda_i, \chi_j[ &= \iota\hbar\varepsilon_{ijk}\chi_k,\\
[\chi_i, \chi_j] &= \iota\hbar\varepsilon_{ijk}\lambda_k.
\end{aligned}\right\} \tag{19}$$

Having characterized the functions from which the probability amplitude for the orientation of a 3-dimensional rotor may be constructed, we shall pass on to a discussion of its dynamics. Our basic assumption will be, that it is possible to construct a Hamiltonian of the form

$$H = H(s_1, s_2, s_3; \zeta_1, \zeta_2, \zeta_3; a), \tag{20}$$

with $a$ referring to a set of external variables which commute with the internal variables $s_i$ and $\zeta_i$. It follows, that

$$[H, s^2] = 0, \tag{21}$$

and hence that the eigenfunctions of $H$ may be written as

$$\psi_k^s = \sum_{i=1}^{(2s+1)^2} \psi_{i,k}\theta_i, \tag{22}$$

where $\theta_i$ ($i = 1, 2, \ldots, (2s+1)^2$) are the functions $D^s_{mn}(\alpha, \beta, \gamma)$, and $\psi_{i,k}$ are functions of the external variables.

Each function space $\Omega_s$ will thus give rise to its own set of eigenfunctions. Inded, it will turn out that the very form of $H$ will depend on the quantum number $s$, and that only for $s = \frac{1}{2}$ is it possible to construct a local Hamiltonian. These results are consequences of the constraints imposed by the theory of special relativity, and discussed in the following section.

## 3. Relativistic description of a spinless particle

The special theory of relativity requires that the laws of physics be invariant under the operations of the inhomogeneous LORENTZ group. Let us, by way of introduction, sketch the implications of this requirement in the case of a free particle without spin.

With

$$x_\mu = (x_1, x_2, x_3, \text{ ict}) \tag{23}$$

denoting a general space-time point, we introduce the operators

$$p_\mu = -\imath\hbar \frac{\partial}{\partial x_\mu} \tag{24}$$

and

$$L_{\mu\nu} = x_\mu p_\nu - x_\nu p_\mu. \tag{25}$$

The following commutator relations are then valid:

$$[x_\mu, p_\nu] = \imath\hbar\delta_{\mu\nu}, \tag{26}$$

$$[p_\mu, p_\nu] = 0, \tag{27}$$

$$[L_{\mu\nu}, L_{\varkappa\lambda}] = \imath\hbar(\delta_{\mu\varkappa}L_{\nu\lambda} + \delta_{\nu\lambda}L_{\mu\varkappa} - \delta_{\nu\varkappa}L_{\mu\lambda} - \delta_{\mu\lambda}L_{\nu\varkappa}), \tag{28}$$

$$[L_{\mu\nu}, p_\lambda] = \imath\hbar(\delta_{\mu\lambda}p_\nu - \delta_{\nu\lambda}p_\mu). \tag{29}$$

We adopt the convention that greek indices take on the values from 1 to 4, italic indices the values from 1 to 3.

The operators $L_{\mu\nu}$ represent the generators of $O(4)$. They are antisymmetric in $\mu$ and $\nu$, and hence one introduces new operators which are all independent, viz.

$$\left.\begin{aligned} l_i &= \tfrac{1}{2}\varepsilon_{ijm} L_{jm}, \\ k_i &= L_{i4}. \end{aligned}\right\} \tag{30}$$

The relations (28) are then replaced by

$$\left.\begin{aligned} [l_i, l_j] &= \iota\hbar\varepsilon_{ijm} l_m, \\ [l_i, k_j] &= \iota\hbar\varepsilon_{ijm} k_m, \\ [k_i, k_j] &= \iota\hbar\varepsilon_{ijm} l_m, \end{aligned}\right\} \tag{31}$$

which are similar to (19).

Next, we define operators for finite transformations:

$$\left.\begin{aligned} F(\boldsymbol{a}) &= \exp(-\iota a_i p_i/\hbar), \\ U(\tau) &= \exp(-\iota\tau p_4/\hbar), \\ R(\boldsymbol{n}, \varepsilon) &= \exp(-\iota\varepsilon_i l_i/\hbar), \\ \Lambda(\boldsymbol{n}', \eta) &= \exp(-\iota\eta_i k_i/\hbar), \end{aligned}\right\} \tag{32}$$

characterized by the six real parameters $a_i$, $\varepsilon_i$, and the four imaginary parameters $\tau$ and $\eta_i$. $\boldsymbol{n}$ and $\boldsymbol{n}'$ are real unit vectors such that $\varepsilon\boldsymbol{n} = (\varepsilon_1, \varepsilon_2, \varepsilon_3)$ and $\eta\boldsymbol{n}' = (\eta_1, \eta_2, \eta_3)$. $F$ generates a spatial translation $\boldsymbol{a}$, $U$ a time displacement $\tau/(ic)$, and $R$ a rotation through the angle $\varepsilon$ about $\boldsymbol{n}$. $\Lambda$ generates a LORENTZ transformation in the direction $\boldsymbol{n}'$ corresponding to the relative velocity $V$ such that

$$\tan\eta = iV/c. \tag{33}$$

The transformations are all independent of the value assigned to the indicator $\iota$.

All $F$ and $U$ and products thereof represent the group $\mathcal{T}$ of translations in MINKOWSKI space. All $R$ and $\Lambda$ and products thereof represent the proper, orthochronous, homogeneous LORENTZ group $\mathcal{L}_0$. The semidirect product of $\mathcal{T}$ and $\mathcal{L}_0$ is the proper, orthochronous, inhomogeneous LORENTZ group $\mathcal{T}\mathcal{L}_0$. The representations of these groups, as well as of the extensions obtained by adding the operators for space and time inversion, have been thoroughly studied. We refer to papers by WIGNER (1939), BARGMANN and WIGNER (1948), and to the books by ROMAN (1960), LYUBARSKII (1960), and LOMONT (1959).

A representation of $\mathcal{T}\mathcal{L}_0$ for a single particle without spin is obtained by constructing a linear function space which is invariant under the operators (24) and (25). As basic functions we may choose eigenfunctions of the commuting operators $p_1, p_2, p_3$, and $p_4$, i.e. functions of the general form

$$|\pi_1, \pi_2, \pi_3, i\pi_0\rangle = \exp(\iota\boldsymbol{\pi}\cdot\boldsymbol{r}/\hbar)\exp(-\iota c\pi_0 t/\hbar). \tag{34}$$

The operator

$$p_\mu p_\mu = \hbar^2\left(\frac{1}{c^2}\frac{\partial^2}{\partial t^2} - \nabla^2\right) \tag{35}$$

commutes with all operators in (24) and (25) and hence with all operators in the set (32). A function space which is irreducible under the operators representing $\mathscr{T}\mathscr{L}_0$ will consequently be characterized by a single eigenvalue of $p_\mu p_\mu$. Since

$$p_\mu p_\mu |\boldsymbol{\pi}, i\pi_0\rangle = (\pi^2 - \pi_0^2)|\boldsymbol{\pi}, i\pi_0\rangle, \tag{36}$$

we have the requirement:

$$\pi_0^2 = \pi^2 + m_0^2 c^2, \tag{37}$$

with $m_0$ being a constant. This constant is identified with the mass of the particle. We further identify $\boldsymbol{\pi}$ with the momentum and $c\pi_0$ with the kinetic energy:

$$E_{kin} = c\pi_0. \tag{38}$$

$m_0$ and $\pi_0$ are, accordingly, assumed to be non-negative; $(\boldsymbol{\pi}, i\pi_0)$ is a time-like four-vector, and

$$\pi_0 = \sqrt{\pi^2 + m_0^2 c^2}. \tag{39}$$

It is easy to verify that all functions of the form (34), with the same $m_0$, may be generated from one function in the set by use of the operators $R$ and $A$ of (32). A convenient choice for the representative function is

$$|0, 0, 0, im_0 c\rangle = \exp(-\iota m_0 c^2 t/\hbar) \qquad \text{when } m_0 > 0, \tag{40}$$

$$|0, 0, 1, i\rangle > \exp[\iota(x_3 - ct)/\hbar] \qquad \text{when } m_0 = 0. \tag{41}$$

We get, for instance:

$$\left.\begin{aligned} A(0, 0, 1, \eta)|0, 0, 0, im_0 c\rangle &= \exp(\iota\pi x_3/\hbar)\exp(-\iota c\sqrt{\pi^2 + m_0^2 c^2}\, t/\hbar) \\ &= |0, 0, \pi, i\pi_0\rangle, \end{aligned}\right\} \tag{42}$$

with

$$\tan\eta = i\pi/\sqrt{\pi^2 + m_0^2 c^2} = ic\pi/E_{kin}. \tag{43}$$

By comparing with (33) we obtain the usual expression for the velocity of the particle:

$$V = c^2\pi/E_{kin}. \tag{44}$$

Similarly we get:

$$A(0,0,1,\eta)|0,0,1,i\rangle = \exp[\imath\pi'(x_3 - ct)/\hbar] = |0,0,\pi',i\pi'\rangle, \tag{45}$$

where

$$\pi' = \exp(-i\eta). \tag{46}$$

Let us now consider the equation of motion for a free spinless particle. The existence of such an equation is, of course, a necessary condition for being able to predict the future from the instantaneous situation. An equation of motion must have the form

$$H\psi = \imath h \frac{\partial \psi}{\partial t}, \tag{47}$$

with $\psi$ being the wavefunction and $H$ a time independent operator, the Hamiltonian of the particle. $H$ and $\imath h \frac{\partial}{\partial t}$ are thus required to be equivalent operators, and this implies that the relations (27)–(29) must remain unaffected by the substitution

$$p_4 \rightarrow \frac{i}{c} H. \tag{48}$$

The relations (27)–(29), with the substitution (48), represent what has been called by DIRAC "relativistic dynamics in the instant form" (DIRAC, 1949). The problem of constructing a dynamical theory is tantamount to finding an $H$ that will satisfy the substituted relations.

The operators $\pm c\sqrt{p^2 + m_0^2 c^2}$, with $m_0$ being an arbitrary constant, will satisfy the relations in our case. $m_0$ is again fixed as the mass of the particle, and a comparison with (34) and (47) shows, that we must choose

$$H = c\sqrt{p^2 + m_0^2 c^2}. \tag{49}$$

The solution for the Hamiltonian is thus unique. Its eigenvalues represent the kinetic energy according to (38).

## 4. The relativistic rotor

We shall now extend the treatment of the previous section to the case of a quantum mechanical rotor, as a model of a particle for which it is possible to talk about an orientation in space. The coordinates $x_\mu$ define the position of the particle by specifying the origin of the coordinate system $S_0$, in space

and time. The EULER angles $\alpha,\beta,\gamma$ specify the orientation of the particle, i.e. the orientation of $S$ with respect to $S_0$.

A first necessary condition for being able to construct a relativistic dynamics for the rotor is the existence of an algebra similar to the one given through the relations (27)–(29). The four-momentum (24) is defined as before, but the operators $L_{\mu\nu}$ must be supplemented with operators built over the internal generators $s_i$ and $\zeta_i$, as given by (7) and (9). Thus we define:

$$J_{\mu\nu} = L_{\mu\nu} + s_{\mu\nu}, \tag{50}$$

and similar to (30):

$$\left.\begin{aligned} J_i &= \tfrac{1}{2}\varepsilon_{ijm}J_{jm}, & s_i &= \tfrac{1}{2}\varepsilon_{ijm}s_{jm}, \\ K_i &= J_{i4}, & \varkappa_i &= s_{i4}. \end{aligned}\right\} \tag{51}$$

The operators $J_{\mu\nu}$ and $p_\mu$ must satisfy the relations (27)–(29) with $J_{\mu\nu}$ substituted for $L_{\mu\nu}$. The operators (51) must satisfy relations similar to (31), in particular:

$$\left.\begin{aligned} [s_i, s_j] &= \iota\hbar\varepsilon_{ijm}s_m, \\ [s_i, \varkappa_j] &= \iota\hbar\varepsilon_{ijm}\varkappa_m, \\ [\varkappa_i, \varkappa_j] &= \iota\hbar\varepsilon_{ijm}s_m. \end{aligned}\right\} \tag{52}$$

We have already, by (18), constructed a set of operators satisfying (52), but they cannot be used for the present purpose, because it is essential that the $s_i$ in (52) be identical with the $s_i$ in (7). This is dictated by the form of the rotation operator (6).

With the $s_i$ fixed by this requirement, it only remains to determine the $\varkappa_i$. The second of the relations (52) shows that $\kappa$ must be equal to $\boldsymbol{s}$ times an operator $b$ commuting with $\boldsymbol{s}$:

$$\kappa = b\boldsymbol{s}, \tag{53}$$

and because of (13) we may take this $b$ to be a function of the $\zeta_i$ alone. The third of the relations (52) shows finally that the condition

$$b^2 = 1 \tag{54}$$

must hold for $b$.

In looking for an operator that will satisfy (54) one must exclude the trivial solutions $b = \pm 1$, since $\boldsymbol{s}$ and $\kappa$ must be linearly independent. This implies, that it is impossible to find a universal expression for $b$, but with (20) and (22) in mind it becomes meaningful to solve (54) within each function space $\Omega_s$ separately (cf. (14)). In this way one obtains the following semigeneral solution, independent of the value assigned to $\iota$:

$$\left.\begin{aligned} b &= \exp(-\pi\iota \boldsymbol{e}\cdot\boldsymbol{s}/\hbar) && \text{for } s \text{ integer,} \\ b &= i\exp(-\pi\iota \boldsymbol{e}\cdot\boldsymbol{s}/\hbar) && \text{for s half-integer,} \end{aligned}\right\} \tag{55}$$

with $\boldsymbol{e}$ being an arbitrary unit vector in the internal coordinate system $S$.

Since no dynamical preference has been given to any of the axes of $S$ so far, we can now introduce such a preference by fixing the direction of $\boldsymbol{e}$. A convenient choice at the present stage is

$$\boldsymbol{e} = \boldsymbol{e}_3. \tag{56}$$

Thus we obtain:

$$\left.\begin{aligned} b &= \frac{2}{\hbar}\frac{\iota}{i}\zeta_3 && \text{for } s = \tfrac{1}{2}, \\ b &= 1 - \frac{2}{\hbar^2}\zeta_3^2 && \text{for } s = 1, \\ &\text{etc.} \end{aligned}\right\} \tag{57}$$

Having determined the operators of the basic algebra we obtain the operators for the finite transformations of $\mathscr{T}\mathscr{L}_0$ by multiplying $R(\boldsymbol{n},\varepsilon)$ in (32) with the operator (6), i.e.

$$Q(\boldsymbol{n},\varepsilon) = \exp(-\iota\varepsilon_i s_i/\hbar). \tag{58}$$

The operator $\Lambda(\boldsymbol{n}',\eta)$ is similarly to be multiplied with

$$\lambda(\boldsymbol{n}',\eta) = \exp(-\iota\eta_i \varkappa_i/\hbar). \tag{59}$$

These operators are again independent of the value assigned to $\iota$.

The operator $p_\mu p_\mu$ of eqn. (35) will also commute with all operators in the new algebra. The irreducible representations of $\mathscr{T}\mathscr{L}_0$ are consequently spanned by functions of the form

$$\psi_j^s = \varphi_j^s(\alpha,\beta,\gamma;\pi,m_0)\,|\,\pi, i\pi_0\rangle \tag{60}$$

where $|\,\pi, i\pi_0\rangle$ is given by (34), and $\varphi_j^s$ are functions of the internal coordinates, depending parametrically on $s$, $\pi$ and $m_0$. The relation (39) is still valid and the energy is given by (38) as before.

Let us assume, in what follows, that $m_0 \neq 0$. The form of $\varphi_j^s$ is then completely given, once it is known for $\pi = \mathbf{0}$. The relation is:

$$\varphi_j^s(\alpha,\beta,\gamma;\pi,m_0) = \lambda(\pi/\pi,\eta)\varphi_j^s(\alpha,\beta,\gamma;\mathbf{0},m_0), \tag{61}$$

with $\eta$ given by (43). We are thus left with the problem of classifying $\varphi_j^s(\alpha,\beta,\gamma;\mathbf{0},m_0)$ further with respect to the symmetry of $\mathscr{T}\mathscr{L}_0$.

At this point we note that there is another operator besides $p_\mu p_\mu$ which commutes with all operators in the basic algebra, namely $w_\mu w_\mu$, where

$$w_\mu = (\boldsymbol{p} \times \boldsymbol{\kappa} + p_4 \boldsymbol{s}, -\boldsymbol{p} \cdot \boldsymbol{s}), \tag{62a}$$

(BARGMANN and WIGNER, 1946). USING (53) and (54) we get, that

$$w_\mu w_\mu = p_\mu p_\mu s_i s_i . \tag{62b}$$

This new invariant gives the mathematical justification for the label $s$ in (60).

The components of $w_\mu$ do not commute with each other. We have, however, the very important result:

$$[w_\mu, p_\nu] = 0, \tag{63}$$

according to which each $\psi_j^s$ may be taken as an eigenfunction for one of the new $w_\mu$ as well. We note, in particular, that $\psi_j^s$ for $\pi = \mathbf{0}$ may be chosen as an eigenfunction of $p_4 s_3$.

For the sake of completeness we also note, that $p_\mu w_\mu$ is an invariant, but since it is identically zero, it is of no use in the present context.

The functions $\varphi_j^s$ are linear combinations of the $(2s+1)^2$ functions $D_{mn}^s(\alpha, \beta, \gamma)$ of section 2, but it is readily seen that the $2s+1$ functions corresponding to a given value of $n$ constitute an invariant function space under all $s_i$ and $\varkappa_i$. Each value of $n$ will thus give rise to an irreducible representation of $\mathscr{T}\mathscr{L}_0$, with the functions $\varphi_j^s$ equal to the functions $D_{mn}^s(\alpha, \beta, \gamma)$, $m = s, s-1, \ldots, -s$.

The $2s+1$ irreducible representations ($n = s, s-1, \ldots, -s$) obtained in this way are, however, all equivalent. This follows from general discussions on the irreducible representations of $\mathscr{T}\mathscr{L}_0$ (see references following eqn. (33)), according to which the representative functions for $\boldsymbol{p} = \mathbf{0}$ are characterized as spanning irreducible representations of $R(3)$, the 3-dimensional real rotation group. $R(3)$ is in this context the little group associated with the four-vector $(0, 0, 0, im_0 c)$.

We have thus arrived at the conclusion, that only for $s = 0$ (which is the case already studied in the previous section) is there no redundant degeneracy in the classification of the rotor states When $s \neq 0$ we are left with a $2s+1$ fold degeneracy.

Any function of the form (60) will satisfy the SCHRÖDINGER equation (47) with the Hamiltonian (49). This is, however, of little interest in the present context, since such a Hamiltonian does not effect the internal coordinates at all. We shall consequently look for a more general Hamiltonian by recon-

sidering the basic algebra and require that it be satisfied with the substitution (48).

The variable $x_4 = ict$ commutes with all operators of the substituted algebra, and may therefore, without loss of generality, be set equal to zero. Thus, we get the substituted operators:

$$\left.\begin{aligned} p_\mu &= \left(p_1, p_2, p_3, \frac{i}{c} H\right), \\ J_i &= l_i + s_i, \\ K_i &= \frac{i}{c} x_i H + \varkappa_i, \end{aligned}\right\} \tag{64}$$

and the algebraic equations involving $H$ become:

$$[H, p_i] = 0, \tag{65}$$

$$[H, J_i] = 0, \tag{66}$$

$$[H, K_i] = \frac{\iota}{i} \hbar c p_i, \tag{67}$$

$$[p_i, K_j] = \frac{\iota}{i} \hbar \delta_{ij} \frac{1}{c} H, \tag{68}$$

$$[J_i, K_j] = \iota \hbar \varepsilon_{ijm} K_m, \tag{69}$$

$$[K_i, K_j] = \iota \hbar \varepsilon_{ijm} J_m. \tag{70}$$

In addition, we have the invariance relation

$$H^2 = c^2 p^2 + m_0^2 c^4. \tag{71}$$

## 5. The local Hamiltonians

In searching for solutions to the above relations we begin by noting, that (65) and (66) imply that $x_1, x_2, x_3$ and $\alpha, \beta, \gamma$ are cyclic coordinates, i.e. $H$ must be of the form

$$H = H(s_i, \zeta_i, p_i; m_0), \tag{72}$$

as alredy anticipated by (20). The relations (68) and (69) are then automatically satisfied, whereas (67) imposes the conditions

$$\frac{i}{c}[H,\varkappa_j] - \frac{1}{c^2}[H,x_j]H = \iota\hbar p_j. \tag{73}$$

The relation (70) is automatically satisfied whenever (73) is.

The necessary conditions on $H$ are thus contained in (66), (71) and (73).

It follows from (71), as well as from (73), that if $H$ is a polynomial in $p_i$, then this polynomial must be of the first degree. Any local Hamiltonian must thus be linear in the momentum operators. The only other conceivable solution is the non-local form

$$H = a\sqrt{c^2p^2 + m_0^2c^4},\ a^2 = 1 \tag{74}$$

with a being a function of the $s_i$ and $\zeta_i$.

A short consideration of (66) and (73) shows, that a must commute with every $s_i$ and $\varkappa_i$, and hence the only possible values are $\pm 1$ and $\pm b$, with $b$ given by (55) and (57).

We shall not, however, consider the non-local Hamiltonians further, but instead confine the attention to local Hamiltonians, as the more satisfactory type of operators from a physical point of view.

A local Hamiltonian is, as mentioned above, necessarily linear in the momentum operators. Hence, we write it as

$$H = \lambda + \mu_j p_j, \tag{75}$$

with $\lambda$ and $\mu_j$ being functions of $s_i$ and $\zeta_i$. Insertion in (68) shows, that $\lambda$ must be a function of the $\zeta_i$ alone, and that $\mu_j = \mu s_j$ with $\mu$ depending only on the $\zeta_i$. Thus we have:

$$H = \lambda(\zeta_i) + \mu(\zeta_i)(\boldsymbol{s}\cdot\boldsymbol{p}). \tag{76}$$

To determine the functions $\lambda$ and $\mu$ we insert (76) in (73) and compare the coefficients of $p_1$, $p_2$ and $p_3$ in turn. It is then found that a necessary condition for (73) to be satisfied is, that $s_1^2 = s_2^2 = s_3^2 =$ a non-vanishing constant. This is only possible if the operators act in the function space $\Omega_{1/2}$, in which case:

$$\left.\begin{aligned} s_is_j + s_js_i &= \tfrac{1}{2}\hbar^2\delta_{ij}, \\ \zeta_i\zeta_j + \zeta_i\zeta_j &= \tfrac{1}{2}\hbar^2\delta_{ij}, \end{aligned}\right\} \tag{77}$$

and

$$\left.\begin{aligned} s_is_j &= \tfrac{1}{2}\hbar\varepsilon_{ijk}s_k, \\ \zeta_i\zeta_j &= -\tfrac{1}{2}\hbar\varepsilon_{ijk}\zeta_k. \end{aligned}\right\} \tag{78}$$

Hence it follows, that it is impossible to turn a 3-dimensional rotor into a relativistic system with a local Hamiltonian, unless it is endowed with an $s$ quantum number of $\frac{1}{2}$.

We proceed, then, by assuming the validity of (77) and (78). $\lambda$ and $\mu$ are then linear function of $\zeta_1,\zeta_2,\zeta_3$. We shall furthermore deviate from (56) and (57) by choosing $\boldsymbol{e}_1$ as the preferred axis when deflning $\kappa$, i.e. we put

$$\boldsymbol{e} = \boldsymbol{e}_1, \tag{79}$$

and hence

$$\kappa = \frac{2}{\hbar}\frac{\iota}{i}\zeta_1 \boldsymbol{s}. \tag{80}$$

Insertion of (77), (78) and (80) in (73) and further comparison of the coefficients of $p_1$, $p_2$ and $p_3$ leads to the unique result

$$\mu = \frac{4c}{\hbar^2}\zeta_1. \tag{81}$$

Finally one obtains, from the terms independent of $p_i$:

$$\lambda\zeta_1 + \zeta_1\lambda = 0. \tag{82}$$

This relation shows, in the light of (77), that $\lambda$ must be a linear combination of $\zeta_2$ and $\zeta_3$, and since no preference has been given to any of the axes perpendicular to $\boldsymbol{e}_1$ we may set

$$\lambda = A\zeta_3, \tag{83}$$

with A being a constant.

Thus we obtain the Hamiltonian

$$H = A\zeta_3 + \frac{4c}{\hbar^2}\zeta_1(\boldsymbol{s}\cdot\boldsymbol{p}). \tag{84}$$

To determine $A$ we square $H$ and compare with (71), while using (77). This leads to the values

$$A = \pm\frac{2}{\hbar}m_0c^2, \tag{85}$$

and hence:

$$H = \pm\frac{2}{\hbar}m_0c^2\zeta_3 + \frac{4c}{\hbar^2}\zeta_1(\boldsymbol{s}\cdot\boldsymbol{p}). \tag{86}$$

The eigenfunctions of $H$ are of the form (22) with $s = \frac{1}{2}$, i.e.

$$\psi_k^{1/2}(\boldsymbol{r}, \alpha, \beta, \gamma) = \sum_{i=1}^{4} \psi_{i,k}(\boldsymbol{r})\,\theta_i(\alpha, \beta, \gamma), \tag{87}$$

where $\theta_1$, $\theta_2$, $\theta_3$, $\theta_4$, are the functions specified by (17). The equation of motion is of the form (47). It becomes identical with the DIRAC equation when transformed to a matrix representation.

## 6. The Dirac equation

The transformation mentioned is obtained by substituting the general expansion

$$\Psi = \sum_{i=1}^{4} \psi_i(\boldsymbol{r}, t)\,\theta_i(\alpha, \beta, \gamma) \tag{88}$$

into the equation of motion (47), i.e.

$$H\Psi = \iota\hbar \frac{\partial \Psi}{\partial t}, \tag{47}$$

with $H$ as given by (86). The inner product is then formed with $\theta_1$, $\theta_2$, $\theta_3$, $\theta_4$ in turn and the orthonormality relations (15) utilized. As a result one obtains:

$$(\pm m_0 c^2 \beta + c\alpha \cdot \boldsymbol{p})\,\psi = \iota\hbar \frac{\partial \psi}{\partial t}, \tag{89}$$

where $\psi$ is a column vector with $\psi_1$, $\psi_2$, $\psi_3$, $\psi_4$, of (88) as components, and

$$\beta = \begin{bmatrix} I & 0 \\ 0 & -I \end{bmatrix}, \quad \alpha_k = \begin{bmatrix} 0 & \sigma_k \\ \sigma_k & 0 \end{bmatrix} \quad (k = 1, 2, 3). \tag{90}$$

$I$ is the two-dimensional unit matrix, and

$$\sigma_1 = \begin{bmatrix} 0 & 1 \\ 1 & 0 \end{bmatrix}, \quad \sigma_2 = \begin{bmatrix} 0 & -\iota \\ \iota & 0 \end{bmatrix}, \quad \sigma_3 = \begin{bmatrix} 1 & 0 \\ 0 & -1 \end{bmatrix} \tag{91}$$

become the PAULI spin matrices when $\iota$ is assigned the value $i$.

Eqn. (89), with the upper sign in front of $m_0 c^2 \beta$ and $\iota = i$, is in fact the DIRAC equation in its Hamiltonian form. The ambiguity in sign of the first term will be commented on in section 13. Until then we shall adopt the plus sign in (86), and write

$$H = m_0 c^2 \zeta_3' + c\zeta_1'(\boldsymbol{s}' \cdot \boldsymbol{p}), \tag{92}$$

where the primed operators, introduced for simplicity, are equal to the corresponding unprimed ones, multiplied by $\frac{2}{\hbar}$.

The present derivation of the DIRAC equation is, of course, rather different from DIRAC's own, since it is based on a model (albeit a very well-defined one) rather than on the purely mathematical properties of hypercomplex numbers. The principles underlying the two derivations are, however, the same, and they may therefore supplement each other in a fruitful way. It is interesting to note, that the 4-dimensional matrices $\sigma_i$ and $\varrho_i$ occurring in DIRAC's paper (DIRAC, 1928) are nothing but the matrix representatives of our $s_i$ and $\zeta_i$ operators multiplied by $\frac{2}{\hbar}$. The sign of $\varrho_2$ is the opposite of ours, though, and the minus sign in the second of the relations (78) is thus absent in DIRAC's equivalent relation.

We shall now consider the solutions of (47) in the light of the previous sections, with the aim of showing the coherence of our approach. We close the present section with the obvious remark, that the functions (88) are independent of the basis chosen in $\Omega_{1/2}$. In other words: if one prefers to take four orthogonal conbinations of the functions (17) as a new basis, then this has no effect upon the analytical form of $\Psi$. The matrix representation of (47) will, however, now be different from (89). The fundamental relations (77) and (78) will, on the other hand, be satisfied by the matrices in any representation. This expresses the so-called representation independence of the DIRAC equation.

## 7. The solutions of the Dirac equation

The solutions of the equation

$$H\Psi = \iota\hbar\frac{\partial\Psi}{\partial t} \tag{47}$$

with $H$ given by (92) are, of course, equivalent to the solutions obtained by the more conventional theory, as presented in wellknown textbooks (e.g. BJORKEN and DRELL, 1964; SAKURAI, 1967). Referring to the discussion in section 4 we may present the results of solving (47) in the following way.

The solutions of (47) span two irreducible representations, $\Gamma$ and $\tilde{\Gamma}$, of $\mathscr{T}\mathscr{L}_0$. These representations become the complex conjugate of each other, when the basis functions spanning them are generated by means of the

operators (32), (58) and (59), starting from the two complex conjugate pairs of functions:

$$\left.\begin{aligned} \Phi_1 &= \theta_1(\alpha,\beta,\gamma)\exp(-\imath m_0 c^2 t/\hbar), \\ \Phi_2 &= \theta_2(\alpha,\beta,\gamma)\exp(-\imath m_0 c^2 t/\hbar), \end{aligned}\right\} \tag{93}$$

and

$$\left.\begin{aligned} \tilde{\Phi}_1 &= \theta_4(\alpha,\beta,\gamma)\exp(\imath m_0 c^2 t/\hbar), \\ \tilde{\Phi}_2 &= -\theta_3(\alpha,\beta,\gamma)\exp(\imath m_0 c^2 t/\hbar). \end{aligned}\right\} \tag{94}$$

Let us construct the functions obtained by performing a homogeneous LORENTZ transformation corresponding to the direction

$$\boldsymbol{e} = \pi/\pi \tag{95}$$

and the parameter $\eta$ given by (43).

The functions $\exp(\pm\imath m_0 c^2 t/\hbar)$ are transormed similar to (42). The $\theta_j$ functions are transformed by means of the operator

$$\lambda(\boldsymbol{e},\eta) = \exp(-\imath\eta\boldsymbol{e}\cdot\kappa/\hbar), \tag{96}$$

with $\kappa$ given by (80). Introducing the primed operator

$$\kappa' = \frac{2}{\hbar}\kappa = \frac{\iota}{i}\zeta_1'\boldsymbol{s}' \tag{97}$$

this becomes

$$\lambda(\boldsymbol{e},\eta) = \cos\frac{\eta}{2} - i\zeta_1'(\boldsymbol{e}\cdot\boldsymbol{s}')\sin\frac{\eta}{2}. \tag{98}$$

Applying standard trigonemetric formulae in connection with the expression (43) for $\tan\eta$ we obtain

$$\left.\begin{aligned} \cos\frac{\eta}{2} &= \left(\frac{|E| + m_0 c^2}{2m_0 c^2}\right)^{\frac{1}{2}}, \\ \sin\frac{\eta}{2} &= i\left(\frac{|E| - m_0 c^2}{2m_0 c^2}\right)^{\frac{1}{2}}, \end{aligned}\right\} \tag{99}$$

where

$$|E| = \sqrt{c^2\pi^2 + m_0^2 c^4}. \tag{100}$$

Thus, we get:

$$\lambda(\boldsymbol{e},\eta) = \cos\frac{\eta}{2}\left[1 + \frac{c}{|E| + m_0 c^2}\zeta_1'(\pi\cdot\boldsymbol{s}')\right]. \tag{101}$$

The functions obtained from (93) and (94) are now readily seen to be

$$\left.\begin{aligned} \Psi_1 &= \cos\frac{\eta}{2}\left[\theta_1 + \frac{c}{|E| + m_0 c^2}(\pi_z\theta_3 + \pi_+\theta_4)\right]\exp(\iota\pi\cdot\boldsymbol{r}/\hbar)\exp(-\iota|E|t/\hbar), \\ \Psi_2 &= \cos\frac{\eta}{2}\left[\theta_2 + \frac{c}{|E| + m_0 c^2}(\pi_-\theta_3 - \pi_z\theta_4)\right]\exp(\iota\pi\cdot\boldsymbol{r}/\hbar)\exp(-\iota|E|t/\hbar), \end{aligned}\right\} \quad (102)$$

and

$$\left.\begin{aligned} \tilde{\Psi}_1 &= \cos\frac{\eta}{2}\left[\theta_4 + \frac{c}{|E| + m_0 c^2}(\pi_-\theta_1 - \pi_z\theta_2)\right]\exp(-\iota\pi\cdot\boldsymbol{r}/\hbar)\exp(\iota|E|t/\hbar), \\ \tilde{\Psi}_2 &= -\cos\frac{\eta}{2}\left[\theta_3 + \frac{c}{|E| + m_0 c^2}(\pi_z\theta_1 + \pi_+\theta_2)\right]\exp(-\iota\pi\cdot\boldsymbol{r}/\hbar)\exp(\iota|E|t/\hbar), \end{aligned}\right\} \quad (103)$$

where

$$\pi_\pm = \pi_1 \pm \iota\pi_2. \quad (104)$$

The functions (102) are eigenfunctions of $H$ and $\boldsymbol{p}$ with eigenvalues $|E|$ and $\pi$, respectively. The functions (103) are eigenfunctions of the same operators with eigenvalues $-|E|$ and $-\pi$.

The function space available for a DIRAC particle is the direct sum $\Omega \oplus \tilde{\Omega}$ of the two spaces $\Omega$ and $\tilde{\Omega}$, obtained by operating with all operators of the form (32), (58) and (59) on the functions (93) and (94), respectively. A function in $\Omega$ represents a particle state, a function in $\tilde{\Omega}$ an antiparticle state. A function with components in both $\Omega$ and $\tilde{\Omega}$ represents a superposition of a particle and an antiparticle state.

## 8. Charge conjugation symmetry

There is a one-to-one correspondence between the functions in the spaces $\Omega$ and $\tilde{\Omega}$ specified in the previous section, two corresponding functions being the complex conjugates of each other. This reflects, that whenever a function $\Psi$ is a solution of (47), then the same is true for the complex conjugate function $\tilde{\Psi}$. The process of complex conjugation is thus an invariance operation of the theory. In the following we shall identify this operation, which we denote by $C$, with the charge conjugation operation of the conventional theory.

The operator effecting the operation $C$ is defined by

$$C_{op}\Psi = \tilde{\Psi} \quad (105)$$

with $\sim$ denoting complex conjugation. It has the obvious property

$$C_{op}^2 = 1. \tag{106}$$

From the explicit expressions (17) we obtain the following relations, already used in passing from (93) to (94):

$$\left.\begin{aligned} \tilde{\theta}_1 &= \theta_4, \\ \tilde{\theta}_2 &= -\theta_3, \\ \tilde{\theta}_3 &= -\theta_2, \\ \tilde{\theta}_4 &= \theta_1. \end{aligned}\right\} \tag{107}$$

Hence, we get for an arbitrary function of the form (88), i.e.

$$\Psi = \theta_1\psi_1 + \theta_2\psi_2 + \theta_3\psi_3 + \theta_4\psi_4, \tag{108}$$

that

$$C_{op}\Psi = \theta_4\psi_1^* - \theta_3\psi_2^* - \theta_2\psi_3^* + \theta_1\psi_4^*, \tag{109}$$

where – in order to facilitate comparisons with the conventional therory – we have used * to denote complex conjugation of a function independent of $\alpha$, $\beta$ and $\gamma$.

This result may conveniently be written as

$$C\Psi = [\theta_1\theta_2\theta_3\theta_4]\begin{bmatrix} 0 & 0 & 0 & 1 \\ 0 & 0 & -1 & 0 \\ 0 & -1 & 0 & 0 \\ 1 & 0 & 0 & 0 \end{bmatrix}\begin{bmatrix} \psi_1^* \\ \psi_2^* \\ \psi_3^* \\ \psi_4^* \end{bmatrix}. \tag{110}$$

The $4\times4$ matrix occurring in this relation is readily identified with DIRAC's $-\gamma_2$. It is equal to $i\gamma^2$ in the tensor notation by e.g. BJORKEN and DRELL (1964). Our simple definition (105) of the charge conjugation operation is then seen to coincide with BJORKEN and DRELL's. It differs from e.g. SAKURAI's (1967) in sign. (Definitions in the literature may vary with an arbitrary phase factor).

The operators (32), (58) and (59), from which the operators of $\mathcal{T}\mathcal{L}_0$ are constructed, are all real (see also (101)). This implies that $C$ commutes with all elements of $\mathcal{T}\mathcal{L}_0$. Hence, we may construct the direct product group $\mathcal{C}\times\mathcal{T}\mathcal{L}_0$, where

$$\mathcal{C} = \{E, C\}, \tag{111}$$

$E$ being the identity operation. The function space $\Omega \oplus \tilde{\Omega}$, which contains the totality of solutions of eqn. (47), defines then a single irreducible representation of $\mathscr{C} \times \mathscr{T}\mathscr{L}_0$. This group is thus an invariance group of the theory.

In the following sections we shall augment this invariance group further by adding the space and time inversion operations.

## 9. Space inversion

The process of space inversion, $P$, replaces $\boldsymbol{r}$ by $-\boldsymbol{r}$ and thus also $\boldsymbol{p}$ by $-\boldsymbol{p}$. To determine its effect on the internal axes of the rotor it is necessary to go beyond the assumption made in section 2, that the vectors $\boldsymbol{r}_1$ and $\boldsymbol{r}_2$ of eqn. (1) merely represent mathematical points. We must now assume, that they in some way or other have a physical significance, such that they are replaced by $-\boldsymbol{r}_1$ and $-\boldsymbol{r}_2$ under inversion.

With this assumption it follows from (2), that the directions of $\boldsymbol{e}_1$ and $\boldsymbol{e}_2$ are reversed under $P$, whereas $\boldsymbol{e}_3$ is left unchanged. The effect on the EULER angles is accordingly:

$$\alpha \to \alpha,\ \beta \to \beta,\ \gamma \to \gamma + \pi. \tag{112}$$

The functions $\theta_1$ and $\theta_2$ in (17) are thus multiplied by $\iota$ under inversion, $\theta_3$ and $\theta_4$ are multiplied by $-\iota$. This result is in accordance with the assumption of the conventional theory, that space inversion is effected by the matrix $a\beta$, where $\beta$ is defined by (90) and $a$ takes one of the four values $\pm 1$, $\pm i$ (see e.g. BJORKEN and DRELL, 1964; SAKURAI, 1967).

Adopting (112) we see from (7), that $s_1$, $s_2$ and $s_3$ are unchanged under inversion. (8), as well as (9), shows that $\zeta_1$ and $\zeta_2$ change sign, whereas $\zeta_3$ remains unaffected.

The relativistic description of a spinless particle is invariant under space inversion, i.e. its symmetry group may be extended from $\mathscr{T}\mathscr{L}_0$ to $\mathscr{T}\mathscr{L}_p$, the orthochronous, inhomogeneous LORENTZ group. Within the algebra defined by the operators (24) and (30) $P$ has the following effect:

$$\boldsymbol{p} \to -\boldsymbol{p},\ p_4 \to p_4,\ \boldsymbol{l} \to \boldsymbol{l},\ \boldsymbol{k} \to -\boldsymbol{k}. \tag{113}$$

The substitution (48) requires that

$$H \to H, \tag{114}$$

a condition which is certainly satisfied by the Hamiltonian (49).

The relations (113) and (114) must likewise hold for the generators associated with the relativistic rotor, if we require that $P$ be a symmetry operation in this case as well. In particular, we must require that

$$\boldsymbol{s} \to \boldsymbol{s}, \; \mathsf{K} \to -\mathsf{K}. \tag{115}$$

$\boldsymbol{s}$ is, in fact, unaffected by $P$. But in order that $\mathsf{K}$ change sign we must require that $b$, as defined by (53), change sign. $\zeta_3$ is unaffected by $P$, and the choice (56) is thus an unacceptable one. For $s = \frac{1}{2}$ we must choose $b$ as a linear combination of $\zeta_1$ and $\zeta_2$ alone, as was in fact done in section 5, by (80).

The fact that (56) is an invalid choice, if $P$ is present as a symmetry operation, does not in any sense make the general conclusions of section 4 invalid, since these only refer to the properties of $\mathscr{T}\mathscr{L}_0$ and its representations.

Considering now the requirement (114), we get a narrowing of the condition on $\lambda$ in passing from (82) to (83), namely that $\lambda$ must be a constant times $\zeta_3$, in accordance with the actual choice (83).

The Hamiltonian (86) is then unaffected by $P$, and the description which we have constructed on the basis of section 5 is invariant under space inversion. This remains true also after the inclusion of the charge conjugation operation, since it is evident that $C$ and $P$ commute. We may thus extend the invariance group of the theory from $\mathscr{C} \times \mathscr{T}\mathscr{L}_0$ to $\mathscr{C} \times \mathscr{T}\mathscr{L}_p$.

## 10. Time inversion

The problem of reversing the direction of time has attracted much attention in the physical literature (see, e.g. Davies, 1974). To-day's discussions of the problem are often based on the so-called time reversal operation $T$ (see, e.g. Bjorken and Drell, 1964), originally introduced by Wigner (1932). Here, we shall define a simpler — and from a relativistic point of view more natural — operation, which we shall denote $T'$ and call the time inversion operation.

The effect of $T'$ on the external coordinates is to replace $t$ by $-t$ and thus also $p_4$ by $-p_4$. Hence, we get the following result for the operators (24) and (30) of the basic algebra for a spinless particle:

$$\boldsymbol{p} \to \boldsymbol{p}, \; p_4 \to -p_4, \; \boldsymbol{l} \to \boldsymbol{l}, \; \boldsymbol{k} \to -\boldsymbol{k}. \tag{116}$$

The substitution (48) requires, that if $T'$ is to be accepted as an invariance operation, then we must demand that

$$H \to -H. \tag{117}$$

This condition is certainly not fulfilled for the Hamiltonian (49). The description of a spinless particle, as developed in section 3, is thus not invariant under time inversion.

For a particle with spin we require that the internal generators be transformed similarly to (116), i.e.

$$\boldsymbol{s} \to \boldsymbol{s}, \kappa \to -\kappa. \tag{118}$$

It is now easy to verify that all three relations (116)–(118), with $H$ as given by (86), are satisfied, if we define $T'$ as the process, which besides transforming $t$ into $-t$ changes the EULER angles according to the scheme:

$$\alpha \to \alpha + \pi, \beta \to \pi - \beta, \gamma \to \pi - \gamma. \tag{119}$$

This corresponds to a 2-fold rotation about the $\boldsymbol{e}_2$-axis, just as (112) corresponds to a 2-fold rotation about the $\boldsymbol{e}_3$-axis. The effect on the $\zeta_i$ operators is:

$$\zeta_1 \to -\zeta_1, \quad \zeta_2 \to \zeta_2, \quad \zeta_3 \to -\zeta_3. \tag{120}$$

The functions (17) are transformed thus:

$$\left.\begin{aligned} \theta_1 &\to \quad \theta_3, \\ \theta_2 &\to \quad \theta_4, \\ \theta_3 &\to -\theta_1, \\ \theta_4 &\to -\theta_2, \end{aligned}\right\} \tag{121}$$

Hence we obtain, from the explicit expressions (102):

$$\left.\begin{aligned} T'\Psi_1 \equiv \Psi_3 &= \cos\frac{\eta}{2}\left[\theta_3 - \frac{c}{|E| + m_0 c^2}(\pi_z\theta_1 + \pi_+\theta_2)\right]\exp(\iota\pi\cdot\boldsymbol{r}/\hbar)\exp(\iota|E|t/\hbar), \\ T'\Psi_2 \equiv \Psi_4 &= \cos\frac{\eta}{2}\left[\theta_4 - \frac{c}{|E| + m_0 c^2}(\pi_-\theta_1 - \pi_z\theta_2)\right]\exp(\iota\pi\cdot\boldsymbol{r}/\hbar)\exp(\iota|E|t/\hbar). \end{aligned}\right\} \tag{122}$$

The functions $\Psi_3$ and $\Psi_4$ may, just as well as the function $\tilde{\Psi}_1$ and $\tilde{\Psi}_2$ in (103), be used as representatives for the function space $\tilde{\Omega}$. $\Psi_3$ and $\Psi_4$ are, in fact, equal to $-\tilde{\Psi}_2$ and $\tilde{\Psi}_1$, respectively, with $-\pi$ substituted for $\pi$. The effect of $T'$ on $\Psi_3$ and $\Psi_4$ is:

$$\left.\begin{aligned} T'\Psi_3 &= -\Psi_1, \\ T'\Psi_4 &= -\Psi_2. \end{aligned}\right\} \tag{123}$$

Hence, the time inversion operation converts a particle state into an anti-particle state and vice versa, the velocity of the LORENTZ frame associated with the particle being reversed during the operation.

Adding the time inversion operation to the operations of $\mathscr{T}\mathscr{L}_p$, leads to the full inhomogeneous LORENTZ group $\mathscr{T}\mathscr{L}$. The charge conjugation operation commutes with $T'$ just as it commutes with all other elements of $\mathscr{T}\mathscr{L}$, and the full invariance group is thus found to be $\mathscr{C} \times \mathscr{T}\mathscr{L}$.

This important result justifies the introduction of $T'$ and demonstrates the fundamental nature of this operation. To anchor it further, let us demonstrate the consistent transformation properties of the 4-vectors of our theory, with respect to space and time inversion.

A 4-vector $a_\mu = (\boldsymbol{a}, a_4)$ is a set of four quantities satisfying a relation similar to (29), viz.

$$[J_{\mu\nu}, a_\lambda] = \iota\hbar(\delta_{\mu\lambda} a_\nu - \delta_{\nu\lambda} a_\mu). \tag{124}$$

The following expressions are readily found to correspond to 4-vectors:

$$x_\mu = (\boldsymbol{r}, \mathrm{ict}), \tag{23}$$

$$p_\mu = (\boldsymbol{p}, p_4), \tag{24}$$

$$w_\mu = (\boldsymbol{p} \times \boldsymbol{\kappa} + p_4 \mathbf{s}, -\boldsymbol{p} \cdot \boldsymbol{s}), \tag{62a}$$

$$\gamma'_\mu = \left( -\zeta'_2 \boldsymbol{s}', \frac{\iota}{i} \zeta'_3 \right). \tag{125}$$

The matrices associated with the operators $\gamma'_\mu$ and the basis (17) are, when $\iota = i$, identical with the $\gamma_\mu$ matrices of the conventional theory, in the notation of DIRAC (1928) and e.g. SAKURAI (1967). The $\gamma'_\mu$ operators turn up in a natural manner, when (47) is multiplied from the left with $\zeta'_3$, to give the equation

$$(m_0 c + \iota \gamma'_\mu p_\mu) \Psi = 0. \tag{126}$$

USING the properties of the $P$ and $T'$ operations as described above, it is easily seen that $x_\mu, p_\mu$ and $\gamma'_\mu$ transform according to the scheme:

$$\left.\begin{aligned} P(\boldsymbol{a}, a_4) &= (-\boldsymbol{a}, a_4), \\ T'(\boldsymbol{a}, a_4) &= (\boldsymbol{a}, -a_4), \end{aligned}\right\} \tag{127}$$

whereas $w_\mu$ transforms as follows:

$$\left.\begin{aligned} P(\boldsymbol{w}, w_4) &= (\boldsymbol{w}, -w_4), \\ T'(\boldsymbol{w}, w_4) &= (-\boldsymbol{w}, w_4). \end{aligned}\right\} \tag{128}$$

These transformation properties characterize $x_\mu$, $p_\mu$ and $\gamma'_\mu$ as ordinary 4-vectors, $w_\mu$ as a pseudo-4-vector. For all four vectors it holds, that

$$PT'a_\mu = T'Pa_\mu = -a_\mu. \tag{129}$$

The "strong inversion" operation $PT' = T'P$ will be the subject matter of the following section.

The possibility of defining a time inversion operation with the above properties in the case of a DIRAC particle suggests, that a similar operator may be defined for other elementary systems as well. Let us, for the moment, assume that this is possible for the electromagnetic field. This field is characterized by a 4-vector

$$A_\mu = (\boldsymbol{A}, i\varphi), \tag{130}$$

where $\boldsymbol{A}$ is the vector potential and $\varphi$ the scalar potential. It is well known, that

$$P(\boldsymbol{A}, i\varphi) = (-\boldsymbol{A}, i\varphi), \tag{131}$$

and comparison with (127) makes us therefore expect, that

$$T'(\boldsymbol{A}, i\varphi) = (\boldsymbol{A}, -i\varphi). \tag{132}$$

Suppose now, that the source of $A_\mu$ is a charged DIRAC particle. The field associated with the corresponding antiparticle must then be $(\boldsymbol{A}, -i\varphi)$. In other words, a particle and its associated antiparticle must have equal, but opposite, charges.

That this is indeed the case is of course well known. The interesting thing in the present context is, that we have tied the conclusion to the properties of the full LORENTZ group, rather than to the properties of the charge conjugation operation. A more appropriate name for the latter, is, in fact, the often used alternative: the particle-antiparticle conjugation operation.

## 11. Strong inversion, alias the PCT-operation

Combining the operations $P$ and $T'$ leads to what we shall call the strong inversion operation, $I$. It changes $x_\mu$ into $-x_\mu$, while the EULER angles undergo the transformation corresponding to a 2-fold rotation about the $\boldsymbol{e}_1$-axis, i.e.

$$\alpha \to \alpha + \pi, \qquad \beta \to \pi - \beta, \qquad \gamma \to -\gamma. \tag{133}$$

Hence, we get:

$$\left.\begin{aligned} & p_\mu \to -p_\mu,\ \boldsymbol{l} \to \boldsymbol{l},\ \boldsymbol{k} \to \boldsymbol{k}, \\ & \boldsymbol{s} \to \mathbf{s},\ \mathsf{K} \to \mathsf{K}, \\ & H \to -H, \\ & w_\mu \to -w_\mu,\ \gamma'_\mu \to -\gamma'_\mu . \end{aligned}\right\} \tag{134}$$

The functions (17) are transformed thus:

$$I[\theta_1\theta_2\theta_3\theta_4)] = -\iota[\theta_3\theta_4\theta_1\theta_2], \tag{135}$$

and for the general function (108) we obtain:

$$I\sum_i \theta_i \psi_i(x_\mu) = -\iota[\theta_1\theta_2\theta_3\theta_4] \begin{bmatrix} 0 & 0 & 1 & 0 \\ 0 & 0 & 0 & 1 \\ 1 & 0 & 0 & 0 \\ 0 & 1 & 0 & 0 \end{bmatrix} \begin{bmatrix} \psi_1(-x_\mu) \\ \psi_2(-x_\mu) \\ \psi_3(-x_\mu) \\ \psi_4(-x_\mu) \end{bmatrix}. \tag{136}$$

The $4\times4$matrix in (136) is the matrix representative of the operator $\zeta'_1$. It is readily identified with the matrix

$$\gamma_5 = \gamma_1\gamma_2\gamma_3\gamma_4 \tag{137}$$

of the conventional theory.

A comparison with e.g. BJORKEN and DRELL (1964) shows us now, that I has the same effect on a general wavefunction as the so-called PCT-operation. Hence, we have arrived at an alternative and simple interpretation of this fundamental operation.

The relation between the operations $P$, $T'$, $I$ and the 2-fold rotations about the three internal axes of the rotor is a nice illustration of the group theoretical fact, that the factor group of $\mathscr{T}\mathscr{L}$ with respect to the invariant subgroup $\mathscr{T}\mathscr{L}_0$ is isomorphic with the group $D_2$.

## 12. Wigner's time reversal operation

Combining the operation $T'$ and $C$ leads to the operation

$$T = CT', \tag{138}$$

which we shall now identify as WIGNER's time reversal operation. The effect of $C$ is to leave $x_\mu$ unaffected, while each operator of the basic algebra (and

thus also $H$) changes its sign. The effect of $T'$ was considered in section 10. Hence we get:

$$\left.\begin{aligned} &\boldsymbol{r}\to\boldsymbol{r},\ t\to -t,\\ &\boldsymbol{p}\to -\boldsymbol{p},\ p_4\to p_4,\ H\to H,\\ &\boldsymbol{l}\to -\boldsymbol{l},\ \boldsymbol{k}\to\boldsymbol{k},\ \boldsymbol{s}\to -\boldsymbol{s},\ \mathsf{K}\to\mathsf{K},\\ &\zeta_1\to\zeta_1,\ \zeta_2\to -\zeta_2,\ \zeta_3\to\zeta_3. \end{aligned}\right\} \tag{139}$$

The effect on the general function (108) is found by combining (121) with (109):

$$T\sum_i \theta_i\psi_i(\boldsymbol{r},t) = [\theta_1\theta_2\theta_3\theta_4]\begin{bmatrix} 0 & 1 & 0 & 0\\ -1 & 0 & 0 & 0\\ 0 & 0 & 0 & 1\\ 0 & 0 & -1 & 0 \end{bmatrix}\begin{bmatrix} \psi_1^*(\boldsymbol{r},-t)\\ \psi_2^*(\boldsymbol{r},-t)\\ \psi_3^*(\boldsymbol{r},-t)\\ \psi_4^*(\boldsymbol{r},-t) \end{bmatrix}. \tag{140}$$

The $4\times4$ matrix in (140) is equal to $\iota$ times the matrix representative of $s_2'$, and equal to the matrix $-\gamma_1\gamma_3$ of the conventional theory.

Thus, the relations (139) and (140) establish the assertion, that the complicated operation known as WIGNER's time reversal operation may be considered as a compound operation, made up of the two elementary operations $C$ and $T'$.

With this result, we have seen that all the symmetry operations of the conventional theory have a simple representation within the rotor model. It is further worth-while noting, that this model leads to a clear understanding of the way in which antilinear operators enter the theory: All operations of the group $\mathscr{T}\mathscr{L}$ correspond to linear operators, the fundamental antilinear operation being the operation $C$.

## 13. Some general remarks

The rotor model as developed so far is a one-particle model, and the comparisons we have made with the conventional theory have, accordingly, not included references to discussions based on field theoretical descriptions. There is, of course, a very extensive literature on the symmetries of the quantized DIRAC field (see e.g. KEMMER et al., 1959; MUIRHEAD, 1965). This literature leaves the general impression, that an operation like the PCT operation has its roots in the connection between spin and statistics (PAULI, 1955; LÜDERS, 1957). We have no reason to doubt that this is true in general,

but would like to stress that the PCT operation as it occurs in the present treatment is a very simple operation. The presence of the letter $C$ in its designation is in fact misleading, since it appears as a genuine operation of the group $\mathscr{T}\mathscr{L}$, of which $C$ is not a member.

As far as $C$ itself is concerned, we may obtain a clearer understanding of its nature by tying it to the presence of the indicator $\iota$, which we have carried through as an unassigned quantity. This is, however, best discussed elsewhere.

Finally, we shall consider the ambiguity in sign of the first term of the Hamiltonian (86). We have so far developed the theory with the plus sign, but it may equally well be developed with the minus sign. The only difference in the resulting wavefunctions is, that the $(\boldsymbol{r},t)$ dependent parts in (102) and (103) are interchanged. In the conventional theory one could talk about an interchange of the large and the small components of the wavefunction, and there would be no basis for believing that one had obtained anything but an alternative description of the same physical situation.

If, however, one adopts the rotor model, then there is no way of transforming the time-dependent wavefunctions corresponding to the two different signs into each other, and the two Hamiltonians must be considered as physically different, i.e. they must be associated with two different types of DIRAC particles. It is, however, easy to see that the two types of particles will behave similarly in an electromagnetic field; the type of interaction which can distinguish between them must be of a different nature.

We are, of course, unable to settle the question as to whether such an interaction exists or not. If it does not, then one is free to choose either sign in the Hamiltonian. If, however, is does exist, then one might perhaps imagine a connection to the electron-muon problem.

## 14. Conclusion

The discussion of sections 7–12 illustrates the type of natural interpretation one obtains by considering a DIRAC particle as a quantum mechanical rotor. The preceding sections taught us, that the only type of behaviour that a relativistic, quantum mechanical rotor can adopt, is that of a DIRAC particle.

Thus, we arrive at the conclusion, that the DIRAC particle and the quantum mechanical rotor are identical dynamical systems. In other words: a DIRAC particle is neither more nor less than a particle, for which it is possible to talk about an orientation in space.

## Acknowledgements

The present paper is dedicated to professor PER-OLOV LÖWDIN in recognition of his outstanding contributions to quantum science. I am greatly indebted to professor BEN R. MOTTELSON for his general interest in the present work and his constructive criticism of the manuscript. I also take the opportunity to thank dr. JOHN AVERY for numerous discussions.

*Department of Chemical Physics*
*Technical University of Denmark*
*DTH 301*
*DK 2800 Lyngby*

## References


Allcock, G. R. (1961). Nuclear Physics **27,** 204.

Bargmann, V., and Wigner, E. (1946). Proc. Natl. Acad. Sci. **34,** 211.

Bhatia, A. K., and Temkin, A. (1964). Rev. Mod. Phys. **36,** 1050.

Bjorken, J. D., and Drell, S. D. (1964). "Relativistic Quantum Mechanics". McGraw-Hill, New York.

Bohm, D., Hillion, P., and Vigiér, J.-P. (1960). Prog. Theor. Phys. **24,** 761.

Bohr, Aa., and Mottelson, B. R. (1969). "Nuclear Structure", Vol. 1. Benjamin, New York.

Bopp, F., and Haag, R. (1950). Z. Naturforschg. **5a,** 644.

Breit, G. (1930). Phys. Rev. **35,** 569.

Corben, H. C. (1968). "Classical and Quantum Theories of Spinning Particles". Holden-Day, San Francisco.

Davies, P. C. W. (1974). "The Physics of Time Asymmetry". University of California Press, Berkeley and Los Angeles.

Dirac, P. A. M. (1928). Proc. Roy. Soc. A**117,** 610.

Dirac, P. A. M. (1949). Rev. Mod. Phys. **21,** 392.

Hillion, P., et Vigiér, J.-P. (1958). Ann. Inst. H. Poincaré **16,** 161, 217.

Hund, F. (1928). Z. Phys. **51,** 1.

Hylleraas, E. (1929). Z. Phys. **54,** 347.

Judd, B. R. (1975). "Angular Momentum Theory for Diatomic Molecules". Academic Press. New York.

Kemmer, N., Polkinghorne, J. C., and Pursey, D. L. (1959). Rep. Progr. Phys. **22,** 368.

Lomont, J. S. (1959). "Applications of Finite Groups". Academic Press, New York.

Lüders, G. (1957). Ann. Phys. **2,** 1.

Lyubarskii, G. Y. (1960). "The Application of Group Theory in Physics". Pergamon, New York.

Muirhead, H. (1965). "The Physics of Elementary Particles". Pergamon, London.

Pauli, W. (1955). "Niels Bohr and the Development of Physics". Pergamon, London.

Roman, P. (1960). "Theory of Elementary Particles". North-Holland, Amsterdam.

Rose, M. E. (1957). "Elementary Theory of Angular Momentum". Wiley, New York.

Sakurai, J. J. (1967). "Advanced Quantum Mechanics". Addison-Wesley, London.

Uhlenbeck, G. E., and Goudsmit, S. (1925). Naturwiss. **13,** 953.

Van Winter, C. (1957). "Space-Time Rotations and Isobaric Spin". Excelsior, Amsterdam.

Whittaker, E. T. (1904). "A treatise on the Analytical Dynamics of Particles and Rigid Bodies". Cambridge.

Wigner, E. P. (1932). Göttinger Nachr. **31,** 546.

Wigner, E. P. (1939). Ann. Math. **40,** 149.


Indleveret til Selskabet april 1977.
Færdig fra trykkeriet oktober 1977.

C. MØLLER

# ON THE CRISIS IN THE THEORY OF GRAVITATION AND A POSSIBLE SOLUTION

Det Kongelige Danske Videnskabernes Selskab
Matematisk-fysiske Meddelelser **39**, 13


Kommissionær: Munksgaard
København 1978

## Synopsis

It is now generally believed that *Einstein's* beautiful *theory of gravitation* under special circumstances leads to inconsistent results. In fact, according to this theory a well-defined physical system may after a finite time pass over into an unphysical state, where the metric is singular and consequently the notions of space and time lose their physical meaning. This inconsistency calls for a generalized theory of gravitation for macroscopic matters which is free of singularities and at the same time retains all the satisfactory features of Einstein's theory. It is shown that such a generalization may possibly be obtained by assuming that the fundamental gravitational variables are, not the metric tensor, but the components of a tetrad field from which the metric of space-time can be derived uniquely. In a *tetrad theory of gravitation* the basic principles of Einstein's theory are still valid exactly, first of all the principle of general relativity, the principle of equivalence, and the fusion of gravity and mechanics. Such a theory also leads to a more satisfactory solution of the energy problem.



Printed in Denmark by Bianco Lunos Bogtrykkeri A/S. ISBN 87-7304-092-4

## 1. Statement of the Problem

During the last two decades all the effects predicted by Einstein's theory of general relativity and gravitation (EGRG) have been experimentally verified with a reasonably high degree of accuracy. It is true that these tests are concerned with cases only where the gravitational field is comparatively weak; but the simplicity and generality of the principles underlying the theory as well as its intrinsic consistency and cogency made it reasonable to assume that the theory be valid for stronger fields also.

However, at the same time investigations concerning the stability of large amounts of mass led to strange results which implied a serious crisis for EGRG, or for physics itself if this theory is taken for gospel truth. In fact it was shown[1] that a sufficiently large amount of matter according to EGRG will undergo a steady contraction under the influence of its own gravitational field. After a finite time as measured on a standard clock following the matter, the system is engulfed in a 'black hole' from which no message can be sent into the outside world, and after a further very short time the system collapses into a singularity, where not only the mass density is infinite, but where the space-time metric itself becomes singular.

Thus, according to Einstein's theory a well-defined physical system may after a finite time pass over into an unphysical state, where the notions of space and time become meaningless. Since these notions enter in an essential way in the formulation of all physical laws this means the breakdown of physics; for one cannot know what will come out of a singularity, and it is then not possible any more to predict the future.

For a long time many physicists (including myself) did not believe that Einstein's otherwise so usccessful theory had such disastrous consequences[2]; but by now there seems to be a consensus of opinion that these space-time singularities are inevitable, whenever the energy-momentum tensor, which in Einstein's theory represents the source of the gravitational field, satisfies certain physically reasonable conditions. Some physicists have tried to maintain that the situation is not so bad; for the final collapse of the system into the singularity is preceded by its passage through the Schwarzschild wall

(the event horizon) that delimits the black hole, and in this state no light or any other signal from the system can penetrate into the outside world, so that the final collapse is totally unobservable from outside. Moreover, an observer at a constant distance $r$ outside the Schwarzschild wall with radius $\alpha$ will strictly speaking never experience the formation of the black hole ; for measured on a standard clock at rest at constant $r > \alpha$ the formation of a black hole will take an infinite time, in contrast to the finite time as measured by a standard clock following the matter. (An extreme example of the relativity of time.) However, this attempt of explaining away the difficulty is not very satisfactory. What about observers that are sitting on the collapsing matter, should the laws of physics not be valid for them? Was it not just one of the main requirements of general relativity that these laws should be of the same form for arbitrarily moving observers?

Other physicists hope that a quantization of the metric field along the lines followed in quantum electrodynamics could prevent the collapse into the singularity, similarly as the introduction of Planck's quantum of action into mechanics and electrodynamics prevents the collapse of the Rutherford model of the atom. Indeed it would seem reasonable to expect quantum gravitational effects to be important for the very strong fields in the small regions of space-time in the vicinity of a singularity. However, in the first place it does not seem possible to carry through the quantization program for the gravitational field along the same lines as in quantum electrodynamics, because the non-linear gravitational field of general relativity is basically non-renormalizable. Moreover the root of the trouble does not seem to lie exclusively in the very small regions near the singularity, but rather in the whole usually macroscopic domain of the black hole.

In a number of interesting papers Hawking[3], Wald[4] and Parker[5] have shown that black holes create and emit particles at a steady rate. It is maintained that this radiation will cause the black hole to lose mass and eventually to disappear, leaving a naked singularity behind. In this situation there is a basic limitation on our ability to predict the future, which Hawking[6] has formulated in a new physical principle—the randomicity principle. According to this principle all configurations for particles emitted from a black hole singularity compatible with the external constraints are equally probable. This means that a complete set of data on a space-like surface is not sufficient in general to determine with certainty the behaviour of a system, since information may disappear into or suddenly appear from a hole singularity.

The randomicity principle implies a much more radical departure from

the deterministic description of classical physics than that which was brought about by the principles of quantum mechanics. In the latter theory it was recognized that the deterministic Newtonian equations of mechanics could not be used to predict the motion of an electron exactly, because this would presuppose that we can know the initial position and momentum of the electron exactly, which is impossible according to Heisenberg's uncertainty principle. On the other hand, the randomicity principle claims that the future state in certain cases may be undetermined even if the initial state is well-defined, which would make physics truly indeterministic.

This is such a serious departure from the philosophy, which has been the mainstay of physics since Galileo, that many physicists will ask if this step is really necessary. Could it not be that Einstein's classical theory of gravitation, on which Hawking's conclusions are based, breaks down in the case of very strong gravitational fields. After all the theory has been experimentally verified for comparatively weak fields only, and surely Einstein's theory like all other theories must be expected to have a limited domain of applicability. In fact, in the past the occurrence of essential singularities in a physical theory has usually been taken as a sign that the theory has been applied in a region that lies outside its domain of applicability.

As an example let us recall the situation concerning the black body radiation which caused Max Planck so much trouble around 1900. If one applies the laws of classical physics in calculating the energy density of the radiation inside a cavity in thermal equilibrium, one obtains the formula of Rayleigh-Jeans, according to which the energy density per unit frequency interval is proportional to the square of the frequency $\nu$. Thus the total energy density, obtained by integrating over all $\nu$, is infinite which obviously is meaningless. This "ultra-violet catastrophe" indicates that we have applied the laws of classical physics to a phenomenon that lies outside their domain of applicability. Using instead the laws of quantum physics, that are valid also for large $\nu$, we are led to Planck's formula for the energy density which gives finite results.

Similarly one would be inclined to think that the occurrence of essential singularities in Einstein's theory indicates that this theory breaks down in the case of very strong gravitational fields—a thought that was not unfamiliar to Einstein himself[7]. This point of view is supported by the circumstance that EGRG actually ceases to be a physical theory connecting measurable physical quantities already before the system passes into the singularity. In order to measure the metric, for instance, we need an instrument which measures the proper time, i.e. a physical clock which shows the same time as the

ideal standard clocks with which one operates in general relativity[8]. It is well-known that an oscillatory system with atomic frequency represents an extremely good standard clock in ordinary gravitational fields. However, as was shown in a recent paper[9] any such clock ceases to give the correct proper time when approaching and before actually reaching a singularity. For this reason we concluded that the proper time and therefore also the metric itself lose their physical meaning already somewhat outside the singularities in question.

Under these circumstances it seems imperative to investigate the possibility of constructing a theory of gravitation for macroscopic matter that is free of singularities and at the same time retains all the satisfactory features of EGRG. According to the preceding discussion this would presumably have to be a theory in which there are no black holes and which gives the same results as Einstein's theory at least for weak fields up to the second order of approximation. However we would have to require more than just that; for there can be no question of returning to the ideas prevailing in physics before 1915. A number of the principles on which Einstein based his theory must be regarded as irrevocable.

In the following we have listed the most fundamental assumptions and properties of EGRG which it would be desirable to retain in a generalized theory:

**A**. *Space-time is a manifold with a pseudo-Riemannian metric. The metric tensor* $g_{ik}$ *is a physical quantity that can be measured in principle by means of standard clocks, and the determinant* $g = \det(g_{ik})$ *is everywhere negative:*

$$g < 0. \tag{1.1}$$

*All physical laws are expressed by equations that are covariant or form-invariant under arbitrary transformations of the space-time coordinates.*

In these equations the measurable quantities $g_{ik}$ enter in an essential way along with the other physical quantities that describe the phenomena in question. The form-invariance of the equations is the mathematical expression of the general principle of relativity, according to which the fundamental laws of nature, obtained by experiments, are of the same form irrespective of the state of motion of the observers. Thus, for the first time in the history of physics a given set of phenomena is described by a uniquely determined set of equations. This inalienable property can be regarded as the crowning touch of a long development of physics from Aristotle over

Galileo and Newton to Einstein—a development that is characterized by a constantly increasing symmetry or form-invariance of the laws of nature under ever wider groups of transformations.

**B**. *Another precious acquisition of EGRG is the fusion of gravitation and mechanics. Einstein's gravitational field equations do not only determine the gravitational field for a given matter distribution, but also the motion of the matter source is determined by these equations: the mechanieal equations of motion are consequences of the field equations.*

For incoherent matter the equations of motion of an infinitesimal piece of matter following from the field equations are identical with the equations of motion of a freely falling test particle.

**C**. A basic assumption in EGRG is *the equivalence principle, according to which the effects of a gravitational field can be 'transformed away' in an infinitesimal region around a given event point P by introducing a system of coordinates that is geodesic at P. Moreover, if this system is locally Lorentzian, all the physical laws at P are of the same form as in special relativity.*

As an immediate consequence of this principle gravity must effect the trajectories of all freely moving particles in exactly the same way independently of the mass of the particle. In the case of the gravitational field of the earth this has now been verified experimentally to the very high accuracy of $10^{-11}$ by Dicke[10] and Bragnisky[11] and their co-workers. Thus at least for weak gravitational fields this consequence of the principle of equivalence can be regarded as well established.

For a matter system with the energy-momentum tensor $T_{ik}$ it follows from the principle of equivalence that the 'conservation laws' in a general system of coordinates must be of the form

$$T_i{}^k{}_{;k} = 0 \tag{1.2}$$

where $;k$ denotes the covariant derivative formed by means of the Christoffel symbols corresponding to the metric tensor $g_{ik}$. Thus according to **B** the equations (1.2) must be consequences of the field equations.

Further it follows from **C** that the world line of a freely falling particle is a geodesic in the 4-space with the metric tensor $g_{ik}$.

**D**. *The gravitational field equations are derivable from a Lagrangean principle* with a Lagrangean density which is a scalar density under the group of general coordinate transformations. In this way the general covariance and the compatibility of the field equations are secured.

**E.** *The field equations are partial differential equations in the field variables of not higher than the second order.* This is essential for obtaining a Cauchy problem of the usual kind.

**F.** *In Einstein's theory the gravitational field is assumed to be exhaustively described by the metric tensor $g_{ik}$ alone.*

According to **D** and **F** the gravitational part of the Lagrangean integral is of the form $\int L\sqrt{-g}\,dx$, where $L$ is a scalar constructed from the $g_{ik}$ and their derivatives. Among the numerous independent scalars of this type, the curvature scalar $R$ plays a special role. In fact, only with $L = R$ do we get field equations of the type **E**. Thus the assumptions **A**–**F** lead uniquely to EGRG, with the field equations

$$G_{ik} = -\varkappa T_{ik}. \tag{1.3}$$

The Einstein tensor $G_{ik}$ is a function of the $g_{ik}$ and their space-time derivatives up to the second order and $T_{ik}$ is the energy-momentum tensor of the matter source, which depends on $g_{ik}$ as well as on the matter variables. On account of the Bianchi identities the divergence of the Einstein tensor vanishes identically, i.e.

$$G_i{}^k{}_{;k} \equiv 0.$$

Hence the "conservation laws" (1.2) are consequences of the field equations in accordance with **B** and **C**.

For incoherent matter we have

$$T_i{}^k = \mu_0 U_i U^k, \tag{1.4}$$

where $\mu_0$ is the proper mass density and $U^i$ is the four-velocity of the matter. With this expression for the energy-momentum tensor the equations (1.2) yield

$$(\mu_0 U^k)_{;k} = 0 \tag{1.5}$$

and

$$\frac{DU_i}{d\tau} \equiv U_{i;k}U^k = 0. \tag{1.6}$$

(1.5) expresses the conservation of proper mass, while (1.6) shows that the world line of a particle in the incoherent matter is a geodesic, as it should be according to **B** and **C** since the particle is freely falling.

The remarkable wholeness of EGRG makes a generalization of this theory a difficult job. At least it would obviously be necessary to give up some of the assumptions contained in **A**–**F**. The properties **A**, **B**, **D** and **E** are so

essential that they hardly can be abandoned and also **C** seems indispensable. The equivalence principle is well established at least for weak gravitational fields. Then remains a possible change of assumption **F**.

We have already mentioned that EGRG is the only possible theory if we assume that the gravitational field is described exclusively by the metric tensor $g_{ik}$. Therefore we shall tentatively assume that there are as yet undiscovered properties of the gravitational field which cannot be described by the metric field only. Thus besides the $g_{ik}$, that certainly describe the field correctly for weak fields, we introduce additional field variables that play a role for strong gravitational fields only. The most primitive assumption is that the new gravitational field variables are independent tensor fields embedded in the Riemannian space with the metric $g_{ik}$. However, as we shall see now, this does not work.

Let us consider the case of an antisymmetric tensor field $\Gamma_{ik}$ which satisfies equations of the same form as the Maxwell equations in general relativity, but with the electric rest charge density replaced by the proper mass density* multiplied by a new universal constant $\lambda$. Then the formalism is entirely analogous with the Einstein-Maxwell equations for electrically charged matter. The field equations for the metric tensor will be influenced by the presence of the $\Gamma$-field since the energy-momentum tensor of the latter field will act as an extra source along with the energy-momentum tensor of the matter. From **B** it follows then that a "freely falling" particle of proper mass $m_0$ is acted upon by a gravitational four-force

$$k_i = \lambda m_0 \Gamma_{ik} U^k / c \tag{1.7}$$

on the analogy of the electromagnetic Lorentz force.

The extra gravitational force between two massive bodies following from (1.7) is repulsive, independent of the sign of $\lambda$, and it increases indefinitely with decreasing distance, which might help preventing a gravitational collapse. On the other hand, the presence of the force $k_i$ means that the equivalence principle **C** is not exactly valid. In a locally Lorentzian system of coordinates the gravitational field is not completely transformed away. However for sufficiently small $\lambda$, **C** may still be approximately valid for weak gravitational fields.

The solutions of the metric field equations are in this case quite analogous with the solutions of the Einstein equations given by Reissner[12] and Weyl[13] for the electromagnetic case. In the empty space outside a spherically sym-

* Strictly speaking this is possible for incoherent matter only. In the general case the proper mass has to be replaced by the conserved "bare mass'.

metric distribution of matter we have therefore in a system of "curvature coordinates" $\{r, \theta, \varphi, ct\}$:

$$ds^2 = a dr^2 + r^2(d\theta^2 + \sin^2\theta d\varphi^2) - bc^2dt^2 \tag{1.8}$$

with

$$b = \frac{1}{a} = 1 - \frac{\alpha}{r} + \frac{\beta^2}{r^2}. \tag{1.9}$$

Here the constant $\alpha$ is approximately equal to the Schwarzschild radius, i.e.

$$\alpha = \frac{\varkappa M c^2}{4\pi} \tag{1.10}$$

and for the constant $\beta$ we get approximately

$$\beta^2 = \alpha^2 \frac{\lambda^2}{2\varkappa c^4}. \tag{1.11}$$

Instead of the single event horizon in the Schwarzschild solution, we have in (1.8) two horizons in general, viz. at the values of $r$ for which $b = 0$. $a$ and $b$ will be everywhere positive only when $\beta^2/\alpha^2 > \frac{1}{4}$, or by (1.11), when the dimensionless quantity $\lambda^2/\varkappa c^4$ satisfies the condition

$$\frac{\lambda^2}{\varkappa c^4} > \tfrac{1}{2} \tag{1.12}$$

in which case black holes would be excluded. However, in order to have agreement with EGRG and the experiments in the case of weak fields in particular as regards the red shift effect, it can be shown that $\lambda^2/\varkappa c^4$ cannot be larger than 0.005, i.e.

$$\lambda^2/\varkappa c^4 \ll 1. \tag{1.13}$$

Since (1.13) is in contradiction with (1.12), the introduction of the $\Gamma$-field does not solve our problem.

Let us now consider the case where the extra gravitational field is described by a scalar $\Psi$ with field equations

$$\Gamma^i{}_{;i} = \lambda\mu_0, \qquad \Gamma_i = -\frac{\partial \Psi}{\partial x^i}. \tag{1.14}$$

Here again $\lambda$ denotes a coupling constant and $\mu_0$ is the proper mass density. In this case we have instead of (1.7) a gravitational four-force

$$k_i = -\lambda m_0 \Gamma_i . \tag{1.15}$$

The corresponding extra gravitational force between two particles is attractive and increases indefinitely with decreasing distance. Therefore there is not much hope of avoiding the singularities of EGRG in this way.

However, a suitable combination of the fields $\Gamma_{ik}$ and $\Gamma_i$ seems to be promising. If the coupling constants $\lambda$ of the two fields are equal we have instead of (1.7) and (1.15)

$$k_i = \lambda m_0 (\Gamma_{ik} U^k / c - \Gamma_i). \tag{1.16}$$

In the Newtonian approximation, i.e. for weak fields and small velocities, it can be shown that the two terms in (1.16) cancel, so that the theory is in accordance with the results of classical celestial mechanics, even if $\lambda^2/\varkappa c^4$ is of order 1. The extra force on a particle at rest in the field of a spherical distribution of matter vanishes for large distances $r$, but for decreasing $r$ this force is increasing and repulsive, so that there is a hope of avoiding collapse with this combination of fields.

A closer investigation of the solution of the metric field equations in the static spherically symmetric case shows that the conditions for the absence of event horizons is again approximately given by (1.12), which in this case is compatible with classical celestial mechanics in the Newtonian approximation. However if we go to the next approximation and consider the perihelion precession of planets, the theory gives a formula for the precession $\Delta\varphi$ that deviates from the expression $\Delta\varphi_E$ in Einstein's theory by a factor $(1 - \lambda^2/\varkappa c^4)$:

$$\Delta\varphi = \Delta\varphi_E (1 - \lambda^2/\varkappa c^4). \tag{1.17}$$

Thus even with the lowest value of $\lambda^2/\varkappa c^4$ compatible with (1.12) we get a value for the perihelion precession in distinct disagreement with the observations.

Another serious difficulty is the following fact. The four-force (1.16) is not a true mechanical force of the Minkowski type[14], since

$$k_i U^i = -\lambda m_0 \Gamma_i U^i = \lambda m_0 \frac{d\Psi}{d\tau} \neq 0. \tag{1.18}$$

This means that the proper mass $m_0$ of a particle is not constant in a gravitational field. Indeed from the equations of motion of a freely falling particle

$$\frac{D m_0 U_i}{d\tau} = k_i \tag{1.19}$$

we get

$$\frac{dm_0}{d\tau} = -\frac{1}{c^2} k_i U^i = -\frac{\lambda m_0}{c^2} \frac{d\Psi}{d\tau}. \tag{1.20}$$

The solution of (1.20) is

$$m_0 = m_0(0) e^{-\frac{\lambda \Psi}{c^2}} \tag{1.21}$$

where $m_0(0)$ is the proper mass for $\Psi = 0$ i.e. in a system of inertia.

Thus the value of the proper mass of an electron, for instance, varies with the scalar gravitational potential $\Psi$. Therefore also the standard frequency of a transition in an atom depends on $\Psi$ and this dependence may even be different in atoms of different constitution. The shift of spectral lines arising from this effect has to be added to the Einstein shift. In the gravitational field of the sun or the earth, and with a $\lambda$ satisfying (1.12), $\lambda\Psi$ is of the same order of magnitude as the Newtonian potential $\chi$, so that this new effect should have been noticed in the experiments of Pound[15] and collaborators, by which Einstein's formula was verified with a high degree of accuracy.

If one goes to more complicated tensor fields than the $\Gamma_{ik}$ and $\Gamma_i$ it seems that it is not even possible to maintain **B**. It was bad enough that **C** could be satisfied approximately only in the just treated cases, but it would seem quite out of question ever to give up **B**. Therefore we have come to the conclusion that a generalization of Einstein's theory in accordance with known facts cannot be obtained by assuming that the metric quantities $g_{ik}$ together with independent tensor fields are the basic gravitational field variables.

These results seem to indicate that EGRG is the only possible theory of gravitation and that the breakdown of physics referred to in the introduction is inevitable. However there is a remaining possibility in assuming that the $g_{ik}$ are not among the truly fundamental gravitational variables, but that the latter are a set of tensor variables from which the metric quantities can be derived uniquely. Such a set of 16 independent variables are the components of so-called tetrad vector fields which determine the 10 metric components $g_{ik}$ by simple algebraic relations.

In a paper[16] from 1961 it was shown that a tetrad description of gravitational fields also allows a more rational treatment of the energy-momentum complex than in a theory based on the metric tensor alone. In 1963 Pellegrini and Plebanski[17] gave a Lagrangean formulation of the theory and a paper[18]

from 1966 contains a survey of all the investigations on the energy-momentum complex in general relativity.

The advantage of using tetrads as gravitational variables is connected with the fact that this allows to construct expressions for the energy-momentum complex which have more satisfactory transformation properties than in a purely metric formulation. However in the just mentioned investigations the admissible Lagrangeans were limited by the assumption that the equations determining the metric tensor should be exactly equal to the field equations of Einstein. In the present situation, where we are looking for metric field equations which deviate from Einstein's field equations in the case of strong gravitational fields, a wider class of Lagrangeans are admissible. In the following sections we shall see that this freedom can be used to construct a consistent theory of gravitation in which all the important properties **A**–**E** are retained and which deviates from Einstein's theory in the case of strong fields only.

## 2. The Basic Notions in a Tetrad Theory of Gravitation

In this section we shall give a survey of the basic notions of tetrad theories already contained in the paper reference 16, to which we shall frequently refer in what follows (the reader is requested to disregard § 6 in ref. 16).

At the out-set, before anything is filled into it, space-time is assumed to be just a continuum of points with arbitrary coordinates $(x^i)$ but without any geometrical properties. A gravitational field in this space is described by four independent *contravariant* vector fields $\underset{a}{h^i}(x)$. Here $a = 1,2,3,4$ is an index numerating the four vectors and $i = 1,2,3,4$ is a contravariant vector index, which means that the $\underset{a}{h^i}$ transform as the coordinate differentials $dx^i$ under all coordinate transformations. There are thus sixteen independent gravitational field variables in this theory in contrast to the ten $g_{ik}$ in EGRG.

Consider the determinant

$$h = det(\underset{a}{h^i}) \tag{2.1}$$

with the element $\underset{a}{h^i}$ in the $a$'th row and the i'th column. We shall assume that this determinant is nowhere zero, i.e.

$$h \neq 0. \tag{2.2}$$

Then we can define a new set of sixteen variables $\overset{a}{h}_i$ by the equations

$$\overset{a}{h}_i \underset{b}{h}^i = \delta^a_b = \text{(Kronecker symbol)}. \tag{2.3}$$

The solutions of these equations are obviously the components of four *covariant* vectors. If $\overset{a}{M}_i$ is the conjugate minor of the element $\underset{a}{h}^i$ in the determinant (2.1) the solutions of the equations (2.3) are

$$\overset{a}{h}_i = \overset{a}{M}_i/h. \tag{2.4}$$

Therefore we also have

$$\underset{a}{h}^i \overset{a}{h}_k = \delta^i_k = \text{(Kronecker symbol)}. \tag{2.5}$$

From (2.3) we get, using a well-known theorem from the theory of determinants,

$$det(\underset{a}{h}^i) \cdot det(\overset{a}{h}_i) = 1, \tag{2.6}$$

where $det(\overset{a}{h}_i)$ is the determinant with $\overset{a}{h}_i$ in the $a$'th row and the $i$'th column.

Let $\varepsilon_a$ be a quantity with components

$$\varepsilon_\alpha = 1, \qquad \alpha = 1,2,3, \qquad \varepsilon_4 = -1, \tag{2.7}$$

equal to the diagonal elements in the constant Minkowski matrix $\eta_{ab} = \eta^{ab}$, i.e.

$$\eta_{ab} = \eta^{ab} = \varepsilon_{a)} \delta^a_b, \tag{2.8}$$

where the parenthesis in a) indicates no summation over $a$ although it appears twice in the expression on the right hand side of (2.8). Now we define two sets of vectors $\overset{a}{h}^i$ and $\underset{a}{h}_i$ by

$$\left.\begin{aligned} \overset{a}{h}^i &= \eta^{ab} \underset{b}{h}^i = \varepsilon_{a)} \underset{a}{h}^i \\ \underset{a}{h}_i &= \eta_{ab} \overset{b}{h}_i = \varepsilon_{a)} \overset{a}{h}_i \end{aligned}\right\} \tag{2.9}$$

and the inverse relations

$$\underset{a}{h}^i = \varepsilon_{a)} \overset{a}{h}^i, \quad \overset{a}{h}_i = \varepsilon_{a)} \underset{a}{h}_i, \tag{2.10}$$

i.e. the tetrad indices $a,b, \ldots$ are lowered and raised by means of the Minkowski matrix.

The presence of a gravitational field $\underset{a}{h}^i(x)$ endows the space-time continuum with definite geometrical properties. In the first place we can define a metric in this space with a metric tensor

$$g_{ik} = \underset{a}{h_i}\overset{a}{h_k} = \varepsilon_a \underset{a}{h_i}\underset{a}{h_k} = g_{ki}, \tag{2.11}$$

which obviously is a symmetric covariant tensor. Its determinant $g = det(g_{ik})$ is

$$g = det(\underset{a}{h_i}) \cdot det(\overset{a}{h_k}) = -\frac{1}{h^2} \tag{2.12}$$

on account of (2.6), (2.1) and the relation

$$det(\underset{a}{h_i}) = -det(\overset{a}{h_i}) \tag{2.13}$$

following from (2.9) and (2.7). According to (2.12) and (2.2) $g$ is always negative which means that the metric of space-time defined by (2.11) is pseudo-Riemannian like in EGRG. By a suitable choice of coordinates $\mathring{x}^i$ it is then always possible to make the values of $\mathring{g}_{ik}$ and their first order derivation at a given event point $P$ equal to the values in a local Lorentzian system of coordinates:

$$\mathring{g}_{ik}(P) = \eta_{ik}, \quad \mathring{g}_{ik,l}(P) = 0. \tag{2.14}$$

From (2.11) and (2.3) we get

$$g_{ik}\underset{a}{h^k} = \underset{b}{h_i}\overset{b}{h_k}\underset{a}{h^k} = \underset{b}{h_i}\delta^b_a = \underset{a}{h_i} \tag{2.15}$$

which shows that $\underset{a}{h_i}$ and $\underset{a}{h^i}$ are the covariant and contravariant components, respectively, of one and the same tetrad vector. The contravariant components of the metric tensor are then

$$g^{ik} = \underset{a}{h^i}\overset{a}{h^k} = \varepsilon_a \underset{a}{h^i}\underset{a}{h^k}. \tag{2.16}$$

Tensor indices are raised and lowered by means of the metric tensor. For a given metric the curvature of space-time can be defined as in EGRG and, as already mentioned, the only usable invariant which can be constructed from the $g_{ik}$ and their derivatives is the curvature scalar $R$.

However the gravitational field $\underset{a}{h^i}$ endows space-time with other geometrical properties besides curvature viz. those connected with the notion of torsion. Thus it is not a simple Riemannian space but rather a space of the type considered first by Weizenböck[19]. If we multiply (2.3) by $\varepsilon_a$ we get

$$\underset{a}{h_i}\underset{b}{h^i} = \varepsilon_a \delta^a_b = \eta_{ab}, \tag{2.17}$$

which shows that the four vectors $\overset{a}{h}{}^{i}$ are mutually orthogonal unit vectors in the space with the metric $g_{ik}$. The vectors $\overset{\alpha}{h}{}^{i}$ ($\alpha = 1,2,3$) have positive norm and are called space-like while the norm of the "time-like" vector $\overset{4}{h}{}^{i}$ is $-1$. Thus space-time can be pictured as a pseudo-Riemannian space with a built-in tetrad lattice.

Since space-time is more general here than in EGRG we can form a larger number of tensors and invariants. In the first place we can form the tensor

$$\gamma_{ikl} = \overset{a}{h}_i \underset{a}{h}_{k;l} = \underset{a}{h}_i \overset{a}{h}_{k;l} = -\gamma_{kil}. \tag{2.18}$$

Here $\underset{a}{h}_{k;l}$ is the usual covariant derivative of the vector $\underset{a}{h}_k$, i.e.

$$\underset{a}{h}_{k;l} = \underset{a}{h}_{k\ l} - \underset{a}{h}_r \Gamma^r_{kl}, \tag{2.19}$$

where $\Gamma^i_{kl}$ is the Christoffel symbol corresponding to the metric $g_{ik}$. The antisymmetry in the indices $i$ and $k$ follows from the vanishing of the covariant derivative of $g_{ik}$:

$$0 = g_{ik;l} = \underset{a}{h}_{i;l} \overset{a}{h}_k + \underset{a}{h}_i \overset{a}{h}_{k;l} = \gamma_{kil} + \gamma_{ikl}. \tag{2.20}$$

Obviously $\gamma_{ikl}$ is a homogeneous linear function of the first order partial derivatives of the tetrad vectors. In fact one has (see ref. 16, B.1, A.11 and A.15)

$$\gamma_{ikl} = \tfrac{1}{2} P_{ikl}{}^{rst} \overset{a}{h}_r \underset{a}{h}_{s,t} = -\tfrac{1}{2} P_{iklr}{}^{st} \underset{a}{h}_s \overset{a}{h}{}^{r},_t \tag{2.21}$$

where

$$P_{ikl}{}^{rst} = \delta^r_i g_{kl}{}^{st} + \delta^r_k g_{li}{}^{st} - \delta^r_l g_{ik}{}^{st} \tag{2.22}$$

and

$$g_{kl}{}^{st} = \delta^s_k \delta^t_l - \delta^s_l \delta^t_k \tag{2.23}$$

are tensors that do not depend on the derivatives of the tetrad vectors. The same holds for the coefficients of $\underset{a}{h}_{s,t}$ and of $\overset{a}{h}{}^{r},_t$ in (2.21). The tensor $\gamma_{ikl}$ is closely related to the Ricci rotation coefficients (ref. 16, 3.8) and to the torsion (ref. 16, 5.14, 5.15).

A space of the Weitzenböck type has teleparallelism (ref. 16, § 5). Two vectors at distant points $P_1$ and $P_2$ may be defined as parallel when they have equal components relative to the tetrad lattice. This leads to a new type of parallel displacement and covariant differentiation of vectors with an affine connection

$$\Delta^i{}_{kl} = \overset{a}{h}{}^i h_{k,l}. \tag{2.24}$$

It differs from the usual affine connection $\Gamma^i_{kl}$ in a pure Riemannian space by the relation (ref. 16, 5.9)

$$\Delta^i{}_{kl} = \Gamma^i_{kl} + \gamma^i{}_{kl}. \tag{2.25}$$

The covariant derivatives of the second kind of a vector field with components $A^i$ and $A_k$ are

$$\left.\begin{aligned} A^i{}_{|\,l} &= A^i{}_{,\,l} + \Delta^i{}_{kl} A^k = A^i{}_{;l} + \gamma^i{}_{kl} A^k \\ A_{k\,|\,l} &= A_{k,\,l} - \Delta^i{}_{kl} A_i = A_{k;l} - \gamma^i{}_{kl} A_i \end{aligned}\right\} \tag{2.26}$$

with obvious generalizations for tensors of higher rank.

When (2.11) is used in the usual expression for the curvature tensor, $R^i_{klm}$ appears as a function of the tensor $\gamma_{ikl}$ and its first order covariant derivatives. In (ref. 16, D. 6) it is given in terms of derivatives of the second kind. In terms of the usual derivatives we have

$$R^i{}_{klm} = \gamma^i{}_{km;l} - \gamma^i{}_{kl;m} + \gamma^i{}_{rl}\gamma^r{}_{km} - \gamma^i{}_{rm}\gamma^r{}_{kl}. \tag{2.27}$$

Further, if $\Phi_k$ is the vector obtained by contraction of $\gamma^i{}_{kl}$

$$\Phi_k = \gamma^i{}_{ki} = -\gamma_k{}^i{}_i = -\overset{a}{h}_k h^i{}_{;i}, \tag{2.28}$$

the curvature scalar $R$ can be written in the form

$$R = -\frac{2}{\sqrt{-g}}(\sqrt{-g}\,\Phi^r)_{,\,r} + \gamma_{rst}\gamma^{tsr} - \Phi_r\Phi^r. \tag{2.29}$$

Here we have used (ref. 16, A. 5–A. 7), (2.28) and

$$\gamma_{rst}\gamma^{tsr} = \overset{a}{h}{}^r{}_{;s}\overset{a}{h}{}^s{}_{;r} \tag{2.30}$$

following from (2.18) and (2.17).

For a given tetrad field $\overset{a}{}{}^i$ the metric field is uniquely given by (2.11), (2.16). However a given metric $g^{ik}$ does not determine the tetrad field completely; for any Lorentz rotation of the tetrads leads to a new set of tetrads $\overset{a}{\lambda}{}^i$ which also satisfy all the relations (2.2–16). Arbitrary point dependent Lorentz rotations of the tetrads are given by

$$\overset{a}{\lambda}{}^i = \overset{a}{\Omega}{}^b_b(x)\overset{b}{h}{}^i, \quad \overset{a}{\lambda}{}^i = {}^a_b\Omega(x)\overset{b}{h}{}^i \tag{2.31}$$

where the rotation coefficients $\underset{a}{\Omega}^{b}(x)$ and the functions

$$\overset{a}{\underset{b}{\Omega}}(x) = \varepsilon_{a)}\,\varepsilon_{b)}\,\underset{a}{\Omega}^{b}(x) \tag{2.32}$$

are scalars satisfying the Lorentz conditions

$$\underset{a}{\Omega}^{c}\,\underset{c}{\Omega}^{b} = \overset{c}{\underset{a}{\Omega}}\,\underset{c}{\Omega}^{b} = \delta^{a}_{b}, \tag{2.33}$$

Hence

$$\underset{a}{\lambda^{i}}\overset{a}{\lambda^{k}} = \underset{a}{\Omega}^{c}\,\overset{a}{\underset{b}{\Omega}}\,\underset{c}{h^{i}}\overset{b}{h^{k}} = \delta^{c}_{b}\underset{c}{h^{i}}\overset{b}{h^{k}} = g^{ik} \tag{2.34}$$

for arbitrary functions $\underset{a}{\Omega}^{b}(x)$ satisfying (2.33).

Since the Lorentz group is a 6-parametric group, the general solution $\underset{a}{h^{i}}(x)$ of (2.16) for a given metric contains six arbitrary functions. Therefore, besides ten equations determining the metric as in EGRG, the field equations in the present theory must contain six further equations. It should be noticed, however, that a Lorentz rotation (2.31) with constant $\underset{a}{\Omega}^{b}$ does not change neither $g_{ik}$ nor $\gamma_{ikl}$. In this case $\underset{a}{\lambda^{i}}$ and $\underset{a}{h^{i}}$ define a space-time with identical curvature and torsion, i.e. the two tetrad lattices describe the same physical situation. However, apart from a constant Lorentz rotation the tetrad field must be completely determined by the field equations.

The situation in special relativity is characterized by a vanishing torsion, i.e.

$$\gamma_{ikl} = 0 \tag{2.35}$$

which by (2.27) entails a vanishing curvature:

$$R_{iklm} = 0 \tag{2.36}$$

This equation allows the introduction of a pseudo-Cartesian system of coordinates with

$$g_{ik} = \eta_{ik} = g^{ik}. \tag{2.37}$$

Then the equation (2.35) gives

$$\underset{a}{h^{i}}{}_{;k} = \underset{a}{h^{i}}{}_{,k} = 0 \tag{2.38}$$

i.e. the $\underset{a}{h^{i}}$ are constant in this system of coordinates and by a suitable constant Lorentz rotation we can make

$$\underset{a}{h^{i}} = \delta^{i}_{a}. \tag{2.39}$$

For an insular matter system, (2.37) and (2.39) can be chosen as the limiting values of $g_{ik}$ and $\underset{a}{h^{i}}$ for spatial distances $r \to \infty$.

### 3. The General Form of the Field Equations

In accordance with **D** we assume that the field equations are derivable from a Lagrangean principle. The gravitational part $\mathfrak{L} = \sqrt{-g}\, L$ of the Lagrangean density must be a scalar density under coordinate transformations, i.e. $L$ is a scalar constructed from the gravitational potentials $\underset{a}{h^i}$ and their derivatives of the first order

$$L = L(\underset{a}{h^i}, \underset{a}{h^i}_{,k}) \tag{3.1}$$

(higher order derivatives in (3.1) would violate condition **E**). Since a constant rotation of the tetrads shall have no physical effect we have to require that $L$ is invariant also under the group of constant Lorentz rotations. According to (2.21) the tensor $\gamma_{ikl}$ is a linear homogeneous function of the first order derivatives of the tetrads and it is invariant under constant Lorentz rotations. Furthermore it is essentially the only tensor with these properties. Therefore $L$ must be a scalar constructed from the $\gamma_{ikl}$ and the metric tensor $g_{ik}$.

The variation of the Lagrangean integral under arbitrary variations $\delta \underset{a}{h^i}$ that vanish at the boundary of the region of integration is

$$\left.\begin{aligned} \delta \int \mathfrak{L}\, dx &= \delta \int L \sqrt{-g}\, dx \\ &= \int \frac{\delta \mathfrak{L}}{\delta \underset{a}{h^i}}\, \delta \underset{a}{h^i} dx, \end{aligned}\right\} \tag{3.2}$$

where

$$\frac{\delta \mathfrak{L}}{\delta \underset{a}{h^i}} = \frac{\partial \mathfrak{L}}{\partial \underset{a}{h^i}} - \left(\frac{\partial \mathfrak{L}}{\partial \underset{a}{h^i}_{,l}}\right)_{,l} \tag{3.3}$$

is the variational derivative of $\mathfrak{L}$ with respect to $\underset{a}{h^i}$. (3.2) may also be written

$$\delta \int \mathfrak{L}\, dx = \int V_{ik} \overset{a}{h}{}^k \delta \underset{a}{h^i} \sqrt{-g}\, dx, \tag{3.4}$$

where $V_{ik}$ is the tensor

$$V_{ik} = \frac{1}{\sqrt{-g}} \frac{\delta \mathfrak{L}}{\delta \underset{a}{h^i}}\, \underset{a}{h_k}. \tag{3.5}$$

From (2.16) we get for the variation of $g^{ik}$ corresponding to the variation $\delta \underset{a}{h^i}$

$$\left.\begin{aligned} \delta g^{ik} &= \overset{a}{h}{}^{i}\delta \overset{a}{h}{}^{k} + \overset{a}{h}{}^{k}\delta \overset{a}{h}{}^{i} \\ &= \overset{a}{h}{}^{i}\delta \overset{a}{h}{}^{k} + \overset{a}{h}{}^{k}\delta \overset{a}{h}{}^{i} = \delta g^{ki}. \end{aligned}\right\} \tag{3.6}$$

If we define a quantity $\delta f^{ik}$ by

$$\delta f^{ik} = \overset{a}{h}{}^{i}\delta \overset{a}{h}{}^{k} - \overset{a}{h}{}^{k}\delta \overset{a}{h}{}^{i} = -\delta f^{ki} \tag{3.7}$$

we have

$$\overset{a}{h}{}^{k}\delta \overset{a}{h}{}^{i} = \tfrac{1}{2}(\delta g^{ik} - \delta f^{ik}). \tag{3.8}$$

Thus (3.4) may be written

$$\delta \int \mathfrak{L} dx = \int (S_{ik}\delta g^{ik} + F_{ik}\delta f^{ik}) \sqrt{-g}\, dx \tag{3.9}$$

with

$$\left.\begin{aligned} S_{ik} &= \tfrac{1}{2} V_{(ik)} = S_{ki} \\ F_{ik} &= -\tfrac{1}{2} V_{[ik]} = -F_{ki}. \end{aligned}\right\} \tag{3.10}$$

As usual $V_{(ik)}$ and $V_{[ik]}$ denote the symmetrical and antisymmetrical combinations, respectively, i.e.

$$\left.\begin{aligned} V_{(ik)} &= \tfrac{1}{2}(V_{ik} + V_{ki}) \\ V_{[ik]} &= \tfrac{1}{2}(V_{ik} - V_{ki}). \end{aligned}\right\} \tag{3.11}$$

By well-known methods we can derive an identity involving $S_{ik}$ and $F_{ik}$ from the invariance of the Lagrangean integral $\int \mathfrak{L} dx$ under arbitrary infinitesimal coordinate transformations

$$\bar{x}^i = x^i + \xi^i(x). \tag{3.12}$$

The corresponding "local" variations of $g^{ik}$ and $\overset{a}{h}{}^{i}$ are

$$\left.\begin{aligned} \delta g^{ik} &= g^{il}\xi^k{}_{,l} + g^{lk}\xi^i{}_{,l} - g^{ik}{}_{,l}\xi^l \\ \delta \overset{a}{h}{}^{i} &= \overset{a}{h}{}^{l}\xi^i{}_{,l} - \overset{a}{h}{}^{i}{}_{,l}\xi^l \end{aligned}\right\} \tag{3.13}$$

and, by (3.7) and (2.16),

$$\left.\begin{aligned} \delta f^{ik} &= g^{il}\xi^k{}_{,l} - g^{kl}\xi^i{}_{,l} \\ &\quad + (\overset{a}{h}{}^{k}\overset{a}{h}{}^{i}{}_{,l} - \overset{a}{h}{}^{i}\overset{a}{h}{}^{k}{}_{,l})\xi^l. \end{aligned}\right\} \tag{3.14}$$

Introduction of (3.13) and (3.14) into (3.9) gives after partial integrations

$$\delta \int \mathfrak{L} dx = 2 \int \{ - S_i{}^k{}_{;k} + F_i{}^k{}_{;k} - F^{kl} \gamma_{kli} \} \xi^i \sqrt{-g}\, dx = 0. \tag{3.15}$$

for arbitrary $\xi^i(x)$ vanishing at the boundary. Hence the identity

$$S_i{}^k{}_{;k} \equiv F_i{}^k{}_{;k} - F^{kl} \gamma_{kli}. \tag{3.16}$$

Let $\mathfrak{L}_m$ denote the usual Lagrangean density of a macroscopic body, which in addition to the matter variables depends on the metric tensor only. Then the variation of the gravitational variables gives

$$\delta \int \mathfrak{L}_m dx = \int T_{ik} \delta g^{ik} \sqrt{-g}\, dx, \tag{3.17}$$

where $T_{ik}$ is the energy-momentum tensor of the matter. By means of (3.9) and (3.17) the Lagrangean principle for the gravitational field in the presence of matter is

$$\left.\begin{aligned} \delta \int (\mathfrak{L} + \mathfrak{L}_m)\, dx &= \delta \int (L + L_m) \sqrt{-g}\, dx \\ = \int \{ S_{ik} + T_{ik}) \delta g^{ik} + F_{ik} \delta f^{ik} \} \sqrt{-g}\, dx &= 0 \end{aligned}\right\} \tag{3.18}$$

for arbitrary variations $\delta \underset{a}{h^i}$ of the 16 functions $\underset{a}{h^i}$. These variations may be written

$$\delta \underset{a}{h^i} = \varepsilon_{ab} \overset{b}{h^i} \tag{3.19}$$

where the

$$\underset{ab}{\varepsilon}(x) = \delta \underset{a}{h^i} \cdot \underset{b}{h_i}(x) \tag{3.20}$$

are 16 independent infinitesimal functions. Writing $\underset{ab}{\varepsilon}$ as a sum of a symmetrical and antisymmetrical part

$$\underset{ab}{\varepsilon} = \underset{ab}{\sigma} + \underset{ab}{\omega}, \qquad \underset{ab}{\sigma} = \underset{(ab)}{\varepsilon} = \underset{ba}{\sigma}, \qquad \underset{ab}{\omega} = \underset{[ab]}{\varepsilon} = -\underset{ba}{\omega}, \tag{3.21}$$

we get

$$\delta \underset{a}{h^i} = \delta_{(d)} \underset{a}{h^i} + \delta_{(r)} \underset{a}{h^i} \tag{3.22}$$

with

$$\left.\begin{aligned} \delta_{(d)} \underset{a}{h^i} &= \underset{ab}{\sigma} \overset{b}{h^i} \\ \delta_{(r)} \underset{a}{h^i} &= \underset{ab}{\omega} \overset{b}{h^i}. \end{aligned}\right\} \tag{3.23}$$

The latter variation is obviously an infinitesimal Lorentz rotation of the type (2.31), (2.33) with

$$\underset{a}{\Omega}^{b} = \delta_a^b + \underset{a}{\omega}^{b} = \delta_a^b + \varepsilon_{b)} \underset{ab}{\omega}, \tag{3.24}$$

which leaves $g^{ik}$ unchanged. In fact we get from (3.6), (3.7) and (3.23)

$$\left.\begin{aligned} \delta_{(r)} g^{ik} &= (\underset{ab}{\omega} + \underset{ba}{\omega}) \overset{a}{h}{}^i \overset{b}{h}{}^k = 0 \\ \delta_{(r)} f^{ik} &= 2 \underset{ab}{\omega} \overset{a}{h}{}^i \overset{b}{h}{}^k \end{aligned}\right\} \tag{3.25}$$

and

$$\left.\begin{aligned} \delta_{(d)} g^{ik} &= 2 \underset{ab}{\sigma} \overset{a}{h}{}^i \overset{b}{h}{}^k \\ \delta_{(d)} f^{ik} &= 0 . \end{aligned}\right\} \tag{3.26}$$

According to (3.22), (3.25), (3.26) a general variation $\delta \underset{a}{h}{}^i$ is composed of 10 independent "dilations" $\delta_{(d)} \underset{a}{h}{}^i$ for which $\delta f^{ik} = 0$ and 6 independent "rotations" $\delta_{(r)} \underset{a}{h}{}^i$ for which $\delta g^{ik} = 0$. Therefore the variational principle (3.18) leads to the field equations

$$S_{ik} + T_{ik} = 0 , \tag{3.27}$$

$$F_{ik} = 0. \tag{3.28}$$

The $10+6$ field equations (3.27), (3.28) determine the 16 tetrad functions apart from arbitrary constant Lorentz rotations. From (3.27) and the identity (3.16) we get

$$T_i{}^k{}_{;k} = -S_i{}^k{}_{;k} = -F_i{}^k{}_{;k} + F^{kl} \gamma_{kli} = 0$$

on account of (3.28), i.e. the usual conservation law (1.2) is a consequence of the field equations as in Einstein's theory.

With an arbitrary $L$ constructed from the $\gamma_{ikl}$ and $g_{ik}$ we have thus a formalism in which all the essential properties **A**–**E** are valid. In particular the equivalence principle is valid exactly and the world line of a freely falling particle is a geodesic in the space with the metric (2.11), but the metric determined by (3.27), (3.28) will of course in general be different from the metric following from Einstein's field equations. Moreover a theory of this type will give a more satisfactory expression for the energy-momentum complex, since the necessary conditions formulated in ref. 18 are satisfied in the present formalism.

## 4. The Choice of Lagrangean

The arbitraryness in the choice of Lagrangean is decisively limited by the essential requirement that the theory must give the same results as EGRG for the gravitational phenomena inside the solar system. Since $L$ is an invariant constructed from the $\gamma_{ikl}$ and $g_{ik}$ the simplest possible independent expressions are

$$\left.\begin{aligned} L^{(1)} &= \Phi_r \Phi^r, \quad L^{(2)} = \gamma_{rst}\gamma^{rst}, \\ L^{(3)} &= \gamma_{rst}\gamma^{tsr} \end{aligned}\right\} \tag{4.1}$$

where $\Phi_k$ is the vector (2.28)

$$\Phi_k = \gamma^i{}_{ki}. \tag{4.2}$$

On account of (2.21) the expressions $L^{(\nu)}$ in (4.1) are homogeneous functions of the first order derivatives $\overset{h^r}{a}{}_{,t}$ of degree 2. The next simplest algebraic expressions are obviously of degree 4 and there are not less than twelve different independent expressions of this type.

In the simplest case $L$ is a linear combination of the quantities (4.1)

$$\mathfrak{L} = \sum_{\nu=1}^{3} \alpha_\nu \mathfrak{L}^{(\nu)}, \quad \mathfrak{L}^{(\nu)} = \sqrt{-g}\, L^{(\nu)}. \tag{4.3}$$

For each $\nu$ we have an equation of the form (3.9)

$$\delta \int \mathfrak{L}^{(\nu)}\, dx = \int (S^{(\nu)}_{ik}\, \delta g^{ik} + F^{(\nu)}_{ik}\, \delta f^{ik}) \sqrt{-g}\, dx, \tag{4.4}$$

and with (4.3) we obtain

$$\left.\begin{aligned} S_{ik} &= \sum_{\nu=1}^{3} \alpha_\nu S^{(\nu)}_{ik} \\ F_{ik} &= \sum_{\nu=1}^{3} \alpha_\nu F^{(\nu)}_{ik}. \end{aligned}\right\} \tag{4.5}$$

A lengthy but elementary calculation gives the following explicit expressions for $S^{(\nu)}_{ik}$ and $F^{(\nu)}_{ik}$:

$$\left.\begin{aligned} S^{(1)}_{ik} &= \tfrac{1}{2}(\Phi_{i;k} + \Phi_{k;}) - \tfrac{1}{2}\Phi_l(\gamma^l{}_{ik} + \gamma^l{}_{ki}) - g_{ik}(\Phi^l{}_{;l} + \tfrac{1}{2}\Phi_l\Phi^l), \\ S^{(2)}_{ik} &= \gamma^l{}_{ik;l} + \gamma^l{}_{ki;l} + \gamma_{rsi}\gamma^{rs}{}_k - \tfrac{1}{2} g_{ik}\gamma_{rst}\gamma^{rst}, \\ S^{(3)}_{ik} &= \tfrac{1}{2}[\gamma^l{}_{ik;l} + \gamma^l{}_{ki;l}] - \tfrac{1}{2}[\gamma_{rsi}\gamma_k{}^{rs} + \gamma_{rsk}\gamma_i{}^{rs}] - \tfrac{1}{2} g_{ik}\gamma_{rst}\gamma^{tsr} \end{aligned}\right\} \tag{4.6}$$

$$\left.\begin{aligned} F^{(1)}_{ik} &= F^{(3)}_{ik} = \tfrac{1}{2}\left[\Phi_{i,k} = \Phi_{k,i} - \Phi_l(\gamma^l{}_{ik} - \gamma^l{}_{ki})\right] \\ F^{(2)}_{ik} &= -\gamma_{ik}{}^l{}_{;\,l}\,. \end{aligned}\right\} \tag{4.7}$$

The Langrangean density

$$\mathfrak{L}^{(0)} = \mathfrak{L}^{(3)} - \mathfrak{L}^{(1)} = \sqrt{-g}\,(\gamma_{rst}\gamma^{tsr} - \Phi_r\Phi^r) \tag{4.8}$$

has the remarkable property that $\int \mathfrak{L}^{(0)} dx$ is invariant under arbitrary infinitesimal Lorentz rotations of the tetrads; for we have, since $F^{(1)}_{ik} = F^{(3)}_{ik}$

$$\delta \int \mathfrak{L}^{(0)} dx = \int (S^{(3)}_{ik} - S^{(1)}_{ik})\,\delta g^{ik} \sqrt{-g}\, dx. \tag{4.9}$$

This is in accordance with the fact shown in (ref. 16, Appendix A), that $\mathfrak{L}^{(0)}$ is equal to the Lagrangean density $\sqrt{-g}\,R$ in Einstein's theory, apart from a usual divergence which can be disregarded in the variations considered. Thus

$$\delta \int \mathfrak{L}^{(0)}\, dx = \delta \int R \sqrt{-g}\, dx = \int G_{ik}\, \delta g^{ik} \sqrt{-g}\, dx \tag{4.10}$$

where $G_{ik}$ is the Einstein tensor in (1.3). A comparison of (4.9) and (4.10) gives

$$G_{ik} = S^{(3)}_{ik} - S^{(1)}_{ik} \tag{4.11}$$

in accordance with (ref. 16, D. 7, D. 8).

We shall now choose the constants $\alpha_\nu$ such that our theory gives the same results as EGRG in the linear approximation of weak fields. In a suitable system of coordinates we have in this case

$$g_{ik} = \eta_{ik} + y_{ik}, \tag{4.12}$$

where the small quantities $y_{ik}$ satisfy the de Donder relations

$$\varepsilon_k y_{ik,k} = \tfrac{1}{2} y,_i, \quad y = \varepsilon_k y_{kk}. \tag{4.13}$$

Then, neglecting terms of the second order in $y_{ik}$, Einstein's equations (1.3) reduce to

$$\tfrac{1}{2}(\Box y_{ik} - \tfrac{1}{2}\eta_{ik}\Box y) = -\varkappa T_{ik}, \tag{4.14}$$

where

$$\Box = \varepsilon_k \frac{\partial^2}{\partial x^{k2}} \tag{4.15}$$

is the usual d'Alembertian.

In the same approximation the tetrads

$$\underset{a}{h_i} = \eta_{ai} + \tfrac{1}{2} y_{ai} \tag{4.16}$$

obviously satisfy (2.11) with $g_{ik}$ given by (4.12), and from (4.16) we get using (4.13)

$$\left.\begin{aligned} \gamma_{ikl} &= \tfrac{1}{2}(y_{kl,i} - y_{il,k}) \\ \Phi_k &= -\tfrac{1}{4} y_{,k}. \end{aligned}\right\} \tag{4.17}$$

These quantities are small of 1. order. Therefore, neglecting terms of 2. order and using (4.13), the equations (4.6) and (4.7) give

$$\left.\begin{aligned} S_{ik}^{(1)} &= \tfrac{1}{2}(\Phi_{i,k} + \Phi_{k,i}) - \eta_{ik}\varepsilon_l \Phi_{l,l} \\ &= \tfrac{1}{4}(\eta_{ik}\Box y - y_{,i,k}), \\ S_{ik}^{(2)} &= 2S_{ik}^{(3)} = \varepsilon_l \gamma_{lik,l} + \varepsilon_l \gamma_{lkl,l} \\ &= \Box y_{ik} - \tfrac{1}{2} y_{,i,k}, \end{aligned}\right\} \tag{4.18}$$

$$\left.\begin{aligned} F_{ik}^{(1)} &= F_{ik}^{(3)} = \tfrac{1}{2}(\Phi_{i,k} - \Phi_{k,i}) = 0 \\ F_{ik}^{(2)} &= -\varepsilon_l \gamma_{ikl,l} = -\tfrac{1}{2}(\varepsilon_l y_{kl,i,l} - \varepsilon_l y_{il,k,l}) \\ &= -\tfrac{1}{4}(y_{,k,i} - y_{,i,k}) = 0. \end{aligned}\right\} \tag{4.19}$$

From the latter equations and (4.5) we see that the expressions (4.16) satisfy the field equations (3.28):

$$F_{ik} = 0, \tag{4.20}$$

and it can be shown (ref. 16, § 4) that (4.16) are the only expressions satisfying (4.20), apart of course from physically unimportant constant Lorentz rotations.

With (4.18) we get for $S_{ik}$ in (4.5)

$$S_{ik} = (2\alpha_2 + \alpha_3)\tfrac{1}{2}\Box y_{ik} + \frac{\alpha_1}{4}\eta_{ik}\Box y - \tfrac{1}{4}(\alpha_1 + 2\alpha_2 + \alpha_3) y_{,i,k}. \tag{4.21}$$

When (4.21) is introduced into the field equations (3.27), it is seen that the latter equations be identical with the linear Einstein equations (4.14), if we choose

$$\alpha_1 = -\frac{1}{\varkappa}, \quad \alpha_2 = \frac{\lambda}{\varkappa}, \quad \alpha_3 = \frac{1}{\varkappa}(1 - 2\lambda) \tag{4.22}$$

with $\lambda$ equal to an arbitrary dimensionless constant. With these values for the $\alpha_\nu$ we get from (4.5), (4.6), (4.7) and (4.11)

$$\left.\begin{aligned} \varkappa S_{ik} &= -S_{ik}^{(1)} + \lambda S_{ik}^{(2)} + S_{ik}^{(3)} - 2\lambda S_{ik}^{(3)} \\ &= G_{ik} + \lambda (S_{ik}^{(2)} - 2S_{ik}^{(3)}), \\ F_{ik} &= -\frac{\lambda}{\varkappa}(2F_{ik}^{(3)} - F_{ik}^{(2)}). \end{aligned}\right\} \tag{4.23}$$

For $\lambda = 0$ the present theory is identical with Einstein's theory, but for $\lambda \neq 0$ the field equations (3.27), (3.28) take the form

$$G_{ik} + H_{ik} = -\varkappa T_{ik}, \tag{4.24}$$

$$2F_{ik}^{(3)} - F_{ik}^{(2)} = \Phi_{i,k} - \Phi_{k,i} - \Phi_l(\gamma^l{}_{ik} - \gamma^l{}_{ki}) + \gamma_{ik}{}^l{}_{;\,l} = 0, \tag{4.25}$$

$$H_{ik} = \lambda[\gamma_{rsi}\gamma^{rs}{}_k + \gamma_{rsi}\gamma_k{}^{rs} + \gamma_{rsk}\gamma_i{}^{rs} + g_{ik}(\gamma_{rst}\gamma^{tsr} - \tfrac{1}{2}\gamma_{rst}\gamma^{rst})]. \tag{4.26}$$

The equations (4.25) are independent of the choice of $\lambda$. On the other hand the term $H_{ik}$, by which (4.24) deviates from Einstein's field equations (1.3) increases with $\lambda$, which can be taken of order 1 without destroying the first order agreement with Einstein's theory in the weak field case. One might hope, therefore, that the metric obtained as solution of (4.24), (4.25) would be quite different from the solution of (1.3) in the case of strong fields and that it be free of singularities. In the next section we shall investigate this point by considering the case of a spherically symmetric system.

## 5. The Spherically Symmetric Case

In the case of a *static* spherically symmetric system the equations (4.24), (4.25) are most easily solved if we use a system of isotropic coordinates $x^i = \{x^\iota, ct\}$. Here the metric is of the form

$$\left.\begin{aligned} g_{ik} &= g_{ii)}\,\delta_{ik}, \quad g^{ik} = \frac{1}{g_{ii)}}\,\delta_{ik}, \\ g_{ii} &= \{a, a, a, -b\}, \end{aligned}\right\} \tag{5.1}$$

where $a$ and $b$ are functions of $r = x^\iota x^\iota$ only. A possible set of tetrads in accordance with (2.11) and (5.1) is

$$\left.\begin{aligned} \underset{a}{h}{}^i &= \frac{1}{\sqrt{|g_{aa)}|}}\,\delta_a{}^i \\ \underset{a}{h}_i &= g_{ii)}\,\underset{a}{h}{}^i = \varepsilon_{a)}\sqrt{|g_{aa}|}\,\delta_{ai} \end{aligned}\right\} \tag{5.2}$$

from which we get the following expression for the tensor (2.18) and the vector (4.2) (see ref. 16, B. 4, B. 8)

$$\left.\begin{aligned} \gamma_{ikl} &= \frac{g'_{ii)}(r)}{2}(n_i\delta_{kl} - n_k\delta_{il}) \\ n_i &= \frac{\partial r}{\partial x^i} = \left\{\frac{x^1}{r}, \frac{x^2}{r}, \frac{x^3}{r}, 0\right\} \end{aligned}\right\} \tag{5.3}$$

and

$$\Phi_k = -(\ln a\sqrt{b})_{,k} = -(\ln a\sqrt{b})' n_k. \tag{5.4}$$

By calculating the functions (4.7) with (5.3), (5.4) and (5.1) one finds (see the corresponding calculations in ref. 16, Appendix B)

$$F_{ik}^{(1)} = F_{ik}^{(2)} = F_{ik}^{(3)} = 0, \quad F_{ik} = 0 \tag{5.5}$$

Thus the tetrads (5.2) satisfy the field equations (4.25), and it can be shown that (5.2) are the only tetrads satisfying these equations, again apart from constant rotations of the tetrads.

Using (5.3) and (5.1) we get for the different terms in (4.26)

$$\left.\begin{aligned} \gamma_{rsi}\gamma^{rs}{}_k &= -2\gamma_{rsi}\gamma_k{}^{rs} = -2\gamma_{rsk}\gamma_i{}^{rs} \\ &= \frac{(g_{ii)}')^2}{2ag_{ii}}\delta_{ik} - \frac{a'^2}{2a^2}n_i n_k \\ \gamma_{rst}\gamma^{rst} &= 2\gamma_{rst}\gamma^{tsr} = \frac{a'^2}{a^3} + \frac{b'^2}{2ab^2} \end{aligned}\right\} \tag{5.6}$$

i.e.

$$H_{ik} = 0. \tag{5.7}$$

Thus, in the static spherically symmetric case the equations (4.24) have the same solutions as Einstein's equations (1.3). In the empty space outside the matter they lead to the following equations for $a(r)$ and $b(r)$:

$$\left.\begin{aligned} a'' + \frac{2a'}{r} - \frac{3}{4}\frac{a'^2}{a} &= 0 \\ \left(\frac{a'}{r} + \frac{2}{r}\right)\frac{b'}{b} + \frac{2a'}{ra} + \frac{a'^2}{2a} &= 0 \end{aligned}\right\} \tag{5.8}$$

with the well-known solutions

$$a = (1 + \alpha/4r)^4, \quad b = \frac{(1 - \alpha/4r)^2}{(1 + \alpha/4r)^2}. \tag{5.9}$$

The functions $a(r)$ and $b(r)$ in (5.9) are everywhere positive except at the Schwarzschild distance $r = \alpha/4$ where $b(r)$ has the minimum value zero. It would seem that only a small change of the equations (5.8) is necessary to make the minimum value of $b(r)$ positive and thus remove the singularity.

So far we have only considered the static case. As an important example of a time-dependent spherical system we shall now consider the case of the non-static homogeneous isotropic universe. In suitable coordinates the metric has the form given by Robertson and Walker, i.e.

$$\left.\begin{aligned} g_{ik} &= g_{ii)}\,\delta_{ik}, \quad g_{ii} = \{a, a, a, -1\} \\ a &= \frac{R(t)^2}{\psi(r)^2}, \quad \psi(r) = 1 + \zeta r^2/4 \\ \zeta &= \begin{cases} 1 \\ 0 \\ -1 \end{cases}. \end{aligned}\right\} \tag{5.10}$$

With tetrads of the form (5.2) we get in this case

$$\gamma_{ikl} = \begin{cases} 0 \quad \text{for} \quad l = 4 \\ \frac{1}{2}\left[a,_i\,\delta_{k\lambda} - a,_k\,\delta_{i\lambda}\right] \quad \text{for} \quad l = \lambda \end{cases} \tag{5.11}$$

and

$$\Phi_k = \gamma^i{}_{ki} = \left(ln\frac{\Psi^2}{R^3}\right)_{,k}. \tag{5.12}$$

Calculating the tensors (4.7) with (5.11) and (5.12) we obtain

$$F^{(1)}_{ik} = F^{(3)}_{ik} = \tfrac{1}{2}F^{(2)}_{ik} = (lnR),_i\,(ln\,\Psi),_k - (lnR),_k\,(ln\Psi),_i, \tag{5.13}$$

which shows that the field equations (4.25) are satisfied with $\underset{a}{h^i}$ given (5.2). Further we get for the different terms in (4.26)

$$\left.\begin{aligned} \gamma_{rsi}\gamma^{rs}{}_k &= -2\gamma_{rsi}\gamma_k{}^{rs} = -2\gamma_{rsk}\gamma_i{}^{rs} \\ &= \begin{cases} 0 \quad \text{for} \quad i = 4 \quad \text{or} \quad k = 4 \\ \dfrac{2}{\Psi^2}\left[(\Psi'^2 - \dot{R}^2)\,\delta_{\iota\varkappa} - \Psi'^2 n_\iota n_\varkappa\right] \quad \text{for} \quad i = \iota,\ k = \varkappa \end{cases} \end{aligned}\right\} \tag{5.14}$$

Thus, $H_{ik}$ vanishes also in this case, and the metric following from the present formalism is again given by the Friedman solution which has a singularity in the far past and for $\zeta = 1$ also in the far future.

As we have seen the simple Lagrangean density

$$\mathfrak{L} = \frac{1}{\varkappa}[\mathfrak{L}^{(0)} + \lambda(\mathfrak{L}^{(2)} - 2\mathfrak{L}^{(3)})], \tag{5.15}$$

which leads to the field equations (4.24)–(4.26), does not solve our problem. However, as mentioned before there is a large variety of possible expressions $\mathfrak{L}^{(4)}$ of degree 4, and with

$$\mathfrak{L} = \frac{1}{\varkappa}\mathfrak{L}^{(0)} + \mathfrak{L}^{(4)} \tag{5.16}$$

the variational principle leads to equations of the form (4.24) with a non-vanishing $H_{ik}$ in the static spherically symmetric case. Instead of (5.8) we get then

$$\left.\begin{aligned} a'' + \frac{2a'}{r} - \frac{3}{4}\frac{a'^2}{a} &= f \\ \left(\frac{a'}{a} + \frac{2}{r}\right)\frac{b'}{b} + \frac{2a'}{ra} + \frac{a'^2}{2a} &= g \end{aligned}\right\} \tag{5.17}$$

where $f$ and $g$ in general are algebraic functions of $a$, $b$, $a'$, $b'$, $a''$ and $b''$ depending on the choice of $\mathfrak{L}^{(4)}$. Besides terms of degree 4, which in the case of weak fields give contributions to $H_{ik}$ that are small of the third order, we may in $\mathfrak{L}^{(4)}$ also include terms of the type $\frac{1}{\varkappa}\sum_{\nu=1}^{3}\lambda_\nu \mathfrak{L}^{(\nu)}$ with sufficiently small dimensionless constants $\lambda_\nu$. It would be surprising if not one of the many possible Lagrangeans would lead to equations (5.17) with everywhere positive solutions $a(r)$, $b(r)$. On the contrary one could rather fear that there are too many Lagrangeans that have singularity free solutions, in which case it would be difficult to obtain a uniquely determined theory without a new guiding principle.

## Conclusion

In the present paper we have not arrived at a definite formalism which can replace Einstein's precise equations. We have shown only that the breakdown of physics predicted by Hawking on the basis of Einstein's theory does not seem to be inevitable. If we admit that the fundamental gravitational field variables are tetrad fields, the way is open for generalizations of Einstein's theory which retain all the satisfactory features **A**–**E** as well as the experimentally and observationally verified results of EGRG. At the same time such a formalism allows a more satisfactory treatment of the energy-momentum complex, in particular as regards the question of the localizability of the energy. It still remains to be seen if the Lagrangean can be chosen in such a way that the field equations in all cases have non-singular solutions.

## References


1) R. Penrose, Phys. Rev. Lett. **14**, 57 (1965).
S. W. Hawking, Proc. Roy. Soc. A **294**, 511 (1966); **295**, 490 (1966); **300**, 187 (1967).
S. W. Hawking and R. Penrose, Proc. Roy. Soc. A **314**, 529 (1970).
2) See f. inst. E. M. Lifshitz and I. M. Khalatnikov, Adv. in Phys. **12**, 185 (1963).
3) S. W. Hawking, Nature **248**, 30 (1974); Commun. Math. Phys. **17** (2), 174.
4) R. M. Wald, On Particle Creation by Black Holes (Preprint, University of Chicago, 1975).
5) L. Parker, Probability Distribution of Particles Created by a Black Hole (Preprint, University of Wisconsin Milwaukee, 1975).
6) S. W. Hawking, Fundamental Breakdown of Physics in Gravitational Collapse. (Orange Aid Preprint, OAP-420, California Institute of Technology, 1975).
7) A. Einstein, The Meaning of Relativity, Princeton University Press 1953, p. 129.
8) See for instance C. Møller, Measurements in General Relativity and the Principle of Relativity in Problems of Theoretical Physics, Ivanenko Festschrift, Moscow 1976.
9) C. Møller, On the Behaviour of Physical Clocks in the Vicinity of Singularities of a Gravitational Field. Report Ettore Majorana School of Physics, Erice, March 1975.
10) P. J. Role, R. Krotkov and R. H. Dicke, Ann. Phys. **26**, 442 (1964).
11) V. B. Braginsky and V. I. Panov, Zh. Eksp. Theor. Fiz. **61**, 873 (1971).
12) H. Reissner, Annln. Phys. **50**, 106 (1916).
13) H. Weyl, Annln. Phys. **54**, 117 (1917).
14) See f. inst. C. Møller, The Theory of Relativity, 2. Edition, Oxford 1972, § 4, 6, p. 104.
15) R. V. Pound and G. A. Rebka, Phys. Rev. Lett. **4**, 337 (1960).
R. V. Pound and J. L. Snider, Phys. Rev. Lett. **13**, 539 (1964).
16) C. Møller, Mat. Fys. Skr. Dan. Vid. Selsk. **1**, no 10 (1961).
17) C. Pellegrini and J. Plebanski, Mat. Fys. Skr. Dan. Vid. Selsk. **2**, no 4 (1963).
18) C. Møller, Mat. Fys. Medd. Dan. Vid. Selsk. **35**, no. 3 (1966).
19) R. Weitzenböck, Invariantentheorie p. 317ff., Groningen 1923; Sber. preuss. Akad. Wiss. 466 (1928).


Indleveret til Selskabet September 1977.
Færdig fra trykkeriet Januar 1978.